



# Kent Academic Repository

**Dolding-Smith, Jessica (2023) *Maturation of the modern human skeleton*. Doctor of Philosophy (PhD) thesis, University of Kent,.**

## Downloaded from

<https://kar.kent.ac.uk/100671/> The University of Kent's Academic Repository KAR

## The version of record is available from

<https://doi.org/10.22024/UniKent/01.02.100671>

## This document version

UNSPECIFIED

## DOI for this version

## Licence for this version

CC BY-ND (Attribution-NoDerivatives)

## Additional information

## Versions of research works

### Versions of Record

If this version is the version of record, it is the same as the published version available on the publisher's web site. Cite as the published version.

### Author Accepted Manuscripts

If this document is identified as the Author Accepted Manuscript it is the version after peer review but before type setting, copy editing or publisher branding. Cite as Surname, Initial. (Year) 'Title of article'. To be published in ***Title of Journal***, Volume and issue numbers [peer-reviewed accepted version]. Available at: DOI or URL (Accessed: date).

### Enquiries

If you have questions about this document contact [ResearchSupport@kent.ac.uk](mailto:ResearchSupport@kent.ac.uk). Please include the URL of the record in KAR. If you believe that your, or a third party's rights have been compromised through this document please see our [Take Down policy](https://www.kent.ac.uk/guides/kar-the-kent-academic-repository#policies) (available from <https://www.kent.ac.uk/guides/kar-the-kent-academic-repository#policies>).

# **Maturation of the modern human skeleton**



**Jessica Anne Moya Dolding-Smith**

Skeletal Biology Research Centre

School of Anthropology and Conservation

University of Kent

A thesis submitted for the degree of Doctor of Philosophy in Anthropology

2<sup>nd</sup> August 2022

Word count: 86, 753, Page count: 653

# ABSTRACT

**Background:** Maturation is the process of becoming mature and reaching the adult state. Maturation occurs in all body systems, but two well-studied maturation processes that occur during modern human growth are skeletal and sexual maturation. Both processes can be studied on dry bone. Variations between individuals and populations are attributed to genetics and environmental influences. Research into maturation can provide new insights into past lives and modern human biology.

**Aim:** This research examines maturation and development in modern humans using archaeological skeletal collections from England and Scotland. This research looks explicitly at epiphyseal fusion and puberty to determine if the age of occurrence and sequence of these growth events changed between the Iron Age ( $\leq 800$  BC) and the Post-Mediaeval (1855 AD) period.

**Materials:** Two hundred and sixty-one skeletons from different periods across England and Scotland were analysed. This included 11 skeletons from Broadstairs (2000 to 350 BC), twenty-four skeletons from Roman Cirencester (69 to 406 AD), thirty-nine skeletons from Anglo-Saxon Chichester, Cirencester, Newcastle, and Auldham (434 to 1178 AD), one hundred and eighty skeletons from Mediaeval Canterbury, Cirencester, York, and Auldham (1000 to 1537 AD), and 7 Post-Mediaeval skeletons from Sheffield and Auldham (1500 to 1855 AD).

**Method:** An average age-at-death was calculated for each skeleton, mainly from dentition. A stage of fusion (Stage 1: unfused, Stage 2: partially fused, and Stage 3: completely fused) was then assessed for various epiphyses found in the skull, neck, shoulder, elbow, wrist, hip, knee and ankle. Age-at-fusion of each epiphyseal site, order of the fusion sequence and pubertal phase (assessed using selected fusion sites and other elements) were then compared between groupings of skeletons based on social status, archaeological site and time period. Statistical

tests were conducted on the data. This included; a goodness-of-fit chi-square to determine if there was a significant relationship between age and fusion, a Mann-Whitney U test to assess significant differences between pubertal phases across the time periods. A binomial logistic regression determined whether age-at-fusion could be distinguished between skeletons of different social statuses. A multiple regression analysis was employed to determine if age-at-fusion could be predicted from multiple variables.

**Results:** Statistically significant associations between age and fusion indicate four sites (anterior arch and posterior synchondrosis of the atlas, the dentocentral and neurocentral junctions of the axis, and metacarpals 2 – 5, proximal and middle phalangeal epiphyses of the hand) which can contribute to age-at-death estimates for Mediaeval skeletons. Age-at-fusion did not differ significantly between high and low-status skeletons from Mediaeval St Gregory's or when compared between Mediaeval archaeological sites. The cervical vertebrae were the exception.

Skeletal maturation was significantly delayed in the proximal radius during the Anglo-Saxon period compared to the Mediaeval period, although several other fusion sites in the Anglo-Saxon appendicular skeleton approached significance. Age at pubertal phase did not differ when compared between the archaeological periods or within the Mediaeval period. Finally, a typical sequence of fusion was discerned: Elbow – (Hip) – Ankle – (Shoulder) – Knee – Wrist. Slight variations in the sequence occurred throughout British history, a similar finding reported by previous research.

**Conclusion:** This is the first in-depth examination of epiphyseal fusion throughout British history. A key strength of this research is that the same methodology was applied throughout, and therefore comparisons made between data are not influenced by methodological bias. Limited variation in age-at-fusion among the Mediaeval sites is likely due, in part, to similarities in the diet of the sites examined here. Delayed maturation in the Anglo-Saxon period coincided with political and economic unrest that could have affected physical development. Results support the idea that age-at-puberty has only begun to decrease for certain pubertal phases. Only the placement of the shoulder in the sequence of fusion differed in this research compared to previous analyses, and this is likely due to a difference in methodology rather than physiology.

# ACKNOWLEDGEMENTS

I would like to thank my supervisors, Dr Patrick Mahoney and Dr Chris Deter, for helping me across the entirety of my PhD journey, from the first email I sent Chris, asking to be her PhD student, to the plethora of worried messages I sent Patrick about my various PhD panics. Little did they know that when first taking me on as a student, they got a PhD student and her Anxiety with a capital *A*. They have both been fabulous and have seen me through the conception of this thesis to its many edits, in which I sometimes look back at the previous drafts and wonder what was going through my head when I wrote it...and more importantly, what Patrick must have been thinking was going through my head when I wrote it. Their support has been unwavering, and I am grateful they took me on as their student.

I want to thank the University of Kent for the Vice Chancellor's Research Scholarship and the top-up funds I was awarded. I would not have been able to go ahead with the PhD without it. I would also like to thank the Skeletal Biology Research Centre for their award of £400 (and joint award with Dr Rosie Pitfield) and the AAPA Pollitzer Travel Award. All of these allowed me to pursue my PhD to its fullest, including the experiences of presenting my work as a poster at anthropological conferences and being able to collect data for my thesis around England and Scotland.

A major part of this research is the skeletons I conducted my research on. Without them, there would be no thesis. I would therefore like to thank all the institutions that allowed me to collect data and the individual people who hosted me during that time. This includes The Corinium Museum and James Harris (including the special tour I was allowed to take my grandma and her partner on), Durham University and Dr Tina Jakob (one of the friendliest people I have ever met), University of Sheffield and Dr Sophie Newman (who was wonderful and invited me to the pub), National Museums Scotland and Dr Alison Sheridan (who was warm and welcoming), the Novium Museum and Amy Roberts (who sat with me for the entire week and kept me company) and finally the University of Kent where I got my largest skeletal sample size.

Finally, I would like to thank Professor Tracey Kivell for her support, Dr Gina McFarlane, for listening to my many ramblings (it always became a wonderful day when Gina was in the lab), and Dr Alastair Key and Dr Rosie Pitfield for being great friends. Alastair and Rosie helped me navigate the academic field and generally were there in the happy, scary, and sad times and I have fond memories of my time at Kent from them. I also want to thank my stepdad, Mark Pollard, for helping fund my thesis's last few years, especially by allowing me to live rent-free while I toiled away the hours in the office upstairs. Lastly, while my grandpa, John Dolding, was not here to witness even the beginnings of my PhD journey, I am forever in his debt. He taught me the joys of science, the hunger for knowledge and the pursuit of dreams. He always wanted to listen to my academic endeavours, and I wish he could have seen what I have achieved so far because of what he saw in me. I am sure he would have loved to have read my results...

# CONTENTS

## Table of Contents

<b>ABSTRACT .....</b>	<b>I</b>
<b>ACKNOWLEDGEMENTS .....</b>	<b>III</b>
<b>CONTENTS .....</b>	<b>V</b>
<b>LIST OF FIGURES.....</b>	<b>XIII</b>
<b>LIST OF TABLES .....</b>	<b>XVIII</b>
<b>INTRODUCTION .....</b>	<b>1</b>
1.1 STRUCTURE OF THESIS .....	1
1.2. STUDY AIMS .....	3
1.3. DEFINITIONS.....	5
<b>LITERATURE REVIEW .....</b>	<b>8</b>
<b>2.1. INTRODUCTION .....</b>	<b>8</b>
2.1.1. PREFACE .....	8
2.1.2. DEFINITIONS AND KEY TERMS .....	9
<b>2.2. BONE GROWTH .....</b>	<b>18</b>
2.2.1. BONE BIOLOGY.....	18
2.2.2. BONE FORMATION .....	26
<b>2.3. EPIPHYSEAL FUSION .....</b>	<b>43</b>
2.3.1. OVERVIEW.....	43
2.3.2. SYMPHYSIS OR SYNCHONDROSIS? .....	45

2.3.3. SEQUENCE OF EPIPHYSEAL FUSION AROUND THE MODERN HUMAN SKELETON .....	46
<b>2.4. INFLUENCES ON SKELETAL MATURATION.....</b>	<b>52</b>
2.4.1. SECULAR TRENDS .....	52
2.4.2. DIFFERENCES BETWEEN THE SEXES .....	55
2.4.3. GENETIC VARIATION IN MATURATION .....	57
<b>2.5. APPLICATIONS OF EPIPHYSEAL FUSION IN ANTHROPOLOGY .....</b>	<b>60</b>
2.5.1. USING EPIPHYSEAL FUSION TO AGE INDIVIDUALS .....	60
2.5.2. USING EPIPHYSEAL FUSION TO SORT COMMINGLED REMAINS.....	70
2.5.3. USING EPIPHYSEAL FUSION TO ASSESS PUBERTY STAGE .....	72
<b>2.6. GROWTH AND MATURATION IN BRITISH HISTORY .....</b>	<b>75</b>
2.6.1. THE IRON AGE.....	75
2.6.2. THE ROMANS.....	76
2.6.3. THE ANGLO-SAXONS .....	78
2.6.4. THE MEDIAEVAL PERIOD.....	80
2.6.5. POST-MEDIAEVAL ERA .....	86
<b>2.7. SUMMARY .....</b>	<b>88</b>
<b><u>MATERIALS .....</u></b>	<b><u>90</u></b>
<b>3.1. THE ARCHAEOLOGICAL SITES .....</b>	<b>90</b>
3.1.1. INTRODUCTION .....	90
3.1.2. BROADSTAIRS AND ST PETER'S.....	91
3.1.3. CANTERBURY .....	92
3.1.4. CHICHESTER.....	95
3.1.5. CIRENCESTER .....	97
3.1.6. EAST LOTHIAN.....	101
3.1.7. NEWCASTLE-UPON-TYNE.....	104
3.1.8. YORK .....	106
3.1.9. SHEFFIELD .....	108
<b>3.2. SKELETAL SAMPLES.....</b>	<b>111</b>
<b><u>METHODS .....</u></b>	<b><u>111</u></b>
<b>4.1. AGE ESTIMATION.....</b>	<b>111</b>
4.1.1. INTRODUCTION .....	111

4.1.2. JUVENILE AGE ESTIMATION .....	111
4.1.3. ADULT AGE ESTIMATION .....	115
<b>4.2. RECORDING EPIPHYSEAL FUSION .....</b>	<b>119</b>
4.2.1. SCORING EPIPHYSEAL FUSION .....	119
4.2.2. THE EPIPHYSEAL SCAR.....	120
<b>4.3. SKELETAL MATURATION .....</b>	<b>122</b>
4.3.1. DETERMINING AGE-AT-FUSION .....	122
4.3.2. DETERMINING THE SEQUENCE OF FUSION .....	124
4.3.3. INTRA-OBSERVER ERROR .....	125
<b>4.4. SKELETAL PUBERTY .....</b>	<b>127</b>
<b>4.5. STATISTICAL ANALYSES.....</b>	<b>129</b>
<b><u>RESULTS.....</u></b>	<b><u>133</u></b>
<b>5.1. RESEARCH QUESTIONS .....</b>	<b>133</b>
<b>5.2. AGE-AT-FUSION IN ST GREGORY'S.....</b>	<b>136</b>
5.2.1. THE AXIAL SKELETON.....	138
5.2.2. THE APPENDICULAR SKELETON.....	143
5.2.3. SUMMARY OF STATISTICAL ANALYSIS .....	159
<b>5.3. AGE-AT-FUSION BETWEEN HIGH AND LOW STATUS .....</b>	<b>161</b>
<b>5.4. SEQUENCE OF FUSION IN ST GREGORY'S .....</b>	<b>164</b>
<b>5.5. PUBERTY IN MEDIAEVAL CANTERBURY .....</b>	<b>165</b>
5.5.1. AGE AT PUBERTY.....	165
5.5.2. THE RELATION OF EPIPHYSEAL FUSION TO PUBERTAL PHASE.....	167
<b><u>RESULTS.....</u></b>	<b><u>172</u></b>
<b>6.1. RESEARCH QUESTIONS .....</b>	<b>172</b>
<b>6.2. MEDIAEVAL CANTERBURY COMPARED TO OTHER BRITISH MEDIAEVAL SITES.....</b>	<b>174</b>
6.2.1. THE AXIAL SKELETON .....	174
6.2.2. THE UPPER APPENDICULAR SKELETON .....	177
6.2.3. THE LOWER APPENDICULAR SKELETON.....	179
6.2.4. SUMMARY OF UNIVARIATE SIGNIFICANT FINDINGS .....	182
6.2.5. MULTIVARIATE ANALYSIS .....	183

<b>6.3. COMPARING AGE-AT-FUSION BETWEEN IRON AGE, ROMAN, ANGLO-SAXON, MEDIAEVAL AND POST-MEDIAEVAL SITES .....</b>	<b>192</b>
6.3.1. THE AXIAL SKELETON .....	192
6.3.2. THE UPPER APPENDICULAR SKELETON .....	196
6.3.3. THE LOWER APPENDICULAR SKELETON .....	202
6.3.4. SUMMARY OF STATISTICALLY SIGNIFICANT UNIVARIATE DIFFERENCES .....	207
6.3.5. MULTIVARIATE ANALYSIS.....	209
<b>6.4. COMPARING SKELETAL MATURATION TO PUBLISHED LITERATURE.....</b>	<b>221</b>
6.4.1. THE AXIAL SKELETON .....	222
6.4.2. THE UPPER APPENDICULAR SKELETON .....	225
6.4.3. THE LOWER APPENDICULAR SKELETON .....	236
<b>6.5. THE SEQUENCE OF FUSION AT BRITISH ARCHAEOLOGICAL PERIODS AND COMPARED TO POST-MEDIAEVAL AND MODERN (18<sup>TH</sup> – 20<sup>TH</sup> CENTURY AD) PUBLISHED DATA .....</b>	<b>246</b>
6.5.1. ARCHAEOLOGICAL SITES .....	246
6.5.2. ARCHAEOLOGICAL SITES COMPARED TO POST-MEDIAEVAL AND MODERN (18 <sup>TH</sup> – 20 <sup>TH</sup> CENTURY) SAMPLES..	246
<b><u>RESULTS.....</u></b>	<b><u>248</u></b>
<b>7.1. RESEARCH QUESTIONS .....</b>	<b>249</b>
<b>7.2. AGE AT PUBERTY COMPARED BETWEEN MEDIAEVAL CANTERBURY AND YORK SAMPLES .....</b>	<b>251</b>
<b>7.3. AGE AT PUBERTY COMPARED BETWEEN ARCHAEOLOGICAL PERIODS.....</b>	<b>253</b>
7.3.1. SUMMARY OF FINDINGS .....	256
7.3.2. MULTIVARIATE ANALYSIS.....	257
<b><u>DISCUSSION .....</u></b>	<b><u>259</u></b>
<b>8.1. INTRODUCTION .....</b>	<b>259</b>
<b>8.2. MATURATION OF THE MEDIAEVAL SKELETON .....</b>	<b>260</b>
8.2.1. AGE-AT-FUSION IN ST GREGORY’S .....	260
8.2.2. AGE-AT-FUSION BETWEEN HIGH AND LOW STATUS .....	262
8.2.3. AGE-AT-FUSION COMPARED BETWEEN MEDIAEVAL CANTERBURY AND YORK .....	263
8.2.4. PATHOLOGIES IN THE MEDIAEVAL SAMPLES.....	264
<b>8.3. MATURATION OF THE MODERN HUMAN SKELETON THROUGH BRITISH ARCHAEOLOGICAL PERIODS .....</b>	<b>268</b>

8.3.1. COMPARING AGE-AT-FUSION BETWEEN IRON AGE, ROMAN, ANGLO-SAXON, MEDIAEVAL AND POST-MEDIAEVAL SITES .....	268
8.3.2. COMPARING SKELETAL MATURATION IN THE ARCHAEOLOGICAL SAMPLE TO POST-MEDIAEVAL AND MODERN PUBLISHED DATA .....	272
<b>8.4. THE SEQUENCE OF FUSION.....</b>	<b>278</b>
8.4.1. THE SEQUENCE OF FUSION IN ST GREGORY’S .....	279
8.4.2. THE SEQUENCE OF FUSION IN BRITISH ARCHAEOLOGICAL PERIODS AND COMPARED TO POST-MEDIAEVAL AND MODERN (18 <sup>TH</sup> – 20 <sup>TH</sup> CENTURY AD) PUBLISHED DATA .....	280
8.4.3. THE SEQUENCE OF FUSION IN THE MODERN HUMAN SKELETON .....	283
<b>8.5. PUBERTY .....</b>	<b>287</b>
8.5.1. PUBERTY IN ST GREGORY’S.....	287
8.5.2. PUBERTY BETWEEN MEDIAEVAL CANTERBURY AND YORK .....	288
8.5.3. PUBERTY COMPARED BETWEEN ARCHAEOLOGICAL GROUPS .....	288
8.5.4. PUBERTY COMPARED TO PUBLISHED ARCHAEOLOGICAL DATA .....	288
<b>8.6. METHODOLOGICAL CONSIDERATIONS.....</b>	<b>294</b>
8.6.1. OSTEOLOGICAL PARADOX.....	294
8.6.2. SAMPLE SIZE .....	295
8.6.3. UNDOCUMENTED COLLECTIONS .....	295
8.6.4. METHODOLOGICAL DIFFERENCES .....	296
<b>8.7. SUMMARY .....</b>	<b>297</b>
<b><u>CONCLUSION .....</u></b>	<b><u>298</u></b>
<b>9.1. CONCLUSION OF RESEARCH .....</b>	<b>298</b>
9.1.1. MATURATION OF THE MEDIAEVAL SKELETON .....	298
9.1.2. MATURATION OF THE MODERN HUMAN SKELETON THROUGH BRITISH ARCHAEOLOGICAL PERIODS .....	299
9.1.3. THE SEQUENCE OF FUSION.....	299
9.1.4. PUBERTY .....	300
<b>9.2. FUTURE DIRECTION .....</b>	<b>301</b>
<b><u>BIBLIOGRAPHY.....</u></b>	<b><u>302</u></b>
<b><u>APPENDICES.....</u></b>	<b><u>343</u></b>
<b>APPENDIX 1: PREVIOUS LITERATURE .....</b>	<b>343</b>

<b>APPENDIX 2: EPIPHYSEAL FUSION SITES.....</b>	<b>355</b>
A2.1. THE AXIAL SKELETON.....	356
A2.2. THE APPENDICULAR SKELETON.....	359
<b>APPENDIX 3: CORRECTIONS FOR MULTIPLE COMPARISONS .....</b>	<b>366</b>
A3.1 AGE-AT-FUSION IN ST GREGORY’S.....	366
A3.2 PUBERTY IN MEDIAEVAL CANTERBURY .....	367
A3.3 MEDIAEVAL CANTERBURY COMPARED TO OTHER BRITISH MEDIAEVAL SITES.....	368
A3.4 COMPARING AGE-AT-FUSION BETWEEN IRON AGE, ROMAN, ANGLO-SAXON, MEDIAEVAL AND POST-MEDIAEVAL SITES .....	368
<b>APPENDIX 4: AGE-AT-FUSION BETWEEN HIGH AND LOW STATUS ST GREGORY’S SKELETAL COLLECTION.....</b>	<b>371</b>
A4.1 THE SKULL.....	371
A4.2. THE CERVICAL VERTEBRAE.....	373
A4.3. THE SACRUM .....	382
A4.4. THE CLAVICLE .....	383
A4.5. THE SCAPULA.....	386
A4.6. THE HUMERUS.....	389
A4.7. THE RADIUS.....	392
A4.8. THE ULNA .....	394
A4.9. THE HAND.....	396
A4.10. THE OS COXAE .....	398
A4.11. THE FEMUR.....	401
A4.12. THE TIBIA.....	404
<b>APPENDIX 5: PUBERTY IN MEDIAEVAL CANTERBURY .....</b>	<b>406</b>
<b>APPENDIX 6: SUMMARY OF CHAPTER 5 .....</b>	<b>414</b>
<b>APPENDIX 7: MEDIAEVAL CANTERBURY COMPARED TO OTHER BRITISH MEDIAEVAL SITES.....</b>	<b>417</b>
A7. 1. THE SKULL.....	417
A7. 2. THE CERVICAL VERTEBRAE .....	420
A7. 3. THE SACRUM .....	430
A7. 4. THE CLAVICLE.....	431
A7. 5. THE SCAPULA.....	434
A7. 6. THE HUMERUS.....	438
A7. 7. THE RADIUS.....	443
A7. 8. THE ULNA .....	446

A7. 9. THE HAND.....	449
A7. 10. THE OS COXAE .....	452
A7. 11. THE FEMUR .....	456
A7. 12. THE TIBIA .....	461
<b>APPENDIX 8: MULTIPLE REGRESSION OF MEDIAEVAL SITES.....</b>	<b>463</b>
A8. 1. AGE RANGE 3 TO 10 YEARS .....	463
A8.2 AGE RANGE 3 TO 15 YEARS.....	466
A8.3 AGE RANGE 13 TO 20 YEARS FOR THE ACROMIAL BORDER OF THE SCAPULA, THE FEMORAL HEAD, GREATER TROCHANTER AND THE PROXIMAL TIBIA.....	469
A8.4 AGE RANGE 13 TO 20 YEARS FOR THE LESSER TROCHANTER AND THE DISTAL FEMUR.....	472
A8.5 AGE RANGE 16 TO 23 YEARS.....	475
A8.6 AGE RANGE 16 TO 30 YEARS.....	478
<b>APPENDIX 9: COMPARING AGE-AT-FUSION THROUGH TIME .....</b>	<b>481</b>
A9. 1. THE SKULL.....	481
A9. 2. THE CERVICAL VERTEBRAE .....	486
A9. 3. THE SACRUM .....	498
A9. 4. THE CLAVICLE.....	500
A9. 5. THE SCAPULA.....	505
A9. 6. THE HUMERUS.....	511
A9. 7. THE RADIUS.....	518
A9. 8. THE ULNA .....	523
A9. 9. THE HAND.....	527
A9. 10. THE OS COXAE .....	532
A9. 11. THE FEMUR .....	536
A9. 12. THE TIBIA .....	544
<b>APPENDIX 10: MULTIVARIATE ANALYSIS OF MULTIPLE FUSION SITES FOUND SIGNIFICANT FROM UNIVARIATE ANALYSIS ON THE ARCHAEOLOGICAL DATA.....</b>	<b>548</b>
A10.1 AGE RANGE 3 TO 10 YEARS.....	548
A10.2 AGE RANGE 3 TO 15 YEARS.....	551
A10.3 AGE RANGE 12 TO 19 YEARS.....	555
A10.4 AGE RANGE 13 TO 20 YEARS FOR THE ACROMIAL BORDER OF THE SCAPULA, THE FEMORAL HEAD, GREATER TROCHANTER AND THE PROXIMAL TIBIA.....	558
A10.5 AGE RANGE 13 TO 20 YEARS FOR THE LESSER TROCHANTER AND THE DISTAL FEMUR .....	561
A10.6 AGE RANGE 16 TO 23 YEARS.....	565

A10.7 AGE RANGE 16 TO 30 YEARS..... 568

**APPENDIX 11: RELATION OF EPIPHYSEAL FUSION TO PUBERTAL PHASE IN THE MEDIAEVAL SAMPLES  
.....571**

**APPENDIX 12: SACRAL BODIES 1 & 2 CROSS-TABULATED WITH PUBERTAL PHASE AND FUSION  
STAGE FOR THE MEDIAEVAL SITES .....572**

**APPENDIX 13: ADDITIONAL INFORMATION PERTAINING TO THE RELATION OF EPIPHYSEAL FUSION  
TO PUBERTAL PHASE IN THE APPENDICULAR SKELETON OF THE MEDIAEVAL SAMPLES ..... 573**

**APPENDIX 14: ADDITIONAL INFORMATION PERTAINING TO THE RELATION OF EPIPHYSEAL FUSION  
TO PUBERTAL PHASE WITHIN THE ARCHAEOLOGICAL SAMPLES .....578**

**APPENDIX 15: MULTIVARIATE ANALYSIS OF PUBERTY WITHIN THE ARCHAEOLOGICAL SITES.....590**

**APPENDIX 16: ROMAN AND MEDIAEVAL AGES AT FUSION COMPARED TO PUBLISHED LITERATURE  
.....595**

**APPENDIX 17: AGE-AT-FUSION ACROSS PERIODS IN FIGURE FORM .....598**

**APPENDIX 18: AGE-AT-FUSION ACROSS PERIODS FOR THE MEDIAL CLAVICLE .....616**

# LIST OF FIGURES

## Chapter Two:

FIGURE 2. 1: THE MAJOR CLASSIFICATIONS OF BONES IN THE HUMAN SKELETON. IMAGE TAKEN FROM BARKER ET AL., (2021).....	19
FIGURE 2. 2: THE ANATOMY OF A FEMUR. SPONGY BONE CAN BE SEEN IN THE PROXIMAL EPIPHYSIS, WHEREAS COMPACT BONE CAN BE VIEWED IN THE SHAFT. IMAGE TAKEN FROM BARKER ET AL., (2021). .....	22
FIGURE 2. 3: THE PERIOSTEUM AND ENDOSTEUM. IMAGE TAKEN FROM BARKER ET AL., (2021). .....	23
FIGURE 2. 4: CROSS-SECTION OF COMPACT BONE, INCLUDING THE MICROSTRUCTURE OF AN OSTEON AND THE PERIOSTEUM STRUCTURE, AS FOUND IN SCHUENKE ET AL., (2020), ON PAGE 35 OF GENERAL ANATOMY AND MUSCULOSKELETAL SYSTEM. ....	24
FIGURE 2. 5: FEMORAL HEAD SHOWING BOTH RED AND YELLOW MARROW. THE YELLOW MARROW STORES FAT, WHEREAS THE RED MARROW PRODUCES RED BLOOD CELLS AND PLATELETS, KNOWN AS HAEMATOPOIESIS. IMAGE AND INFORMATION TAKEN FROM BARKER ET AL., (2021). .....	25
FIGURE 2. 6: DORSAL VIEW OF A HUMAN EMBRYO AT 4 WEEKS. BOTH SOMITES AND THE NEURAL TUBE CAN BE SEEN. IMAGE TAKEN FROM DEQUÉANT AND POURQUIÉ, (2008), PAGE 371 OF 'SEGMENTAL PATTERNING OF THE VERTEBRAE EMBRYONIC AXIS. .	26
FIGURE 2. 7: SHOWS THE FORMING OF THE NEURAL TUBE WITHIN 24 HOURS IN A CHICK EMBRYO (HUMANPATH.COM, 2007).....	28
FIGURE 2. 8: THE DIAGRAM SHOWS THE NEURAL CREST AND TUBE IN A HUMAN EMBRYO. THE LEFT IMAGE IS A DORSAL AND TRANSVERSE SECTION AT 22 DAYS. THE MIDDLE IMAGE IS AT 23 DAYS. THE RIGHT IMAGE SHOWS A HEALTHY NEWBORN BABY WITH THE NUMBERS DENOTING REGIONS OF THE NEURAL TUBE. (HUMANPATH.COM, 2007). .....	29
FIGURE 2. 9: EARLY BONE FORMATION SUMMARISED IN CHART FORMAT (STEMPLE, 2005; MITCHELL AND SHARMA, 2009; DERUITER AND DOTY, 2011; MACCORD, 2013; BERENDSEN AND OLSEN, 2015; HALL, 2015; DERUITER, 2018; HAMILTON AND MANTON, 2019; TIKKANEN, 2022; MUHR AND ACKERMAN, 2022; THE EDITORS OF ENCYCLOPAEDIA BRITANNICA, 2022) .....	30
FIGURE 2. 10: THIS IMAGE SHOWS HOW SPONGY BONE IS MADE UP OF TRABECULAE. IN TURN, THE TRABECULAE CONTAIN OSTEOCYTES AND RED MARROW MAY FILL IN THE SPACES BETWEEN. IMAGE AND INFORMATION TAKEN FROM BARKER ET AL., (2021). .....	33
FIGURE 2. 11: SHOWS THE STAGES OF INTRAMEMBRANOUS OSSIFICATION. IMAGE TAKEN FROM BARKER ET AL., (2021). .....	34
FIGURE 2. 12: SHOWS THE ZONES DEFINED AT THE GROWTH PLATE AS A BONE, SUCH AS THE FEMUR, GROWS IN LENGTH VIA ENDOCHONDRAL OSSIFICATION. IMAGE TAKEN FROM BARKER ET AL., (2021). .....	38
FIGURE 2. 13: ENDOCHONDRAL OSSIFICATION IS PICTURED HERE. IMAGE FROM BARKER ET AL., (2021). .....	41
FIGURE 2. 14: THE DIAGRAM SHOWS A GROWING FEMUR VERSUS A MATURE FEMUR. THE EPIPHYSIS, METAPHYSIS AND DIAPHYSIS ARE LABELLED. IMAGE FROM BARKER ET AL., (2021). .....	43

FIGURE 2. 15: THE FOUR TYPES OF EPIPHYSES ARE PICTURED HERE. (A) DEPICTS PRESSURE AND TRACTION EPIPHYSES, (B) AND (D) DEPICTS ATAVISTIC EPIPHYSES, (C) DEPICTS AN ABERRANT EPIPHYSIS. IMAGE TAKEN FROM KAUSHAL,(2019). .....	45
FIGURE 2. 16: THE SEQUENCE OF UNION AS RECORDED BY STEVENSON, (1924) ON PAGE 88 .....	47
FIGURE 2. 17: SEQUENCE OF SKELETAL FUSION TAKEN FROM SCHAEFER AND BLACK,(2007) ON PAGE 281.....	49
FIGURE 2. 18: SEQUENCE OF COMPLETE FUSION FOR A SAMPLE OF EUROPEAN SKELETONS TAKEN FROM LENOVER AND ŠEŠELJ, (2019) ON PAGE 387.....	51

### Chapter Three:

FIGURE 3. 1: BROADSTAIRS AND ST PETER’S IS PINNED ON THE MAP. IMAGE TAKEN FROM GOOGLE MAPS. ....	91
FIGURE 3. 2: MAP OF CANTERBURY PROVIDED BY GOOGLE MAPS. AS REFERENCE, BROADSTAIRS LIES TO THE UPPER RIGHT OF THIS MAP. ....	92
FIGURE 3. 3: THIS SHOWS A MORE IN-DEPTH VIEW OF CANTERBURY AND PINNED IS WHERE THE NORTHGATE AREA IS. WHEN SCALED IN, AS SHOWN ON THE PICTURE ON THE RIGHT-HAND SIDE, ROADS SUCH AS ‘HIGH STREET ST GREGORY’S CAN BE SEEN. IMAGES TAKEN FROM GOOGLE MAPS. ....	94
FIGURE 3. 4: CHICHESTER IS MAPPED HERE. AS A REFERENCE, IF THE COAST IS FOLLOWED UP TO THE RIGHT, CANTERBURY AND BROADSTAIRS CAN BE LOCATED. IMAGE PROVIDED BY GOOGLE MAPS. ....	95
FIGURE 3. 5: COMPTON IS SHOWN ON THE RED PIN IN REFERENCE TO CHICHESTER ON THE RIGHT-HAND SIDE MAP. A CLOSER LOOK IS PROVIDED ON THE LEFT. IMAGES PROVIDED BY GOOGLE MAPS. ....	96
FIGURE 3. 6: MAP OF CIRENCESTER. AS A REFERENCE, LONDON IS TO THE EAST-SOUTHEAST OF CIRENCESTER, AND CHICHESTER IS SOUTH-SOUTH-EAST. IMAGE PROVIDED BY GOOGLE MAPS.....	97
FIGURE 3. 7: ST JAMES’ PLACE IS CIRCLED IN BLACK ON THE MAP AND SCALED IN ON THE LEFT-HAND IMAGE. THE SCALED-IN IMAGE SHOWS THE ROADS OLD TETBURY ROAD AND HAMMOND WAY, WHICH ARE VITAL ROADS FOR BOTH FORMER BRIDGES GARAGE/ ST JAMES’ PLACE AND BATH GATE. THE RED CIRCLE ON THE RIGHT-HAND IMAGE HIGHLIGHTS WHERE THE ROMAN AMPHITHEATRE USED TO BE, WHEREAS THE RED CIRCLE ON THE LEFT-HAND IMAGE GIVES AN IDEA OF WHERE BATH GATE – THE OLD ROMAN GATE IS. IMAGES PROVIDED BY GOOGLE MAPS.....	99
FIGURE 3. 8: MAP OF LECHLADE. THE SCALED-IN IMAGE IS TO THE LEFT. IMAGES PROVIDED BY GOOGLE MAPS. ....	101
FIGURE 3. 9: THE EAST LOTHIAN AREA IS SHOWN WITHIN THE RED LINE. IMAGE PROVIDED BY GOOGLE MAPS.....	102
FIGURE 3. 10: THE RED PIN IN THE RIGHT-HAND MAP SHOWS THE PLACEMENT OF AULDHAME IN THE EAST LOTHIAN AREA. THE IMAGE IS THEN SCALED IN ON THE LEFT-HAND MAP. IMAGES PROVIDED BY GOOGLE MAPS. ....	103
FIGURE 3. 11: MAP OF NEWCASTLE-UPON-TYNE. IMAGE PROVIDED BY GOOGLE MAPS. ....	104
FIGURE 3. 12: MAP OF YORK. IMAGE PROVIDED BY GOOGLE MAPS. ....	107
FIGURE 3. 13: THE RED PIN HIGHLIGHTS THE CITY OF SHEFFIELD. TO THE NORTHEAST OF SHEFFIELD IS YORK, WHICH CAN BE SEEN IN THE TOP RIGHT. IMAGE PROVIDED BY GOOGLE MAPS.....	109
FIGURE 3. 14: CARVER STREET IS SHOWN WITHIN THE RED-DOTTED LINES. IMAGE PROVIDED BY GOOGLE MAPS. ....	110

## Chapter Four:

- FIGURE 4. 1: AN EXAMPLE OF HOW TEETH WERE USED TO ESTIMATE AGE. THE LEFT-HAND SIDE OF THE ILLUSTRATION SHOWS DEVELOPING TEETH STILL WITHIN THE ALVEOLAR BONE AND THE ASSOCIATED AGE. THE RIGHT SIDE SHOWS A DEVELOPING TOOTH CROWN AND ROOT WITH ATTAINMENT STAGES AND ASSOCIATED AGES IN THE TABLE BELOW. ALL IMAGES ARE TAKEN FROM ALQAHTANI ET AL., (2010). ..... 112
- FIGURE 4. 2: A FLOW CHART OF THE METHODOLOGY USED IN THIS THESIS IS PRESENTED HERE. THE FUSION SITES USED TO HELP IN AGE ESTIMATION ARE ALSO PRESENTED HERE. THESE FUSION SITES ARE SEPARATE TO THE FUSION SITES USED TO ANALYSE SKELETAL MATURATION. ALL FUSION SITES LISTED ON THE RIGHT-HAND SIDE THAT WERE PRESENT ON THE SKELETON WERE STUDIED, IN NO PARTICULAR ORDER. WHEN ANALYSING ADULT SKELETONS, AGEING METHODS TO LOOK AT DEGRADATION OF THE SKELETON ARE APPLIED ..... 114
- FIGURE 4. 3: PHOTOGRAPHS OF VARIOUS BONES IN DIFFERENT STAGES OF FUSION. (A) LEFT FEMUR. CLEARLY SHOWS BILLOWING OF A GROWING CHILD. LABELLED AS STAGE 1 = NO FUSION, (B) RIGHT ULNA. A FAIRLY WIDE GAP BETWEEN THE SHAFT AND PROXIMAL EPIPHYSIS. LABELLED AS STAGE 2 = PARTIAL FUSION, (C) LEFT AND RIGHT FEMURS FROM ONE INDIVIDUAL. BILLOWING PRESENT AND SEPARATED EPIPHYSES. LABELLED AS STAGE 1 = NO FUSION, (D) SACRUM. A GAP CAN BE SEEN BETWEEN BODIES 1 & 2 BUT WITH FILLING IN ALSO PRESENT. LABELLED AS STAGE 2 = PARTIAL FUSION, (E) LEFT TIBIA. A GAP CAN STILL BE SEEN BETWEEN THE PROXIMAL EPIPHYSIS AND THE SHAFT. POST-MORTEM DAMAGE CAN BE SEEN ON THE PROXIMAL EPIPHYSIS BUT DOES NOT AFFECT THE VISIBILITY OF THE EPIPHYSEAL LINE. LABELLED AS STAGE 2 = PARTIAL FUSION, (F) RIGHT ILIUM. A LARGE GAP IS STILL PRESENT BETWEEN THE ILIUM AND THE ILIAC CREST. LABELLED AS STAGE 2 = PARTIAL FUSION, (G) RIGHT ULNA. IT LOOKS TO HAVE REACHED MATURITY IN TERMS OF PROXIMAL EPIPHYSEAL FUSION. LABELLED AS STAGE 3 = COMPLETE FUSION, (H) RIGHT FEMUR. FULLY MATURE. LABELLED AS STAGE 3 = COMPLETE FUSION. PHOTOGRAPHS TAKEN BY J.A.M. DOLDING-SMITH ON THE ST GREGORY'S SKELETAL COLLECTION HELD AT THE UNIVERSITY OF KENT ..... 120
- FIGURE 4. 4: PHOTOGRAPHS OF FEMURS WITH CLEAR EPIPHYSEAL LINES AROUND THE PROXIMAL EPIPHYSES AND AROUND THE GREATER TROCHANTER IN THE RIGHT PHOTOGRAPH. ALTHOUGH THE LINES ARE STILL EVIDENT, EPIPHYSEAL LINES CAN PERSIST FOR DECADES AFTER FUSION. THE GREATER TROCHANTER HAS A PARTIAL GAP BUT IS MAINLY INFILLED. THUS, ALL THE FUSION SITES IN THESE PHOTOGRAPHS WOULD BE LABELLED AS STAGE 3 = COMPLETE FUSION. PHOTOGRAPHS TAKEN BY J.A.M. DOLDING-SMITH FROM THE ST GREGORY'S SKELETAL COLLECTION HELD AT THE UNIVERSITY OF KENT ..... 121

## Chapter Five:

- FIGURE 5. 1: AGE-AT-FUSION IN THE ST GREGORY'S SKELETAL COLLECTION. BLUE AND BLACK TEXT IS ONLY USED TO HELP READABILITY. .... 137
- FIGURE 5. 2: EPIPHYSEAL FUSION (STAGES 2 AND 3) OF THE AXIAL SKELETON (ALONG WITH THE MEDIAL CLAVICLE) IS PLOTTED AS TO WHERE IT FALLS DURING PUBERTY FOR THE LOW-STATUS MEDIAEVAL ST GREGORY'S SKELETAL COLLECTION ..... 168
- FIGURE 5. 3: GROWTH CHART FOR ST GREGORY'S SKELETAL COLLECTION. GROWTH STAGES ARE SHOWN BY BOXES. AGES ARE GIVEN BY BUBBLES ON THE LEFT. FUSION SITES ARE PLACED NEXT TO THE AGE THAT THE ENTIRE SAMPLE COMPLETED FUSION. COLOURS

OF FUSION SITES AND AGE BUBBLES DENOTE PUBERTAL PHASE. IF A FUSION SITE COULD FUSE DURING MULTIPLE PUBERTAL PHASES, FOLLOWING PUBERTAL PHASES WERE GIVEN ON THE RIGHT-HAND SIDE. ....	171
---	-----

## Chapter Six:

FIGURE 6. 1: TIMING OF FUSION OF THE OSSICULUM TERMINALE TO THE DENS BETWEEN MEDIAEVAL GROUPS. MEDIAEVAL YORK ONLY HAD ONE INDIVIDUAL AT AGE 8 YEARS IN PARTIAL FUSION (STAGE 2). ....	176
FIGURE 6. 2: SCATTER PLOT OF THE FUSION STAGE OF THE OSSICULUM TERMINALE OF THE AXIS COMPARED TO THE AGE-AT-DEATH IN YEARS OF EACH SKELETON FROM EACH RESPECTIVE MEDIAEVAL SITE. ....	190
FIGURE 6. 3: SCATTER PLOT OF THE FUSION OF THE LESSER TROCHANTER OF THE FEMUR BY AGE IN YEARS, SEPARATED BY ARCHAEOLOGICAL PERIOD. ....	220
FIGURE 6. 4: SCATTER PLOT OF THE FUSION OF THE DISTAL EPIPHYSIS OF THE FEMUR BY AGE IN YEARS, SEPARATED BY ARCHAEOLOGICAL PERIOD. ....	220

## Chapter Eight:

FIGURE 8. 1: THE ATLAS OF THE CERVICAL VERTEBRAE WITH COMPLETE BIPARTITION. PHOTOGRAPH WAS TAKEN BY J.A.M DOLDING-SMITH FROM THE ST GREGORY'S SKELETAL COLLECTION HELD AT THE UNIVERSITY OF KENT. ....	266
FIGURE 8. 2: THE AXIS OF THE CERVICAL VERTEBRAE WITH A CREVICE AT THE DENTOCENTRAL JUNCTION. AGES AT FUSION THAT OCCURS DURING THE CHILDHOOD PHASE OF MODERN HUMAN GROWTH IS GIVEN IN THE BLACK BOXES FOR ST GREGORY'S SKELETAL COLLECTION. PHOTOGRAPH WAS TAKEN BY J.A.M DOLDING-SMITH FROM THE FISHERGATE SKELETAL COLLECTION HELD AT THE UNIVERSITY OF DURHAM. ....	267
FIGURE 8. 3: FUSION OF THE PARS LATERALIS TO PARS BASILARIS COMPARED BETWEEN ARCHAEOLOGICAL GROUPS. AGE IN YEARS IS GIVEN IN COLOURED CIRCLES. MODERN DATA IS FROM LISBON, PORTUGAL, 1908-1984AD (BIRTHS AND DEATHS), DRY BONE (CARDOSO ET AL., 2013B). ....	273
FIGURE 8. 4: FUSION OF THE SPHENO-OCCIPITAL SYNCHONDROSIS COMPARED BETWEEN ARCHAEOLOGICAL GROUPS. AGE IN YEARS IS GIVEN IN COLOURED CIRCLES. MODERN DATA IS FROM COIMBRA, PORTUGAL, 1826-1938AD (BIRTHS AND DEATHS), DRY BONE (COQUEUGNIOT AND WEAVER, 2007). ....	274
FIGURE 8. 5: FUSION OF THE MEDIAL CLAVICLE COMPARED BETWEEN ARCHAEOLOGICAL GROUPS. AGE IN YEARS IS GIVEN IN COLOURED CIRCLES. MODERN DATA IS FROM BOSNIA, 1995AD (WAR VICTIMS FROM THE FALL OF SREBRENICA), MALES ONLY, DRY BONE (SCHAEFER, 2008B). ....	276
FIGURE 8. 6: SEQUENCE OF FUSION FOR ST GREGORY'S SKELETAL COLLECTION. THE MODAL SEQUENCE IS ON THE LEFT, WHEREAS OUTLIERS ARE DENOTED BY PINK ARROWS (N/ TOTAL) E.G., 1 OUT 3 SEQUENCES, THE PROXIMAL RADIUS COMES AFTER THE DISTAL HUMERUS AND BEFORE THE ACETABULUM. ....	279

FIGURE 8. 7: SEQUENCE OF FUSION FOR THE ROMAN, ANGLO-SAXON AND MEDIAEVAL ARCHAEOLOGICAL GROUPS, AS WELL AS THE BOSNIAN (SCHAEFER AND BLACK, 2007) AND EUROPEAN (LENOVER AND ŠEŠELJ, 2019) MODAL SEQUENCES FOR COMPLETE FUSION. FUSION SITES WITH A YELLOW LINE AND NOT AN ARROW DICTATE WHERE THE ORDER IN THE SEQUENCE IS UNKNOWN. GAPS REPRESENT NO DATA. COLOURS UNDERNEATH HEADERS AT THE TOP ARE AS FOLLOWS: GREY = OCCIPITAL BONES, ORANGE = BONES/EPIPHYSES THAT MAKE UP THE PELVIS AND HIP, DARK BLUE = EPIPHYSES THAT MAKE UP THE ELBOW, GREEN = EPIPHYSES THAT MAKE UP THE PECTORAL GIRDLE, PURPLE = EPIPHYSES THAT MAKE UP THE ANKLE, RED = EPIPHYSES THAT MAKE UP THE KNEE, AND LIGHT BLUE = EPIPHYSES THAT MAKE UP THE WRIST..... 281

FIGURE 8. 8: SUMMARY OF THE SEQUENCE OF FUSION FOR THE MODERN HUMAN SKELETON..... 286

# LIST OF TABLES

## Chapter Two:

TABLE 2. 1: A SIMPLIFIED VERSION OF INTRAMEMBRANOUS OSSIFICATION. TAKEN FROM: (A) (MADER, 2008; WIGLEY ET AL., 2008; LONG, 2011; CUNNINGHAM ET AL., 2016; BARKER ET AL., 2021), (B) (BARKER ET AL., 2021), (C) (WIGLEY ET AL., 2008), (D) (BARKER ET AL., 2021) .....	35
TABLE 2. 2: SIMPLIFIED STEPS OF ENDOCHONDRAL OSSIFICATION. REFERENCES: (A) (MADER, 2008; LITTLE ET AL., 2011; BARKER ET AL., 2021), (B) (MADER, 2008; WIGLEY ET AL., 2008; BARKER ET AL., 2021), (C) (LITTLE ET AL., 2011; CUNNINGHAM ET AL., 2016; BARKER ET AL., 2021), (D) (WIGLEY ET AL., 2008), (E)(BARKER ET AL., 2021), (F) (ROCHE, 1978).....	42

## Chapter Three:

TABLE 3. 1: ALL SKELETONS AND THEIR CORRESPONDING SITES USED. * = DATES GIVEN IN CENTURIES AND APPROXIMATED BY JAM DOLDING-SMITH INTO EARLY, MID- AND LATE CENTURIES BY DIVIDING 100 YEARS BY 3, ** = APPROXIMATE COLLECTIVE. ACTUAL PHASES ARE LISTED HERE. SK. 327 (PHASE 3), SK. 345 (PHASES 2 – 3), SK. 467 (PHASE 2), SK. 663 (PHASE 2), SK. 742 (PHASE 3), SK. 834 (PHASES 1 – 2) AND SK. 868 (PHASE 3). PHASE 1 = 650 – 1000 AD, PHASE 2 = 1000 – 1200 AD, PHASE 3 = 1200 – 1400 AD, AND PHASE 4 = 1500 – 1700 AD .....	90
TABLE 3. 2: TOTAL SAMPLE SIZE, SPLIT BY LOCATION, ARCHAEOLOGICAL SITE, AND AGE GROUP. ....	112

## Chapter Four:

TABLE 4. 1: FUSION SITES USED TO HELP DETERMINE AGE-AT-DEATH. THE AGE RANGES WERE TAKEN FROM SCHAEFER ET AL., (2009). THE FUSION SITES LISTED HERE WERE USED FOR AGE ESTIMATION ONLY. ....	113
TABLE 4. 2: CRITERIA USED TO ESTIMATE SEX FOR AGE ESTIMATION IN ADULT SKELETONS. REFERENCES USED ARE AS FOLLOWS: A (BUIKSTRA AND UBELAKER, 1994; NIKITA, 2017), B (SCHUTKOWSKI, 1993), C (BRUZEK, 2002), D (BASS, 2005), E (PHENICE, 1967; NIKITA, 2017), F(ROGERS, 2009). ....	116
TABLE 4. 3 LIST OF FUSION SITES RECORDED FOR THE METHODOLOGY USED TO DETERMINE AGE AT FUSION .....	123
TABLE 4. 4: LIST OF FUSION SITES RECORDED FOR THE METHODOLOGY USED TO DETERMINE THE SEQUENCE OF FUSION .....	124

TABLE 4. 5: THE TABLE BELOW SHOWS THE Z SCORES AND P VALUES FOR THE INTRA-OBSERVER ERROR TEST ON AGE AND FUSION SITES BETWEEN A FIRST AND SECOND RECORDING OF FOURTEEN SKELETONS. Z SCORES AND P VALUES ARE BASED ON A WILCOXON SIGNED RANK TEST PERFORMED IN IBM® SPSS® STATISTICS 26 (2019) .....	126
TABLE 4. 6: CRITERIA USED TO ESTIMATE PUBERTAL STAGE. BASED ON THE TABLE GIVEN IN LEWIS ET AL., (2016). BLACK BARS REPRESENT NO FURTHER STAGES. ....	127
TABLE 4. 7: CHOICE OF TEST FOR UNIVARIATE STATISTICAL TESTS USED IN THIS THESIS .....	130
TABLE 4. 8: CHOICE OF TEST USED IN THIS THESIS.....	131
TABLE 4. 9: CHOICE OF TEST FOR MULTIVARIATE STATISTICAL TESTS USED IN THIS THESIS.....	132

## Chapter Five:

TABLE 5. 1: AGE IN YEARS/STAGE OF UNION OF THE OCCIPITAL OF THE SKULL FOR ST GREGORY'S SKELETAL COLLECTION. THE STAGES OF UNION ARE RECORDED AS PERCENTAGES .....	138
TABLE 5. 2: AGE AT YEARS/STAGE OF UNION OF THE ATLAS OF THE CERVICAL VERTEBRAE FOR ST GREGORY'S SKELETAL COLLECTION. THE STAGES OF UNION ARE RECORDED AS PERCENTAGES. ....	140
TABLE 5. 3: AGE IN YEARS/STAGE OF UNION OF THE AXIS OF THE CERVICAL VERTEBRAE FOR ST GREGORY'S SKELETAL COLLECTION. THE STAGES OF UNION ARE RECORDED AS PERCENTAGES.....	141
TABLE 5. 4: AGE IN YEARS/STAGE OF UNION OF THE SACRUM FOR ST GREGORY'S SKELETAL COLLECTION. THE STAGES OF UNION ARE RECORDED AS PERCENTAGES .....	143
TABLE 5. 5: AGE IN YEARS/STAGE OF UNION OF THE CLAVICLE FOR ST GREGORY'S SKELETAL COLLECTION. THE STAGES OF UNION ARE RECORDED AS PERCENTAGES .....	144
TABLE 5. 6: AGE IN YEARS/STAGE OF UNION OF THE SCAPULA FOR ST GREGORY'S SKELETAL COLLECTION. THE STAGES OF UNION ARE RECORDED AS PERCENTAGES .....	145
TABLE 5. 7: AGE IN YEARS/STAGE OF UNION OF THE HUMERUS FOR ST GREGORY'S SKELETAL COLLECTION. THE STAGES OF UNION ARE RECORDED AS PERCENTAGES .....	148
TABLE 5. 8: AGE IN YEARS/STAGE OF UNION OF THE RADIUS FOR ST GREGORY'S SKELETAL COLLECTION. THE STAGES OF UNION ARE RECORDED AS PERCENTAGES. ....	150
TABLE 5. 9: AGE IN YEARS/STAGE OF UNION OF THE ULNA FOR ST GREGORY'S SKELETAL COLLECTION. THE STAGES OF UNION ARE RECORDED AS PERCENTAGES. ....	151
TABLE 5. 10: AGE IN YEARS/STAGE OF UNION OF THE HAND FOR ST GREGORY'S SKELETAL COLLECTION. THE STAGES OF UNION ARE RECORDED AS PERCENTAGES. ....	152
TABLE 5. 11: AGE IN YEARS/STAGE OF UNION OF THE OS COXAE FOR ST GREGORY'S SKELETAL COLLECTION. THE STAGES OF UNION ARE RECORDED AS PERCENTAGES. ....	154
TABLE 5. 12: AGE IN YEARS/STAGE OF UNION OF THE FEMUR FOR ST GREGORY'S SKELETAL COLLECTION. THE STAGES OF UNION ARE RECORDED AS PERCENTAGES. ....	156
TABLE 5. 13: AGE IN YEARS/STAGE OF UNION OF THE TIBIA FOR ST GREGORY'S SKELETAL COLLECTION. THE STAGES OF UNION ARE RECORDED AS PERCENTAGES. ....	158

TABLE 5. 14: FUSION OF EACH SITE AND THE ASSOCIATION WITH AGE. RESULTS WERE PRODUCED FROM A GOODNESS-OF-FIT CHI-SQUARE. ** = STATISTICALLY SIGNIFICANT, † = FAILED THE CHI-SQUARE TEST BUT WAS STATISTICALLY SIGNIFICANT WHEN A FISHER-FREEMAN-HALTON EXACT TEST WAS RUN ON THE DATA ( $P = 0.041$ ).....	160
TABLE 5. 15: ASSUMPTIONS FOR THE BINOMIAL LOGISTIC REGRESSIONS TEST. OUTLIERS WERE MINIMAL AND WERE LEFT IN THE ANALYSIS. ....	161
TABLE 5. 16: BINOMIAL LOGISTIC REGRESSION TO TEST IF AGE-AT-FUSION DIFFERED BETWEEN THE HIGH AND LOW STATUS OF ST GREGORY'S SKELETAL COLLECTION. GREY BOXES ARE ALTERNATED WITH WHITE TO MAKE READABILITY EASIER. ....	163
TABLE 5. 17: AGE AT PUBERTY FOR LOW AND HIGH-STATUS INDIVIDUALS FROM MEDIAEVAL CANTERBURY. THE STAGES OF UNION ARE RECORDED AS PERCENTAGES. ....	166
TABLE 5. 18: EPIPHYSEAL FUSION (STAGES 2 AND 3) OF THE AXIAL SKELETON IS PLOTTED AS TO WHERE IT FALLS DURING PUBERTY FOR THE LOW-STATUS MEDIAEVAL ST GREGORY'S SKELETAL COLLECTION. GREY SHADING SHOWS WHERE FUSION TAKES PLACE. BLUE SHADING SHOWS WHERE FUSION HAS COMPLETED. ....	167
TABLE 5. 19: EPIPHYSEAL FUSION (STAGES 2 AND 3) OF THE APPENDICULAR SKELETON IS PLOTTED AS TO WHERE IT FALLS DURING PUBERTY FOR THE LOW-STATUS MEDIAEVAL ST GREGORY'S SKELETAL COLLECTION. GREY SHADING SHOWS WHERE FUSION TAKES PLACE. ....	170

## Chapter Six:

TABLE 6. 1: AGE AND PHASE FOR THE FUSION OF THE AXIAL SKELETON OF MEDIAEVAL SKELETONS FOR YORK AND CANTERBURY. GREY = STAGE 1 UNFUSED. GREEN = STAGE 2 PARTIAL FUSION. YELLOW = STAGE 3 COMPLETE FUSION. THE FUSION SITES ARE: OCCIPITAL OF THE SKULL: (1) PARS LATERALIS TO PARS BASILARIS, (2) SPHENO-OCCIPITAL SYNCHONDROSIS, ATLAS OF THE CERVICAL VERTEBRAE: (3) ANTERIOR ARCH, (4) POSTERIOR SYNCHONDROSIS, AXIS OF THE CERVICAL VERTEBRAE: (5) OSSICULUM TERMINALE TO THE DENS, (6) DENTONEURAL SYNCHONDROSIS, (7) DENTOCENTRAL & NEUROCENTRAL JUNCTIONS .....	175
TABLE 6. 2: AGE AND PHASE FOR THE FUSION OF THE UPPER APPENDICULAR SKELETON OF MEDIAEVAL SKELETONS FOR YORK, CANTERBURY AND AULDHAME. GREY = STAGE 1 UNFUSED. GREEN = STAGE 2 PARTIAL FUSION. YELLOW = STAGE 3 COMPLETE FUSION. THE FUSION SITES INCLUDE, SCAPULA: (1) CORACOID PROCESS, (2) INFERIOR BORDER, HUMERUS: (3) MEDIAL EPICONDYLE, (4) DISTAL COMPOSITE EPIPHYSIS, RADIUS: (5) PROXIMAL EPIPHYSIS, ULNA: (6) PROXIMAL AND (7) DISTAL EPIPHYSES, HAND: (8) DISTAL PHALANGES.....	178
TABLE 6. 3: AGE AND PHASE FOR THE FUSION OF THE LOWER APPENDICULAR SKELETON OF MEDIAEVAL SKELETONS FOR YORK, CANTERBURY AND AULDHAME. GREY = STAGE 1 UNFUSED. GREEN = STAGE 2 PARTIAL FUSION. YELLOW = STAGE 3 COMPLETE FUSION. THE FUSION SITES INCLUDE, OS COXAE: (1) ISCHIO-PUBIC RAMUS, (2) ILIAC CREST, (3) ACETABULUM, FEMUR: (4) FEMORAL HEAD, (5) GREATER AND (6) LESSER TROCHANTERS, (7) DISTAL EPIPHYSIS .....	181
TABLE 6. 4: AGE AND PHASE FOR THE FUSION OF THE PROXIMAL AND DISTAL TIBIA OF MEDIAEVAL SKELETONS FOR YORK, CANTERBURY AND AULDHAME. GREY = STAGE 1 UNFUSED. GREEN = STAGE 2 PARTIAL FUSION. YELLOW = STAGE 3 COMPLETE FUSION. .	182
TABLE 6. 5: DATA TESTED PRIOR TO CARRYING OUT THE MULTIPLE REGRESSION. ....	183

TABLE 6. 6: DATA TESTED PRIOR TO CARRYING OUT THE MULTIPLE REGRESSION. ....	184
TABLE 6. 7: DATA TESTED PRIOR TO CARRYING OUT THE MULTIPLE REGRESSION. FUSION SITES LISTED IN SHORT-HAND ARE THE FOLLOWING: 1. MEDIAL EPICONDYLE OF THE HUMERUS, 2. SPHENO-OCCIPITAL SYNCHONDROSIS, AND 3. DISTAL PHALANGEAL EPIPHYSES OF THE HAND. ....	185
TABLE 6. 8: DATA TESTED PRIOR TO CARRYING OUT THE MULTIPLE REGRESSION. ....	186
TABLE 6. 9: DATA TESTED PRIOR TO CARRYING OUT THE MULTIPLE REGRESSION. ....	187
TABLE 6. 10: DATA TESTED PRIOR TO CARRYING OUT THE MULTIPLE REGRESSION. ....	188
TABLE 6. 11: MULTIPLE REGRESSION RESULTS FOR MEDIAEVAL CANTERBURY, YORK AND AULDHAME, BETWEEN THE AGES OF 3 TO 10 YEARS AND 3 TO 15 YEARS. ** = STATISTICALLY SIGNIFICANT. ....	190
TABLE 6. 12: MULTIPLE REGRESSION RESULTS FOR MEDIAEVAL CANTERBURY, YORK AND AULDHAME, BETWEEN THE AGES OF 13 TO 20 FOR THE PROXIMAL EPIPHYSES OF THE LEG, ALONG WITH THE ACROMIAL BORDER OF THE SCAPULA, AND THE GREATER TROCHANTER, 13 TO 20 FOR THE LESSER TROCHANTER AND THE DISTAL FEMUR, 16 TO 23, AND 16 TO 30 YEARS. ** = STATISTICALLY SIGNIFICANT. ....	191
TABLE 6. 13: AGE AND PHASE OF THE PARS LATERALIS TO THE PARS BASILARIS OF THE SKULL FOR ROMAN, ANGLO-SAXON, AND MEDIAEVAL GROUPS COLLECTED FROM BRITISH ARCHAEOLOGICAL COLLECTIONS. GREY = STAGE 1 UNFUSED. GREEN = STAGE 2 PARTIAL FUSION. YELLOW = STAGE 3 COMPLETE FUSION. ....	192
TABLE 6. 14: AGE AND PHASE FOR THE FUSION OF THE AXIAL SKELETON FOR ROMAN, ANGLO-SAXON, MEDIAEVAL AND POST-MEDIAEVAL GROUPS COLLECTED FROM BRITISH ARCHAEOLOGICAL COLLECTIONS. GREY = STAGE 1 UNFUSED. GREEN = STAGE 2 PARTIAL FUSION. YELLOW = STAGE 3 COMPLETE FUSION. THE FUSION SITES ARE: THE SKULL: (1) SPHENO-OCCIPITAL SYNCHONDROSIS, ATLAS OF THE CERVICAL VERTEBRAE: (2) ANTERIOR ARCH, (3) POSTERIOR SYNCHONDROSIS, AXIS OF THE CERVICAL VERTEBRAE: (4) OSSICULUM TERMINALE, (5) DENTONEURAL SYNCHONDROSIS, (6) DENTOCENTRAL & NEUROCENTRAL JUNCTIONS, (7) POSTERIOR SYNCHONDROSIS ....	193
TABLE 6. 15: AGE AND PHASE FOR THE FUSION OF BODIES 1 AND 2 OF THE SACRUM FOR ROMAN, ANGLO-SAXON, AND MEDIAEVAL GROUPS COLLECTED FROM BRITISH ARCHAEOLOGICAL COLLECTIONS. GREY = STAGE 1 UNFUSED. GREEN = STAGE 2 PARTIAL FUSION. YELLOW = STAGE 3 COMPLETE FUSION. ....	195
TABLE 6. 16: AGE AND PHASE FOR THE FUSION OF THE UPPER APPENDICULAR SKELETON FOR THE IRON AGE, ROMAN, ANGLO-SAXON, MEDIAEVAL AND POST-MEDIAEVAL GROUPS COLLECTED FROM BRITISH ARCHAEOLOGICAL COLLECTIONS. GREY = STAGE 1 UNFUSED. GREEN = STAGE 2 PARTIAL FUSION. YELLOW = STAGE 3 COMPLETE FUSION. THE FUSION SITES ARE: THE CLAVICLE: (1) MEDIAL AND (2) LATERAL, AND THE SCAPULA: (1) THE CORACOID AND THE (2) ACROMIAL EPIPHYSIS ....	197
TABLE 6. 17: AGE AND PHASE FOR THE FUSION OF THE (1) MEDIAL BORDER AND (2) INFERIOR ANGLE OF THE SCAPULA FOR THE ANGLO-SAXON AND MEDIAEVAL GROUPS COLLECTED FROM BRITISH ARCHAEOLOGICAL COLLECTIONS. GREY = STAGE 1 UNFUSED. GREEN = STAGE 2 PARTIAL FUSION. YELLOW = STAGE 3 COMPLETE FUSION. ....	198
TABLE 6. 18: AGE AND PHASE FOR THE FUSION OF THE UPPER APPENDICULAR SKELETON FOR THE IRON AGE, ROMAN, ANGLO-SAXON AND MEDIAEVAL GROUPS COLLECTED FROM BRITISH ARCHAEOLOGICAL COLLECTIONS. GREY = STAGE 1 UNFUSED. GREEN = STAGE 2 PARTIAL FUSION. YELLOW = STAGE 3 COMPLETE FUSION. THE FUSION SITES ARE: HUMERUS: (1) MEDIAL EPICONDYLE, (2) DISTAL COMPOSITE EPIPHYSIS, (3) PROXIMAL EPIPHYSIS, RADIUS: (4) PROXIMAL AND (5) DISTAL, ULNA: (6) PROXIMAL	199
TABLE 6. 19: AGE AND PHASE FOR THE FUSION OF THE UPPER APPENDICULAR SKELETON FOR THE IRON AGE, ROMAN, ANGLO-SAXON, MEDIAEVAL AND POST-MEDIAEVAL GROUPS COLLECTED FROM BRITISH ARCHAEOLOGICAL COLLECTIONS. GREY = STAGE 1	

<i>UNFUSED. GREEN = STAGE 2 PARTIAL FUSION. YELLOW = STAGE 3 COMPLETE FUSION. THE FUSION SITES ARE: ULNA: (1) DISTAL EPIPHYSIS, HAND: (2) METACARPALS 2 – 5 AND THE PROXIMAL AND MIDDLE PHALANGEAL EPIPHYSES, (3) DISTAL PHALANGEAL EPIPHYSES.....</i>	<i>201</i>
<i>TABLE 6. 20: AGE AND PHASE FOR THE FUSION OF THE LOWER APPENDICULAR SKELETON FOR THE IRON AGE, ROMAN, ANGLO-SAXON AND MEDIAEVAL GROUPS COLLECTED FROM BRITISH ARCHAEOLOGICAL COLLECTIONS. GREY = STAGE 1 UNFUSED. GREEN = STAGE 2 PARTIAL FUSION. YELLOW = STAGE 3 COMPLETE FUSION. THE FUSION SITES ARE: OS COXAE: (1) ILIAC CREST, (2) ACETABULUM, FEMUR: (3) FEMORAL HEAD, AND (4) THE GREATER TROCHANTER.....</i>	<i>203</i>
<i>TABLE 6. 21: AGE AND PHASE FOR THE FUSION OF THE LOWER APPENDICULAR SKELETON FOR THE IRON AGE, ROMAN, ANGLO-SAXON AND MEDIAEVAL GROUPS COLLECTED FROM BRITISH ARCHAEOLOGICAL COLLECTIONS. GREY = STAGE 1 UNFUSED. GREEN = STAGE 2 PARTIAL FUSION. YELLOW = STAGE 3 COMPLETE FUSION. THE FUSION SITES ARE: FEMUR: (1) LESSER TROCHANTER AND (2) THE DISTAL EPIPHYSIS, TIBIA: (3) PROXIMAL AND (4) DISTAL EPIPHYSES .....</i>	<i>206</i>
<i>TABLE 6. 22: SIGNIFICANT RESULTS FROM THE MANN WHITNEY U TESTS WHEN ARCHAEOLOGICAL PERIODS WERE COMPARED. ALL RESULTS WITHIN THE TABLE ABOVE ARE FROM ANALYSES CONDUCTED ON STAGES 2 AND 3 DATA COMBINED. ....</i>	<i>208</i>
<i>TABLE 6. 23: DATA TESTED PRIOR TO CARRYING OUT THE MULTIPLE REGRESSION. ....</i>	<i>210</i>
<i>TABLE 6. 24: DATA TESTED PRIOR TO CARRYING OUT THE MULTIPLE REGRESSION. ....</i>	<i>211</i>
<i>TABLE 6. 25: DATA TESTED PRIOR TO CARRYING OUT THE MULTIPLE REGRESSION. ....</i>	<i>212</i>
<i>TABLE 6. 26: DATA TESTED PRIOR TO CARRYING OUT THE MULTIPLE REGRESSION. ....</i>	<i>213</i>
<i>TABLE 6. 27: DATA TESTED PRIOR TO CARRYING OUT THE MULTIPLE REGRESSION. ....</i>	<i>214</i>
<i>TABLE 6. 28: DATA TESTED PRIOR TO CARRYING OUT THE MULTIPLE REGRESSION. ....</i>	<i>215</i>
<i>TABLE 6. 29: DATA TESTED PRIOR TO CARRYING OUT THE MULTIPLE REGRESSION. ....</i>	<i>216</i>
<i>TABLE 6. 30: MULTIPLE REGRESSION FOR ALL ARCHAEOLOGICAL PERIODS (IRON AGE, ROMAN, ANGLO-SAXON, MEDIAEVAL, AND POST-MEDIAEVAL) FOR MULTIPLE AGE RANGES. ** = STATISTICALLY SIGNIFICANT.....</i>	<i>218</i>
<i>TABLE 6. 31: MULTIPLE REGRESSION FOR ALL ARCHAEOLOGICAL PERIODS (IRON AGE, ROMAN, ANGLO-SAXON, MEDIAEVAL, AND POST-MEDIAEVAL) FOR MULTIPLE AGE RANGES. ** = STATISTICALLY SIGNIFICANT.....</i>	<i>219</i>
<i>TABLE 6. 32: FUSION OF THE PARS LATERALIS TO THE PARS BASILARIS OF THE OCCIPITAL BONE OF THE SKULL SPLIT BY PRIMARY DATA COLLECTED FOR THIS THESIS AND SECONDARY DATA, WHICH WAS TAKEN FROM PUBLISHED LITERATURE. REFERENCES ARE BELOW. LIGHT GREY = UNFUSED (STAGE 1). DARK GREY = PARTIAL FUSION (STAGE 2). BLACK = COMPLETE FUSION (STAGE 3), SOMETIMES STAGES OF FUSION OVERLAP DUE TO VARIATION IN INDIVIDUALS. TO KEEP THE TABLE SIMPLE, OVERLAP OF FUSION STAGES IS DENOTED BY THE WHITE TEXT. THE REFERENCE SAMPLE IS SHOWN IN BLUE AS PARTIAL FUSION (STAGE 2) AND COMPLETE FUSION (STAGE 3) ARE NOT DISTINGUISHED IN THE TEXT. REFERENCES: (A) MODERN, LISBON, PORTUGAL, 1908-1984AD (BIRTHS AND DEATHS), DRY BONE (CARDOSO ET AL., 2013B), (B) MODERN, COLOGNE, GERMANY, 1970s, EMBEDDED BONE AND RADIOGRAPHS* (TILLMANN AND LORENZ, 1978), (C)REFERENCE SAMPLE (SCHAEFER ET AL., 2009)222</i>	<i>222</i>
<i>TABLE 6. 33: FUSION OF THE SPHENO-OCCIPITAL SYNCHONDROSIS SPLIT BY PRIMARY DATA COLLECTED FOR THIS THESIS AND SECONDARY DATA, WHICH WAS TAKEN FROM PUBLISHED LITERATURE. REFERENCES ARE BELOW. LIGHT GREY = UNFUSED (STAGE 1). DARK GREY = PARTIAL FUSION (STAGE 2). BLACK = COMPLETE FUSION (STAGE 3), SOMETIMES STAGES OF FUSION OVERLAP DUE TO VARIATION IN INDIVIDUALS. TO KEEP THE TABLE SIMPLE, OVERLAP OF FUSION STAGES IS DENOTED BY THE WHITE TEXT. THE REFERENCE SAMPLE IS SHOWN IN BLUE AS PARTIAL FUSION (STAGE 2) AND COMPLETE FUSION (STAGE 3) ARE NOT DISTINGUISHED IN THE TEXT. REFERENCES: (A) MODERN, COIMBRA, PORTUGAL, 1826-1938AD (BIRTHS AND DEATHS), DRY</i>	

BONE (COQUEUGNIOT AND WEAVER, 2007), (B) MODERN, FORENSIC DATA BANK, UNITED STATES OF AMERICA, 1950-1990 AD (BIRTHS ONLY), DRY BONE (SHIRLEY AND JANTZ, 2011), (C) MODERN, LIVING PATIENTS, NIIGATA, JAPAN, CT SCANS\* (OKAMOTO ET AL., 1996), (D) REFERENCE SAMPLE (SCHAEFER ET AL., 2009)..... 223

TABLE 6. 34: FUSION OF BODIES 1 & 2 OF THE SACRUM SPLIT BY PRIMARY DATA COLLECTED FOR THIS THESIS AND SECONDARY DATA, WHICH WAS TAKEN FROM PUBLISHED LITERATURE. REFERENCES ARE BELOW. LIGHT GREY = UNFUSED (STAGE 1). DARK GREY = PARTIAL FUSION (STAGE 2). BLACK = COMPLETE FUSION (STAGE 3), SOMETIMES STAGES OF FUSION OVERLAP DUE TO VARIATION IN INDIVIDUALS. TO KEEP THE TABLE SIMPLE, OVERLAP OF FUSION STAGES IS DENOTED BY THE WHITE TEXT. THE REFERENCE SAMPLE IS SHOWN IN BLUE AS PARTIAL FUSION (STAGE 2) AND COMPLETE FUSION (STAGE 3) ARE NOT DISTINGUISHED IN THE TEXT. REFERENCES: (A) MODERN, COIMBRA, PORTUGAL, 1826-1938AD (BIRTHS AND DEATHS), DRY BONE (COQUEUGNIOT AND WEAVER, 2007), (B) MODERN, COIMBRA, PORTUGAL, EARLY 20<sup>TH</sup> CENTURY, DRY BONE (BELCASTRO ET AL., 2008), (C) MODERN, LISBON, PORTUGAL, LATE 19<sup>TH</sup> TO EARLY 20<sup>TH</sup> CENTURY, DRY BONE (RIOS ET AL., 2008), (D) MODERN, SARDINIA, ITALY, EARLY 20<sup>TH</sup> CENTURY, DRY BONE (BELCASTRO ET AL., 2008), (E) REFERENCE SAMPLE (SCHAEFER ET AL., 2009) ..... 224

TABLE 6. 35: FUSION OF THE MEDIAL EPIPHYSIS OF THE CLAVICLE SPLIT BY PRIMARY DATA COLLECTED FOR THIS THESIS AND SECONDARY DATA, WHICH WAS TAKEN FROM PUBLISHED LITERATURE. REFERENCES ARE BELOW. LIGHT GREY = UNFUSED (STAGE 1). DARK GREY = PARTIAL FUSION (STAGE 2). BLACK = COMPLETE FUSION (STAGE 3), SOMETIMES STAGES OF FUSION OVERLAP DUE TO VARIATION IN INDIVIDUALS. TO KEEP THE TABLE SIMPLE, OVERLAP OF FUSION STAGES IS DENOTED BY THE WHITE TEXT. THE REFERENCE SAMPLE IS SHOWN IN BLUE AS PARTIAL FUSION (STAGE 2) AND COMPLETE FUSION (STAGE 3) ARE NOT DISTINGUISHED IN THE TEXT. REFERENCES: (A) POST-MEDIAEVAL, LONDON, ENGLAND, 1646-1859AD, DRY BONE, ORIGINAL METHOD USED FIVE PHASES WHICH WERE GROUPED DOWN INTO THREE PHASES FOR THE PURPOSE OF THIS TABLE USING THE METHODOLOGY IN THIS STUDY, (BLACK AND SCHEUER, 1996), (B) POST-MEDIAEVAL, LONDON, ENGLAND, 1650-1700AD, DRY BONE, ORIGINAL METHOD USED FIVE PHASES WHICH WERE GROUPED DOWN INTO THREE PHASES FOR THE PURPOSE OF THIS TABLE USING THE METHODOLOGY IN THIS STUDY, (BLACK AND SCHEUER, 1996), (C) MODERN, LISBON, PORTUGAL, 1805-1975AD (BIRTHS AND DEATHS), DRY BONE, ORIGINAL METHOD USED FIVE PHASES WHICH WERE GROUPED DOWN INTO THREE PHASES FOR THE PURPOSE OF THIS TABLE USING THE METHODOLOGY IN THIS STUDY, (BLACK AND SCHEUER, 1996), (D) MODERN, COIMBRA, PORTUGAL, 1826-1938AD (BIRTHS AND DEATHS), DRY BONE, (COQUEUGNIOT AND WEAVER, 2007), (E) MODERN, USA, 1912-1938AD, DRY BONE, (LANGLEY-SHIRLEY AND JANTZ, 2010), (F) MODERN, LOS ANGELES, USA, 1977-1979AD (AUTOPSIES), (WEBB AND SUCHY, 1985), (G) MODERN, EAST TENNESSEE, USA, 1986-1998AD, DRY BONE, (LANGLEY-SHIRLEY AND JANTZ, 2010), (H) MODERN, BOSNIA, 1995AD (WAR VICTIMS FROM THE FALL OF SREBRENICA), MALES ONLY, DRY BONE (SCHAEFER, 2008B), (I) MODERN, BERLIN, GERMANY, LIVING PATIENTS, RADIOGRAPHS\*, ORIGINAL METHOD USED FIVE PHASES WHICH WERE GROUPED DOWN INTO THREE PHASES FOR THE PURPOSE OF THIS TABLE USING THE METHODOLOGY IN THIS STUDY, (SCHMELING ET AL., 2004), (J) REFERENCE SAMPLE, (SCHAEFER ET AL., 2009) ..... 227

TABLE 6. 36: FUSION OF THE LATERAL EPIPHYSIS OF THE CLAVICLE SPLIT BY PRIMARY DATA COLLECTED FOR THIS THESIS AND SECONDARY DATA, WHICH HAS COME FROM PUBLISHED LITERATURE AND ARE REFERENCED BELOW. LIGHT GREY REFERS TO SKELETONS RECORDED AS UNFUSED ONLY. DARK GREY REFERS TO SKELETONS RECORDED IN PARTIAL FUSION, WITH THE NUMBERS IN WHITE, LISTING IF DATA WAS ALSO RECORDED FOR STAGE 1 OR 3. BLACK REFERS TO SKELETONS THAT WERE RECORDED AS COMPLETELY FUSED ONLY. BLUE IS BASED OFF PUBLISHED LITERATURE THAT ALSO LOOKED AT MULTIPLE

- SECONDARY DATA SOURCES TO DETERMINE AN AGE-AT-FUSION FOR SKELETONS. FINALLY, THE ASTERISK REFERS TO DATA THAT USED COMPUTER IMAGING TECHNOLOGY. REFERENCES: (A) MODERN, EAST TENNESSEE, USA, 1986-1998AD, DRY BONE, (LANGLEY, 2016), (B) MODERN, EAST TENNESSEE, USA, 1986-1998AD, DRY BONE, (LANGLEY, 2016)..... 228
- TABLE 6. 37: FUSION OF THE CORACOID PROCESS TO THE BODY OF THE SCAPULA SPLIT BY PRIMARY DATA COLLECTED FOR THIS THESIS AND SECONDARY DATA, WHICH WAS TAKEN FROM PUBLISHED LITERATURE. REFERENCES ARE BELOW. LIGHT GREY = UNFUSED (STAGE 1). DARK GREY = PARTIAL FUSION (STAGE 2). BLACK = COMPLETE FUSION (STAGE 3), SOMETIMES STAGES OF FUSION OVERLAP DUE TO VARIATION IN INDIVIDUALS. TO KEEP THE TABLE SIMPLE, OVERLAP OF FUSION STAGES IS DENOTED BY THE WHITE TEXT. THE REFERENCE SAMPLE IS SHOWN IN BLUE AS PARTIAL FUSION (STAGE 2) AND COMPLETE FUSION (STAGE 3) ARE NOT DISTINGUISHED IN THE TEXT. REFERENCES: (A) MODERN, COIMBRA, PORTUGAL, 1826-1938AD (BIRTHS AND DEATHS), DRY BONE (COQUEUGNIOT AND WEAVER, 2007), (B) MODERN, LISBON, PORTUGAL, 1887-1975AD (BIRTHS AND DEATHS), DRY BONE (CARDOSO, 2008A), (C) MODERN, BOSNIA, 1995AD (WAR VICTIMS FROM THE FALL OF SREBRENICA), MALES ONLY, DRY BONE (SCHAEFER, 2008B), (D) REFERENCE SAMPLE (SCHAEFER ET AL., 2009)..... 228
- TABLE 6. 38: FUSION OF THE ACROMION PROCESS TO THE BODY OF THE SCAPULA SPLIT BY PRIMARY DATA COLLECTED FOR THIS THESIS AND SECONDARY DATA, WHICH WAS TAKEN FROM PUBLISHED LITERATURE. REFERENCES ARE BELOW. LIGHT GREY = UNFUSED (STAGE 1). DARK GREY = PARTIAL FUSION (STAGE 2). BLACK = COMPLETE FUSION (STAGE 3), SOMETIMES STAGES OF FUSION OVERLAP DUE TO VARIATION IN INDIVIDUALS. TO KEEP THE TABLE SIMPLE, OVERLAP OF FUSION STAGES IS DENOTED BY THE WHITE TEXT. THE REFERENCE SAMPLE IS SHOWN IN BLUE AS PARTIAL FUSION (STAGE 2) AND COMPLETE FUSION (STAGE 3) ARE NOT DISTINGUISHED IN THE TEXT. REFERENCES: (A) MODERN, COIMBRA, PORTUGAL, 1826-1938AD (BIRTHS AND DEATHS), DRY BONE (COQUEUGNIOT AND WEAVER, 2007), (B) MODERN, LISBON, PORTUGAL, 1887-1975AD (BIRTHS AND DEATHS), DRY BONE (CARDOSO, 2008A), (C) MODERN, USA, 1950-1952AD (WAR VICTIMS FROM THE KOREAN WAR), MALES ONLY, DRY BONE (MCKERN AND STEWART, 1957), (D) MODERN, BOSNIA, 1995AD (WAR VICTIMS FROM THE FALL OF SREBRENICA), MALES ONLY, DRY BONE (SCHAEFER, 2008B), (E) REFERENCE SAMPLE (SCHAEFER ET AL., 2009)..... 229
- TABLE 6. 39: FUSION OF THE MEDIAL BORDER OF THE SCAPULA SPLIT BY PRIMARY DATA COLLECTED FOR THIS THESIS AND SECONDARY DATA, WHICH WAS TAKEN FROM PUBLISHED LITERATURE. REFERENCES ARE BELOW. LIGHT GREY = UNFUSED (STAGE 1). DARK GREY = PARTIAL FUSION (STAGE 2). BLACK = COMPLETE FUSION (STAGE 3), SOMETIMES STAGES OF FUSION OVERLAP DUE TO VARIATION IN INDIVIDUALS. TO KEEP THE TABLE SIMPLE, OVERLAP OF FUSION STAGES IS DENOTED BY THE WHITE TEXT. THE REFERENCE SAMPLE IS SHOWN IN BLUE AS PARTIAL FUSION (STAGE 2) AND COMPLETE FUSION (STAGE 3) ARE NOT DISTINGUISHED IN THE TEXT. REFERENCES: (A) MODERN, USA, 1950-1952AD (WAR VICTIMS FROM THE KOREAN WAR), MALES ONLY, DRY BONE (MCKERN AND STEWART, 1957), (B) MODERN, BOSNIA, 1995AD (WAR VICTIMS FROM THE FALL OF SREBRENICA), MALES ONLY, DRY BONE (SCHAEFER, 2008B), (C) REFERENCE SAMPLE (SCHAEFER ET AL., 2009)..... 229
- TABLE 6. 40: FUSION OF THE INFERIOR BORDER TO THE BODY OF THE SCAPULA SPLIT BY PRIMARY DATA COLLECTED FOR THIS THESIS AND SECONDARY DATA, WHICH HAS COME FROM PUBLISHED LITERATURE AND ARE REFERENCED BELOW. LIGHT GREY REFERS TO SKELETONS RECORDED AS UNFUSED ONLY. DARK GREY SECONDARY DATA, WHICH WAS TAKEN FROM PUBLISHED LITERATURE. REFERENCES ARE BELOW. LIGHT GREY = UNFUSED (STAGE 1). DARK GREY = PARTIAL FUSION (STAGE 2). BLACK = COMPLETE FUSION (STAGE 3), SOMETIMES STAGES OF FUSION OVERLAP DUE TO VARIATION IN INDIVIDUALS. TO KEEP THE TABLE SIMPLE, OVERLAP OF FUSION STAGES IS DENOTED BY THE WHITE TEXT. THE REFERENCE SAMPLE IS SHOWN IN BLUE AS PARTIAL FUSION (STAGE 2) AND COMPLETE FUSION (STAGE 3) ARE NOT DISTINGUISHED IN THE TEXT. REFERENCES: (A) POST-MEDIAEVAL, LISBON, PORTUGAL, 1887-1975AD (BIRTHS AND DEATHS), DRY BONE (CARDOSO, 2008A), (B) MODERN, USA, 1950-

<i>1952AD (WAR VICTIMS FROM THE KOREAN WAR), MALES ONLY, DRY BONE (MCKERN AND STEWART, 1957), (C) MODERN, BOSNIA, 1995AD (WAR VICTIMS FROM THE FALL OF SREBRENICA), MALES ONLY, DRY BONE (SCHAEFER, 2008B) .....</i>	<i>230</i>
--	------------

<b>TABLE 6. 41: FUSION OF THE MEDIAL EPICONDYLE OF THE HUMERUS SPLIT BY PRIMARY DATA COLLECTED FOR THIS THESIS AND SECONDARY DATA, WHICH WAS TAKEN FROM PUBLISHED LITERATURE. REFERENCES ARE BELOW. LIGHT GREY = UNFUSED (STAGE 1). DARK GREY = PARTIAL FUSION (STAGE 2). BLACK = COMPLETE FUSION (STAGE 3), SOMETIMES STAGES OF FUSION OVERLAP DUE TO VARIATION IN INDIVIDUALS. TO KEEP THE TABLE SIMPLE, OVERLAP OF FUSION STAGES IS DENOTED BY THE WHITE TEXT. THE REFERENCE SAMPLE IS SHOWN IN BLUE AS PARTIAL FUSION (STAGE 2) AND COMPLETE FUSION (STAGE 3) ARE NOT DISTINGUISHED IN THE TEXT. REFERENCES: (A) MODERN, COIMBRA, PORTUGAL, 1826-1938AD (BIRTHS AND DEATHS), DRY BONE (COQUEUGNIOT AND WEAVER, 2007), (B) MODERN, LISBON, PORTUGAL, 1887-1975AD (BIRTHS AND DEATHS), DRY BONE (CARDOSO, 2008A), (C) MODERN, BOSNIA, 1995AD (WAR VICTIMS FROM THE FALL OF SREBRENICA), MALES ONLY, DRY BONE (SCHAEFER, 2008B), (D) MODERN, CHANDIGARH, INDIA, LIVING PATIENTS, RADIOGRAPHS*, (SAHNI ET AL., 1995), (E) REFERENCE SAMPLE (SCHAEFER ET AL., 2009) .....</b>	<b>232</b>
--	------------

<b>TABLE 6. 42: FUSION OF THE DISTAL COMPOSITE EPIPHYSIS TO THE SHAFT OF THE HUMERUS SPLIT BY PRIMARY DATA COLLECTED FOR THIS THESIS AND SECONDARY DATA, WHICH WAS TAKEN FROM PUBLISHED LITERATURE. REFERENCES ARE BELOW. LIGHT GREY = UNFUSED (STAGE 1). DARK GREY = PARTIAL FUSION (STAGE 2). BLACK = COMPLETE FUSION (STAGE 3), SOMETIMES STAGES OF FUSION OVERLAP DUE TO VARIATION IN INDIVIDUALS. TO KEEP THE TABLE SIMPLE, OVERLAP OF FUSION STAGES IS DENOTED BY THE WHITE TEXT. THE REFERENCE SAMPLE IS SHOWN IN BLUE AS PARTIAL FUSION (STAGE 2) AND COMPLETE FUSION (STAGE 3) ARE NOT DISTINGUISHED IN THE TEXT. REFERENCES: (A) MODERN, COIMBRA, PORTUGAL, 1826-1938AD (BIRTHS AND DEATHS), DRY BONE (COQUEUGNIOT AND WEAVER, 2007), (B) MODERN, LISBON, PORTUGAL, 1887-1975AD (BIRTHS AND DEATHS), DRY BONE (CARDOSO, 2008A), (C) MODERN, BOSNIA, 1995AD (WAR VICTIMS FROM THE FALL OF SREBRENICA), MALES ONLY, DRY BONE (SCHAEFER, 2008B), (D) REFERENCE SAMPLE (SCHAEFER ET AL., 2009) .....</b>	<b>233</b>
--	------------

<b>TABLE 6. 43: FUSION OF THE PROXIMAL EPIPHYSIS OF THE HUMERUS SPLIT BY PRIMARY DATA COLLECTED FOR THIS THESIS AND SECONDARY DATA, WHICH WAS TAKEN FROM PUBLISHED LITERATURE. REFERENCES ARE BELOW. LIGHT GREY = UNFUSED (STAGE 1). DARK GREY = PARTIAL FUSION (STAGE 2). BLACK = COMPLETE FUSION (STAGE 3), SOMETIMES STAGES OF FUSION OVERLAP DUE TO VARIATION IN INDIVIDUALS. TO KEEP THE TABLE SIMPLE, OVERLAP OF FUSION STAGES IS DENOTED BY THE WHITE TEXT. THE REFERENCE SAMPLE IS SHOWN IN BLUE AS PARTIAL FUSION (STAGE 2) AND COMPLETE FUSION (STAGE 3) ARE NOT DISTINGUISHED IN THE TEXT. REFERENCES: (A) MODERN, COIMBRA, PORTUGAL, 1826-1938AD (BIRTHS AND DEATHS), DRY BONE (COQUEUGNIOT AND WEAVER, 2007), (B) MODERN, LISBON, PORTUGAL, 1887-1975AD (BIRTHS AND DEATHS), DRY BONE (CARDOSO, 2008A), (C) MODERN, BOSNIA, 1995AD (WAR VICTIMS FROM THE FALL OF SREBRENICA), MALES ONLY, DRY BONE (SCHAEFER, 2008B), (D) MODERN, CENTRAL INDIA, INDIA, LIVING PATIENTS, RADIOGRAPHS, FEMALES ONLY (TIRPUDE ET AL., 2014), (E) REFERENCE SAMPLE (SCHAEFER ET AL., 2009) .....</b>	<b>233</b>
--	------------

<b>TABLE 6. 44: FUSION OF THE PROXIMAL EPIPHYSIS OF THE RADIUS SPLIT BY PRIMARY DATA COLLECTED FOR THIS THESIS AND SECONDARY DATA, WHICH WAS TAKEN FROM PUBLISHED LITERATURE. REFERENCES ARE BELOW. LIGHT GREY = UNFUSED (STAGE 1). DARK GREY = PARTIAL FUSION (STAGE 2). BLACK = COMPLETE FUSION (STAGE 3), SOMETIMES STAGES OF FUSION OVERLAP DUE TO VARIATION IN INDIVIDUALS. TO KEEP THE TABLE SIMPLE, OVERLAP OF FUSION STAGES IS DENOTED BY THE WHITE TEXT. THE REFERENCE SAMPLE IS SHOWN IN BLUE AS PARTIAL FUSION (STAGE 2) AND COMPLETE FUSION (STAGE 3) ARE NOT DISTINGUISHED IN THE TEXT. REFERENCES: (A) MODERN, COIMBRA, PORTUGAL, 1826-1938AD (BIRTHS AND DEATHS), DRY BONE (COQUEUGNIOT AND WEAVER, 2007), (B) MODERN, LISBON, PORTUGAL, 1887-1975AD (BIRTHS AND DEATHS), DRY BONE (CARDOSO, 2008A), (C) MODERN, BOSNIA, 1995AD (WAR VICTIMS FROM THE FALL OF SREBRENICA), MALES ONLY, DRY BONE (SCHAEFER, 2008B), (D) MODERN, CHANDIGARH, INDIA, LIVING PATIENTS, RADIOGRAPHS*, (SAHNI ET AL., 1995), (E) REFERENCE SAMPLE (SCHAEFER ET AL., 2009) .....</b>	<b>233</b>
--	------------

<i>BONE (CARDOSO, 2008A), (C) MODERN, BOSNIA, 1995AD (WAR VICTIMS FROM THE FALL OF SREBRENICA), MALES ONLY, DRY BONE (SCHAEFER, 2008B), (D) REFERENCE SAMPLE (SCHAEFER ET AL., 2009) .....</i>	<i>234</i>
<i>TABLE 6. 45: FUSION OF THE DISTAL EPIPHYSIS OF THE RADIUS SPLIT BY PRIMARY DATA COLLECTED FOR THIS THESIS AND SECONDARY DATA, WHICH WAS TAKEN FROM PUBLISHED LITERATURE. REFERENCES ARE BELOW. LIGHT GREY = UNFUSED (STAGE 1). DARK GREY = PARTIAL FUSION (STAGE 2). BLACK = COMPLETE FUSION (STAGE 3), SOMETIMES STAGES OF FUSION OVERLAP DUE TO VARIATION IN INDIVIDUALS. TO KEEP THE TABLE SIMPLE, OVERLAP OF FUSION STAGES IS DENOTED BY THE WHITE TEXT. THE REFERENCE SAMPLE IS SHOWN IN BLUE AS PARTIAL FUSION (STAGE 2) AND COMPLETE FUSION (STAGE 3) ARE NOT DISTINGUISHED IN THE TEXT. REFERENCES: (A) MODERN, COIMBRA, PORTUGAL, 1826-1938AD (BIRTHS AND DEATHS), DRY BONE (COQUEUGNIOT AND WEAVER, 2007), (B) MODERN, LISBON, PORTUGAL, 1887-1975AD (BIRTHS AND DEATHS), DRY BONE (CARDOSO, 2008A), (C) MODERN, BOSNIA, 1995AD (WAR VICTIMS FROM THE FALL OF SREBRENICA), MALES ONLY, DRY BONE (SCHAEFER, 2008B), (D) REFERENCE SAMPLE (SCHAEFER ET AL., 2009) .....</i>	
<i>TABLE 6. 46: FUSION OF THE PROXIMAL EPIPHYSIS OF THE ULNA SKULL SPLIT BY PRIMARY DATA COLLECTED FOR THIS THESIS AND SECONDARY DATA, WHICH WAS TAKEN FROM PUBLISHED LITERATURE. REFERENCES ARE BELOW. LIGHT GREY = UNFUSED (STAGE 1). DARK GREY = PARTIAL FUSION (STAGE 2). BLACK = COMPLETE FUSION (STAGE 3), SOMETIMES STAGES OF FUSION OVERLAP DUE TO VARIATION IN INDIVIDUALS. TO KEEP THE TABLE SIMPLE, OVERLAP OF FUSION STAGES IS DENOTED BY THE WHITE TEXT. THE REFERENCE SAMPLE IS SHOWN IN BLUE AS PARTIAL FUSION (STAGE 2) AND COMPLETE FUSION (STAGE 3) ARE NOT DISTINGUISHED IN THE TEXT. REFERENCES: (A) MODERN, COIMBRA, PORTUGAL, 1826-1938AD (BIRTHS AND DEATHS), DRY BONE (COQUEUGNIOT AND WEAVER, 2007), (B) MODERN, LISBON, PORTUGAL, 1887-1975AD (BIRTHS AND DEATHS), DRY BONE (CARDOSO, 2008A), (C) MODERN, BOSNIA, 1995AD (WAR VICTIMS FROM THE FALL OF SREBRENICA), MALES ONLY, DRY BONE (SCHAEFER, 2008B), (D) REFERENCE SAMPLE (SCHAEFER ET AL., 2009) .....</i>	<i>234</i>
<i>TABLE 6. 46: FUSION OF THE PROXIMAL EPIPHYSIS OF THE ULNA SKULL SPLIT BY PRIMARY DATA COLLECTED FOR THIS THESIS AND SECONDARY DATA, WHICH WAS TAKEN FROM PUBLISHED LITERATURE. REFERENCES ARE BELOW. LIGHT GREY = UNFUSED (STAGE 1). DARK GREY = PARTIAL FUSION (STAGE 2). BLACK = COMPLETE FUSION (STAGE 3), SOMETIMES STAGES OF FUSION OVERLAP DUE TO VARIATION IN INDIVIDUALS. TO KEEP THE TABLE SIMPLE, OVERLAP OF FUSION STAGES IS DENOTED BY THE WHITE TEXT. THE REFERENCE SAMPLE IS SHOWN IN BLUE AS PARTIAL FUSION (STAGE 2) AND COMPLETE FUSION (STAGE 3) ARE NOT DISTINGUISHED IN THE TEXT. REFERENCES: (A) MODERN, COIMBRA, PORTUGAL, 1826-1938AD (BIRTHS AND DEATHS), DRY BONE (COQUEUGNIOT AND WEAVER, 2007), (B) MODERN, LISBON, PORTUGAL, 1887-1975AD (BIRTHS AND DEATHS), DRY BONE (CARDOSO, 2008A), (C) MODERN, BOSNIA, 1995AD (WAR VICTIMS FROM THE FALL OF SREBRENICA), MALES ONLY, DRY BONE (SCHAEFER, 2008B), (D) REFERENCE SAMPLE (SCHAEFER ET AL., 2009) .....</i>	
<i>TABLE 6. 47: FUSION OF THE DISTAL EPIPHYSIS OF THE ULNA SPLIT BY PRIMARY DATA COLLECTED FOR THIS THESIS AND SECONDARY DATA, WHICH WAS TAKEN FROM PUBLISHED LITERATURE. REFERENCES ARE BELOW. LIGHT GREY = UNFUSED (STAGE 1). DARK GREY = PARTIAL FUSION (STAGE 2). BLACK = COMPLETE FUSION (STAGE 3), SOMETIMES STAGES OF FUSION OVERLAP DUE TO VARIATION IN INDIVIDUALS. TO KEEP THE TABLE SIMPLE, OVERLAP OF FUSION STAGES IS DENOTED BY THE WHITE TEXT. THE REFERENCE SAMPLE IS SHOWN IN BLUE AS PARTIAL FUSION (STAGE 2) AND COMPLETE FUSION (STAGE 3) ARE NOT DISTINGUISHED IN THE TEXT. REFERENCES: (A) MODERN, COIMBRA, PORTUGAL, 1826-1938AD (BIRTHS AND DEATHS), DRY BONE (COQUEUGNIOT AND WEAVER, 2007), (B) MODERN, LISBON, PORTUGAL, 1887-1975AD (BIRTHS AND DEATHS), DRY BONE (CARDOSO, 2008A), (C) MODERN, BOSNIA, 1995AD (WAR VICTIMS FROM THE FALL OF SREBRENICA), MALES ONLY, DRY BONE (SCHAEFER, 2008B), (D) MODERN, CHANDIGARH, INDIA, LIVING PATIENTS, RADIOGRAPHS*, (SAHNI ET AL., 1995), (E) REFERENCE SAMPLE (SCHAEFER ET AL., 2009) .....</i>	<i>235</i>
<i>TABLE 6. 48: FUSION OF THE ILIAC CREST OF THE OS COXAE SPLIT BY PRIMARY DATA COLLECTED FOR THIS THESIS AND SECONDARY DATA, WHICH WAS TAKEN FROM PUBLISHED LITERATURE. REFERENCES ARE BELOW. LIGHT GREY = UNFUSED (STAGE 1). DARK GREY = PARTIAL FUSION (STAGE 2). BLACK = COMPLETE FUSION (STAGE 3), SOMETIMES STAGES OF FUSION OVERLAP DUE TO VARIATION IN INDIVIDUALS. TO KEEP THE TABLE SIMPLE, OVERLAP OF FUSION STAGES IS DENOTED BY THE WHITE TEXT. THE REFERENCE SAMPLE IS SHOWN IN BLUE AS PARTIAL FUSION (STAGE 2) AND COMPLETE FUSION (STAGE 3) ARE NOT DISTINGUISHED IN THE TEXT. REFERENCES: (A) MODERN, COIMBRA, PORTUGAL, 1826-1938AD (BIRTHS AND DEATHS), DRY BONE (COQUEUGNIOT AND WEAVER, 2007), (B) MODERN, LISBON, PORTUGAL, 1930-1960AD (DEATHS), DRY BONE (CARDOSO, 2008B), (C) MODERN, BOSNIA, 1995AD (WAR VICTIMS FROM THE FALL OF SREBRENICA), MALES ONLY, DRY</i>	

<p>BONE (SCHAEFER, 2008B), (D) MODERN, LOS ANGELES, USA, 1977-1979AD (AUTOPSIES), (WEBB AND SUCHY, 1985),  (E) REFERENCE SAMPLE (SCHAEFER ET AL., 2009) .....</p>	238
<p>TABLE 6. 49: FUSION OF THE ACETABULUM OF THE OS COXAE SPLIT BY PRIMARY DATA COLLECTED FOR THIS THESIS AND SECONDARY DATA, WHICH WAS TAKEN FROM PUBLISHED LITERATURE. REFERENCES ARE BELOW. LIGHT GREY = UNFUSED (STAGE 1). DARK GREY = PARTIAL FUSION (STAGE 2). BLACK = COMPLETE FUSION (STAGE 3), SOMETIMES STAGES OF FUSION OVERLAP DUE TO VARIATION IN INDIVIDUALS. TO KEEP THE TABLE SIMPLE, OVERLAP OF FUSION STAGES IS DENOTED BY THE WHITE TEXT. THE REFERENCE SAMPLE IS SHOWN IN BLUE AS PARTIAL FUSION (STAGE 2) AND COMPLETE FUSION (STAGE 3) ARE NOT DISTINGUISHED IN THE TEXT. REFERENCES: (A) MODERN, LISBON, PORTUGAL, 1930-1960AD (DEATHS), DRY BONE (CARDOSO, 2008B), (B) MODERN, BOSNIA, 1995AD (WAR VICTIMS FROM THE FALL OF SREBRENICA), MALES ONLY, DRY BONE (SCHAEFER, 2008B), (C) REFERENCE SAMPLE (SCHAEFER ET AL., 2009).....</p>	
	239
<p>TABLE 6. 50: FUSION OF THE FEMORAL HEAD SPLIT BY PRIMARY DATA COLLECTED FOR THIS THESIS AND SECONDARY DATA, WHICH WAS TAKEN FROM PUBLISHED LITERATURE. REFERENCES ARE BELOW. LIGHT GREY = UNFUSED (STAGE 1). DARK GREY = PARTIAL FUSION (STAGE 2). BLACK = COMPLETE FUSION (STAGE 3), SOMETIMES STAGES OF FUSION OVERLAP DUE TO VARIATION IN INDIVIDUALS. TO KEEP THE TABLE SIMPLE, OVERLAP OF FUSION STAGES IS DENOTED BY THE WHITE TEXT. THE REFERENCE SAMPLE IS SHOWN IN BLUE AS PARTIAL FUSION (STAGE 2) AND COMPLETE FUSION (STAGE 3) ARE NOT DISTINGUISHED IN THE TEXT. REFERENCES: (A) MODERN, COIMBRA, PORTUGAL, 1826-1938AD (BIRTHS AND DEATHS), DRY BONE (COQUEUGNIOT AND WEAVER, 2007), (B) MODERN, LISBON, PORTUGAL, 1930-1960AD (DEATHS), DRY BONE (CARDOSO, 2008B), (C) MODERN, BOSNIA, 1995AD (WAR VICTIMS FROM THE FALL OF SREBRENICA), MALES ONLY, DRY BONE (SCHAEFER, 2008B), (D) MODERN, WESTERN AUSTRALIA, LIVING PATIENTS, MDCT SCANS* (SULLIVAN ET AL., 2017), (E) REFERENCE SAMPLE (SCHAEFER ET AL., 2009) .....</p>	
	240
<p>TABLE 6. 51: FUSION OF THE GREATER TROCHANTER OF THE FEMUR SPLIT BY PRIMARY DATA COLLECTED FOR THIS THESIS AND SECONDARY DATA, WHICH WAS TAKEN FROM PUBLISHED LITERATURE. REFERENCES ARE BELOW. LIGHT GREY = UNFUSED (STAGE 1). DARK GREY = PARTIAL FUSION (STAGE 2). BLACK = COMPLETE FUSION (STAGE 3), SOMETIMES STAGES OF FUSION OVERLAP DUE TO VARIATION IN INDIVIDUALS. TO KEEP THE TABLE SIMPLE, OVERLAP OF FUSION STAGES IS DENOTED BY THE WHITE TEXT. THE REFERENCE SAMPLE IS SHOWN IN BLUE AS PARTIAL FUSION (STAGE 2) AND COMPLETE FUSION (STAGE 3) ARE NOT DISTINGUISHED IN THE TEXT. REFERENCES: (A) MODERN, COIMBRA, PORTUGAL, 1826-1938AD (BIRTHS AND DEATHS), DRY BONE (COQUEUGNIOT AND WEAVER, 2007), (B) MODERN, LISBON, PORTUGAL, 1930-1960AD (DEATHS), DRY BONE (CARDOSO, 2008B), (C) MODERN, BOSNIA, 1995AD (WAR VICTIMS FROM THE FALL OF SREBRENICA), MALES ONLY, DRY BONE (SCHAEFER, 2008B), (D) MODERN, WESTERN AUSTRALIA, LIVING PATIENTS, MDCT SCANS* (SULLIVAN ET AL., 2017), (E) REFERENCE SAMPLE .....</p>	
	241
<p>TABLE 6. 52: FUSION OF THE LESSER TROCHANTER OF THE FEMUR SPLIT BY PRIMARY DATA COLLECTED FOR THIS THESIS AND SECONDARY DATA, WHICH WAS TAKEN FROM PUBLISHED LITERATURE. REFERENCES ARE BELOW. LIGHT GREY = UNFUSED (STAGE 1). DARK GREY = PARTIAL FUSION (STAGE 2). BLACK = COMPLETE FUSION (STAGE 3), SOMETIMES STAGES OF FUSION OVERLAP DUE TO VARIATION IN INDIVIDUALS. TO KEEP THE TABLE SIMPLE, OVERLAP OF FUSION STAGES IS DENOTED BY THE WHITE TEXT. THE REFERENCE SAMPLE IS SHOWN IN BLUE AS PARTIAL FUSION (STAGE 2) AND COMPLETE FUSION (STAGE 3) ARE NOT DISTINGUISHED IN THE TEXT. REFERENCES: (A) MODERN, COIMBRA, PORTUGAL, 1826-1938AD (BIRTHS AND DEATHS), DRY BONE (COQUEUGNIOT AND WEAVER, 2007), (B) MODERN, LISBON, PORTUGAL, 1930-1960AD (DEATHS), DRY BONE (CARDOSO, 2008B), (C) MODERN, BOSNIA, 1995AD (WAR VICTIMS FROM THE FALL OF SREBRENICA), MALES ONLY, DRY</p>	

	BONE (SCHAEFER, 2008b), (d) MODERN, WESTERN AUSTRALIA, LIVING PATIENTS, MDCT SCANS* (SULLIVAN ET AL., 2017), (E) REFERENCE SAMPLE (SCHAEFER ET AL., 2009) .....	242
TABLE 6. 53:	FUSION OF THE DISTAL EPIPHYSIS OF THE FEMUR SPLIT BY PRIMARY DATA COLLECTED FOR THIS THESIS AND SECONDARY DATA, WHICH WAS TAKEN FROM PUBLISHED LITERATURE. REFERENCES ARE BELOW. LIGHT GREY = UNFUSED (STAGE 1). DARK GREY = PARTIAL FUSION (STAGE 2). BLACK = COMPLETE FUSION (STAGE 3), SOMETIMES STAGES OF FUSION OVERLAP DUE TO VARIATION IN INDIVIDUALS. TO KEEP THE TABLE SIMPLE, OVERLAP OF FUSION STAGES IS DENOTED BY THE WHITE TEXT. THE REFERENCE SAMPLE IS SHOWN IN BLUE AS PARTIAL FUSION (STAGE 2) AND COMPLETE FUSION (STAGE 3) ARE NOT DISTINGUISHED IN THE TEXT. REFERENCES: (A) MODERN, COIMBRA, PORTUGAL, 1826-1938AD (BIRTHS AND DEATHS), DRY BONE (COQUEUGNIOT AND WEAVER, 2007), (B) MODERN, LISBON, PORTUGAL, 1930-1960AD (DEATHS), DRY BONE (CARDOSO, 2008b), (C) MODERN, USA, 1950-1952AD (WAR VICTIMS FROM THE KOREAN WAR), MALES ONLY, DRY BONE (MCKERN AND STEWART, 1957), (D) MODERN, BOSNIA, 1995AD (WAR VICTIMS FROM THE FALL OF SREBRENICA), MALES ONLY, DRY BONE (SCHAEFER, 2008b), (E) MODERN, CORK, IRELAND, LIVING PATIENTS, RADIOGRAPHS*, (O'CONNOR ET AL., 2008), (F) MODERN, DELTA STATE, NIGERIA, LIVING PATIENTS, RADIOGRAPHS*, (EBEYE ET AL., 2016), (G) REFERENCE SAMPLE (SCHAEFER ET AL., 2009) .....	243
TABLE 6. 54:	FUSION OF THE PROXIMAL EPIPHYSIS OF THE TIBIA SPLIT BY PRIMARY DATA COLLECTED FOR THIS THESIS AND SECONDARY DATA, WHICH WAS TAKEN FROM PUBLISHED LITERATURE. REFERENCES ARE BELOW. LIGHT GREY = UNFUSED (STAGE 1). DARK GREY = PARTIAL FUSION (STAGE 2). BLACK = COMPLETE FUSION (STAGE 3), SOMETIMES STAGES OF FUSION OVERLAP DUE TO VARIATION IN INDIVIDUALS. TO KEEP THE TABLE SIMPLE, OVERLAP OF FUSION STAGES IS DENOTED BY THE WHITE TEXT. THE REFERENCE SAMPLE IS SHOWN IN BLUE AS PARTIAL FUSION (STAGE 2) AND COMPLETE FUSION (STAGE 3) ARE NOT DISTINGUISHED IN THE TEXT. REFERENCES: (A) MODERN, COIMBRA, PORTUGAL, 1826-1938AD (BIRTHS AND DEATHS), DRY BONE (COQUEUGNIOT AND WEAVER, 2007), (B) MODERN, LISBON, PORTUGAL, 1930-1960AD (DEATHS), DRY BONE (CARDOSO, 2008b), (C) MODERN, USA, 1950-1952AD (WAR VICTIMS FROM THE KOREAN WAR), MALES ONLY, DRY BONE (MCKERN AND STEWART, 1957), (D) MODERN, BOSNIA, 1995AD (WAR VICTIMS FROM THE FALL OF SREBRENICA), MALES ONLY, DRY BONE (SCHAEFER, 2008b), (E) MODERN, CORK, IRELAND, LIVING PATIENTS, RADIOGRAPHS*, (O'CONNOR ET AL., 2008), (F) MODERN, DELTA STATE, NIGERIA, LIVING PATIENTS, RADIOGRAPHS*, (EBEYE ET AL., 2016), (G) REFERENCE SAMPLE (SCHAEFER ET AL., 2009) .....	244
TABLE 6. 55:	FUSION OF THE DISTAL EPIPHYSIS OF THE TIBIA SPLIT BY PRIMARY DATA COLLECTED FOR THIS THESIS AND SECONDARY DATA, WHICH WAS TAKEN FROM PUBLISHED LITERATURE. REFERENCES ARE BELOW. LIGHT GREY = UNFUSED (STAGE 1). DARK GREY = PARTIAL FUSION (STAGE 2). BLACK = COMPLETE FUSION (STAGE 3), SOMETIMES STAGES OF FUSION OVERLAP DUE TO VARIATION IN INDIVIDUALS. TO KEEP THE TABLE SIMPLE, OVERLAP OF FUSION STAGES IS DENOTED BY THE WHITE TEXT. THE REFERENCE SAMPLE IS SHOWN IN BLUE AS PARTIAL FUSION (STAGE 2) AND COMPLETE FUSION (STAGE 3) ARE NOT DISTINGUISHED IN THE TEXT. REFERENCES: (A) MODERN, COIMBRA, PORTUGAL, 1826-1938AD (BIRTHS AND DEATHS), DRY BONE (COQUEUGNIOT AND WEAVER, 2007), (B) MODERN, LISBON, PORTUGAL, 1930-1960AD (DEATHS), DRY BONE (CARDOSO, 2008b), (C) MODERN, BOSNIA, 1995AD (WAR VICTIMS FROM THE FALL OF SREBRENICA), MALES ONLY, DRY BONE (SCHAEFER, 2008b), (D) REFERENCE SAMPLE (SCHAEFER ET AL., 2009) .....	245
TABLE 6. 56:	THE SEQUENCE OF OSSIFICATION SITES COMPLETING FUSION BY PERIOD OF ROMAN, ANGLO-SAXON AND MEDIAEVAL SAMPLES COMPARED TO PREVIOUS STUDIES. THE MODAL SEQUENCE IS THE MOST COMMON ORDER OF FUSION FOUND IN BOTH THE TIME PERIOD SAMPLES AND THE COMPARISON STUDIES. OUTLIERS ARE OSSIFICATION SITES THAT COMPLETED FUSION IN A	

DIFFERENT SEQUENCE TO THE MODAL SEQUENCE OF THE SAMPLES AND ARE LISTED BELOW. THE KEY IS TAKEN FROM LENOVER AND ŠEŠELJ, (2019), FROM THE OSSIFICATION SITES THAT WERE USED IN BOTH THE PARTIAL AND COMPLETE MODAL SEQUENCES OF THAT STUDY FOR THEIR EUROPEAN SAMPLES. FOR THE COMPARISON STUDIES, GROUPED OSSIFICATION SITES – SHOWN VIA A COLLECTIVE COLOUR – ARE OSSIFICATION SITES THAT COMPLETED FUSION TOGETHER. FOR THE TIME PERIOD SAMPLES, GROUPED OSSIFICATION SITES EITHER ARE OSSIFICATION SITES THAT COMPLETED FUSION TOGETHER OR HAD A LOW SAMPLE SIZE THAT THE OSSIFICATION SITES COULD BE PROPERLY PLACED BETWEEN OTHER SITES, BUT COULD NOT BE SORTED INDIVIDUALLY E.G. THE SEQUENCE OF SITE A AND SITE B MAY BE FOUND TO SIT BETWEEN SITE C AND D, BUT LOW SAMPLE SIZES MAY NOT SHOW WHETHER SITE A OR SITE B IS FIRST. NUMBERS WITH A LINE NEXT TO THEM E.G. “(1) –” MEANS THAT THE SITE WAS NOT INCLUDED IN THAT SAMPLE. NAMES OF OSSIFICATION SITES DIFFER BETWEEN STUDIES BASED ON WHAT WAS WRITTEN IN THE ORIGINAL STUDY. REFERENCES: (A) EUROPEAN SAMPLE INCLUDES SKELETONS FROM LONDON, ENGLAND (18<sup>TH</sup>-19<sup>TH</sup> CENTURY), LISBON, PORTUGAL (19<sup>TH</sup>-20<sup>TH</sup> CENTURY) AND CLEVELAND, USA (EARLY 20<sup>TH</sup> CENTURY), AGE KNOWN (LENOVER AND ŠEŠELJ, 2019), (B) BOSNIAN SAMPLE INCLUDES SKELETONS WHO WERE BOSNIAK (BOSNIAK MUSLIM) MALES, AGE KNOWN (SCHAEFER AND BLACK, 2007) ..... 247

## Chapter Seven:

TABLE 7. 1: AGE AT PUBERTY FOR MEDIAEVAL CANTERBURY AND MEDIAEVAL YORK. THE STAGES OF UNION ARE RECORDED AS PERCENTAGES. ....	252
TABLE 7. 2: AGE AT PUBERTY FOR ALL ARCHAEOLOGICAL GROUPS. THE STAGES OF UNION ARE RECORDED AS PERCENTAGES. ....	255
TABLE 7. 3: AGE-AT-DEATH PER PUBERTAL PHASE FOR THE ARCHAEOLOGICAL PERIODS.....	256
TABLE 7. 4: ASSUMPTIONS CARRIED OUT FOR THE MULTIPLE REGRESSION. ....	257
TABLE 7. 5: MULTIPLE REGRESSION TO EXAMINE IF AGE AT PUBERTAL PHASE COULD BE PREDICTED BY ARCHAEOLOGICAL PERIOD. ..	258

## Chapter Eight:

TABLE 8. 1: SIGNIFICANT ASSOCIATIONS BETWEEN AGE AND STAGES 1 – 3. * = ANOMALOUS INDIVIDUALS NOT INCLUDED, ** = MORE LIKELY TO BE UNDER 8 YEARS OF AGE, *** = MORE LIKELY TO BE BETWEEN 8 – 10 YEARS .....	261
TABLE 8. 2: AGE-AT-DEATH PER PUBERTAL PHASE FOR THE PRIMARY DATA OF IRON AGE AND ROMAN GROUPS WITH THE ROMAN SECONDARY DATA. PUBERTAL PHASES ARE NAMED AS FOUND. REFERENCE: (I) ROMAN, ENGLAND, 1 <sup>ST</sup> -5 <sup>TH</sup> CENTURY, DRY BONE (ARTHUR ET AL., 2016) .....	289
TABLE 8. 3: AGE-AT-DEATH PER PUBERTAL PHASE FOR THE PRIMARY DATA OF ANGLO-SAXON AND MEDIAEVAL GROUPS WITH THE MEDIAEVAL SECONDARY DATA. PUBERTAL PHASES ARE NAMED AS FOUND. REFERENCES: (I) MEDIAEVAL, YORK, ENGLAND, 950-1700AD, DRY BONE (LEWIS ET AL., 2016), (II) MEDIAEVAL, BARTON-UPON-HUMBER, ENGLAND, 950-1700AD, DRY BONE (LEWIS ET AL., 2016), (III) MEDIAEVAL, ST MARY SPITAL, LONDON, ENGLAND, 950-1500AD, DRY BONE (LEWIS ET AL., 2016), (IV) MEDIAEVAL, MURCIA, SPAIN, 11 <sup>TH</sup> -13 <sup>TH</sup> CENTURIES, DRY BONE (DOE ET AL., 2017).....	291

---

*TABLE 8. 4: AGE-AT-DEATH PER PUBERTAL PHASE FOR THE PRIMARY DATA OF THE POST-MEDIAEVAL GROUP WITH SECONDARY POST-MEDIAEVAL AND MODERN DATA. PUBERTAL PHASES ARE NAMED AS FOUND. REFERENCES: (I) POST-MEDIAEVAL/MODERN, COIMBRA, PORTUGAL, EARLY 20<sup>TH</sup> CENTURY, DRY BONE, (HENDERSON AND PADEZ, 2017)., (II) POST-MEDIAEVAL/MODERN, MIDDENBEEEMSTER, NETHERLANDS, 1829-1966AD, DRY BONE (BLOM ET AL., 2021), (III) MODERN, COPENHAGEN, DENMARK, 1930-1970AD, MEASUREMENTS ON LIVING CHILDREN (AKSGLAED ET AL., 2008)..... 292*

## CHAPTER 1

## INTRODUCTION

## 1.1 STRUCTURE OF THESIS

Epiphyseal fusion is important in anthropology because it is useful in estimating the age of juvenile skeletons, sorting commingled juvenile remains, understanding growth and development in modern humans and providing an insight into the lives of historic populations. Juvenile remains are less well represented in the archaeological record than adult remains. However, contrary to popular belief, this is not due to poor preservation (Lewis, 2011).

Studies of fusion in living children have analysed various aspects of the skeleton, but many have focussed on the hand and wrist (Calfee et al., 2010; Duren et al., 2015; Boeyer et al., 2018). This thesis explores the maturation and development of the modern human juvenile skeleton throughout British history from approximately  $\leq 800$  BC to 1855 AD (800 BC has been given as a starting date, as this is the defined date of the Iron Age (University of Bradford, 2022)). However, the earliest skeletal samples used in this study are thought to range from the Bronze Age to the Iron Age but are grouped here under the term *Iron Age*). This thesis aims to provide the first in-depth examination of skeletal maturation and development within England and Scotland, using the same methodology throughout.

This thesis is structured to firstly present an understanding of the current literature and themes on skeletal maturation, to provide new information on the topic via new data that are analysed with statistical tests, and to finally address how this data fits in with current knowledge. This study is split into eleven chapters. Each chapter is described in brief below:

**Chapter One:** Introduction and definitions.

**Chapter Two:** A literature review. This includes the biology of bone and its growth, histological analysis of the growth plate, influences on epiphyseal fusion, secular trends, and the applications of epiphyseal fusion in biological anthropology.

**Chapter Three:** Materials used to conduct the research.

**Chapter Four:** Methodology used within the thesis.

**Chapter Five:** Results. Maturation of the Mediaeval skeleton. This chapter looks exclusively at the St Gregory's Mediaeval skeletal sample. This sample was the largest ( $n = 135$ ) compared to the other skeletal collections used for this study. The results consider the age at which the epiphyses fuse in the St Gregory's collection, variation in age-at-fusion between high and low-status individuals, the order in which the epiphyses fused, and finally, the age at each pubertal phase.

**Chapter Six:** Results. Maturation of the modern human skeleton compared between archaeological periods. There are two parts to Chapter six. Firstly, maturation in Mediaeval Canterbury (composed of the St Gregory sample) is compared to other Mediaeval sites collected for this thesis. Secondly, maturation is explored throughout the British archaeological periods, covering the Iron Age, Roman, Anglo-Saxon, Mediaeval and Post-Mediaeval eras. These archaeological groups are then compared to other published studies that have previously analysed epiphyseal fusion in other skeletal collections. Finally, the sequence of fusion for these archaeological groups is examined.

**Chapter Seven:** Results. Age at puberty compared amongst Mediaeval sites and between archaeological periods.

**Chapter Eight:** Discussion of Chapters Five to Seven.

**Chapter Nine:** Conclusion of this thesis.

**Chapter Ten:** Bibliography.

**Chapter Eleven:** Appendices.

## 1.2. STUDY AIMS

This study aims to provide an in-depth analysis of skeletal maturation and development across British archaeological periods. The research questions are:

**Chapter Five:** Maturation of the Mediaeval skeleton. Exploring growth and development in St Gregory's cemetery and priory.

*At what age did skeletal fusion occur at Mediaeval St Gregory's?*

Age-at-fusion will be examined in the Mediaeval Canterbury sample.

*Are there differences in age-at-fusion between the high and low-status skeletons?*

Age-at-fusion will be compared between the skeletons buried in the priory and those buried in the cemetery.

*What is the sequence of skeletal fusion at Mediaeval St Gregory's?*

The order of each fusion site will be charted to produce a modal sequence – the most common pattern.

*What is the age at puberty phases in Mediaeval Canterbury?*

Age at each pubertal phase is charted for St Gregory's skeletal collection.

**Chapter Six:** Maturation of the modern human skeleton compared between archaeological periods.

*Are there differences in the age-at-fusion between Mediaeval Canterbury and other British Mediaeval sites?*

Age-at-fusion is compared between St Gregory's skeletal collection and other Mediaeval collections acquired for this thesis.

*Are there differences in age-at-fusion between British archaeological periods?*

Age-at-fusion is compared between British archaeological periods (Iron Age, Roman, Anglo-Saxon, Mediaeval and Post-Mediaeval groups) collected for this thesis.

***How does skeletal maturation within this thesis compare to published literature?***

Data from previous studies that analysed age-at-fusion in either skeletons or living patients are compared to the data collected for this thesis.

***What is the sequence of fusion for the archaeological groups within this thesis, and do the sequences differ from previous literature?***

The sequence of fusion is charted once more but with all the archaeological data collected for this thesis. The data is then compared to published modal sequences from previous studies.

**Chapter Seven:** Age at puberty compared amongst Mediaeval sites and between archaeological periods.

***Does age at puberty differ between Mediaeval Canterbury and Mediaeval York?***

The puberty data produced in Chapter 5 for St Gregory's skeletal collection is compared to the age at puberty produced for the Mediaeval York sample.

***Does the age at which each pubertal phase is attained change when compared between archaeological periods?***

All data collected for this thesis is placed into an archaeological period and age at each pubertal phase is compared between groups.

### 1.3. DEFINITIONS

Brief definitions presented here are covered in greater detail in Chapter two. Historical periods of British history are taken from the University of Bradford and English Heritage's glossary of British Archaeological periods of time (University of Bradford, 2022).

*Adolescence:* The period in-between childhood and adulthood. It involves the development of sexual, social, and cognitive maturation, which is required to conceive and rear offspring successfully (Marshall and Tanner, 1986; Mauras, 2001; Sisk and Foster, 2004; Buck Louis et al., 2008; Hochberg and Belsky, 2013; Dwyer and Quinton, 2019).

*Adolescent growth spurt:* This occurs during the adolescent period, although it is not a necessary prerequisite to achieving full adult stature. The body undergoes a dramatic increase in growth, leading to gains in stature and weight. These occur through a period in which growth accelerates until it reaches a maximum rate of growth before decelerating until growth in stature is complete (Marshall and Tanner, 1986; Bogin and Smith, 2000; Ellison and Reiches, 2012; Lewis et al., 2016).

*Adrenarche:* The maturation of the adrenal glands (Dorn and Biro, 2011). Children may grow body hair, among other changes. This occurs a few years before puberty but does not include the maturation of secondary sexual characteristics or reproductive organs (Malina, 1974; Malina et al., 2004; Swerdloff et al., 2009; Bogin, 2012; Hermanussen, 2016; Willacy, 2016).

*Anglo-Saxon:* A period in British history lasting from 410 AD to 1066 AD.

*Catch-up growth:* A recovery period for the body in which the body goes through a duration of rapid growth to catch up to its original growth trajectory before the incident that caused growth to slow or cease. Catch-up growth can occur if the detrimental effect is not too severe or goes on for too long (Golden, 1994; Cameron and Demerath, 2002; Gosman, 2012; Hauspie and Roelants, 2012; Doe et al., 2017).

*Childhood:* This is between 3 to 6.9 years for modern human children (Bogin, 2015). However, the word "*child*" can refer to a person who has yet to reach adulthood.

*Development:* Progression of one form into a more complex structure.

*Growth:* An increase in size and mass (Bogin, 1999a; Cameron, 2012a). This oscillatory process fluctuates between periods of expansion and arrest (Lampl et al., 1992; Goldsmith et al., 2003; Malina et al., 2004; Noonan et al., 2004; Lampl, 2009; Lejarraga, 2012; Maqsood et al., 2020). The growth of modern humans can be split into segments. Adolescence is the most well-known segment due to puberty and the growth spurt.

*Iron Age:* A period in British history lasting from 800 BC to 43 AD.

*Juvenile skeleton:* Also known as ‘sub-adult or ‘non-adult.’ For archaeological samples, the term refers to modern human skeletons that had not completed most epiphyseal fusion before death (Buikstra and Ubelaker, 1994; Nikita, 2017).

*Juvenile stage:* This occurs between 7 to 10 years for girls and between 7 to 12 years for boys in modern human children (Bogin, 2015).

*Maturation:* The process of reaching the adult state. Maturity occurs throughout the body, as well as behaviourally. Each child matures at its own rate, determined by genetics and influenced by the environment (Malina et al., 2004; O’Connor et al., 2008; Hauspie and Roelants, 2012; Steckel, 2012; Weaver and Fuchs, 2013; Cunningham et al., 2016; Lampl and Schoen, 2017).

*Mediaeval:* Also known as the Middle Ages. It is a period in British history lasting from 1066 AD until 1540 AD.

*Modern:* Within this research, the word “modern” will either be capitalised (Modern) or in lower-case (modern) to separate the two terms. A capitalised “M” refers to a period of time – the present era that began in 1901 AD up until this moment in time. A lowercase “m” refers to modern humans, meaning *Homo sapiens* and not other hominins considered human, such as *Homo neanderthalensis*.

*Neonatal period:* The period between birth and twenty-eight days after delivery (Bogin, 2015).

*Post-Mediaeval*: A period in British history lasting from 1540 AD until 1901 AD.

*Puberty*: Changes within the body that lead to an individual becoming fertile (Malina et al., 2004). It is when children begin to mature sexually, including the development of secondary sexual characteristics and reproductive organs (Marshall and Tanner, 1986; Bogin, 2012; Ellison and Reiches, 2012; Dwyer and Quinton, 2019). This occurs during the adolescent period (Sisk and Foster, 2004; Hochberg and Belsky, 2013). The sexes experience puberty differently.

*Roman*: A period in British history lasting from 43 AD until 410 AD.

*Sexual maturation*: A biological process that enables an organism to become fertile and reproduce. This occurs during adolescence for modern humans (Bogin and Smith, 2000; Malina et al., 2004; Bogin, 2012).

*Skeletal maturation*: The process of the bones of the skeleton reaching an adult state. This involves the growth and ossification of bones and the eventual fusion of primary and secondary ossification centres (Buikstra and Ubelaker, 1994; Malina et al., 2004).

## CHAPTER 2

# LITERATURE REVIEW

## GROWTH AND MATURATION

### 2.1. INTRODUCTION

#### 2.1.1. Preface

Chapter two provides information on the maturation and growth of modern humans. Summary definitions and key terms presented in Chapter one are expanded upon in **Section 2.1.2.** In **Section 2.2.**, bone biology is discussed, including bone growth. A key point within this section is that longitudinal growth ceases before epiphyseal fusion (Cutler, 1997; Parfitt, 2002).

**Section 2.3.** reviews epiphyseal fusion. In particular, **Section 2.3.** considers the sequence of modern human fusion and the variation that may occur across individuals and groups. **Section 2.4.** goes into detail surrounding the influences upon skeletal maturation, such as secular trends and differences between the sexes, including how the hormone oestrogen affects the sexes differently.

**Section 2.5.** presents applications of epiphyseal fusion in anthropology and reviews previous literature. Although medical imaging methods are used to study epiphyseal fusion, the main focus of the literature review is on dry bone studies (including autopsies as they use the same methodology as dry bone studies) as this is the focus of this thesis. Thus, dry bone epiphyseal fusion studies are outlined from their origin in the 1920s to the present day.

### 2.1.2. Definitions and Key Terms

#### A) *Maturation*

Maturation is the process of becoming mature. It has been argued that maturation is a continuous process that lasts from birth until death (Malina et al., 2004; Cameron, 2012b). However, within the context of this thesis, maturation can be defined as the process of reaching the adult state (Malina et al., 2004; Cameron, 2012b). Becoming a healthy adult involves biological and behavioural maturity (Roche, 1992; Cameron, 2012a). Maturity, therefore, occurs throughout the body, including all organs and tissues (Roche, 1992; Cameron, 2012a).

Maturation is often measured by how fast or slow (tempo) the individual takes to reach the adult state, as well as when each event (timing) takes place (Malina et al., 2004). Maturation differs between populations – both contemporary and through time – and between individuals (Malina et al., 2004; O'Connor et al., 2008; Cunningham et al., 2016). Maturation can vary greatly between individuals within a population, regardless of their chronological age (Malina et al., 2004; O'Connor et al., 2008; Cunningham et al., 2016). For example, two children may be of the same chronological age but not necessarily at the same maturity stage (Kaprio et al., 1995; Malina et al., 2004). Individual differences in maturity stage can be due to a host of factors, including genetics, diet, socioeconomics and overall environmental influences (Hauspie and Roelants, 2012; Steckel, 2012; Weaver and Fuchs, 2013; Cunningham et al., 2016; Lampl and Schoen, 2017).

Maturation occurs in all body systems, but two maturity processes that have been studied most thoroughly are sexual and skeletal maturation. Sexual maturation is when an individual reaches the point at which they can reproduce and raise offspring successfully (Malina et al., 2004). Skeletal maturation is when the bones have fully ossified, and all epiphyses have fused, leading to the adult form (Malina et al., 2004). Some academics may divide skeletal maturity into the development of the primary ossification centres and the development and fusion of the epiphyses (Buikstra and Ubelaker, 1994).

Skeletal maturation is valuable for assessing maturity because it spans the entire period of modern human growth (Malina et al., 2004; O'Connor et al., 2008). The hormones that regulate skeletal maturity also regulate sexual and somatic maturation (Malina, 2012). *Somatic* refers to the body, and therefore *somatic maturation* refers to the maturation of the body, which is measured via the age of onset of the adolescent growth spurt and age at PHV (Peak Height Velocity, Beunen et al., 2006). The processes that define skeletal maturation, therefore, define other maturity processes. Puberty, in particular, is a major biological event in which both

skeletal maturation and growth accelerate (Hewitt and Acheson, 1961a; Gasser et al., 2001). During this period, most bones reach the full extent of their growth and cease growing, therefore allowing the epiphyses to close (Malina et al., 2004; Lampl and Schoen, 2017).

### *B) Growth*

Growth is an increase in size and mass (Bogin, 1999a; Cameron, 2012a). Height and weight increase, and tissues and organs get larger during the growth period (Malina et al., 2004). Rather than a continuous process, the growth process oscillates between short growth bursts and periods of arrest (Lampl et al., 1992; Goldsmith et al., 2003; Malina et al., 2004; Noonan et al., 2004; Lampl, 2009; Lejarraga, 2012; Maqsood et al., 2020). Growth spurts occur at biologically defined times, such as the mid-growth or juvenile growth spurt and pubertal or adolescent growth spurt (Gasser et al., 2001; Lejarraga, 2012), as well as being seasonal. For example, stature tends to increase more so during the spring and summer months for some but not all populations (Malina et al., 2004).

### The stages of growth

Growth can be divided into stages. The neonatal period extends from birth to twenty-eight days after birth (Bogin, 2015). This is the most rapid period of postnatal growth and maturation (Bogin, 2015). The growth rate is still rapid during infancy – the period after the neonatal stage – until three years of age, but a steep deceleration is included within this period (Gosman, 2012; Bogin, 2015). Infancy is characterised by developmental milestones - biologically, cognitively and behaviourally (Bogin, 2015).

Childhood extends from 3 to 6.9 years (Bogin, 2015). Both infancy and childhood are when the brain grows rapidly (Bogin, 2012, 2015). The brain completes most of its growth at the end of childhood (Bogin, 2012, 2015), but recent evidence suggests that the brain continues to remodel into adolescence (Herting and Sowell, 2017; Vijayakumar et al., 2018). Although brain growth is overall complete, the child is not yet socially or cognitively mature (Hochberg and Belsky, 2013). Childhood is a much steadier period of growth than infancy and the neonatal period (Bogin, 2015). However, some children may enter a mid-growth spurt.

Adrenarche occurs before puberty and is thought to cause the mid-growth spurt at around the ages of 6 to 8 years (Malina, 1974; Malina et al., 2004; Swerdloff et al., 2009; Bogin, 2012; Hermanussen, 2016). Adrenarche is the maturation of the adrenal glands (Dorn and Biro, 2011). The maturity of the adrenal glands causes androgens to be secreted – specifically dehydroepiandrosterone (DHEA) and DHEA-sulphate (DHEA-S, Bogin and

Campbell, n.d.). Androgens are known as the ‘male hormone’ but are secreted in girls and boys (Willacy, 2016). Children are affected differently by adrenarche (Willacy, 2016). For some children, adrenarche can result in the growth of armpit and pubic hair, the production of adult body odour, changes to the skin resulting in acne, and/or mood swings (Willacy, 2016). In contrast, other children are left unaffected (Willacy, 2016). Androgens have to reach high enough concentrations for reactions to occur, such as hair follicles to grow (Dorn and Biro, 2011). Adrenarche leads into pubarche (Buck Louis et al., 2008). Puberty occurs a few years later from adrenarche (Willacy, 2016). Puberty is different to adrenarche because this is when a child begins sexual maturity, such as breast and testicular growth (Willacy, 2016).

The Juvenile period occurs between approximately 7 to 10 years for girls and 7 to 12 years for boys (Bogin, 2015). This is a slow-growth period (Bogin, 2015). Growth is thought to be slow to allow a period of learning, as well as to either delay reproduction in the child or to reduce metabolic costs to prevent competition with older individuals (Bogin, 1990, 2012; Janson and Van Schaik, 1993; Walker et al., 2006a; Stone, 2007). In living studies, Childhood and Juvenility may be more easily distinguished. However, in dry bone studies, these two stages are usually combined as it is challenging to discriminate between set ages in undocumented skeletons (Buikstra and Ubelaker, 1994; Nikita, 2017).

Adolescence is the final stage before adulthood (Bogin, 2015). The adolescent stage lasts for a significant period of a person’s life, often for their entire second decade (Malina, 1974; Bogin and Smith, 2000). For example, adolescence can last until 18 to 20 years of age for females, whereas adolescence can last until 21 to 25 years for males (Bogin, 2015). In dry bone studies, the adolescent period is generally set between 12 to 20 years (Buikstra and Ubelaker, 1994; Nikita, 2017). Modern human adolescence is unusual in the animal kingdom because of the length of this stage (Bogin, 1999b, 1999a, 2012, 2015). There are 5 to 10 years between puberty onset and age-at-first-birth (Bogin, 1999b, 1999a, 2012, 2015). This lengthy period before age-at-first-birth is most likely a strategy to increase reproductive success (Bogin, 2003).

Modern human adolescence is characterised by a rapid growth spurt, followed by slower growth until adulthood (Bogin and Smith, 2000; Ford et al., 2012). The endocrine system plays a pivotal role via the reactivated hypothalamic-pituitary-gonadal axis (HPG-axis) that matures the gonads (Sisk and Foster, 2004; Hochberg and Belsky, 2013). The HPG-axis is first activated when the individual is a foetus (Dwyer and Quinton, 2019). It is then reactivated at birth and silenced once again at three months (Dwyer and Quinton, 2019). The third reactivation of the HPG-axis happens at puberty (Dwyer and Quinton, 2019). The HPG-

axis is required for human reproduction (Dwyer and Quinton, 2019). It includes a range of neuroendocrine networks that coordinate reproductive competence (Dwyer and Quinton, 2019).

In some studies, puberty is defined as the reactivation of the HPG-axis (Sisk and Foster, 2004; Hochberg and Belsky, 2013) and, therefore, puberty is a concise event that lasts only a few days or weeks during adolescence (Bogin and Smith, 2000). In contrast, other studies use 'puberty' and 'adolescence' interchangeably (Hochberg and Belsky, 2013). Therefore puberty is an event between childhood and adulthood that is neither singular nor discreet (Malina et al., 2004). Within this thesis, puberty can be defined as ending when individuals reach their full reproductive capacity and can successfully conceive (Marshall and Tanner, 1986; Murras, 2001; Buck Louis et al., 2008; Dwyer and Quinton, 2019). Puberty, therefore, includes the adolescent growth spurt and the formation of secondary sexual characteristics (Ellison and Reiches, 2012).

The adolescent growth spurt starts with an acceleration of growth, known as the acceleration phase (Marshall and Tanner, 1986; Bogin and Smith, 2000; Lewis et al., 2016). Growth accelerates until it reaches a maximum rate of growth, known as Peak Height Velocity (PHV, Marshall and Tanner, 1986; Bogin and Smith, 2000; Lewis et al., 2016). After PHV has been achieved, growth will decelerate until it eventually ceases and the adult form has been realised (Marshall and Tanner, 1986; Bogin and Smith, 2000; Ellison and Reiches, 2012; Lewis et al., 2016). At the end of this period, girls achieve menarche, whereas boys' voices fully mature (Hägg and Taranger, 1982; Shapland and Lewis, 2013) and both sexes become reproductively mature (Bogin, 1999a). Adolescence typically commences in females before males (Beunen et al., 2006).

The adolescent growth spurt influences most skeletal dimensions and internal organs (Marshall and Tanner, 1986; Bogin, 1999b). However, the adolescent growth spurt does not occur uniformly across the body (Marshall and Tanner, 1986; Bogin, 1999b). For example, the feet reach PHV and obtain adult proportions before any other region of the body (Marshall and Tanner, 1986). The legs, and particularly the lower legs, tend to reach PHV before the trunk, but the trunk increases in length more so during this time than the legs (Marshall, 1978).

Growth hormone (GH) and insulin-like growth factor-I (IGF-1) in early adolescence and the sex steroid oestrogen are the primary hormones during puberty. Oestrogen is responsible for promoting growth and preventing growth (Ellison and Reiches, 2012). During the acceleration phase, oestrogen stimulates chondrocyte proliferation (Ellison and Reiches,

2012). During the deceleration phase, oestrogen stimulates the mineralisation of osteoblasts while preventing osteoclasts from demineralising (Ellison and Reiches, 2012).

Oestrogen levels spike during foetal development and puberty (Alonso and Rosenfield, 2002). As oestrogen levels are similar for the foetus and the adolescent, the foetal stage is often referred to as a mini-puberty (Alonso and Rosenfield, 2002). Low doses of oestrogen are thought to activate the Growth Hormone – Insulin-like Growth Factor-1 axis (GH-IGF-1 axis, Börjesson et al., 2010; Shim, 2015). This may be done through oestrogen stimulating the secretion of GH (Juul, 2001). GH is an essential hormone required for linear growth (Juul, 2001). GH equally stimulates IGF-1 (Karimian et al., 2012), which is needed to encourage the rate of cell division (Ballock and O’Keefe, 2003). The activation of the GH-IGF-1 axis is essential for the adolescent growth spurt in early puberty (Börjesson et al., 2010; Shim, 2015). GH and IGF-1 stimulate longitudinal growth during puberty, increase bone mass in prepuberty and maintain bone homeostasis throughout life (Shim, 2015). Low concentrations of oestrogen are also required to stimulate chondrocyte growth in the proliferation zone of the growth plate (Juul, 2001).

High concentrations of oestrogen are believed to instigate the senescence of the growth plate that leads to epiphyseal fusion by inducing cell death for hypertrophic chondrocytes (Juul, 2001). A higher concentration of oestrogen also stimulates osteoblasts to invade the growth plate (Juul, 2001). The G-protein-coupled oestrogen receptor is found within the growth plate's hypertrophic zone (Karimian et al., 2012). Thus, high doses of oestrogen are required for epiphyseal closure by binding oestrogen to its receptors found in the growth plate cartilage (Börjesson et al., 2010; Shim, 2015). Over the pubertal period, the receptor decreases in expression (Karimian et al., 2012).

Precocious puberty can cause premature epiphyseal fusion and, thus, short stature (Shim, 2015). However, for early epiphyseal fusion, the growth plates must (a) be nearing senescence and (b) be exposed to high doses of oestrogen for some time (Weise et al., 2001). The amount of body fat has been known to influence pubertal growth (Perry et al., 2008). Adipose tissue is a target for oestrogen signalling and a source of it (Alonso and Rosenfield, 2002). Higher oestrogen concentrations in children early on inhibit growth and allow for the epiphyses' premature closure (Alonso and Rosenfield, 2002).

### Catch-up growth

Children grow and mature at different rates (Hauspie and Roelants, 2012). Attained adult stature is determined by genetics but can be affected by the environment (Hauspie and

Roelants, 2012). Too much negative environmental stimuli can have detrimental effects upon final adult height (Prader et al., 1963; Golden, 1994; Gosman, 2012; Hauspie and Roelants, 2012). However, the body has a level of plasticity. If the adverse conditions are not too severe or long-lasting, the body can recover (Golden, 1994; Cameron and Demerath, 2002; Gosman, 2012; Hauspie and Roelants, 2012; Doe et al., 2017). Growth and maturation rate may slow during the adverse period and then go through a period of rapid growth to catch up to its original growth trajectory, once conditions improve (Golden, 1994; Cameron and Demerath, 2002; Gosman, 2012; Hauspie and Roelants, 2012; Doe et al., 2017). Illness and nutrition deficiency are two adverse conditions that may postpone growth (Nilsson et al., 2005). They may cause insulin-like growth factor 1 and thyroid hormone levels to drop, inhibiting growth and slowing growth plate senescence (Nilsson et al., 2005). Other external factors to cause growth arrest and short stature include body deformations, psychosocial deprivation, and drug use, including administered drugs like adrenal steroids used to treat asthma (Lejarraga, 2012).

### Early and Late Maturation

Some studies have found that children who begin the adolescent growth spurt later tend to be taller on average than children who mature earlier (Hauspie et al., 1977; Hägg and Taranger, 1991). The later the adolescent growth spurt occurs, the more intense and shorter the spurt is (Abassi, 1998; Bogin, 2012). Contrastingly, other studies have found no correlation between final height and maturation rate (Largo et al., 1978; Bielicki and Hauspie, 1994; Abassi, 1998; Hauspie and Roelants, 2012). Hence, these studies argue that the timing of the adolescent growth spurt does not affect adult stature (Largo et al., 1978; Bielicki and Hauspie, 1994; Abassi, 1998; Hauspie and Roelants, 2012). In this regard, those that mature early can reach a similar height to those that mature late by having a more intense growth spurt (Hauspie and Roelants, 2012).

Some studies have found that girls that reach menarche early on are, on average, shorter in stature than girls who sexually mature much later (Biro et al., 2001; Onland-Moret et al., 2005; Schooling et al., 2010; Kang et al., 2019; Dewitte and Lewis, 2020). Other studies have found that girls that reach menarche early are taller on average (Chun and Shin, 2018). In contrast, several studies have found no correlation between sexual maturation rate and final height (Ersoy et al., 2004).

Populations that are in the process of improving their living conditions tend to shift in the direction of allowing for optimal growth and reproduction (Dewitte and Lewis, 2020). For example, children that emigrate from an economically poor to a wealthier country tend to be

taller and larger than children that remained behind (Franzen and Smith, 2009). For girls, improving living conditions causes them to reach menarche earlier and grow taller (Dewitte and Lewis, 2020). In comparison, industrialised populations tend to have a positive association between sexual maturation rate and final height (Dewitte and Lewis, 2020). Girls who reach menarche early tend to be shorter on average than girls who reach menarche later (Dewitte and Lewis, 2020). The reason for this may be that as living conditions improve, children can begin to reach their genetically determined height (McIntyre, 2011). Improved growth conditions and rapid growth, in turn, triggers early puberty (McIntyre, 2011). Due to the biphasic effect of oestrogen (Ellison and Reiches, 2012), this may cause growth to stop earlier (McIntyre, 2011). However, the overall impact still shows a negative correlation because the younger generation is still becoming taller on average than their parents (McIntyre, 2011). Once living conditions are improved, height plateaus (McIntyre, 2011).

Over-nutrition has been found to cause early puberty in some studies, but not all (McIntyre, 2011). Early maturing children have been associated with a heavier weight and a higher body mass index (BMI), either at pubertal onset or in adulthood (Tanner, 1962; van Lenthe et al., 1996; Biro et al., 2001; Cameron and Demerath, 2002; Demerath et al., 2004a; Hauspie and Roelants, 2012; Tremblay and Larivière, 2020). Rapid weight gain in infants has been linked to advanced skeletal maturation in childhood (Demerath et al., 2009). Rapid maturation was found in both sexes in children from Amsterdam who were termed obese (van Lenthe et al., 1996). Hence, those that enter sexual maturation early may have their growth stunted (McIntyre, 2011). A weaker relationship between age at menarche and final height should be found in countries where living standards fall behind fully industrialised societies (Dewitte and Lewis, 2020).

Low birth weight has been linked to an early age at menarche and shorter stature (Cooper et al., 1996; Ibáñez et al., 2000; Romundstad et al., 2003; Opdahl et al., 2008; Morris et al., 2010; Dossus et al., 2012). In comparison, high birth weight has been associated with delayed menarche (Dossus et al., 2012). Low birth weight has been correlated with short stature in men (Tuvemo et al., 1999). Low birth weight and shorter femoral height in males have been linked to a higher retzius periodicity found within the enamel (Luyer and Mahoney, 2017; Mahoney et al., 2018). Chances of being short in adulthood are increased twofold if an individual is born prematurely (Tuvemo et al., 1999), and premature babies have been found to have the highest retzius periodicity (Luyer and Mahoney, 2017). Thus, factors at birth significantly impact an individual's life, so much so that individuals tend to die around the time

of their birth month, most likely due to an annual periodicity of imprinted birth stress (Vaiserman et al., 2003).

### *C) Development*

Development is both biological and behavioural (Malina et al., 2004). Biological development is the differentiation of stem cells into different cell types (Malina et al., 2004). These cell types eventually become functional biological units (Malina et al., 2004). Behavioural development allows a child to learn how to interact within their society and culture (Malina et al., 2004). Some academics do not differentiate between maturation and development and define both as changes in a system that progresses from an immature state to a specialised, mature state (Bogin, 1999a; Cameron, 2012b). However, those who define the terms separately argue that maturation is a part of development and relates to progressive increases in complexity (Roche, 1992). Still, all individuals who reach adulthood reach the same level of maturity (Roche, 1992). In this regard, maturation is defined as developmental changes that end the same way in all adults (Roche, 1992). For example, all adults reach a final adult stature, and all modern human skeletons change and achieve an adult skeletal status (Roche, 1992). In this study, development refers to the progression of one form into a more complex structure, and thus maturation is a part of development.

### *D) Sexual maturation*

Sexual maturation is the process of reaching sexual maturity. It is when an organism becomes fertile and can reproduce (Malina et al., 2004). In modern humans, sexual maturation occurs during adolescence (Bogin and Smith, 2000; Bogin, 2012). This is also when individuals reach social maturity (Bogin and Smith, 2000; Bogin, 2012).

### *E) The link between puberty and skeletal maturation*

In females, secondary sexual characteristics are the development of the breasts, pelvic remodelling, the adjustment of the reproductive organs, and the start of menstruation (Marshall and Tanner, 1986; Ellison and Reiches, 2012). In boys, secondary sexual characteristics include increased testicular volume, growth of the penis, muscles and facial hair, deepening of the voice and seminal emission (Bogin, 2012; Ellison and Reiches, 2012; Dwyer and Quinton, 2019). Both sexes gain pubic and axillary hair and change body composition (Marshall and Tanner, 1986; Ellison and Reiches, 2012). Thus, if the words ‘puberty’ and ‘adolescence’ are considered separate terms, puberty is the maturation and development of the physical body,

such as secondary sexual characteristics. Adolescence thus includes puberty and cognitive and social maturation, which are equally needed to reproduce successfully (Sisk and Foster, 2004; Hochberg and Belsky, 2013).

Secondary sexual characteristics cannot be viewed on dry bone, but various studies have looked at how puberty can be studied from the skeleton (Hewitt and Acheson, 1961b, 1961a; Grave and Brown, 1976; Houston, 1980; Coutinho et al., 1993; Hassel and Farman, 1995; Legge, 2005; Lai et al., 2008; Shapland and Lewis, 2013, 2014; Arthur et al., 2016; Lewis et al., 2016; Lacoste Jeanson et al., 2016). Puberty stages can be studied from dry bone because puberty plays a crucial role in skeletal development (Vanderschueren et al., 2005). For example, oestrogen and androgens are hormones required for puberty and the adolescent growth spurt (Vanderschueren et al., 2005).

An illustration of the link between puberty and skeletal maturation is the development of the hook of hamate of the hand. A developing hook of hamate can indicate the acceleration phase of the adolescent growth spurt, whereas a mature hook of hamate can indicate that PHV has been achieved (Shapland and Lewis, 2013). The maturation of the cervical vertebrae has been found to correlate with six stages of the adolescent growth spurt (Shapland and Lewis, 2014). Whereas fusion of the iliac crest can indicate that PHV has passed, and in females, it can signal that menarche has been achieved (Shapland and Lewis, 2013). An indication that menarche has occurred has also been associated with premolar tooth stages (Lacoste Jeanson et al., 2016). As age-at-menarche has been described as comparable in heritability to height and skeletal maturation, it can be suggested that there is a close relationship between menarche and the skeleton (Loesch et al., 1995; Ellison and Reiches, 2012).

The relationship between puberty and the skeleton is of consequence because of the demands that puberty places upon the skeleton through growth and bone modelling (Vanderschueren et al., 2005). Puberty thus plays a significant role in the acquisition of bone mass, bone turnover and the closing of the epiphyses (Riis et al., 1985; Blumsohn et al., 1994; Saggese et al., 2002; van Coeverden et al., 2002; Eastell, 2005; Shapland and Lewis, 2014). Moreover, this also means that the onset of puberty, the obtainment of adult stature, and the maturation of the skeleton are all subject to environmental influences (Ellison and Reiches, 2012; Hochberg and Belsky, 2013).

## 2.2. BONE GROWTH

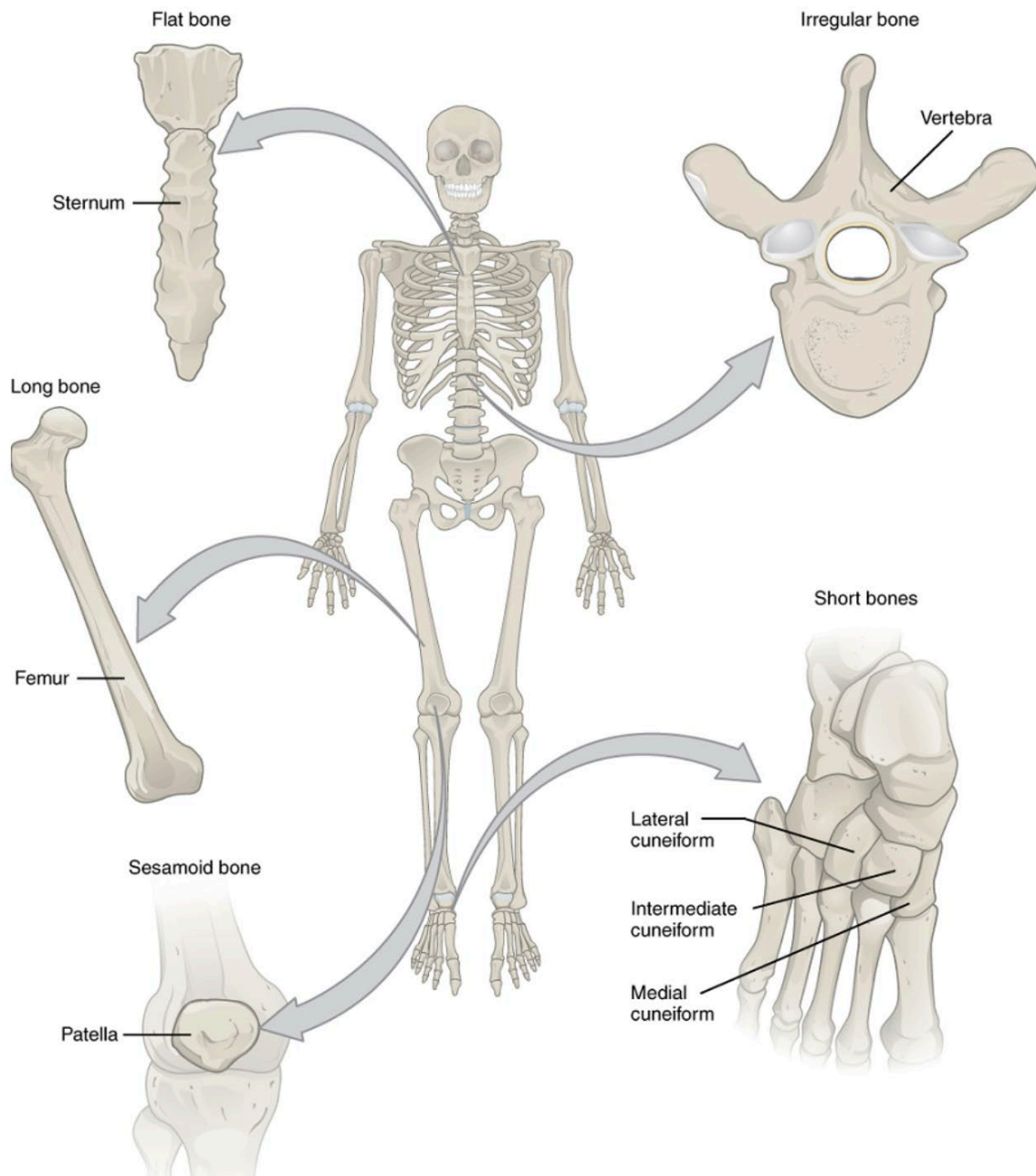
### 2.2.1. Bone Biology

Skeletal tissue is thought to have evolved around three-quarters of a billion years ago (Hall, 2015). The evolutionary lineage of cartilage is even older (Hall, 2015). The role of bone is to provide protection and support for the body and act as a reservoir for fat storage, growth factors, and mineral salts, such as calcium ions for muscle contractions (Betts et al., 2016; Jennings and Premanandan, 2018). Bone is also the site of blood cell production (Betts et al., 2016).

Various types of bones are named according to shape (Halim, 2008) and are illustrated in **Figure 2. 1**. Bones that make up the limbs, fingers and toes are long bones because their length exceeds their breadth (Halim, 2008; Betts et al., 2016). These bones act as levers and move under muscle contractions (Betts et al., 2016). Carpal and tarsal bones are known as short bones (Halim, 2008). They are cube-like, with their length, width and thickness being of equal dimensions (Betts et al., 2016). Short bones provide support and stability and have limited motion (Betts et al., 2016). Bones of the skull, the scapula and the sternum are known as flat bones (Halim, 2008; Betts et al., 2016). These bones protect internal organs, such as the brain, and act as muscle attachment sites (Betts et al., 2016).

Irregular bones do not fit within the above criterion (Halim, 2008; Betts et al., 2016). Irregular bones include the pelvis, vertebrae and the sphenoid (Halim, 2008; Betts et al., 2016). Bones such as the frontal bone that contain air-filled spaces are known as Pneumatic bones, whereas bones that are not always present in the skeleton, such as Wormian bones, are known as accessory or supernumerary bones (Halim, 2008). Finally, sesamoid bones are formed in the tendons of muscles, where large amounts of pressure are generated (Halim, 2008; Betts et al., 2016). These bones act to protect the tendons from stress (Betts et al., 2016). Sesamoid bones are known as such because they are sesame-seed shaped and are found in the hands, feet and knees (Betts et al., 2016).

Figure 2. 1: The major classifications of bones in the human skeleton. Image taken from Barker et al., (2021).



Cartilage is a flexible and robust material consisting of the protein chondrin secreted by chondrocytes (Clegg and Mackean, 2000). Cartilage matrix is gel-like and contains many elastic and collagen fibres (Mader, 2008). Unlike bone, cartilage is not penetrated by blood vessels, and instead, nutrients and waste move via diffusion (Clegg and Mackean, 2000). The most common form of cartilage – hyaline cartilage – is found on the surfaces of bones at the joints, the connectors to the ribs and sternum, and the rings that hold the trachea and bronchi open in adults (Clegg and Mackean, 2000). Hyaline cartilage is a connective tissue that is high in the protein collagen. Hyaline cartilage forms the entire skeleton in modern human embryos,

which is gradually replaced by bone as the embryo grows (Clegg and Mackean, 2000). Other cartilage forms include fibro-cartilage and elastic cartilage. Fibro-cartilage is shock-absorbing and is located between the vertebrae (Clegg and Mackean, 2000). Fibro-cartilage is stronger than hyaline cartilage because it contains more collagen fibres (Mader, 2008). Elastic cartilage can be found in the pinna of the ear and the epiglottis (Clegg and Mackean, 2000). Elastic cartilage is more flexible than hyaline cartilage, allowing the ear's pinna to bend easily (Mader, 2008).

Bone is strong and rigid (Clegg and Mackean, 2000). It comprises 70.0% mineral and 30.0% organic matter (Clegg and Mackean, 2000). Bone cells are responsible for forming, resorption, and maintaining bone (Nanci, 2008). There are three main types of bone cells. Osteoblasts are bone-forming cells and are formed from mesenchymal cells (Jennings and Premanandan, 2018). They produce the organic matrix of bone, as well as secreting cytokines (Nanci, 2008). Cytokines are glycoproteins (Kassab et al., 2019). They synchronise the immune system when the body is invaded by foreign microbes (Kassab et al., 2019). Osteoblasts also produce growth factors, including IGF and fibroblastic growth factor, which regulate bone formation and cellular function (Nanci, 2008).

Osteocytes are osteoblasts that have become trapped in the bone matrix they produce (Nanci, 2008). When osteocytes become trapped, they decrease in size, and the space they occupy is named a lacunae (Nanci, 2008). They lose their ability to divide and instead maintain bone (Resnick and Kransdorf, 1996). In general terms, the more rapid the bone formation, the more osteoblasts present, and therefore more osteocytes are trapped (Nanci, 2008).

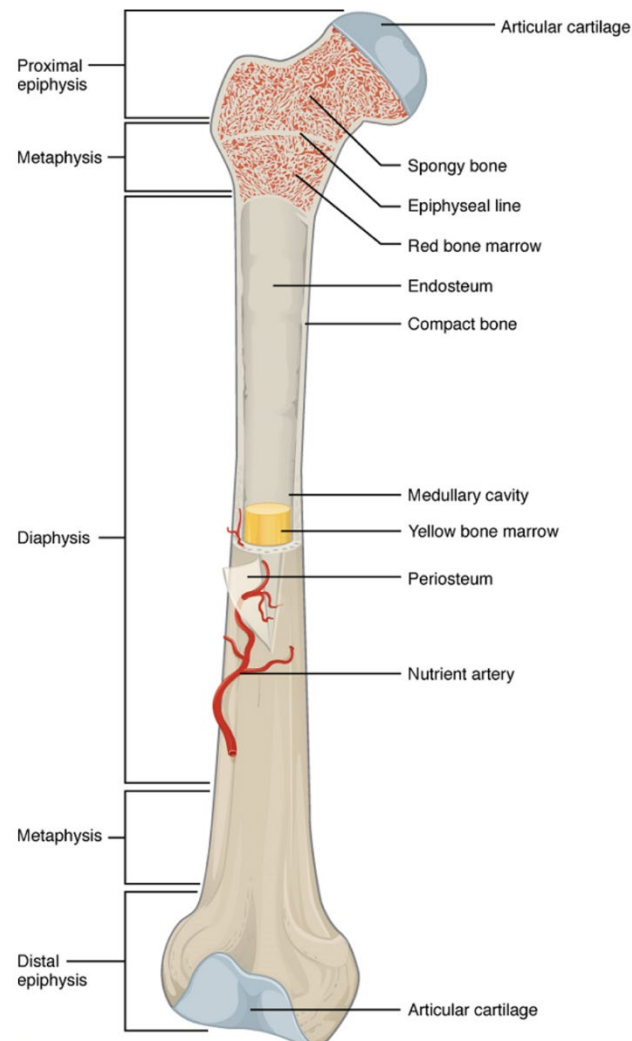
Lacunae are small cavities within bone (Jennings and Premanandan, 2018). Lacunae send out enclosed channels into bone called canaliculi, which allow osteocytes to maintain contact with neighbouring osteocytes and osteoblasts (Nanci, 2008). Canaliculi allow osteocytes to detect and respond to changing mechanical loads (Nanci, 2008). Like osteocytes, bone-lining cells are thought to originate from osteoblasts (Resnick and Kransdorf, 1996). Bone-lining cells are believed to be osteoblasts that have become inactive (Resnick and Kransdorf, 1996). They line the bone's surface and are flat in appearance (Resnick and Kransdorf, 1996). Their role is unknown, but they communicate with osteocytes and may be involved with either maintenance or differentiation into osteoblasts (Resnick and Kransdorf, 1996).

Osteoclasts are the third primary type of bone cell. They are bone-resorbing cells. They are haematopoietic-derived, like blood cells (Jennings and Premanandan, 2018). Osteoclasts are usually found in depressions known as Howship's lacunae (Nanci, 2008). To resorb and

break down bone, osteoclasts attach themselves to a bone's mineralised surface (Nanci, 2008). They then demineralise the bone by creating an acidic environment, which exposes the organic matrix (Nanci, 2008). Acid phosphatase and cathepsin B are released to degrade the matrix, which is then removed from the area (Nanci, 2008). Osteoclasts return the mineral phosphate and calcium into the bloodstream (Mader, 2008).

Bone has two forms, compact and spongy. Spongy bone is also known as trabecular bone. This is illustrated in **Figure 2. 2**. Compact bone is a highly organised structure and is very dense (Clegg and Mackean, 2000; Mader, 2008). Compact bone can be found on the diaphysis, also known as the shaft, of long bones. The compact bone of the diaphysis is covered with a tough, fibrous membrane made from dense, connective tissue called the periosteum (Clegg and Mackean, 2000). The periosteum is a point of attachment for tendons, ligaments and contains blood vessels, nerves and lymphatic vessels (Betts et al., 2016). The periosteum is essential for bone repair and appositional growth (Clarke, 2008). See **Section 2.2.2** below for information on appositional growth. The periosteum contains arterioles and capillaries, and these pierce the compact bone, known as the cortex, and enter the medullary canal, providing the blood supply to the bone (Resnick and Krandorf, 1996).

Figure 2. 2: The anatomy of a femur. Spongy bone can be seen in the proximal epiphysis, whereas compact bone can be viewed in the shaft. Image taken from Barker et al., (2021).

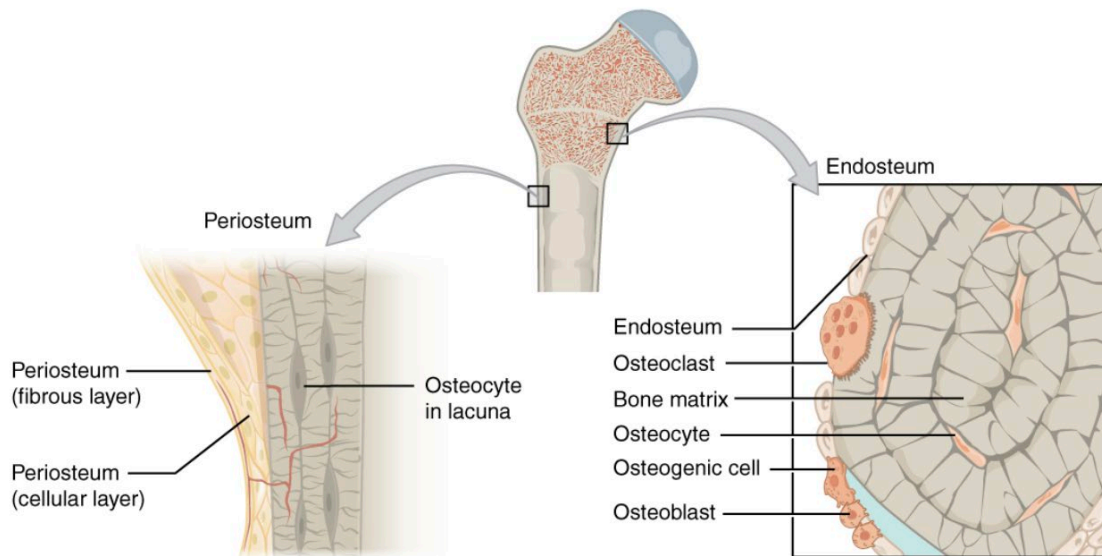


The periosteum attaches to the bone's outer cortical surface via Sharpey fibres, which are thick and extend into the underlying bone tissue (Clarke, 2008). The periosteum is illustrated in **Figure 2. 3**. In children, the periosteum is only loosely attached, with two defined layers (a fibrous outer layer and an inner osteogenic layer) whereas, in adults, it is thinner, more firmly attached, with the two layers fused (Resnick and Kransdorf, 1996). The osteogenic layer is also known as the cambium layer, which contains undifferentiated mesenchymal cells for bone and cartilage formation (Ito et al., 2001; O'Driscoll et al., 2001; Schuenke et al., 2020).

The endosteum lines the marrow cavity of the bone and is a soft connective tissue like that of the periosteum (Spatola et al., 2020). The endosteum is less well-defined than the periosteum (Resnick and Kransdorf, 1996). The periosteum is continuous apart from the

epiphyses, as the epiphyses are covered with cartilage or a synovial membrane (Resnick and Kransdorf, 1996).

Figure 2. 3: The periosteum and endosteum. Image taken from Barker et al., (2021).

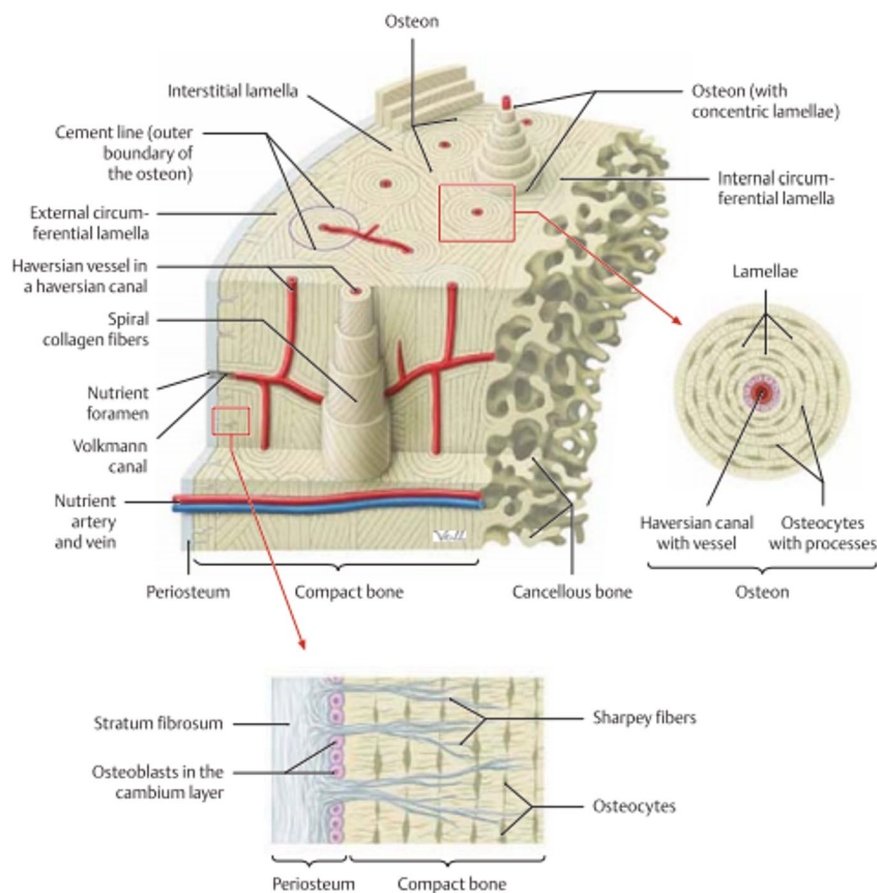


Compact bone is composed of osteons (also known as haversian systems), which are cylindrical in shape (Mader, 2008). See **Figure 2. 4** for the Haversian system. Each osteon consists of rings of calcified bone matrix – lamellae (singular, lamella) - and embedded osteocytes within their lacunae surrounding a haversian canal (Clegg and Mackean, 2000; Mader, 2008). The haversian canal contains nerves, veins, arteries, and capillaries (Clegg and Mackean, 2000). Osteocytes nearest to the haversian canals pass on nutrients and collect waste nutrients from outer osteocytes via gap junctions (Mader, 2008). Gap junctions make up part of intercellular channels that allow for the transfer of ions and small molecules directly from cell to cell and are found in most solid tissue cells (Goodenough and Paul, 2009). On the outside of the osteon is a cement line, which is more mineralised than the rest of the osteon (Schuenke et al., 2020; Spatola et al., 2020). Volkmann canals connect the haversian canals to each other and the periosteum (Spatola et al., 2020).

Osteons are continually remodelled throughout life, leading to some osteons not being as cylindrical as others (Spatola et al., 2020). The inner lamella is always the youngest and newest part of the osteon (Spatola et al., 2020). Spiral collagen fibres are present in each lamella (Schuenke et al., 2020). These fibres are responsible for bone's resistance to traction, bending and pressure (Spatola et al., 2020). Due to osteons being circular, the space between osteons is

filled with the interstitial lamellae system (Spatola et al., 2020). This system is the residue of degraded osteons that were once circular and have been remodelled over time (Spatola et al., 2020). They still contain osteocytes and lacuna but have a higher level of mineralisation because they are older (Spatola et al., 2020). Directly underneath the periosteum is the external circumferential lamella (Schuenke et al., 2020). There is also an internal circumferential lamella (Schuenke et al., 2020). These lamellae are arranged around the surface of the bone (Schuenke et al., 2020). For example, they would be placed concentrically in the diaphysis of a long bone (Schuenke et al., 2020). The external circumferential lamella contains Sharpey fibres (Spatola et al., 2020).

Figure 2. 4: Cross-section of compact bone, including the microstructure of an osteon and the periosteum structure, as found in Schuenke et al., (2020), on page 35 of *General Anatomy and Musculoskeletal system*.

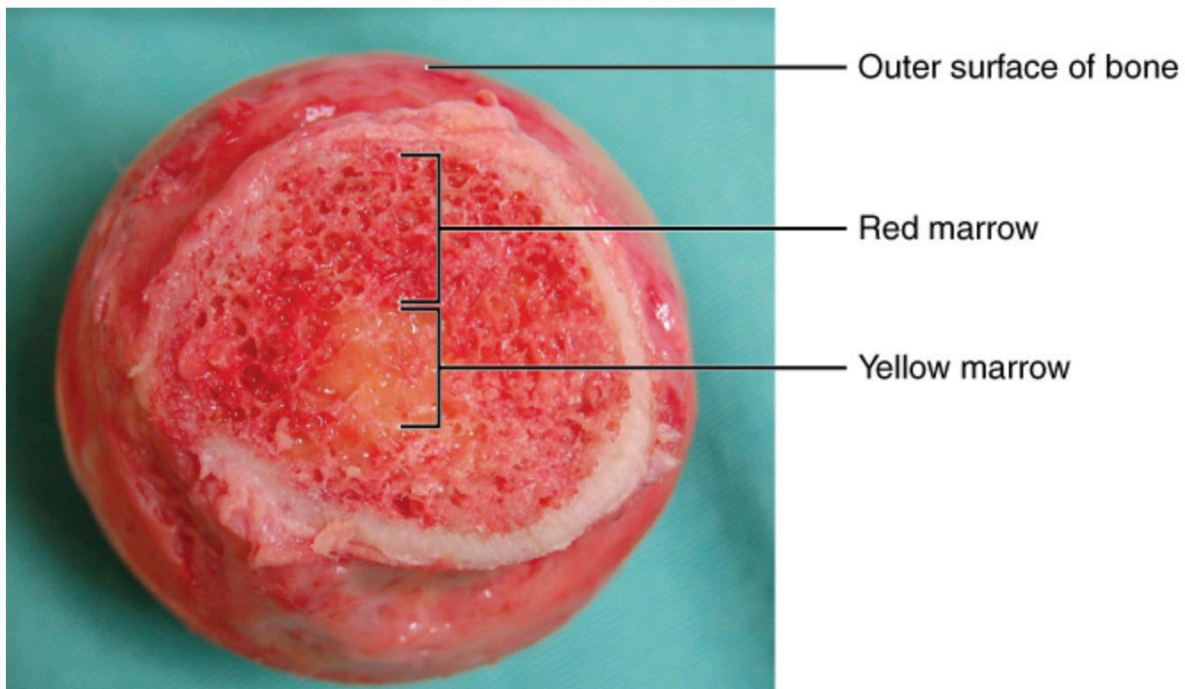


Underneath the compact bone of the diaphysis lies a mesh of spongy bone and interconnecting spaces (Resnick and Kransdorf, 1996). The interconnecting spaces may contain myeloid, fatty marrow or both (Resnick and Kransdorf, 1996). Myeloid tissue is also known as red marrow,

and fatty marrow is also known as yellow marrow. Red marrow is named for its high erythrocyte content, whereas yellow marrow has a high-fat cell content (Małkiewicz and Dziedzic, 2012). When a child is born, all their bone marrow is red, and over time approximately half of that will be converted into yellow marrow (Małkiewicz and Dziedzic, 2012).

The medullary cavity of the diaphysis contains fat-containing, yellow bone marrow that fills in the spaces between the spongy bone (Clegg and Mackean, 2000; Mader, 2008). The epiphyses contain mostly red bone marrow, where blood cells are made (Clegg and Mackean, 2000; Mader, 2008). Red and yellow marrow can be seen in **Figure 2. 5**. The epiphyses are primarily composed of spongy bone, although spongy bone is always surrounded by compact bone (Clegg and Mackean, 2000; Mader, 2008). Spongy bone appears unorganised and is arranged in haphazard thin bars known as trabeculae separated by large spaces (Clegg and Mackean, 2000; Mader, 2008). Osteocytes are trapped in the trabeculae, and the areas between the trabeculae contain red bone marrow (Clegg and Mackean, 2000). Canaliculi bring nutrients to the irregularly placed osteocytes (Mader, 2008). Trabeculae are lighter than compact bone because they contain less inorganic material (Clegg and Mackean, 2000; Mader, 2008).

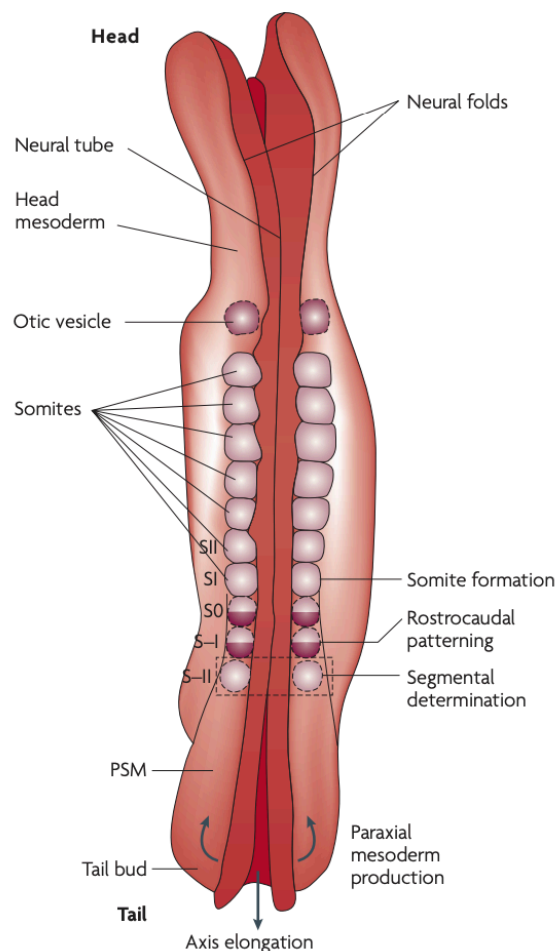
*Figure 2. 5: Femoral head showing both red and yellow marrow. The yellow marrow stores fat, whereas the red marrow produces red blood cells and platelets, known as haematopoiesis. Image and information taken from Barker et al., (2021).*



### 2.2.2. Bone formation

Formation of the skeleton starts with the condensation of mesenchymal cells that are driven by genes and regulatory factors (Weaver and Fuchs, 2013). Mesenchymal cells are stem cells that make bone, fat and cartilage cells (EuroStemCell, 2016). Mesenchymal cells stem from various embryonic cell lineages depending on the bone they are forming (Weaver and Fuchs, 2013). During vertebrae embryonic development, the embryo is made up of blocks of mesoderm, called somites, that sit either side of a neural tube (Dequéant and Pourquié, 2008; DeRuiter, 2018), as seen in **Figure 2. 6**. Mesoderm is one of the three germ layers that will give rise to organs and tissues as the germ layers interact with one another (Dequéant and Pourquié, 2008; DeRuiter, 2018). Mesoderm is the middle layer (Dequéant and Pourquié, 2008; DeRuiter, 2018).

*Figure 2. 6: Dorsal view of a human embryo at 4 weeks. Both somites and the neural tube can be seen. Image taken from Dequéant and Pourquié, (2008), page 371 of 'Segmental patterning of the vertebrae embryonic axis.*



The neural tube eventually becomes the central nervous system (Barnes, 2018). The neural tube is formed from the folding and thickening of the neural plate to create neural folds (Gilbert, 2000). In the centre of the neural plate forms a neural groove that divides the embryo into left and right sides (Gilbert, 2000). The neural folds migrate to the neural groove and fuse to form the neural tube (Gilbert, 2000). The dorsal most portion of the neural tube differentiates into neural crest cells (Gilbert, 2000). Eventually, the neural crest separates from the neural tube and migrates away (Barnes, 2018). The folding of the neural tube can be viewed in **Figure 2.7** and **Figure 2.8**. Neural crest cells are cells that can differentiate into certain other cell types (Barnes, 2018). Mesenchymal cells that form the craniofacial bones are derived from the neural crest (Weaver and Fuchs, 2013).

The somites that sit on either side of the neural tube eventually become the vertebrae, ribs, skin dermis, and skeletal muscles (Gilbert, 2000; DeRuiter, 2018). However, once the somites mature, they cannot deviate from their role. For example, mature somites that form into the cervical vertebrae cannot develop into the ribs (Gilbert, 2000). The somite formation is dependent on what region it is placed in the embryo (Gilbert, 2000). Somites are split into three regions – sclerotome, dermatome and myotome - and each area forms a different part of the body (Gilbert, 2000). The axial skeleton is formed from the sclerotome (Weaver and Fuchs, 2013).

Somites are formed from the paraxial mesoderm (Gilbert, 2000). The intermediate mesoderm is lateral to the paraxial mesoderm, and on either side of the intermediate mesoderm sits the lateral plate mesoderm (Gilbert, 2000; LePace, 2016). Mesenchymal cells that form the appendicular skeleton come from the lateral plate mesoderm (Weaver and Fuchs, 2013). The lateral plate mesoderm splits into two layers, the somatic mesoderm and the splanchnic mesoderm (LePace, 2016). The somatic mesoderm attaches to the inner surface of the ectoderm (one of the three germ layers that will give rise to organs and tissues as the germ layers interact with one another. It is the outer layer) and forms the somatopleure (Matson, 2021). Primitive limb buds develop in the core of the mesenchyme from unsegmented somatopleuric mesoderm, and the mesenchyme eventually transforms into cartilaginous precursors of their future bones (Hamilton and Manton, 2019). Except for the clavicle, which is formed through intramembranous ossification (Hamilton and Manton, 2019; Barker et al., 2021). The limb buds of the pectoral girdle are first to develop, then the pelvic girdle develops, and finally the limbs in order of their proximity to the axial skeleton (Hamilton and Manton, 2019).

Figure 2. 7: Shows the forming of the neural tube within 24 hours in a chick embryo (Humanpath.com, 2007)

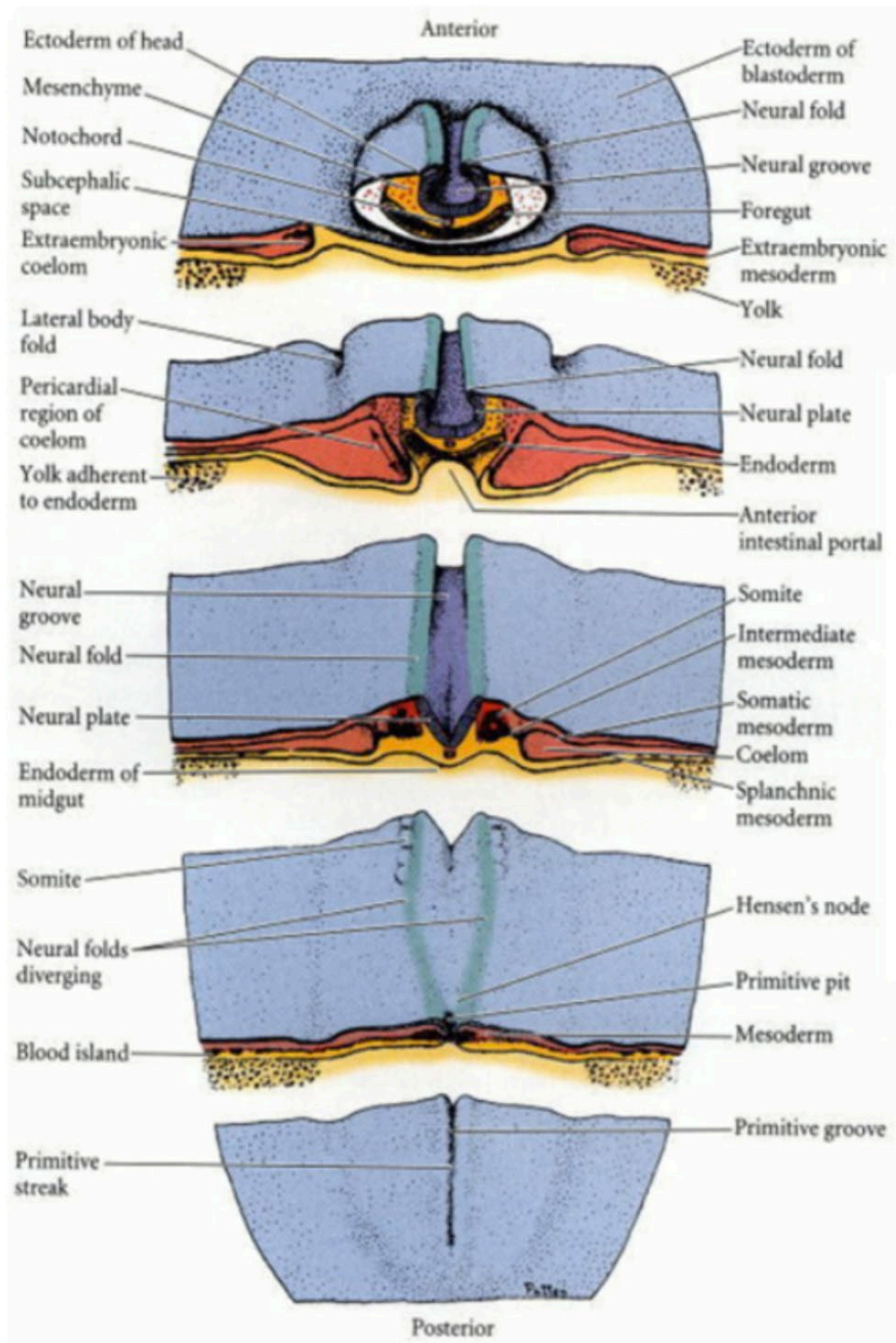
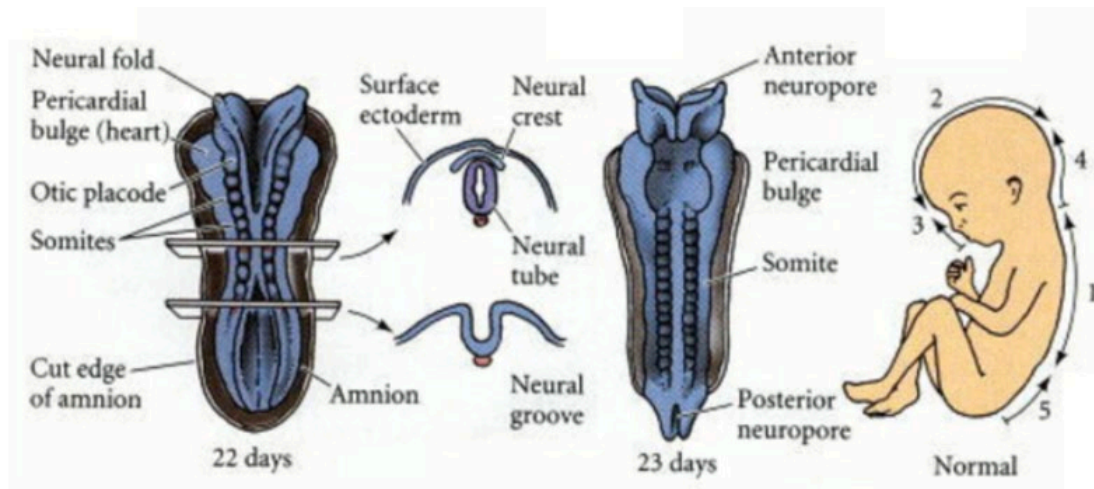
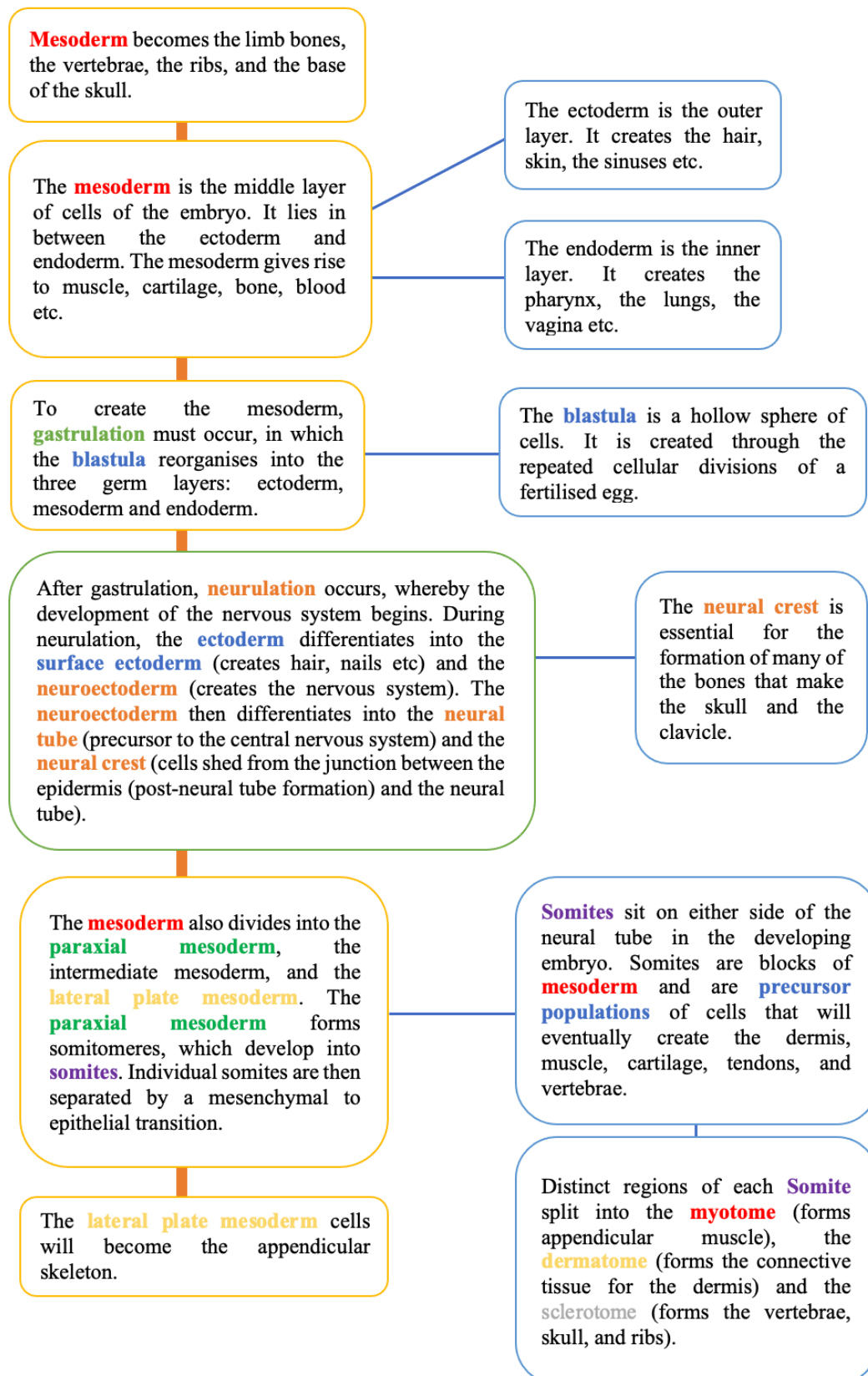


Figure 2. 8: The diagram shows the neural crest and tube in a human embryo. The left image is a dorsal and transverse section at 22 days. The middle image is at 23 days. The right image shows a healthy newborn baby with the numbers denoting regions of the neural tube. (Humanpath.com, 2007).



Osteogenesis is the region in which bones will eventually form (Cunningham et al., 2016). The cellular interactions and locally generated growth factors instruct the mesenchymal cells to migrate to the sites of osteogenesis (Cunningham et al., 2016). The formation of bone, known as ossification, will form either through intramembranous or endochondral ossification, depending on the bone (Mader, 2008). **Figure 2. 9** illustrates the early stages of bone development within the embryo in chart format.

Figure 2. 9: Early bone formation summarised in chart format (Stemple, 2005; Mitchell and Sharma, 2009; DeRuiter and Doty, 2011; MacCord, 2013; Berendsen and Olsen, 2015; Hall, 2015; DeRuiter, 2018; Hamilton and Manton, 2019; Tikkanen, 2022; Muhr and Ackerman, 2022; The Editors of Encyclopaedia Britannica, 2022)



The **lateral plate mesoderm** separates into the **somatopleuric mesoderm** (the outer layer, and the origins of the appendicular skeleton) and the splanchnopleuric mesoderm (the inner layer, which sits against the endoderm)

For the vertebral column, the **sclerotome cells** migrate medially to the notochord (sits in the middle of many vertebrates and signals the position of organs etc) and meet the sclerotome cells from the other side to make the vertebrae.

**Mesenchyme** is derived from the **somatopleuric mesoderm**. The **mesenchymal cells** migrate to the sites of future bones of the appendicular skeleton. The primitive limb buds develop in the core of the mesenchyme. The **mesenchyme** condenses to form blastemal masses that resemble the future limb bones. The **mesenchyme** is then transformed into **cartilaginous precursors** which maps out the size and shape of the bone. The clavicle is the exception to the rule.

#### *A) Intramembranous ossification*

Intramembranous ossification is the direct formation of bone instead of endochondral ossification that forms bone from a cartilaginous model (Wigley et al., 2008; Hall, 2015). However, some evidence suggests that a cartilaginous phase exists in the early stages of intramembranous ossification (Hall, 2015). Although the majority of long bones are formed through endochondral ossification, the periosteal (the membrane surrounding the bone) and endosteal (a layer of cells that line the medullary cavity) membranes are formed through perichondral intramembranous ossification (Maggiano, 2012). However, they are longitudinally extended via endochondral ossification (Maggiano, 2012). As the bone grows in length, the periosteal collar matches the bone by increasing in length and diameter through the secretion of the bone matrix by osteoblasts, which is then calcified (Mader, 2008; Wigley et al., 2008).

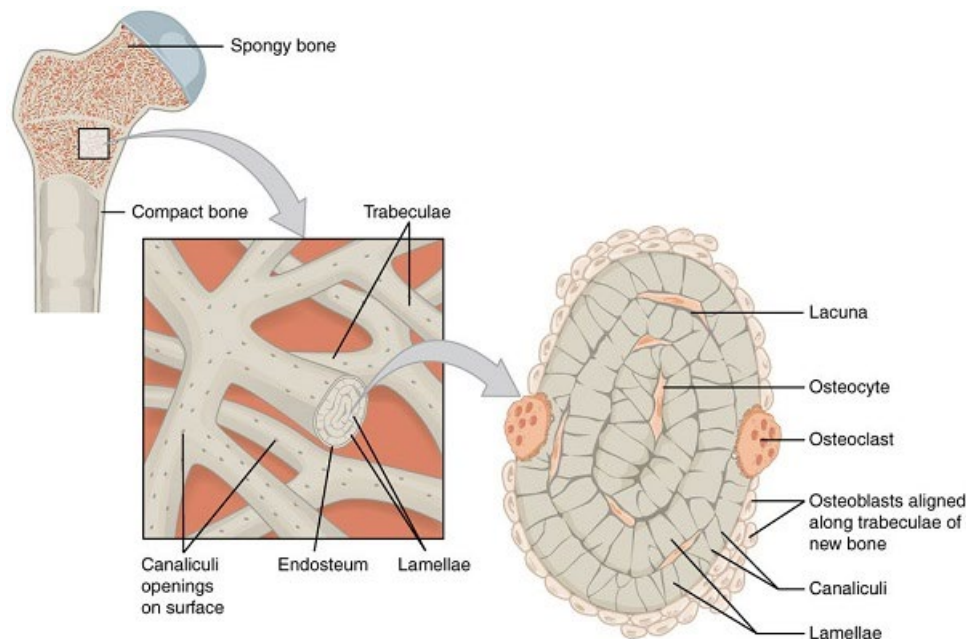
Intramembranous ossification forms bone from mesenchymal tissue through two processes: dermal and perichondral (Cunningham et al., 2016). Bones such as the parietal, frontal and squamous portion of the occipital are formed by dermal intramembranous

ossification. In contrast, the os coxae and the diaphyses of the long bones primary centres are created via perichondral intramembranous ossification (Cunningham et al., 2016).

In intramembranous ossification, mesenchymal stem cells transform into osteoprogenitor cells – precursor cells to osteoblasts or chondrocytes – around capillaries (Mader, 2008; Wigley et al., 2008; Cunningham et al., 2016). The osteoprogenitor cells become osteoblasts in a small number of sites called ossification centres (Mader, 2008; Wigley et al., 2008; Long, 2011; Cunningham et al., 2016). Osteoblasts secrete a matrix of collagen fibrils and mucopolysaccharides (known as osteoid) that calcify once calcium salts are added to the matrix (Mader, 2008). Mucopolysaccharides are long chains of sugar molecules with repeating disaccharide units (Lukacs, 2008; Edens Hurst, 2019). Mucopolysaccharides tend to be found in the fluid around the joints and mucus (Edens Hurst, 2019). Mucopolysaccharides are also known as glycosaminoglycans (Lukacs, 2008).

Calcification of osteoid creates light and porous, spongy bone (Mader, 2008). As more layers of the calcified matrix are deposited, the osteoblasts become trapped within primitive lacunae – the space occupied by an osteocyte (the term for a trapped osteoblast, Wigley et al., 2008). The osteocytes maintain intercellular contact through their dendrites (cytoplasmic processes), forming into canaliculi as the matrix condenses and the dendrites elongate (Wigley et al., 2008). The trabeculae (the tissue of the bone that looks like it is composed of small beams) thicken through the process of matrix secretion (Wigley et al., 2008). Calcification and the final entrapment of the osteoblasts continues, leading to intervening vascular spaces becoming narrower (Wigley et al., 2008). How trabeculae make up spongy bone can be viewed in **Figure 2. 10**.

Figure 2. 10: This image shows how spongy bone is made up of trabeculae. In turn, the trabeculae contain osteocytes and red marrow may fill in the spaces between. Image and information taken from Barker et al., (2021).



Spongy bone forms slowly (Wigley et al., 2008). Haemopoietic tissue fills in any gaps (Wigley et al., 2008). Spongy bone can be found ‘sandwiched’ within flat bones (Mader, 2008). Where bone becomes compact bone, such as the formation of the periosteum, the trabeculae will thicken, and the vascular spaces will narrow (Wigley et al., 2008). The spaces become narrowed because the collagen fibres are secreted on the walls of the already formed trabeculae, and these collagen fibres are organised into either longitudinal, parallel or spiral bundles that enclose the osteocytes in concentric sequential rows through the replacement of more mature lamellar bone (Wigley et al., 2008; Long, 2011). A simplified version of intramembranous ossification is given in **Figure 2. 11** and **Table 2. 1**.

Figure 2. 11: Shows the stages of intramembranous ossification. Image taken from Barker et al., (2021).

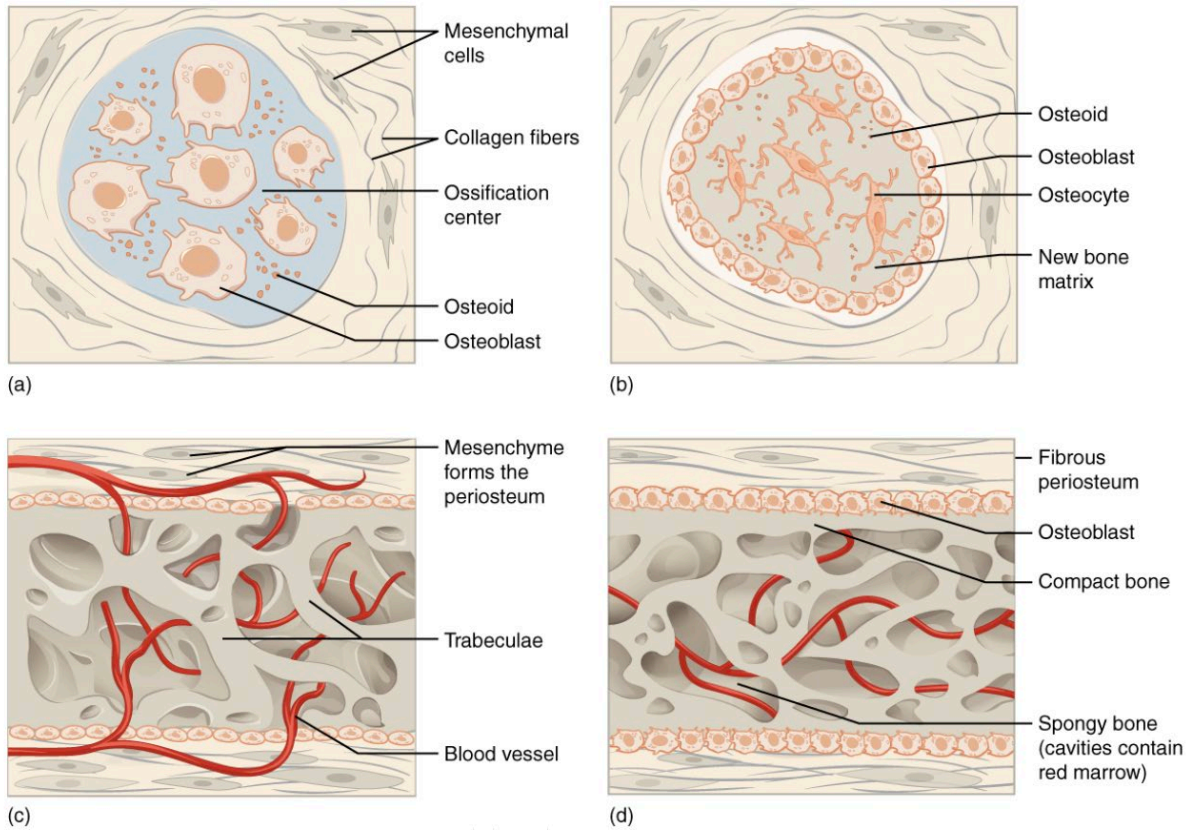


Table 2. 1: A simplified version of intramembranous ossification. Taken from: (A) (Mader, 2008; Wigley et al., 2008; Long, 2011; Cunningham et al., 2016; Barker et al., 2021), (B) (Barker et al., 2021), (C) (Wigley et al., 2008), (D) (Barker et al., 2021)

Stage	Description
1	Mesenchymal cells gather and differentiate into osteoprogenitor cells around capillaries. The osteoprogenitor cells become osteoblasts in clusters called ossification centres <sup>A</sup>
2	The osteoblasts secrete osteoid. When the osteoid hardens, it traps the osteoblasts in it. The trapped osteoblasts become osteocytes. As this occurs, osteoprogenitor cells surrounding the connective tissue become new osteoblasts <sup>B</sup>
3	The thickening of the matrix causes trabeculae to form. Spongy bone has many gaps, whereas compact bone is formed through the secretion of collagen fibres on the trabeculae <sup>C</sup>
4	In spongy bone, the blood vessels are crowded around by trabeculae, and so the blood vessels condense to form red marrow <sup>D</sup>

## *B) Endochondral ossification*

### Primary ossification centre

Endochondral ossification is critical for linear growth of long bones and the healing of fractures (Little et al., 2011; Gosman, 2012). Endochondral ossification begins with undifferentiated mesenchymal cells that secrete a hyaline (translucent) cartilage-like matrix before turning into chondrocytes (Mader, 2008; Little et al., 2011). Chondrocytes are cartilage-forming cells. The cartilage model is shaped in the form of the future bone (Mader, 2008; Wigley et al., 2008). The perichondrium then begins to develop around the cartilage model (Barker et al., 2021). Matrix continues to be secreted to increase the size of the cartilage model (Barker et al., 2021). The cartilage is calcified and prevents nutrients from reaching the chondrocytes, causing them to die (Mader, 2008; Little et al., 2011; Barker et al., 2021).

Next, a vascular bud penetrates the periosteal collar and forms an irruption canal that allows osteoblasts and osteoclasts to penetrate the model's core (Little et al., 2011; Cunningham et al., 2016). Capillaries also penetrate the model, and the perichondrium becomes the periosteum (Barker et al., 2021). The osteoblasts form new bone by attaching themselves to the calcified walls and producing osteoid (Wigley et al., 2008). This first formed bone is spongy bone, known as the primary ossification centre, which will eventually form the diaphysis (Mader, 2008).

Some of the first-formed bone is removed by osteoclasts to create a primitive medullary cavity (Mader, 2008; Wigley et al., 2008). However, the primitive medullary cavity still retains some trabeculae, with a central core of calcified cartilage, to support the developing marrow tissue (Wigley et al., 2008). Eventually, the trabeculae will be removed and replaced with either marrow or mature bone (Wigley et al., 2008). The bone will continue to grow in length through endochondral ossification and in thickness and width (Wigley et al., 2008). Width is achieved by depositing the bone matrix from cells derived from the perichondral collar (Wigley et al., 2008).

### Secondary ossification centres

Later in the process, secondary ossification centres form, which is more typical for modern humans during the postnatal development stage (Mader, 2008; Wigley et al., 2008; Cunningham et al., 2016). The secondary ossification centres will eventually form the epiphyses (the ends of the bone). For some bones, several epiphyses will form (Roche, 1978). The epiphyses develop through the clustering of chondrocytes that then enlarge (Wigley et al.,

2008). Vascular mesenchyme invades the inner sections of the growing epiphyses and supplies the internal areas with osteoblasts and osteoclasts that ossify into spongy bone (Wigley et al., 2008). The increasing inner sections of the epiphyses are filled with spongy bone and red bone marrow that persists for an extended period (Mader, 2008). While the inner area of the epiphysis is spongy bone, the outer periphery remains cartilaginous and is known as articular cartilage (Mader, 2008; Wigley et al., 2008).

#### The growth plate during the period of growth

The growth plate is where new bone growth in children is achieved. The growth plate occurs between the epiphysis and diaphysis. Cartilage is present at the growth plate, allowing the diaphysis to grow in length (Mader, 2008). There are two types of growth plates, horizontal for longitudinal growth and spherical for epiphysis growth (Little et al., 2011). As long as growth plates are present, the bone will grow in length (Mader, 2008).

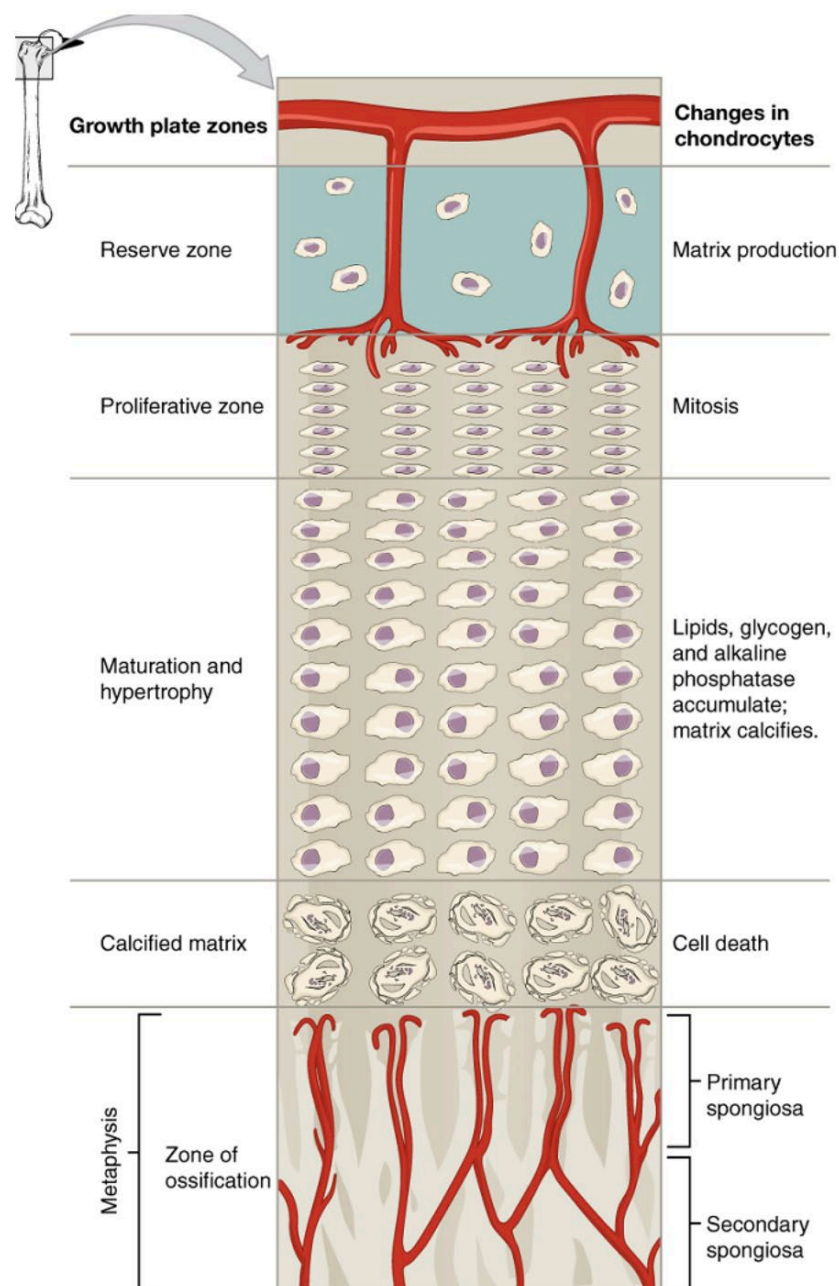
The growth plate is divided into three zones (Little et al., 2011). These zones are depicted in **Figure 2. 12**. The first zone – the resting zone (or reserve zone) - is closest to the epiphysis and contains dormant undifferentiated cells (Wigley et al., 2008; Little et al., 2011). Chondrocytes are irregularly scattered in the resting zone's cartilage matrix (Abad et al., 2002; Kannian and Ryan, 2019). Epiphyseal, metaphyseal and perichondral vessels help nourish the chondrocytes via a canalicular system (Delgado-Martos et al., 2013).

The perichondral ring of LaCroix and the ossification groove of Ranvier sit around the growth plate. The ossification groove of Ranvier is wedge-shaped and contains chondrocyte progenitor cells that are given to the resting zone so that the physis may expand in width as the bone grows in length (Ballock and O'Keefe, 2003). The perichondral fibrous ring of LaCroix is a band of fibrous tissue merged with the periosteum (Ballock and O'Keefe, 2003). It provides structural support to the growth plate (Ballock and O'Keefe, 2003) and anchors the growth plate to the metaphysis at the periphery (Little et al., 2011).

The second zone – the proliferative zone illustrated in **Figure 2. 12** – is where cellular proliferation and matrix production occurs (Little et al., 2011). The cells arrange themselves and form columns of chondrocytes that produce new cartilage (Mader, 2008; Little et al., 2011). Within this zone, chondrocytes divide by mitosis (Abad et al., 2002; Kannian and Ryan, 2019). Their daughter cells then line up into rows along the bone's long axis (Abad et al., 2002; Kannian and Ryan, 2019). The daughter cells produce collagen II and XI (Ballock and O'Keefe, 2003; Karimian et al., 2012). It is unknown how the daughter cells line up, but the

line-up determines the direction of growth (Abad et al., 2002), but it may be possible that primary cilia are responsible (Karimian et al., 2012).

Figure 2. 12: Shows the zones defined at the growth plate as a bone, such as the femur, grows in length via endochondral ossification. Image taken from Barker et al., (2021).



The third zone is the hypertrophic zone. The hypertrophic zone is nearest to the metaphysis (Abad et al., 2002). The hypertrophic zone is sometimes divided into three zones (Little et al., 2011). The maturation zone (zone 1) is where the chondrocytes swell in size. Chondrocyte

enlargement is responsible for approximately 44.0 to 59.0% of long bone growth (Ballock and O'Keefe, 2003). About 41.0 to 56.0% of long bone growth is due to chondrocyte proliferation and matrix synthesis (Ballock and O'Keefe, 2003). Variation in hypertrophic chondrocyte height may be responsible for variation in long bone height (Ballock and O'Keefe, 2003). For example, the femur is a bone that grows rapidly, which may be due to the speed of chondrocyte proliferation (Ballock and O'Keefe, 2003).

The degeneration zone (zone 2) is where the chondrocytes accumulate calcium and finally release the calcium into the matrix as they undergo programmed cell death to form calcified cartilaginous bars in zone 3 (Little et al., 2011). The calcified cartilage provides the template for osteoblasts to form bone (Ballock and O'Keefe, 2003). Ossification is initiated via blood vessels and bone cells invading the area calcified by the chondrocytes from the metaphysis (Abad et al., 2002; Ballock and O'Keefe, 2003; Little et al., 2011).

The metaphysis is the region between the epiphysis and the diaphysis. It is made primarily from primary and secondary spongiosa (Little et al., 2011). Primary spongiosa comprises mineralised cartilage and the early ossification of a true bone matrix (Kronenberg, 2003; Jennings and Premanandan, 2018). No chondrocytes are present in the primary spongiosa (Kronenberg, 2003).

Osteoblasts that invade the hypertrophic zone originate from the bone marrow and lay down spongy bone (Emons et al., 2010). Chondroclasts and osteoclasts remove the cartilage for the osteoblasts to lay down bone (Wigley et al., 2008; Little et al., 2011). The ossification process is regulated by GH and IGF-1, (Kannian and Ryan, 2019). The newly formed spongy bone is remodelled into the mature spongy bone in the secondary spongiosa (Jennings and Premanandan, 2018). The secondary spongiosa is closest to the diaphysis and reflects the bone's compression and tension (Jennings and Premanandan, 2018).

Having chondrocytes continuing cell division near where the epiphyses will eventually fuse means that the bone can continue to grow longitudinally (Wigley et al., 2008). The exact process in the diaphysis also occurs inside the epiphysis's articular cartilage, allowing the epiphysis to grow and match the growth of the diaphysis (Mader, 2008; Wigley et al., 2008). When linear growth finally ceases, the epiphyses can close (Cutler, 1997; Parfitt, 2002).

#### The growth plate at the end of the growth period

Growth stops when the cells at the epiphyseal plate lose their hyperplastic (increased cell production) growth potential (Bogin, 1999a; Nilsson and Baron, 2004). During the growth period, the number and size of the chondrocytes at the growth plate decline (Turner et al., 1994;

Weise et al., 2001). This causes the growth plate to shrink (Turner et al., 1994; Weise et al., 2001). The chondrocytes become more widely spaced over time (Lazarus et al., 2007). Eventually, resorption of cartilage and the vascular invasion of calcified cartilage begins to exceed cartilage expansion (Turner et al., 1994). Over time, the growth plate is resorbed, and any remaining chondrocytes are replaced by bone and bone marrow (Naski et al., 1998; Weise et al., 2001; Ballock and O'Keefe, 2003). The replacement occurs through the chondrocytes dying, vascularisation, and the replacement of the calcified matrix by osteoblasts (Naski et al., 1998; Weise et al., 2001; Ballock and O'Keefe, 2003). The growth plate is then perforated, and growth stops (Turner et al., 1994).

When growth stops, a layer of bone is created between the epiphysis and the diaphysis, decreasing the growth plate's size (Roche, 1978). Over months or years, depending on the maturation site, the bone created is resorbed (Roche, 1978). All cartilage at the growth plate is replaced by bone. The cartilage is replaced at the periphery first (Roche, 1978). The last cartilage to be replaced is at the circumferential margin (Roche, 1978). This is why, in dry bone, an epiphyseal scar may still be seen where the cartilage had not yet reached completion (Roche, 1978). Once the growth period has been completed, osteoblasts and osteoclasts continue to remodel the bone (Little et al., 2011), allowing bone to increase in width (Mader, 2008). **Figure 2. 13** shows a diagram of endochondral ossification. **Table 2. 2** is a simplified version of endochondral ossification.

Figure 2. 13: Endochondral ossification is pictured here. Image from Barker et al., (2021).

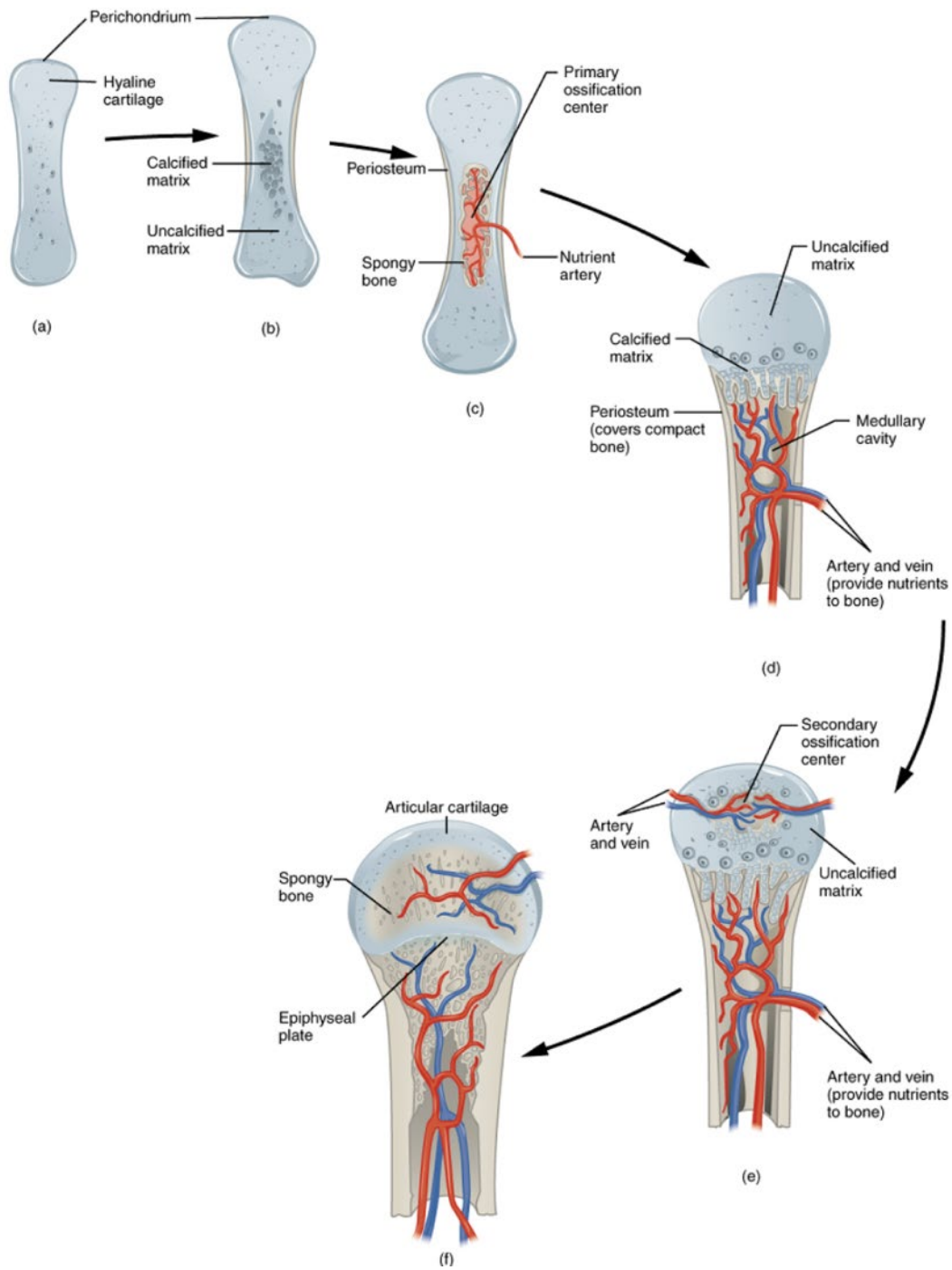


Table 2. 2: Simplified steps of endochondral ossification. References: (A) (Mader, 2008; Little et al., 2011; Barker et al., 2021), (B) (Mader, 2008; Wigley et al., 2008; Barker et al., 2021), (C) (Little et al., 2011; Cunningham et al., 2016; Barker et al., 2021), (D) (Wigley et al., 2008), (E)(Barker et al., 2021), (F) (Roche, 1978)

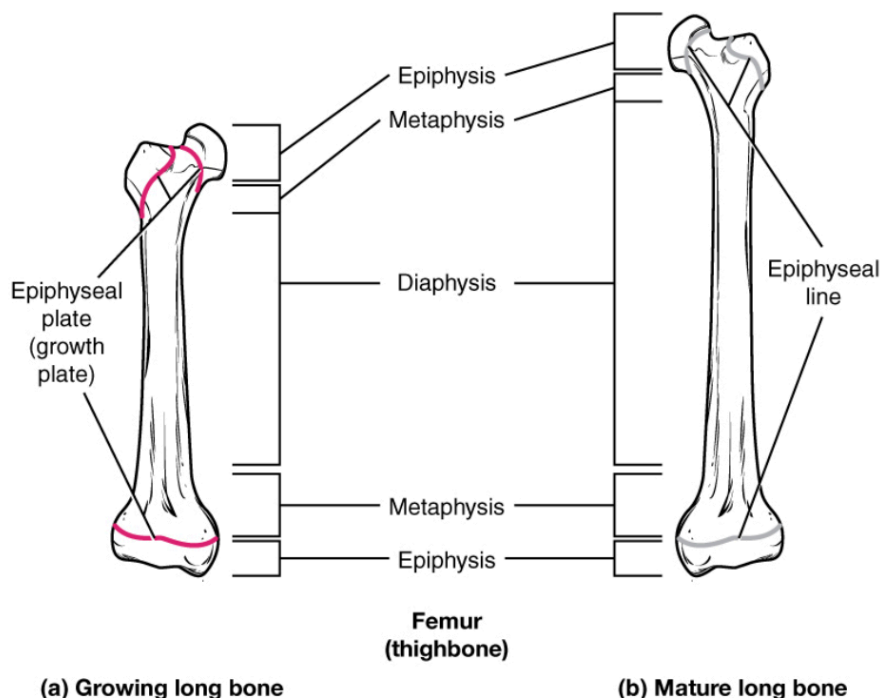
Stage	Description
1	Undifferentiated mesenchymal cells secrete hyaline cartilage and then differentiate into chondrocytes. This is the primary ossification centre <sup>A</sup>
2	A cartilage model forms that represents the shape of the future bone it will become. The perichondrium forms around the model. Calcification occurs <sup>B</sup>
3	The chondrocytes die, and a vascular bud penetrates the periosteal collar to allow in capillaries, osteoblasts and osteoclasts to the model. The perichondrium becomes the periosteum <sup>C</sup>
4	New bone is laid down. A primitive medullary cavity is created. The bone increases in length at the growth plate <sup>D</sup>
5	Secondary ossification centres begin to develop that will eventually become the epiphyses <sup>E</sup>
6	Chondrocyte proliferation begins to slow down and eventually stops. The cartilage is replaced with bone, and the epiphyses fuse, preventing any more longitudinal growth <sup>F</sup>

## 2.3. EPIPHYSEAL FUSION

### 2.3.1. Overview

An epiphysis is a bone that grows and fuses to another bone (Lewin, 1929). The word ‘epiphysis’ first appeared in English medical literature in 1634 AD (Nicholson and Nixon, 1961). An epiphysis forms from a secondary centre of ossification, whereas the diaphysis forms from a primary centre (Halim, 2008). The diaphysis makes up the shaft of a long bone. The metaphysis is at the end of the diaphysis and faces the epiphyseal cartilage (Halim, 2008). When the epiphysis is separate from the diaphysis, a layer of cartilaginous tissue exists, known as the epiphyseal cartilage (see **Section 2.2.B.**, Lewin, 1929). The epiphyseal cartilage is also referred to as the epiphyseal plate or the growth plate. The epiphyses function to serve in the development of joints, as attachments for tendons and muscles, and to allow the bones to grow in length before fusion (Lewin, 1929). A diagram of a labelled long bone is given in **Figure 2.14**.

*Figure 2. 14: The diagram shows a growing femur versus a mature femur. The epiphysis, metaphysis and diaphysis are labelled. Image from Barker et al., (2021).*



There are four types of epiphyses. Pressure and traction epiphyses form at the end of long bones (Hall, 2015; Cunningham et al., 2016). Pressure epiphyses develop in pressure areas (Parsons,

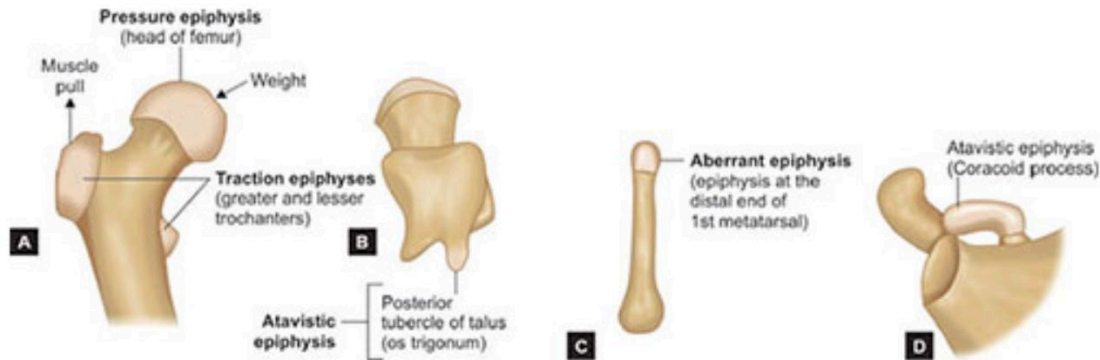
1904; Hall, 2015; Cunningham et al., 2016). For example, the femoral and humeral heads are considered pressure epiphyses (Halim, 2008; Cunningham et al., 2016). Pressure epiphyses are created through endochondral ossification, have a thin, compact bone shell that forms around a spongy bone inside, and usually establishes themselves at the articular ends of a bone (Cunningham et al., 2016).

Traction epiphyses tend to develop from perichondral ossification and are of various sizes and shapes (Cunningham et al., 2016). They are thought to have evolved from sesamoid structures (Parsons, 1908; Lewin, 1929; Hall, 2015). Traction epiphyses are the epiphyses that insert into tendons and ligaments and are involved with the pull of the muscles (Parsons, 1904; Hall, 2015; Cunningham et al., 2016). Examples include the iliac crest, the inferior angle of the scapula, and the tuberosities and trochanters of the humerus and femur (Parsons, 1904; Halim, 2008; Hall, 2015; Cunningham et al., 2016).

Atavistic epiphyses are bones that were once independent of the diaphysis but became one bone during the evolution of *Homo sapiens* (Kaushal, 2019). An example of an atavistic epiphysis is the coracoid process to the scapula (Kaushal, 2019). In modern humans, the coracoid fuses to the body of the scapula and becomes one single bone during the growth period (Kaushal, 2019). However, in many four-legged mammals, the coracoid remains an independent bone distinct from the scapula body (Kaushal, 2019).

Pressure, traction and atavistic epiphyses were first labelled and divided by Parsons, (1904). The fourth epiphysis is known as a pseudo or aberrant epiphysis (Cunningham et al., 2016). Pseudo-epiphyses are not true epiphyses and are deviations from normal skeletal anatomy and, therefore, are not always present in a modern human skeleton (Cunningham et al., 2016; Kaushal, 2019). They tend to be a regular occurrence in children (Nakashima and Furukawa, 1997; Cunningham et al., 2016). Pseudo-epiphyses tend to be found at the non-epiphyseal ends of the bones of the hands and feet (Nakashima and Furukawa, 1997; Cunningham et al., 2016). **Figure 2. 15** depicts the four types of epiphyses.

Figure 2. 15: The four types of epiphyses are pictured here. (A) Depicts pressure and traction epiphyses, (B) and (D) depicts atavistic epiphyses, (C) depicts an aberrant epiphysis. Image taken from Kaushal, (2019).



Epiphyses are formed from secondary ossification centres that eventually fuse with the diaphysis. Epiphyseal fusion of the modern human skeleton can span three decades of life and occurs once the bone has ceased growing (Halim, 2008; Cunningham et al., 2016). The majority of longitudinal bone growth ends during adolescence (Bogin, 1999a; Malina, 2012; Lewis et al., 2016; Doe et al., 2017, 2019). Longitudinal growth can no longer occur once chondrocyte proliferation stops and epiphyseal fusion occurs (Halim, 2008). At that time, the diaphysis and the epiphysis become one continuous bone (Halim, 2008).

### 2.3.2. Symphysis or synchondrosis?

Cartilaginous joints are bones that have been united by fibro-cartilage to form a symphysis, such as the pubic symphysis, or by hyaline cartilage, such as the sphenoid-occipital synchondrosis (Cendekiawan et al., 2010; Betts et al., 2016). Fibro-cartilage comprises of collagen fibre bundles, giving the joint flexibility and cushioning between vertebral joints (Betts et al., 2016). A symphysis can be narrow or wide (Betts et al., 2016).

A synchondrosis can be temporary or permanent (Betts et al., 2016). The growth plate in long bones are examples of temporary synchondroses, as the cartilage is eventually replaced by bone (Betts et al., 2016). As cartilage is softer than bone, damage to the growth plate can prevent longitudinal growth (Betts et al., 2016). Permanent synchondroses, such as the first sternocostal joint, retain their hyaline cartilage throughout life (Betts et al., 2016).

### 2.3.3. Sequence of epiphyseal fusion around the modern human skeleton

Different systems of the body grow, develop and mature at different rates (Humphrey, 1998). The brain and eyes mature early during childhood, whereas body weight and other major organs reach adult proportions after puberty (Humphrey, 1998). The skeleton grows and matures in response to organ development (Humphrey, 1998; Schaefer and Black, 2007; Lenover and Šešelj, 2019). For example, the majority of the skull bones mature in early childhood to accommodate rapid brain growth (Humphrey, 1998). Before puberty, growth is concentrated on the appendicular skeleton (Singh et al., 2011). In contrast, the axial skeleton accelerates growth during early puberty (Singh et al., 2011). Thus, after the fusion of the majority of the skull, the elbow is next to fuse, then the majority of the lower limbs, next the wrist, proximal humerus, and finally the iliac crest (Schaefer and Black, 2007; Lenover and Šešelj, 2019).

For most long bones, except for the fibula, the first epiphysis to form – the growing end - is the last to unite (Lewin, 1929; Halim, 2008). Pressure epiphyses usually fuse before traction epiphyses, and an epiphysis made up of multiple secondary centres will fuse before they fuse to the diaphysis (Halim, 2008). Again, much of this sequence is to do with functionality. For instance, the growing end is first to form and last to unite because it requires a more extended period of growth (Halim, 2008). Thus, the non-growing sites, such as the medial humeral epicondyle and ankle, fuse before growing sites like the knee and wrist (Lenover and Šešelj, 2019). Bones under a lot of pressure will also be more consistent in the fusion sequence than bones that are not (Lenover and Šešelj, 2019). However, it is unknown why some fusion sites, such as the medial epiphysis of the clavicle, take so long to fuse (Cunningham et al., 2016). Although, it should be noted that variation in the sequence of fusion of the skeleton occurs both within and between populations (Lenover and Šešelj, 2019).

Two central studies have looked at the sequence of fusion around the skeleton. Although studies before this, such as Stevenson, (1924) and Stewart, (1934), have equally looked at epiphyseal fusion, some of these earlier studies were unsubstantiated. For example, Stevenson, (1924) thought that little variability existed in the sequence of union between individuals and that the sequence of fusion was set and never changing. Other flaws included the simplification of epiphyseal fusion, including the removal of deviations from the sequence, and the use of non-human primates to fill in gaps in the fusion sequence (McKern and Stewart, 1957; Webb and Suchey, 1985).

However, early studies such as Stevenson, (1924) paved the way for more in-depth analyses on the timing of union. **Figure 2. 16** shows the sequence of fusion charted by Stevenson, (1924). In contrast, the work by Stewart, (1934) showed that population differences and socioeconomics could affect the sequence of fusion. However, he failed to account for individual variation, commenting that there was a constant epiphyseal order. At the same time, the author noted that variation between individuals was too great to determine the order of sequence of some fusion sites (Stewart, 1934).

*Figure 2. 16: The sequence of union as recorded by Stevenson, (1924) on page 88*

*An early study that recorded the sequence of fusion summarised the sequence as follows (brackets are believed to show when the author of the study found variation in a skeleton, although he writes that “the sequence of union among the various epiphyses is observed to be exactly the same in every individual”):*

*Distal extremity of the humerus*

*(Medial epicondyle of the humerus)*

*Coracoid process of the scapula*

*Three primary elements of the innominate bone*

*Head of the radius*

*(Olecranon of the radius)*

*Head of the femur*

*(Lesser and greater trochanters of the femur)*

*(Tuberosities of the ribs)*

*Distal extremity of the tibia and fibula*

*Proximal extremity of the tibia*

*(Proximal extremity of the fibula)*

*Distal extremity of the femur*

*Tuberosity of the ischium*

*Distal extremities of the radius and ulna*

*Head of the humerus*

*Crest of the ilium*

*Heads of the ribs*

*Ramal epiphysis of the pelvis*

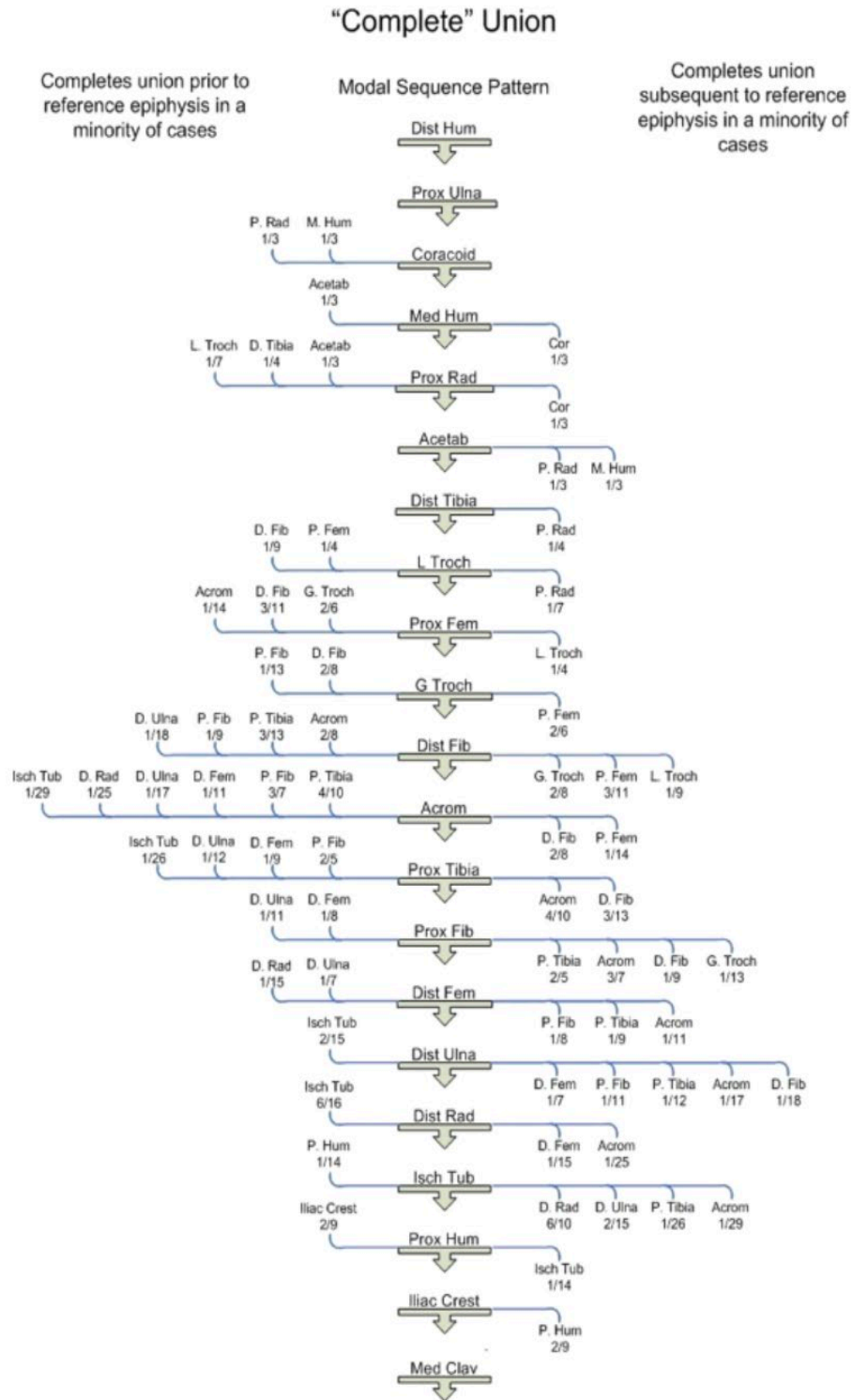
*Clavicle*

Schaefer & Black (2007) and Schaefer (2008) looked at Bosnian Muslim males (known as Bosniaks) who had died between the ages of 14 to 30 years. Schaefer & Black (2007) charted

the modal sequence (the sequence the majority of the sample followed) for ‘beginning’ and ‘complete’ fusion for twenty-one epiphyses. The start of fusion was recorded as an epiphysis that had begun fusion, whereas complete fusion was recorded as a bone that had fused (Schaefer and Black, 2007).

**Figure 2. 17** shows the sequence for complete fusion for modern day Bosniak males in Schaefer & Black (2007) and Schaefer (2008). **Figure 2. 17** indicates that Bosniak males always complete fusion of their distal humerus before any other of the twenty-one epiphyses assessed, whereas the medial clavicle is always last to fuse (Schaefer and Black, 2007). **Figure 2. 17** illustrates the deviations in the fusion sequence in the blue lines that spread out from the main tree (Schaefer and Black, 2007). For example, two skeletons out of nine of the Bosniak sample completed fusion of the iliac crest before the proximal humerus (Schaefer and Black, 2007).

Figure 2. 17: Sequence of skeletal fusion taken from Schaefer and Black,(2007) on page 281



Lenover and Šešelj, (2019) analysed the modal sequence of fusion for forty-three sites around the skeleton. They studied 524 Post-Mediaeval and Modern juvenile skeletons from collections representing European, African, and Asian ancestry, as well as pre-historic Native Americans (Lenover and Šešelj, 2019). They recorded when fusion commenced and when it was complete. **Figure 2. 18** shows the modal sequence for complete fusion for Lenover and Šešelj, (2019) European samples.

Lenover and Šešelj, (2019) included more fusion sites than Schaefer & Black (2007) and found that the thoracic arch was the first to fuse, whereas the medial clavicle was the last to fuse. Lenover and Šešelj, (2019) found that the acromion, spheno-occipital synchondrosis, and distal humerus were the most variable fusion sites between the geographic groups. They also found that beginning fusion was more variable across the geographic groups than complete fusion, with complete fusion trajectories having less inter-population variation (Lenover and Šešelj, 2019). Finally, Lenover and Šešelj, (2019) compared their European sample to the Bosniak sample from Schaefer & Black (2007). They found that the sequence order varied more for the early fusing sites, whereas the later-fusing sites deviated little from the modal trajectory (Lenover and Šešelj, 2019). They concluded that the Bosniak sample and their European data were “generally similar”, but some differences were found and believed to be due to local or regional populational variation (Lenover and Šešelj, 2019).

Although the work by Cardoso and colleagues (Cardoso, 2008a, 2008b; Cardoso et al., 2014) can be used to formulate a sequence of fusion, their primary task was to provide ages-at-fusion. Lenover and Šešelj, (2019) established the modal sequence within Cardoso and his colleagues’ work and found that the sequence was similar to their European data. However, this was to be expected as a large part of Lenover, and Šešelj, (2019) sample used the same skeletal collection as the work by Cardoso. Thus, although the work by the early scholars, such as Stevenson, (1924) and Stewart, (1934) was rudimentary, and did not take into account individual variation in the sequence of fusion, they reported a sequence of fusion that was generally similar when compared between modern human groups.

Figure 2. 18: Sequence of complete fusion for a sample of European skeletons taken from Lenover and Šešelj, (2019) on page 387

	Completes union prior to reference epiphysis in a minority of cases (n/total)	Modal sequence	Completes union subsequent to reference epiphysis in a minority of cases (n/total)	
Sequence of fusion		Thoracic arch-arch		
		Cervical arch-arch		
		Occipital lateral-squama		
		Thoracic arch-centrum		
		Cervical arch-centrum		
		Occipital basilar-lateral		
		Coracoid (1/20)	Ischiopubic ramus	
		Coracoid (2/5)	Ischium-ilium	
		P. ulna (1/6), d. humerus (1/16)	Coracoid	
		D. humerus (1/4)	Ischium-pubis (acet.)	Coracoid (1/4)
		D. humerus (1/14)	Ilium-pubis	Coracoid (1/4)
		D. humerus (2/14)	P. ulna/	Coracoid (1/7)
		D. humerus (4/18)	p. radius/	Ilium-pubis (1/4), ischium-pubis (acet.) (1/4), coracoid (2/7)
		D. humerus (4/12)	m. humeral epicondyle	
		D. humerus (4/12)	Fem. head/	P. radius (1/8), coracoid (1/11)
		D. humerus (4/12)	g. trochanter	P. radius (1/8), coracoid (1/12), ischiopubic ramus (1/32)
		D. humerus (4/11)	D. tibia/	P. radius (1/9), coracoid (1/13)
		D. humerus (4/11)	l. trochanter	Fem. head (1/3), coracoid (1/13)
		D. humerus (4/10)	D. fibula	L. trochanter (1/3), p. radius (1/10)
		Acromion (1/4)	D. humerus/	P. ulna (2/13)
		Ischial tuberosity (1/3)	p. tibia	D. fibula (1/4), coracoid (1/16)
		D. radius (1/3), ischial tuberosity (2/5), d. ulna (1/4)	P. fibula	D. humerus (2/6), coracoid (1/19)
		Ischial tuberosity (3/5), p. humerus (1/6)	Acromion	D. humerus (3/8), l. trochanter (1/6), p. radius (1/13), coracoid (1/17), ischiopubic ramus (1/29)
		Ischial tuberosity (1/3)	D. radius/	D. humerus (1/5), coracoid (1/19)
			d. femur	Acromion (2/4), d. humerus (2/6), coracoid (1/18)
			Ischial tuberosity	D. humerus (2/7)
		D. ulna	D. humerus (1/6), coracoid (1/20)	
		P. humerus	D. humerus (1/9)	
		Iliac crest		
		M. clavicle	Iliac crest (2/14)	

## 2.4. INFLUENCES ON SKELETAL MATURATION

### 2.4.1. Secular trends

#### *A) Overview*

Secular trends are a change in the rate and level of maturation and growth in a population over time (van Wieringen, 1978; de Muinck Keizer-Schrama and Mul, 2001; Malina et al., 2004). For example, the change in haemoglobin levels or the rate of dental development in a population (Garn and Russell, 1971; van Wieringen, 1978; Arthur et al., 2016). A secular trend can be positive or negative in a population or absent altogether (van Wieringen, 1978; de Muinck Keizer-Schrama and Mul, 2001; Malina et al., 2004). While genetics determine the rate and level of maturation and growth, trends can be determined by the environment that acts upon epigenetics (Malina et al., 2004; Fudvoye and Parent, 2017).

Positive secular trends (earlier maturation and increases in size, Malina, 1990) in earlier skeletal maturation have been identified, particularly in the hand and wrist. The hand and wrists of 1990s American children were found to mature earlier than those of UK children from the 1960s (Tanner et al., 1997). Separate studies have also found this positive secular trend in skeletal maturation in American children (Calfee et al., 2010; Duren et al., 2015; Boeyer et al., 2018), as well as in urban black South African children (Hawley et al., 2009), Taiwanese children (Hsieh et al., 2013), and Chinese children (So and Yen, 1990). However, not all maturity indicators are equal. For example, Duren et al., (2015) found that some bone maturity indicators developed at a later age, whereas the epiphyses fused earlier in the 1965 to 2001 AD cohort than the 1930 to 1964 AD group.

Two environmental factors that influence positive secular trends in a population are nutrition and access to health care, as optimal growth occurs when a child is healthy and well-nourished (Gafni and Baron, 2000). When a child is malnourished or incurs an illness, the body will down-regulate growth to preserve itself (Gafni and Baron, 2000). If the problem is resolved, catch-up growth will occur (Gafni and Baron, 2000). This is where growth exceeds the growth rate the child would have experienced if the insult had never happened (Gafni and Baron, 2000). However, catch-up growth seldom achieves the child's full adult stature (Gafni and Baron, 2000).

Poor growth during childhood has long-term effects into adulthood, with a higher chance of mortality and morbidity (Jones et al., 2015). Poor growth during childhood can affect

all major organs of the body and stunt linear growth (Hoddinott et al., 2013). Poor socioeconomic status and poor access to health care can result in short stature, increased risk of diabetes, high cholesterol and early morbidity (Malina et al., 1985; Nyström and Vågerö, 1989; Silventoinen and Rahkonen, 1999; Jousilahti et al., 2000; Silventoinen, 2003; Kemkes-Grottenthaler, 2005). In some studies, a connection between obesity, early onset of puberty and accelerated bone maturation has been found (Klein et al., 1998; Wang, 2002; Golub et al., 2008; Kaplowitz, 2008; Schooling et al., 2010). An earlier pubertal onset has been argued to cause health complications during childhood through disturbed early development (Golub et al., 2008). Early maturation has equally been linked to a higher risk of reproductive organ cancers and depression (Tanner, 1962; van Lenthe et al., 1996; Biro et al., 2001; Cameron and Demerath, 2002; Demerath et al., 2004a; Hauspie and Roelants, 2012; Tremblay and Larivière, 2020).

Different populations can experience different environments that help or hinder growth. Children born and raised in a suitable environment tend to mature earlier and are larger on average than children from poor socioeconomic backgrounds (Malina et al., 1985). If the socioeconomic background changes, such as an increase in income, the family or population may afford better nutrition (Steckel, 2012). Future generations will reflect this through growth indicators, like increased stature (Steckel, 2012).

Genetics are a factor in causing maturational differences between modern human populations. For example, Portuguese children were more skeletally advanced than Belgian children, except for in carpal maturity (Freitas et al., 2004). The reason could not be explained socioeconomically (Freitas et al., 2004), and therefore could be due to genetic differences. For instance, some studies have found that black American girls tend to enter PHV earlier than white American girls (Berkey et al., 1994; Biro et al., 2001; Rogol et al., 2002). They also tend to be more advanced skeletally, taller and heavier than white American girls (Berkey et al., 1994; Biro et al., 2001; Rogol et al., 2002). However, some studies suggest these differences between black and white children are socioeconomic rather than genetic (Schmeling et al., 2004). For example, children from a more impoverished background may eat more cheap, unhealthy, energy-dense foods that could increase adiposity (Pechey and Monsivais, 2016). A correlation exists between greater adiposity and early maturation (Biro et al., 2001).

### *B) Studies on skeletal maturation*

A positive secular trend in skeletal maturation was found in urban black South African children from 1962 to 2001 AD, but not in white South African children (Hawley et al., 2009). Initially,

urban black children did not have the same access to healthcare and nutrition as white children (Hawley et al., 2009). The white children had, most likely, skeletally advanced at an earlier period in time because of advantages in nutrition and healthcare granted to them (Hawley et al., 2009). By the time that black South African children gained access to stable housing and electricity and begun to skeletally advance, the white children had, in all probability, already reached their full genetic potential (Hawley et al., 2009). However, many black South Africans remain behind white South Africans in skeletal maturation (Hawley et al., 2009).

In China, children from higher socioeconomic backgrounds have better access to nutrition, healthcare, parental care, and overall living conditions than Chinese children from low socioeconomic backgrounds (Low et al., 1964; So and Yen, 1990). These children have also matured skeletally faster than children from lower socioeconomic classes (Low et al., 1964; So and Yen, 1990). Ossification rate can be affected by the socioeconomic development of a population (Schmelting et al., 2000). For example, in a predominately rural country, increased commerce, the introduction of education and increased medical care will affect the quality of life in the towns first before filtering down into the villages (Forbes et al., 1971). Thus, the finding that Japanese children from Tokyo are more skeletally advanced than children from Nomozaki – a rural fishing village (Takai and Akiyoshi, 1983) may be due to the socioeconomic differences between urban and rural environments in Japan.

Skeletal maturation was delayed in Modern Indian children compared to American children from the 1930s (Patil et al., 2012). Specifically, Indian males had more delayed skeletal maturation than Indian females (Patil et al., 2012). Malnutrition and/or socioeconomic status were thought to be contributing factors (Patil et al., 2012).

Taiwanese children from the mid-2000s were more skeletally advanced than Taiwanese children from the mid-1960s (Hsieh et al., 2013). Taiwan in the 1960s was largely an agricultural economy with poor economic growth and a poor diet that consisted of mainly sweet potatoes (Hsieh et al., 2013). In contrast, in the mid-2000s, Taiwanese children had a high-calorie diet, such as burgers and pizza (Hsieh et al., 2013). Advanced skeletal maturation was also found in American children born in 1995 AD compared to American children born in 1935 AD (Boeyer et al., 2018). Although the authors (Boeyer et al., 2018) did not detail the possible reasons behind the secular change, it would not be unexpected if it were also due to socioeconomic advancement in America. While not every secular change can be explained through socioeconomic change (e.g. Freitas et al., 2004), it is clear that better nutrition, housing, and healthcare can exert an influence on the timing of skeletal maturation.

### 2.4.2. Differences between the sexes

Major differences between females and males are hormonally induced and this has a large impact on growth, maturation, and the maintenance of the skeleton. Oestrogen is a key hormone for both sexes. Females produce oestrogen from their ovaries and adrenal glands (Sylvia et al., 2002; Ellison and Reiches, 2012), except postmenopausal females, in which oestrogen is converted from adrenal androgens found in the peripheral tissues via the P450 aromatase enzyme (Sylvia et al., 2002). In males, the testes synthesise some oestrogen, but the majority of men's oestrogen is locally produced in other tissues, such as the brain, skin and bone, whereby oestrogen is synthesised through the aromatisation of testosterone by the P450 enzyme (Perry et al., 2008; Cooke et al., 2017).

Androgens are also necessary and these hormones are used to maintain cancellous bone mass and regulate the differentiation and proliferation of epiphyseal chondrocytes (Vanderschueren et al., 2004). Little research has been done on the effect of androgens on the female growth plate (Vanderschueren et al., 2004), but no sex differences have yet been found regarding androgen receptor expression in the chondrocytes in the modern human growth plate (Clarke and Khosla, 2009). Thus, the growth plate is likely the same for both sexes. The production of the sex hormones from the gonads are therefore a crucial component that induces differences in bone maturation and growth – shorter stature in women from higher circulating oestrogen levels and higher bone mass in males due to higher levels of circulating androgens (Vanderschueren et al., 2004).

When aromatase enzymes or oestradiol receptors are not functional in boys, a growth spurt does not occur (Ellison and Reiches, 2012). The lack of function can allow males to continue growing linearly into the third decade of their life (Ellison and Reiches, 2012). In castrated boys, the pituitary gland still produces growth hormone, but this is not balanced out by testosterone (Peschel and Peschel, 1987; Barbier, 1998). Due to the removal of the testes, castrated boys are more susceptible to enlarged breasts, osteoporosis, tall stature, and reduced secondary sexual characteristics because of hyperplasia of the pituitary gland (Wilson and Roehrborn, 1999; Eng et al., 2010; Kessler et al., 2016).

#### *A) Birth and childhood*

Sex differences in skeletal maturation between modern humans are present before birth (Rogol et al., 2002). At birth, female babies are 4 to 6 weeks more skeletally mature than males (Rogol

et al., 2002). Both sexes tend to mature at similar rates during childhood (Humphrey, 1998; Rogol et al., 2002). For example, the fusion of the pars basilaris to the pars lateralis of the occipital occurs at approximately 5 to 7 years of age for all children (Schaefer et al., 2009).

### *B) Puberty*

Sexual dimorphism reoccurs once again when children enter adolescence. On average, females enter puberty at an earlier age (typically one to two years) than males (Rogol et al., 2002). For example, the fusion of the spheno-occipital synchondrosis occurs earlier in females than it does in males (Schaefer et al., 2009). Puberty is thought to start and finish earlier in females than males because prepubertal females have 8x more oestradiol (a form of oestrogen) than prepubertal males of the same age (Cutler, 1997; Dunsworth, 2020).

Oestrogen stimulates and stops growth, and higher concentrations in girls would naturally cause an earlier start to the adolescent growth spurt and earlier growth arrest than in boys (Dunsworth, 2020). Locally produced oestrogen may explain why girls begin the adolescent growth spurt before breast budding, which requires high levels of circulating oestrogen produced by the ovaries (Öz et al., 2001). Oestrogen is required for ovulation and menstruation in women, incurring costs to the body (Dunsworth, 2020). This is potentially why stature (and age at menarche) is correlated with nutritional costs and disease more so in females than males (Biro et al., 2001; Onland-Moret et al., 2005; Baer et al., 2006; Walker et al., 2006b; Schooling et al., 2010; Kang et al., 2019; Dewitte and Lewis, 2020).

Due to the higher levels of oestradiol found in the female body, the earlier growth spurt could potentially be why women are shorter than men on average (Dunsworth, 2020). As men have lower oestradiol levels, their biology requires longer to reach the desired concentrations to accelerate and cease growth. Therefore they have a more extended period in which to grow taller (Dunsworth, 2020). This would explain why trunk length is similar in both sexes, but not limb length (Seeman, 1998; Singh et al., 2011) and why no sex differences have been found in oestrogen and androgen receptors found at the growth plate (Nilsson et al., 2003).

Children without reproductive organs and late-maturing children do not have a growth spurt at puberty (Prader, 1982; Bogin, 2003). Instead, these children will experience linear growth at a prepubertal rate (Turner et al., 1994). Not all epiphyseal fusion occurs at puberty, but most adult height is attained at this time (Shim, 2015). The pubertal growth spurt comprises approximately 15.0 to 20.0% of adult height attainment, which proceeds epiphyseal fusion (Carel et al., 2004). It is widely believed that epiphyseal fusion ceases longitudinal growth, but growth stops at the growth plate before fusion occurs (Bogin, 1999a; Parfitt, 2002; Nilsson and

Baron, 2004). Some children never experience epiphyseal fusion but will eventually stop growing (Bogin, 1999a; Parfitt, 2002; Nilsson and Baron, 2004). The adolescent growth spurt is therefore not required to reach final adult height (Bogin, 2003).

### 2.4.3. Genetic variation in maturation

The timing and tempo of skeletal maturation and bone ossification are highly heritable between siblings (Towne et al., 2012). Skeletal maturation timing heritability is approximately 0.49 between siblings (Hewitt, 1957). Heritability ( $H^2 - V_G/V_P$ ) is always measured from 0 to 1 and is the proportion of how much the phenotype varies from the population average (phenotypic variance), which is due to genetic factors (Wray and Visscher, 2008). Heritability is highest between identical twins (Kimura, 1981).

Genetic defects can impact growth and skeletal maturation. If the gene that regulates sex steroid production is affected, skeletal maturation may be delayed, and bone density will be low (Vanderschueren et al., 2005). If the gene affected is critical for growth plate function, then the likely outcome is skeletal dysplasia and idiopathic short stature (Baron et al., 2015). However, if the gene affected is crucial for protein function at the growth plate but is not critical for growth plate function, bone morphology remains normal, and the child will only have short stature (Baron et al., 2015).

#### *A) Short Stature Homeobox gene*

The Short Stature Homeobox (*SHOX*) gene is essential for skeletal development, and copies are found on both the X and Y chromosome (Genetic Home Reference, 2012). Sometimes, the number of *SHOX* gene copies is reduced on the sex chromosomes, resulting in short stature (Baron et al., 2015). Langer mesomelic dysplasia is usually caused by deletions of this gene, whereby not enough *SHOX* protein is produced and results in short stature, short long bones in the arms and the legs, and deformities at the wrist and forearm (Genetic Home Reference, 2012). Since the *SHOX* genes are found on the sex chromosomes, a missing or reduced X chromosome means copies of the *SHOX* gene are reduced (Genetic Home Reference, 2012). Again, this results in short stature and unusual rotations found at the wrist and elbow (Genetic Home Reference, 2012). Finally, too many copies of the *SHOX* gene results in Klinefelter syndrome (Baron et al., 2015). The outcome of this is tall stature (Baron et al., 2015).

### *B) Indian Hedgehog and PTHrP*

Indian Hedgehog is one of the many critical proteins required for bone development (Maeda et al., 2007; Karimian et al., 2012). Mutations of Indian Hedgehog can cause acrocapitofemoral dysplasia (Zhang et al., 1998; Kindblom et al., 2002; Hellemans et al., 2003; Karimian et al., 2012). This disease is characterised by short stature, short limbs, delayed bone maturation and a narrow thorax (GARD, 2021). Mutations of PTHrP can cause Blomstrand dysplasia (Zhang et al., 1998; Kindblom et al., 2002; Hellemans et al., 2003; Karimian et al., 2012). This disease causes premature ossification of the skeleton and advanced maturation that is lethal (Hoogendam et al., 2007). Mutations of both Indian Hedgehog and PTHrP can cause premature epiphyseal fusion (Zhang et al., 1998; Kindblom et al., 2002; Hellemans et al., 2003; Karimian et al., 2012).

### *C) Fibroblast growth factors*

Fibroblast growth factors are cell-signalling proteins (Naski et al., 1998; Karimian et al., 2012). They are involved with Indian Hedgehog and PTHrP (Naski et al., 1998; Ballock and O'Keefe, 2003). Fibroblast growth factors are thought to be involved in growth plate senescence and, thus, involved in determining the size of the adult skeleton (Karimian et al., 2012). Fibroblast growth factor receptor genes are expressed during every stage of endochondral ossification (Naski et al., 1998; Karimian et al., 2012).

Overexpression of Fibroblast growth factor receptor 3 (FGFR3) can cause reduced proliferation at the growth plate (Naski et al., 1998; Ballock and O'Keefe, 2003). Mutations of the FGFR3 gene can lead to growth disorders, such as achondroplasia and hypochondroplasia (Naski et al., 1998; Lazarus et al., 2007; Karimian et al., 2012). Achondroplasia prevents the cartilage at the growth plate of long bones from ossifying (GARD, 2017). This leads to dwarfism, with limited elbow movement and small fingers but a large head (GARD, 2017). Hypochondroplasia is like achondroplasia but milder yet still characterised by very short stature (GARD, 2018). Dwarfism is a common outcome of gene and protein mutations that affect growth plate regulation. For instance, disruption to the genes that encode for natriuretic peptide receptor 2 and C-type natriuretic peptide can result in impaired endochondral ossification and dwarfism (Tamura et al., 2004; Karimian et al., 2012).

### *D) Epigenetics*

Socioeconomic status can affect the genes required for growth and skeletal maturation. This may be caused by environmental conditions affecting DNA methylation (McDade et al., 2019).

DNA methylation is an epigenetic marker that alters gene expression, gene regulation, and the control of the gene but does not change the nucleotide sequence (Mortier and Vanden Berghe, 2012; McDade et al., 2019). During critical periods of development, changes in the environment may permanently alter the epigenome through activating or silencing specific genes (Mortier and Vanden Berghe, 2012). This then changes how the gene is expressed, altering the structure and function of the tissues controlled by the gene (Mortier and Vanden Berghe, 2012).

## 2.5. APPLICATIONS OF EPIPHYSEAL FUSION IN ANTHROPOLOGY

Epiphyseal fusion may be used in anthropology to (1) estimate age in developing individuals, (2) sort commingled remains and (3) infer puberty.

### 2.5.1. Using epiphyseal fusion to age individuals

#### *A) Introduction*

Many studies of archaeological and living samples have attempted to correlate chronological age with the timing of epiphyseal fusion (O'Connor et al., 2008). Examples of studied population samples include knee radiographs in a living Irish sample (O'Connor et al., 2008) and several epiphyseal fusion sites sampled in human remains from Lisbon in the 1920s (Cardoso, 2008a, 2008b).

Medical imaging studies that examine skeletal maturation often use x-rays of the hand and wrist (e.g. So and Yen, 1990; Tanner et al., 1997; Hawley et al., 2009; Hsieh et al., 2013). Dry bone studies may look at a specific fusion site, such as the clavicle (Webb and Suchey, 1985; MacLaughlin, 1990; Black and Scheuer, 1996; Langley-Shirley and Jantz, 2010; Langley, 2016) or the entire skeleton (McKern and Stewart, 1957; Coqueugniot and Weaver, 2007; Cardoso, 2008a, 2008b; Schaefer, 2008b).

McKern and Stewart, (1957) have made significant contributions to the timing of epiphyseal fusion in archaeological samples. Equally, Buikstra and Ubelaker, (1994), Cunningham et al., (2016) and Schaefer et al., (2009) have also provided extensive research on age at ossification and epiphyseal fusion, which underpins the three-stage scoring system (see **Appendix 1**).

#### *B) Literature review*

##### Radiographic studies

Medical imaging modalities, such as x-rays, have been used to study epiphyseal fusion (Corron et al., 2021). As the hand and wrist have multiple ossification sites, this part of the body is often chosen for maturation studies (Introna and Campobasso, 2006). Because of this, many methodologies have been applied to the hand and wrist. The Greulich and Pyle radiographic

atlas is a common methodology to assess the hand and wrist (Introna and Campobasso, 2006). It was created between 1931 to 1942 AD and used hand and wrist radiographs from 1,000 white Americans from Cleveland, Ohio, from a middle to upper social class background (Cavallo et al., 2021). It is an efficient method but largely imprecise because of the dataset used (Introna and Campobasso, 2006; Cavallo et al., 2021). For instance, the method does not apply well to populations outside of the original dataset, including modern white Americans (Introna and Campobasso, 2006; Cavallo et al., 2021).

An alternative to the Greulich and Pyle method is the Tanner-Whitehouse radiographic system (Introna and Campobasso, 2006). One thousand, nine hundred and thirty European children were used for this method (Cavallo et al., 2021). An advantage of this system is that the process involves generating a maturation score differentiated by sex, unlike the Greulich and Pyle method (Cavallo et al., 2021). Another advantage is that the Tanner-Whitehouse system has been revised and improved over the years and now includes the ability to apply the method to non-European populations (Cavallo et al., 2021). The Tanner-Whitehouse method can be used on dry bone, but this can be problematic as x-rays can produce a more advanced maturation score (Introna and Campobasso, 2006).

The third well-known radiographic method is the Fels method developed by Roche (Cavallo et al., 2021). This was created from a longitudinal study that x-rayed 13,823 left hands and wrists of 677 children from their first month of life to 22 years of age (Cavallo et al., 2021). All the children were born between 1928 to 1974 AD (Cavallo et al., 2021). It is a very accurate age estimation method but is time-consuming (Cavallo et al., 2021).

Not all studies use the hand and wrist. For example, some studies have looked at the shoulder (Tirpude et al., 2014) or the knee (Ebeye et al., 2016). These studies tend to use scoring techniques similar to those used on dry bone. Like dry bone studies, each paper may use a different variation of scoring. For example, Crowder and Austin, (2005) used a four-stage scoring method, in which an extra stage is placed between unfused and partial fusion. Schmeling et al., (2003) used a five-stage method in which stages 1 and 2 included the ossification of the epiphysis.

### Dry bone studies

The study of dry bone epiphyseal fusion has primarily been attributed to Stevenson, (1924), Paterson, (1926), Todd and D'Errico, (1928), and Todd, (1930a, 1930b; Schaefer and Black, 2007). The work most well-known on epiphyseal fusion was the data collected by McKern & Stewart (1957), who had been influenced by Theodore D. McCown's work on age-related

changes in skeletons (Powell et al., 2006). McKern & Stewart (1957) have been cited in several progeny studies (e.g. Schaefer and Black, 2005; O'Connor et al., 2008; Schaefer, 2008b; Schaefer et al., 2009; Ebeye et al., 2016).

### *1920s – 1930s*

Although epiphyseal fusion was considered before Stevenson, (1924), Paul H. Stevenson's paper – Age Order of Epiphyseal Union in Man – is often cited as a defining paper on the study of epiphyseal fusion. This is because it was one of the first non-radiographic studies examining epiphyseal fusion on a large dataset (Yaşar İşcan and Steyn, 2013). Previous analyses by archaeologists, anatomists and medico-legal experts were based upon anatomy books that were not entirely correct, in that ages detailed for epiphyseal fusion were simplified and unsubstantiated (Stevenson, 1924; McKern and Stewart, 1957). The source of the error on epiphyseal fusion is said to date back to a German manuscript from 1871 AD by J. Henle (Todd, 1930a).

Anatomists, such as T. Wingate Todd, sought to rectify the erroneous information through the re-examination of skeletal maturation (McKern and Stewart, 1957). Todd directed Stevenson to research and write the 1924 AD paper (Todd, 1930a). This paper most likely paved the way for future epiphyseal studies by charting four stages of recording epiphyseal union – (1) no union, (2) beginning union, (3) Recent union, and (4) Complete union, each with a corresponding description.

Todd's research into skeletal maturation continued with Todd and D'Errico's 1928 AD paper. However, only the clavicle was reviewed (Todd and D'Errico, 1928). While the long fusion timing of the medial clavicle was well-known even before Stevenson, (1924), the lateral epiphysis of the clavicle was thought to be fictitious or at least a rare occurrence (Todd and D'Errico, 1928). The work by Todd and D'Errico, (1928) stated the timing and existence of the lateral epiphysis of the clavicle at approximately twenty years of age.

Todd simplified epiphyseal fusion (McKern and Stewart, 1957) and Krogman simplified this further in 1939 AD for the FBI, whereby age estimates for epiphyseal fusion and natural modern human variation were reproduced as limited ranges (McKern and Stewart, 1957). Furthermore, the known age of the skeletons used by Todd and his associates was not always reliable (Webb and Suchey, 1985). To exacerbate matters, skeletons that were found to deviate from the standard skeletal maturation data of that time were excluded from the studies (Webb and Suchey, 1985).

Certain flaws within these papers were already recognised at the time. Stewart, (1934) noted that the article by Stevenson, (1924) had very few skeletons under the age of twenty and that Stevenson, (1924) had used non-human primates to fill in the missing data. Stewart, (1934) commented on the inconsistencies in the work between Stevenson and Todd. The study by Stewart, (1934) used juvenile skeletons sampled from Native American and Inuit groups to study the sequence of epiphyseal fusion. Stewart, (1934) found greater variation in the sequence of epiphyseal fusion compared to the work of Stevenson (Yaşar İşcan and Steyn, 2013). A second reform in skeletal maturation would be required to redress skeletal maturation, but this would not come until 1957 AD.

### *1950s – 1970s*

In 1957 AD, McKern and Stewart produced a report for the US army intended to aid in identifying American soldiers killed in battle. The US Army Secretary requested the information (McKern and Stewart, 1957). The project required the analysis of 450 American male skeletons of known age that had been repatriated from North Korea in the autumn of 1954 AD under Operation Glory (McKern and Stewart, 1957). This analysis aimed to improve previous ageing methodology, particularly for American males of military age (McKern and Stewart, 1957). The reform was required because, although Todd had made improvements to the study of skeletal maturation, analyses on epiphyseal fusion between 1952 to 1955 AD had found age estimations for epiphyseal fusion to differ significantly from the research performed by Todd (McKern and Stewart, 1957). However, due to a lack of data available to specialists, epiphyseal fusion age standards were still based upon Todd's work (McKern and Stewart, 1957). McKern and Stewart, (1957) provided a five-phase system – (1) no union, (2) beginning union, (3) active union, (4) recent union, and (5) complete union – established from the system given in the paper by Todd and D'Errico, (1928; Langley-Shirley and Jantz, 2010).

The report by McKern and Stewart, (1957) was possibly the most influential paper on epiphyseal fusion. However, there were other works on fusion during this period. Redfield, (1970) was one such paper. Redfield, (1970) sought to aid in ageing immature remains from the occipital bone. The reasoning behind this was that the occipital bone, particularly the pars basilaris, is a robust bone during early development that is most likely to be found intact (Redfield, 1970). Redfield, (1970) argued that the development of the occipital bone is less affected by the environment.

During the 1960s, Johnston, (1961) studied epiphyseal fusion in Native Americans excavated from the Indian Knoll archaeological site. He noted that most studies before his had

centred on Modern white populations (Johnston, 1961). Johnston, (1961) used a three-stage system to chart epiphyseal fusion and looked at sex differences in epiphyseal fusion, variation in sequence and age at union between his findings and previous studies.

Papers, such as the work by Redfield, (1970) and Johnston, (1961), therefore provided age estimates for juvenile skeletons outside the demographic presented by McKern and Stewart, (1957). Although McKern and Stewart, (1957) data sought to provide a more substantiated account of epiphyseal fusion, their dataset was limited. Their research focused on mostly white American males of military war age (McKern and Stewart, 1957). The given ages in their report would later become out-of-date for forensic cases, as the demographic was that of men born in the late 1930s.

### ***1980s***

In 1985 AD, Webb and Suchey, (1985) analysed 800 Los Angeles autopsies from the late 1970s to provide modern standards for American forensic anthropologists (Langley-Shirley and Jantz, 2010). Their analysis only focused on the anterior iliac crest and medial clavicle, but they did include both sexes of various ancestry between the ages of 11 to 40 years (Webb and Suchey, 1985). It had the largest sample size since McKern and Stewart, (1957) study and had four stages – (1) no union and no epiphysis, (2) no union with epiphysis present, (3) partial union, and (4) complete union.

Again, the work by Webb and Suchey, (1985) was another attempt to reform the standards of skeletal maturation. Criteria were now based upon Stevenson, (1924), Todd and D'Errico, (1928), and McKern and Stewart, (1957), but these standards were either unreliable or underrepresented specific demographics (Webb and Suchey, 1985). In particular, Webb and Suchey, (1985) wanted to represent individuals who had died in their twenties. This specific age group made up a large proportion of unidentified deaths in forensic cases (Webb and Suchey, 1985). They were keen to use dry bone rather than radiographs as this presented a more likely scenario for a forensic investigator (Webb and Suchey, 1985). To give credit to the work by McKern and Stewart, (1957), Webb and Suchey, (1985) found that their male sample did not differ much in age at epiphyseal fusion for the medial clavicle.

However, Webb and Suchey, (1985) were not the only scholars working on the medial clavicle. Szilvássy, (1980) methodology was adapted into English during this period from his previous paper - Szilvássy, (1968) – whereby developmental changes of the medial end of the clavicle were documented in picture form. Szilvássy, (1980) established a three-phase system

specifically for the medial end of the clavicle with an age range for fusion times. Yet, this paper remains more in obscurity than the well-known paper by Webb and Suchey, (1985).

In his work, Ubelaker, (1984, 1987) detailed the problems of identification of juvenile skeletons in forensic investigations. Ubelaker, (1987) was keen to emphasise the use of comparing epiphyseal union timings between studies to gain a variety of age estimations. Although the work by Ubelaker, (1987) only summarised previous articles on epiphyseal fusion and factors to be considered when estimating age from juvenile human remains, his work paved the way for his and Jane E. Buikstra's later work in 1994 AD.

### ***1990s***

In 1994 AD Buikstra and Ubelaker produced: 'Standards: For data collection from Human Skeletal Remains.' The book contained several devices for recording skeletal remains, including recording juvenile human remains (Buikstra and Ubelaker, 1994). However, the publication did not give fusion data for a particular sample population, although it gave estimated ages of epiphyseal closure (Buikstra and Ubelaker, 1994). Instead, their manual gave the three-phase system of recording epiphyseal fusion – (0) no union, (1) partial union, and (2) complete union – which has been reproduced in many subsequent studies of skeletal maturation (Buikstra and Ubelaker, 1994). Although Buikstra and Ubelaker were not the first to create the three-phase system – for example Johnston, (1961) and Szilvássy, (1980) – they are the most well-known. The three-phase system is argued to be the preferable method, as it removes the majority of subjective error that increases with increasing scoring stages (Schaefer and Black, 2007; Cardoso, 2008a).

The three-stage scoring method made popular by Buikstra and Ubelaker, (1994) did not become a necessary standard within the literature. Black and Scheuer, (1996) studied age changes in the clavicle through measurements. They used a five-stage method (Black and Scheuer, 1996) based upon the paper by MacLaughlin, (1990). MacLaughlin, (1990) studied a known-age skeletal sample from Lisbon, Portugal. Black and Scheuer, (1996) took this further. They analysed four skeletal samples – three known-age London samples and the same sample as MacLaughlin from Lisbon (Black and Scheuer, 1996). Whereas the early years of studying skeletal maturation attempted to simplify the process of epiphyseal fusion, the 1990s explored variation in skeletal development. Much of this work provided age estimates to help with ageing skeletons of unknown age – both archaeological and forensic (Black and Scheuer, 1996).

### ***2000s – Present day***

In 2005 AD, Maureen Schaefer and Sue M. Black compared the epiphyseal union times given in McKern and Stewart, (1957) with Bosniak men who had died in the fall of Srebrenica (Schaefer and Black, 2005). The same stages used by McKern and Stewart, (1957) were used by Schaefer and Black, (2005), and they found that the older Bosniak males completed fusion earlier than the American soldiers. In contrast, the younger Bosniak males completed fusion later than the American soldiers (Schaefer and Black, 2005).

Following this, Schaefer, (2008b) concentrated on the Bosniak soldiers exclusively. She reduced the stages from five to three (Schaefer, 2008b). Within her 2008 AD paper, she sought to improve on the studies by Stevenson, (1924), Todd, (1930) and McKern and Stewart, (1957) by increasing the age range studied and reporting the full extent of fusion of a large sample, rather than only reporting on average development (Schaefer, 2008b). She noted that more research on dry bone, and not radiographic material, would be required to make meaningful conclusions on secular change, socioeconomics and the genetics of skeletal maturation (Schaefer, 2008b). Maureen Schaefer has also created two key texts on juvenile osteology, along with her seniors, Louise Scheuer, Sue M. Black and Craig Cunningham, named *Developmental Juvenile Osteology* and *Juvenile Osteology: A Laboratory and Field Manual* (Schaefer et al., 2009; Cunningham et al., 2016).

Coqueugniot and Weaver, (2007) have studied a known-age skeletal sample from Coimbra, Portugal and charted various fusion points with a three-phase system. They followed this with a later paper on a probabilistic approach to age estimation for a skeletal sample (Coqueugniot et al., 2010). Hugo F.V. Cardoso has produced extensive work on epiphyseal fusion in the Lisbon skeletal collection. Cardoso and colleagues have produced analyses on age-at-fusion for the ischiopubic ramus (Cardoso et al., 2013a), the occipital bone (Cardoso et al., 2013b), the upper limb and pectoral girdle (Cardoso, 2008a), the sacrum (Cardoso et al., 2014), the os coxae and lower limb (Cardoso, 2008b), and the hands and feet (Cardoso and Severino, 2010). Cardoso used a three-phase system which he credited Johnston, (1961; Cardoso and Severino, 2010). In a more recent paper (Belcastro et al., 2019), the epiphyseal scar was added as a phase. The paper designated the phases as degrees – degree 0: no union, degree 1: <50% fusion, degree 2: >50% fusion, degree 3: complete union with scar, and degree 4: complete union (Belcastro et al., 2019). They found that degree 3 was a good indicator of skeletons younger than 35 years of age (Belcastro et al., 2019).

Modern studies may also focus on individual bones, such as the sacrum (Belcastro et al., 2008; Rios et al., 2008), the spheno-occipital synchondrosis (Shirley and Jantz, 2011) and

the clavicle (Langley-Shirley and Jantz, 2010; Langley, 2016). When studying the clavicle, Langley and Jantz (2010) wanted to update the age estimates for Modern Americans. Langley and Jantz (2010) used two scoring systems – a five and a three-phase system. They found that inter-observer error was lower for the three-stage system (Langley-Shirley and Jantz, 2010). They also found that Modern Americans fused four years earlier for the medial clavicle than Americans from the 20<sup>th</sup> century (Langley-Shirley and Jantz, 2010). In her second paper, Langley (2016) looked at the lateral end of the clavicle using only the three-phase system. She found that age at fusion for the lateral clavicle was similar to previous studies. Thus, research into epiphyseal fusion has been extensive.

### **Overview**

The 1920s to 1930s could be considered the beginning of the study into modern human epiphyseal fusion by providing the first non-radiographic analysis on the subject. However, as described above, there were scientific costs, including the exclusion of modern human variation and the use of non-human primates to fill in missing data, which most likely created a younger growth profile for humans as chimpanzees achieve skeletal maturity before that of humans (Brimacombe, 2017). Regardless, the works of Stevenson, (1924) and Todd, (1930a) are considered revolutionary (Kern, 2006) and paved the way for future studies, as well as generating new insights into the field. For example, Todd found that there was a connection between dental eruption and epiphyseal fusion (Kern, 2006). However, this period also suffered from misconceptions, such that Todd believed that only stature, and not skeletal maturation, was variable (Roche, 1992). Thus, the 1920s and 1930s can be considered pivotal in the study of epiphyseal fusion but ultimately flawed.

The 1950s to 1970s was a time of multiple scientific outputs, as the World Wars and the Korean War had generated a large number of skeletons to study, along with the skeletal collections already amassed by the previous generation, such as Todd (Işcan, 1981). McKern and Stewart, (1957) are the most recognised academics for studying epiphyseal fusion during this time and are highly cited. In the Stevenson, (1924) study, he used a sample size of 90 males and 20 females. McKern and Stewart, (1957) increased their sample to 450 males and had better documentation of the age-at-death compared with Stevenson, (1924) and Todd and D'Errico, (1928). While the sample size was generous, the sample was composed of only male, mostly white skeletons of military age, meaning that earlier fusing epiphyses were not as well represented as later fusing epiphyses (Webb and Suchey, 1985; Cunningham et al., 2016).

The limited demographic of McKern and Stewart, (1957) was rectified in the 1980s by Webb and Suchey, (1985). Their sample size consisted of 605 autopsied males and 254 autopsied females that included individuals from different ancestral backgrounds but who lived in Los Angeles, had reliable age-at-death data, and were recently deceased, meaning the sample was representative of 1980s Los Angeles, and included younger individuals to account for earlier fusing epiphyses (Webb and Suchey, 1985). However, they only studied the medial clavicle and the anterior iliac crest (Webb and Suchey, 1985). Their reasoning behind the limited epiphyses used was that they wanted epiphyses that were easily accessible in autopsied individuals and that did not obstruct the embalming process (Webb and Suchey, 1985). However, while their study was for a forensic application, the limited epiphyses used meant that the methodology was not as applicable to skeletonised remains in general. In particular, their four-phase system of recording the stage of fusion is set up for soft tissue remains, albeit the recording system is not difficult to apply to hard tissue. Szilvássy, (1980) was also republished at this time, which included a three-phase system, but again, his work only looked at the medial clavicle. The 1980s was, therefore, an era in which scientific endeavour was applied thoroughly, especially for the purpose of forensic anthropology, but suffered from a lack of enquiry into multiple epiphyseal sites.

This trend in analysing a restricted number of fusion sites was carried on into the 1990s, with Black and Scheuer, (1996) study on the medial clavicle. They studied 37 males and 30 females (Black and Scheuer, 1996). Although a much lower sample size than their predecessors, they provided age-at-fusion data for archaeological collections from London, England and Lisbon, Portugal, and therefore provided variation data (Black and Scheuer, 1996). However, while research into specific epiphyses can mean greater attention to detail – for instance, Black and Scheuer, (1996) also looked at maximum clavicular length – it also meant that many other epiphyses were largely overlooked since the 1980s. MacLaughlin, (1990) also only looked at epiphyseal fusion for the medial clavicle. Buikstra and Ubelaker, (1994) did provide age-at-fusion for a wide range of epiphyses during this period, but their data was a compilation of previous fusion data, including that of McKern and Stewart, (1957). Compilation data is an asset for those wanting to access data quickly and efficiently but may also come with the caveat of including the problems of the original data, such as potential incorrect age information and in the case of McKern and Stewart, (1957), only male ages at fusion.

Male-only collections appear to be more prominent because wars are fought mainly by men. The collection analysed by McKern and Stewart, (1957) was American soldiers killed in

the Korean War, and the skeletal collection analysed by Maureen Schaefer in the 2000s was of Bosniak soldiers killed in the fall of Srebrenica (Schaefer and Black, 2005; Schaefer, 2008b). Again, this meant that the sample was a male-only collection with a limited age range (17 to 30 years) but provided a comparison to the 1950s American soldiers (Schaefer and Black, 2005; Schaefer, 2008b). Schaefer also provided compilation data from previous studies, including her own, like that of Buikstra and Ubelaker, (1994), but separated each study and included more female data (Schaefer et al., 2009). Like the eras before them, the 2000s and 2010s included more epiphyseal fusion data on specific sites, such as the clavicle (Langley-Shirley and Jantz, 2010; Langley, 2016) or the sacrum (Belcastro et al., 2008; Rios et al., 2008). However, other studies of this time have been more thorough.

Coqueugniot and Weaver, (2007) provided a meticulous examination of many fusion sites for both sexes on the Coimbra, Portugal collection. Although their methodology is questionable in that they recorded glued epiphyses as unfused (Coqueugniot and Weaver, 2007). Hugo Cardoso has also been prolific in the study of epiphyseal fusion and has produced several papers on the Lisbon, Portugal skeletal collection detailing ages-at-fusion for various epiphyses (Cardoso, 2008a, 2008b; Cardoso and Severino, 2010; Cardoso et al., 2013b, 2013a, 2014), as well as looking at the link between dental and skeletal maturation that began with Todd in the 1930s (Cardoso, 2007; Conceição and Cardoso, 2011). Cardoso has also offered opinions on comparing epiphyseal fusion studies and the need for a standard methodology that has been lacking in this area of osteology (Cardoso, 2008a). All of this work has therefore been invaluable to the study of epiphyseal fusion. It is hoped that future work into epiphyseal fusion will continue to produce extensive work on skeletal collections, as well as establishing a standard method of recording that can allow for comparisons and interpretations to be carried out with ease.

### *C) Problems concerning the study of epiphyseal fusion for age*

The first papers that attempted to reform epiphyseal fusion on dry bone in the 1920s suffered from simplifying the process of skeletal maturation (Stewart, 1934; McKern and Stewart, 1957; Webb and Suchey, 1985). Although the study of epiphyseal fusion has come far, a standard methodology does not exist. Comparisons between radiographic studies and dry bone studies are advised against because earlier stages of fusion tend to be more easily seen on x-rays, and partial fusion on dry bone can appear completely fused on radiographs, which can lead to more advanced scoring in radiographic examinations (Introna and Campobasso, 2006; Cardoso, 2008b; Schaefer, 2008a; Fojas et al., 2015; Corron et al., 2021). However, strict comparisons

between dry bone studies can prove difficult when no standard methodology exists between them (Cardoso, 2008a; Cardoso et al., 2013b).

The three-stage system is considered the preferred method of recording epiphyseal fusion in dry bone as – (1) no union, (2) partial union, and (3) complete union (Schaefer and Black, 2007; Cardoso, 2008a). This is due to the three-stage method removing the majority of subjective error that increases with successive phases (Schaefer and Black, 2007; Cardoso, 2008a). Langley-Shirley and Jantz, (2010) found that inter-observer error was lower when scoring fusion of the medial clavicle using a three-stage method rather than a five-stage method. However, multiple stages continue to be used in studies, creating barriers in the ability to compare them. For example, Belcastro et al., (2019) added two extra phases for examining the epiphyseal scar on dry bone. This complicated matters by dividing complete union into three separate phases – (3) <50% union, (4) >50% union and (5) the presence of a scar. Not only does this increase inter-observer error, but this is also not easily applied to other studies whereby fusion criteria differ.

The study of secular trends and population studies tends to be carried out on the skeleton using medical imaging studies (So and Yen, 1990; Matsuoka et al., 1999; Hawley et al., 2009; Hsieh et al., 2013; Duren et al., 2015; Boeyer et al., 2018), whereas dry bone studies comparing populations are more limited (Black and Scheuer, 1996; Belcastro et al., 2008, 2019). Dry bone studies tend to focus more on using known age skeletons to help with age estimations (McKern and Stewart, 1957; Webb and Suchey, 1985; Coqueugniot and Weaver, 2007). This can lead to misunderstandings within the literature, i.e., the belief that epiphyseal fusion causes the end of adolescent growth (Parfitt, 2002; Nilsson and Baron, 2004). Modern times have seen the use of epiphyseal fusion to discuss more than just estimating age, such as the sorting of comingled remains (Schaefer and Black, 2007; Schaefer, 2008a, 2014; Lenover and Šešelj, 2019), puberty (Shapland and Lewis, 2013, 2014; Arthur et al., 2016; Lewis et al., 2016) and biology (Dunsworth, 2020).

### **2.5.2. Using epiphyseal fusion to sort comingled remains**

#### *A) Introduction*

The comingling of human remains is when human remains become mixed, usually due to a mass fatality, such as an explosion, a plane crash or war (Schaefer and Black, 2007). It is a

forensic concern because it can lead to a person's misidentification (Schaefer and Black, 2007). Understanding the sequence of fusion is essential in this respect because it can aid in sorting the minimum number of young persons within a disaster or mass grave (Schaefer, 2008a, 2014; Lenover and Šešelj, 2019), along with other techniques, such as visual pair matching and taphonomy (L'Abbe, 2005). Variation in the sequence of fusion between populations occurs, and this is important to note when sorting commingled remains, as well as when studying external environmental factors between populations (Stewart, 1934; Garn and Rohmann, 1960; Garn et al., 1961; Roche, 1992; Lenover and Šešelj, 2019).

### *B) Literature Review*

During the 1920s, Stevenson, (1924) provided research on the age-at-fusion for secondary ossification centres in modern humans and the sequence of fusion around the body. However, Stevenson, (1924) believed that the sequence of fusion was set and never-changing between individuals. This thought process was also true of his colleague, Todd, (1930a, 1930b), who reported slightly different fusion sequence patterns to Stevenson, (1924) but maintained that the sequence of fusion was identical among every human being (Schaefer and Black, 2007). The work by Stewart, (1934) in the 1930s contended this statement by studying the sequence of union between Inuit and Native Americans. Stewart, (1934) then compared his sequence with that of Stevenson, (1924). Stewart, (1934) agreed with the work by Stevenson, (1924) but suggested that the order of fusion may vary between ancestry and socioeconomics, and that beginning union was more variable than complete union. However, the work by Stewart, (1934) did not change the popular opinion that the fusion sequence was unvaried.

Nonetheless, in the 1960s, Johnston, (1961) argued that the sequence of fusion was not fixed. He argued that more research on the sequence of fusion should be performed on “non-whites” (Johnston, 1961). Johnston, (1961) analysed the Indian Knoll collection, a Native American archaeological site. He (Johnston, 1961) found that the sequence of union was closest to the Native American data provided by Stewart, (1934) but that there was no statistical significance. Johnston, (1961) was keen to test the sequence of fusion between Native Americans and Caucasians. Since he found no significant differences in his correlations, he concluded that racial variation could not be inferred.

Also, during the 1960s, Garn and Rohmann, (1960) studied the ossification of the hand and wrist. They concluded that the order of ossification varied between groups and by individual (Garn and Rohmann, 1960). This opinion was in opposition to the majority of the literature at the time, such as the work by Greulich and Pyle, (1950). William Greulich was a

student of Todd (Kern, 2006). Garn and Rohmann, (1960) suggested that in a healthy population, minor deviations to the sequence of fusion are standard and a product of the environment and chance, but larger deviations to the sequence of fusion are a product of population genetics.

Earlier works only sought to discover a fusion sequence and whether that sequence was identical in every human, but later works, with human variation established, wanted to use the sequence to help in commingled remains. Epiphyseal fusion can help separate commingled remains because any inconsistencies found in the fusion sequence can aid in collating juveniles into whole individuals, who are usually mixed with other skeletons as a result of war or mass disasters (Schaefer and Black, 2007). The work by Schaefer and colleagues (Schaefer and Black, 2007; Schaefer, 2008a, 2014) thus sought to improve on previous studies by providing a fusion sequence for dry bone for a wide variety of fusion sites around the body. However, a potential flaw was that the fusion sequence was only based upon Bosniak males (Schaefer and Black, 2007). Later, Lenover and Šešelj, (2019) updated the fusion sequence to incorporate fusion sequences from skeletal collections representing Africans, Asians, Europeans and Native Americans.

### **2.5.3. Using epiphyseal fusion to assess puberty stage**

#### *A) Introduction*

Skeletal and sexual maturation are closely linked (Shapland and Lewis, 2014). In species such as modern humans and rabbits, the majority of epiphyseal fusion occurs at the time of puberty (Hirai et al., 2011). Growth plate senescence and epiphyseal fusion are affected by the timing of the adolescent growth spurt (Cunningham et al., 2016). Furthermore, epiphyseal fusion can direct the osteologist to the skeleton's pubertal stage. For example, the fusion of the phalangeal epiphyses of the hand is closely linked to peak height velocity (Grave and Brown, 1976; Shapland and Lewis, 2013).

#### *B) Literature Review*

The seminal work on puberty in human remains was produced by Shapland and Lewis (2013), who adapted and collated previous research into a format which allowed the osteologist to assess the pubertal phase a skeleton was in at the time of their death. To determine this,

Shapland and Lewis, (2013) used the ossification of the hand and the wrist, the ossification of the iliac crest, and the epiphyseal fusion of the distal radius. Each fusion site's progression is associated with a pubertal phase (Shapland and Lewis, 2013). For example, a developing hook of hamate of the hand can be attributed to an acceleration of the growth spurt, whereas a fully matured hamate corresponds with PHV having been achieved (Shapland and Lewis, 2013). Shapland and Lewis, (2014) later added cervical vertebrae maturation to their methodology. The maturation of the cervical vertebrae corresponded to each stage of the adolescent growth spurt (Shapland and Lewis, 2014).

Since then, a multitude of papers has been written assessing archaeological puberty based upon the works of Shapland and Lewis, (2013, 2014). In 2016 AD, Arthur et al., (2016) used Shapland and Lewis' methodology to study puberty in Roman England. They found that pubertal onset was the same for Modern European adolescents but that Romans experienced a longer duration of puberty compared with Modern teens (Arthur et al., 2016). Around the same time, Mary Lewis and Fiona Shapland co-authored a paper with Rebecca Watts to use their puberty research on Mediaeval collections from England (Lewis et al., 2016). They found similar results to Arthur et al., (2016) and concluded that physical exertion, a poor diet and infections could have contributed to Mediaeval adolescent's delayed development (Lewis et al., 2016).

The following year, Henderson and Padez, (2017) used the methods by Shapland and Lewis, (2013, 2014) to test puberty in a 20th-century Portuguese skeletal collection. The Coimbra collection is a vital assemblage to anthropology because it includes detailed documentation of the skeleton's age-at-death, sex, occupation and cause of death (Henderson and Padez, 2017). They found that females completed puberty before males, and the age at menarche for girls was older than expected based upon historical data (Henderson and Padez, 2017). Such a collection would have been ideal for testing puberty in human remains, but a small sample size meant that the results gleaned were reduced (Henderson and Padez, 2017).

That same year, Doe et al., (2017) studied the pubertal phase of skeletons at the San Nicolás Maqbara burial site in Murcia, Spain, using the same methodology. Again, the onset of puberty was similar to Modern Spaniards but was delayed in reaching later pubertal phases compared to contemporary adolescents (Doe et al., 2017). Danielle Doe later applied the Shapland and Lewis procedure to six skeletons from a Spanish Bronze Age site – El Cerro de la Encantada (Doe et al., 2019). It was reasoned that puberty has remained relatively unchanged since prehistoric times (Doe et al., 2019).

Finally, Blom et al., (2021) analysed puberty in a Dutch Post-Mediaeval collection from Middenbeemster and compared their data to previous puberty studies. They also found puberty to be of longer duration than today (Blom et al., 2021). Their data overall agreed with previous studies, but they found the female Dutch skeletons to have experienced pubertal onset at a much earlier age (Blom et al., 2021). Thus, the methodology set out by Shapland and Lewis, (2013, 2014) has been of great importance and has led to the understanding of puberty in history. To test the efficiency of this methodology, however, it would be preferable to evaluate the methods on more Modern skeletal collections.

## 2.6. GROWTH AND MATURATION IN BRITISH HISTORY

As this thesis draws upon samples from British history and prehistory, this section will review previous literature on potential environmental effects on historical populations. The focus will be on three main environmental influences that can affect childhood growth and maturation, which are nutrition, disease and war. These are discussed in detail below.

### 2.6.1. The Iron Age

The Iron Age is considered one of the shortest archaeological periods in British and Irish prehistory, but it is seen as a period of great social change (Pryor, 2004). By 300 BC, the population was growing quickly, and contact with the rest of Europe was more frequent (Pryor, 2004). Population growth may have come about from a return to a warmer and drier climate that was not present during the Late Bronze age to the Early Iron age, which allowed for the development of new farming technology (Oliver, 2012). Social systems became more hierarchical, and early kingdoms that minted their own coinage began to form (Pryor, 2004). Women most likely held authoritarian and martial positions, and many graves were not gendered (Pope and Ralston, 2011).

It is expected that there may have been some warring between peoples as evinced by hillforts, which would protect the farmers when land became scarce from population increases (Schama, 2009). However, there is also evidence that trading occurred, and therefore a level of peace would have had to have been in place (Schama, 2009).

The Iron Age British diet most likely relied on meat and milk from sheep, as there is evidence that there was a heavy reliance on sheep husbandry before the Roman invasion (Albarella et al., 2008). However, cattle and pigs were also kept, with cattle use decreasing throughout the Iron Age period (Albarella et al., 2008). Pigs were also not as frequent in Britain compared to the rest of Europe, and it has been suggested that meat consumption may have been lower in Britain than in Europe, with a greater reliance on crop production (Albarella et al., 2008).

Isotopic evidence at Wetwang in Yorkshire suggested that the Iron Age inhabitants had a diet high in either meat or dairy products and low in marine animals (Jay and Richards, 2006). The isotopic evidence, along with a lack of archaeological evidence for fishing equipment or

fish bones, may indicate that marine foods were probably not a dietary staple in the Iron Age (Jay, 2008). That may have been due in part to the Iron age beliefs and rituals centred around water (Redfern et al., 2010). In support of a more egalitarian community, isotopic evidence suggests that the diet of Wetwang varied little between individuals and throughout their lives (Jay and Richards, 2006) and this is supported by a similarity in the degree of dental wear, carious lesions and abscesses between the elite and non-elite (Peck, 2013). A difference in grave goods at the site may show that society was stratified to a degree (Jay and Richards, 2006). Weaning practices at Wetwang were also identified, and it is thought that the mother's milk was supplemented early on in Iron Age children with either a mix of animal and human milk or plant foods (Jay et al., 2008).

Relationships between these aspects of diet and the growth and maturation of Iron Age children is poorly understood, due to a combination of the number of Iron Age cemeteries available, excavation techniques used, taphonomy, and the funerary rites used throughout the period (Redfern, 2007). However, in a study that compared Iron Age and Romano-British children, it was found that Romano-British children were taller from infancy to childhood but had more evidence of metabolic disease. In contrast, the Iron Age children were taller from childhood (Redfern, 2007). Both cohorts reached a similar height at age 20 years. This evidence suggests that growing up in Iron Age Britain may have been subject to fewer environmental stressors than in Roman Britain (Redfern, 2007).

### **2.6.2. The Romans**

Rome had attempted to invade Britain twice (55 BC and 54 BC) before prevailing in 43 BC (Miles, 2006). The cultural and social change that Romanisation brought appears to have influenced the growth and maturation of children. Although Romanisation was not a complete takeover of the indigenous cultures present in Britain, with societies being allowed to express their ethnic and cultural identities, skeletal studies, as detailed above, do show there was an effect on biological functions (Redfern, 2007; Albarella et al., 2008; Redfern and Dewitte, 2011). It is also of note that the incorporation of Britain into the Roman empire began after the attack by Julius Caesar in 55 to 54 BC (Redfern and Dewitte, 2011), but trading between Britain and the rest of Europe had been occurring for many years beforehand (Miles, 2006).

For some British communities, dietary changes occurred, such as marine consumption (Locker, 2007; Redfern and Dewitte, 2011; Redfern et al., 2012; Van der Veen, 2014), whereas

for other communities, no such change occurred. This is most likely because Romanisation affected different parts of the country and social statuses independently (Cheung et al., 2012). Diet can affect dental health, prevention or susceptibility to infectious or metabolic diseases, and growth in childhood (Redfern and Dewitte, 2011). An increase in population density and urbanisation can incur deleterious effects on the body, which some communities experienced (Redfern and Dewitte, 2011). Potential changes to the treatment of children may have also occurred with Roman rule and medicinal practices, such that colostrum was advised to be withheld, and instead, the infant was prescribed a mixture of water and honey (Redfern, 2007). This would have increased the probability of mortality in the infant (Redfern, 2007).

New settlement types may have also increased diseases, which could affect the very young (Redfern and Dewitte, 2011). Thus, after the Roman conquest, physiological stress and frailty are argued to have increased, leading to a higher risk of death (Redfern and Dewitte, 2011). Higher exposure to new people, food, pathogens and parasites from the continent would have increased with the Roman occupation of Britain (Redfern and Dewitte, 2011).

At the same time, agriculture and landscape management improved and intensified, and new, more efficient technologies were implemented, including innovations in cooking (Redfern and Dewitte, 2011; Cheung et al., 2012). Yet overall, Romanisation was found to have deleterious effects on the most vulnerable groups, the elderly and children (Redfern and Dewitte, 2011). Unlike the Iron Age, which appears to have had a more egalitarian society, Roman culture had a hierarchical system, which put children and the elderly at the margins of society (Redfern and Dewitte, 2011).

Society and culture have a significant impact on health and can determine effects on the body throughout one's life, including an individual's growth potential (Redfern, 2008). In skeletal samples from Dorset, mean stature was found to significantly decrease in females and males from the Iron Age to the Roman era (Redfern, 2008). Thus, while housing and food production may have improved, the impact of other environmental influences brought by the Romans meant that growth was affected (Redfern, 2008). However, the range of stature increased during the Roman occupation so that the tallest British-Roman individuals were taller than the Iron Age individuals, but the shortest Roman-British individuals were shorter than Iron Age individuals, showing the interplay of various environmental factors (Redfern, 2008).

### 2.6.3. The Anglo-Saxons

Far from the initial Roman invasions in 55 and 54 BC and the revolt by Boudicca in 60 AD (Schama, 2009), England's alliance lay with Rome three centuries later (Jenkins, 2012). However, Rome was under attack from the Visigoths during this era and had left England undefended, which allowed raiders from across the seas and land to pillage (Jenkins, 2012). This included the Picts from central and northern Scotland, the Gaelic Dal Riata from Ireland (Schama, 2009), the Jutes from Denmark, the Frisians from the Netherlands, and the Angles and Saxons from different areas of Germany (Jenkins, 2012). The Jutes took over Kent and the Isle of Wight, the Angles gave name to East Anglia, and the Saxons formed territories in Essex, Middlesex, Wessex and Sussex (Jenkins, 2012). From this, the English were named the 'Saeson', Sassenach' and "Sawsnek' by the Welsh, Gaelic and Cornish peoples (Jenkins, 2012). Movement was also occurring within Britain and Ireland as a whole. For example, some Dal Riata are thought to have moved to Scotland (Miles, 2006). The Dal Riata was known as the 'Scoti' – the origin of Scotland's name (Miles, 2006).

The Saxons brought back paganism and displaced Christianity, although the Gaelic countries of Britain retained Christianity (Jenkins, 2012). However, between 600 to 800 AD, England was once again made Christian (Jenkins, 2012). The Saxons changed the cultural landscape of England. Rather than give their allegiance to a far-off power, like Rome, the Saxons were more family orientated, whereby each settlement had a communal hall and ceorls (free farmers) would be subordinate to ealdormen (chiefs, Jenkins, 2012).

During this period, the several Kings of England were expanding their reigns – King Raedwald of East Anglia expanded to create the Kingdom of Mercia (600 to 624 AD), King Aethelfrith of Bernicia defeated the Dal Riata Scots in 603 AD, took over the Kingdom of Mercia and seized Cumbria in 615 AD (Simpson, 2022). More wars ensued when Raedwald killed Aethelfrith in 616 AD at the battle at Bawtry, and northern rivals attacked Edwin, King of Deira (Simpson, 2022). The Meicen Kingdom at Hatfield and the Anglian Kingdom at Lincolnshire were later captured by Edwin, as well as the West Saxons in 626 AD at the Battle of Wessex (Simpson, 2022). Edwin was then dispatched at the battle of Hatfield Chase in Yorkshire by Penda of Mercia and the Welsh leader, Cadwallon of Gwynedd in 633 AD (Jenkins, 2012). The Welsh having got their name from the Anglo-Saxon word for 'foreigner' – *Wealsh* (Miles, 2006). Differences between the Welsh and Central England are supported by genetic (Y chromosome) evidence, in which living Central English Anglo-Saxons were found to be indistinguishable from Friesland and Norway, whereas two North Welsh towns were found to be distinct from each other and the Central English towns (Weale et al., 2002).

The many wars of this period ended with a plague that broke out in England and Ireland in 664 AD (Creighton, 1981). After the synod at Whitby in 664 AD and the rise to power of King Offa in 757 AD, it may be suggested that a level of peace came to England, but this was short-lived (Jenkins, 2012), and within Scotland, war was still occurring between the Picts and Dal Riata (Miles, 2006).

The first recorded raid of the Vikings was in 787 AD, and after King Offa's death, warring began once more with Ecgbeht of Wessex invading Cornwall in 814 AD, along with the battle of Ellandune, near Swindon, in 825 AD (Jenkins, 2012). Rebellion occurred between the East Anglians and King Beornwulf of Mercia, but Ecgbeht succeeded in taking Mercia and Northumbria (englishmonarchs.co.uk, 2022).

Viking attacks became more regular, and the Cornish and Devon peoples allied with the Danes against Ecgbeht (englishmonarchs.co.uk, 2022). Mercia became an independent state once more (englishmonarchs.co.uk, 2022). The Vikings succeeded in taking York, Mercia, East Anglia (Jenkins, 2012), Shetland and Orkney, among others (Miles, 2006). In Ireland, women were stolen from their homes, and invasions occurred frequently down the river systems (Miles, 2006). Irish infighting was also happening at this time, like that of King Feidlimid mac Crimthainn of Munster, who attacked and massacred the monks at the Clonmacnoise and Durrow monasteries (Miles, 2006). Between 866 to 1016 AD, fighting between the English and Vikings occurred with the taking, losing and retaking of land (Jenkins, 2012; York Museums Trust, 2022). Viking attacks affected everyone, with many of the attacks coordinated to occur during festivals so that goods could be plundered from everyone (Dyer, 2002). The Anglo-Saxon age ended with the infamous 1066 AD.

During the Anglo-Saxon period, culture became Anglo-Saxon, too (Miles, 2006). Anglo-Saxon children tended to be weaned quickly at approximately one year of age when they would be introduced to an adult diet (Haydock et al., 2013). Children may have been seen differently after they could speak around the ages of two or three, and this corresponded with a change in treatment towards the child and total immersion into the adult diet (Haydock et al., 2013). Compared to the Roman period, the duration of introductory foods appeared longer for Romano-British children than Anglo-Saxon children ( $\geq 2$  years for Romans, 1 year for Anglo-Saxons, Haydock et al., 2013).

Rather than the urban centres of Roman times, Anglo-Saxon settlements were scattered communities, including subsistence farmers (Mays and Beavan, 2012). Although aspects of Romanisation existed, it is thought that the economy became more localised once more, and therefore people cultivated and ate from the lands that surrounded them rather than having a

great reliance on imported foods (Holmes, 2016). This is implied by carbon ( $\delta^{13}\text{C}$ ) isotope signatures, in which plant diet composition of Anglo-Saxons from 400 to 550 AD was different to the Anglo-Saxons from 600 to 700 AD, and this is thought to be because of the collapse of the Roman trading network (Sakai, 2017).

Boys attained adulthood at age twelve, and a person's social rank was determined by their wealth (Miles, 2006). There were free people and those that were "unfree", yet the consumption of meat and marine animals was not a privilege of any one group (Privat et al., 2002). However, based on isotope nitrogen values ( $\delta^{15}\text{N}$ ), it has been argued that at specific sites, men over the age of thirty years consumed more lower-status foods, such as freshwater animals or pork, compared to males under the age of 30 years (Privat et al., 2002; Mays and Beavan, 2012). It is thought this may have occurred because younger men would have been more politically and militarily active than the older men and, therefore, would be seen as superior to the more senior men (Privat et al., 2002). This dietary difference might have contributed to growth for Anglo-Saxon male adolescents, although there is limited data for either sex from this period in time. However, stress markers appear to be greater in Anglo-Saxon subadults than in Mediaeval subadults. This is thought to be from the Anglo-Saxon subadults being exposed to more continuous and systematic stress than Mediaeval subadults (Ribot and Roberts, 1996). This stress could be due to the continual warring and invasions as described above. War can generate conditions, such as poor nutrition, an increase in disease, and negative psychological effects that can greatly influence and impact growth and maturation in the child (Prebeg and Bralić, 2000).

#### **2.6.4. The Mediaeval Period**

The Mediaeval period began with the Norman conquest of 1066 AD and the harrowing of the North in 1069 AD (Jenkins, 2012). By the 1070s, approximately 4,000 Saxons were replaced by 200 Norman barons, bishops and abbots (Jenkins, 2012). This left only 5.0% of England under Saxon rule (Jenkins, 2012). From this, around 200,000 Normans, Flemish and French peoples emigrated to England and a fifth of the English population was starved or slaughtered (Jenkins, 2012). However, the Norman conquest is considered similar to the Roman conquest centuries before, where everyday life was barely disturbed, but society and politics were slowly changed (Gies and Gies, 1990). In contrast, the Anglo-Saxon period was constant invasions where there were mass migrations and displacement of whole regional populations (Gies and

Gies, 1990). Instead, the Normans replaced only the English who owned estates. In contrast, the lower levels of society were left to their customs and practices as these individuals would generate an income for the upper classes (Dyer, 2002).

The Norman period brought about a change of status for the lowest rung of society. Where many individuals were slaves before the Norman conquest, the Normans wanted to install Norman landholders who would provide military service (Jones and Ereira, 2004). However, the Normans did not want to work their land and therefore used the English to provide labour service for the manor, and in return, provided the English with small pockets of land in which to grow their own food so that the Normans did not have to feed the English themselves (Jones and Ereira, 2004).

The Norman lords often owned multiple manors and therefore had to leave their estates unattended for periods of time. So that the manor could run when the lord was away, the peasants, named “villeins”, had to maintain the keep (Jones and Ereira, 2004). Although the lord’s steward presided over the villeins, it was the villeins that minded the manor, giving them a level of power (Jones and Ereira, 2004). The lord could be fined if unjust, regulations could sometimes be ignored or manipulated, and the lord would keep the villeins happy with seasonal holidays, like Christmas or Easter, that included time off and feasts (Jones and Ereira, 2004). Many families lived in nuclear units around the manor in two-room houses with a ditch or fence to provide privacy from neighbours (Jones and Ereira, 2004).

New towns were also established and attracted peasants by having fixed cash rents or a five-year respite on the rent (Dyer, 2002). These new towns were associated with castles, such as Newcastle (Dyer, 2002). Towns also attracted country women to become servants, especially if they would inherit little from their families, as well as tradesmen who were skilled in smithing or tanning (Dyer, 2002). Towns required migrants because few children survived to adulthood when raised in an urban environment. Still, towns also attracted the poor because handouts of food from monasteries and wealthy households occurred more so in towns (Dyer, 2002).

The use of unsanitary rags and horns to feed babies in London was one of the factors that led to high infant mortality rates (Hanawalt, 1993). However, where city children were more at risk of disease-related deaths, country children were more at risk of accident-related deaths as their parents worked the fields and therefore left them alone or with older siblings (Hanawalt, 1993). Women were also more at risk of dying in urban environments compared to rural settings, but this may have been a consequence of more women moving to urban environments from rural compared to men (Walter et al., 2016).

Wars, crusades, revolts and invasions were still prominent at this time and continued into the 1150s and beyond (Jenkins, 2012). However, the 1150s also saw a gentler climate, where harvests were abundant, more land was made available for farming, and technology was improving (Schama, 2009). There were also more markets and fairs; long-distance travel became safer and commercial connections became more profitable in Britain (Schama, 2009). The economy allowed for a population boom, which continued into the 14<sup>th</sup> century, with 4 million British by 1300 AD (Schama, 2009).

Food was generally healthy for low-status individuals. Fruit and vegetables were considered food for peasants, as it was believed fruit led to dysentery (Jones and Ereira, 2004). However, fruits and vegetables were still consumed by the upper classes (Dyer, 1994). Bread was brown and often had peas and beans baked into it (Jones and Ereira, 2004). However, the poorest individuals usually ate pottage (a type of soup that changed with the seasons) rather than bread, as it required no milling and was therefore not taxed (Gies and Gies, 1990). Harvest workers and their families were supplied with the best diet by the manor lord, and many peasants had a healthy diet provided by offal, herrings, and dairy produce (Dyer, 1994). However, individuals may not have had access to this all year round (Dyer, 1994), and malnutrition was a problem (Ward, 2006). Bread, milk and cheese became more available after the black death (Gies and Gies, 1990), as well as a range of different meats (Dyer, 1994).

The consumption of marine foods rose compared to the Anglo-Saxon period (Müldner and Richards, 2005; Mays and Beavan, 2012), and this most likely came from religious ideology in which Christian fasting regulations prevented individuals from consuming meat for half of the year (Müldner and Richards, 2005, 2007). The lack of marine consumption in the Anglo-Saxon period appears similar to the potential reasons why marine foods were not consumed in the Iron Age, due to a religious affinity with the water (Redfern et al., 2010), as paganism was brought back to England during the Anglo-Saxon era.

Breastfeeding in Mediaeval times tended to occur for children up to one or two years of age, allowing infants to grow at a similar pace to today (Mays, 2010). However, after the removal of breast milk, growth could falter for some Mediaeval children (Mays, 2010). Nutrition is suspected to have been poor at sites such as Wharram Percy, as height-for-age for children was low, and acquisition of cortical bone during the growth period was found to be much lower when compared to Modern children (Mays, 2010). Stress indicators, such as dental enamel hypoplasias and porotic hyperostosis, were high in this population (Mays, 2010).

Isotope data on Wharram Percy suggests that they ate a diet of cereal and animal protein, whether that be meat or dairy, which is similar to the diet of British prehistoric

populations (Müldner and Richards, 2006). Equally, isotopic evidence has shown that food consumed was overall similar between areas and social groups (Müldner and Richards, 2005), and evidence points to children receiving a similar diet regardless of status (Reitsema and Vercellotti, 2012; Dawson and Brown, 2013; Mahoney et al., 2016). Femoral length in Mediaeval children between 1 to 15 years of age was found to be shorter than Modern children, suggesting a diet that was of less nutritional value compared to the present (Waldron, 2006). Mediaeval females were on average just over 5 ft, which is slightly below Modern standards for height, potentially reflecting a lower standard of living compared to Modern times (Shapland et al., 2015). Growth data of Mediaeval girls suggests that puberty and epiphyseal fusion were delayed by approximately two or three years, allowing the girls to catch up in stature (Shapland et al., 2015). Overall, data suggest that wealthy peasants had a reasonably good diet, which was the amplest during the harvest season (Woolgar et al., 2006), but may have become poorer at other times of the season. Stress markers in the adults of Wharram Percy point to potential periods of low nutrition but high physical labour (Mays, 2010).

Certain areas of Mediaeval life continued to improve with a defining moment in 1215 AD when the Magna Carter was signed by King John (Jenkins, 2012). The Magna Carter supported the civil liberties of the people (Jenkins, 2012). However, as soon as the Magna Carter was signed, King John asked for it to be annulled (Jenkins, 2012). This made the barons furious, and they asked the French King for help (Jenkins, 2012). Realising that King John was in trouble, Scotland and Wales took advantage of this by moving their forces into England (Jenkins, 2012).

King John's son, Henry III accrued a large debt with the pope in the 1250s (Jenkins, 2012). This debt relied on the people to pay taxes, who were already suffering from famine and harvest failures, and then in 1265 AD, the battle of Evesham occurred, in which parliament went to war with the King (Jenkins, 2012). However, peace came in 1267 AD for England through the Statute of Marlborough (Jenkins, 2012), and the 13<sup>th</sup> century also saw a rise in trade jobs (Dyer, 2002). Trade jobs meant that the everyday person did not have to work the fields and could earn a living from crafts and retail (Dyer, 2002). This meant that people could start a family earlier, and this helped with the population boom (Dyer, 2002).

Wales fared differently compared to England. When Llywelyn, the Welsh ruler, failed to attend King Edward's (Henry III's son) coronation, Edward took that as an act of rebellion (Jenkins, 2012). Edward I invaded north Wales in 1277 AD (Jenkins, 2012) with 800 knights and 15,000-foot soldiers, of which 9,000 were Welsh (Schama, 2009). Edward I then turned his sights towards Scotland (Jenkins, 2012). Many Scottish lost their lives during this period.

For example, over three days at Berwick, approximately 11,000 men, women and children were murdered, and Berwick was burnt to the ground (Schama, 2009).

. For Britain as a whole, the spoils of the 12<sup>th</sup> and 13<sup>th</sup> centuries that caused a population explosion began to take its toll in the 14<sup>th</sup> century, and a great famine from 1315 to 1316 AD was followed by diseases in British cattle and sheep (Schama, 2009). The famine was most likely not helped by a great frost that occurred in 1306 AD and then again in 1309 AD and 1312 to 1317 AD, which caused fish, birds and cattle to die (Mount, 2016). There were also heavy summer rains that caused dried-out marshlands to be sodden, and corn did not ripen (Jones and Ereira, 2004). Along with the royal wars and a large population pressing for resources, land and grain prices soared (Schama, 2009). The poor became poorer, crime increased, and tensions were high (Schama, 2009). People were laid off from their jobs and could not afford to buy extravagances, which put more businesses under (Dyer, 2002).

Increased enamel defects are found in the 13<sup>th</sup> to 15<sup>th</sup>-century populations (Roberts, 2009). Enamel defects in teeth can sometimes relate to dietary problems during the growth period (Roberts, 2009), but can also be due to emotional stress or disease (Dawson-Hobbs, 2016). Those targeted the worst by famines, are the poorest individuals, children and the elderly (Yaussy and Dewitte, 2018). In juvenile remains from Mediaeval London, a positive association was found between linear enamel hypoplasia and famine burials, meaning that physiological insults to a growing body affected frailty and, thus, increased the chances of mortality and morbidity (Yaussy and Dewitte, 2018).

Children who grew up during the Great Famine were more likely to have stress markers than children pre-famine (Dewitte and Slavin, 2013). During the famine, shorter females were found to have increased frailty than taller women and were, therefore, more likely to die during this time (Dewitte and Slavin, 2013). Variation in stature then decreased after the Great Famine because of a higher mortality in shorter women (Dewitte and Slavin, 2013).

The Great Famine was succeeded by the Hundred Year War in 1337 AD. Places such as Winchelsea on the south coast of England were regularly attacked by the French, with women and children raped and murdered (Mount, 2016). The English were also at war with Scotland, which meant that taxes were higher for civilians to help fund the wars (Gies and Gies, 1990). This most likely did not help with the recovery from the Great Famine.

Malnutrition and disease are prime factors for preventing a child from achieving full adult stature (Mays, 2018). Malnutrition also weakens the body's immune system, making the body more susceptible to disease or parasitic infection (Yaussy and Dewitte, 2018). For example, the famine of 1257 to 1258 AD was followed by an outbreak of an infectious disease

in 1259 AD (Yaussy and Dewitte, 2018). The higher susceptibility to infection caused by famines and high taxes, along with a large population particularly cramped in cities such as London and Bristol, made an excellent petri dish for when the Bubonic plague landed on British shores in 1348 AD (Schama, 2009; Jenkins, 2012).

Survival analyses of Mediaeval Londoners have shown that survivorship decreased prior to the Black Death (Dewitte, 2015). Some places became ghost towns because of the number of people who died, and it is estimated that the population fell from five and half million to four million (Jenkins, 2012). It took eighteen months for half of the British population to be killed off by the bacillus *Yersinia pestis* (Schama, 2009). The youngest, elderly and poorest had the least resistance and were the first victims to die (Schama, 2009). William Dene, who witnessed the plague, wrote that parents would carry the bodies of their children to church on their shoulders before having to throw them into a mass plague grave, and in some cases, those that died could not get their last rites, as much of the clergy had died out too (Schama, 2009).

Although adults aged between 20 to 40 years would be the least affected group by the plague, there was still mortality occurring among these ages, and this caused a decrease in the breeding population (Dyer, 2002). While people in England were dying, Scotland mounted an invasion, but before they could attack, the plague struck the camp. The men that survived returned to Scotland and took the plague with them (Schama, 2009). The plague returned in 1361 AD and again every twenty to twenty-five years, with the last wave in 1375 AD (Schama, 2009).

The plague caused a high death toll in England which coincided with rising wages while food and rent prices fell (Schama, 2009; Jenkins, 2012). The government attempted to place wages back to pre-pandemic levels, but this caused a revolt in 1381 AD (Gies and Gies, 1990; Schama, 2009; Jenkins, 2012). A higher frequency of periosteal lesions in post-Black Death Mediaeval London skeletons showed that the population was healthier in terms of longevity, as periosteal lesions are positively associated with age, and an increase in older adults was found in the post-Black Death Mediaeval London skeletal collection compared to the pre-Black Death sample (Dewitte, 2014). A healthier post-Black Death population could partly be due to improvements in diet and living conditions (Dewitte, 2014, 2018).

When separated by sex, survivorship for both sexes decreased before the Black Death (Dewitte, 2018). For males, a pattern of increasing linear enamel hypoplasia and decreasing stature occurred before the Black Death, with this pattern reversed after the plague (Dewitte, 2018). The poor health of the pre-Black Death individuals showed that health was declining in

the population two generations before the arrival of the plague (Dewitte, 2018). This may be due to the famine that occurred beforehand and may explain the decreased stature of males at this time (Dewitte, 2018). As mentioned above, malnutrition *in utero* and early childhood can stunt growth and affect immune function, increasing the risk of death by infectious diseases in adulthood (Dewitte, 2018).

Female survivorship was similar to males pre and post-plague, yet linear enamel hypoplasia did not drop significantly after the plague for females, and stature decreased (Dewitte, 2018). The decrease in height is thought to be from improved conditions after the plague that induced an earlier age at menarche, which in turn would have induced growth to stop earlier and closure of the growth plates (Dewitte, 2018; Dewitte and Lewis, 2020).

The 15<sup>th</sup> century witnessed a return to the prosperous Middle Ages, made good by the reduction in the population in the previous century (Gies and Gies, 1990). Peasants could afford to construct houses with masonry foundations and add a second floor or additional rooms (Gies and Gies, 1990).

The Wars of the Roses occurred between 1455 to 1485 AD (Jenkins, 2012). The wars culled much of the nobility. It is estimated that 75,000 men were present at the battle at Towton, representing 10.0% of the fighting-age male population (Jenkins, 2012). Another 28,000 men were slaughtered in the Wars of the Roses, and 150 noble families either died or lost their land (Jenkins, 2012). The wars ended with the Battle of Bosworth and the marrying of the two roses: Henry VII and Elizabeth of York (Jenkins, 2012).

Henry VII's son, Henry VIII, brought about changes to the church and demolished and stripped many monasteries (Jenkins, 2012). This was good for individuals of non-noble blood, as the monastic land was sold to anyone willing to buy it, and this created a merchant class in Britain who could now hold land (Jenkins, 2012).

### **2.6.5. Post-Mediaeval Era**

The beginning of the Post-Mediaeval Era, mainly the 17<sup>th</sup> century AD, was a period of civil war, pestilence, crowded, urban living and poor nutrition (History Extra, 2016; Morrill, 2016; Zuvich, 2016; Appleby and Stahl-Timmins, 2018; Murel, 2021; English Heritage, 2022). This was also a period of industrialisation in the 18<sup>th</sup> century, and the greater urbanisation of Britain meant that living conditions were unhygienic, with the urban population having little access to fresh fruit and vegetables (Nitsch et al., 2011; Mant and Roberts, 2015; Eggington, 2020). With

industrialisation, women joined the workforce, leading to parents taking up artificial weaning practices (Nitsch et al., 2011). This resulted in many children lacking essential dietary components, which caused poor health and growth attainment (Nitsch et al., 2011).

The diet of the upper social class was nutritionally poor. Their diet was high in carcinogens and sugar, with a reliance on tea, coffee, hot chocolate, and milled flour (Corbett and Moore, 1976; Rando et al., 2014; Mant and Roberts, 2015). An increase in caries and a decrease in mandibular measurements from a sugar-rich and soft diet occurred compared to the Mediaeval period (Corbett and Moore, 1976; Rando et al., 2014). Detrimental fashionable child-rearing practices of the rich, such as preventing children from going out into the sunlight, meant that children would be subject to nutrient deficiency (Newman and Gowland, 2017; Newman et al., 2019). This led to stunted growth, poor health and increased mortality in children due to industrialisation, compared to children of the Anglo-Saxon and Mediaeval periods (Lewis, 1999, 2002, 2013; Pinhasi et al., 2006).

Weaning age was reduced to 7 months, compared to the age of 1 to 2 years for the Mediaeval period (Pinhasi et al., 2006). However, instead of growth faltering after the child was weaned, growth for Post-Mediaeval children was found to falter *in utero* or at birth. It is thought that this relates to the mother being malnourished and immunodeficient (Pinhasi et al., 2006). Although the diet of the rich could result in poor growth in children, the lower classes were subject to more extreme poverty, with many living in high-density timber shacks that had poor sanitary conditions and lacked sufficient heating (Pinhasi et al., 2006). This would have significantly affected the growth of the child (Pinhasi et al., 2006). Growth disruptions experienced by the child led to an increased risk of mortality in adulthood (Watts, 2015).

## 2.7. SUMMARY

The aim of this thesis is to examine skeletal and sexual maturation in British archaeological skeletal remains from the Iron Age to the Post-Mediaeval era. This will include looking at age-at-fusion and the sequence of fusion. **Section 2.3.** of the literature review covered the sequence of fusion, and the studies given in that section will be compared to the findings of this study. **Section 2.1.** and **2.2.** gave definitions and introduced the reader to bone growth, which is necessary for understanding epiphyseal fusion.

**Section 2.4.** looked at influences on skeletal maturation, including secular trends. A secular trend is a change in the rate and level of maturation and growth in a population over time (van Wieringen, 1978; de Muinck Keizer-Schrama and Mul, 2001; Malina et al., 2004). Although genetics is the determining factor in the rate and level of maturation and growth, environmental influences have an effect on the phenotype, and this is what causes secular trends in a population (Malina et al., 2004; Fudvoye and Parent, 2017). Studies that have looked at secular trends of skeletal maturation have mostly found that Modern children tend to mature earlier than children of the past (So and Yen, 1990; Tanner et al., 1997; Hawley et al., 2009; Calfee et al., 2010; Hsieh et al., 2013; Duren et al., 2015; Boeyer et al., 2018), and two main environmental influences thought to have contributed to this positive secular trend is better nutrition and better access to healthcare (Gafni and Baron, 2000).

The technological gains that have accumulated throughout the past until now have had a significant effect on food production and healthcare but have also produced negative effects, such as industrialisation. These effects have been shown to have influenced growth, as seen in **Section 2.6.** whereby, for example, stature changed during Roman times compared to the Iron Age, from the interplay of positive effects, such as improved agricultural and landscape management, but negative effects, such as higher exposure to pathogens from migration and globalisation (Redfern and Dewitte, 2011; Cheung et al., 2012). However, as seen in **Section 2.6.** the past is far from a linear progression of improvements and is interspersed with periods of war, pestilence and political unrest that are reversed by moments of better climates, social change, and agricultural improvements, all of which may have affected the skeleton.

Finally, **Section 2.5.** reviewed previous literature on epiphyseal fusion studies. Two points of interest from **Section 2.5.** are the lack of age-at-fusion studies for archaeological skeletal collections before the Post-Mediaeval era – most likely because age-at-death records for skeletal collections are found more so in Post-Mediaeval and Modern populations – and the

absence of a standard methodology in epiphyseal fusion studies. This thesis plans to rectify this by using a standard methodology throughout to study epiphyseal fusion in archaeological skeletal collections.

## CHAPTER 3

## MATERIALS

## 3.1. THE ARCHAEOLOGICAL SITES

## 3.1.1. Introduction

This chapter lists the archaeological sites and skeletal remains that are the focus of this study. Each section starts with an overview of the region, followed by the archaeological site and the number of skeletons used. The total number of skeletons examined for this thesis was two hundred and sixty-one. A summary of the archaeological sites used is given in **Table 3. 1**.

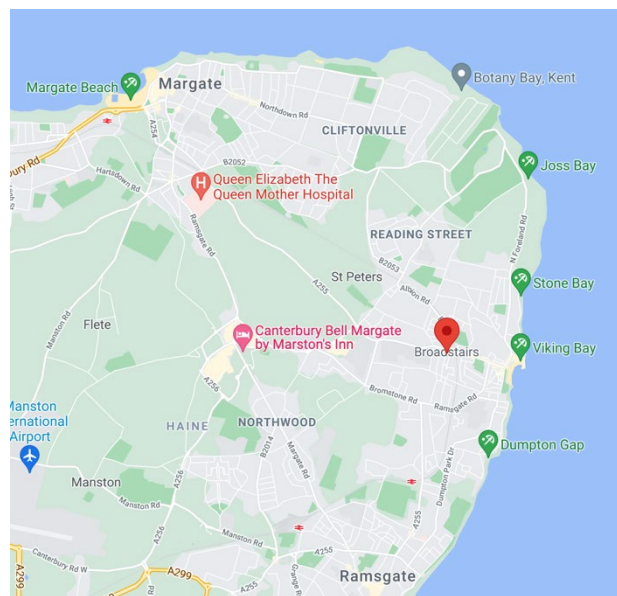
*Table 3. 1: All skeletons and their corresponding sites used. \* = Dates given in centuries and approximated by JAM Dolding-Smith into early, mid- and late centuries by dividing 100 years by 3, \*\* = Approximate collective. Actual phases are listed here. Sk. 327 (Phase 3), Sk. 345 (Phases 2 – 3), Sk. 467 (Phase 2), Sk. 663 (Phase 2), Sk. 742 (Phase 3), Sk. 834 (Phases 1 – 2) and Sk. 868 (Phase 3). Phase 1 = 650 – 1000 AD, Phase 2 = 1000 – 1200 AD, Phase 3 = 1200 – 1400 AD, and Phase 4 = 1500 – 1700 AD*

Country	Region	Site	Archaeological period and approximate dates	Number of Skeletons
England	Broadstairs and St Peter's	South Dumpton Down	Middle/Late Bronze Age to Iron Age (2000 – 350 BC)	11
		Canterbury	St Gregory's priory	Mediaeval (1084 – 1537 AD)
	Chichester	Apple Down	Anglo-Saxon (468 – 601 AD)*	10
	Cirencester	Bath Gate	Roman (69 – 406 AD)	13
		Former Bridges Garage	Roman (69 – 301 AD)*	7
		St James' Place		4
		Butler's Field	Anglo-Saxon (434 – 701 AD)*	10
	Newcastle-upon-Tyne	Abbey of St Mary		5
			Black Gate	Anglo-Saxon (800 – 1178 AD)
		York	Fishergate House	Mediaeval (1334 – 1434 AD)*
All Saint's church			Mediaeval (1000 – 1300 AD)*	13
Sheffield	Carver Street	Post-Mediaeval (1806 – 1855 AD)	6	
Scotland	East Lothian	Auldham	Anglo-Saxon (650 – 1000 AD)	2
			Mediaeval (1000 – 1400 AD)**	7
			Post-Mediaeval (1500 – 1700 AD)	1

### 3.1.2. Broadstairs and St Peter's

Broadstairs and St Peter's is a town in the county of Kent in England (**Figure 3. 1**). The town is situated on the Isle of Thanet. The Isle of Thanet was reported to be where Hengist (an Anglo-Saxon settler) landed in the 5<sup>th</sup> century (Rodriguez, 2017). As well as where the Regulbium and Rutupiae Roman forts were situated, which guarded the Wantsum Channel and Ebbs Fleet (Rodriguez, 2017). The earliest known record of Broadstairs is from 1435 AD, in which the town is listed as *Brodsteyr*, from the Old English *brad staegger*, meaning the broad stairway (Poulton-Smith, 2013). It is now a well-known seaside town.

Figure 3. 1: Broadstairs and St Peter's is pinned on the map. Image taken from Google maps.



#### A) South Dumpton Down in Thanet

**South Dumpton Down** was excavated in the early 1990s by the Trust for Thanet Archaeology and is a site adjacent to Dumpton Gap Road (Perkins, 1995; Moody, 2008). The skeletons are now in the care of the University of Kent. It is thought that there were three phases of human settlement at South Dumpton Down: Phase I (Late Neolithic – Early Bronze Age, 2000 BC), Phase II (Middle Bronze Age, 1200 to 1000 BC) and Phase III (Early Iron Age, 550 – 350 BC, Perkins, 1995). It is believed that South Dumpton Down represented a network of interlinked settlements that ranged across the upland areas of eastern Kent (Moody, 2008; Rowing, 2011). Eleven skeletons were examined for this thesis, aged between 3 to 35 years. This archaeological site is grouped under the historical period of the *Iron Age*.

### 3.1.3. Canterbury

Canterbury is a city in the English county of Kent (**Figure 3. 2**). Archaeological finds suggest that Canterbury has been in use since the Bronze Age (Lyle, 2013). During Roman times, Canterbury was known as *Durovernum Cantiacorum* and was a typical tribal capital for the Cantiaci (Lyle, 2013). In the Saxon period, Canterbury, then known as *Cantwaraburh*, had a unique religious status (Lyle, 2013) and was the capital for the Kentish king, Aethelberht I, in the late 6<sup>th</sup> century (Lotha, 2019a). During this time, St Augustine established Canterbury cathedral, which was initially called Christ Church (Lotha, 2019a).

During the Viking period, Canterbury managed to survive two waves of attacks between 835 to 851 AD and between 991 to 1012 AD (Lyle, 2013). Canterbury also survived William the Conqueror (Lyle, 2013). Throughout these periods, the more affluent citizens of Canterbury gained wealth from investments, such as in international trade (Lyle, 2013). After the assassination of Thomas Beckett, Canterbury became religiously renowned and was as famous as Rome as a place of pilgrimage (Lyle, 2013). This caused a population boom from 6,000 to 10,000 people in the 1200s (Lyle, 2013). By 1300 AD Canterbury had become a prosperous town, holding diplomatic visits and parliamentary elections (Lyle, 2013). However, by 1348 AD, the bubonic plague arrived and reduced the population down to 3,000 by the early sixteenth century (Lyle, 2013). Destruction only increased with the loss of monastic buildings (Lyle, 2013). However, there was a revival in the 18<sup>th</sup> century (Lyle, 2013). Canterbury is now a tourist town and home to students from the various universities situated there (Lotha, 2019a).

Figure 3. 2: Map of Canterbury provided by Google maps. As reference, Broadstairs lies to the upper right of this map.



*A) St Gregory's Priory in Canterbury*

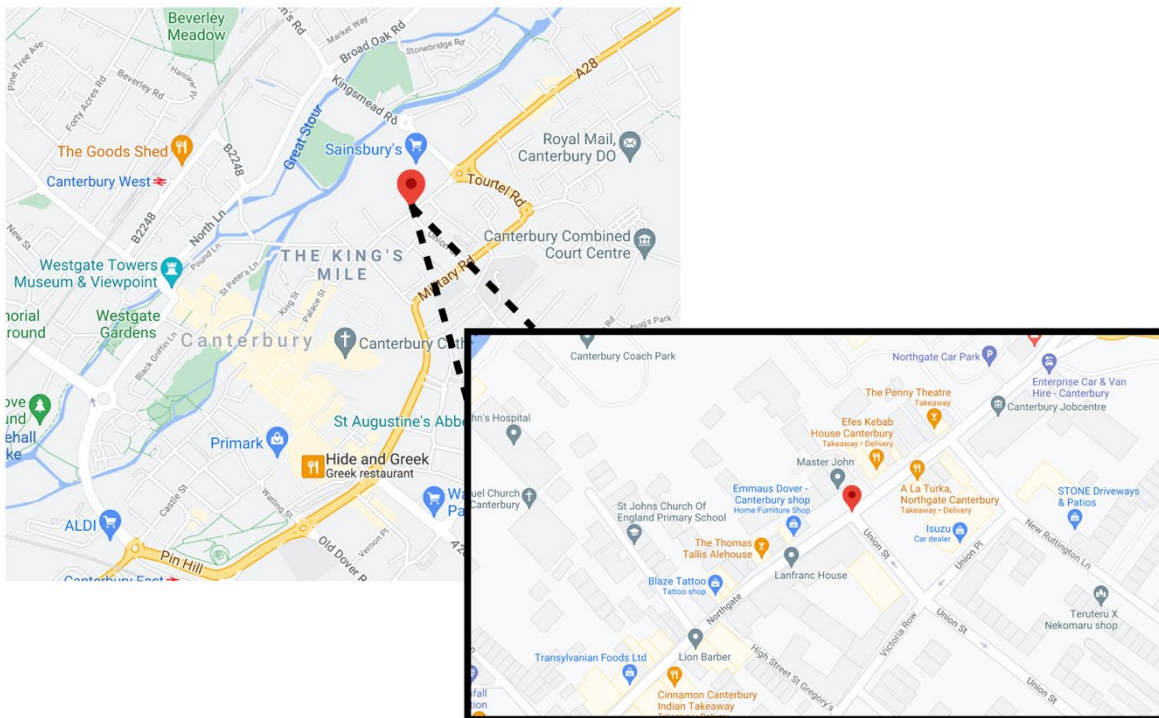
**St Gregory's Priory** was excavated by the Canterbury Archaeological Trust between the years of 1988 to 1991 AD (Hicks and Hicks, 2001). The site was found in the Northgate area of Canterbury (**Figure 3. 3**). The site would have been situated beyond the Mediaeval walls, but would have been an important thoroughfare for both the Mediaeval people and the Romans before them (Hicks and Hicks, 2001).

St Gregory's Priory is composed of two ecclesiastical establishments (Hicks and Hicks, 2001). St Gregory's church was founded in 1084 AD by Archbishop Lanfranc to become the sister establishment to St John's Hospital that sat on the opposite side of the road (Hicks and Hicks, 2001). The cemetery of St Gregory's was placed to the south (Hicks and Hicks, 2001). In 1133 AD, St Gregory's was enlarged and became a priory, but parts of the building were destroyed by a fire in 1145 AD (Hicks and Hicks, 2001). The fire most likely provided the opportunity to rebuild a grander priory under the patronage of Archbishop Theobald (Hicks and Hicks, 2001). Building work began in 1181 AD and continued into the 13<sup>th</sup> century (Hicks and Hicks, 2001). In 1537 AD, the priory was dissolved; however, some of the building was left standing into the mid-19<sup>th</sup> century (Hicks and Hicks, 2001).

The burials found in the cemetery consisted of 1,251 low-status individuals (Hicks and Hicks, 2001). High-status burials were deposited within the church and priory or directly outside the west front of Archbishop Theobald's Priory church (Anderson and Andrews, 2001; Hicks and Hicks, 2001). Ninety-one high-status skeletons were obtained during the excavation (Anderson and Andrews, 2001; Hicks and Hicks, 2001). The presence of women and children buried within the building are thought to represent the allowance of lay benefactors and their families to be interred within the Priory (Anderson and Andrews, 2001).

The skeletons remain in the care of the University of Kent. Overall preservation was excellent, with many skeletons being almost complete and juveniles well-preserved (Anderson and Andrews, 2001). Juvenile mortality was found to be 40.0% higher in the cemetery, which was statistically significant, compared to the church and priory (Anderson and Andrews, 2001). One hundred and seventeen low-status skeletons and eighteen high-status skeletons were examined for this thesis. The estimated ages were between 3 to 35 years.

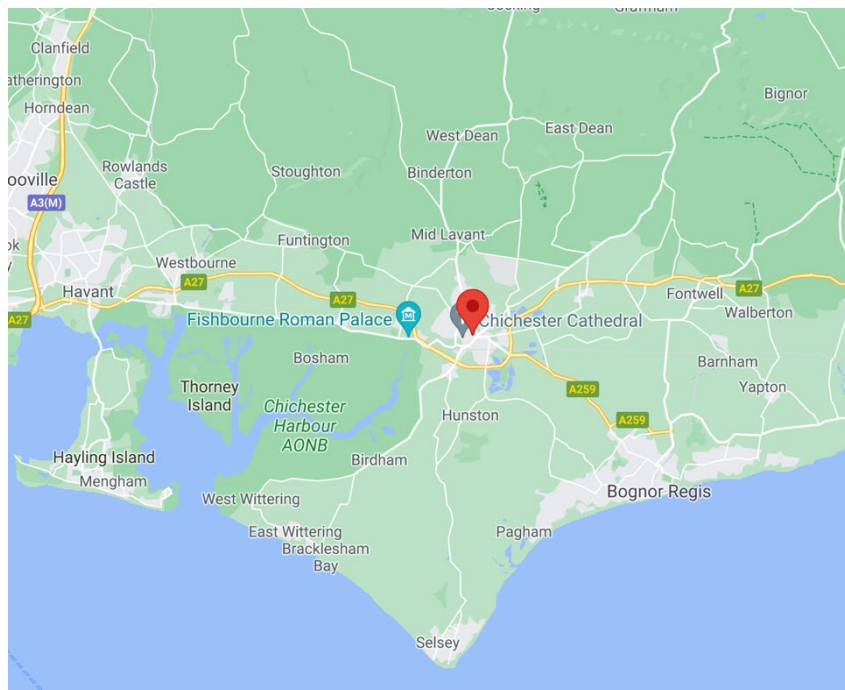
Figure 3. 3: This shows a more in-depth view of Canterbury and pinned is where the Northgate area is. When scaled in, as shown on the picture on the right-hand side, roads such as 'High Street St Gregory's' can be seen. Images taken from Google maps.



### 3.1.4. Chichester

Chichester has been an essential part of English history and has played a significant role during the Roman, Saxon and Mediaeval periods (Down and Welch, 1990). Chichester is a city located in West-Sussex in the South-East of England (**Figure 3. 4**). Chichester began as entrenchments dating back to the Late Iron Age that may have signified a transition or cooperation between a hierarchical and communal organisation (Garland, 2012). During the Roman conquest, Chichester is believed to have been a client kingdom, with the village Fishbourne possibly being the more active site (Garland, 2012). It is thought that the native Britons accepted Roman annexation, and the cooperation of the British and Romans created the beginnings of a hybrid Romano-British town, known as *Noviomagus Reginorum*, situated in present-day Chichester (Garland, 2012). During the Anglo-Saxon period, it is believed that Chichester was a key city during king Aethelwealh's reign (Down and Welch, 1990). Today, Chichester is a tourist town and boasts a Roman Palace in the village of Fishbourne.

Figure 3. 4: Chichester is mapped here. As a reference, if the coast is followed up to the right, Canterbury and Broadstairs can be located. Image provided by Google maps.



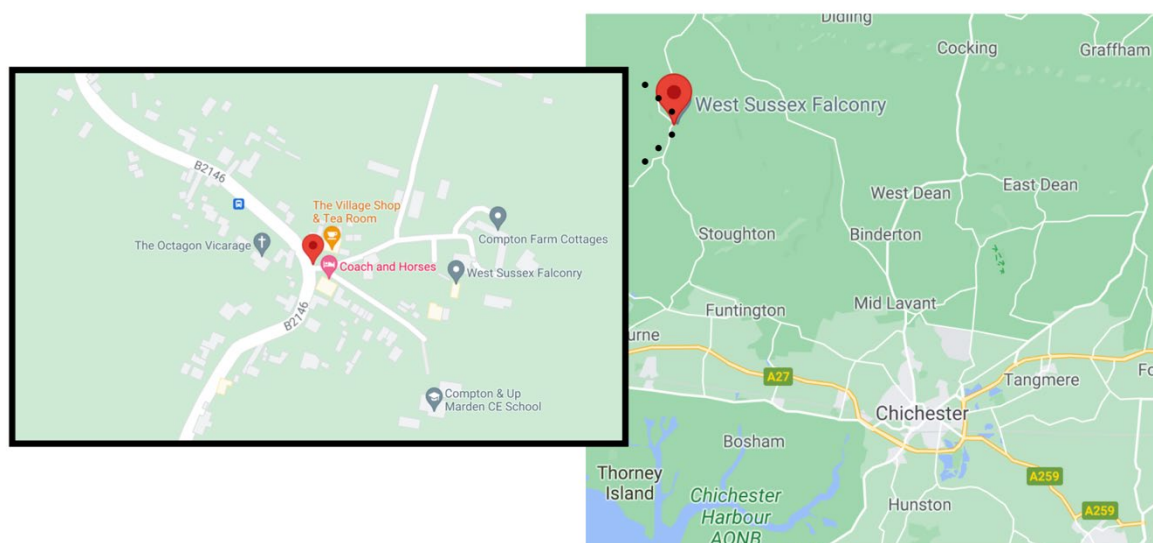
### A) Apple Down in Chichester

**Apple Down** is an Anglo-Saxon burial site located in Compton, West Sussex, on a dip slope of the South Downs (Down and Welch, 1990). A map is provided in **Figure 3. 5**. Compton was known initially as *Cumtun*, meaning ‘valley farm’ (Livitt, 1990). Compton is documented in 1015 AD when Aethelstan Aetheling gifted Compton to Godwin, son of Wulfnoth (Livitt, 1990).

The Chichester Excavation Unit excavated Apple Down (Down and Welch, 1990). The remains are now in the care of the Novium Museum. The majority of the human remains had their bodies laid south to north or west to east, and the skeletons were buried over two cemetery sites (Down and Welch, 1990). A total of 121 inhumations and 64 cremations were recovered from cemetery one, with possible family plots discovered (Down and Welch, 1990). The burials were dated to the late 5<sup>th</sup> to early 6<sup>th</sup> century, and it is known that the cemetery remained in use until the late 7<sup>th</sup> century or later (Down and Welch, 1990).

Evidence from burials point to possible native British burial customs remaining within an ethnically diverse population at the time (Down and Welch, 1990). In contrast, later plots suggest possible baptised Christian burials (Down and Welch, 1990). Cemetery two was found isolated from the first cemetery and had only eleven graves and may have been the ancestors of a small hamlet in Up Marden (Down and Welch, 1990). Ten skeletons were examined for this thesis, with estimated ages between 7 to 22 years.

*Figure 3. 5: Compton is shown on the red pin in reference to Chichester on the right-hand side map. A closer look is provided on the left. Images provided by Google maps.*

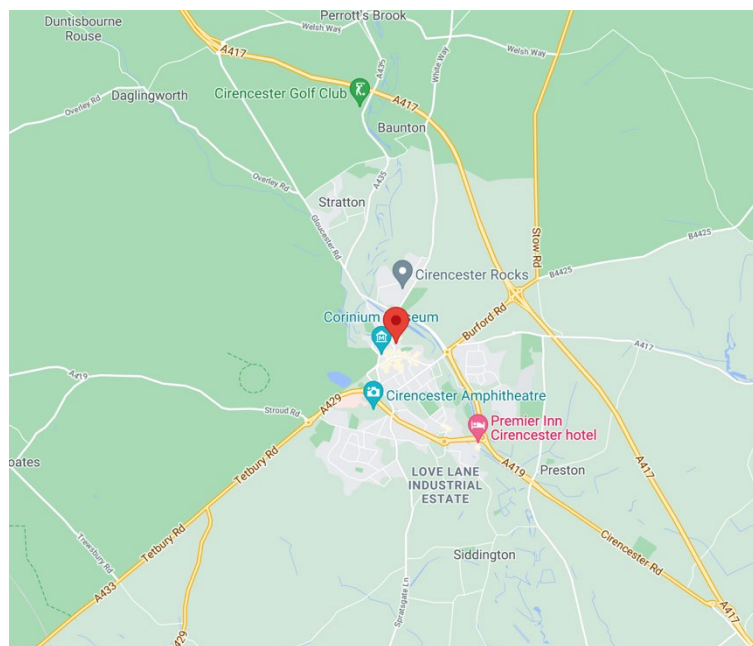


### 3.1.5. Cirencester

The Romans invaded Britain in 43 AD (Cheung et al., 2012) and established a fort at present-day Cirencester (**Figure 3. 6**) in approximately 45 AD (Wacher, 1982; Holbrook, 2012). There is no evidence of a pre-existing Iron Age community before the settlement (Holbrook, 2012; Moore, 2014). However, Cirencester is close to the town of Bagendon. The town of Bagendon is still in use today but is thought to have its origins as a social and political centre for the Dobunni tribe during the Iron Age (Holbrook, 2012; Moore, 2014). Evidence of this has been provided by pre-Roman coin minting and ancient industrial activity (Holbrook, 2012; Moore, 2014).

After the establishment of the Roman fort at Cirencester, it later became a town and was named *Corinium* or *Corinium Dobunorum* (Buckman and Newmarch, 1850; Copeland, 2011). Corinium became the administrative centre for the Dobunni (Buckman and Newmarch, 1850; Copeland, 2011). It was a thriving urban town with well-connected road and river routes (Copeland, 2011; Cheung et al., 2012) and was the second-largest enclosed area via walls after Londinium (London) within the province (Holbrook, 2012). By the fifth century, urban life appeared to decline (McWhirr et al., 1982; Holbrook, 2012). However, today Cirencester is a tourist and agricultural centre (Wallenfeldt, 2014). Cirencester is located in the Cotswold Hills, at the south-eastern end in a long-dip slope (McWhirr et al., 1982).

Figure 3. 6: Map of Cirencester. As a reference, London is to the East-Southeast of Cirencester, and Chichester is South-South-East. Image provided by Google maps.



*A) Bath Gate Cemetery in Cirencester*

**Bath Gate Cemetery** is a Roman burial ground that lies to the west of Bath Gate - a Roman town gate (McWhirr et al., 1982). It sits on either side of the Fosse Way – a Roman road linking Exeter to Lincoln (McWhirr et al., 1982) - which linked Corinium to the amphitheatre (Viner and Leech, 1982). Excavations in the area occurred between 1969 to 1976 AD and 1978 AD by the Cirencester Excavation Committee, with the recovery of over 453 Romano-British individuals from the Bath Gate cemetery (McWhirr et al., 1982; Viner and Leech, 1982). The skeletons are under the care of the Corinium Museum in Cirencester.

Complete skeletons made up 26.9% of remains recovered (Viner and Leech, 1982). The low percentage may be due to the cemetery having been used for an extended period of time, as well as from Roman grave diggers (Viner and Leech, 1982). However, 24.7% of the entire Bath Gate cemetery was labelled as ‘nearly complete’ (Viner and Leech, 1982). The majority of the burials were laid in a north-south alignment parallel with a ditch (Viner and Leech, 1982). Due to a build-up of mixed burial-earth, excavations could not be removed according to the strict stereographical principles (Viner and Leech, 1982). Coins were used to date some of the burials, with the earliest coin dated to approximately 69 to 76 AD and the latest coins dated to approximately 395 to 406 AD, with the majority of coins dated to 310 to 360 AD (Viner and Leech, 1982). Thirteen skeletons were examined for this thesis, with estimated ages between 9 to 25 years.

*B) Former Bridges Garage & St James’ Place in Cirencester*

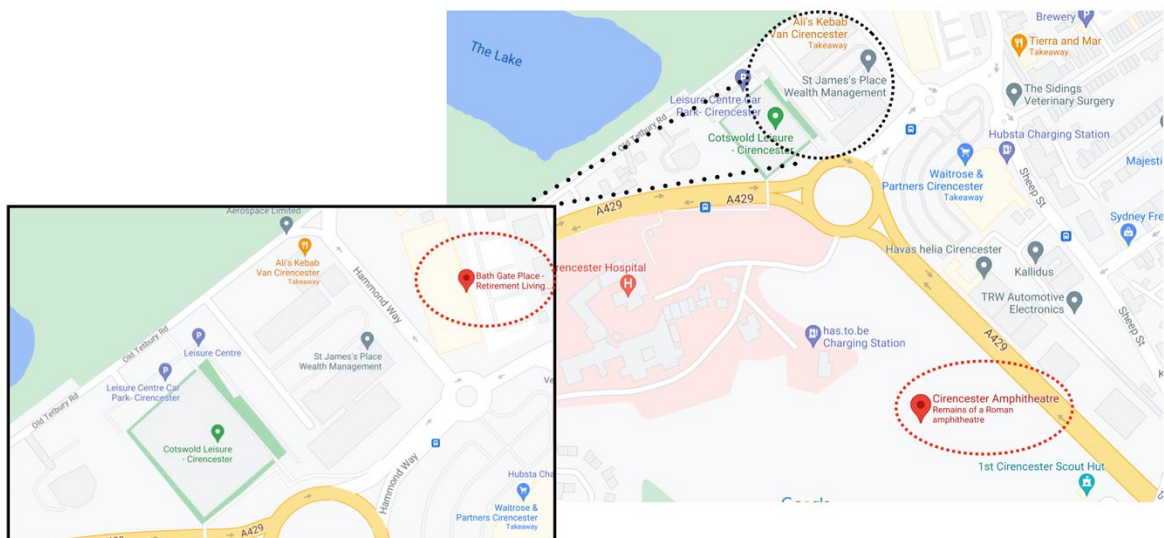
**Former Bridges Garage and St James’ Place** were excavated between 2011 and 2015 AD on the site of the former Bridges Garage, the site owned by St James’ Place Wealth Management, which is situated in the corner formed by Tetbury road and Hammond Way/A429 (Wright et al., 2017). **Figure 3. 7** shows the placement of this site. Tetbury road may have been a track or a minor road up to the town defences (Wright et al., 2017).

The cemetery was excavated in two phases (Wright et al., 2017). The first phase began when the Cotswold District Council gave planning permission to demolish a garage to build a temporary car park in 2010 AD (Wright et al., 2017). Excavations of phase one continued until Christmas Eve 2011 AD when planning permission was granted for a new office development to be built on the site of the temporary car park (Wright et al., 2017). Phase two, therefore, began with the examination of the areas which would be disturbed by the office block and had not been thoroughly examined back in 2011 AD (Wright et al., 2017).

The Roman cemetery found at this site was in use between the late 1<sup>st</sup> century or the middle of the 2<sup>nd</sup> century and most likely continued into the late 3<sup>rd</sup> to 4<sup>th</sup> century (Holbrook, 2017a, 2017b). A total of 118 skeletons were excavated with the addition of 8 cremation burials (Holbrook, 2017a). These were added to the eight inhumation and forty-six cremation burials recorded in 1960 AD (Holbrook, 2017a). The human remains are now in the care of the Corinium Museum.

The cemetery was walled and would have been a prominent monument during the Roman period and a place for wealthy individuals to bury their dead (Holbrook, 2017b). However, some individuals had been buried prone and bound at the cemetery's edge (Holbrook, 2017b). Seven skeletons from Former Bridges Garage and four St James' Place skeletons were examined for this thesis, with estimated ages between 6 to 26 years.

*Figure 3. 7: St James' Place is circled in black on the map and scaled in on the left-hand image. The scaled-in image shows the roads Old Tetbury road and Hammond way, which are vital roads for both Former Bridges Garage/ St James' Place and Bath Gate. The red circle on the right-hand image highlights where the Roman amphitheatre used to be, whereas the red circle on the left-hand image gives an idea of where Bath Gate – the old Roman gate is. Images provided by Google maps.*



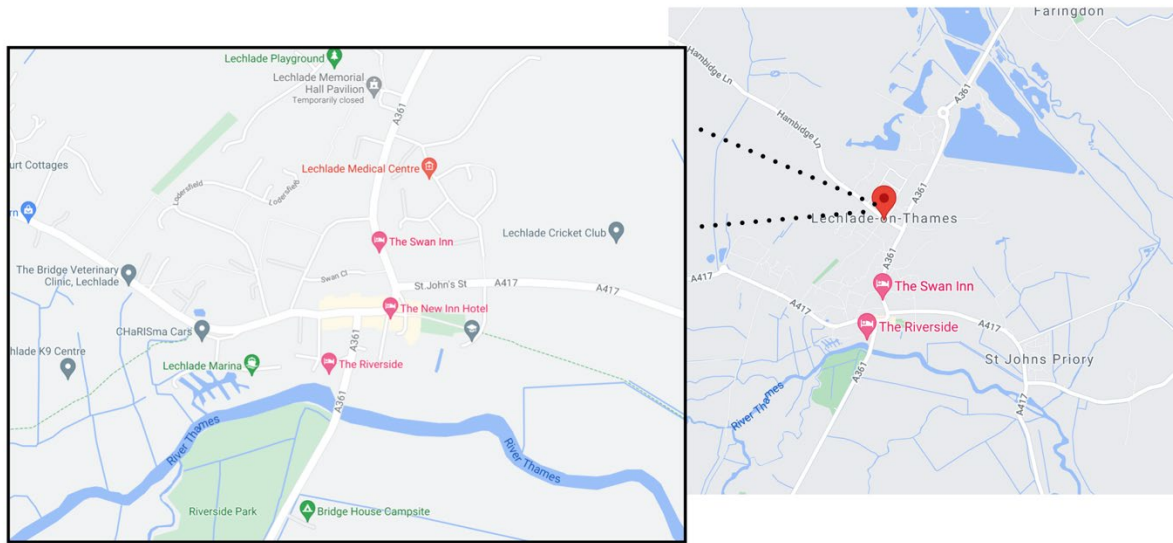
*C) Butler's Field in Cirencester*

**Butler's Field** is an Anglo-Saxon cemetery in Lechlade, Gloucestershire (Boyle and Palmer, 1998). The Oxford Archaeological Unit excavated the site in 1985 AD (Boyle and Palmer, 1998). Lechlade is between the English towns of Oxford and Swindon and located on the north bank of the River Thames and near to the river Leach (Boyle and Palmer, 1998). Lechlade is situated approximately 18 minutes by car from Cirencester. A map of Lechlade is shown in **Figure 3. 8**.

The excavation recovered a total of 219 inhumed individuals, consisting of 89 females, 50 males, 5 unsexed adults and 75 juveniles, which are now in the care of the Corinium Museum in Cirencester (Boyle, 1998; Boyle and Palmer, 1998). The grave goods associated with the burials suggested that the cemetery was in use between the mid or late 5<sup>th</sup> century until the late 7<sup>th</sup> or early 8<sup>th</sup> century (Boyle, 1998; Boyle and Palmer, 1998). Therefore, the longevity of the cemetery is a unique aspect of Butler's Field (Boyle, 1998).

Two phases throughout the cemetery's use were identified via a shift in grave goods and positioning of the remains, with the graves positioned north-east to south-west in phase one (mid to late 5<sup>th</sup>-6<sup>th</sup> century) and north-west to the south-east in the second phase (7<sup>th</sup> to early 8<sup>th</sup> century, Boyle, 1998). The local setting of the site is uncertain as no securely dated settlement from the Anglo-Saxon period has been excavated in the area, as well as Roman sites within the area showing no evidence of continued occupation (Boyle and Palmer, 1998). Preservation at the site was reasonably good, with 71.0% of the human remains labelled in good condition (Harman, 1998). Ten skeletons were examined for this thesis, with estimated ages between 7 to 23 years.

Figure 3. 8: Map of Lechlade. The scaled-in image is to the left. Images provided by Google maps.



#### D) Abbey of St Mary in Cirencester

**Abbey of St Mary** was an Augustinian abbey in Cirencester (McWhirr, 1998). The site was excavated by the Cirencester Excavation Committee in 1964 to 1966 AD and is now in the care of the Corinium museum (McWhirr, 1998). The abbey of St Mary was founded in the early 12<sup>th</sup> century by Henry I (Bryant and Heighway, 1998). Building work is thought to have begun in either 1117 or 1130 AD (Bryant and Heighway, 1998) and was demolished in 1539 AD (McWhirr, 1998). A 13<sup>th</sup>-century burial site that included juvenile skeletons was found west of the abbey (Bryant and Heighway, 1998). Total burials of the abbey came to 60 individuals (Heighway et al., 1998). Some of the graves were pits reminiscent of Mediaeval plague pits (Heighway et al., 1998). Five skeletons were examined for this thesis, with estimated ages between 6 to 14 years.

#### 3.1.6. East Lothian

East Lothian is a council area and county in Scotland and is situated on the southern coast of the Firth of Forth (**Figure 3. 9**, Wallenfeldt, 2018). East Lothian was also known as *Haddingtonshire* until the 20<sup>th</sup> century and was part of a broader region known as Lothian (Wallenfeldt, 2018). During the 14<sup>th</sup> to 16<sup>th</sup> centuries, East Lothian suffered much destruction at the hands of English invaders (Wallenfeldt, 2018). This resulted in the erection of feudal

castles at the time (Wallenfeldt, 2018). The 18<sup>th</sup> century saw the development of the agricultural industry, and new market towns were established through that development (Wallenfeldt, 2018). Today, East Lothian is mainly composed of residential suburbs and manufactures food and beverages (Wallenfeldt, 2018).

Figure 3. 9: The East Lothian area is shown within the red line. Image provided by Google maps.



#### *A) Auldhame in East Lothian*

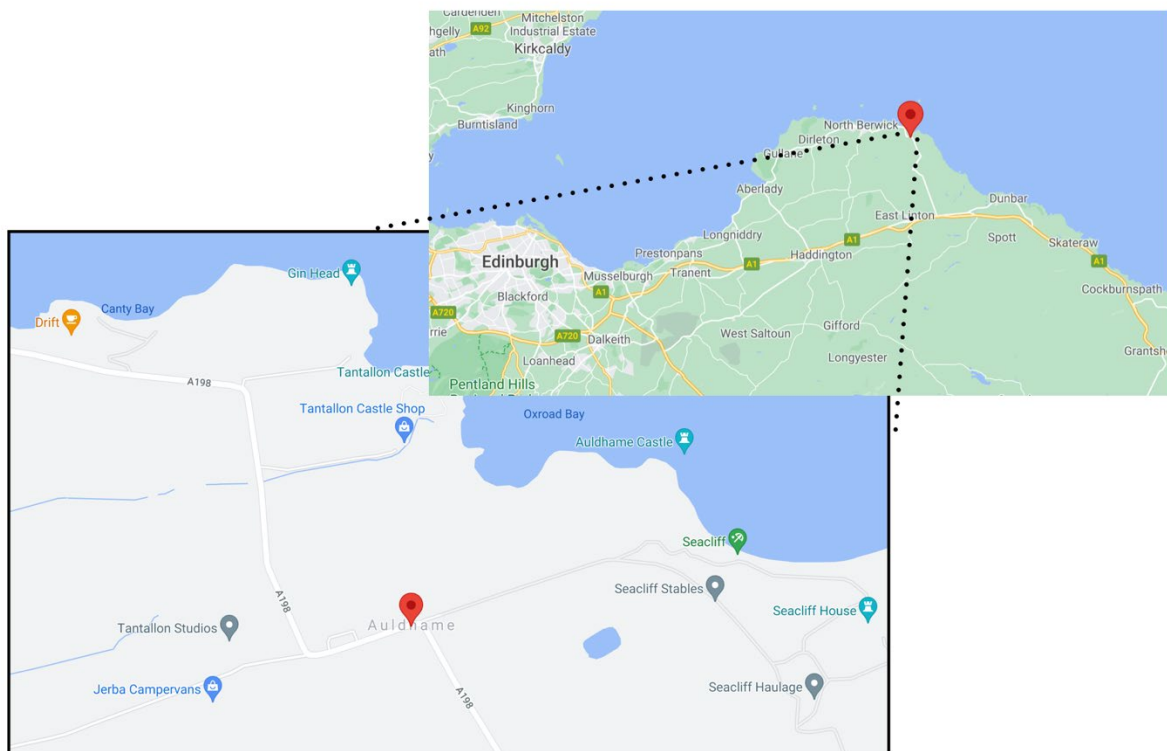
**Auldhame** is a hamlet in East Lothian in Scotland (**Figure 3. 10**). It is believed that between the mid-7<sup>th</sup> and mid-9<sup>th</sup> century, there was a monastic settlement on the headland (Crone and Hindmarch, 2016). Towards the end of the 9<sup>th</sup> century, the monastic settlement appeared to have gone into disuse, but was later revived as a church and graveyard for the parish of Auldhame (Crone and Hindmarch, 2016). While there were periods of disuse for the church, the church lasted over seven centuries, including a brief period of Viking presence (Crone and Hindmarch, 2016). Therefore, the site at Auldhame served as an Anglian monastic settlement and a Mediaeval parish church (Crone and Hindmarch, 2016).

The settlement was found when ploughing in preparation for planting potatoes, and this led to the discovery of human bone in February 2005 AD (Crone and Hindmarch, 2016). Historic Scotland commissioned the AOC archaeology group to investigate (Crone and

Hindmarch, 2016). In January 2008 AD, the site was accidentally ploughed again, which unearthed further human remains (Crone and Hindmarch, 2016). A total of 242 skeletons were recovered, with 66 known burials that Historic Scotland left interred (Crone and Hindmarch, 2016). Due to a mix of burial activity over a millennium, ploughing and soil erosion, the unearthed skeletons had a completeness of about 58.0% (Crone and Hindmarch, 2016). The skeletons remain in the care of National Museums Scotland.

As the settlement spanned a millennium, some skeletons could be dated to distinct phases (Barber, 2016). Eighteen skeletons belonged to Phase 1, dated from 650 to 1000 AD (Barber, 2016). Eleven skeletons belonged to Phase 2 dated from 1000 to 1200 AD, whereas ten skeletons belonged to Phase 3 from 1200 to 1400 AD (Barber, 2016). Finally, Phase 4 was dated at 1500 to 1700 AD and had four burials (Barber, 2016). Ten skeletons were chosen and examined for this thesis. Dated skeletons were required for the types of questions posed in this research, but the ten skeletons had to be selected across the time periods from this site due to external limitations. Out of the ten chosen skeletons, two were labelled as Anglo-Saxon, seven were labelled as Mediaeval, and one was labelled as Post-Mediaeval. The skeletons were estimated to be between 11 to 33 years of age.

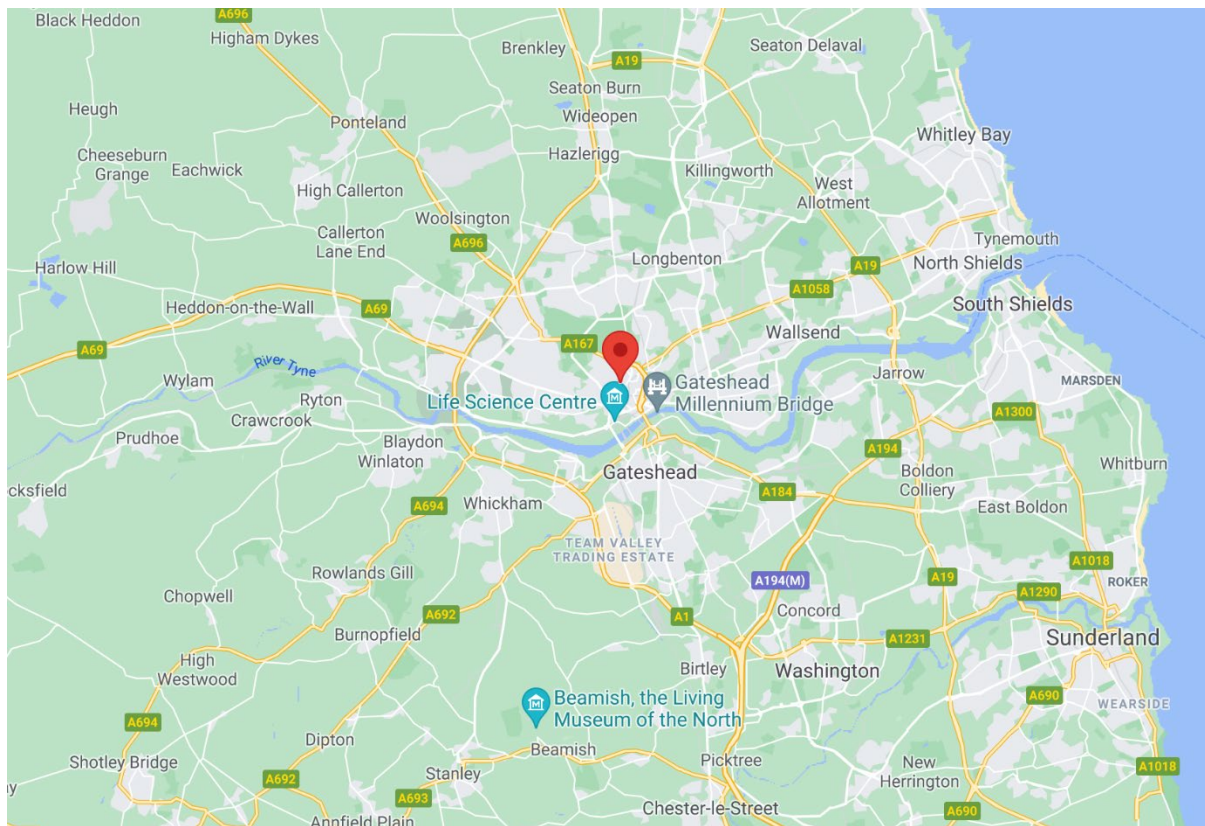
Figure 3. 10: The red pin in the right-hand map shows the placement of Auldhame in the East Lothian area. The image is then scaled in on the left-hand map. Images provided by Google maps.



### 3.1.7. Newcastle-Upon-Tyne

Newcastle-upon-Tyne, also known as Newcastle, is a northeast English city in Tyne and Wear (**Figure 3. 11**). Newcastle's origins began when the New Castle upon the river Tyne was supposedly constructed on the Christian community of Monkchester in 1080 AD, by Robert Curthose, son of William I (Nolan et al., 2010). However, Newcastle's past goes back much further. It was the Roman fort – *Pons Aelius* – in the 2<sup>nd</sup> century, which was abandoned in the late 4<sup>th</sup> or early 5<sup>th</sup> century, and part of the kingdom of Bernicia in the 6<sup>th</sup> and early 7<sup>th</sup> centuries (Nolan et al., 2010). Bernicia was later united with Deira to the south to form the Anglian kingdom of Northumbria under Bernicia's last pagan ruler – Aethelfrith (Nolan et al., 2010). Today, Newcastle-upon-Tyne is a large metropolitan city (Lotha, 2019b).

Figure 3. 11: Map of Newcastle-upon-Tyne. Image provided by Google maps.



*A) Black Gate Cemetery in Newcastle*

**Black Gate Cemetery** is an early Mediaeval cemetery dated to the late 7<sup>th</sup> to 12<sup>th</sup> century (Nolan et al., 2010). It is, therefore, often dated as an Anglo-Saxon site (Nolan et al., 2010). Excavations on the cemetery were carried out between 1977 and 1992 AD by Newcastle Archaeology Unit, with 679 individuals exhumed (Nolan et al., 2010). Approximately a third of those burials were juveniles (Nolan et al., 2010). The human remains are now in the care of the University of Sheffield. Black gate cemetery is recorded as having the largest number of burials of Christian Anglo-Saxon and Saxo-Norman origin to have been excavated from one single site in northeast England (Nolan et al., 2010). These individuals were exhumed from the cemetery level of the twelfth-century keep – the New Castle (Nolan et al., 2010).

Black Gate cemetery is thought to have originated from a 7<sup>th</sup> century monastic settlement, although no evidence for this settlement has been found (Nolan et al., 2010). Although many monasteries began to decline during the mid-9<sup>th</sup> century, the Black Gate cemetery remained well established into the 10<sup>th</sup> century (Nolan et al., 2010). It is thought that by 1000 AD, a church had been built in the cemetery (Nolan et al., 2010).

When the New Castle upon Tyne was constructed in 1080 AD, part of the castle ditch cut through the cemetery, and the rest of the cemetery was enclosed by the bailey (Nolan et al., 2010). Individuals continued to be buried in the part of the cemetery surrounded within the bailey after the construction of the castle (Nolan et al., 2010). It is believed that these individuals would have been members of the castle garrison and their families using the church instead of a continuation of local civilian burial activity (Nolan et al., 2010).

The later rebuilding of the Castle by Henry II disturbed more of the cemetery, contracting the cemetery more so and removing some of the human remains (Nolan et al., 2010). Evidence suggests that a small number of people continued to be buried in the cemetery during the 12<sup>th</sup> century to as late as the 13<sup>th</sup> century (Nolan et al., 2010). Reliable dating of the burials had not been entirely possible, so that some post-1080 AD burials may have been interpreted as pre-1080 AD burials (Nolan et al., 2010). The burials were broadly arranged from west to east, a common but not exclusive Christian practice (Nolan et al., 2010). Seventeen skeletons were examined for this thesis, with estimated ages between 4 to 18 years.

### 3.1.8. York

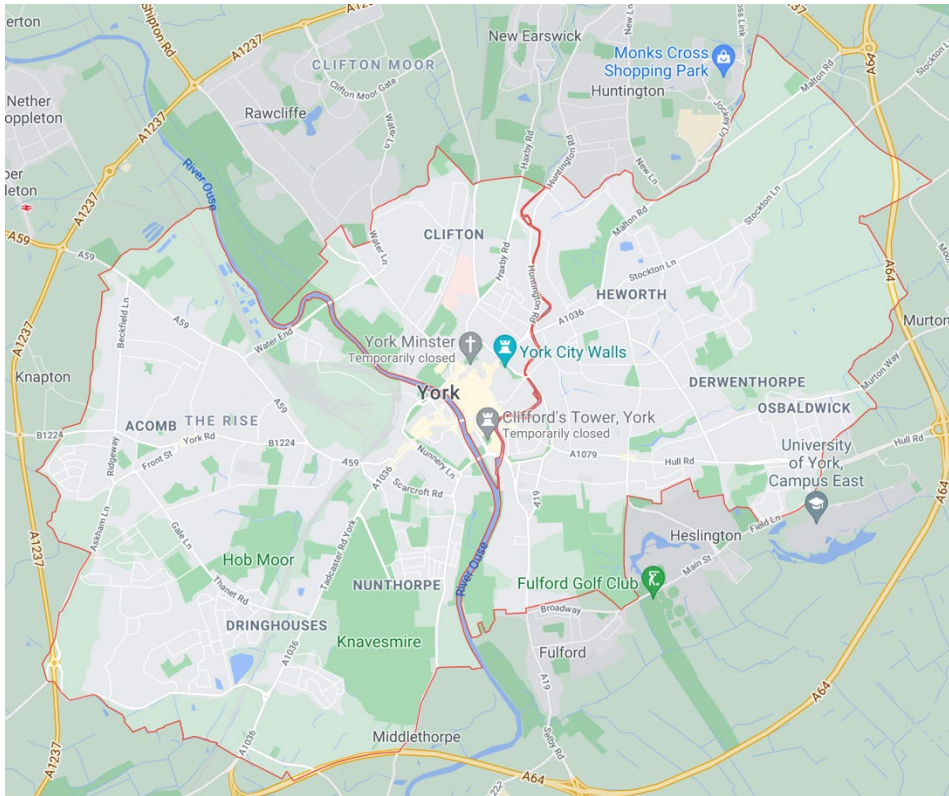
York is a city in North Yorkshire, England (**Figure 3. 12**). Evidence of a prehistoric settlement located in the Vale of York shows York's historical value (Hudson-Edwards et al., 1999; Roskams and Neal, 2020). Roman York was founded in approximately 71 AD, when Roman commander, Petilius Cerialis, of Hispana (the Ninth Legion), erected a legionary fortress on the northeast bank of the River Ouse, with the intentions of conquering the Brigantes tribe (Hudson-Edwards et al., 1999; Ottaway, 2004). This eventually led to the settlement of *Eboracum* –believed to have derived from its native name meaning either ‘the place of the yew trees’ or ‘estate of Eburos’ (Hudson-Edwards et al., 1999; Ottaway, 2004; Palliser, 2014). *Eboracum* was prosperous and was elevated to the Roman-British capital of the north, becoming a world centre of domestic and industrial goods (Hudson-Edwards et al., 1999; Ottaway, 2004; Palliser, 2014; McIntyre, 2016). Even after the Roman empire faded away, the dominance and prosperity of *Eboracum* continued to loom over the north (Ottaway, 2004).

Over time, *Eboracum* became *Eorfwic* during the Anglo-Saxon era, although little is known about what occurred at *Eorfwic* (Spall and Toop, 2005; Mainman, 2019). However, *Eorfwic* was captured and settled by the Viking's Great Army in 866 AD and renamed *Jorvik* in 876 AD (Addyman, 1980; Hudson-Edwards et al., 1999). When William the Conqueror invaded in 1066 AD, York was not so easily defeated. Anglo-Saxon nobles revolted against the invasion and King Swein of Denmark was asked to bring his fleet of ships (Daniell, 2007). This led to the ‘Harrying of the North’, in which William devastated the Yorkshire countryside and in his later years, regretted such a heinous act (Daniell, 2007).

During King Richard II rule, York was elevated to county status in 1396 AD (Dobson, 2007). York fared well, becoming a popular metropolitan city that was the second-largest in England and important in Mediaeval financial, political and clerical realms (Gillingham and Griffiths, 2000; Dobson, 2007; Burt, 2013). At the time, York had one of the largest international trading centres (Gillingham and Griffiths, 2000; Burt, 2013).

York appears to have always had a flair for independence and in 1644 AD it was used as a stronghold for the Royalists against Oliver Cromwell during England's civil war (McIntyre and Bruce, 2010). York is now a university city, has a thriving tourist industry and manufactures a variety of products, from railway cars to sweets (Gaur, 2017).

Figure 3. 12: Map of York. Image provided by Google maps.



### A) Fishergate House in York

**Fishergate House** was excavated between 2000 and 2001 AD by Field Archaeology Specialists Ltd on behalf of Mike Griffiths Associates (Spall and Toop, 2005). Fishergate lies away from the central core of York but has been occupied since the Roman period and became a Mediaeval suburb (Spall and Toop, 2005). During the 8<sup>th</sup> century, Eorfwic (Anglo-Saxon York) was a major religious and royal centre of the kingdom of Deira (Spall and Toop, 2005). Fishergate played a part in this through long-distance trade and craft working (Spall and Toop, 2005). By the 10<sup>th</sup> century, the Fishergate suburb was well-established and had several churches, including All Saint's (Spall and Toop, 2005). However, these fell out of use during the Mediaeval period (Spall and Toop, 2005).

Life, work and death appear to have gone hand in hand at Fishergate House, with occupants of the suburb potentially burying their dead close to where they lived and worked (Spall and Toop, 2005). Some of the skeletons exhumed from Fishergate House are from the early 8<sup>th</sup> century and early 10<sup>th</sup> to 11<sup>th</sup> centuries (Spall and Toop, 2005). However, the primary skeletal collection was dated to approximately mid-14<sup>th</sup> to mid-15<sup>th</sup> century (Spall and Toop,

2005). The Mediaeval cemetery discovered was previously unknown, and 250 individuals were excavated, including several infants (Spall and Toop, 2005). This skeletal collection is now in the care of the Fenwick Human Osteology Lab at Durham University. The Mediaeval cemetery is thought to belong to the church of St Helen's, which would have been established before the 11<sup>th</sup> century and abandoned in the 16<sup>th</sup> century (Spall and Toop, 2005). Its existence was then forgotten, and Fishergate House was built upon it during the 19<sup>th</sup> century (Spall and Toop, 2005). Twenty skeletons were examined for this thesis, with estimated ages between 5 to 16 years.

#### *B) All Saint's Church in York*

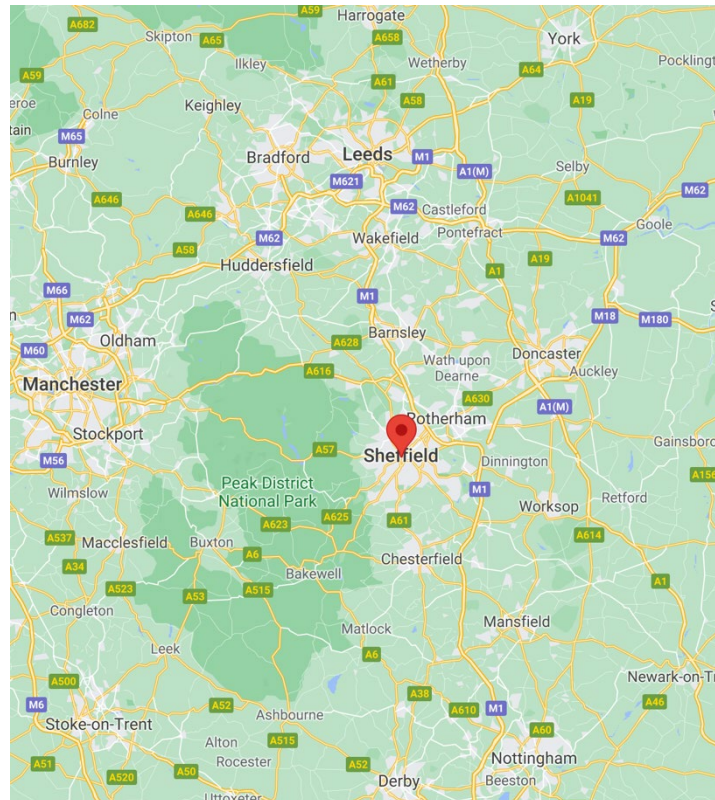
**All Saint's Church, Fishergate ("The Barbican")** was excavated between 2007 and 2008 AD by On-Site Archaeology (McIntyre and Bruce, 2010). Little evidence exists for the church, but it was referenced between 1091 and 1095 AD when it was given to Whitby Abbey (McIntyre and Bruce, 2010). When Henry VIII dissolved the monasteries, the church suffered the same fate (McIntyre and Bruce, 2010). The church is Mediaeval in origin and had been in use for over 400 years, but through excavation, remains of a Roman cemetery, a possible pre-Norman church and some post-Mediaeval burials were also found (McIntyre and Bruce, 2010). The human remains included 7 Roman skeletons, 547 Mediaeval (11<sup>th</sup> to 14<sup>th</sup> century) and 10 English Civil war mass graves containing over 100 skeletons (17<sup>th</sup> century, McIntyre and Bruce, 2010; McIntyre, 2016). The Mediaeval graves were laid with their heads facing west and were civilians from the York population (McIntyre and Bruce, 2010). The human remains now lie in the care of the University of Sheffield. Thirteen Mediaeval skeletons were examined for this thesis, with estimated ages between 5 to 18 years.

#### **3.1.9. Sheffield**

Sheffield is a town, city and metropolitan borough of South Yorkshire and lies to the north-central of England (**Figure 3. 13**, Lotha, 2017). It was recorded as an Anglo-Saxon village named *Escafeld* in the 1086 AD Domesday Book (Lotha, 2017). By the early 12<sup>th</sup> century, Sheffield had a parish and a castle built by the Norman lord William de Lovetot (Lotha, 2017). During Mediaeval times, an industry was created around the local ore and charcoal deposits (Lotha, 2017). By the 15<sup>th</sup> century, the streams around Sheffield were used to help power the grinding and forging of metal (Lotha, 2017). By the 17<sup>th</sup> century, Sheffield became a powerful

rival to London in the cutlery industry (Lotha, 2017). Sheffield gained a monopoly over this industry within England by 1700 AD (Lotha, 2017). Sheffield became the world centre of high-grade steel manufacturing by 1830 AD and created stainless steel by approximately 1912 AD (Lotha, 2017).

Figure 3. 13: The red pin highlights the city of Sheffield. To the northeast of Sheffield is York, which can be seen in the top right. Image provided by Google maps

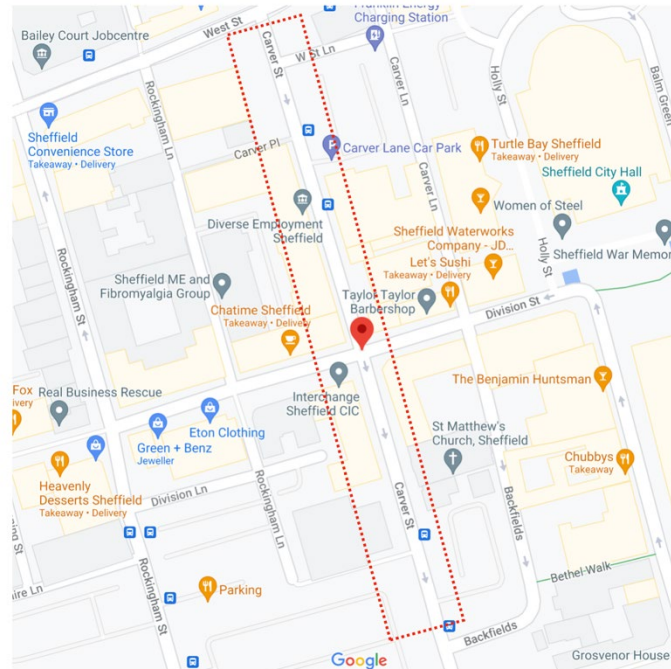


#### A) Carver Street Methodist Chapel in Sheffield

**Carver Street Methodist Chapel** was excavated in 1999 AD when the chapel was converted into a public house (The University of Sheffield, 2003). Carver Street is shown in **Figure 3. 14**. The chapel was located in Sheffield city centre and built in 1805 AD (The University of Sheffield, 2003). The chapel served a large congregation and was a place for non-conformist, middle to low-status individuals (The University of Sheffield, 2003). Records indicate that burials most likely occurred between 1806 to 1855 AD and is, therefore, a 19<sup>th</sup>-century industrial northern skeletal collection (The University of Sheffield, 2003). A total of 74 adult and 32 juveniles were exhumed and are now in the care of The University of Sheffield (The

University of Sheffield, 2003). Six skeletons were examined for this thesis, with ages between 7 to 17 years of age.

Figure 3. 14: Carver Street is shown within the red-dotted lines. Image provided by Google maps.



### 3.2. SKELETAL SAMPLES

The total sample examined for this thesis can be found in **Table 3. 2**. Each data chapter draws from this sample to answer specific questions posed within this thesis. Skeletons were selected from an age range of 3 to 35 years, which had to be estimated, as all skeletal collections were undocumented. The lower age limit of 3 years was set because this is usually the earliest age a permanent tooth's crown fully forms (Reid and Dean, 2006; AlQahtani et al., 2010; Pitfield, 2019). The upper limit of 35 years was set because the medial epiphysis of the clavicle is said to fuse between 17 to 30 years of age (Schaefer et al., 2009). Age 35 years was therefore picked to allow for possible deviations to epiphyseal fusion. Three skeletons that could not be aged were included in areas of this thesis that did not require age specific data i.e., estimating the sequence of fusion. All skeletons were required to come from historically dated collections as to represent the various time periods of Britain.

Table 3. 2: Total sample size, split by location, archaeological site, and age group.

Location	Site	Period	Child 3 – 12 yrs	Adolescent 13 – 20 yrs	Young Adult 21 – 34 yrs	Middle Adult 35 – 49 yrs	Not aged	Total
Broadstairs and St Peter's	South Dumpton Down	Iron Age	1	3	5	2	0	11
Canterbury	St Gregory's priory	Mediaeval						
	<i>High status</i>		10	3	3	0	2	18
	<i>Low status</i>		50	32	23	11	1	117
Chichester	Apple Down	Anglo- Saxon	5	3	2	0	0	10
Cirencester	Bath Gate	Roman	3	6	4	0	0	13
	FBG		3	2	2	0	0	7
	St James' Place		1	1	2	0	0	4
	Butler's Field	Anglo- Saxon	6	3	1	0	0	10
	Abbey of St Mary	Mediaeval	3	2	0	0	0	5
East Lothian	Auldhame	Anglo- Saxon	0	0	2	0	0	2
		Mediaeval	1	2	4	0	0	7
		Post- Mediaeval	0	1	0	0	0	1
Newcastle- Upon-Tyne	Black Gate	Anglo- Saxon	11	6	0	0	0	17
York	Fishergate House	Mediaeval	12	8	0	0	0	20
	All Saint's Church		7	6	0	0	0	13
Sheffield	Carver Street	Post- Mediaeval	3	3	0	0	0	6
<b>Total</b>			<b>116</b>	<b>81</b>	<b>48</b>	<b>13</b>	<b>3</b>	<b>261</b>

## CHAPTER 4

## METHODS

## METHODS IN EPIPHYSEAL FUSION

## 4.1. AGE ESTIMATION

## 4.1.1. Introduction

The skeletal samples are referred to as *sub-adult/ juvenile remains* and *adult* skeletons. An adult skeleton is a skeleton that has reached the majority of its skeletal maturity before death and is usually over the age of 18 years (White et al., 2012). The term *Sub-adult* is used interchangeably with *juvenile skeleton* to mean a skeleton that did not reach adulthood in life and was still growing and maturing skeletally (White et al., 2012). This study estimated all skeletal ages from the dentition and certain skeletal age cues. Often, an age range was estimated rather than a specific age. This is because no ageing technique can account for all sex-specific and populational variations in growth and degenerative changes that would give an exact chronological age (Hunter and Cox, 2005). However, on occasion, the AlQahtani et al., (2010) dental method used for ageing juveniles would point to a specific age. Therefore, a mean of each age range was assigned to each skeleton by taking the middle age of the estimated age range. This is standard practice in archaeological studies of juvenile growth (Shapland and Lewis, 2013, 2014; Arthur et al., 2016).

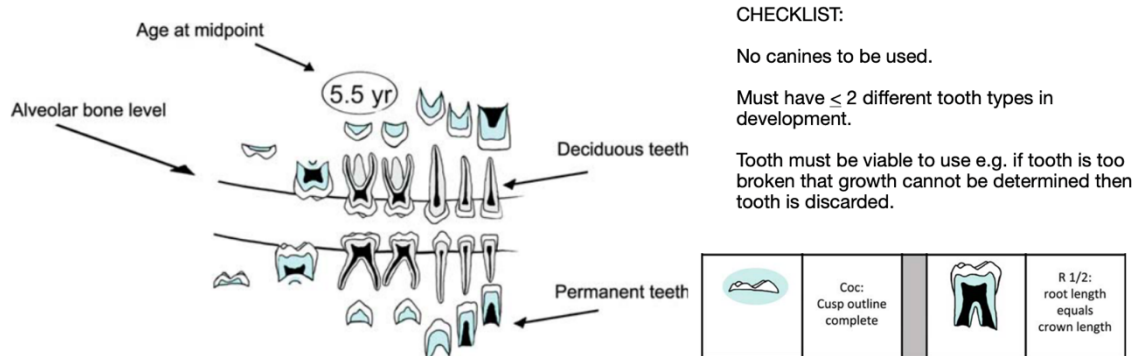
## 4.1.2. Juvenile age estimation

Dental development is the most favoured method for estimating age in juvenile skeletons because of the strong correlation with chronological age. Additionally, environmental and nutritional factors have less effect on dental development relative to the development of bones (Cardoso, 2007; Shapland and Lewis, 2013). However, the accuracy of dental development decreases as age increases, particularly when age estimation through dentition becomes reliant on the development and eruption of the third molar (Shapland and Lewis, 2014).

If dental development could not be employed as an age estimation technique, occasionally, epiphyseal fusion **not used in the main research** was used to estimate. This

same practice was used in the work of Lewis et al., (2016), in which pubertal phase was assigned to skeletons from specific skeletal markers separate from the skeletal markers used to estimate an average age-at-death. Thus, juvenile age estimation was based mainly on dental development, and where dentition was not present or could not be scored, epiphyseal fusion was used. **Figure 4. 1** gives the dental ageing criteria involved in this thesis' methodology.

*Figure 4. 1: An example of how teeth were used to estimate age. The left-hand side of the illustration shows developing teeth still within the alveolar bone and the associated age. The right side shows a developing tooth crown and root with attainment stages and associated ages in the table below. All images are taken from AlQahtani et al., (2010).*



Age (years)	Tooth	Number of teeth	Maxilla			Mandible				
			Tooth formation stage			Tooth formation stage				
			Minimum	Median	Maximum	Minimum	Median	Maximum		
1.5 <sup>a</sup>	i <sup>1</sup>	5	R ¼	R ¾	R ¾	i <sub>1</sub>	7	R ¾	R ¾	Re
	i <sup>2</sup>	6	Ri	R ½	R ¾	i <sub>2</sub>	7	R ¾	R ¾	Re
	c <sup>1</sup>	6	Cr <sub>c</sub>	Ri	R ½	c <sub>1</sub>	7	Cr ¾	Ri	R ½
	m <sup>1</sup>	7	Ri	R ½	R ¾	m <sub>1</sub>	8	Ri	R ½	R ¾
	m <sup>2</sup>	8	Cr <sub>c</sub>	Ri	R ¼	m <sub>2</sub>	8	Cr ¾	Ri	R ¼
	I <sup>1</sup>	6	Cr ½	Cr ½	Cr ½	I <sub>1</sub>	6	Cr 1/2	Cr ½	Cr ¾
	I <sup>2</sup>	4	–	Coc	Coc	I <sub>2</sub>	6	Coc	Cr ½	Cr ½
	C <sup>1</sup>	8	Coc	Coc	Coc	C <sub>1</sub>	4	–	Coc	Coc
	M <sup>1</sup>	4	–	Coc	Cr ½	M <sub>1</sub>	8	Cco	Coc	Cr ½

*A) Methods used to estimate the age of individuals under the age of 18 years*

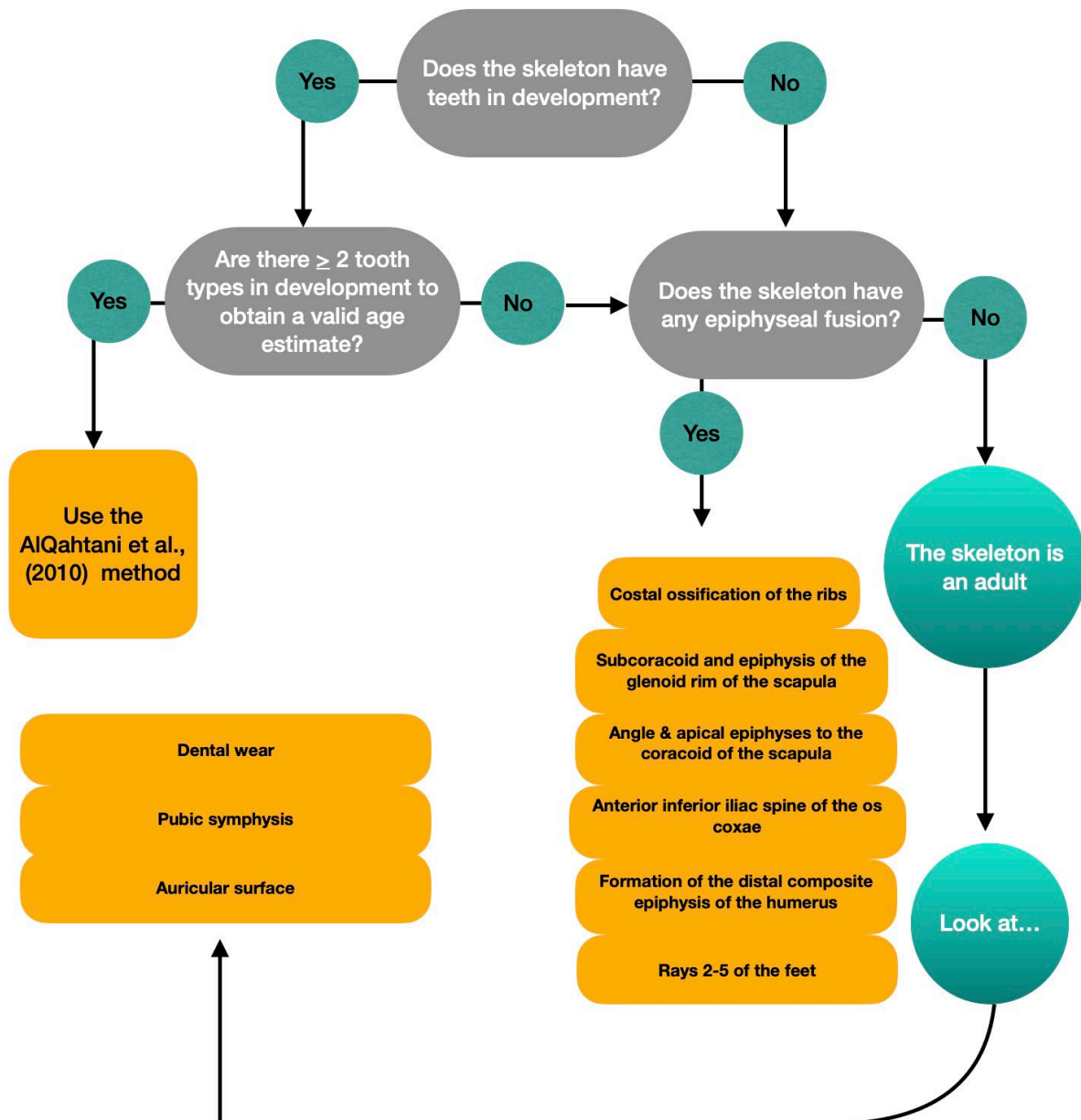
Dental development was used to estimate age in juvenile skeletons. All teeth were used, except for the mandibular canine. This is because the mandibular canine is a key component in assessing pubertal phase in a juvenile skeleton (Coutinho et al., 1993; Shapland and Lewis, 2013, 2014). To obtain an age-at-death estimate from the dentition, the development of the root and crown, as well as eruption timing was examined (AlQahtani et al., 2010).

If the dentition could not be used, fusion sites listed in **Table 4. 1** were applied. Sites were chosen because they fuse between 11 to 25 years of age in modern humans (Schaefer et al., 2009). The epiphyses employed here were **not** used in the main study. The methodology used was determined by the preservation and maturation of each skeleton. The methodology was systematically performed step-by-step and illustrated in **Figure 4. 2**.

*Table 4. 1: Fusion sites used to help determine age-at-death. The age ranges were taken from Schaefer et al., (2009). The fusion sites listed here were used for age estimation only.*

<b>Bone</b>	<b>Fusion site</b>	<b>Age range</b>
Rib cage	Costal ossification centres	17 – 25 years
Scapula	Subcoracoid and epiphyses for the glenoid rim of the body	15 – 18 years
	The angle and apical epiphyses of the coracoid	16 – 20 years
Humerus	Formation of the distal composite epiphysis: medial part of the trochlea, capitulum, and the lateral condyle	12 – 14 years
Os Coxae	Anterior inferior iliac spine	14 – 18 years
Feet	Metatarsals, and middle and distal phalanges of the foot rays 2 – 5	11 – 16 years

Figure 4. 2: A flow chart of the methodology used in this thesis is presented here. The fusion sites used to help in age estimation are also presented here. These fusion sites are separate to the fusion sites used to analyse skeletal maturation. All fusion sites listed on the right-hand side that were present on the skeleton were studied, in no particular order. When analysing adult skeletons, ageing methods to look at degradation of the skeleton are applied



### 4.1.3. Adult age estimation

Adult age estimation is dependent on degenerative changes in the skeleton. Dental wear was used in conjunction with skeletal wear. The upper age limit was set at 35 years. Some adult ageing methods require differentiation by sex. Biological sex was therefore estimated to assist in the accuracy of age-at-death for adults. Criteria for the estimation of sex for the purpose of adult age estimation is given in **Table 4. 2**.

Although methods are available for estimating sex in juvenile skeletons (Schutkowski, 1993; Bruzek, 2002; Bass, 2005; Rogers, 2009), estimating sex in juveniles is imprecise, especially in prepubertal children (White et al., 2012; Doe et al., 2017; Nikita, 2017). This is due to the low levels of sex hormones circulating in pre-pubescent children, which are responsible for the secondary sexual characteristics (White et al., 2012; Doe et al., 2017; Nikita, 2017).

When adult biological sex could not be determined due to unclear observable features or poor preservation, sex-specific ageing criteria were observed and averaged for both sexes (Arthur et al., 2016). Each sex-based feature was scored as either female, male or intermediate (Arthur et al., 2016; Lewis et al., 2016). Biological sex was estimated from the category that was most scored (Bruzek, 2002). However, priority was given to the os coxae, which is considered to be the most reliable sex indicator for modern humans (Arthur et al., 2016).

Table 4. 2: Criteria used to estimate sex for age estimation in adult skeletons. References used are as follows: A (Buikstra and Ubelaker, 1994; Nikita, 2017), B (Schutkowski, 1993), C (Bruzek, 2002), D (Bass, 2005), E (Phenice, 1967; Nikita, 2017), F(Rogers, 2009).

Bone	Skeletal Feature	Criteria
Skull <sup>A</sup>	Glabella	Prominent in males
	Mastoid process	Larger in males
	Nuchal crest	More protruding in males
	Supraorbital margin	Sharper in females
	Mental eminence	Larger projection in males
Pelvis	Composite arc <sup>B</sup>	Females have a double curve, and males have a single curve
	Greater sciatic notch <sup>B</sup>	Asymmetrical in males
	Pre-auricular sulcus <sup>C</sup>	Present in females
	Auricular surface elevation <sup>D</sup>	Elevated in females
	Ventral arc <sup>E</sup>	Present in females
	Sub-pubic concavity <sup>E</sup>	Present in females
Humerus <sup>F</sup>	Medial ischio-pubic ramus <sup>E</sup>	Narrow & sharp in females and wide & dull in males
	Ischio-pubic proportion <sup>C</sup>	Females have a pubis longer than the ischium, vice versa indicates male
	Trochlear notch	More symmetrical and bowtie shaped in females
	Olecranon fossa	Deep & oval in females and a shallow triangle in males
	Medial epicondyle	Raised in females and parallel to the surface in males

#### *A) Methods used to estimate the age of individuals over the age of 18*

Adult age estimation methods were: (1) occlusal dental wear (Brothwell, 1981), (2) the pubic symphysis (Brooks and Suchey, 1990) and (3) the auricular surface (Lovejoy et al., 1985; Buckberry and Chamberlain, 2002). The use of dental wear to estimate age is based on the premise that the older the individual, the greater the dental wear (Brothwell, 1981). Dental wear was only analysed on molars, and the degree of wear placed skeletons into three age categories: (1) 17 to 25 years, (2) 25 to 35 years, (3) 33 to 45 years and (4) 45+ years (Brothwell, 1981). The dental wear methodology was based on Prehistoric to Mediaeval English skeletal collections (Brothwell, 1981), which was suitable for the study of English and Scottish skeletal samples from archaeological collections.

The pubic symphysis and auricular surface were used in conjunction with dental wear to estimate age. Estimating age in adults is a process of studying the gradual effects of

degradation, which occurs as the body ages. This is made more difficult because genes, culture, and the environment all play a part in how age-related changes affect the body, as well as age marker variability increasing with age (Cunha et al., 2009; Millán et al., 2013). It is suggested that when dentition is missing in skeletonised remains, adult age should be estimated from the pubic symphysis, ribs, and/or the auricular surface, and that cranial suture closure should be avoided (Cunha et al., 2009).

The pubic symphysis is considered one of the most reliable adult age estimating techniques (Buikstra and Ubelaker, 1994; Garvin et al., 2012). The application of the Suchey-Brooks (Brooks and Suchey, 1990) method over the Todd pubic symphysis scoring system (Todd, 1920; T Wingate Todd, 1921a, 1921b; T. Wingate Todd, 1921) was preferred because of the use of available casts, which were accessible for this thesis. The Suchey-Brooks method is also considered to be the best method for age estimation of the pubic symphysis and is most widely used in forensic and palaeoanthropology (Cunha et al., 2009; Millán et al., 2013).

While it has been found that the Suchey-Brooks method is not as versatile outside of American populations, nearly all the methods available have been based on American populations (Millán et al., 2013). Equally, the versatility of this method tends to drop at  $\geq 40$  years of age (Millán et al., 2013), which is not applicable to this thesis as this study attempted to only use skeletons  $\sim 35$  years or under. Regardless, it is considered appropriate to account for age variability by employing various age-estimating techniques (Brooks and Suchey, 1990; Millán et al., 2013), which this study did.

Images and descriptions from Brooks and Suchey, (1990), along with casts distinguished six stages of pubic symphyseal surface wear with a corresponding mean age at death. Symphyseal wear was sex-specific (Brooks and Suchey, 1990). The more worn the surface, the older the individual. As the adult ages, the billowing found on younger adults' pubic symphyses is filled in by bone (Garvin et al., 2012). By middle age, the pubic symphysis becomes more defined (Garvin et al., 2012). As the adult ages past this, the pubic symphysis begins to break down and has more lipping and erosion on the bone (Garvin et al., 2012). Each phase is given a mean age and an age range, which increases with each phase (Brooks and Suchey, 1990). For example, the mean age for phase 1 in females is 19.4 years, with an age range of 15 to 24 years (Brooks and Suchey, 1990). Whereas the mean age for phase 5 in females is 48.1 years, with an age range of 25 to 83 years (Brooks and Suchey, 1990).

As for the auricular surface, a scoring system was applied, giving a composite score (Lovejoy et al., 1985; Buckberry and Chamberlain, 2002). The composite score would determine an age range at death. Like the pubic symphysis, the auricular surface is billowed

in youth (Garvin et al., 2012). Over time, the auricular surface becomes striated, and the billowing is reduced (Garvin et al., 2012). During middle age, the auricular surface becomes granulated, and there is an appearance of micro- and macroporosity (Garvin et al., 2012). Finally, the auricular surface is worn away and is characterised by lipping and erosion in old age (Garvin et al., 2012).

In the Buckberry and Chamberlain method (Buckberry and Chamberlain, 2002), each component, such as granulation or microporosity, is given an independent score, which is added at the end to give a score that is assigned an age range (Garvin et al., 2012). The Buckberry and Chamberlain method have seven stages (Buckberry and Chamberlain, 2002). Like the Suchey-Brooks method, the age range gets more convoluted as age increases, with stage 1 having a median age of 17 years and an age range of 16 to 19 years, whereas stage 5 has a median age of 62 years but an age range of 29 to 88 years (Buckberry and Chamberlain, 2002).

The Lovejoy method (Lovejoy et al., 1985) on the auricular surface has been found to be difficult to apply and can suffer from repeatability problems (Millán et al., 2013). While problems have been found with the Buckberry and Chamberlain method (Buckberry and Chamberlain, 2002), it was developed on a London Post-Mediaeval skeletal collection and, therefore, can be considered suitable for this thesis. However, the use of the auricular surface for age estimation can be advantageous as it is fairly durable in skeletonised remains and may not be subject to variation from sex or ancestry (Garvin et al., 2012). All three techniques – dentition, pubic symphysis and the auricular surface - will be applied to the adult skeleton of this study and determine an age range. A mean age would then be applied.

## 4.2. RECORDING EPIPHYSEAL FUSION

Fusion sites were scored as either (1) unfused, (2) partially fused or (3) completely fused. This three-phase scoring method was based upon the work by Johnston, (1961), Szilvássy, (1980) and Buikstra and Ubelaker, (1994) that was reviewed in Chapter two. All epiphyseal fusion sites scored in this thesis can be viewed in **Appendix 2**.

### 4.2.1. Scoring epiphyseal fusion

When available, both left and right elements of the fusion site were scored. In cases where both sides are intact, but one side on one individual is more advanced in its fusion stage than the other side, the most advanced stage would be recorded (Schaefer and Black, 2007; Schaefer, 2008b). Although advanced fusion on one side can occur, it is a rare event (Schaefer, 2008b). Severely damaged bones were removed from the study unless the epiphysis or diaphysis were intact and showed clear billowing. The site could then be recorded as unfused.

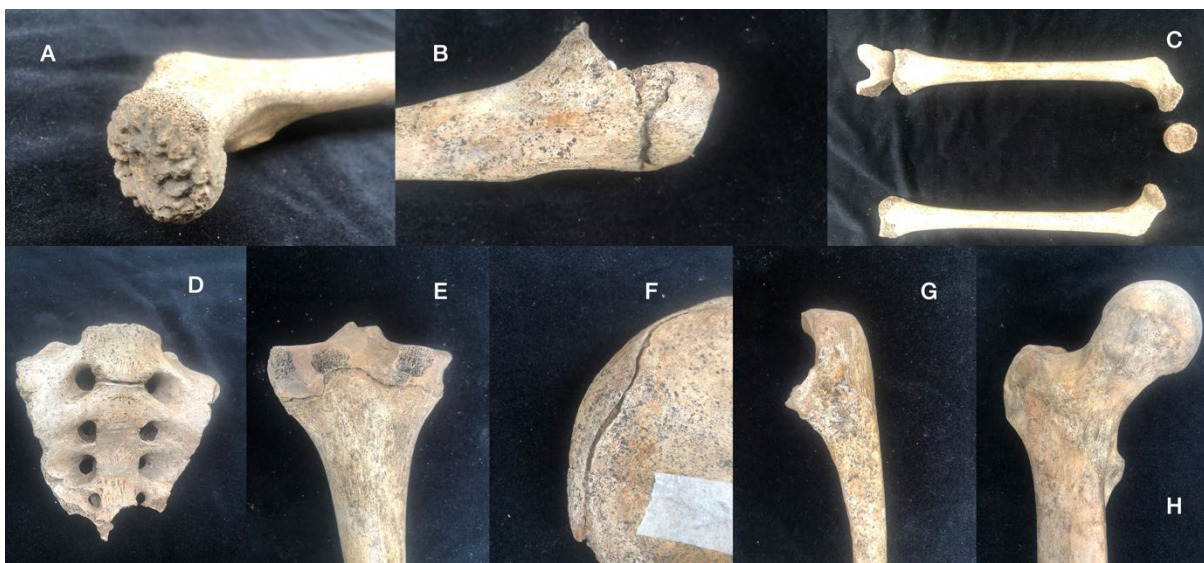
The scoring of each fusion site was based on three distinct phases (**Figure 4. 3**).

**Stage one:** There is no bony union between the diaphysis and epiphysis, and the two bony elements remain separate (Buikstra and Ubelaker, 1994).

**Stage two:** Partial bone union.

**Stage three:** The two bone elements have completely fused, and there may be complete obliteration of the epiphyseal line, or the site may display an epiphyseal scar or line (Buikstra and Ubelaker, 1994; Schaefer and Black, 2007; Cardoso, 2008b; Schaefer, 2014). An epiphyseal scar should not be confused with partial fusion and should be scored as Stage three (Buikstra and Ubelaker, 1994; Schaefer and Black, 2007; Cardoso, 2008b; Schaefer, 2014).

Figure 4. 3: Photographs of various bones in different stages of fusion. (A) Left femur. Clearly shows billowing of a growing child. Labelled as Stage 1 = no fusion, (B) Right ulna. A fairly wide gap between the shaft and proximal epiphysis. Labelled as Stage 2 = partial fusion, (C) Left and right femurs from one individual. Billowing present and separated epiphyses. Labelled as Stage 1 = no fusion, (D) Sacrum. A gap can be seen between bodies 1 & 2 but with filling in also present. Labelled as Stage 2 = partial fusion, (E) Left tibia. A gap can still be seen between the proximal epiphysis and the shaft. Post-mortem damage can be seen on the proximal epiphysis but does not affect the visibility of the epiphyseal line. Labelled as Stage 2 = partial fusion, (F) Right ilium. A large gap is still present between the ilium and the iliac crest. Labelled as Stage 2 = partial fusion, (G) Right ulna. It looks to have reached maturity in terms of proximal epiphyseal fusion. Labelled as Stage 3 = complete fusion, (H) Right femur. Fully mature. Labelled as Stage 3 = complete fusion. Photographs taken by J.A.M. Dolding-Smith on the St Gregory's skeletal collection held at the University of Kent



#### 4.2.2. The epiphyseal scar

The epiphyseal scar or line can appear as a band of bone that is much thicker than the bony structures on either side of it due to previous fusion between the epiphysis and metaphysis (Davies et al., 2015; Faisant et al., 2015). **Figure 4. 4** gives photographic examples of fusion sites labelled as Stage three, even though a line can be viewed between the proximal epiphyses and the shaft of the two femurs.

In radiographic studies, the epiphyseal scar occurs even in elderly patients (Cope, 1920; Davies et al., 2013, 2015; Faisant et al., 2015). The persistence of the scar is thought to be due to both localised and systematic factors, such as the rate of remodelling and the amount of mechanical load the site receives, rather than age (Cope, 1920; Davies et al., 2013, 2015; Faisant et al., 2015). While some have argued that an epiphyseal scar is only visible on radiographs and in cross-sections (Davies et al., 2013), others have noted the presence of the epiphyseal scar on dry bone (Schaefer and Black, 2007; Cardoso, 2008b,

2008a; Schaefer, 2008b). Cardoso, (2008a) found that the epiphyseal scar can persist for several years externally after the bone has fused.

*Figure 4. 4: Photographs of femurs with clear epiphyseal lines around the proximal epiphyses and around the greater trochanter in the right photograph. Although the lines are still evident, epiphyseal lines can persist for decades after fusion. The greater trochanter has a partial gap but is mainly infilled. Thus, all the fusion sites in these photographs would be labelled as Stage 3 = complete fusion. Photographs taken by J.A.M. Dolding-Smith from the St Gregory's skeletal collection held at the University of Kent*



To distinguish between partial fusion (Stage 2) and an epiphyseal scar, a largely unfilled gap (see images B, D – F in **Figure 4. 3** for reference) would denote partial fusion (Stage 2). The boundary between Stages two and three can be precarious (Stevenson, 1924). However, to resolve the issue, a flat instrument can be inserted into the unfilled area, such as the tip of a pair of callipers. If the instrument can be inserted, it is an indication that the bone was partially fusing at the time of death.

Schaefer, (2008a) denoted that if additional chondral ossification appeared to be required at the fusion site, she would label the bone as ‘partially fused’. However, if she deemed that the fusion site only required a shallow infill, she would mark the bone as having completed fusion (Schaefer, 2008b). In **Figure 4. 4**, the proximal femurs are shown to be filled in. The greater trochanter in the right photograph of **Figure 4. 4** shows a small gap. However, most of the greater trochanter remains filled in and would be recorded as having completed fusion (Stage 3).

### 4.3. SKELETAL MATURATION

#### 4.3.1. Determining AGE-at-fusion

Previous studies by Coqueugniot and Weaver, (2007), Schaefer, (2008a), Cardoso, (2008a, 2008b) and Cardoso et al., (2013) have produced standards for studying skeletal maturation in past populations. This study is based upon these. To reconstruct age from fusion, each skeleton would be examined for the 33 fusion sites (**Table 4. 3**) and scored according to the methodology in **Section 4.2**.

Table 4. 3 List of fusion sites recorded for the methodology used to determine age at fusion

<b>Bone</b>	<b>Fusion sites</b>
1. Occipital	1a. Pars lateralis to the pars basilaris 1b. Spheno-occipital synchondrosis
2. Cervical vertebrae	2a. Anterior arch of the atlas 2b. Posterior synchondrosis of the atlas 2c. Ossiculum terminale to the dens 2d. Dentoneural synchondrosis of the axis 2e. Dentocentral and neurocentral junctions of the axis 2f. Posterior synchondrosis of the axis
3. Sacrum	3a. Sacral bodies 1 and 2
4. Clavicle	4a. Medial epiphysis 4b. Lateral epiphysis
5. Scapula	5a. Coracoid 5b. Acromial epiphysis 5c. Medial epicondyle 5d. Inferior angle epiphysis to the body
6. Humerus	6a. Medial epicondyle 6b. Distal composite epiphysis 6c. Proximal epiphysis
7. Radius	7a. Proximal epiphysis 7b. Distal epiphysis
8. Ulna	8a. Proximal epiphysis 8b. Distal epiphysis
9. Hand	9a. Heads of the metacarpals 2 – 5, proximal and middle phalangeal epiphyses 9b. Distal phalangeal epiphyses
10. Os coxae	10a. Ischiopubic ramus 10b. Iliac crest 10c. Union of the acetabulum
11. Femur	11a. Femoral head 11b. Greater trochanter 11c. Lesser trochanter 11d. Distal epiphysis
12. Tibia	12a. Proximal epiphysis 12b. Distal epiphysis

### 4.3.2. Determining the sequence of fusion

This methodology was developed from previous studies by Schaefer, (2008, 2014), Schaefer and Black, (2007) and Lenover and Šešelj, (2019), and examines the order in which bones fused. Twenty-three fusion sites were used (**Table 4. 4**). The fusion sites were chosen based upon similar fusion sites used by Lenover and Šešelj, (2019). Each site was scored via the three-phase scoring methodology (See **Section 4.2**).

*Table 4. 4: List of fusion sites recorded for the methodology used to determine the sequence of fusion*

<b>Bone</b>	<b>Fusion site</b>
1. Occipital	1a. Pars lateralis to pars basilaris 1b. Pars lateralis to squama 1c. Spheno-occipital synchondrosis
2. Sacrum	2a. Sacral bodies 1 & 2
3. Clavicle	3a. Medial epiphysis
4. Scapula	4a. Coracoid 4b. Acromial epiphysis
5. Humerus	5a. Proximal epiphysis 5b. Medial humeral epicondyle 5c. Distal composite epiphysis
6. Radius	6a. Proximal epiphysis 6b. Distal epiphysis
7. Ulna	7a. Proximal epiphysis 7b. Distal epiphysis
8. Os coxae	8a. Ischiopubic ramus 8b. Iliac crest 8c. Union of the acetabulum
9. Femur	9a. Femoral head 9b. Greater trochanter 9c. Lesser trochanter 9d. Distal epiphysis
10. Tibia	10a. Proximal epiphysis 10b. Distal epiphysis

### 4.3.3. Intra-observer error

Fourteen skeletons were selected at random from each sample. Age-at-fusion was recorded twice for each of these skeletons. A Wilcoxon Signed-Rank test (Wilcoxon, 1945) was used to compare age and fusion scores. A non-parametric Wilcoxon Signed-Rank test was used as it is suitable for paired samples, it does not assume normality, and it is suitable for small sample sizes (Lund and Lund, 2020a, 2020b). The two related groups are the 14 skeletons, which were examined and then re-examined again at a later date. It is expected that the information taken from each skeleton should be the same, such as estimated age and fusion score, as it was the same skeleton, but it is also understandable that certain aspects of skeletal information, such as the fusion score, are partly subjective. The period of time between retesting each skeleton differed depending on the skeletal collection, as some collections were recorded in a more limited time frame. Thus, the retesting of skeletons could occur anywhere between four days to a couple of months. No statistically significant changes occurred between the two sets of recordings ( $Z \leq 1.000$ ,  $p \geq 0.083$ ). Individual Z scores and p values can be found in **Table 4. 5**.

Table 4. 5: The table below shows the Z scores and p values for the intra-observer error test on age and fusion sites between a first and second recording of fourteen skeletons. Z scores and p values are based on a Wilcoxon Signed Rank test performed in IBM® SPSS® Statistics 26 (2019)

<b>Variable</b>	<b>Z score</b>	<b>P value</b>
Age	-1.190	0.234
Pars lateralis to squama	0.000	1.000
Pars lateralis to pars basilaris	-1.732	0.083
Spheno-occipital synchondrosis	0.000	1.000
Anterior arch of C1	0.000	1.000
Posterior synchondrosis of C1	0.000	1.000
Dens of the C2	1.000	0.317
Dentoneural synchondrosis of C2	0.000	1.000
Dentocentral & neurocentral junctions of the C2	0.000	1.000
Posterior synchondrosis of C2	0.000	1.000
Sacral bodies 1 – 2	0.000	1.000
Medial epiphysis of the clavicle	-1.000	0.317
Lateral epiphysis of the clavicle	0.000	1.000
Coracoid of the scapula	0.000	1.000
Acromial epiphysis of the scapula	0.000	1.000
Medial border of the scapula	0.000	1.000
Interior angle epiphysis	0.000	1.000
Medial humeral epicondyle	0.000	1.000
Distal composite epiphysis	0.000	1.000
Humeral head	0.000	1.000
Proximal epiphysis of the radius	0.000	1.000
Distal epiphysis of the radius	0.000	1.000
Proximal epiphysis of the ulna	0.000	1.000
Distal epiphysis of the ulna	0.000	1.000
Heads of the metacarpals 2 – 5, proximal and middle phalangeal epiphyses of the hand	0.000	1.000
Distal phalanges of the hand	0.000	1.000
Iliac crest	0.000	1.000
Acetabulum	0.000	1.000
Femoral head	0.000	1.000
Greater trochanter	0.000	1.000
Lesser trochanter	0.000	1.000
Distal epiphysis of the femur	0.000	1.000
Proximal epiphysis of the tibia	0.000	1.000
Distal epiphysis of the tibia	0.000	1.000

#### 4.4. SKELETAL PUBERTY

The puberty phases are based on Lewis et al., (2016). These are: (1) Pre-puberty – those who have not yet entered the pubertal process, (2) Acceleration – the acceleration of the adolescent growth spurt, (3) PHV – the maximum rate of growth, (4) Deceleration – the deceleration of the adolescent growth spurt, (5) Maturation - some epiphyses remain partially fused and are in the process of maturing, and (6) Completion – puberty is finished, and the epiphyses involved in puberty are all complete.

The fusion sites used to determine the pubertal stage were as follows: (1) the iliac crest, (2) the hook of hamate, (3) the distal phalanges of the hand, (4) the distal radius, (5) the proximal ulna, (6) the cervical vertebrae, and (7) the mandibular canine (Shapland and Lewis, 2013, 2014; Arthur et al., 2016; Lewis et al., 2016). Fusion sites used to estimate the pubertal stage are given in **Table 4. 6**.

Table 4. 6: Criteria used to estimate pubertal stage. Based on the table given in Lewis et al., (2016). Black bars represent no further stages.

STAGE	Iliac crest	Hamate hook	Distal phalanges	Distal radius	Proximal ulna	Cervical vertebrae	Mandibular Canine
<b>Pre-puberty</b>	Unfused	Absent	Unfused	Unfused	Unfused	Stage 1	Stage F
<b>Acceleration</b>	Unfused	Appeared	Unfused	Unfused	Unfused	Stage 2	Stage G/H
<b>PHV</b>	Unfused	Complete	Unfused	Unfused	Fusion complete	Stage 3	Stage H
<b>Deceleration</b>	Unfused or partial union		Partial union or Fused	Unfused		Stages 4 – 5	
<b>Maturation</b>	Partial union		Partial union or fused	Partial union		Stages 5 – 6	
<b>Completion</b>	Fusion complete		Fusion complete	Fusion complete		Stage 6	

As an example, if an individual skeleton had a complete hook of hamate, unfused distal phalanges, a fused ulna, an unfused distal radius, and a mandibular canine in Stage H, then the pubertal stage would be set as PHV. Three or more features had to be observed to record a valid puberty score (Lewis et al., 2016).

Lewis et al., (2016), had additional ossification stages for the iliac crest. However, due to the preservation of the skeletons used in this study, the iliac crest was simplified to the three-stage method given by Buikstra and Ubelaker, (1994). The scoring method in **Section 4.2** was applied here.

The cervical vertebrae and mandibular canine were recorded differently from the other fusion sites. Observation of the growth of the third or fourth cervical vertebrae can be divided into six steps of maturation: (1) the vertebrae body is wedge-shaped, and the inferior border is flat, (2) the vertebrae body is almost rectangular, and the inferior border begins to cave in, (3) the vertebrae body is rectangular shaped, and the concavity of the inferior border is more developed, (4) the vertebrae is almost square, and the concavity of the inferior border is distinct, (5) the vertebrae body is square-shaped, and the concavity of the inferior border is accentuated, (6) the vertebrae body is taller than it is wide and the inferior border has a deep concavity (Shapland and Lewis, 2014).

The mandibular canine was recorded in three stages. Stage F was recorded when the mandibular canine root was half-formed (Shapland and Lewis, 2013). Stage G was recorded when the root was almost complete, and Stage H equalled a mature mandibular canine (Shapland and Lewis, 2013).

#### 4.5. STATISTICAL ANALYSES

Data were analysed in IBM® SPSS® Statistics 26 (2019). A Goodness-of-fit Chi-square (Pearson, 1900) was used to examine age-at-fusion in St Gregory's skeletal collection. If the test was violated, a Fisher's Exact Test (Fisher, 1934) or a Fisher-Freeman-Halton Exact Test (Freeman and Halton, 1951) was performed on the data. See **Table 4.7 - Table 4.9** for details. A Mann-Whitney U test (Mann and Whitney, 1947) was used to compare age-at-fusion between two archaeological sites, two periods or high and low-status individuals, as well as between epiphyseal fusion and pubertal phase of high and low-status skeletons. A Mann-Whitney U was also used to analyse the difference in age at pubertal phase between Mediaeval Canterbury and York. To analyse age at pubertal phase between archaeological periods, a Kruskal Wallis test (Kruskal and Wallis, 1952) was carried out. A binomial logistic regression (Berkson, 1944) was used to predict whether the age-at-fusion could determine the status of a skeleton. Similarly, a multiple regression (Verhulst, 1838, 1845; Bravais, 1846; Galton, 1894; Pearson, 1938; Wilson and Worcester, 1943; Berkson, 1944; Cox, 1966) was used to examine whether age-at-fusion could predict archaeological site or pubertal phase. Contingency tables were used to look at the sequence of fusion, as per previous methodology (Schaefer and Black, 2007; Schaefer, 2008a, 2014; Lenover and Šešelj, 2019). Bonferroni corrections were performed on many of the statistical tests and can be found in **Appendix 3**. These corrections were employed to correct for multiple comparisons.

Table 4. 7: Choice of test for univariate statistical tests used in this thesis

Statistical test	Test assumptions	Questions posed	Variables	Choice of test	Adjustments
Mann-Whitney U	1. The data is ordinal (ordered categories, e.g., 1, 2, 3) 2. The data is quantitative 3. The data is not normally distributed 4. The independent variable has two categories 5. There is no relationship between the two groups (Witte and Witte, 2017; Lund and Lund, 2020c)	1. Is there a difference between age-at-fusion and high and low-status?	<i>Dependent variable:</i> Fusion stages 1 – 3 <i>Independent variable:</i> High and low-status	Allows for the comparison of high and low-status	
		2. What pubertal phase did the fusion of the epiphyses occur at for the high and low-status skeletons?	<i>Dependent variable:</i> Pubertal phases 1-6 <i>Independent variable:</i> High and low-status	The pubertal phase (ordinal data) at which each epiphysis fuses is compared between high and low-status skeletons	
		2. Are there differences in age-at-fusion between Mediaeval sites?	<i>Dependent variable:</i> Fusion stages 1 – 3 <i>Independent variable:</i> York and Canterbury	Fusion (either stages 2 and 3 together or stage 2 alone, depending on sample size) for a set age is compared between York and Canterbury	Only the ages that fusion (Stages 2 and 3) take place are selected for this test.
		3. Are there differences in age-at-fusion between historical periods?	<i>Dependent variable:</i> Fusion stages 1 – 3 <i>Independent variable:</i> Historical periods, tested one by one e.g., Roman vs Mediaeval	Fusion (either stages 2 and 3 together or stage 2 alone, depending on sample size) for a set age range is compared between two archaeological sites	Only the ages that fusion (Stages 2 and 3) take place are selected for this test.
		4. Is there a difference in the age at pubertal phase between Mediaeval Canterbury and York	<i>Dependent variable:</i> Pubertal phases 1-6 <i>Independent variable:</i> Canterbury and York	This is similar to the other tests, except pubertal phase replaces fusion stage.	

Table 4. 8: Choice of test used in this thesis

Statistical test	Test assumptions	Questions posed	Variables	Choice of test	Adjustments
Kruskal-Wallis test	1. One dependent variable that is continuous or ordinal 2. One independent variable that has two or more categorical, independent groups 3. There is independence of observations (Lund and Lund, 2013a)	1. Is there a difference between age at pubertal phase when compared between archaeological period?	<i>Dependent variable:</i> Puberty phase <i>Independent variable:</i> Archaeological groups	It is a non-parametric test and looks at whether there are statistical significant differences of ordinal or continuous data between groups.	
Chi-square test: one sample goodness of fit	1. One categorical variable, which can be dichotomous (such as female/male), nominal or ordinal) 2. No relationship exists between cases 3. "There must be at least 5 expected frequencies in each group..." of the categorical variable (A. Lund and Lund, 2018a)	1. Was there a significant association between age and fusion in St Gregory's skeletal collection?	<i>Categorical variable:</i> Fusion stages	The distribution of age of the skeletons can be compared to fusion stage, so see if a significant association can be made between a certain age when fusion occurred	Caution is placed on certain epiphyses that do not meet all assumptions, and a Fisher's Exact test (Fisher, 1934) or a Fisher-Freeman-Halton Exact Test (Freeman and Halton, 1951) are run on those results.
Binomial logistic regression	1. The dependent variable is composed of two categories 2. The independent and dependent variables are mutually exclusive 3. The independent variables can be continuous, nominal or ordinal 4. There must be a linear relationship between continuous independent variables (A. Lund and Lund, 2018b)	1. Does age-at-fusion differ between high and low-status?	<i>Dependent variable:</i> High and low status <i>Independent variable:</i> Combined fusion sites	Binomial logistic regression tests are good for predicting the probability of whether the independent variables fall into one of the two categories (A. Lund and Lund, 2018b). This was therefore a good test to see if age-at-fusion differed between high and low status	Only the age range that fusion was occurring was included.

Table 4. 9: Choice of test for multivariate statistical tests used in this thesis.

Statistical test	Test assumptions	Questions posed	Variables	Choice of test	Adjustments
Multiple regression	1. One dependent variable that is continuous 2. Independent variables can be continuous or nominal, or an ordinal variable that is listed as nominal 3. There must be independence of observation 4. A linear relationship must exist between the variables 5. The data must show homoscedasticity 6. The data must not show multicollinearity 7. Data should not have any significant outliers, high leverage points or highly influential points 8. Errors are normally distributed (Lund and Lund, 2013b)	1. Does age-at-fusion differ between Mediaeval archaeological site?	<i>Dependent variable:</i> Age <i>Independent variables:</i> Fusion stage and archaeological site	Multiple regression can be used to understand how variables affect one another.	Some assumptions were seen as cautionary, and a note would be made. Some assumptions meant that the data available had to be changed to proceed or to abandon the test altogether. More information will be provided on what assumptions were changed or not in the Results sections.  Scatterplots were not performed on independent variables because they were not continuous variables (Lund and Lund, 2013b)
		2. Can age-at-fusion be distinguished between archaeological period?	<i>Dependent variable:</i> Age <i>Independent variables:</i> Fusion stage and historical period		
		3. Can age at pubertal phase be distinguished by archaeological period?	<i>Dependent variable:</i> Age <i>Independent variables:</i> Archaeological period and pubertal phase		

## CHAPTER 5

## RESULTS

MATURATION OF THE MEDIAEVAL SKELETON. EXPLORING GROWTH AND  
DEVELOPMENT IN ST GREGORY'S CEMETERY AND PRIORY

## 5.1. RESEARCH QUESTIONS

There are four research questions.

**Question 1. At what age did skeletal fusion occur at Mediaeval St Gregory's?**

The goal of the first research question is to establish the age at which bones fused in skeletons from St Gregory's Priory and Cemetery. These results are presented in **Section 5.2**.

**Question 2. Are there differences in age-at-fusion between the high and low-status skeletons?**

St Gregory's skeletal collection can be divided into low-status individuals buried in the cemetery and high-status individuals buried in the priory or directly outside the west front of Archbishop Theobald's Priory church (Anderson and Andrews, 2001; Hicks and Hicks, 2001). Children from higher socioeconomic backgrounds tend to mature skeletally faster than children from impoverished areas because of better living conditions, better parental care and a lower sibling count (Low et al., 1964; So and Yen, 1990). Based on the literature review (**Section 2.4**) it is predicted that epiphyseal fusion may occur earlier in the high-status sample compared to the low-status sample. Results are presented in **Section 5.3**.

**Question 3. What is the sequence of skeletal fusion at Mediaeval St Gregory's?**

Research into the sequence of fusion has found that, contrary to previous assertions (Stevenson, 1924; Todd, 1930b, 1930a), the sequence of fusion can vary between populations (Stewart, 1934; Lenover and Šešelj, 2019). Knowledge of the sequence of fusion in historical populations is limited. Results are presented in **Section 5.4**.

#### **Question 4. What is the age at puberty phases in Mediaeval Canterbury?**

It has been found that many bones fuse at certain pubertal phases (Hewitt and Acheson, 1961b, 1961a; Grave and Brown, 1976; Houston, 1980; Coutinho et al., 1993; Hassel and Farman, 1995; Legge, 2005; Lai et al., 2008; Shapland and Lewis, 2013, 2014; Arthur et al., 2016; Lewis et al., 2016; Lacoste Jeanson et al., 2016). Selected fusion sites in skeletons from St Gregory's will be recorded to determine in which pubertal phase they fused. Comparisons will be undertaken from high and low-status areas at St Gregory's. The age at puberty will also be recorded. Results will be presented in **Section 5.5**.

\*\*\*

**A note on statistics:** A Chi-square test was performed on age-at-fusion for the St Gregory's skeletal collection. A binomial logistic regression was undertaken on the high and low-status groups to test whether age-at-fusion could distinguish between these two social groups. The sequence of fusion in St Gregory's skeletal collection was examined through contingency tables. A Mann Whitney U was used to compare age-at-fusion between the high and low-status of St Gregory's.

Assumptions for a Goodness-of-fit chi-square test include: (1) There is one categorical variable, which can be dichotomous, nominal or ordinal, (2) No relationship exists between the cases, and (3) There must be at least five expected frequencies in each group of the categorical variable (A. Lund and Lund, 2018a). The Goodness-of-fit test on the St Gregory's skeletal collection met these assumptions by (1) Fusion stage can be classed as ordinal data, and (2) No skeleton could be in multiple fusion stages at once. However, some tests did fail the third assumption. In this case, a Fisher's Exact test or a Fisher-Freeman-Halton-Exact test was performed on the data.

Assumptions for the binomial logistic regression included (1) The dependent variable is composed of two categories, (2) The independent variable and dependent variables are mutually exclusive, (3) The independent variables can be continuous, nominal, or ordinal, and (4) There must be a linear relationship between continuous independent variables (A. Lund and Lund, 2018b). The assumptions for this test were met in that (1) The dependent variable was two groups, high and low status, (2) Skeletons could either be high or low status and not both, (3) The independent variables were age (continuous) and fusion stage (ordinal) of selected epiphyses, and (4) There was only one continuous independent variable, which was age, and a linear relationship was found to exist. Other assumptions for this test, such as sample size was

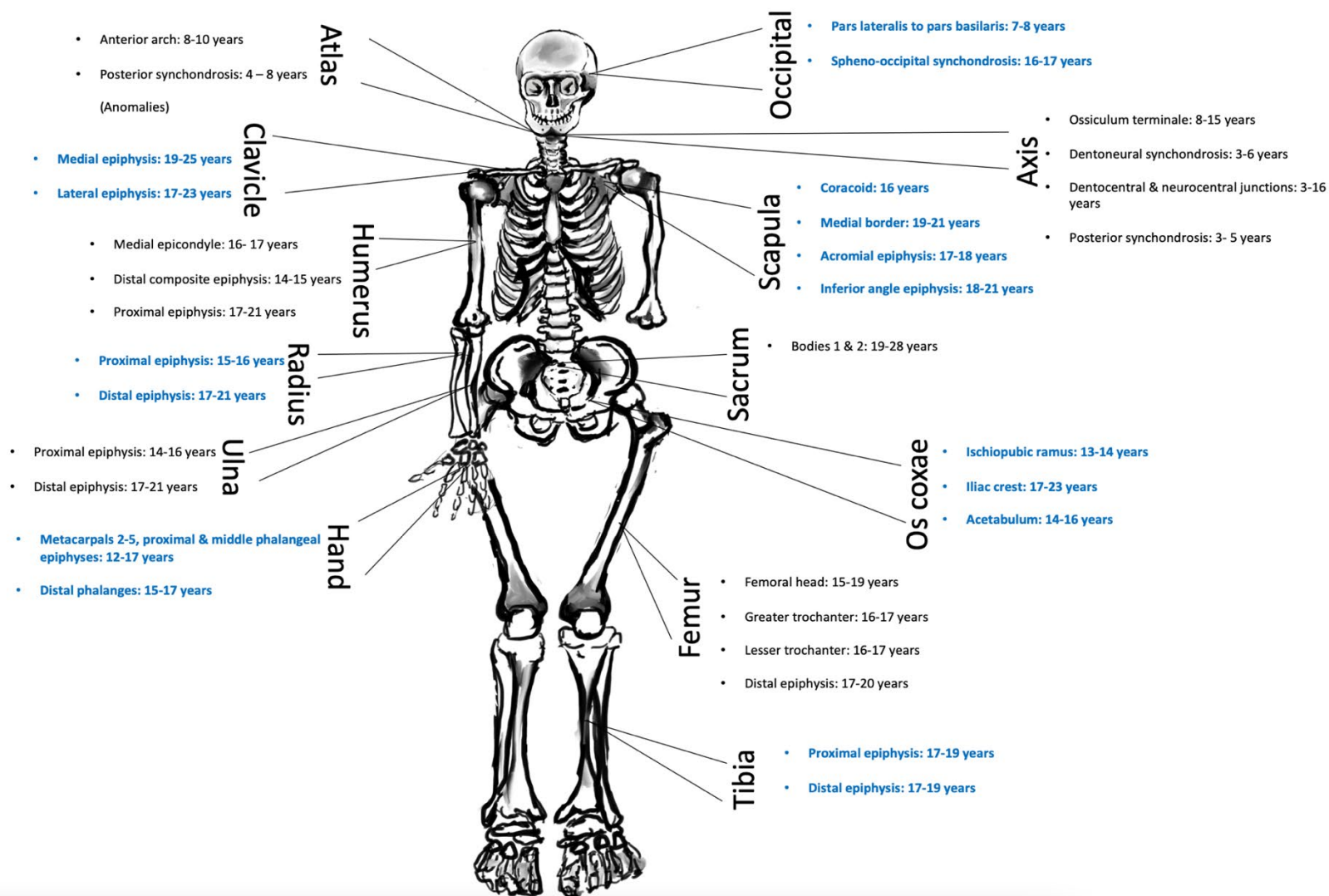
met. Other assumptions required to carry out a binomial logistic regression were tested before the binomial logistic regression was carried out and these can be found in **Section 5.3**.

The assumptions for a Mann Whitney U include (1) The data is ordinal, (2) The data is quantitative, (3) The data is not normally distributed, (4) The independent variable has two categories, and (5) There is no relationship between the two groups (Witte and Witte, 2017; Lund and Lund, 2020c). Assumptions for these tests were met in that (1) Fusion stage, and puberty phase are both ordinal data, (2) The data is quantitative, (3) The sample sizes are small and therefore are not normally distributed, (4) The independent variable is high vs low status, and (5) Skeletons cannot be both high and low status. More information on these tests is presented with the results throughout this chapter. As a final note on statistics, when comparing the high and low-status groups, the high-status sample size was far lower than the low-status sample size.

## 5.2. AGE-AT-FUSION IN ST GREGORY'S

**Figure 5. 1** is a summary of the results and illustrates the range of skeletal fusion ages at Mediaeval Canterbury.

Figure 5. 1: Age-at-fusion in the St Gregory's skeletal collection. Blue and black text is only used to help readability.



### 5.2.1. The Axial Skeleton

#### A) The Skull: Occipital

**Table 5. 1** provides the age-at-fusion for the pars lateralis to pars basilaris of the occipital bone and the fusion of the spheno-occipital synchondrosis. Complete fusion (Stage 3) of the **pars lateralis to pars basilaris** had occurred for 100.0% of juveniles by age 9 years. On average these bones were still unfused (Stage 1) for some individuals between 7 to 8 years of age. The mean age at complete fusion (Stage 3) was 8 years (mean age = 7.71, sd = 0.49). However, there was no significant association ( $X^2(1) = 2.778, p = 0.096$ ) between the age group: 7 to 8 years and complete fusion (Stage 3). As two cells in this test had frequencies less than five, a Fisher's Exact Test was conducted on the data. Again, no association was found between the age range of 7 to 8 years and fusion of the pars lateralis to pars basilaris of the occipital ( $p = 1.000$ ).

Table 5. 1: Age in years/stage of union of the occipital of the skull for St Gregory's skeletal collection. The stages of union are recorded as percentages

		Age	n	Stage of union		
				1	2	3
The occipital	Pars lateralis to pars basilaris	4	5	100.0		-
		5	4	100.0		-
		6	3	100.0		-
		7	3	33.3		66.7
		8	6	16.7		83.3
		9	4	-		100.0
		10	2	-		100.0
		11	3	-		100.0
	Spheno- occipital Synchondrosis	Age	n	1	2	3
		14	3	100.0	-	-
		15	6	100.0	-	-
16		5	80.0	20.0	-	
17		1	-	-	100.0	
19		4	-	-	100.0	

**Pars lateralis to pars basilaris:**

Earliest age at complete fusion: 7 years

All complete fusion at age 9 years

Partial fusion (Stage 2) of the **spheno-occipital synchondrosis** began at age 16 years for some adolescents, and complete fusion (Stage 3) had occurred at 17 years. There was no significant ( $X^2(2) = 3.000, p = 0.223$ ) association between the age group 16 to 17 years and fusion (Stages 2 and 3). As three cells had frequencies less than five, a Fisher-Freeman-Halton Exact Test was performed on the data. Again, no association was found between the age range of 16 to 17 years and fusion of the spheno-occipital synchondrosis ( $p = 0.333$ ).

**Spheno-occipital synchondrosis:**

Earliest age at complete fusion: 17 years

No more unfused after 16 years

*B) Cervical vertebrae: Atlas*

**Table 5. 2** provides the age-at-fusion for the anterior arch and posterior synchondrosis of the atlas of the cervical vertebrae. Of the individuals aged between 12 to 15 years, just two individuals were found to be unfused (Stage 1) for their **anterior arch** of the atlas. A significant association ( $X^2(2) = 45.355, p < 0.001$ ) between the age group: 8 to 15 years and fusion (Stages 2 and 3) was found for the anterior arch of the atlas. This result remained statistically significant when a Bonferroni corrections test was performed on the data. (See **Appendix 3**).

The **posterior synchondrosis** of the atlas had completely fused (Stage 3) for most Mediaeval juveniles by 8 years of age, except for three individuals who remained unfused (Stage 1) after this age. A significant association ( $X^2(1) = 11.919, p < 0.001$ ) was found between the age group 4 to 15 years and complete fusion (Stage 3) of the posterior synchondrosis of the atlas. This result remained statistically significant when a Bonferroni corrections test was performed on the data. (See **Appendix 3**).

**Posterior synchondrosis of the atlas:**

Earliest age at complete fusion: 4 years

All complete fusion at age 8 years

Table 5. 2: Age at years/stage of union of the atlas of the cervical vertebrae for St Gregory's skeletal collection. The stages of union are recorded as percentages.

		Stage of union						
		Age	n	1	2	3		
The Atlas	Anterior arch	5	4	100.0	-	-		
		6	5	100.0	-	-		
		7	1	100.0	-	-		
		8	3	-	-	100.0		
		9	4	-	25.0	75.0		
		10	1	-	-	100.0		
		11	3	-	-	100.0		
		12	6	16.7	-	83.3		
		13	3	-	-	100.0		
		14	2	-	-	100.0		
		15	9	11.1	-	88.9		
		16	3	-	-	100.0		
		17	2	-	-	100.0		
		18	1	-	-	100.0		
				Age	n	1	2	3
			Posterior synchondrosis	3	7	100.0	-	-
				4	4	75.0	-	25.0
				5	2	100.0	-	-
	8	4		-	-	100.0		
	9	4		25.0	-	75.0		
	10	1		-	-	100.0		
	11	3		-	-	100.0		
	12	6		16.7	-	83.3		
	13	3		-	-	100.0		
	14	2		-	-	100.0		
	15	8	12.5	-	87.5			
	16	3	-	-	100.0			
	17	2	-	-	100.0			

### C) Cervical vertebrae: Axis

**Table 5. 3** provides the age-at-fusion for the ossiculum terminale to the dens, the dentoneural synchondrosis, dentocentral and neurocentral junctions and the posterior synchondrosis of the axis of the cervical vertebrae. The **ossiculum terminale** fused to the dens between the ages of 8 to 15 years. On average, juveniles were 11 years of age (mean age = 10.89, s.d. = 2.26) when partial fusion (Stage 2) was underway, and 14 years (mean age = 13.45, s.d. = 1.57) when complete fusion (Stage 3) occurred. A significant association ( $X^2(2) = 8.450, p = 0.015$ ) was found between the age group: 8 to 15 years and fusion (Stages 2 and 3) of the ossiculum terminale of the dens. However, this data was not statistically significant when a Bonferroni corrections test was conducted. (See **Appendix 3**).

Table 5. 3: Age in years/stage of union of the axis of the cervical vertebrae for St Gregory's skeletal collection. The stages of union are recorded as percentages

			Stage of union			
	Age	n	1	2	3	
<b>Ossiculum terminale to the dens</b>	5	3	100.0	-	-	
	6	5	100.0	-	-	
	7	4	100.0	-	-	
	8	7	85.7	14.3	-	
	9	3	33.3	66.7	-	
	10	2	-	100.0	-	
	11	4	25.0	-	75.0	
	12	7	-	28.6	71.4	
	13	3	-	33.3	66.7	
	14	4	25.0	-	75.0	
	15	10	-	10.0	90.0	
	16	5	-	-	100.0	
	17	2	-	-	100.0	
	18	2	-	-	100.0	
	<b>Dentoneural synchondrosis</b>	3	6	83.3	-	16.7
		4	5	60.0	-	40.0
		5	5	60.0	-	40.0
		6	5	40.0	20.0	40.0
7		4	-	-	100.0	
8		7	-	-	100.0	
<b>Dentocentral &amp; neurocentral junctions</b>	3	4	75.0	25.0	-	
	4	5	60.0	40.0	-	
	5	4	25.0	50.0	25.0	
	6	5	20.0	80.0	-	
	7	3	-	66.7	33.3	
	8	7	-	57.1	42.9	
	9	4	-	50.0	50.0	
	10	2	-	50.0	50.0	
	11	4	-	-	100.0	
	12	7	-	71.4	28.6	
	13	3	-	33.3	66.7	
	14	4	-	25.0	75.0	
	15	10	-	-	100.0	
	16	5	-	20.0	80.0	
<b>Posterior synchondrosis</b>	3	7	28.6	-	71.4	
	4	5	-	-	100.0	
	5	5	20.0	-	80.0	
	6	5	-	-	100.0	
	7	4	-	-	100.0	
	8	7	-	-	100.0	

**Ossiculum terminale:**

Earliest age at complete fusion: 11 years

No more unfused after 14 years

The **dentoneural synchondrosis** fused between 3 to 6 years (mean age = 4.88, sd = 1.13). A significant association ( $X^2 (2) = 10.286, p = 0.006$ ) was found between the age group: 3 to 6 years and fusion (Stages 2 and 3) of the dentoneural synchondrosis of the axis. However, this data was found to not be statistically significant when a Bonferroni corrections test was applied to the data. (See **Appendix 3**).

The **dentocentral and neurocentral junctions** fused between the ages of 3 to 16 years. On average, individuals from Mediaeval Canterbury were 9 years of age (mean = 8.54, sd = 3.44) when fusion was underway (Stage 2). A significant association ( $X^2 (2) = 14.896, p < 0.001$ ) was found between the age group: 3 to 16 years and fusion (Stages 2 and 3) of the dentocentral and neurocentral junctions of the axis. This data remained statistically significant when a Bonferroni corrections test was applied. (See **Appendix 3**).

The **posterior synchondrosis** of the axis was completely fused (Stage 3) in all individuals by the age of 6 years. A significant association ( $X^2 (1) = 7.118, p = 0.008$ ) was found between the age group: 3 to 5 years and complete fusion (Stage 3) of the posterior synchondrosis of the axis. However, this data was not statistically significant when a Bonferroni corrections test was applied (See **Appendix 3**).

**Dentoneural synchondrosis:**

Earliest age at complete fusion: 3 years

All complete fusion at age 7 years

**Posterior synchondrosis:**

Earliest age at complete fusion: 3 years

All complete fusion at age 6 years

**Dentocentral & neurocentral junctions:**

Earliest age at complete fusion: 5 years

No individuals remain unfused past age 6 years

## D) Sacrum: Bodies 1 and 2

**Table 5. 4** provides the age-at-fusion for bodies 1 and 2 of the sacrum. Bodies 1 and 2 of the sacrum are completely fused (Stage 3) in all individuals by 28 years of age. Partial fusion (Stage 2) occurred between the ages of 19 to 25 years. On average, individuals from Mediaeval Canterbury were 21 years old (mean age = 21.25, sd = 0.579) when fusion was underway (Stage 2). No significant association ( $X^2(1) = 1.316, p = 0.251$ ) was found between the age group: 19 to 28 years and fusion (Stages 2 and 3) of the sacral bodies 1 and 2.

Table 5. 4: Age in years/stage of union of the sacrum for St Gregory's skeletal collection. The stages of union are recorded as percentages

		Stage of union				
		Age	n	1	2	3
<b>Sacrum</b>	<b>Bodies 1 &amp; 2</b>	16	3	100.0	-	-
		19	4	-	75.0	25.0
		21	8	-	75.0	25.0
		22	1	-	100.0	-
		23	1	-	-	100.0
		24	1	-	-	100.0
		25	2	-	100.0	-
		28	2	-	-	100.0

**Sacral bodies 1 & 2:**

Earliest age at complete fusion: 19 years

All complete fusion at age 28 years

### 5.2.2. The Appendicular Skeleton

## A) The Clavicle

**Table 5. 5** provides the age-at-fusion for the medial and lateral epiphyses of the clavicle. The **medial epiphysis** fused between the ages of 19 to 25 years. On average, individuals from Mediaeval Canterbury were 22 years of age (mean = 21.50, sd = 2.52) when fusion of the medial epiphysis was underway (Stage 2). No significant association ( $X^2(2) = 3.440, p = 0.179$ )

**Medial clavicle:**

Earliest age at complete fusion: 19 years

No more left unfused after age 24 years

was found between the age group: 19 to 25 years and fusion (Stages 2 and 3) of the medial epiphysis of the clavicle.

Table 5. 5: Age in years/stage of union of the clavicle for St Gregory's skeletal collection. The stages of union are recorded as percentages

		Age	n	Stage of union			
				1	2	3	
The Clavicle	Medial epiphysis	16	5	100.0	-	-	
		17	2	100.0	-	-	
		18	2	100.0	-	-	
		19	5	60.0	20.0	20.0	
		20	2	50.0	-	50.0	
		21	7	42.9	28.6	28.6	
		22	1	100.0	-	-	
		23	4	25.0	-	75.0	
		24	1	100.0	-	-	
		25	5	-	20.0	80.0	
		28	2	-	-	100.0	
		Age	n	1	2	3	
		Lateral epiphysis	14	4	100.0	-	-
			15	7	100.0	-	-
			16	3	100.0	-	-
			17	2	50.0	50.0	-
			18	2	100.0	-	-
			19	5	20.0	-	80.0
			20	1	-	-	100.0
			21	4	-	-	100.0
	22		1	-	100.0	-	
	23	4	-	-	100.0		
	25	3	-	-	100.0		

The **lateral epiphysis** fused between the ages of 17 to 23 years. Individuals from Mediaeval Canterbury were 20 years of age (mean = 19.50, sd = 3.54) when fusion of the lateral epiphysis was underway (Stage 2). A significant association ( $\chi^2 (2) = 10.842, p = 0.004$ ) was found between the age group: 17 to 23 years and fusion (Stages 2 and 3) of the lateral epiphysis of the clavicle. However, this data was not statistically significant when a Bonferroni corrections test was applied (See **Appendix 3**).

**Lateral clavicle:**

Earliest age at complete fusion: 19 years

All complete fusion at age 23 years

No more unfused past the age of 19 years

## B) The Scapula

**Table 5. 6** provides the age-at-fusion for the coracoid, medial border, acromial epiphysis and inferior angle epiphysis of the scapula. Fusion of the **coracoid** was underway (Stage 2) at age 16 years and completely fused by age 17 years.

**Coracoid:**  
 Earliest age at complete fusion: 16 years  
 All complete fusion at age 17 years

Table 5. 6: Age in years/stage of union of the scapula for St Gregory's skeletal collection. The stages of union are recorded as percentages

		Stage of union				
		Age	n	1	2	3
The scapula	Coracoid	13	3	100.0	-	-
		14	5	100.0	-	-
		15	9	100.0	-	-
		16	3	-	33.3	66.7
		17	2	-	-	100.0
		18	2	-	-	100.0
		19	5	-	-	100.0
		Age	n	1		3
		Medial border	16	3	100.0	
	19		1	-		100.0
	21		2	50.0		50.0
	25		1	-		100.0
	Acromial epiphysis	Age	n	1		3
		14	2	100.0		-
		15	9	100.0		-
		16	4	100.0		-
		17	2	50.0		50.0
		18	2	50.0		50.0
		19	4	-		100.0
		20	2	-		100.0
21	7	-		100.0		
Inferior angle epiphysis	Age	n	1		3	
	15	6	100.0		-	
	16	3	100.0		-	
	17	1	100.0		-	
	18	1	-		100.0	
	19	2	50.0		50.0	
	21	5	60.0		40.0	
	22	1	-		100.0	
	23	1	-		100.0	

The **medial border** fused between the ages of 19 to 21 years. On average, individuals from Mediaeval Canterbury were 20 years old (sd = 1.41) when complete fusion (Stage 3) occurred. No Stage 2 was recorded for the fusion of the medial border to the scapula. No significant association ( $\chi^2 (1) = 0.333, p = 0.564$ ) was found between age group: 19 to 21 years and complete fusion (Stage 3) for the medial border of the scapula. As two cells had expected frequencies less than five and therefore failed one of the assumptions of the Chi-square, a Fisher's Exact test was performed. Again, no association was found between the age range of 19 to 21 years of age and fusion of the medial border of the scapula ( $p = 1.000$ ).

**Medial border:**

Earliest age at complete fusion: 19 years

No more unfused after age 21 years

Fusion of the **acromial border** occurred somewhere between ages of 17 to 18 years. On average, individuals from Mediaeval Canterbury were 18 years of age (mean = 17.50, sd = 0.71) when complete fusion occurred (Stage 3). No Stage 2 was recorded for the acromial epiphysis to the scapula. No significant association ( $\chi^2 (1) = 0.000, p = 1.000$ ) was found between the age group: 17 to 18 years and complete fusion (Stage 3) of the acromial epiphysis to the scapula. As two cells had expected frequencies less than five and therefore failed one of the assumptions of the Chi-square, a Fisher's Exact test was performed. Again, no association was found between the age range of 17 to 18 years and fusion of the acromial border of the scapula ( $p = 1.000$ ).

**Acromial epiphysis:**

Earliest age at complete fusion: 17 years

All complete fusion at age 19 years

**Inferior angle epiphysis:**

Earliest age at complete fusion: 18 years

All complete fusion at age 22 years

The **inferior angle epiphysis** fused between 18 to 21 years. On average, individuals from Mediaeval Canterbury were 20 years old (mean = 19.75, sd = 1.50) when complete fusion (Stage 3) had occurred. No Stage 2 was recorded for the inferior angle epiphysis to the scapula. No significant association ( $X^2(1) = 0.000, p = 1.000$ ) was found between the age group: 18 to 21 years and complete fusion (Stage 3) of the inferior angle epiphysis of the scapula. As two cells had expected frequencies less than five and therefore failed one of the assumptions of the Chi-square, a Fisher-Freeman-Halton Exact test was performed. Again, no association was found between the age range of 18 to 21 years of age and fusion of the inferior angle of the scapula was found ( $p = 1.000$ ).

### *C) The Humerus*

**Table 5. 7** provides the age-at-fusion for the medial epicondyle, distal composite epiphysis and proximal epiphysis of the humerus. Partial fusion (Stage 2) of the **medial epicondyle** occurred for some adolescents at age 16 years, and complete fusion (Stage 3) had occurred by 17 years. No significant association ( $X^2(2) = 0.400, p = 0.819$ ) was found between the age group 16 to 17 years and fusion (Stages 2 and 3) of the medial humeral epicondyle. As three cells had expected frequencies less than five and therefore failed one of the assumptions of the Chi-square, a Fisher-Freeman-Halton Exact test was performed. Again, no association was found between the age range of 16 to 17 years of age and fusion of the medial humeral epicondyle ( $p = 0.200$ ).

**Medial humeral epicondyle:**

No more unfused past the age of 16 years

Complete fusion occurs at age 17 years

Table 5. 7: Age in years/stage of union of the humerus for St Gregory's skeletal collection. The stages of union are recorded as percentages

		Stage of union				
		Age	<i>n</i>	1	2	3
The humerus	Medial epicondyle	13	3	100.0	-	-
		14	5	100.0	-	-
		15	10	100.0	-	-
		16	3	66.7	33.3	-
		17	2	-	-	100.0
		18	1	-	-	100.0
		19	6	-	-	100.0
		20	2	-	-	100.0
		Age	<i>n</i>	1	2	3
	Distal composite epiphysis to the shaft	11	5	100.0	-	-
		12	7	100.0	-	-
		13	3	100.0	-	-
		14	5	80.0	-	20.0
		15	10	40.0	10.0	50.0
		16	3	-	-	100.0
		17	2	-	-	100.0
		18	2	-	-	100.0
		Age	<i>n</i>	1	2	3
	Proximal epiphysis	14	5	100.0	-	-
		15	10	100.0	-	-
		16	4	100.0	-	-
		17	2	50.0	-	50.0
		18	2	50.0	50.0	-
		19	4	25.0	25.0	50.0
20		2	-	50.0	50.0	
21		7	-	28.6	71.4	
22		1	-	-	100.0	
23		3	-	-	100.0	
24	1	-	-	100.0		

The **distal composite epiphysis** fused (Stages 2 and 3) to the shaft of the humerus between 14 to 15 years of age. No significant association ( $X^2(2) = 5.200, p = 0.074$ ) was found between the age group: 14 to 15 years and fusion (Stages 2 and 3) of the distal composite epiphysis to the humerus.

**Distal composite epiphysis:**

Earliest age at complete fusion: 14 years

All complete fusion at age 16 years

Fusion of the **proximal epiphysis** occurred between the ages of 17 to 21 years. On average, individuals from Mediaeval Canterbury were 20 years of age (mean age = 19.80, sd = 1.30) when fusion was underway (Stage 2). No significant association ( $X^2(2) = 3.294, p = 0.193$ )

was found between the age group: 17 to 21 years and fusion (Stages 2 and 3) of the proximal epiphysis of the humerus.

**Proximal humeral epiphysis:**

Earliest age at complete fusion: 17 years

All complete fusion at age 22 years

*D) The Radius*

**Table 5. 8** provides the age-at-fusion for the proximal and distal epiphyses of the radius. Partial fusion (Stage 2) occurred between the ages of 15 to 16 years for the **proximal epiphysis** of the radius. On average, individuals from Mediaeval Canterbury were 16 years old (mean = 15.67, sd = 0.58) when fusion was underway (Stage 2). Fusion had not occurred in any individual up to the age of 14 years old. No significant association ( $X^2(2) = 2.462, p = 0.292$ ) was found between the age group: 15 to 16 years and fusion (Stages 2 and 3) of the proximal epiphysis of the radius. As three cells had expected frequencies less than five and therefore failed one of the assumptions of the Chi-square, a Fisher-Freeman-Halton Exact test was performed. This time, there was an association between age range and fusion ( $p = 0.041$ ). However, when a Bonferroni correction was performed on the data, this result was non-significant.

Fusion (Stages 2 and 3) occurred between 17 to 21 years for the **distal epiphysis** of the radius. On average, individuals from Mediaeval Canterbury were 19 years (mean = 19.33, sd = 1.53) when fusion was underway (Stage 2). Fusion had not occurred in any individual up to the age of 16 years. No significant association ( $X^2(2) = 4.333, p = 0.115$ ) was found between the age group: 17 to 21 years and fusion (Stages 2 and 3) of the distal epiphysis of the radius.

**Proximal radius:**

Earliest age at complete fusion: 15 years

All complete fusion at age 17 years

**Distal radius:**

Earliest age at complete fusion: 17 years

All complete fusion at age 22 years

Table 5. 8: Age in years/stage of union of the radius for St Gregory's skeletal collection. The stages of union are recorded as percentages.

		Stage of union				
		Age	n	1	2	3
The radius	Proximal epiphysis	12	7	100.0	-	-
		13	3	100.0	-	-
		14	5	100.0	-	-
		15	9	77.8	11.1	11.1
		16	4	-	50.0	50.0
		17	2	-	-	100.0
		18	2	-	-	100.0
		19	5	-	-	100.0
		Age	n	1	2	3
	Distal epiphysis	14	5	100.0	-	-
		15	5	100.0	-	-
		16	3	100.0	-	-
		17	2	50.0	-	50.0
		18	2	50.0	50.0	-
		19	5	20.0	20.0	60.0
		20	2	50.0	-	50.0
		21	7	14.3	14.3	71.4
		22	1	-	-	100.0
		23	3	-	-	100.0
		24	1	-	-	100.0

### E) The Ulna

**Table 5. 9** provides the age-at-fusion for the proximal and distal epiphyses of the ulna. Fusion (Stages 2 and 3) occurred between 14 to 16 years of age for the **proximal epiphysis** of the ulna. On average, individuals from Mediaeval Canterbury were 15 years old (sd = 0.50) when partial fusion was underway (Stage 2). Fusion had not occurred in any individual up to the age of 13 years old. A significant association ( $X^2(2) = 9.875, p = 0.007$ ) was found between the age group: 14 to 16 years and fusion (Stages 2 and 3) of the proximal epiphysis of the ulna. However, this data was not statistically significant when a Bonferroni corrections test was applied (See **Appendix 3**).

Table 5. 9: Age in years/stage of union of the ulna for St Gregory's skeletal collection. The stages of union are recorded as percentages.

		Stage of union				
		Age	n	1	2	3
The ulna	Proximal epiphysis	11	5	100.0	-	-
		12	7	100.0	-	-
		13	3	100.0	-	-
		14	5	80.0	20.0	-
		15	8	62.5	37.5	-
		16	3	66.7	-	33.3
		17	2	-	-	100.0
		18	2	-	-	100.0
		19	6	-	-	100.0
		Age	n	1	2	3
	Distal epiphysis	14	4	100.0	-	-
		15	7	100.0	-	-
		16	1	100.0	-	-
		17	2	50.0	-	50.0
		18	2	50.0	50.0	-
		19	5	20.0	20.0	60.0
		20	2	50.0	-	50.0
		21	2	16.7	-	83.3
		22	1	-	-	100.0
		23	2	-	-	100.0
		24	1	-	-	100.0

Fusion (Stages 2 and 3) of the **distal epiphysis** of the ulna occurred between 17 to 21 years. On average, individuals from Mediaeval Canterbury were 19 years old (mean = 18.50, sd = 0.71) when fusion was underway (Stage 2). Fusion had not occurred in any individual up to the age of 16 years of age. Significance was approached ( $\chi^2 (2) = 5.765, p = 0.056$ ) for the association between the age group: 17 to 21 years and fusion (Stages 2 and 3) of the distal epiphysis of the ulna.

**Proximal ulna:**

Earliest age at complete fusion: 16 years

All complete fusion at age 17 years

**Distal ulna:**

Earliest age at complete fusion: 17 years

All complete fusion at age 22 years

## F) The Hand

**Table 5. 10** provides the age-at-fusion for the metacarpals 2 – 5, proximal and middle phalangeal epiphyses and the distal phalangeal epiphyses of the hand. Fusion (Stages 2 and 3) occurred between the ages of 12 to 17 years for **metacarpals 2 – 5 and the proximal and middle phalangeal epiphyses** of the hand. On average, individuals from Mediaeval Canterbury were 14 years of age (sd = 2.83) when fusion was underway (Stage 2). Fusion had not occurred in any individual up to the age of 11 years old. A significant association ( $X^2(2) = 24.100, p < 0.001$ ) was found between the age group: 12 to 17 years and fusion (Stages 2 and 3) of the metacarpals 2 to 5, proximal and middle phalangeal epiphyses of the hand. This data was still statistically significant when a Bonferroni corrections test was applied. (See **Appendix 3**).

Of the individuals examined, 100% had fused their **distal phalanges** of the hand by 17 years of age. No significant association ( $X^2(1) = 1.800, p = 0.180$ ) was found between the age group: 15 to 17 years and complete fusion (Stage 3) of the distal phalangeal epiphyses of the hand. As two cells had expected frequencies less than five and therefore failed one of the assumptions of the Chi-square, a Fisher's Exact test was performed. Again, no association between the age range 15 to 17 years and fusion of the distal phalanges of the hand were found ( $p = 0.200$ ).

Table 5. 10: Age in years/stage of union of the hand for St Gregory's skeletal collection. The stages of union are recorded as percentages.

		Age	n	Stage of union		
				1	2	3
The hand	Metacarpals 2-5, proximal and middle phalangeal epiphyses	9	2	100.0	-	-
		10	1	100.0	-	-
		11	4	100.0	-	-
		12	5	80.0	20.0	-
		13	2	100.0	-	-
		14	3	100.0	-	-
		15	6	100.0	-	-
		16	3	66.7	33.3	-
		17	1	-	-	100.0
		18	2	-	-	100.0
	19	5	-	-	100.0	
		Age	n	1		3
		Distal phalanges	14	3	100.0	-
			15	4	100.0	-
			17	1	-	100.0
			19	4	-	100.0
			20	1	-	100.0
			21	3	-	100.0

**Metacarpals 2 – 5, proximal and middle  
phalangeal epiphyses:**

Earliest age at complete fusion: 17 years

All complete fusion at age 18 years

**Distal phalangeal epiphyses:**

Complete fusion occurs at age 17 years

*G) The Os coxae*

**Table 5. 11** provides the age-at-fusion for the ischiopubic ramus, iliac crest and the acetabulum of the os coxae. Only a few individuals were available for examination of the **ischiopubic ramus**. Of these, fusion occurred somewhere between the ages of 13 to 14 years, although an ischiopubic ramus displaying Stage 2 was not present. No significant association ( $X^2 (1) = 0.333, p = 0.564$ ) was found between the age group: 13 to 14 years and complete fusion (Stage 3) of the ischiopubic ramus. As two cells had expected frequencies less than five and therefore failed one of the assumptions of the Chi-square, a Fisher's Exact test was performed. Again, no association was found between the age range of 13 to 14 years and fusion of the ischiopubic ramus ( $p = 1.000$ ).

**Ischiopubic ramus:**

Earliest age at complete fusion: 13 years

All complete fusion at age 16 years

Fusion of the **iliac crest** (Stages 2 and 3) occurred between 17 to 23 years of age. On average, individuals from Mediaeval Canterbury were 20 years of age (mean = 19.75, sd = 1.82) when fusion was underway (Stage 2). Fusion had not occurred in any individual up to the age of 16 years old. No significant association ( $X^2 (2) = 5.250, p = 0.072$ ) was found between the age group: 17 to 23 years and fusion (Stages 2 and 3) of the iliac crest.

**Iliac crest:**

Earliest age at complete fusion: 19 years

All complete fusion at age 24 years

Table 5. 11: Age in years/stage of union of the os coxae for St Gregory's skeletal collection. The stages of union are recorded as percentages.

		Stage of union				
		Age	n	1	2	3
The os coxae	Ischiopubic ramus	12	1	100.0	-	-
		13	1	-	-	100.0
		14	2	50.0	-	50.0
		16	1	-	-	100.0
	Iliac crest	14	5	100.0	-	-
		15	8	100.0	-	-
		16	4	100.0	-	-
		17	2	50.0	50.0	-
		18	2	-	100.0	-
		19	6	-	66.7	33.3
		20	2	50.0	-	50.0
		21	8	12.5	37.5	50.0
22		1	-	100.0	-	
23		3	-	33.3	66.7	
24		1	-	-	100.0	
25		5	-	-	100.0	
Acetabulum	11	5	100.0	-	-	
	12	6	100.0	-	-	
	13	3	100.0	-	-	
	14	5	80.0	20.0	-	
	15	7	57.1	28.6	14.3	
	16	3	-	33.3	66.7	
	17	2	-	-	100.0	
	18	1	-	-	100.0	
	19	6	-	-	100.0	

Fusion was underway in the **acetabulum** between the ages of 14 to 16 years. On average, individuals from Mediaeval Canterbury were 15 years of age (sd = 0.82) when fusion was underway (Stage 2). Fusion had not occurred in any individual up to the age of 13 years of age. No significant association ( $X^2(2) = 2.800, p = 0.247$ ) was found between the age group: 14 to 16 years and fusion (Stages 2 and 3) of the acetabulum.

**Acetabulum:**

Earliest age at complete fusion: 15 years

All complete fusion at age 17 years

*H) The Femur*

**Table 5. 12** provides the age-at-fusion for the femoral head, the greater and lesser trochanters and the distal epiphysis of the femur. Partial fusion (Stage 2) occurred between 15 to 19 years for the **femoral head**. On average, individuals from Mediaeval Canterbury were 17 years of age (mean = 17.25, sd = 1.71) when fusion was underway (Stage 2). Fusion had not occurred in any individual up to the age of 14 years. No significant association ( $X^2 (2) = 3.263, p = 0.196$ ) was found between the age group: 15 to 19 years and fusion (Stages 2 and 3) of the proximal epiphysis of the femur.

**Femoral head:**

Earliest age at complete fusion: 17 years

All complete fusion at age 20 years

As for the **greater trochanter**, partial fusion (Stage 2) occurred between 16 to 17 years. On average, individuals from Mediaeval Canterbury were 17 years of age (mean = 16.50, sd = 0.71) when fusion was underway (Stage 2). Fusion had not occurred in any individual up to the age of 15 years old. Partial fusion (Stage 2) of the **lesser trochanter** occurred at age 16 years, and complete fusion (Stage 3) occurred in all individuals by age 17 years. No significant association ( $X^2 (2) = 0.400, p = 0.819$ ) was found between the age group: 16 to 17 years and fusion (Stages 2 and 3) of the greater or lesser trochanters.

**Greater & lesser trochanters:**

Earliest age at complete fusion: 17 years

Table 5. 12: Age in years/stage of union of the femur for St Gregory's skeletal collection. The stages of union are recorded as percentages.

		Stage of union					
		Age	n	1	2	3	
The femur	Femoral head	12	7	100.0	-	-	
		13	3	100.0	-	-	
		14	5	100.0	-	-	
		15	8	87.5	12.5	-	
		16	3	100.0	-	-	
		17	2	-	50.0	50.0	
		18	1	-	100.0	-	
		19	5	-	20.0	80.0	
		20	2	-	-	100.0	
		21	8	-	-	100.0	
		22	1	-	-	100.0	
		Age	n	1	2	3	
		Greater trochanter	13	3	100.0	-	-
			14	5	100.0	-	-
			15	8	100.0	-	-
			16	3	66.7	33.3	-
			17	2	-	50.0	50.0
			18	1	-	-	100.0
			19	5	-	-	100.0
		20	2	-	-	100.0	
		Age	n	1	2	3	
		Lesser trochanter	13	3	100.0	-	-
			14	5	100.0	-	-
	15		8	100.0	-	-	
	16		3	66.7	33.3	-	
	17		2	-	-	100.0	
	18		1	-	-	100.0	
	19	5	-	-	100.0		
	Age	n	1	2	3		
	Distal epiphysis	14	4	100.0	-	-	
		15	7	100.0	-	-	
		16	3	100.0	-	-	
		17	2	50.0	-	50.0	
		18	1	100.0	-	-	
		19	5	-	20.0	80.0	
		20	2	-	50.0	50.0	
		21	6	-	-	100.0	
		22	1	-	-	100.0	
	23	2	-	-	100.0		

Fusion (Stages 2 and 3) of the **distal epiphysis** of the femur occurred between 17 to 20 years. On average, individuals from Mediaeval Canterbury were 20 years of age (mean = 19.50, sd = 0.71) when fusion was underway (Stage 2). No significant association ( $X^2(2) = 3.200, p = 0.202$ ) was found between the age group: 17 to 20 years and fusion (Stages 2 and 3) of the distal epiphysis of the femur. As three cells had expected frequencies less than five and therefore failed one of the assumptions of the Chi-square, a Fisher-Freeman-Halton Exact test was performed. Again, no association between the age range of 17 to 20 years and the fusion of the distal epiphysis of the femur was found ( $p = 0.367$ ).

**Distal femur:**

Earliest age at complete fusion: 17 years

All complete fusion at age 21 years

I) *The Tibia*

**Table 5. 13** provides the age-at-fusion for the proximal and distal epiphyses of the tibia. Partial fusion (Stage 2) of the **proximal epiphysis** of the tibia occurred between 17 to 19 years. On average, individuals from Mediaeval Canterbury were 18 years old (mean = 18.33, sd = 1.16) when fusion was underway (Stage 2). Fusion had not occurred in any individual up to the age of 16 years old. No significant association ( $X^2 (2) = 1.750, p = 0.417$ ) was found between the age group: 17 to 19 years and fusion (Stages 2 and 3) of the proximal epiphysis of the tibia. As three cells had expected frequencies less than five and therefore failed one of the assumptions of the Chi-square, a Fisher-Freeman-Halton Exact test was performed. Again, no association was found between the age range of 17 to 19 years and fusion of the proximal epiphysis of the tibia ( $p = 0.536$ ). (See **Appendix 3**).

Partial fusion of the **distal epiphysis** of the tibia occurred between 17 to 18 years. On average, individuals from Mediaeval Canterbury were 18 years of age (mean = 17.50, sd = 0.71) when fusion was underway (Stage 2). Fusion had not occurred in any individual up to the age of 16 years old. No significant association ( $X^2 (1) = 0.333, p = 0.564$ ) was found between the age group: 17 to 18 years and fusion (Stages 2 and 3) of the distal epiphysis of the tibia. As two cells had expected frequencies less than five and therefore failed one of the assumptions of the Chi-square, a Fisher's Exact test was performed. Again, no association was found between the age range of 17 to 18 years of age and fusion of the distal epiphysis of the tibia ( $p = 1.000$ ).

Table 5. 13: Age in years/stage of union of the tibia for St Gregory's skeletal collection. The stages of union are recorded as percentages.

		Age	n	Stage of union		
				1	2	3
The tibia	Proximal epiphysis	14	3	100.0	-	-
		15	7	100.0	-	-
		16	2	100.0	-	-
		17	2	-	50.0	50.0
		18	1	100.0	-	-
		19	5	-	40.0	60.0
		20	2	-	-	100.0
		21	6	-	-	100.0
		22	1	-	-	100.0
		Age	n	1	2	3
	Distal epiphysis	14	3	100.0	-	-
		15	6	100.0	-	-
		16	2	100.0	-	-
		17	2	-	50.0	50.0
		18	1	-	100.0	-
		19	4	-	-	100.0
		20	2	-	-	100.0
		21	6	-	-	100.0

**Proximal tibia:**

Earliest age at complete fusion: 17 years

All complete fusion at age 20 years

**Distal tibia:**

Earliest age at complete fusion: 17 years

All complete fusion at age 19 years

### 5.2.3. Summary of statistical analysis

A summary of the Goodness-of-fit Chi-square results can be found in **Table 5. 14**. There was a significant association between the age of an individual and bone fusion at nine sites. These sites were the cervical vertebrae, the lateral clavicle, the proximal ulna and the metacarpals and proximal and middle phalangeal epiphyses of the hand. The proximal radius was also found to be statistically significant when a Fisher-Freeman-Halton Exact Test was run on the data ( $p = 0.041$ ).

The anterior arch of the atlas and the ossiculum terminale of the axis fused (Stages 2 and 3) between the ages of 8 to 15 years. The posterior synchondrosis of the atlas fused between the ages of 4 to 15 years and the dentocentral and neurocentral junctions of the axis fused between 3 to 16 years. The dentoneural synchondrosis (3 to 6 years) and posterior synchondrosis (3 to 5 years) of the axis fused in childhood only. The significant results for the appendicular skeleton occurred mostly during the adolescent period.

Bonferroni corrections tests were conducted on the data. Only four out of the ten sites remained statistically significant. These were the anterior arch and the posterior synchondrosis of the atlas, the dentocentral and neurocentral junctions of axis, and the metacarpals 2 – 5 and the proximal and middle phalangeal epiphyses of the hand. The anterior arch and posterior synchondrosis of the atlas had individuals that remained unfused (Stage 1) past the age that many other skeletons had completed fusion (Stage 3). This most likely contributed to a significant result after a Bonferroni test was performed. The dentocentral and neurocentral junctions of the axis had a large range of skeletons in partial fusion (Stage 2) compared to many of the other fusion sites. Finally, metacarpals 2 – 5 and the proximal and middle phalangeal epiphyses of the hand had more individuals unfused (Stage 1) than in partial fusion (Stage 2) or in complete fusion (Stage 3), and the weighted results towards one stage more than the other stages could have contributed to a statistically significant result.

Table 5. 14: Fusion of each site and the association with age. Results were produced from a goodness-of-fit chi-square. \*\* = statistically significant, † = failed the chi-square test but was statistically significant when a Fisher-Freeman-Halton Exact Test was run on the data ( $p = 0.041$ )

Fusion site	Age group	Fusion stages considered	Significance
Pars lateralis to pars basilaris	7 – 8 years	Stage 3	0.096
Spheno-occipital synchondrosis	16 to 17 years	Stages 2 and 3	0.223
Anterior arch (atlas)	8 to 15 years	Stages 2 and 3	<u>&lt; 0.001</u> **
Posterior synchondrosis (atlas)	4 to 15 years	Stage 3	<u>&lt; 0.001</u> **
Ossiculum terminale (axis)	8 to 15 years	Stages 2 and 3	<u>0.015</u> **
Dentoneural synchondrosis (axis)	3 to 6 years	Stages 2 and 3	<u>0.006</u> **
Dentocentral and neurocentral junctions (axis)	3 to 16 years	Stages 2 and 3	<u>&lt; 0.001</u> **
Posterior synchondrosis (axis)	3 to 5 years	Stage 3	<u>0.008</u> **
Sacral bodies 1 and 2	19 to 28 years	Stages 2 and 3	0.251
Medial clavicle	19 to 25 years	Stages 2 and 3	0.179
Lateral clavicle	17 to 23 years	Stages 2 and 3	<u>0.004</u> **
Medial border (scapula)	19 to 21 years	Stage 3	0.564
Acromial border (scapula)	17 to 18 years	Stage 3	1.000
Inferior angle (scapula)	18 to 21 years	Stage 3	1.000
Medial humeral epicondyle	16 to 17 years	Stages 2 and 3	0.819
Distal composite epiphysis (humerus)	14 to 15 years	Stages 2 and 3	0.074
Proximal humerus	17 to 21 years	Stages 2 and 3	0.193
Proximal radius	15 to 16 years	Stages 2 and 3	0.292†
Distal radius	17 to 21 years	Stages 2 and 3	0.115
Proximal ulna	14 to 16 years	Stages 2 and 3	<u>0.007</u> **
Distal ulna	17 to 21 years	Stages 2 and 3	0.056
Metacarpals and the proximal and middle phalangeal epiphyses (hand)	12 to 17 years	Stages 2 and 3	<u>&lt;0.001</u> **
Distal phalanges (hand)	15 to 17 years	Stage 3	0.180
Ischiopubic ramus	13 to 14 years	Stage 3	0.564
Iliac crest	17 to 23 years	Stages 2 and 3	0.072
Acetabulum	14 to 16 years	Stages 2 and 3	0.247
Femoral head	15 to 19 years	Stages 2 and 3	0.196
Greater and lesser trochanters	16 to 17 years	Stages 2 and 3	0.819
Distal femur	17 to 20 years	Stages 2 and 3	0.202
Proximal tibia	17 to 19 years	Stages 2 and 3	0.417
Distal tibia	17 to 18 years	Stages 2 and 3	0.564

### 5.3. AGE-AT-FUSION BETWEEN HIGH AND LOW STATUS

No statistically significant differences existed between the high and low-status groups in the St Gregory's Mediaeval skeletal collection. The timing of fusion, the age-at-fusion of the sub-samples and statistical analyses are provided in **Appendix 4**. A binomial logistic regression was carried out on the data (**Table 5. 16**), along with assumptions tested first (**Table 5. 15**), but no statistically significant differences were found.

*Table 5. 15: Assumptions for the binomial logistic regressions test. Outliers were minimal and were left in the analysis.*

Age Group (years)	Linear relationship exists		Case wise diagnostics	Model fit	
3 - 10	0.416	✓	No case wise diagnostics	0.995	✓
3 - 15	1.000	✓		1.000	✓
11 - 18	No data available for high status individuals				
12 - 19	0.509	✓	There was 1 standardised residual with a value of 4.241 standard deviations	0.940	✓
13 - 20	0.567	✓	There was 1 standardised residual with a value of 2.972 standard deviations	0.852	✓
13 - 20	0.620	✓	There were 2 standardised residuals with values of 3.576 and 2.214 standard deviations	0.980	✓
16 - 23	0.998	✓	There was 1 standardised residual with a value of 1.840 standard deviations	0.893	✓
16 - 30	0.296	✓	There was 1 standardised residual with a value of 2.562 standard deviations	0.334	✓

Apart from ages 11 to 18 years, all the tests passed the assumptions for a binomial logistic regression. The age range chosen and the fusion sites that were grouped were based on when each epiphysis fused, and therefore, some fusion sites are found in multiple tests as they fuse over a longer age range or were split over multiple tests to pass the assumptions. A Bonferroni corrections test was not required because there was only one continuous independent variable (A. Lund and Lund, 2018b). It is of note that due to the small sample size of the high-status group, the lack of significant findings in both the Mann Whitney U and the binomial logistic regression could potentially be due to a lack of data.

In **Table 5. 16** the Nagelkerke  $r^2$  relates to the explained variation of the dependent variable (A. Lund and Lund, 2018b). As an example, in the age group 3 to 10 years, 59.1% of the status of the skeletons can be explained by the model of the binomial logistic regression output. The Classification section of the table shows the probability of a skeleton being high or low status. When the independent variables are added into the age group 3 to 10 years: age and fusion stage, the model can now correctly classify 77.8% of cases, on whether they are high or low-status (A. Lund and Lund, 2018b). Variable significance shows whether the independent variables add significantly to the model (A. Lund and Lund, 2018b). As individual variables, none of these added anything significant to the model.

While a non-statistically significant  $p$ -value showed that a linear relationship existed between the data and that the models fit well based on a non-significant Hosmer and Lemeshow goodness-of-fit test (**Table 5. 15**), none of the independent variables was significant (**Table 5. 16**). The models explained 14.8 to 86.0% (Nagelkerke  $r^2$ ) of the variance in the status of St Gregory's. The model also correctly classified between 77.8 to 92.6% of cases. Overall, the model determined if there was a difference in age-at-fusion between the high and low status of St Gregory's. Results revealed no difference between these social groupings.

Table 5. 16: Binomial logistic regression to test if age-at-fusion differed between the high and low status of St Gregory's skeletal collection. Grey boxes are alternated with white to make readability easier.

Age Group (years)	Nagelkerke r <sup>2</sup>	Classification %		Variable significance (p value)	
3 - 10	0.591	Low-Status	92.3	Age	0.457
		High-Status	40.0	Pars lateralis to pars basilaris	0.999
		Overall	77.8	Posterior synchondrosis C1	1.000
				Dentoneural synchondrosis	1.000
3 - 15	0.860	Low-Status	88.9	Age	0.999
		High-Status	100.0	Anterior arch C1	0.999
		Overall	92.3	Posterior synchondrosis C1	1.000
				Ossiculum terminale	1.000
				Dentocentral and neurocentral junctions	1.000
12 - 19	0.199	Low-Status	100.0	Age	0.482
		High-Status	0.00	Medial humeral epicondyle	1.000
		Overall	91.9		
13 - 20	0.185	Low-Status	100.0	Age	0.882
		High-Status	0.00	Acromial border	1.000
		Overall	89.5	Proximal tibia	1.000
				Greater trochanter	1.000
				Femoral head	1.000
13 - 20	0.148	Low-Status	100.0	Age	0.591
		High-Status	0.00	Lesser trochanter	1.000
		Overall	92.6	Distal femur	1.000
16 - 23	0.384	Low-Status	93.3	Age	0.865
		High-Status	0.00	Proximal humerus	0.999
		Overall	77.8	Lateral clavicle	0.999
				Iliac crest	1.000
16 - 30	0.234	Low-Status	100.0	Age	0.711
		High-Status	25.0	Lateral clavicle	0.999
		Overall	88.9	Medial clavicle	0.999

#### 5.4. SEQUENCE OF FUSION IN ST GREGORY'S

Twenty-three fusion sites were analysed and sequenced. The occipital bone of the skull was the first to fuse in the sequence, beginning with the **pars lateralis** fusing to the **pars squama** (1<sup>st</sup>) and then the **pars lateralis** fusing to the **pars basilaris** (2<sup>nd</sup>). The third site to fuse was the **ischiopubic ramus** (3<sup>rd</sup>) and then the **distal humerus** (4<sup>th</sup>). Overall, the **acetabulum** (5<sup>th</sup>) fuses next and then the **proximal radius** (6<sup>th</sup>), but in some occurrences, the proximal radius will fuse before the acetabulum. The **coracoid** (7<sup>th</sup>) of the scapula tends to fuse after the proximal radius, but in rarer cases, the coracoid will fuse before the proximal radius. No differences could be discerned between whether the coracoid or the **proximal ulna** (7<sup>th</sup>) fused first and are therefore recorded as fusing at a similar time in the sequence. In 8<sup>th</sup> place in the sequence, the **medial humeral epicondyle**, the **lesser trochanter** of the femur and the **spheno-occipital synchondrosis** (8<sup>th</sup>) fuse around the same time. The **greater trochanter** (9<sup>th</sup>) fuses after this. The **distal epiphysis of the tibia** and the **acromion** of the scapula (10<sup>th</sup>) fuse in tenth place and then the **femoral head**, **proximal epiphysis of the tibia** and the **distal epiphysis of the femur** (11<sup>th</sup>) fuse in eleventh place. The **distal epiphysis of the radius**, **distal epiphysis of the ulna** and **proximal epiphysis of the humerus** (12<sup>th</sup>) are grouped together in twelfth place. Next fuses the **iliac crest** (13<sup>th</sup>), **sacral bodies 1 – 2** (14<sup>th</sup>) and finally the sequence ends with the **medial clavicle** (15<sup>th</sup>).

## 5.5. PUBERTY IN MEDIAEVAL CANTERBURY

### 5.5.1. Age at puberty

**Table 5. 17** shows the pubertal stage recorded and estimated age for the low-status, and a small sample of high-status Mediaeval Canterbury skeletons. All low-status Mediaeval children remained in **Pre-puberty** until age 8 years, with some remaining in this stage until age 12 years. The **Acceleration** phase commenced for some low-status juveniles at age 9 years while others were 16 years of age when this phase commenced. The low-status individuals entered **PHV** between 14 to 21 years of age. The mean age to enter PHV was 15 years (mean age = 14.94, s.d. = 0.73) for the low-status sample.

**Deceleration** occurred between the ages of 16 to 21 years for the low-status group. The mean age to enter this phase was 18 years (s.d. = 2.11). The **Maturation** phase occurred between 17 to 25 years for the low-status individuals, with a mean age of 19 years (mean age = 19.44, s.d. = 1.42). Low-status individuals **completed** puberty between 19 to 25 years of age (mean age = 22.10, s.d. 2.30).

The high-status group had limited data. One high-status child commenced the acceleration phase at 11 years of age and one individual was recorded as having completed puberty at 23 years. Although the data is limited, the table shows a clear distinction between the phases, with each phase showing ever increasing age ranges.

Table 5. 17: Age at puberty for low and high-status individuals from Mediaeval Canterbury. The stages of union are recorded as percentages.

		Age at puberty for Mediaeval Canterbury							
	Age	<i>n</i>	Pre-puberty	Acceleration	PHV	Deceleration	Maturation	Completion	
<i>Low status</i>	3	7	100.0	–	–	–	–	–	
	4	4	100.0	–	–	–	–	–	
	5	5	100.0	–	–	–	–	–	
	6	5	100.0	–	–	–	–	–	
	7	4	100.0	–	–	–	–	–	
	8	6	100.0	–	–	–	–	–	
	9	5	40.0	60.0	–	–	–	–	
	10	2	100.0	–	–	–	–	–	
	11	4	25.0	75.0	–	–	–	–	
	12	7	57.1	42.9	–	–	–	–	
	13	3	–	100.0	–	–	–	–	
	14	5	–	80.0	20.0	–	–	–	
	15	9	–	44.4	55.6	–	–	–	
	16	5	–	20.0	60.0	20.0	–	–	
	17	2	–	–	50.0	–	50.0	–	
	18	1	–	–	–	100.0	–	–	
	19	5	–	–	–	20.0	40.0	40.0	
	20	2	–	–	–	50.0	–	50.0	
	21	8	–	–	12.5	12.5	25.0	50.0	
	22	1	–	–	–	–	–	100.0	
	23	2	–	–	–	–	–	100.0	
	24	1	–	–	–	–	–	100.0	
	25	6	–	–	–	–	16.7	83.3	
	28	2	–	–	–	–	–	100.0	
	<i>High status</i>	3	2	100.0	–	–	–	–	–
		4	3	100.0	–	–	–	–	–
		5	1	100.0	–	–	–	–	–
		6	1	100.0	–	–	–	–	–
7		1	100.0	–	–	–	–	–	
8		1	100.0	–	–	–	–	–	
11		1	–	100.0	–	–	–	–	
15		1	–	100.0	–	–	–	–	
18		1	–	–	–	–	100.0	–	
19		1	–	–	–	–	100.0	–	
23		1	–	–	–	–	–	100.0	
25	1	–	–	–	–	–	100.0		

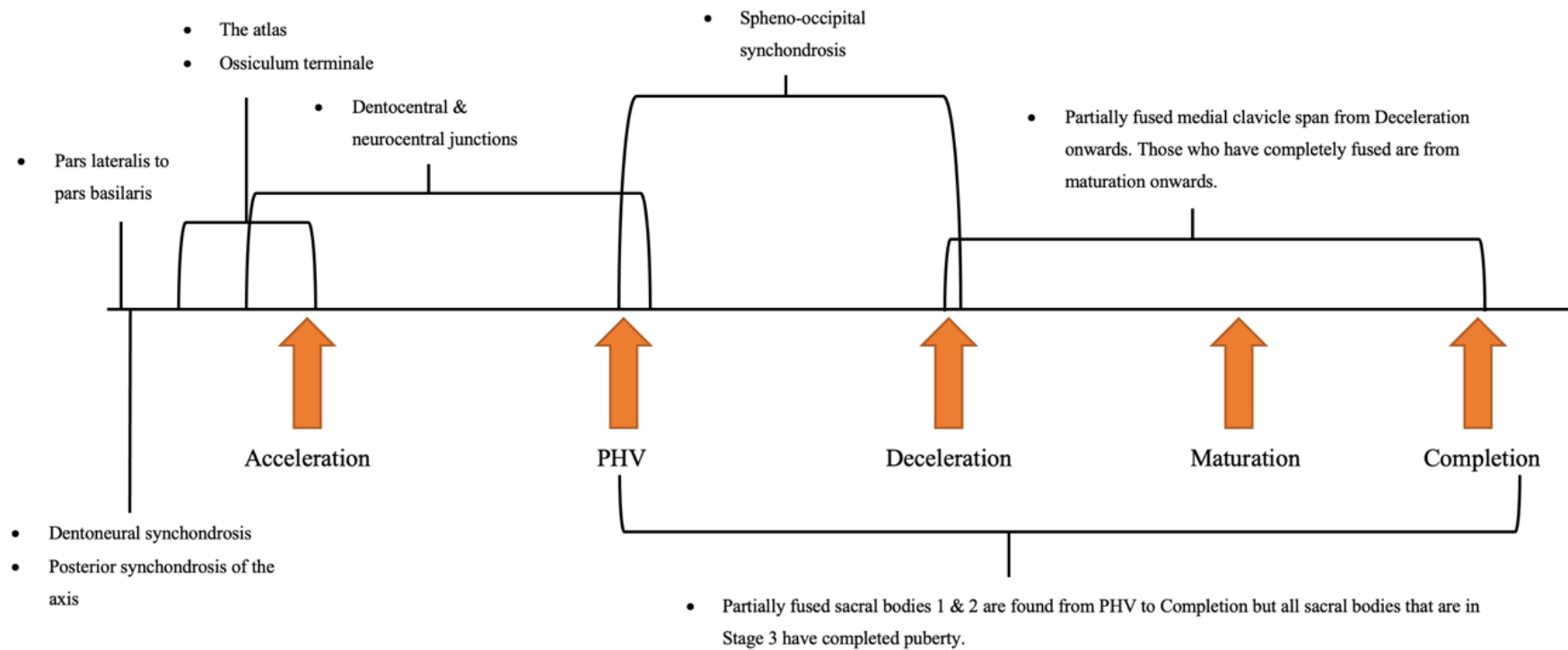
### 5.5.2. The relation of epiphyseal fusion to pubertal phase

**Table 5. 18** illustrates the pubertal phases in which epiphyseal fusion takes place, for the axial skeleton of the low-status individuals from Mediaeval Canterbury. This same information is also represented in figure form below in **Figure 5. 2**.

*Table 5. 18: Epiphyseal fusion (Stages 2 and 3) of the axial skeleton is plotted as to where it falls during puberty for the low-status Mediaeval St Gregory's skeletal collection. Grey shading shows where fusion takes place. Blue shading shows where fusion has completed.*

	Pre-puberty	Acceleration	PHV	Deceleration	Maturation	Completion
Pars lateralis to pars basilaris						
Spheno-occipital synchondrosis						
Anterior arch (atlas)						
Posterior synchondrosis (atlas)						
Ossiculum terminale to the dens						
Dentoneural synchondrosis (axis)						
Dentocentral & neurocentral junctions (axis)						
Posterior synchondrosis (axis)						
Bodies 1 & 2 of the sacrum						

Figure 5. 2: Epiphyseal fusion (Stages 2 and 3) of the axial skeleton (along with the medial clavicle) is plotted as to where it falls during puberty for the low-status Mediaeval St Gregory's skeletal collection



The information for **Table 5. 18** and **Figure 5. 2** can be found in **Appendix 5**, including pubertal information on the high-status Mediaeval group. However, some points of interest are detailed here. Firstly, the **ossiculum terminale** to the dens of the axis was significant. In low-status skeletons, partial fusion (Stage 2) and complete fusion (Stage 3) occurred in the first two pubertal phases. The mean pubertal phase at fusion (Stages 2 and 3) was Acceleration (mean phase = 1.55, s.d. = 0.51). As for the high-status group, no unfused (Stage 1) skeletons went past the Pre-puberty phase. All partially fused high-status skeletons were in the Acceleration phase. All completely fused high-status individuals were in the Acceleration phase and above. The pubertal phase at fusion (Stages 2 and 3) for the high-status juveniles was PHV (s.d. = 1.73). The high-status group, therefore, fused at a later pubertal phase when compared to the low-status group. This was statistically significantly different ( $p = 0.047$ ,  $U = 11.000$ ). This data was not statistically significant when a Bonferroni corrections test was performed (See **Appendix 3**).

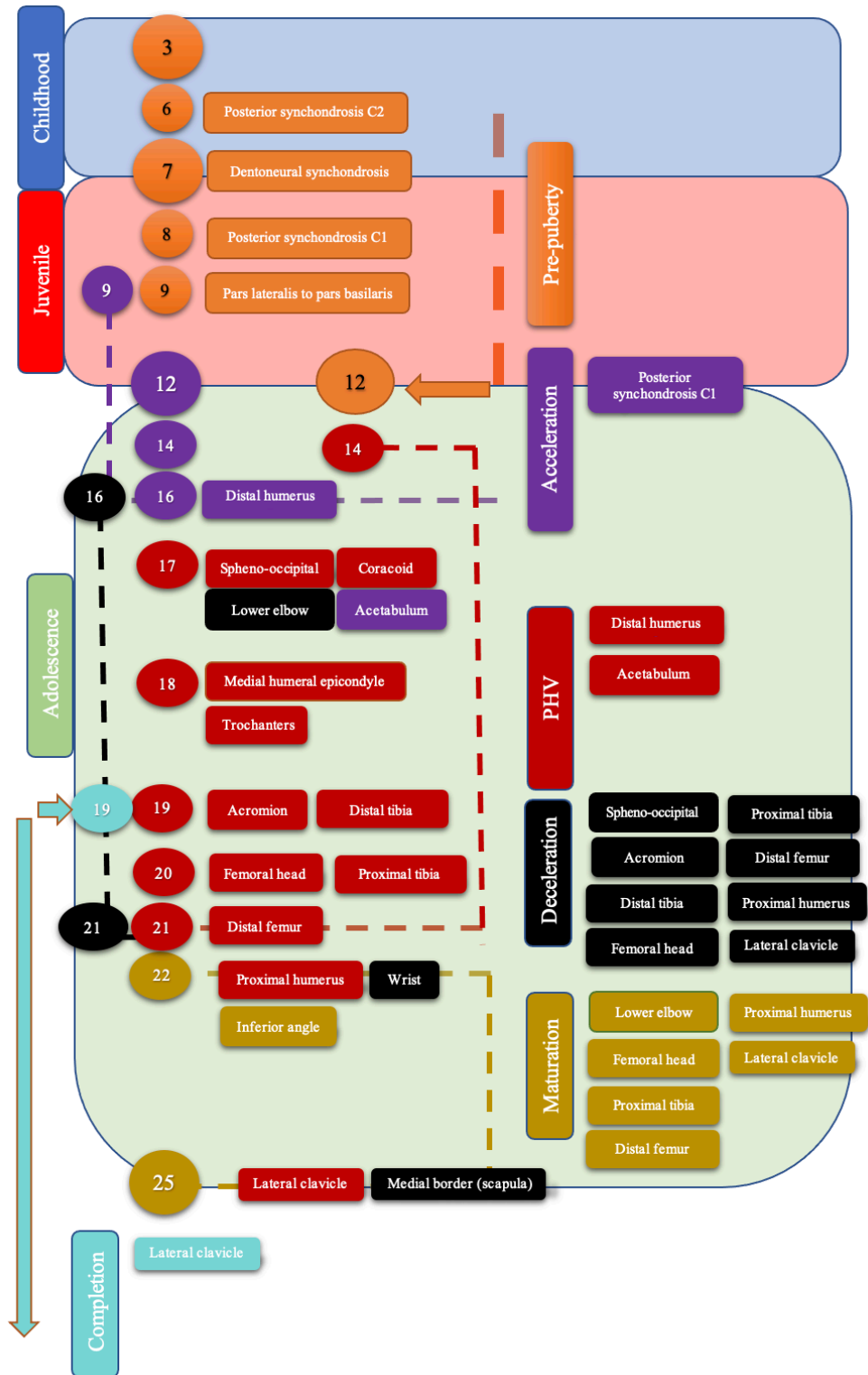
The **sacral bodies 1 and 2** were also of importance. Low-status individuals who were partially fused at death were found in pubertal stages PHV to Completion. Mean pubertal phase for those in partial fusion (Stage 2) was the Maturation phase (mean phase = 5.18, s.d. = 0.98). All low-status individuals who had completed fusion of sacral bodies 1 and 2 had also completed puberty (**Appendix 5**). The high-status 19-year-old was also found to have completed puberty. Thus, the fusion process for sacral bodies 1 and 2 can start from PHV onwards. Nevertheless, complete fusion of the sacral bodies 1 and 2 is only associated with the individual having completed puberty.

**Table 5. 19** illustrates in which pubertal phases epiphyseal fusion takes place for the low-status individuals of Mediaeval Canterbury for the appendicular skeleton. This same information is also represented in figure form below in **Figure 5. 3**, along with the results of **Section 5.5**. Chapter Five is summarised in table format in **Appendix 6**.

*Table 5. 19: Epiphyseal fusion (Stages 2 and 3) of the appendicular skeleton is plotted as to where it falls during puberty for the low-status Mediaeval St Gregory's skeletal collection. Grey shading shows where fusion takes place.*

	Pre-puberty	Acceleration	PHV	Deceleration	Maturation	Completion
Medial clavicle						
Lateral clavicle						
Coracoid						
Medial border of scapula						
Acromial epiphysis						
Inferior angle of scapula						
Medial humeral epicondyle						
Distal composite epiphysis to the shaft of the humerus						
Proximal epiphysis of humerus						
Proximal radial epiphysis						
Distal epiphysis of the ulna						
Metacarpals 2-5, proximal & middle phalangeal epiphyses						
Acetabulum						
Femoral head						
Greater & lesser trochanters						
Distal femoral epiphysis						
Proximal tibial epiphysis						
Distal tibial epiphysis						

Figure 5. 3: Growth chart for St Gregory’s skeletal collection. Growth stages are shown by boxes. Ages are given by bubbles on the left. Fusion sites are placed next to the age that the entire sample completed fusion. Colours of fusion sites and age bubbles denote pubertal phase. If a fusion site could fuse during multiple pubertal phases, following pubertal phases were given on the right-hand side.



## CHAPTER 6

**RESULTS**MATURATION OF THE MODERN HUMAN SKELETON COMPARED BETWEEN  
ARCHAEOLOGICAL PERIODS**6.1. RESEARCH QUESTIONS****Question 1. Are there differences in the age-at-fusion between Mediaeval Canterbury and other British Mediaeval sites?**

Age-at-fusion will be compared between Mediaeval children from York in the north of England, Mediaeval children from Canterbury in the south of England and Mediaeval children from Auldhame in Scotland (**Section 6.2.**).

**Question 2. Are there differences in age-at-fusion between British archaeological periods?**

Age-at-fusion is compared between archaeological sites grouped by historical period (Iron age, Roman, Anglo-Saxon, Mediaeval and Post-Mediaeval) across England and Scotland (**Section 6.3.**).

**Question 3. How does skeletal maturation within this thesis compare to published literature?**

Age-at-fusion for the archaeological data recorded in this thesis is compared to age-at-fusion for historical and modern data samples that have been taken from the published literature (**Section 6.4.**).

**Question 4. What is the sequence of fusion for the archaeological groups within this thesis, and do the sequences differ from previous literature?**

Following on from previous studies (Schaefer and Black, 2007; Schaefer, 2008a, 2014; Lenover and Šešelj, 2019), the sequence of fusion determined for the Mediaeval group in **Section 5.4.**, and the archaeological groups of Roman and Anglo-Saxon are compared to the published data (**Section 6.5.**).

\*\*\*

**A note on statistics:** The statistical tests used in this chapter include a Mann Whitney U, a multiple regression, and contingency tables. The Mann-Whitney U was used to test age-at-fusion between Mediaeval sites and between archaeological periods. The assumptions for a Mann Whitney U are found in **Section 5.1**. The multiple regression was used to test whether the age-at-fusion of epiphyses could predict which Mediaeval site or archaeological period the skeleton came from. The contingency tables looked at the sequence of fusion.

The assumptions for a multiple regression are (1) One dependent variable is continuous, (2) The independent variables can be continuous or nominal, or an ordinal variable that is listed as nominal, (3) There must be independence of observation, (4) A linear relationship exists between the variables, (5) The data must show homoscedasticity, (6) The data must not show multicollinearity, (7) Data should not have any significant outliers, high leverage points or highly influential points, and (8) Errors are normally distributed (Lund and Lund, 2013b). The assumptions were met in that (1) Age was the continuous variable, and (2) Fusion stage is ordinal data but can be considered nominal for this test, and Mediaeval site or archaeological period is nominal. The other assumptions were tested using statistical tests before the multiple regression was carried out. Whether the assumption was met and whether the test was carried out was done on a case-by-case basis and can be reviewed within this chapter.

As a final note on statistics, when comparing between Mediaeval sites and between archaeological groups, the Mediaeval Canterbury and Mediaeval archaeological samples were far larger than the Mediaeval York, Mediaeval Auldham and archaeological period samples. This may have potentially skewed the data and shown significant or non-significant differences where there may not have been if the sample sizes had been more equally distributed. For example, the Iron Age and Post-Mediaeval samples were extremely small, and this may have had a consequential effect on the few significant differences found for these groups. Furthermore, the greater sample of the Mediaeval group may have meant that significant differences were found where there should not have been, as the Mediaeval sample would have covered greater skeletal variation compared to a smaller sample size. These problems are kept in mind when discussing and testing the data. Future studies could aim to collect more samples and run the tests again to see if the results are a true representation.

## 6.2. MEDIAEVAL CANTERBURY COMPARED TO OTHER BRITISH MEDIAEVAL SITES

### 6.2.1. The axial skeleton

Age-at-fusion and age distribution data for all sites can be found in **Appendix 7**. This subsection gives the results of age-at-fusion for the axial skeleton in Mediaeval York and Mediaeval Canterbury (**Table 6. 1**). Mediaeval York included the combined archaeological sites of All Saint's church and Fishergate House. Mediaeval Canterbury included both high and low-status skeletons from St Gregory's cemetery and priory. Auldham was only included when the sample size was large enough, whereas Cirencester was excluded due to a low sample size.

#### *A) The Skull*

Complete fusion (Stage 3) occurred at age 7 years for Mediaeval York for the **pars lateralis to pars basilaris**, and between 7 to 8 years for Mediaeval Canterbury. The **spheno-occipital synchondrosis** had completed fusion (Stage 3) by age 16 years in Mediaeval York but remained unfused (Stage 1) for one adolescent at age 18 years. Fusion was underway (Stage 2) at age 16 years for Mediaeval Canterbury and completely fused (Stage 3) by age 17 years.

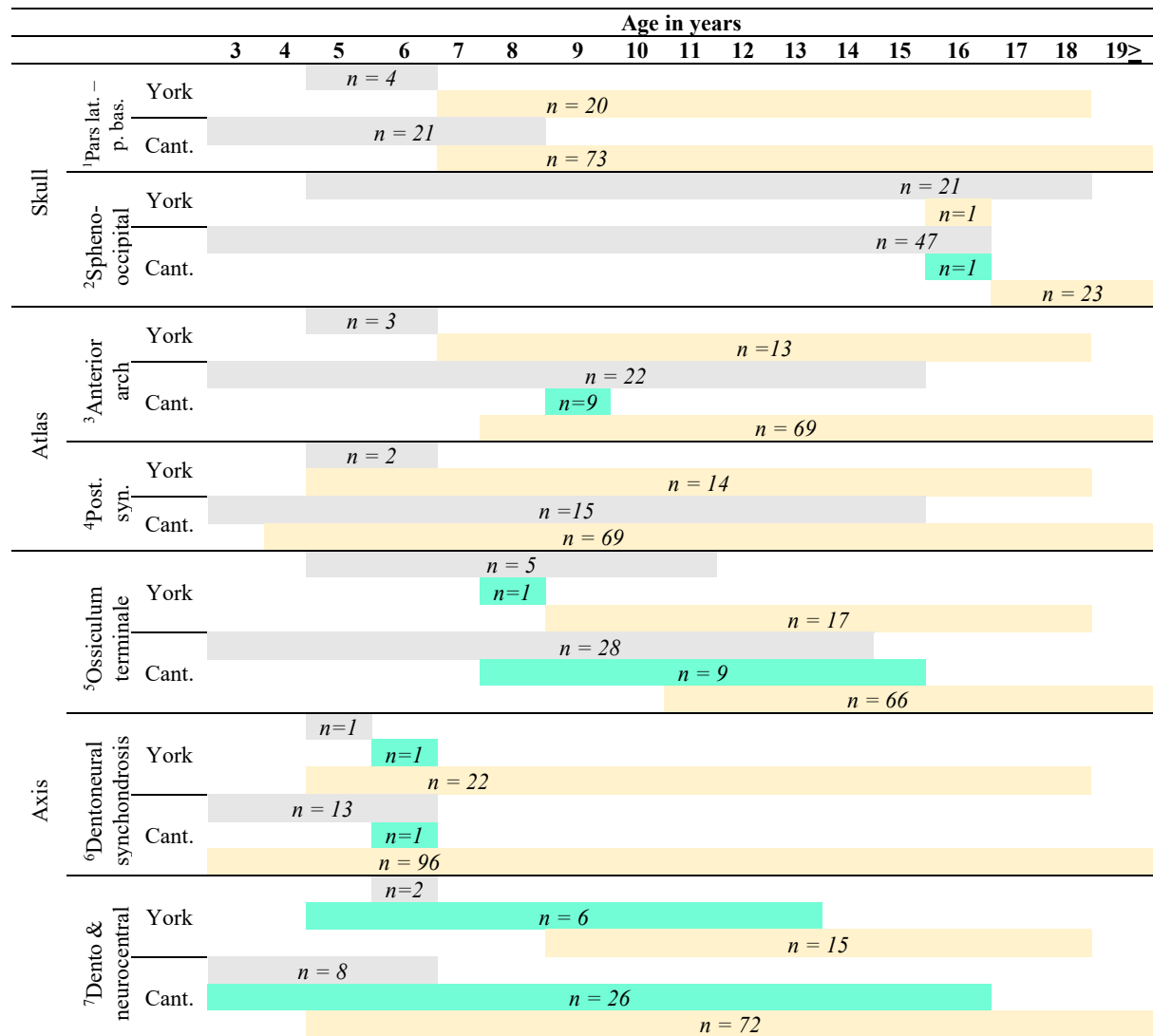
#### *B) Cervical vertebrae*

##### The Atlas

Complete fusion (Stage 3) of the **anterior arch** of the atlas occurred at age 7 years for Mediaeval York. The earliest age that Mediaeval Canterbury skeletons completed fusion (Stage 3) was 8 years. However, one individual was unfused (Stage 1) at age 12 years and another at age 15 years. Fusion was underway (Stage 2) for one individual at age 9 years.

Complete fusion (Stage 3) occurred at the earliest age of 5 years for the **posterior synchondrosis** for Mediaeval York, although one individual remained unfused (Stage 1) at age 6 years. Complete fusion (Stage 3) occurred at the earliest age of 4 years for Mediaeval Canterbury. Most Canterbury juveniles appeared to have completed fusion (Stage 3) by age 8 years, but three individuals remained unfused (Stage 1) at ages nine, twelve and fifteen years.

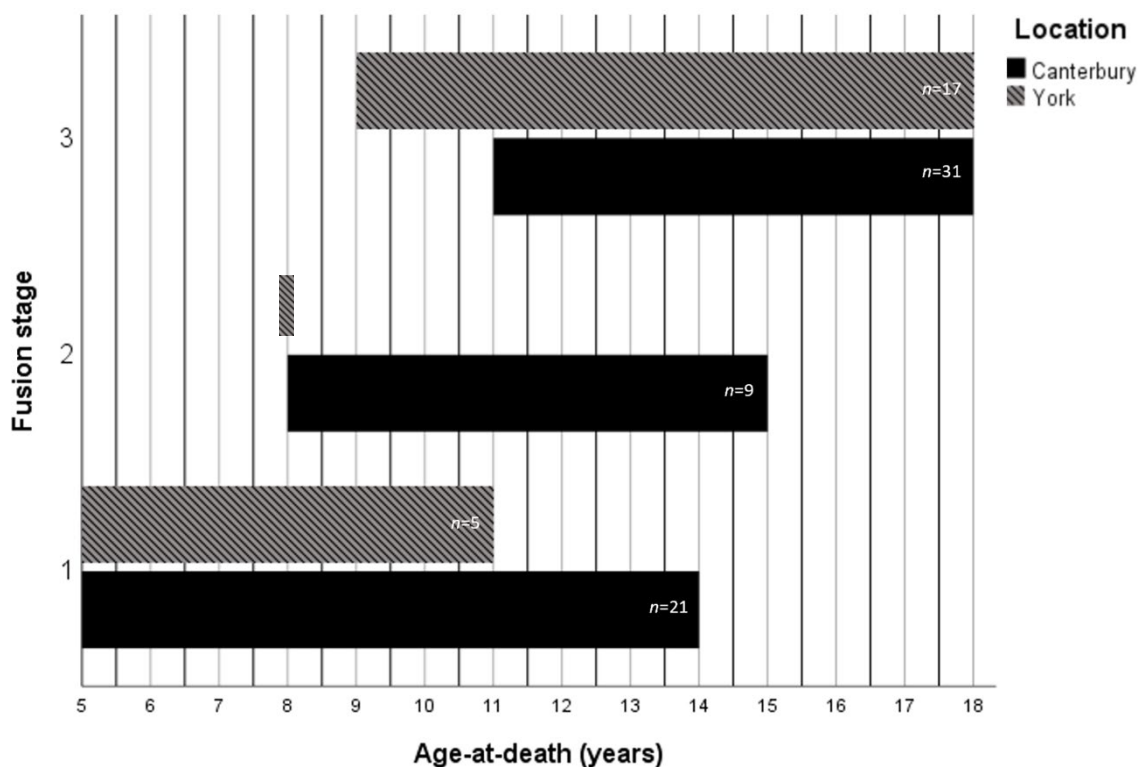
Table 6. 1: Age and phase for the fusion of the axial skeleton of Mediaeval skeletons for York and Canterbury. Grey = Stage 1 unfused. Green = Stage 2 partial fusion. Yellow = Stage 3 complete fusion. The fusion sites are: Occipital of the skull: (1) pars lateralis to pars basilaris, (2) spheno-occipital synchondrosis, Atlas of the cervical vertebrae: (3) Anterior arch, (4) Posterior synchondrosis, Axis of the cervical vertebrae: (5) Ossiculum terminale to the dens, (6) Dentoneural synchondrosis, (7) Dentocentral & neurocentral junctions



### The Axis

Fusion was underway (Stage 2) at age 8 years for Mediaeval York for the **ossiculum terminale** to the dens. Most juveniles had completed fusion (Stage 3) by age 9 years, but one individual remained unfused at age 11 years. In comparison, fusion was underway (Stage 2) between 8 to 15 years in the Canterbury sample. However, some individuals remained unfused (Stage 1) up until age 14 years. Complete fusion (Stage 3) did not occur for the entire sample until age 16 years. When the two groups were compared, it was revealed that fusion (Stages 2 and 3) occurred at a significantly younger age in York than Canterbury ( $U=17.000, p=0.005$ ). This is illustrated in **Figure 6. 1**. This remained statistically significant when a Bonferroni correction test was performed on the data (See **Appendix 3**).

Figure 6. 1: Timing of fusion of the ossiculum terminale to the dens between Mediaeval groups. Mediaeval York only had one individual at age 8 years in partial fusion (Stage 2).



Fusion was underway (Stage 2) at age 6 years ( $n = 1$ ) for the **dentoneural synchondrosis** in Mediaeval York, but some children had already completed fusion (Stage 3) at age 5 years ( $n = 2$ ). Fusion (Stages 2 and 3) occurred between 3 to 6 years for Mediaeval Canterbury, with complete fusion (Stage 3) occurring for the entire sample by 7 years. When fusion (Stages 2

and 3) was compared between the two groups, no significant differences were revealed ( $U=9.500$ ,  $p=0.251$ ).

Fusion was underway (Stage 2) between 5 to 13 years for the **dentocentral and neurocentral junctions** in Mediaeval York. Complete fusion (Stage 3) occurred at the earliest of 9 years and for the entire sample by 15 years. The range of ages over which fusion was underway (Stage 2) was much wider in Canterbury (3 to 16 years) compared to York. However, there were no significant differences between the groups for when fusion was underway (Stage 2,  $U=70.000$ ,  $p=0.698$ ), nor overall fusion (Stages 2 and 3,  $U=348.00$ ,  $p=0.602$ ).

### 6.2.2. The upper appendicular skeleton

Age-at-fusion for the upper appendicular skeleton is presented in **Table 6. 2**.

#### *A) The Scapula*

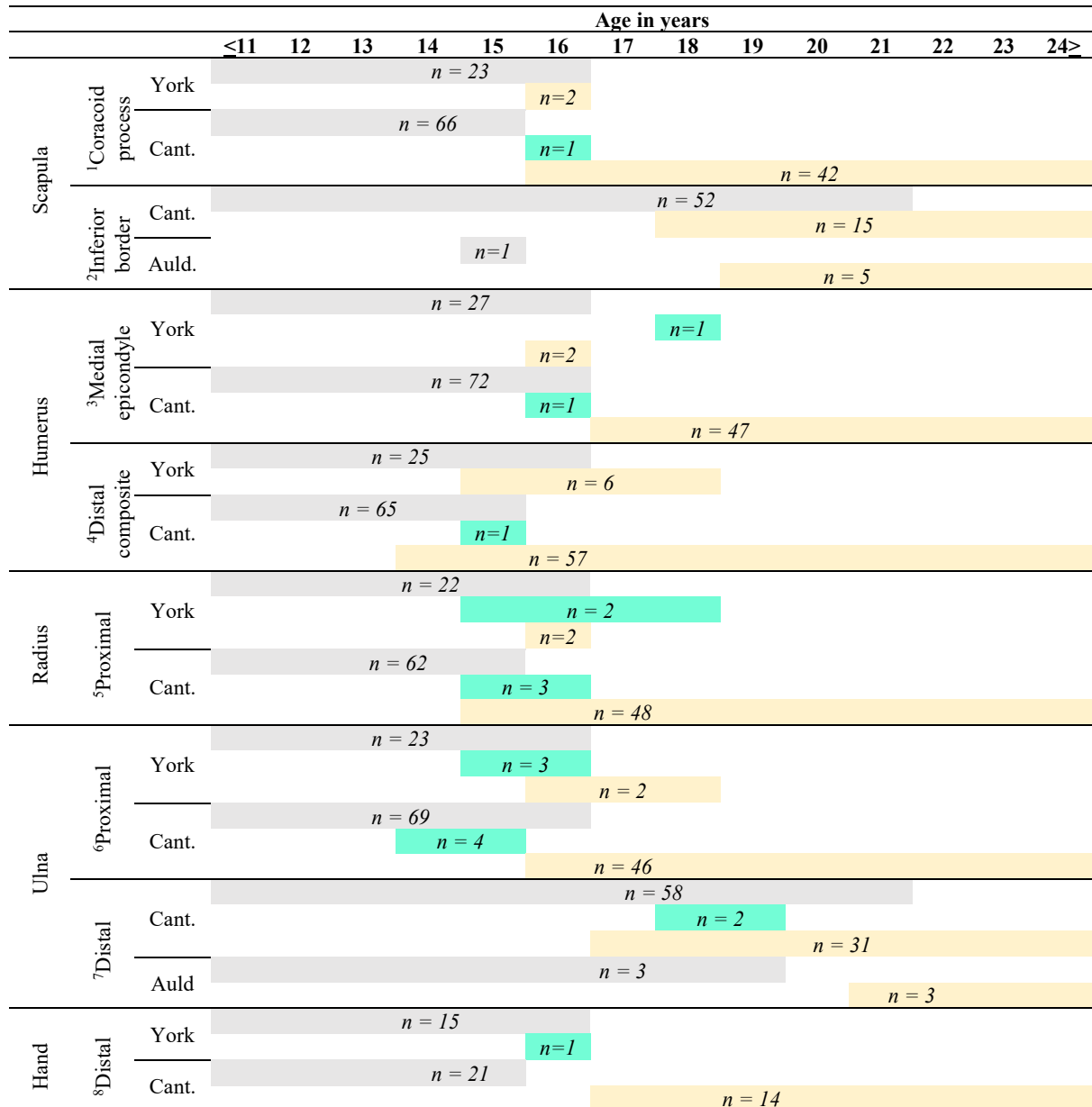
At age 16 years, Mediaeval York adolescents were either unfused (Stage 1,  $n = 2$ ) or had completed fusion (Stage 3,  $n = 2$ ) for the **coracoid process**. Fusion was found to be underway (Stage 2) at age 16 years for Mediaeval Canterbury. The entire Canterbury sample had completed fusion (Stage 3) by age 17 years.

Individuals remained unfused (Stage 1) for the **inferior border** in the Canterbury sample up until age 21 years. Some adolescents completed fusion (Stage 3) at age 18 years, but the entire sample did not complete fusion (Stage 3) until age 22 years. One skeleton was recorded as unfused (Stage 1) at 15 years in the Auldham sample. Three Auldham skeletons, aged at nineteen, twenty-one and twenty-two were recorded as having completed fusion (Stage 3).

#### *B) The Humerus*

Fusion occurred (Stages 2 and 3) between 16 to 18 years for the **medial epicondyle** in the Mediaeval York sample and between 16 to 17 years for Canterbury. When fusion (Stages 2 and 3) was compared between the two groups, no significant differences were revealed ( $U = 4.000$ ,  $p=0.814$ ). Some York adolescents had completed fusion (Stage 3) of the **distal composite epiphysis** by 15 years, but the entire sample did not complete fusion until age 18 years. Fusion (Stages 2 and 3) occurred between 14 to 15 years for the Canterbury sample.

Table 6. 2: Age and phase for the fusion of the upper appendicular skeleton of Mediaeval skeletons for York, Canterbury and Auldham. Grey = Stage 1 unfused. Green = Stage 2 partial fusion. Yellow = Stage 3 complete fusion. The fusion sites include, Scapula: (1) coracoid process, (2) inferior border, Humerus: (3) medial epicondyle, (4) distal composite epiphysis, Radius: (5) proximal epiphysis, Ulna: (6) proximal and (7) distal epiphyses, Hand: (8) distal phalanges



*C) The Radius*

Fusion was underway (Stage 2) for the **proximal epiphysis** between 15 to 18 years in the Mediaeval York sample and 15 to 16 years in the Mediaeval Canterbury sample. The mean age for when fusion was underway (Stage 2) was therefore similar between the two groups, as no significant differences were found ( $U=2.500, p=0.761$ ).

*D) The Ulna*

Fusion was underway (Stage 2) for the **proximal epiphysis** between 15 to 16 years in the Mediaeval York sample. Whereas fusion (Stages 2 and 3) occurred between 14 to 16 years for Mediaeval Canterbury. The mean age of when fusion was underway (Stage 2) was similar between the two groups, as no significant differences were found ( $U=1.500, p=0.076$ ). Fusion (Stages 2 and 3) occurred between 17 to 21 years for the **distal epiphysis** in the Mediaeval Canterbury sample. Auldhame skeletons were unfused (Stage 1) at  $\leq 19$  years ( $n = 3$ ) and had completed fusion (Stage 3) at  $\geq 21$  years ( $n = 3$ ).

*E) The Hand*

Fusion was underway (Stage 2) for the **distal phalanges** of the hand at 16 years in the York sample. In the Canterbury sample, skeletons  $\leq 15$  years ( $n = 21$ ) were unfused and skeletons  $\geq 17$  years ( $n = 14$ ) had completed fusion (Stage 3).

**6.2.3. The lower appendicular skeleton**

Age-at-fusion for the lower appendicular skeleton is presented in **Table 6. 3**.

*A) The Os coxae*

One skeleton, aged at 10 years, was found to have an unfused (Stage 1) **ischiopubic ramus** in the Mediaeval York sample, while all other individuals between 9 to 14 years had completed fusion (Stage 3). Canterbury skeletons between 9 to 14 years were found unfused (Stage 1), whereas those aged between 13 to 16 years had completed fusion (Stage 3).

Some Canterbury individuals remained unfused for their **iliac crest** until 21 years. Fusion was underway (Stage 2) between 17 to 23 years and the entire sample completed fusion (Stage 3) by 24 years. Fusion was underway (Stage 2) at age 19 years for Auldhame and the

entire sample had completed fusion (Stage 3) by 21 years. When fusion (Stages 2 and 3) was compared between the two groups, no significant differences were found ( $U=25.500, p=0.586$ ).

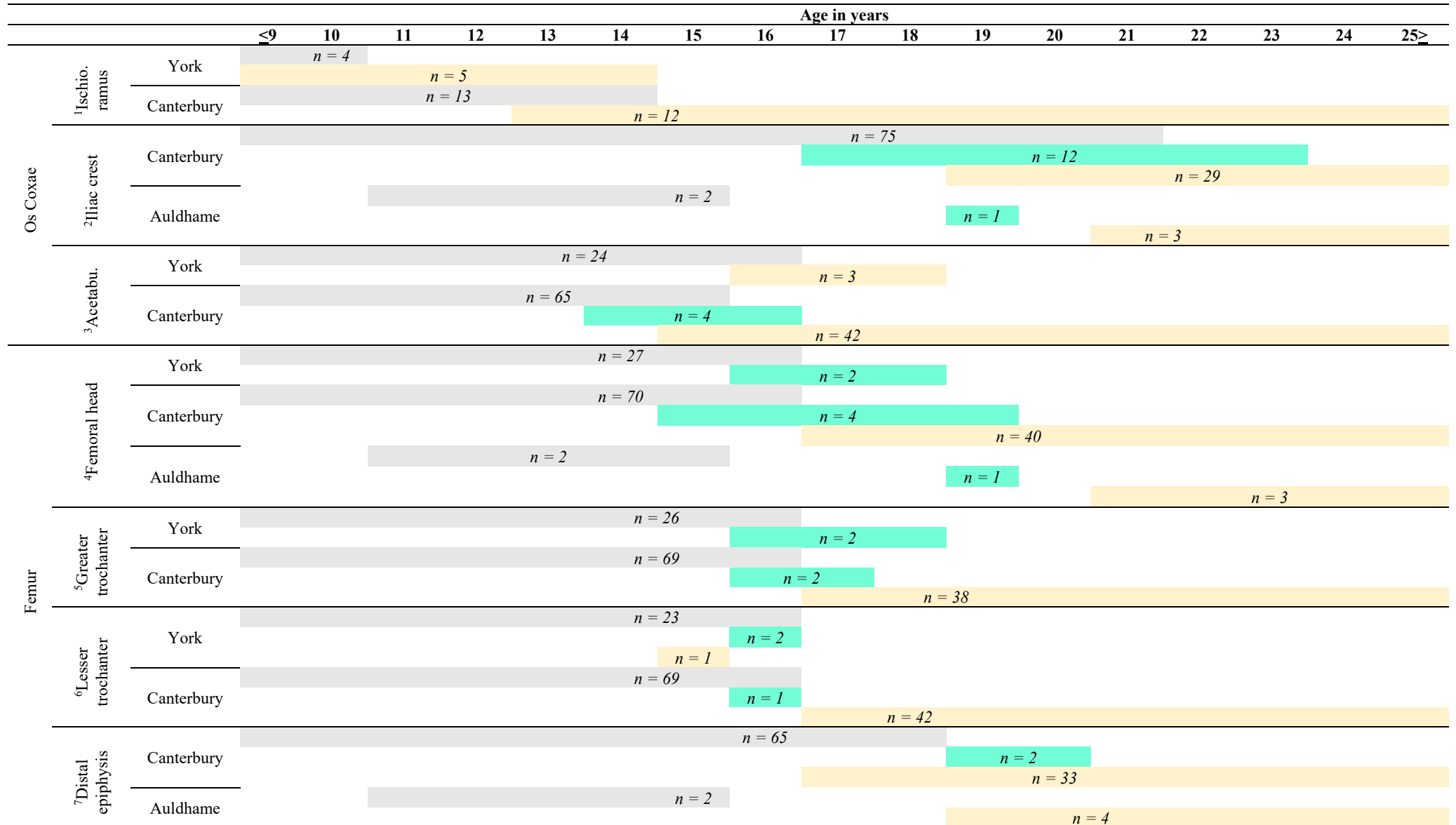
At age  $\leq 15$  years, all York skeletons ( $n = 24$ ) were unfused (Stage 1) for the **acetabulum**. At age 16 years, individuals were found both unfused ( $n = 1$ , Stage 1) and having completed fusion ( $n = 2$ , Stage 3). Fusion was underway (Stage 2) between 14 to 16 years for Canterbury. The entire sample had completed fusion (Stage 3) by age 17 years.

### *B) The Femur*

Fusion was underway (Stage 2) between 16 to 18 years for the **femoral head** in Mediaeval York. Fusion was underway (Stage 2) between 15 to 19 years for Mediaeval Canterbury. The femoral head was unfused (Stage 1) at  $\leq 15$  years ( $n = 2$ ) in Auldhame and had completed fusion (Stage 3) by  $\geq 21$  years ( $n = 3$ ), with fusion underway (Stage 2) in one individual aged 19 years.

Fusion was underway (Stage 2) for the **greater trochanter** between 16 to 18 years for York and between 16 to 17 years for Canterbury. When partial fusion (Stage 2) was compared between the two groups, no significant differences were found ( $U=1.500, p=0.683$ ). Meanwhile, fusion (Stages 2 and 3) occurred between 15 to 16 years for the **lesser trochanter** in the York sample and between 16 to 17 years for Canterbury. When fusion (Stages 2 and 3) was compared between the two groups, no significant differences were found ( $U=1.000, p=0.099$ ). Fusion occurred (Stages 2 and 3) between 17 to 20 years for the **distal epiphysis** in the Mediaeval Canterbury sample. One Auldhame skeleton was recorded as unfused (Stage 1) at age 15 years, whereas skeletons aged at nineteen, twenty-one and twenty-two were recorded as having completed fusion (Stage 3).

Table 6. 3: Age and phase for the fusion of the lower appendicular skeleton of Mediaeval skeletons for York, Canterbury and Auldham. Grey = Stage 1 unfused. Green = Stage 2 partial fusion. Yellow = Stage 3 complete fusion. The fusion sites include, Os coxae: (1) ischiopubic ramus, (2) iliac crest, (3) acetabulum, Femur: (4) Femoral head, (5) greater and (6) lesser trochanters, (7) distal epiphysis



### C) The Tibia

Fusion was underway (Stage 2) for the **proximal epiphysis** of the tibia between 17 to 19 years in the Mediaeval Canterbury sample (**Table 6. 4**). As for Auldhame, skeletons aged at  $\leq 15$  years ( $n = 2$ ) were unfused (Stage 1). Fusion was recorded as having completed (Stage 3) at  $\geq 19$  years ( $n = 4$ ). The fusion of the **distal epiphysis** was underway (Stage 2) at age 16 years ( $n = 2$ ) for Mediaeval York. Fusion was underway (Stage 2) between 17 to 18 years for Canterbury ( $n = 2$ ).

Table 6. 4: Age and phase for the fusion of the proximal and distal tibia of Mediaeval skeletons for York, Canterbury and Auldhame. Grey = Stage 1 unfused. Green = Stage 2 partial fusion. Yellow = Stage 3 complete fusion.

		Age in years										
		<14	15	16	17	18	19	20	21	22	≥	
Tibia	Proximal	Cant.	n = 59			n = 3		n = 30				
		Auld.	n = 2		n = 4							
	Distal	York	n = 18		n = 2							
		Cant.	n = 53			n = 2		n = 30				

#### 6.2.4. Summary of univariate significant findings

The ossiculum terminale fused (Stages 2 and 3) to the dens of the axis on the cervical vertebrae at a significantly older age in the Mediaeval Canterbury sample compared to York. Other non-significant trends were observed. These included an earlier age-at-fusion in the Canterbury sample compared to either Auldhame or York for the dentocentral and neurocentral junctions of the axis (York), the distal ulna (Auldhame), femoral head (Auldhame), distal femur (Auldhame) and the proximal tibia (Auldhame). It is possible that the lack of differences could be due in part to the smaller sample for Mediaeval York and Auldhame compared to Canterbury.

### 6.2.5. Multivariate Analysis

A multiple regression was performed on the data to determine if Mediaeval Canterbury, York and Auldham could be distinguished by the age at which fusion occurred. Before carrying out the regression, test assumptions were checked. These assumptions are presented in **Table 6. 5 - Table 6. 10**. The age range chosen and the fusion sites that were grouped were based on when each epiphysis fused, and therefore, some fusion sites are found in multiple tests as they fuse over a longer age range or were split over multiple tests to pass the assumptions. Some tests that were violated meant that the test could not be carried out, whereas other tests were cautionary (Lund and Lund, 2013b). This is given in the tables below.

Table 6. 5: Data tested prior to carrying out the multiple regression.

Assumption	Test	Fusion sites	Age range (years)	Result	Pass or fail of test
Independence of observation	Durbin-Watson		3 - 10	2.047	✓
A linear relationship exists between the variables	Scatter plot between Studentised Deleted Residual and Studentised Residual	Dentoneural synchondrosis C2 Posterior synchondrosis of C1 & C2		See <b>Appendix 8</b>	✓
The data must show homoscedasticity	Studentised Residual				✓
The data must not show multicollinearity	Collinearity Statistics			Initially, the test failed. The pars lateralis to pars basilaris, and the anterior arch of the atlas was removed, and the test was run again.	
Data should not have any significant outliers, high leverage points or highly influential points	Case wise diagnostics			No case wise diagnostic	✓
	Leverage points			See <b>Appendix 8</b>	✓
	Cook's Distance Values				✓
Errors are normally distributed	Histogram				✓

Table 6. 6: Data tested prior to carrying out the multiple regression.

Assumption	Test	Fusion sites	Age range (years)	Result	Pass or fail of test
Independence of observation	Durbin-Watson		3 - 15	1.841	✓
A linear relationship exists between the variables	Scatter plot between Studentised Deleted Residual and Studentised Residual	Anterior arch C1 Posterior synchondrosis C1 Ossiculum terminale C2 Dentocentral & neurocentral junctions C2		See <b>Appendix 8</b>	✓
The data must show homoscedasticity	Collinearity Statistics				✓
The data must not show multicollinearity	Case wise diagnostics			No case wise diagnostic	✓
Data should not have any significant outliers, high leverage points or highly influential points	Leverage points			See <b>Appendix 8</b>	✓
	Cook's Distance Values				✓
Errors are normally distributed	Histogram				✓

Table 6. 7: Data tested prior to carrying out the multiple regression. Fusion sites listed in short-hand are the following: 1. Medial epicondyle of the humerus, 2. Spheno-occipital synchondrosis, and 3. Distal phalangeal epiphyses of the hand.

Assumption	Test	Fusion sites	Age range (years)	Result	Pass or fail of test
Independence of observation	Durbin-Watson		11 - 18	2.000	✓
A linear relationship exists between the variables	Scatter plot between Studentised Deleted Residual and Studentised Residual	Acetabulum Ischiopubic ramus Distal humerus Metacarpals		The data failed both tests. The data was transformed but continued to fail the test. This age range was therefore abandoned.	
The data must show homoscedasticity					
The data must not show multicollinearity	Collinearity Statistics	1. MedHum 2. SphenoOc 3. DistalPhala	12 - 19	The test failed the test on all fusion sites. The test was abandoned.	
Independence of observation	Durbin-Watson		13 - 20	2.001	✓
A linear relationship exists between the variables	Scatter plot between Studentised Deleted Residual and Studentised Residual			See <b>Appendix 8</b>	✓
The data must show homoscedasticity					✓
The data must not show multicollinearity	Collinearity Statistics	Acromial border Proximal tibia Greater trochanter Femoral head			✓
Data should not have any significant outliers, high leverage points or highly influential points	Case wise diagnostics Leverage points Cook's Distance Values			No case wise diagnostic Six data points are listed as cautionary. See <b>Appendix 8</b>	✓
Errors are normally distributed	Histogram				✓

Table 6. 8: Data tested prior to carrying out the multiple regression.

Independence of observation	Durbin-Watson		13 - 20	2.027	✓
A linear relationship exists between the variables	Scatter plot between Studentised Deleted Residual and Studentised Residual			See <b>Appendix 8</b>	✓
The data must show homoscedasticity	Studentised Residual				✓
The data must not show multicollinearity	Collinearity Statistics	Lesser trochanter Distal femur		Initially, the test failed. The distal tibia was removed, and the tests rerun.	
Data should not have any significant outliers, high leverage points or highly influential points	Case wise diagnostics			No case wise diagnostic	✓
	Leverage points			Three data points are listed as cautionary	
	Cook's Distance Values			See <b>Appendix 8</b>	✓
Errors are normally distributed	Histogram				✓

Table 6. 9: Data tested prior to carrying out the multiple regression.

Assumption	Test	Fusion sites	Age range (years)	Result	Pass or fail of test
Independence of observation	Durbin-Watson		16 - 23	2.720	This can be considered slightly cautionary.
A linear relationship exists between the variables	Scatter plot between Studentised Deleted Residual and Studentised Residual	Lateral clavicle Inferior angle of scapula Iliac crest		See <b>Appendix 8</b>	✓
The data must show homoscedasticity					✓
The data must not show multicollinearity	Collinearity Statistics			Initially, the test failed. The distal radius and the proximal humerus were removed and the tests rerun.	
Data should not have any significant outliers, high leverage points or highly influential points	Case wise diagnostics			No case wise diagnostic	✓
	Leverage points			See <b>Appendix 8</b>	✓
	Cook's Distance Values				✓
Errors are normally distributed	Histogram				✓

Table 6. 10: Data tested prior to carrying out the multiple regression.

Assumption	Test	Fusion sites	Age range (years)	Result	Pass or fail of test
Independence of observation	Durbin-Watson		16 – 30	1.827	✓
A linear relationship exists between the variables	Scatter plot between Studentised Deleted Residual and Studentised Residual			See <b>Appendix 8</b>	✓
The data must show homoscedasticity	Studentised Residual				✓
The data must not show multicollinearity	Collinearity Statistics	Lateral clavicle Medial clavicle Sacral bodies 1 & 2		Initially, this test failed, but the iliac crest and medial border of the scapula were removed and the tests rerun	
Data should not have any significant outliers, high leverage points or highly influential points	Case wise diagnostics Leverage points Cook's Distance Values			No case wise diagnostic See <b>Appendix 8</b>	✓ Some points are approaching dangerous levels. ✓
Errors are normally distributed	Histogram				✓

If the variables passed the assumptions, a multiple regression was run on those variables and presented in **Table 6. 11 - Table 6. 12**. When analysing the tables,  $r$  shows if the data is a good fit or not. The closer  $r$  is to one, the better the fit. All results presented show a good fit with the data. The Adjusted  $r^2$  shows whether the independent variables explain the dependent variable (M. Lund and Lund, 2018). Many of the Adjusted  $r^2$  shows that around 56.4 to 74.1% of the independent variables explain the dependent variable: age, with fusion sites in the leg showing the highest percentage with age.

A few independent variables were found to be significant. The posterior synchondrosis of the atlas (**Table 6. 11**) was found to be significantly associated ( $p = 0.016$ ) with the age group: 3 to 10 years. The posterior synchondrosis of the atlas had Canterbury individuals unfused (Stage 1) at later ages than York. The ossiculum terminale ( $p < 0.001$ ) and Mediaeval site ( $p = 0.034$ ) were found to be significantly associated with the age group: 3 to 15 years. As age increases, more Canterbury skeletons would be present, and fusion of the ossiculum terminale would be further advanced. When the data is represented in a scatter diagram (**Figure 6. 2**), the multiple regression is most likely suggesting that partial fusion (Stage 2) of the ossiculum terminale is found in greater numbers and at a more advanced age in Mediaeval Canterbury than in York or Auldham. This fits with the univariate analysis above that found that fusion (Stages 2 and 3) occurred at a significantly younger age in York than in Canterbury.

The fusion of the greater trochanter of the femur in the age group: 13 to 20 years (**Table 6. 12**) was found to be significant ( $p = 0.022$ ), as well as the lesser trochanter ( $p < 0.001$ ) and distal epiphysis of the femur ( $p = 0.0011$ ) in the same age group. These fusion sites had a greater variation of fusion in the Canterbury skeletons compared with York or Auldham, and this may have contributed to these significant results. This may also have been why the fusion sites of the leg had the best fit for the model. A Bonferroni corrections test was performed on the data and only the ossiculum terminale and lesser trochanter of the femur remained statistically significant (see **Appendix 3**).

Table 6. 11: Multiple regression results for Mediaeval Canterbury, York and Auldham, between the ages of 3 to 10 years and 3 to 15 years. \*\* = statistically significant.

Age range (years)	Independent variables	B	p	ANOVA	r	Adjusted $r^2$
3 - 10	Mediaeval Site	0.669	0.411			
	Posterior synchondrosis of atlas	1.317	<b>0.016**</b>			
	Dentoneural synchondrosis of axis	0.816	0.162	$F(4, 21)$ 11.244, $p < 0.001$	0.826	0.621
	Posterior synchondrosis of axis	0.456	0.597			
3 - 15	Mediaeval Site	-1.635	<b>0.034**</b>			
	Anterior arch of atlas	1.183	0.141			
	Posterior synchondrosis of atlas	0.044	0.951	$F(5, 39)$ 19.568, $p < 0.001$	0.846	0.678
	Ossiculum terminale	2.214	<b>&lt;0.001**</b>			
	Dentocentral & neurocentral junctions	0.697	0.319			

Figure 6. 2: Scatter plot of the fusion stage of the ossiculum terminale of the axis compared to the age-at-death in years of each skeleton from each respective Mediaeval site.

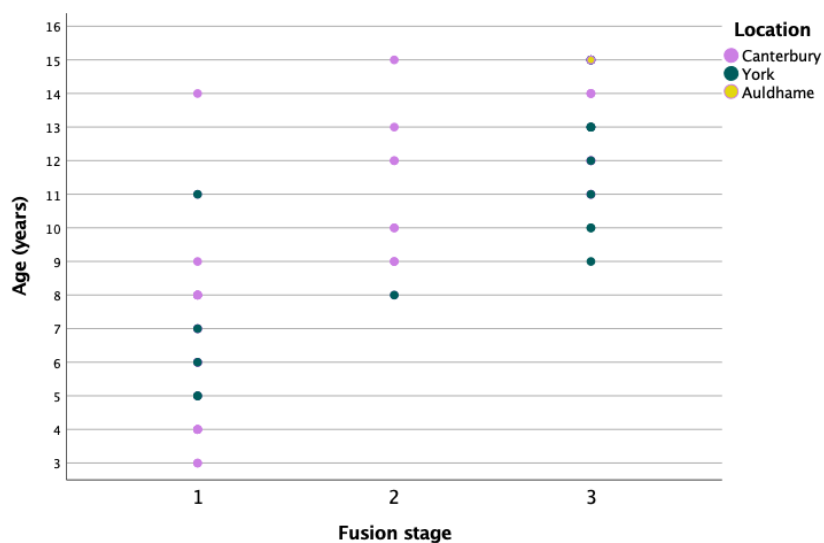


Table 6. 12: Multiple regression results for Mediaeval Canterbury, York and Auldham, between the ages of 13 to 20 for the proximal epiphyses of the leg, along with the acromial border of the scapula, and the greater trochanter, 13 to 20 for the lesser trochanter and the distal femur, 16 to 23, and 16 to 30 years. \*\* = statistically significant.

Age range (years)	Independent variables	B	p	ANOVA	r	Adjusted r <sup>2</sup>
13 - 20	Mediaeval Site	0.109	0.781			
	Acromial border of scapula	0.337	0.617			
	Femoral head	0.037	0.959	F (5, 22) 16.447, p<0.001	0.888	0.741
	Greater trochanter	1.493	<b>0.022**</b>			
	Proximal tibia	0.205	0.782			
13 - 20	Mediaeval Site	-0.051	0.869			
	Lesser trochanter	1.307	<b>&lt;0.001**</b>	F (3, 34) 34.913, p,<0.001	0.869	0.733
	Distal Femur	0.930	<b>0.011**</b>			
16 - 23	Mediaeval Site	0.013	0.984			
	Lateral clavicle	0.900	0.178			
	Inferior Angle of the Scapula	0.544	0.333	F (4, 9) 5.208, p = 0.019	0.836	0.564
16 - 30	Iliac Crest	1.215	0.519			
	Mediaeval Site	-0.196	0.825			
	Lateral clavicle	.0433	0.642			
	Medial clavicle	1.419	0.163	F (4, 16) 8.088, p<0.001	0.818	0.586
	Sacral bodies 1 & 2	2.170	0.122			

### 6.3. COMPARING AGE-AT-FUSION BETWEEN IRON AGE, ROMAN, ANGLO-SAXON, MEDIAEVAL AND POST-MEDIAEVAL SITES

#### 6.3.1. The axial skeleton

Age-at-fusion and age distribution for all sites can be found in **Appendix 9**. This sub-section gives the results of age-at-fusion for the axial skeleton for all archaeological groups (**Table 6. 13 to Table 6. 15**).

##### A) The Skull

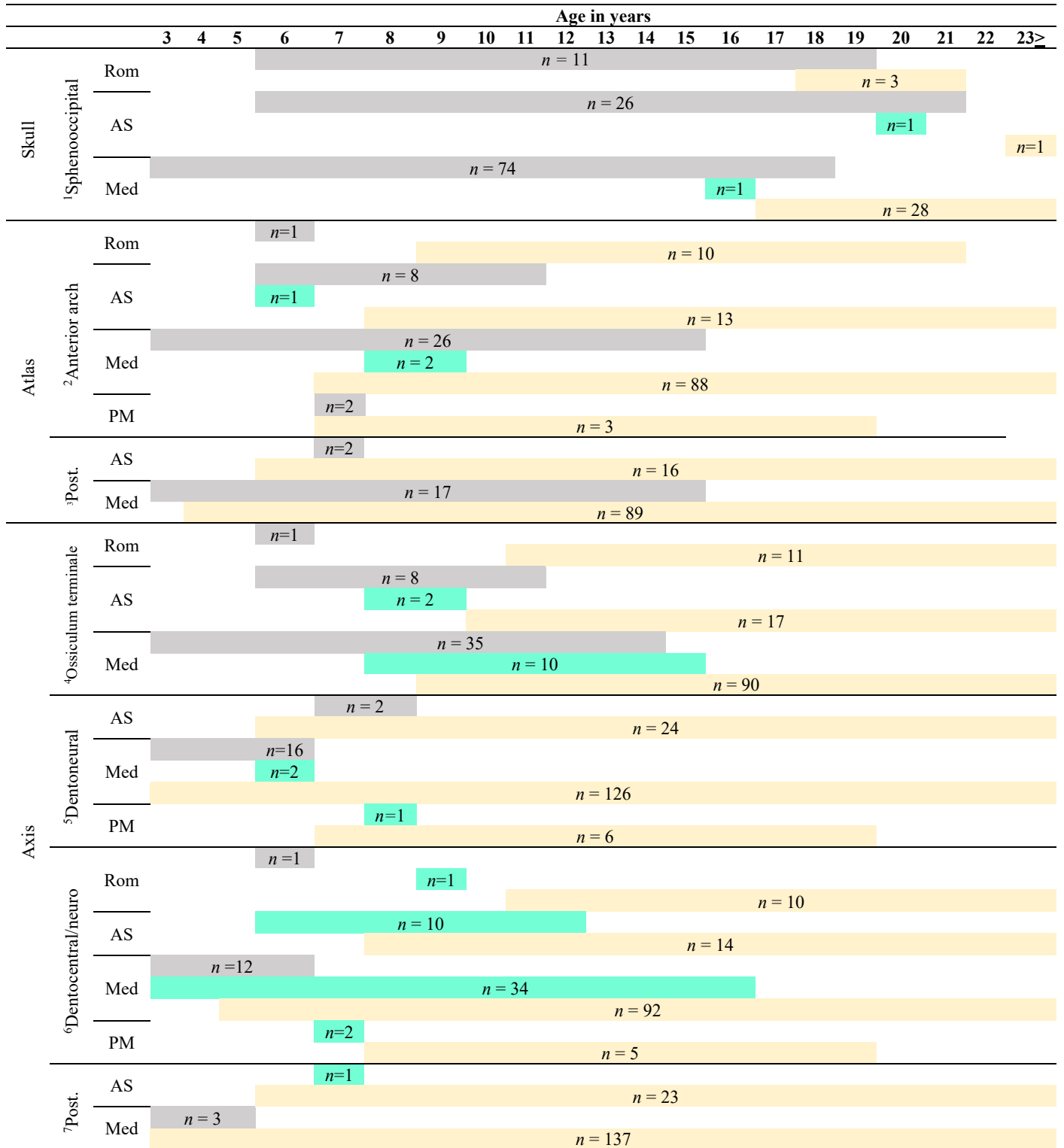
Fusion was underway (Stage 2) for the **pars lateralis to pars basilaris** of the occipital of the skull between 6 to 8 years for the Anglo-Saxon sample and completely fused (Stage 3) for the entire sample by 9 years (**Table 6. 13**). No Mediaeval skeletons had a partially fused (Stage 2) pars lateralis to pars basilaris.

Table 6. 13: Age and phase of the pars lateralis to the pars basilaris of the skull for Roman, Anglo-Saxon, and Mediaeval groups collected from British archaeological collections. Grey = Stage 1 unfused. Green = Stage 2 partial fusion. Yellow = Stage 3 complete fusion.

		Age in years																	
		3	4	5	6	7	8	9	10	11	12	13	14	15	16	17	18	19	≥
Skull	Pars lat. to bas.																		
	Rom				n=1														
	AS				n=5	n=3													
	Med				n=28														

Complete fusion (Stage 3) of the **spheno-occipital synchondrosis** (**Table 6. 14**) had occurred by the age of 9 years for the Roman sample. Fusion was underway (Stage 2) between 6 to 8 years for the Anglo-Saxon sample, with the earliest age at complete fusion (Stage 3) occurring at age 7 years. Mediaeval individuals were found unfused (Stage 1) and completely fused (Stage 3) between the ages of 7 to 8 years. Fusion (Stages 2 and 3) of the spheno-occipital synchondrosis occurred in the Anglo-Saxon sample at a significantly later age than the Mediaeval group ( $U = 0.000$ ,  $p = 0.032$ ). This was not statistically significant when a Bonferroni corrections test was conducted on the data (See **Appendix 3**).

Table 6. 14: Age and phase for the fusion of the axial skeleton for Roman, Anglo-Saxon, Mediaeval and Post-Mediaeval groups collected from British archaeological collections. Grey = Stage 1 unfused. Green = Stage 2 partial fusion. Yellow = Stage 3 complete fusion. The fusion sites are: The skull: (1) Spheno-occipital, Atlas of the cervical vertebrae: (2) Anterior arch, (3) Posterior synchondrosis, Axis of the cervical vertebrae: (4) Ossiculum terminale, (5) Dentoneural synchondrosis, (6) Dentocentral & neurocentral junctions, (7) Posterior synchondrosis



*B) The Atlas*

Complete fusion (Stage 3) occurred at age 9 years for the Roman group for the **anterior arch** of the atlas. Fusion (Stages 2 and 3) for the Anglo-Saxon group occurred between 6 to 11 years and between 7 to 15 years for the Mediaeval group. Complete fusion (Stage 3) occurred at the earliest age of 7 years for some Post-Mediaeval children. The mean age in which the Anglo-Saxon group completed fusion (Stage 3) of the anterior arch of the atlas was significantly younger compared to the Mediaeval sample ( $U = 30.000, p = 0.037$ ). This was not statistically significant when a Bonferroni corrections test was conducted on the data (See **Appendix 3**).

Two Anglo-Saxon children had an unfused (Stage 1) **posterior synchondrosis** of the atlas at age 7 years, whereas complete fusion (Stage 3) of this site had occurred in all other children from 6 years onwards. Some skeletons from the Mediaeval sample were found to be unfused (Stage 1) up until the age of 15 years. Most Mediaeval skeletons were completely fused (Stage 3) from age 3 years onwards.

*C) The Axis*

Fusion (Stages 2 and 3) of the **ossiculum terminale** of the axis occurred between age 8 to 11 years for the Anglo-Saxon group. Some Mediaeval individuals remained unfused (Stage 1) until age 14 years. Fusion was underway (Stage 2) between 8 to 15 years for Mediaeval skeletons, with the earliest age at complete fusion (Stage 3) being 9 years. The ossiculum terminale fused at a significantly later age in the Mediaeval group compared to the Anglo-Saxon group ( $U = 33.500, p = 0.009$ ). This was not statistically significant when a Bonferroni corrections test was conducted on the data (See **Appendix 3**).

Complete fusion (Stage 3) of the **dentoneural synchondrosis** occurred at the earliest age of 6 years for the Anglo-Saxon group. Complete fusion occurred at the earliest age of 3 years for the Mediaeval group, although complete fusion had not occurred for the entire sample until age 7 years. Fusion was underway (Stage 2) for one Post-Mediaeval juvenile at age 8 years.

Fusion of the **dentocentral and neurocentral junctions** was underway at age 9 years for the Roman sample, with complete fusion (Stage 3) occurring at age 11 years. Fusion was underway (Stage 2) for the Anglo-Saxon sample between 6 to 12 years. Complete fusion (Stage 3) occurred for the entire sample at age 14 years. No Mediaeval skeletons remained unfused (Stage 1)  $\geq 7$  years. Fusion was underway (Stage 2) between 3 to 16 years and complete fusion (Stage 3) for the entire Mediaeval sample occurred at age 17 years. Two Post-Mediaeval

children were found to be in Stage two at age 7 years, with complete fusion (Stage 3) occurring at age 8 years for the entire sample.

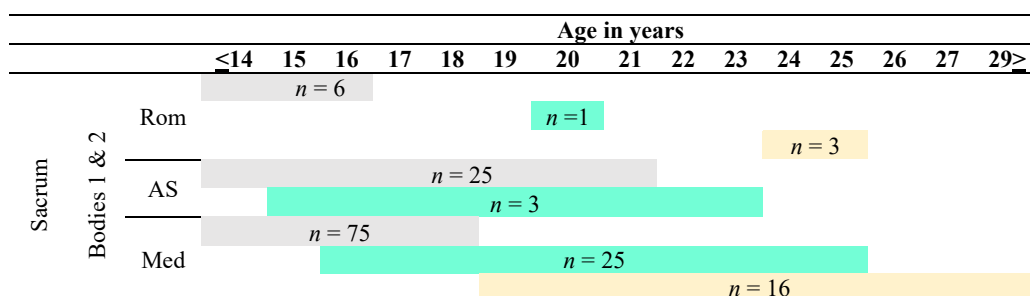
When the mean age-at-fusion (Stages 2 and 3) of the dentocentral and neurocentral junctions was compared between the Anglo-Saxon and Mediaeval samples, the Mediaeval group was found to fuse at a significantly later age than the Anglo-Saxons ( $U = 379.000$ ,  $p = 0.037$ ). This was not statistically significant when a Bonferroni corrections test was run on the data (See **Appendix 3**). Mean age-at-fusion did not differ significantly between the Anglo-Saxons and the Post-Mediaeval groups ( $U = 13.000$ ,  $p = 0.304$ ), nor the Mediaeval and Post-Mediaeval groups ( $U = 45.500$ ,  $p = 0.062$ ). There were also no statistically significant differences in the mean age in which fusion was underway (Stage 2) between the Anglo-Saxon and Mediaeval groups ( $U = 162.000$ ,  $p = 0.822$ ). The Post-Mediaeval group did not differ significantly when compared to the Anglo-Saxon group ( $U = 7.000$ ,  $p = 0.502$ ) or the Mediaeval group ( $U = 23.000$ ,  $p = 0.445$ ).

Fusion of the **posterior synchondrosis** was underway for some Anglo-Saxon children at age 7 years, but some children had already completed fusion (Stage 3) at age 6 years. The earliest age to complete fusion for the Mediaeval group was 3 years, but the entire sample did not complete fusion until age 6 years.

#### D) The sacrum

Fusion was underway (Stage 2) for the Anglo-Saxon sample for the **sacral bodies 1 and 2** between 15 to 23 years, whereas fusion was underway for the Mediaeval sample between 16 to 25 years (**Table 6. 15**). When Stage 2 was compared between these two groups, no significant differences were found ( $U = 22.500$ ,  $p = 1.000$ ).

Table 6. 15: Age and phase for the fusion of bodies 1 and 2 of the sacrum for Roman, Anglo-Saxon, and Mediaeval groups collected from British archaeological collections. Grey = Stage 1 unfused. Green = Stage 2 partial fusion. Yellow = Stage 3 complete fusion.



### 6.3.2. The upper appendicular skeleton

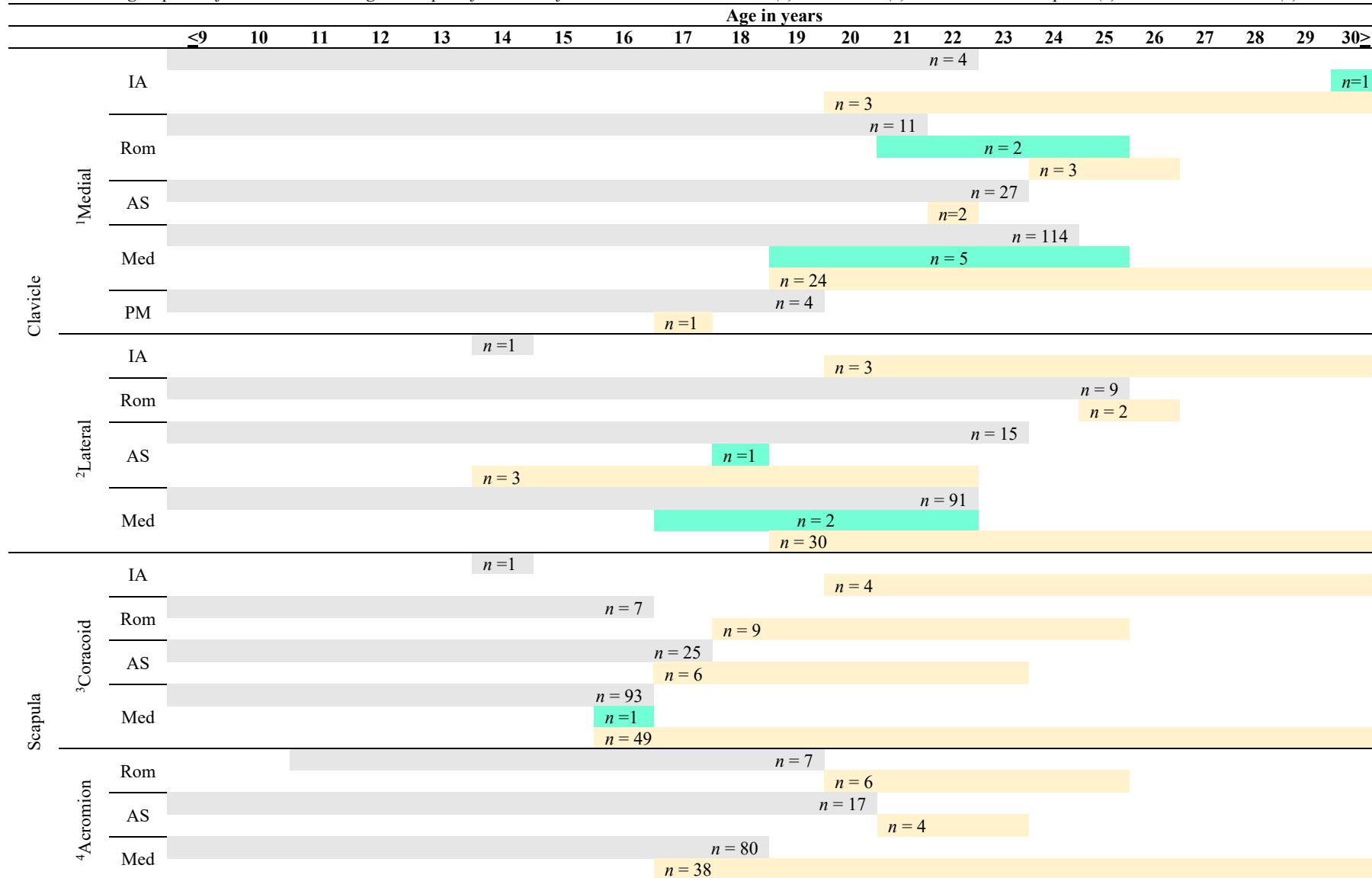
#### *A) The Clavicle*

Fusion was underway (Stage 2) for the **medial clavicle** between 21 to 25 years of age for the Roman sample and between 19 to 25 years for the Mediaeval sample (**Table 6. 16**). The mean age-at-fusion (Stages 2 and 3) was compared between these two groups, but no significant differences were found ( $U = 20.500, p = 0.259$ ). As for the **lateral clavicle**, fusion (Stages 2 and 3) occurred between 14 to 23 years for the Anglo-Saxon sample and between 17 to 22 years for the Mediaeval sample. No statically significant differences were found in the mean age-at-fusion between these two groups ( $U = 24.000, p = 0.442$ ).

#### *B) The Scapula*

Within the Roman sample, the **coracoid** completed fusion (Stage 3) for the entire sample by 18 years of age. Fusion was underway (Stage 2) at age 16 years for the Mediaeval group, with the entire sample having completed fusion (Stage 3) by age 17 years. The entire Roman sample had completed fusion of the **acromial epiphysis** by 20 years and 21 years for the Anglo-Saxons. The earliest age at complete fusion for the Mediaeval sample was 17 years, but the entire sample did not complete fusion until age 19 years.

Table 6. 16: Age and phase for the fusion of the upper appendicular skeleton for the Iron Age, Roman, Anglo-Saxon, Mediaeval and Post-Mediaeval groups collected from British archaeological collections. Grey = Stage 1 unfused. Green = Stage 2 partial fusion. Yellow = Stage 3 complete fusion. The fusion sites are: the clavicle: (1) medial and (2) lateral, and the scapula: (1) the coracoid and (2) the acromion



Complete fusion (Stage 3) of the **medial border** of the scapula (**Table 6. 17**) occurred at age 22 years for the Anglo-Saxon sample. Although complete fusion occurred at the earliest age of 19 years for the Mediaeval sample, the entire sample did not complete fusion until age 25 years. Complete fusion of the **inferior angle** occurred at age 22 years for the Anglo-Saxons. The earliest age for complete fusion to occur in the Mediaeval sample was 18 years, but the entire sample did not complete fusion until age 22 years.

Table 6. 17: Age and phase for the fusion of the (1) medial border and (2) inferior angle of the scapula for the Anglo-Saxon and Mediaeval groups collected from British archaeological collections. Grey = Stage 1 unfused. Green = Stage 2 partial fusion. Yellow = Stage 3 complete fusion.

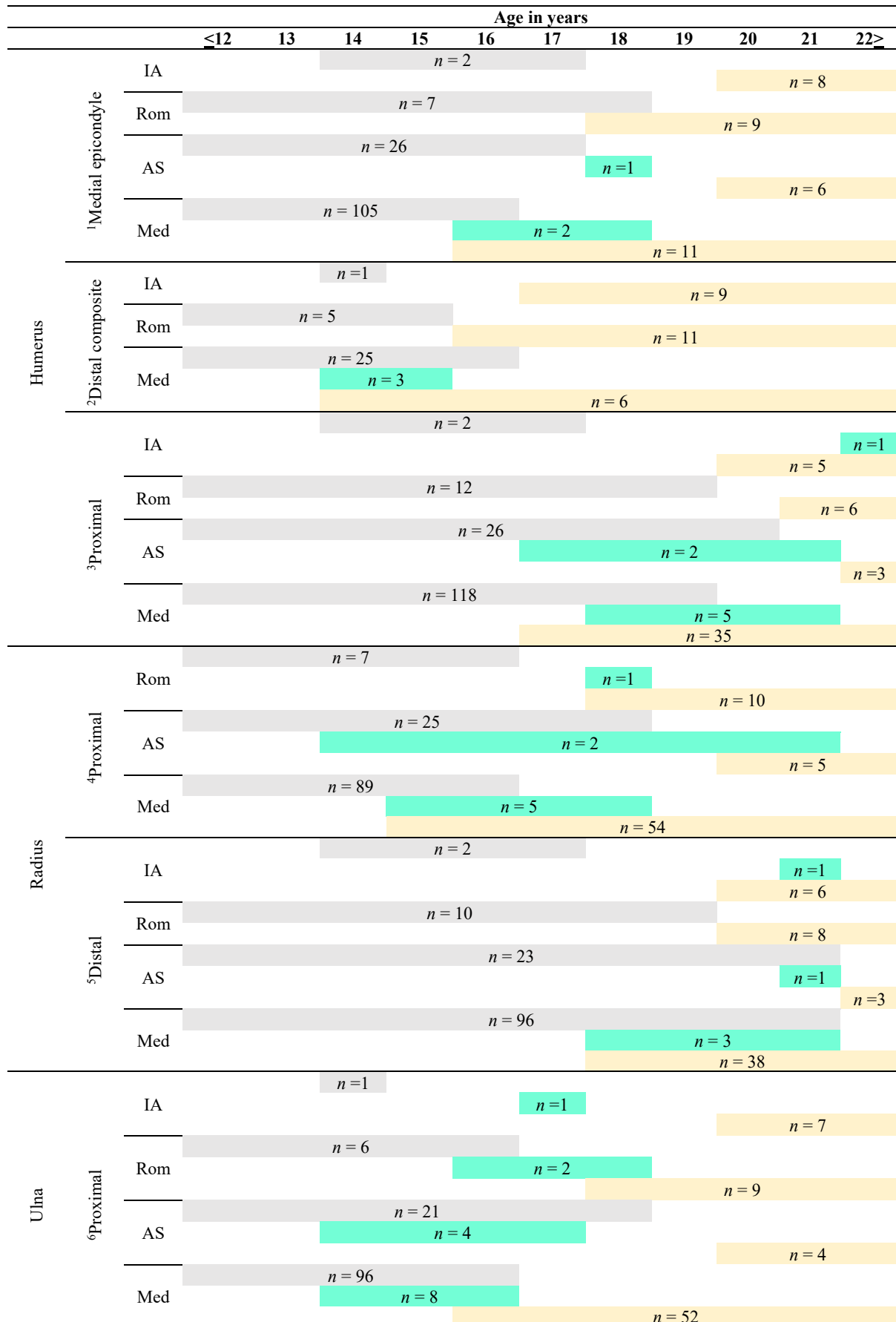
		Age in years															
		≤ 10	11	12	13	14	15	16	17	18	19	20	21	22	23	24	25≥
Scapula	<sup>1</sup> Medial	AS	n = 13													n = 2	
		Med	n = 48													n = 8	
	<sup>2</sup> Inferior	AS	n = 12													n = 2	
		Med	n = 72													n = 20	

### C) The Humerus

The mean age-at-fusion (Stages 2 and 3) for the **medial humeral epicondyle** was similar across the groups (**Table 6. 18**). The earliest age at complete fusion (Stage 3) for the Roman group was 18 years, with the entire sample completing fusion at age 19 years. Evidence of fusion at age 19 years was missing for the Anglo-Saxon sample. However, fusion was underway (Stage 2) at age 18 years and evidence of complete fusion (Stage 3) was present by the age of 20 years. Fusion was underway (Stage 2) between 16 to 18 years for the Mediaeval group and complete fusion (Stage 3) occurred for the entire sample at age 19 years. When the mean age-at-fusion (Stages 2 and 3) was compared between the Anglo-Saxon and Mediaeval groups, no statistically significant differences were present ( $U = 1.000, p = 0.068$ ).

Complete fusion (Stage 3) of the **distal composite epiphysis** occurred at age 17 years for the Iron Age group and age 16 years for the Romans. Fusion was underway (Stage 2) between 14 to 18 years for the Anglo-Saxons and between 14 to 15 years for the Mediaeval group. Complete fusion (Stage 3) occurred for the entire Mediaeval sample at age 14 years.

Table 6. 18: Age and phase for the fusion of the upper appendicular skeleton for the Iron Age, Roman, Anglo-Saxon and Mediaeval groups collected from British archaeological collections. Grey = Stage 1 unfused. Green = Stage 2 partial fusion. Yellow = Stage 3 complete fusion. The fusion sites are: Humerus: (1) medial epicondyle, (2) distal composite epiphysis, (3) proximal epiphysis, Radius: (4) proximal and (5) distal, Ulna: (6) proximal



Fusion (Stages 2 and 3) of the **proximal epiphysis** of the humerus occurred between the ages of 20 to 22 years for the Iron Age sample and between 17 to 22 years for the Anglo-Saxons. Fusion (Stages 2 and 3) occurred between 17 to 21 years for the Mediaeval group. There were no statistically significant differences in the mean age-at-fusion (Stages 2 and 3) when the Anglo-Saxon and Mediaeval samples were compared ( $U = 18.500, p = 0.688$ ).

#### *D) The Radius*

Fusion was underway (Stage 2) for the **proximal epiphysis** of the radius in the Roman sample at 18 years of age, and the entire Roman sample had completed fusion (Stage 3) by the age of 19 years. Fusion was underway (Stage 2) between 14 to 21 years for the Anglo-Saxon sample and between 15 to 18 years for the Mediaeval group. The mean age-at-fusion (Stages 2 and 3) occurred at a significantly younger age in the Roman group, compared with the Anglo-Saxons ( $U = 0.000, p = 0.047$ ). This was not statistically significant when a Bonferroni corrections test was run on the data (See **Appendix 3**). Similarly, fusion (Stages 2 and 3) occurred at a significantly younger age in the Mediaeval group compared to the Anglo-Saxons ( $U = 0.000, p = 0.001$ ). This result remained statistically significant after a Bonferroni corrections test was run on the data (See **Appendix 3**). However, no significant differences were found between the Roman and Mediaeval samples ( $U = 3.000, p = 0.067$ ), though the value approached significance.

Fusion was underway (Stage 2) for the **distal epiphysis** of the radius at age 21 years for both the Iron Age and Anglo-Saxon samples. Complete fusion (Stage 3) occurred at age 20 years for the Roman sample. Fusion was underway (Stage 2) for the Mediaeval sample between 17 to 21 years. No significant differences in the mean age-at-fusion (Stages 2 and 3) were found between the Iron Age and Anglo-Saxon samples ( $U = 1.000, p = 0.099$ ), nor the Iron Age and Mediaeval samples ( $U = 14.500, p = 0.371$ ). However, the mean age-at-fusion was found to occur at a significantly younger age for the Mediaeval group compared to the Anglo-Saxons ( $U = 3.500, p = 0.019$ ). This was not statistically significant when a Bonferroni corrections test was run on the data (See **Appendix 3**).

#### *E) The Ulna*

Fusion of the **proximal epiphysis** of the ulna (**Table 6. 11**) was underway (Stage 2) at age 17 years for the Iron Age sample and between 16 to 18 years of age for the Roman sample. Fusion was underway (Stage 2) between the ages of 14 to 17 years for the Anglo-Saxon sample, with

one unfused (Stage 1) individual at age 18 years. Fusion was underway (Stage 2) between 14 to 16 years for the Mediaeval sample. No significant differences were found in the mean age of Stage 2 fusion when the Romans were compared to the Anglo-Saxons ( $U = 1.000, p = 0.159$ ), or the Mediaeval sample ( $U = 1.000, p = 0.055$ ). Neither did the Anglo-Saxon sample differ significantly when compared to the Mediaeval sample ( $U = 15.000, p = 0.855$ ).

Fusion (Stages 2 and 3) of the **distal epiphysis** of the ulna (**Table 6. 19**) occurred between 20 to 21 years for the Romans, between 21 to 22 years for the Anglo-Saxons, and between 17 to 21 years for the Mediaeval sample. No significant differences in the mean age-at-fusion (Stages 2 and 3) were found between the Roman and Anglo-Saxon samples ( $U = 1.000, p = 0.099$ ), nor the Roman and Mediaeval samples ( $U = 12.500, p = 0.310$ ). However, the mean age-at-fusion was found to be significantly younger in the Mediaeval sample compared to the Anglo-Saxons ( $U = 3.000, p = 0.019$ ). This was not statistically significant when a Bonferroni corrections test was run on the data (See **Appendix 3**).

Table 6. 19 : Age and phase for the fusion of the upper appendicular skeleton for the Iron Age, Roman, Anglo-Saxon, Mediaeval and Post-Mediaeval groups collected from British archaeological collections. Grey = Stage 1 unfused. Green = Stage 2 partial fusion. Yellow = Stage 3 complete fusion. The fusion sites are: Ulna: (1) Distal epiphysis, Hand: (2) Metacarpals 2 – 5 and the proximal and middle phalangeal epiphyses, (3) Distal phalangeal epiphyses

		Age in years																	
		<9	10	11	12	13	14	15	16	17	18	19	20	21	22	23>			
Ulna	<sup>1</sup> Distal	Rom	n = 8											n = 1	n = 5				
		AS	n = 16											n = 1	n = 3				
	Med	n = 82											n = 2		n = 34				
		IA	n = 2											n = 6					
Hand	<sup>2</sup> Metacarpals	Rom	n = 5											n = 4					
		AS	n = 25											n = 1	n = 5				
		Med	n = 78											n = 2		n = 41			
	<sup>3</sup> Distal	PM	n = 1											n = 2					
		AS	n = 14											n = 6					
		Med	n = 38											n = 1	n = 18				

### *F) The Hand*

Complete fusion (Stage 3) of the **metacarpals 2 – 5, proximal and middle phalangeal epiphyses** of the hand was found to occur at age 20 years for the entire sample of the Iron Age and Roman groups. Fusion (Stages 2 and 3) occurred between 20 to 22 years of age for the Anglo-Saxon group, between 12 to 18 years for the Mediaeval group, and between 16 to 19 years for the Post-Mediaeval group. The mean age-at-fusion (Stages 2 and 3) was significantly younger in the Mediaeval sample, compared to the Anglo-Saxons ( $U = 0.000$ ,  $p = 0.024$ ). The mean age-at-fusion was also significantly younger in the Post-Mediaeval sample compared to the Anglo-Saxons ( $U = 0.000$ ,  $p = 0.046$ ), but not when the Mediaeval and Post-Mediaeval samples were compared ( $U = 6.000$ ,  $p = 0.649$ ). However, none of these results remained statistically significant when a Bonferroni corrections test was run on the data (See **Appendix 3**). Complete fusion (Stage 3) of the **distal phalangeal epiphyses** occurred for the entire Anglo-Saxon sample by 20 years of age. Fusion was underway (Stage 2) at 16 years of age in the Mediaeval sample and had completed fusion (Stage 3) for the entire sample by age 17 years.

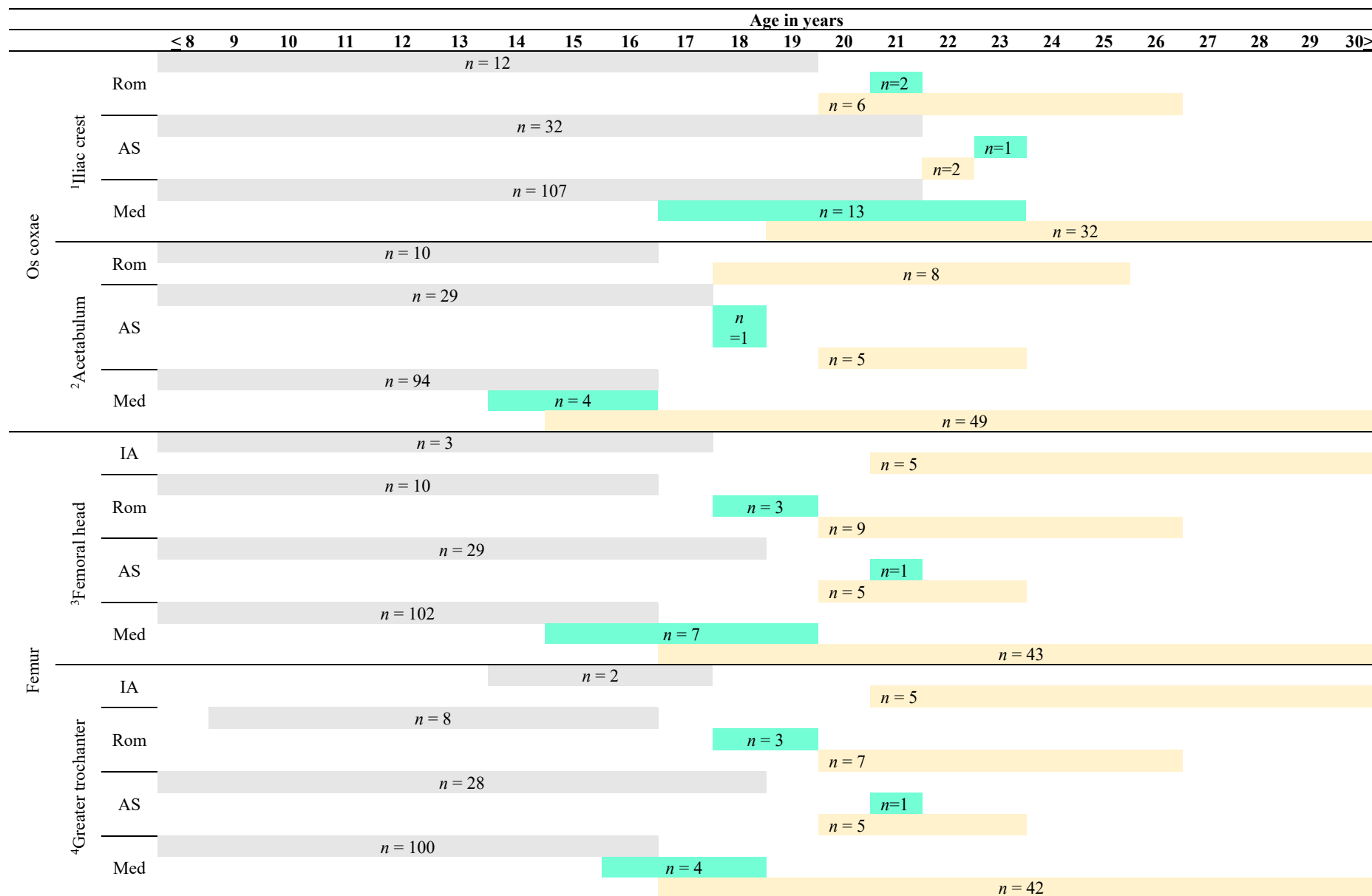
### **6.3.3. The lower appendicular skeleton**

#### *A) The Os coxae*

Fusion (Stages 2 and 3) of the **iliac crest** of the os coxae (**Table 6. 20**) occurred between 20 to 24 years for the Roman sample, between 21 to 23 years for the Anglo-Saxons, and between 17 to 23 years for the Mediaeval sample. The mean age-at-fusion (Stages 2 and 3) was significantly younger in the Mediaeval sample compared to the Anglo-Saxons ( $U = 9.500$ ,  $p = -0.036$ ). This was not statistically significant when a Bonferroni corrections test was run on the data (See **Appendix 3**). However, neither the Roman or Anglo-Saxon samples ( $U = 3.000$ ,  $p = 0.280$ ), nor the Roman and Mediaeval groups ( $U = 31.500$ ,  $p = 0.263$ ) differed significantly from each other.

Complete fusion (Stage 3) of the **acetabulum** of the os coxae occurred at age 18 years for the entire Roman sample. Fusion was underway (Stage 2) at age 18 years for the Anglo-Saxon sample and between 14 to 16 years for the Mediaeval group. The mean age-at-fusion (Stages 2 and 3) was significantly younger in the Mediaeval group compared to the Anglo-Saxon group ( $U = 0.000$ ,  $p = 0.025$ ). This was not statistically significant when a Bonferroni corrections test was run on the data (See **Appendix 3**).

Table 6. 20: Age and phase for the fusion of the lower appendicular skeleton for the Iron Age, Roman, Anglo-Saxon and Mediaeval groups collected from British archaeological collections. Grey = Stage 1 unfused. Green = Stage 2 partial fusion. Yellow = Stage 3 complete fusion. The fusion sites are: Os coxae: (1) Iliac crest, (2) acetabulum, Femur: (3) Femoral head, and (4) the Greater trochanter



### B) The Femur

Complete fusion (Stage 3) of the **proximal femur** (Table 6. 20) occurred at age 21 years for the Iron Age sample. Fusion was underway (Stage 2) between 18 to 19 years for the Romans, age 18 years for the Anglo-Saxons, and between 15 to 19 years for the Mediaeval sample. The mean age-at-fusion (Stages 2 and 3) was significantly younger for the Roman group compared to the Anglo-Saxon sample ( $U = 0.500, p = 0.046$ ), and was significantly younger for the Mediaeval sample compared to the Anglo-Saxons ( $U = 0.000, p = 0.007$ ). However, none of these results remained statistically significant when a Bonferroni corrections test was run on the data (See Appendix 3). No significant differences were found between the Roman and Mediaeval samples ( $U = 17.000, p = 0.371$ ).

Fusion of the **greater trochanter** was underway (Stage 2) between 18 to 19 years for the Romans, with complete fusion (Stage 3) for the entire sample at age 20 years. Complete fusion (Stage 3) occurred at 20 years of age for the Anglo-Saxon sample also, and 21 years of age for the Iron Age group. Fusion was underway (Stage 2) for the Mediaeval group between 16 to 18 years with the earliest age at complete fusion (Stage 3) being 17 years of age. Complete fusion for the entire sample occurred at age 19 years. The mean age-at-fusion (Stages 2 and 3) was found to be significantly younger for the Mediaeval sample compared to the Romans ( $U = 2.000, p = 0.027$ ). This was not statistically significant when a Bonferroni corrections test was run on the data (See Appendix 3).

Fusion of the **lesser trochanter** (Table 6. 21) was underway (Stage 2) between 18 to 19 years of age for the Roman sample. Fusion (Stages 2 and 3) occurred between 14 to 20 years for the Anglo-Saxons and between 15 to 17 years for the Mediaeval group. The mean age-at-fusion (Stages 2 and 3) was significantly younger for the Mediaeval sample compared to the Roman sample ( $U = 0.000, p = 0.018$ ). This was not statistically significant when a Bonferroni corrections test was run on the data (See Appendix 3). No significant differences were found between the Roman and Anglo-Saxon samples ( $U = 2.500, p = 0.767$ ), nor the Anglo-Saxon and Mediaeval samples ( $U = 6.000, p = 1.000$ ) when the mean age-at-fusion was compared.

Complete fusion (Stage 3) of the **distal epiphysis** occurred for the entire sample at age 21 years for the Iron Age group and age 20 years for the Romans. Fusion was underway (Stage 2) between 20 to 21 years for the Anglo-Saxon group. Fusion (Stages 2 and 3) occurred between 17 to 20 years for the Mediaeval group. The mean age-at-fusion (Stages 2 and 3) was significantly younger in the Mediaeval group when compared to the Anglo-Saxons ( $U = 1.000,$

$p = 0.005$ ). This was not statistically significant when a Bonferroni corrections test was run on the data (See **Appendix 3**).

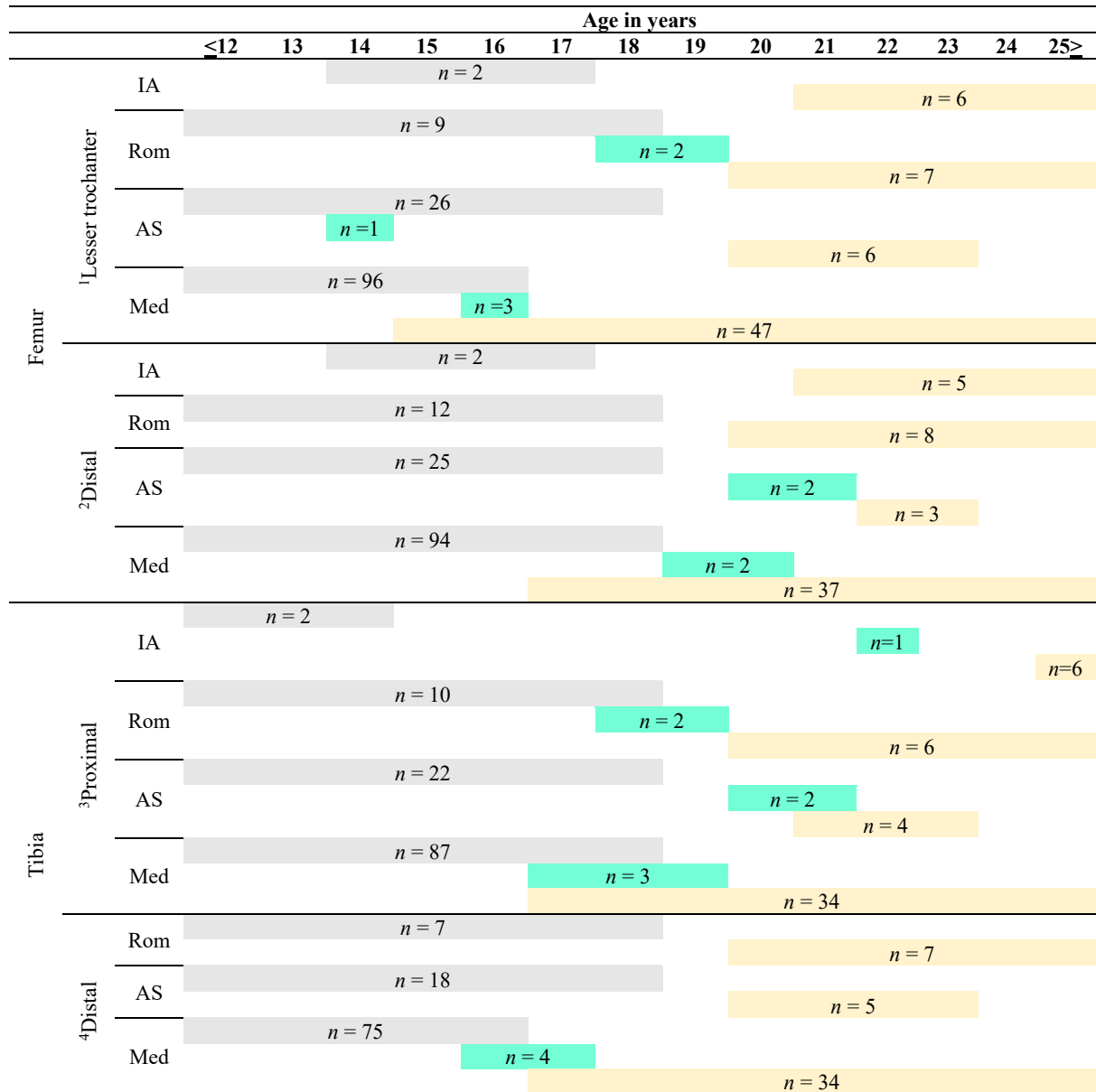
### *C) The Tibia*

The **proximal epiphysis** of the tibia fused (Stages 2 and 3) between the ages of 21 to 22 years for the Iron Age group. Fusion was underway (Stage 2) between 18 to 19 years of age for the Roman group, with complete fusion (Stage 3) occurring for the entire sample by the age of 20 years. The Anglo-Saxons had later ages, with fusion underway (Stage 2) between 20 to 21 years. The earliest age complete fusion (Stage 3) occurred was 21 years, with the entire sample completing fusion a year later at age 22 years. Fusion was underway (Stage 2) between 17 to 19 years of age for the Mediaeval sample. The earliest age complete fusion (Stage 3) occurred was 17 years, with the entire Mediaeval sample completing fusion at age 20 years.

The mean age-at-fusion (Stages 2 and 3) was significantly younger in the Roman sample compared to the Iron Age group ( $U = 0.000$ ,  $p = 0.046$ ), and significantly younger in the Mediaeval sample compared to the Iron Age group ( $U = 0.000$ ,  $p = 0.007$ ). The mean age-at-fusion was also significantly younger in the Mediaeval sample compared to the Anglo-Saxons ( $U = 0.00$ ,  $p = 0.007$ ), but not when the Iron Age and Anglo-Saxon samples were compared ( $U = 2.000$ ,  $p = 0.197$ ). Neither did the Romans differ significantly when compared to the Anglo-Saxon group ( $U = 0.500$ ,  $p = 0.072$ ), or the Mediaeval group ( $U = 9.000$ ,  $p = 0.477$ ). None of these results remained statistically significant when a Bonferroni corrections test was conducted on the data (See **Appendix 3**).

Complete fusion (Stage 3) of the **distal epiphysis** of the tibia occurred for the entire sample at age 20 years for the Roman, Anglo-Saxon, and Mediaeval groups. Fusion was underway (Stage 2) between 16 to 18 years for the Mediaeval sample, with the earliest age at complete fusion (Stage 3) occurring at 17 years.

Table 6. 21: Age and phase for the fusion of the lower appendicular skeleton for the Iron Age, Roman, Anglo-Saxon and Mediaeval groups collected from British archaeological collections. Grey = Stage 1 unfused. Green = Stage 2 partial fusion. Yellow = Stage 3 complete fusion. The fusion sites are: Femur: (1) Lesser trochanter and (2) the distal epiphysis, Tibia: (3) Proximal and (4) distal epiphyses



#### 6.3.4. Summary of statistically significant univariate differences

**Table 6. 22** gives all the significant  $p$  values from the above section. Most significant differences occurred when the Mediaeval and Anglo-Saxon samples were compared. Overall, the axial skeleton of the Mediaeval sample fused at an older age when compared to the Anglo-Saxon group. The exception to this rule was the spheno-occipital synchondrosis, in which this trend was reversed. As for the appendicular skeleton, both the Anglo-Saxon and Iron Age groups were older when fusion occurred, compared to the Roman, Mediaeval and Post-Mediaeval groups. Finally, the greatest variation in fusion ages occurred when the proximal tibia was compared between archaeological periods. When a Bonferroni corrections test was applied to the data, only the proximal radius was found to be statistically significant between the Anglo-Saxon and Mediaeval groups (See **Appendix 3**). The large dataset for the Mediaeval sample and the smaller samples for the other archaeological groups, especially the Iron Age and Post-Mediaeval data, could have potentially skewed the data, whereby greater sample sizes present greater variation in age-at-fusion.

Table 6. 22: Significant results from the Mann Whitney U tests when archaeological periods were compared. All results within the table above are from analyses conducted on Stages 2 and 3 data combined.

<b>Fusion site</b>	<b>Groups tested</b>	<b>Mean ages (years)</b>	<b><i>p</i></b>
Spheno-occipital synchondrosis	Anglo-Saxon	22	0.032
	Mediaeval	18	
Anterior arch of the atlas	Anglo-Saxon	9	0.037
	Mediaeval	12	
Ossiculum terminale of the dens	Anglo-Saxon	10	0.009
	Mediaeval	13	
Dentocentral & neurocentral junctions	Anglo-Saxon	9	0.037
	Mediaeval	11	
Proximal radius	Roman	18	0.047
	Anglo-Saxon	21	
	Anglo-Saxon Mediaeval	21 16	0.001
Distal radius	Anglo-Saxon	22	0.019
	Mediaeval	20	
Distal ulna	Anglo-Saxon	22	0.019
	Mediaeval	20	
Heads of metacarpals 2 – 5 and the proximal and middle phalangeal epiphyses	Anglo-Saxon	21	0.024
	Mediaeval	16	
	Anglo-Saxon Post-Mediaeval	21 17	0.046
Iliac crest	Anglo-Saxon	22	-0.036
	Mediaeval	20	
Acetabulum	Anglo-Saxon	19	0.025
	Mediaeval	15	
Femoral head	Roman	19	0.046
	Anglo-Saxon	21	
	Anglo-Saxon Mediaeval	21 18	0.007
Greater trochanter	Roman	19	0.027
	Mediaeval	17	
Lesser trochanter	Roman	19	0.018
	Mediaeval	16	
Distal femoral epiphysis	Anglo-Saxon	21	0.005
	Mediaeval	19	
Proximal tibia	Iron Age	21	0.046
	Roman	19	
	Iron Age	21	0.007
	Mediaeval	19	
	Anglo-Saxon Mediaeval	21 19	0.007

### **6.3.5. Multivariate analysis**

A multiple regression was performed on the data to determine if the different archaeological periods (Iron Age, Roman, Anglo-Saxon, Mediaeval and Post-Mediaeval) could be distinguished by the age at which fusion occurred. Before carrying out the regression, test assumptions had to be met. These assumptions are presented in **Table 6. 23 - Table 6. 29**. The age range chosen and the fusion sites that were grouped were based on when each epiphysis fused, and therefore, some fusion sites are found in multiple tests as they fuse over a longer age range or were split over multiple tests to pass the assumptions. Some tests that were violated meant that the test could not be carried out, whereas other tests were cautionary (Lund and Lund, 2013b). This information is given in the tables below.

Table 6. 23: Data tested prior to carrying out the multiple regression.

Assumption	Test	Fusion sites	Age range (years)	Result	Pass or fail of test
Independence of observation	Durbin-Watson		3 - 10	1.982	✓
A linear relationship exists between the variables	Scatter plot between Studentised Deleted Residual and			See <b>Appendix 10</b>	✓
The data must show homoscedasticity	Studentised Residual				✓
The data must not show multicollinearity	Collinearity Statistics	Pars lateralis to pars basilaris Dentoneural synchondrosis C2 Posterior synchondrosis C1			✓
Data should not have any significant outliers, high leverage points or highly influential points	Case wise diagnostics			No case wise diagnostics	✓
	Leverage points			One data point was extremely large. This individual was removed, and the tests were rerun. Due to this, the test removed the posterior synchondrosis of the axis. Some cautionary leverage points have been left in but are not as high as the data point removed.	
	Cook's Distance Values			Initially, there was a value over one. This skeleton was removed, and the tests rerun.	
Errors are normally distributed	Histogram			See <b>Appendix 10</b>	✓

Table 6. 24: Data tested prior to carrying out the multiple regression.

Assumption	Test	Fusion sites	Age range (years)	Result	Pass or fail of test
Independence of observation	Durbin-Watson		3 - 15	1.660	✓
A linear relationship exists between the variables	Scatter plot between Studentised Deleted Residual and Studentised Residual	Anterior arch C1 Posterior synchondrosis C1 Ossiculum terminale C2 Dentocentral & neurocentral junctions C2		See <b>Appendix 10</b>	✓
The data must show homoscedasticity	Collinearity Statistics			✓	
The data must not show multicollinearity	Case wise diagnostics			Sk. 27 from the Mediaeval Canterbury sample was listed in the case-wise diagnostics. It was decided to keep the data point and list as cautionary. A few data points could be considered cautionary.	
Data should not have any significant outliers, high leverage points or highly influential points	Leverage points				
	Cook's Distance Values			See <b>Appendix 10</b>	✓
Errors are normally distributed	Histogram				✓
A linear relationship exists between the variables	Scatter plot between Studentised Deleted Residual and Studentised Residual	Distal humerus Proximal ulna Metacarpals Acetabulum Ischiopubic ramus	11 - 18	The test continued to fail, even when the data was transformed. This test was therefore abandoned.	

Table 6. 25: Data tested prior to carrying out the multiple regression.

Assumption	Test	Fusion sites	Age range (years)	Result	Pass or fail of test
Independence of observation	Durbin-Watson		12 – 19	2.192	✓
A linear relationship exists between the variables	Scatter plot between Studentised Deleted Residual and Studentised Residual	Medial humeral epicondyle Spheno-occipital synchondrosis		See <b>Appendix 10</b>	✓
The data must show homoscedasticity	Studentised Residual				✓
The data must not show multicollinearity	Collinearity Statistics			Initially, the test failed. However, the distal phalangeal epiphyses of the hand were removed from the test, and the test was rerun.	
Data should not have any significant outliers, high leverage points or highly influential points	Case wise diagnostics			No case wise diagnostics	✓
	Leverage points			See <b>Appendix 10</b>	✓
	Cook's Distance Values				✓
Errors are normally distributed	Histogram				✓

Table 6. 26: Data tested prior to carrying out the multiple regression.

Assumption	Test	Fusion sites	Age range (years)	Result	Pass or fail of test
Independence of observation	Durbin-Watson		13 - 20	2.315	✓
A linear relationship exists between the variables	Scatter plot between Studentised Deleted Residual and Studentised Residual			See <b>Appendix 10</b>	✓
The data must show homoscedasticity				This could be considered slightly cautionary but was decided that the test could continue.	
The data must not show multicollinearity	Collinearity Statistics	Acromial border Proximal tibia Greater trochanter Proximal femur		See <b>Appendix 9</b>	✓
Data should not have any significant outliers, high leverage points or highly influential points	Case wise diagnostics			No case wise diagnostics	✓
	Leverage points			Some results approach cautionary levels.	
	Cook's Distance Values			See <b>Appendix 10</b>	✓
Errors are normally distributed	Histogram				✓

Table 6. 27: Data tested prior to carrying out the multiple regression.

Assumption	Test	Fusion sites	Age range (years)	Result	Pass or fail of test
Independence of observation	Durbin-Watson		13 – 20	2.070	✓
A linear relationship exists between the variables	Scatter plot between Studentised Deleted Residual and Studentised Residual			See <b>Appendix 10</b>	✓
The data must show homoscedasticity	Studentised Residual				✓
The data must not show multicollinearity	Collinearity Statistics	Lesser trochanter Distal femur		Initially, this test failed. However, the distal tibia was removed, and the tests rerun.	
Data should not have any significant outliers, high leverage points or highly influential points	Case wise diagnostics			No case wise diagnostics	✓
	Leverage points			See <b>Appendix 10</b>	✓
	Cook's Distance Values				✓
Errors are normally distributed	Histogram				✓

Table 6. 28: Data tested prior to carrying out the multiple regression.

Assumption	Test	Fusion sites	Age range (years)	Result	Pass or fail of test
Independence of observation	Durbin-Watson		16 - 23	2.014	✓
A linear relationship exists between the variables	Scatter plot between Studentised Deleted Residual and Studentised Residual			See <b>Appendix 10</b>	✓
The data must show homoscedasticity	Studentised Residual				✓
The data must not show multicollinearity	Collinearity Statistics	Proxial humerus Lateral clavicle Inferior angle epiphysis Iliac crest		The distal radius was removed, and the tests rerun.	
Data should not have any significant outliers, high leverage points or highly influential points	Case wise diagnostics			No case wise diagnostics	✓
	Leverage points			Some cautionary data points.	
	Cook's Distance Values			One data point belonging to Sk. 742 from Auldhame was high. Usually, this skeleton would be removed, and the data rerun. However, this caused multicollinearity, and therefore would make the test unusable. It was therefore decided to leave in the datapoint to keep the test.	
Errors are normally distributed	Histogram			See <b>Appendix 10</b>	✓

Table 6. 29: Data tested prior to carrying out the multiple regression.

Assumption	Test	Fusion sites	Age range (years)	Result	Pass or fail of test
Independence of observation	Durbin-Watson		16 - 30	2.202	✓
A linear relationship exists between the variables	Scatter plot between Studentised Deleted Residual and Studentised Residual			See <b>Appendix 10</b>	✓
The data must show homoscedasticity	Studentised Residual				✓
The data must not show multicollinearity	Collinearity Statistics	Lateral clavicle Medial border Medial clavicle Sacral bodies 1 & 2		The iliac crest was removed, and the test rerun	
Data should not have any significant outliers, high leverage points or highly influential points	Case wise diagnostics Leverage points Cook's Distance Values			No case wise diagnostics Two leverage points were very high. However, when they were removed, it caused there to be a lot of multicollinearities. It was therefore decided to leave the points to keep the test intact. See <b>Appendix 10</b>	✓
Errors are normally distributed	Histogram				✓

If the variables passed the assumptions, a multiple regression was run on those variables and are presented in **Table 6. 30 - Table 6. 31**. When analysing the tables,  $r$  shows if the data is a good fit or not. The closer  $r$  is to one, the better the fit. All results presented show a good fit with the data, with the age range 3 to 10 years and 16 to 30 years showing the best fit with the fusion data. The Adjusted  $r^2$  shows whether the independent variables explain the dependent variable (M. Lund and Lund, 2018). Many of the Adjusted  $r^2$  shows that around 57.9 to 81.3% of the independent variables explain the dependent variable: age, with fusion sites that fuse between the ages of 3 to 10 years showing the highest fit with the data.

Some fusion sites were found to be significant with a specific age range, including the pars lateralis to pars basilaris ( $p<0.001$ ), and the dentoneural synchondrosis of the axis ( $p=0.027$ ) between the age range 3 to 10 years, the ossiculum terminale ( $p<0.001$ ) and the dentocentral and neurocentral junctions of the axis ( $p=0.031$ ) between the age range 3 to 15 years, the medial epicondyle of the humerus ( $p<0.001$ ) between the age range 12 to 19 years, the greater trochanter of the femur ( $p<0.001$ ) between the age range 13 to 20 years, and sacral bodies 1 and 2 ( $p=0.018$ ) between the age range 16 to 30 years. However, only one age range tested was found to be significantly associated with an archaeological period and certain fusion sites. This was the age range 13 to 20 years ( $p=0.021$ ) and the lesser trochanter ( $p<0.001$ ) and distal femur ( $p=0.015$ ).

The data showed that age decreased as the archaeological period moved from the Iron Age to the Post-Mediaeval periods, whereas the fusion stages of the lesser trochanter increased as did age. However, rather than showing variation in fusion between archaeological periods, it is more likely that the sampling of the skeletons for the lesser trochanter caused the association between the data. This is shown in **Figure 6. 3** with more Anglo-Saxon skeletons found in Fusion stages 1 and 2, Roman skeletons only found in Stage 2, and Post-Mediaeval skeletons found only in Stage 3. This is even more apparent when looking at the fusion of the distal femur (**Figure 6. 4**), as the Mediaeval sample dominates the scatter plot, with only Post-Mediaeval data found in Stage 2 of fusion. A Bonferroni corrections test was performed on the data and only the pars lateralis to pars basilaris of the occipital (3 to 10 years), the ossiculum terminale of the axis (3 to 15 years), the medial humeral epicondyle (12 to 19 years), the greater trochanter (13 to 20 years), and the lesser trochanter of the femur (13 to 20 years) remained statistically significant (See **Appendix 3**).

Table 6. 30: Multiple regression for all archaeological periods (Iron Age, Roman, Anglo-Saxon, Mediaeval, and Post-Mediaeval) for multiple age ranges. \*\* = statistically significant.

Age range (years)	Independent variables	B	p	ANOVA	r	Adjusted r <sup>2</sup>
3 - 10	Period	0.207	0.562			
	Pars lateralis to pars basilaris of the occipital	1.870	<0.001**			
	Dentoneural synchondrosis of the axis	0.829	0.027**	<i>F</i> (4, 23) 30.261, <i>p</i> <0.001	0.917	0.813
	Posterior synchondrosis of the atlas	-0.365	0.304			
3 - 15	Period	0.141	0.795			
	Anterior arch of the atlas	0.739	0.184			
	Posterior synchondrosis of the atlas	0.151	0.783			
	Ossiculum terminale of the axis	2.101	<0.001**	<i>F</i> (5, 53) 26.361, <i>p</i> <0.001	0.845	0.686
12 - 19	Dentocentral and neurocentral junctions of the axis	1.211	0.031**			
	Period	0.096	0.731			
	Spheno-occipital synchondrosis	0.542	0.157	<i>F</i> (3, 48) 24.383, <i>p</i> <0.001	0.777	0.579
13 - 20	Medial epicondyle of the humerus	1.790	<0.001**			
	Period	-0.394	0.078			
	Acromial border of the scapula	-0.342	0.403			
	Femoral head	0.116	0.844	<i>F</i> (5,35) 27.851, <i>p</i> <0.001	0.894	0.770
	Greater trochanter	1.821	<0.001**			
	Proximal tibia	0.599	0.299			

Table 6. 31: Multiple regression for all archaeological periods (Iron Age, Roman, Anglo-Saxon, Mediaeval, and Post-Mediaeval) for multiple age ranges. \*\* = statistically significant.

Age range (years)	Independent variables	B	p	ANOVA	r	Adjusted r <sup>2</sup>
13 - 20	Period	-0.463	<b>0.021**</b>	<i>F</i> (3, 55) 34.620, <i>p</i> <0.001	0.809	0.635
	Lesser trochanter	1.331	<b>&lt;0.001**</b>			
	Distal femur	0.950	<b>0.015**</b>			
16 - 23	Period	-0.431	0.344	<i>F</i> (5, 14) 7.351, <i>p</i> = 0.001	0.851	0.626
	Lateral Clavicle	0.193	0.702			
	Inferior angle of the scapula	-0.553	0.464			
	Proximal humerus	1.285	0.134			
16 - 30	Iliac crest of the os coxae	1.330	0.110	<i>F</i> (5, 6) 9.211, <i>p</i> = 0.009	0.941	0.789
	Period	-0.651	0.422			
	Medial Clavicle	2.015	0.123			
	Lateral Clavicle	0.351	0.672			
	Medial border of Scapula	-0.767	0.360			
Sacral bodies 1 & 2	3.393	<b>0.018**</b>				

Figure 6. 3: Scatter plot of the fusion of the lesser trochanter of the femur by age in years, separated by archaeological period

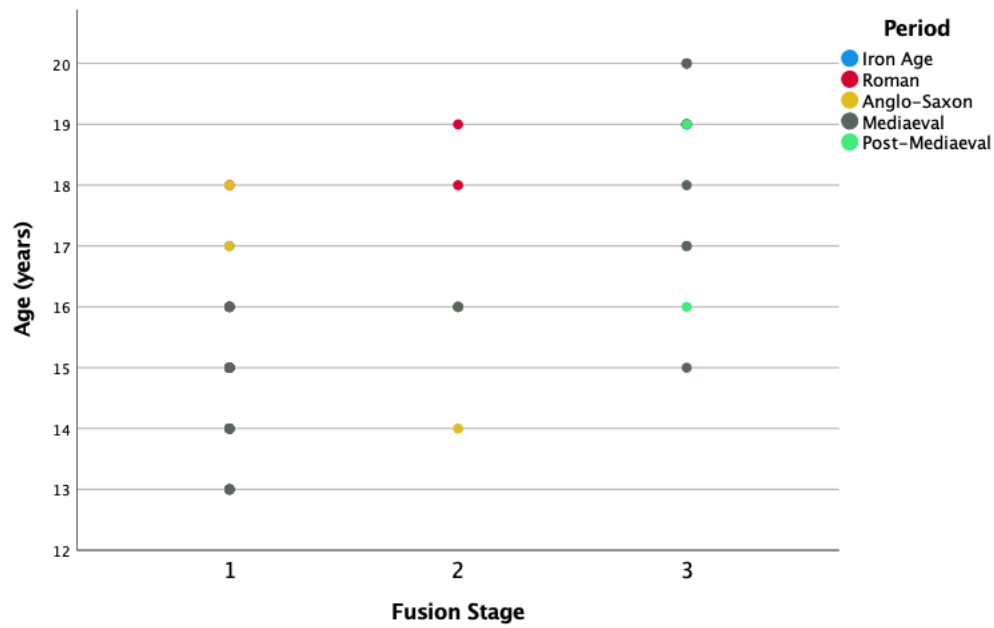
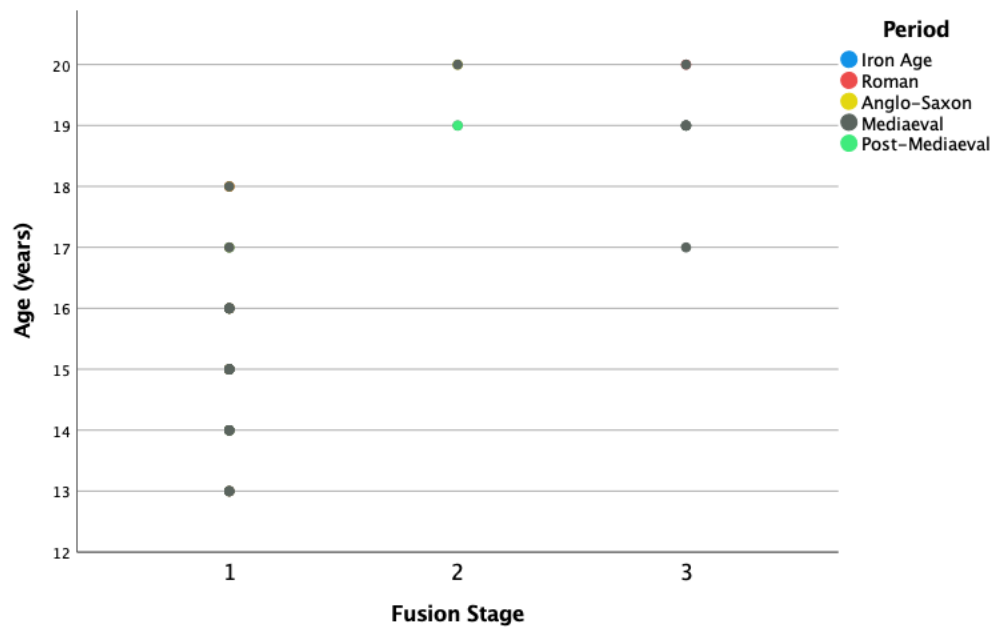


Figure 6. 4: Scatter plot of the fusion of the distal epiphysis of the femur by age in years, separated by archaeological period



#### 6.4. COMPARING SKELETAL MATURATION TO PUBLISHED LITERATURE

This section compares the data collected from the archaeological sites (Iron age, Roman, Anglo-Saxon, Mediaeval and Post-Mediaeval) presented above in **Section 6.3.** to fusion data from more recent Post-Mediaeval and Modern human samples. All the Post-Mediaeval and Modern data has been taken from published literature. Data from Schaefer et al., (2009) has also been included in each table as a Reference sample. In their book, 'Juvenile Osteology: A Laboratory and Field Manual', Schaefer et al., (2009) gives morphological summaries of each bone, including the age-at-fusion. Their morphological summaries are based on the research of previous studies from mainly Modern populations (Schaefer et al., 2009), many of which have been detailed independently in the tables below. The tabled data is presented in summarised form. Summary findings from **Section 6.4.** are detailed in the text beneath.

##### Summary Findings:

- **Skull:** The archaeological samples entered fusion (Stages 2 and 3) at a later age compared to the Modern published data. This was found for both the pars lateralis to pars basilaris and the spheno-occipital synchondrosis.
- **Sacrum:** The archaeological and Post-Mediaeval and Modern published samples entered fusion (Stages 2 and 3) at a similar time for the sacral bodies 1 and 2. However, the Modern published data had some individuals remain unfused (Stage 1) or partially fused (Stage 2) into the fifth decade of life, whereas complete fusion (Stage 3) for the entire sample had occurred by the age of 25 years for most of the archaeological samples.
- **Clavicle:** The range of fusion ages for the medial clavicle was much greater for the later Post-Mediaeval and Modern datasets compared to the archaeological samples. In particular, partial fusion (Stage 2) continued into the third decade of life for some individuals in the Modern samples, whereas partial fusion did not continue past the age of 25 years for many of the archaeological samples.
- **Scapula:** Complete fusion (Stage 3) of the medial border of the scapula occurred at an earlier age in the Modern published samples compared to the archaeological samples. The Post-Mediaeval published data for the inferior angle completed fusion for the entire sample earlier than the archaeological or Modern data.
- **Tibia:** Age-at-fusion (Stages 2 and 3) of the proximal tibia was earlier for the Post-Mediaeval and Modern published data, compared to the archaeological samples.

Overall, the Post-Mediaeval and Modern published data was found to be similar in the ages at fusion (Stages 2 and 3) to archaeological data for the appendicular skeleton. Only fusion sites from the pectoral girdle and the proximal epiphysis of the tibia in the appendicular skeleton differed between the published and archaeological data. The sites of the skull and the sacrum of the axial skeleton showed some deviations between the archaeological material and Post-Mediaeval and Modern published data.

### 6.4.1. The axial skeleton

#### A) The Skull

Overall, the archaeological data from this study showed that fusion (Stages 2 and 3) occurred at a later age when compared to the fusion ages reported for more recent periods (1908 AD to the present). The **pars lateralis to pars basilaris** (Table 6. 32) remained unfused (Stage 1) and partially fused (Stage 2) at a much later age (7 to 8 years) in the archaeological sites (Roman, Anglo-Saxon, Mediaeval and Post-Mediaeval) when compared to the published data. The oldest that the Modern samples remained in partial fusion (Stage 2) was between 6 to 7 years. The earliest age at complete fusion (Stage 3) occurred at age 7 years for the Anglo-Saxon and Mediaeval samples, with complete fusion occurring for the entire sample (Roman, Anglo-Saxon and Mediaeval) at age 9 years. This is much older than the comparative data, in which the earliest age at complete fusion occurred at 5 years for the Lisbon sample, and complete fusion for the entire sample occurred between 7 to 8 years for the published data (Lisbon and Cologne).

Table 6. 32: Fusion of the pars lateralis to the pars basilaris of the occipital bone of the skull split by primary data collected for this thesis and secondary data, which was taken from published literature. References are below. Light grey = unfused (Stage 1). Dark grey = partial fusion (Stage 2). Black = complete fusion (Stage 3). Sometimes stages of fusion overlap due to variation in individuals. To keep the table simple, overlap of fusion stages is denoted by the white text. The Reference Sample is shown in blue as partial fusion (Stage 2) and complete fusion (Stage 3) are not distinguished in the text. References: (a) Modern, Lisbon, Portugal, 1908-1984AD (births and deaths), dry bone (Cardoso et al., 2013b), (b) Modern, Cologne, Germany, 1970s, embedded bone and radiographs\* (Tillmann and Lorenz, 1978), (c) Reference sample (Schaefer et al., 2009)

		Age in years								
		Dataset	3	4	5	6	7	8	9	10
Pars lateralis to pars basilaris	This study	Roman								
		Anglo-Saxon				1 - 2	1 - 3	1 - 3		
		Mediaeval					1 & 3	1 & 3		
		Post-Mediaeval								
	Published data	(a) 1908 - 1984AD, Lisbon			2 - 3	2 - 3	2 - 3			
		(b) 1970s, Cologne*								
		(c) Reference sample								

Complete fusion (Stage 3) of the **spheno-occipital synchondrosis** (Table 6. 33) occurred at later ages in the archaeological data compared to Post-Mediaeval and Modern samples that date from 1826 AD to the present. The Anglo-Saxon sample had the oldest age at complete fusion, which did not occur until age 23 years. The earliest ages at which complete fusion occurred in the Post-Mediaeval and Modern samples was between 11 to 14 years (Coimbra, USA and Niigata). The earliest age of complete fusion in the archaeological data occurred between 15 to 16 years of age (Mediaeval and Post-Mediaeval).

Table 6. 33: Fusion of the spheno-occipital synchondrosis split by primary data collected for this thesis and secondary data, which was taken from published literature. References are below. Light grey = unfused (Stage 1). Dark grey = partial fusion (Stage 2). Black = complete fusion (Stage 3). Sometimes stages of fusion overlap due to variation in individuals. To keep the table simple, overlap of fusion stages is denoted by the white text. The Reference Sample is shown in blue as partial fusion (Stage 2) and complete fusion (Stage 3) are not distinguished in the text. References: (a) Modern, Coimbra, Portugal, 1826-1938AD (births and deaths), dry bone (Coqueugniot and Weaver, 2007), (b) Modern, Forensic Data Bank, United States of America, 1950-1990 AD (births only), dry bone (Shirley and Jantz, 2011), (c) Modern, living patients, Niigata, Japan, CT scans\* (Okamoto et al., 1996), (d) Reference sample (Schaefer et al., 2009)

		Age in years																	
Dataset		8	9	10	11	12	13	14	15	16	17	18	19	20	21	22	23	24	
Spheno-occipital synchondrosis	This study	Roman																	
		Anglo-Saxon																	
		Mediaeval																	
		Post-Mediaeval																	
	Published data	(a) 1826-1938AD, Coimbra																	
		(b) 1950-1990AD, USA																	
		(c) 1996AD, Niigata*																	
		(d) Reference sample																	

### B) The Sacrum

The range of ages that the **sacral bodies 1 and 2** (Table 6. 34) either partially fused (Stage 2) in or completely fused (Stage 3) in, in the Modern samples that dated from the 19<sup>th</sup> to 20<sup>th</sup> century was much greater compared to the archaeological data. None of the archaeological sites displayed evidence of partial fusion (Stage 2) beyond the age of 25 years. Published data from Modern Coimbra, Lisbon and Sardinia revealed that partial fusion (Stage 2) for some individuals continued into their fifth decade of life.

Table 6. 34: Fusion of bodies 1 & 2 of the sacrum split by primary data collected for this thesis and secondary data, which was taken from published literature. References are below. Light grey = unfused (Stage 1). Dark grey = partial fusion (Stage 2). Black = complete fusion (Stage 3). Sometimes stages of fusion overlap due to variation in individuals. To keep the table simple, overlap of fusion stages is denoted by the white text. The Reference Sample is shown in blue as partial fusion (Stage 2) and complete fusion (Stage 3) are not distinguished in the text. References: (a) Modern, Coimbra, Portugal, 1826-1938AD (births and deaths), dry bone (Coqueugniot and Weaver, 2007), (b) Modern, Coimbra, Portugal, early 20<sup>th</sup> century, dry bone (Belcastro et al., 2008), (c) Modern, Lisbon, Portugal, late 19<sup>th</sup> to early 20<sup>th</sup> century, dry bone (Rios et al., 2008), (d) Modern, Sardinia, Italy, early 20<sup>th</sup> century, dry bone (Belcastro et al., 2008), (e) Reference sample (Schaefer et al., 2009)

		Age in years																							
Dataset		13	14	15	16	17	18	19	20	21	22	23	24	25	26	27	28	29	30-34	35-39	40-44	45-49	50-54	55-59	
<b>This study</b>	<b>Roman</b>				1-2				2-3				3												
	<b>Anglo-Saxon</b>									1-2	2-3	3													
	<b>Mediaeval</b>				1-2		1-2	1-2	2-3	3	2-3	3	3	3	3			3							
	<b>Post-Mediaeval</b>								2-3																
<b>Sacral bodies 1 &amp; 2</b>	<b>(a) 1826-1938AD, Coimbra</b>	1-2	1-2	1-2	1-2	1-2	1-2	1-2	1-2	1-3	1-3	1-3	1-3	1-3	1-3	1-3	2-3							♀	
	<b>(b) 20th century, Coimbra</b>							1-2	1-2	1-2	1-2	1-2	1-2	1-3	1-3	1-3	1-3	1-3	2-3	2-3	2-3	2-3	2-3	2-3	♀
	<b>(c) 19th-20th century, Lisbon</b>								1-2	1-2	1-2	1-2	1-2	1-3	1-3	1-3	1-3	1-3	2-3	2-3	2-3	2-3	2-3	2-3	♀
	<b>(d) 20th century, Sardinia</b>								1-3	1-3	1-3	1-3	1-3	1-3	1-3	1-3	1-3	1-3	1-3	1-3	1-3	1-3	1-3	2-3	♀
	<b>(e) Reference sample</b>																								♀
		<b>(e) Reference sample</b>																							

### 6.4.2. The upper appendicular skeleton

#### *A) The Clavicle*

Overall, the archaeological sites completed fusion (Stage 3) of the **medial clavicle** at an earlier age compared to the Post-Mediaeval and Modern data (**Table 6. 35**). The Post-Mediaeval archaeological data had the earliest age at complete fusion of 17 years. Certain Modern groups (Los Angeles and Tennessee) had a few individuals where complete fusion had occurred by 20 years of age, which is close to the Iron age (20 years) and Mediaeval (19 years) archaeological data. The Post-Mediaeval and Modern data displayed a greater range of ages for partial fusion (Stage 2) compared to the archaeological data.

Complete fusion (Stage 3) of the **lateral clavicle** occurred in some Anglo-Saxon individuals by the age of 14 years (**Table 6. 36**). This was the earliest age-at-fusion recorded compared to all other datasets. The other archaeological sites (Iron age, Roman and Mediaeval) completed fusion at a later age (19 to 25 years) when compared to the Modern data, in which the earliest age at complete fusion occurred at age 17 years for 20<sup>th</sup> century Tennessee.

#### *B) The Scapula*

Partial (Stage 2) and complete (Stage 3) fusion of the **coracoid process** occurred from age 11 years and between the ages of 11 to 14 years respectively in the Post-Mediaeval data from Coimbra and Lisbon (**Table 6. 37**). The earliest age at complete fusion of the Modern sample from Bosnia occurred at age 16 years, which is the same age as when the Mediaeval sample first entered Stage three.

Complete fusion of the **acromion** occurred at the earliest ages of 16 to 17 years for the Post-Mediaeval and Modern data from 1826 to the 1990s AD (**Table 6. 38**). The earliest age the Mediaeval sample entered complete fusion was 17 years. Complete fusion for the entire sample occurred between 19 to 23 years for the published data (Coimbra, Lisbon, USA and Bosnia) and between 19 to 21 years for the archaeological data.

Complete fusion of the **medial border** of the scapula occurred at an earlier age in the Modern data compared to the archaeological data (**Table 6. 39**). The Modern data from the USA and Bosnia entered complete fusion at the earliest ages of 17 and 18 years respectively. The Mediaeval archaeological sample completed fusion at the earliest age of 19 years. Complete fusion for the entire Modern data occurred at age 23 years. This was similar to the

ages in which the Anglo-Saxon and Mediaeval archaeological data completed fusion for the entire sample from 21 to 22 years.

The Post-Mediaeval 1887 to 1975 AD Lisbon female skeletal collection and the archaeological Mediaeval sample first entered complete fusion of the **inferior angle** at age 18 years (**Table 6. 40**). The Post-Mediaeval Lisbon males and the Modern data first entered complete fusion a year earlier at 17 years. Some individuals remained unfused (Stage 1) at age 21 years in the Anglo-Saxon and Mediaeval archaeological samples and the Modern samples. Complete fusion (Stage 3) occurred for the entire sample by age 19 to 21 years for the Post-Mediaeval data, 22 years for the archaeological data and finally, the Modern data completed fusion for the entire sample by age 23 years.

Table 6. 35: Fusion of the medial epiphysis of the clavicle split by primary data collected for this thesis and secondary data, which was taken from published literature. References are below. Light grey = unfused (Stage 1). Dark grey = partial fusion (Stage 2). Black = complete fusion (Stage 3). Sometimes stages of fusion overlap due to variation in individuals. To keep the table simple, overlap of fusion stages is denoted by the white text. The Reference Sample is shown in blue as partial fusion (Stage 2) and complete fusion (Stage 3) are not distinguished in the text. References: (a) Post-Mediaeval, London, England, 1646-1859AD, dry bone, original method used five phases which were grouped down into three phases for the purpose of this table using the methodology in this study, (Black and Scheuer, 1996), (b) Post-Mediaeval, London, England, 1650-1700AD, dry bone, original method used five phases which were grouped down into three phases for the purpose of this table using the methodology in this study, (Black and Scheuer, 1996), (c) Modern, Lisbon, Portugal, 1805-1975AD (births and deaths), dry bone, original method used five phases which were grouped down into three phases for the purpose of this table using the methodology in this study, (Black and Scheuer, 1996), (d) Modern, Coimbra, Portugal, 1826-1938AD (births and deaths), dry bone, (Coqueugniot and Weaver, 2007), (e) Modern, USA, 1912-1938AD, dry bone, (Langley-Shirley and Jantz, 2010), (f) Modern, Los Angeles, USA, 1977-1979AD (autopsies), (Webb and Suchey, 1985), (g) Modern, East Tennessee, USA, 1986-1998AD, dry bone, (Langley-Shirley and Jantz, 2010), (h) Modern, Bosnia, 1995AD (war victims from the fall of Srebrenica), males only, dry bone (Schaefer, 2008b), (i) Modern, Berlin, Germany, living patients, radiographs\*, original method used five phases which were grouped down into three phases for the purpose of this table using the methodology in this study, (Schmelting et al., 2004), (j) Reference sample, (Schaefer et al., 2009)

		Age in years																						
Dataset		13	14	15	16	17	18	19	20	21	22	23	24	25	26	27	28	29	30	31	32	33	34	
This study	Iron Age								Black	Light grey				Black					Dark grey					
	Roman								Light grey	1-2			Black	2-3	Black									
	Anglo-Saxon								Light grey		Black	Light grey												
	Mediaeval							Light grey	1-3	1&3	1-3	Light grey	1&3	Light grey	2-3		Black							
	Post-Mediaeval					Black		Light grey																
Medial clavicle Published data	(a) 1646-1859AD, London									Light grey	1-2				2-3	2-3								
	(b) 1650-1700AD, London													2-3	2-3	2-3	2-3							
	(c) 1805-1975AD, Lisbon							Light grey	1-2	1-2	1-2												Black	
	(d) 1826-1938AD, Coimbra				Light grey	1-2	1-2	1-2	1-2	1-2	1-2	1-2	1-2	1-2	2-3	2-3	2-3	2-3	2-3					
	(e) 1912-1938AD, USA					1-2	1-2	1-2	1-2	1-2	1-3	1-3	1-3	1-3	2-3	2-3	2-3	2-3	2-3	2-3				
	(f) 1977-1979AD, Los Angeles					1-2	1-2	1-2	2-3	1-2	2-3	2-3	2-3	2-3	2-3	2-3	2-3	2-3	2-3	2-3	2-3	2-3	2-3	Black ♀
	(g) 1986-1998AD, E. Tennessee	1-2	1-2	1-2	1-2	1-2	1-2	1-2	2-3	2-3	2-3	2-3	2-3	2-3	2-3	2-3	2-3	2-3	2-3	2-3	2-3	2-3	2-3	2-3
	(h) 1995AD, Bosnia				Light grey	1-2	1-2	1-2	1-2	1-3	1-3	1-3	2-3	2-3	2-3	2-3	2-3	2-3	2-3				Black ♂	
	(i) 2004AD, Berlin*																							
	(j) Reference sample																							

Table 6. 36: Fusion of the lateral epiphysis of the clavicle split by primary data collected for this thesis and secondary data, which has come from published literature and are referenced below. Light grey refers to skeletons recorded as unfused only. Dark grey refers to skeletons recorded in partial fusion, with the numbers in white, listing if data was also recorded for Stage 1 or 3. Black refers to skeletons that were recorded as completely fused only. Blue is based off published literature that also looked at multiple secondary data sources to determine an age-at-fusion for skeletons. Finally, the asterisk refers to data that used computer imaging technology. References: (a) Modern, East Tennessee, USA, 1986-1998AD, dry bone, (Langley, 2016), (b) Modern, East Tennessee, USA, 1986-1998AD, dry bone, (Langley, 2016).

		Age in years													
Dataset		14	15	16	17	18	19	20	21	22	23	24	25	26	
Lateral clavicle	This study	Iron Age													
		Roman												1 & 3	
		Anglo-Saxon													
	Published data	Mediaeval				1 - 2		1 & 3			1 - 2				
		(a) 1986-1998AD, E. Tennessee		1 - 2		1 - 3	1 - 3	1 - 3	1 - 3	2 - 3	2 - 3	2 - 3	2 - 3		
		(b) Reference sample													

Table 6. 37: Fusion of the coracoid process to the body of the scapula split by primary data collected for this thesis and secondary data, which was taken from published literature. References are below. Light grey = unfused (Stage 1). Dark grey = partial fusion (Stage 2). Black = complete fusion (Stage 3). Sometimes stages of fusion overlap due to variation in individuals. To keep the table simple, overlap of fusion stages is denoted by the white text. The Reference Sample is shown in blue as partial fusion (Stage 2) and complete fusion (Stage 3) are not distinguished in the text. References: (a) Modern, Coimbra, Portugal, 1826-1938AD (births and deaths), dry bone (Coqueugniot and Weaver, 2007), (b) Modern, Lisbon, Portugal, 1887-1975AD (births and deaths), dry bone (Cardoso, 2008a), (c) Modern, Bosnia, 1995AD (war victims from the fall of Srebrenica), males only, dry bone (Schaefer, 2008b), (d) Reference sample (Schaefer et al., 2009)

		Age in years														
Dataset		10	11	12	13	14	15	16	17	18	19	20	21	22	23	
Coracoid process of the scapula	This study	Roman														
		Anglo-Saxon														
		Mediaeval														
	Published data	(a) 1826-1938AD, Coimbra		1 - 2			2 - 3	2 - 3	2 - 3	2 - 3						♂
		(b) 1887-1975AD, Lisbon		1 & 3		2 - 3	1 & 3									
		(c) 1995AD, Bosnia		1 - 2			1 - 2	2 - 3	2 - 3							
(d) Reference sample																

Table 6. 38: Fusion of the acromion process to the body of the scapula split by primary data collected for this thesis and secondary data, which was taken from published literature. References are below. Light grey = unfused (Stage 1). Dark grey = partial fusion (Stage 2). Black = complete fusion (Stage 3), Sometimes stages of fusion overlap due to variation in individuals. To keep the table simple, overlap of fusion stages is denoted by the white text. The Reference Sample is shown in blue as partial fusion (Stage 2) and complete fusion (Stage 3) are not distinguished in the text. References: (a) Modern, Coimbra, Portugal, 1826-1938AD (births and deaths), dry bone (Coqueugniot and Weaver, 2007), (b) Modern, Lisbon, Portugal, 1887-1975AD (births and deaths), dry bone (Cardoso, 2008a), (c) Modern, USA, 1950-1952AD (war victims from the Korean war), males only, dry bone (McKern and Stewart, 1957), (d) Modern, Bosnia, 1995AD (war victims from the fall of Srebrenica), males only, dry bone (Schaefer, 2008b), (e) Reference sample (Schaefer et al., 2009)

		Age in years											
		13	14	15	16	17	18	19	20	21	22	23	
Acromion of scapula	This study	Roman											
		Anglo-Saxon											
		Mediaeval											
	Published data	(a) 1826-1938AD, Coimbra											
		(b) 1887-1975AD, Lisbon											
		(c) 1950-1952AD, USA											
	(d) 1995AD, Bosnia												
	(e) Reference sample												

Table 6. 39: Fusion of the medial border of the scapula split by primary data collected for this thesis and secondary data, which was taken from published literature. References are below. Light grey = unfused (Stage 1). Dark grey = partial fusion (Stage 2). Black = complete fusion (Stage 3), Sometimes stages of fusion overlap due to variation in individuals. To keep the table simple, overlap of fusion stages is denoted by the white text. The Reference Sample is shown in blue as partial fusion (Stage 2) and complete fusion (Stage 3) are not distinguished in the text. References: (a) Modern, USA, 1950-1952AD (war victims from the Korean war), males only, dry bone (McKern and Stewart, 1957), (b) Modern, Bosnia, 1995AD (war victims from the fall of Srebrenica), males only, dry bone (Schaefer, 2008b), (c) Reference sample (Schaefer et al., 2009)

		Age in years										
		16	17	18	19	20	21	22	23	24	25	
Medial border of scapula	This study	Roman										
		Anglo-Saxon										
		Mediaeval										
	Published data	1950-1952AD, USA										
		1995AD, Bosnia										
		Reference sample										

Table 6. 40: Fusion of the inferior border to the body of the scapula split by primary data collected for this thesis and secondary data, which has come from published literature and are referenced below. Light grey refers to skeletons recorded as unfused only. Dark grey secondary data, which was taken from published literature. References are below. Light grey = unfused (Stage 1). Dark grey = partial fusion (Stage 2). Black = complete fusion (Stage 3). Sometimes stages of fusion overlap due to variation in individuals. To keep the table simple, overlap of fusion stages is denoted by the white text. The Reference Sample is shown in blue as partial fusion (Stage 2) and complete fusion (Stage 3) are not distinguished in the text. References: (a) Post-Mediaeval, Lisbon, Portugal, 1887-1975AD (births and deaths), dry bone (Cardoso, 2008a), (b) Modern, USA, 1950-1952AD (war victims from the Korean war), males only, dry bone (McKern and Stewart, 1957), (c) Modern, Bosnia, 1995AD (war victims from the fall of Srebrenica), males only, dry bone (Schaefer, 2008b)

		Age in years									
Dataset		15	16	17	18	19	20	21	22	23	
Inferior angle of the scapula	This study	Anglo-Saxon									
		Mediaeval					1 & 3		1 & 3		
	Published data	(a) 1887-1975AD, Lisbon			1 - 2			1 & 3		♀	
		(b) 1950-1952AD, USA		1 - 2	1 & 3	1 & 3		♂			
		(c) 1995AD, Bosnia	♂		1 - 3	1 - 3	1 - 3	1 - 3	1 & 3	2 - 3	
		(d) Reference sample									

### C) The Humerus

The earliest age at complete fusion (Stage 3) of the **medial humeral epicondyle** was between 11 to 14 years for the Post-Mediaeval Coimbra and Lisbon females and the Modern Chandigarh radiographic data from living patients (**Table 6. 41**). The male data from 1826 AD to the present day and the unsexed Mediaeval archaeological data completed fusion at the earliest age of 16 years. Complete fusion for the entire sample occurred between 19 to 21 years of age for the archaeological, Post-Mediaeval and Modern samples, except for the Post-Mediaeval Lisbon females and the Modern Chandigarh data that completed fusion for the entire sample earlier at 16 to 17 years.

The earliest age at complete fusion of the **distal composite epiphysis** of the humerus occurred between 11 to 12 years for the Post-Mediaeval female data (**Table 6. 42**). The earliest age-at-fusion (Stages 2 and 3) for the Anglo-Saxon and Mediaeval archaeological samples and the Post-Mediaeval Lisbon male sample was 14 years. The Iron age archaeological site, as well as the Post-Mediaeval Coimbra and Modern Bosnian male data were close behind, with some individuals partially fused (Stage 2) or completely fused (Stage 3) between 15 to 17 years.

Individuals entering partial fusion (Stage 2) of the **proximal humerus** occurred between 13 to 16 years for the Post-Mediaeval and Modern data, except for the Post-Mediaeval Coimbra group (**Table 6. 43**). The Mediaeval archaeological sample completed fusion (Stage 3) at the earliest age of 17 years. This age was much earlier than the age that the Post-Mediaeval Coimbra skeletal collection first completed fusion at age 20 years. The archaeological samples completed fusion for the entire sample between 21 to 22 years.

Many of the Post-Mediaeval and Modern samples completed fusion for the entire dataset between 22 to 24 years. Only the 2014 AD Central Indian study (18 years) and the 1887 to 1975 AD Lisbon female study (20 years) completed fusion for their entire datasets much earlier compared to the other groups.

#### *D) The Radius*

Partial fusion (Stage 2) and complete fusion (Stage 3) of the **proximal radius** occurred between 11 to 12 years for the Post-Mediaeval female data (**Table 6. 44**). Many of the other groups, both archaeological and from 1826 AD to the present entered fusion (Stages 2 and 3) at the earliest ages of 14 to 16 years. Complete fusion (Stage 3) of the entire sample occurred between 17 to 22 years for the archaeological, Post-Mediaeval and Modern data.

The earliest age-at-fusion (Stages 2 and 3) of the **distal radius** occurred between 16 to 17 years for many of the archaeological, Post-Mediaeval and Modern data (**Table 6. 45**). The exception to this was the Post-Mediaeval Coimbra males who entered partial fusion (Stage 2) at the earliest age of 19 years and the Lisbon females who entered partial fusion at the earliest age of 14 years. Complete fusion (Stage 3) first occurred in the Iron age and Roman archaeological samples at age 20 years. Complete fusion for the entire sample occurred between 20 to 23 years for all groups.

#### *E) The Ulna*

Partial fusion (Stage 2) of the **proximal ulna** occurred at age 11 years for the Post-Mediaeval Lisbon skeletal collection (**Table 6. 46**). This was an earlier age at partial fusion than the archaeological data, the Post-Mediaeval Coimbra data and the Modern Bosnian data. The Anglo-Saxon and Mediaeval archaeological data entered partial fusion at age 14 years, and this was earlier than the Post-Mediaeval Coimbra males and the Modern Bosnian males.

The Post-Mediaeval Lisbon and Modern radiographic Chandigarh groups entered partial fusion of the **distal ulna** earlier (14 to 15 years of age) than the archaeological data and the other Post-Mediaeval and Modern data (**Table 6. 47**). The Mediaeval sample, Post-Mediaeval Coimbra females and Modern Bosnian males entered fusion (Stages 2 and 3) at age 17 years. Except for the Post-Mediaeval Lisbon females and the Modern Chandigarh living patients, who completed fusion (Stage 3) for the entire sample much earlier (19 to 20 years), all other groups completed fusion for the entire sample between 21 to 22 years.

Table 6. 41: Fusion of the medial epicondyle of the humerus split by primary data collected for this thesis and secondary data, which was taken from published literature. References are below. Light grey = unfused (Stage 1). Dark grey = partial fusion (Stage 2). Black = complete fusion (Stage 3). Sometimes stages of fusion overlap due to variation in individuals. To keep the table simple, overlap of fusion stages is denoted by the white text. The Reference Sample is shown in blue as partial fusion (Stage 2) and complete fusion (Stage 3) are not distinguished in the text. References: (a) Modern, Coimbra, Portugal, 1826-1938AD (births and deaths), dry bone (Coqueugniot and Weaver, 2007), (b) Modern, Lisbon, Portugal, 1887-1975AD (births and deaths), dry bone (Cardoso, 2008a), (c) Modern, Bosnia, 1995AD (war victims from the fall of Srebrenica), males only, dry bone (Schaefer, 2008b), (d) Modern, Chandigarh, India, living patients, radiographs\*, (Sahni et al., 1995), (e) Reference sample (Schaefer et al., 2009)

		Age in years												
Dataset		10	11	12	13	14	15	16	17	18	19	20	21	
Medial humeral epicondyle	This study	Iron Age												
		Roman												
		Anglo-Saxon												
		Mediaeval												
	Published data	(a) 1826-1938AD, Coimbra												
		(b) 1887-1975AD, Lisbon												
		(c) 1995AD, Bosnia												
		(d) 1995AD, Chandigarh*												
		(e) Reference sample												

Table 6. 42: Fusion of the distal composite epiphysis to the shaft of the humerus split by primary data collected for this thesis and secondary data, which was taken from published literature. References are below. Light grey = unfused (Stage 1). Dark grey = partial fusion (Stage 2). Black = complete fusion (Stage 3). Sometimes stages of fusion overlap due to variation in individuals. To keep the table simple, overlap of fusion stages is denoted by the white text. The Reference Sample is shown in blue as partial fusion (Stage 2) and complete fusion (Stage 3) are not distinguished in the text. References: (a) Modern, Coimbra, Portugal, 1826-1938AD (births and deaths), dry bone (Coqueugniot and Weaver, 2007), (b) Modern, Lisbon, Portugal, 1887-1975AD (births and deaths), dry bone (Cardoso, 2008a), (c) Modern, Bosnia, 1995AD (war victims from the fall of Srebrenica), males only, dry bone (Schaefer, 2008b), (d) Reference sample (Schaefer et al., 2009)

		Age in years									
Dataset		10	11	12	13	14	15	16	17	18	19
This study	Iron Age										
	Roman										
	Anglo-Saxon										
	Mediaeval										
Published data	(a) 1826-1938AD, Coimbra										
	(b) 1887-1975AD, Lisbon										
	(c) 1995AD, Bosnia										
	(d) Reference sample										

Table 6. 43: Fusion of the proximal epiphysis of the humerus split by primary data collected for this thesis and secondary data, which was taken from published literature. References are below. Light grey = unfused (Stage 1). Dark grey = partial fusion (Stage 2). Black = complete fusion (Stage 3). Sometimes stages of fusion overlap due to variation in individuals. To keep the table simple, overlap of fusion stages is denoted by the white text. The Reference Sample is shown in blue as partial fusion (Stage 2) and complete fusion (Stage 3) are not distinguished in the text. References: (a) Modern, Coimbra, Portugal, 1826-1938AD (births and deaths), dry bone (Coqueugniot and Weaver, 2007), (b) Modern, Lisbon, Portugal, 1887-1975AD (births and deaths), dry bone (Cardoso, 2008a), (c) Modern, Bosnia, 1995AD (war victims from the fall of Srebrenica), males only, dry bone (Schaefer, 2008b), (d) Modern, Central India, India, living patients, radiographs, females only (Tirpude et al., 2014), (e) Reference sample (Schaefer et al., 2009)

		Age in years											
Dataset		13	14	15	16	17	18	19	20	21	22	23	24
This study	Iron Age												
	Roman												
	Anglo-Saxon												
	Mediaeval												
Published data	(a) 1826-1938AD, Coimbra												
	(b) 1887-1975AD, Lisbon												
	(c) 1995AD, Bosnia												
	(d) 2014AD, Central India*												
	(e) Reference sample												

Table 6. 44: Fusion of the proximal epiphysis of the radius split by primary data collected for this thesis and secondary data, which was taken from published literature. References are below. Light grey = unfused (Stage 1). Dark grey = partial fusion (Stage 2). Black = complete fusion (Stage 3). Sometimes stages of fusion overlap due to variation in individuals. To keep the table simple, overlap of fusion stages is denoted by the white text. The Reference Sample is shown in blue as partial fusion (Stage 2) and complete fusion (Stage 3) are not distinguished in the text. References: (a) Modern, Coimbra, Portugal, 1826-1938AD (births and deaths), dry bone (Coqueugniot and Weaver, 2007), (b) Modern, Lisbon, Portugal, 1887-1975AD (births and deaths), dry bone (Cardoso, 2008a), (c) Modern, Bosnia, 1995AD (war victims from the fall of Srebrenica), males only, dry bone (Schaefer, 2008b), (d) Reference sample (Schaefer et al., 2009)

		Age in years												
Dataset		10	11	12	13	14	15	16	17	18	19	20	21	22
This study	Iron Age					Light grey			Dark grey			Black		
	Roman							Light grey		2 - 3	Black			
	Anglo-Saxon				Light grey	1 - 2		Light grey				Black	2 - 3	Black
	Mediaeval					Light grey	1 - 3	1 - 3	Dark grey	2 - 3	Black			
Published data	(a) 1826-1938AD, Coimbra		Light grey	1 - 2	Dark grey	Dark grey	Dark grey	Dark grey	2 - 3	Black	♀			
	(b) 1887-1975AD, Lisbon	Light grey	1 & 3		1 - 3	1 & 3	2 - 3	2 - 3	Dark grey	♀				♂
	(c) 1995AD, Bosnia						1 - 3	1 - 3	Dark grey	2 - 3	Black			♂
	(d) Reference sample			Blue	Blue	Blue	Blue	Blue	Blue	Blue	Blue			

Table 6. 45: Fusion of the distal epiphysis of the radius split by primary data collected for this thesis and secondary data, which was taken from published literature. References are below. Light grey = unfused (Stage 1). Dark grey = partial fusion (Stage 2). Black = complete fusion (Stage 3). Sometimes stages of fusion overlap due to variation in individuals. To keep the table simple, overlap of fusion stages is denoted by the white text. The Reference Sample is shown in blue as partial fusion (Stage 2) and complete fusion (Stage 3) are not distinguished in the text. References: (a) Modern, Coimbra, Portugal, 1826-1938AD (births and deaths), dry bone (Coqueugniot and Weaver, 2007), (b) Modern, Lisbon, Portugal, 1887-1975AD (births and deaths), dry bone (Cardoso, 2008a), (c) Modern, Bosnia, 1995AD (war victims from the fall of Srebrenica), males only, dry bone (Schaefer, 2008b), (d) Reference sample (Schaefer et al., 2009)

		Age in years											
Dataset		13	14	15	16	17	18	19	20	21	22	23	
This study	Iron Age					Light grey			Black	2 - 3			
	Roman							Light grey		Black			
	Anglo-Saxon								Light grey	1 - 2	Black		
	Mediaeval				Light grey	1 & 3	1 - 2	1 - 3	1 & 3	1 - 3	Black		
Published data	(a) 1826-1938AD, Coimbra				Light grey	1 - 2	1 - 2	1 - 2	2 - 3	2 - 3	2 - 3	Black	♀
	(b) 1887-1975AD, Lisbon	Light grey	1 - 2	1 - 2	1 - 2	2 - 3	2 - 3		1 - 2	1 - 3	1 - 3	Black	♂
	(c) 1995AD, Bosnia				1 - 2	1 - 3	Light grey	2 - 3	2 - 3	2 - 3		Black	♂
	(d) Reference sample		Blue	Blue	Blue	Blue	Blue	Blue	Blue	Blue	Blue		

Table 6. 46: Fusion of the proximal epiphysis of the ulna skull split by primary data collected for this thesis and secondary data, which was taken from published literature. References are below. Light grey = unfused (Stage 1). Dark grey = partial fusion (Stage 2). Black = complete fusion (Stage 3). Sometimes stages of fusion overlap due to variation in individuals. To keep the table simple, overlap of fusion stages is denoted by the white text. The Reference Sample is shown in blue as partial fusion (Stage 2) and complete fusion (Stage 3) are not distinguished in the text. References: (a) Modern, Coimbra, Portugal, 1826-1938AD (births and deaths), dry bone (Coqueugniot and Weaver, 2007), (b) Modern, Lisbon, Portugal, 1887-1975AD (births and deaths), dry bone (Cardoso, 2008a), (c) Modern, Bosnia, 1995AD (war victims from the fall of Srebrenica), males only, dry bone (Schaefer, 2008b), (d) Reference sample (Schaefer et al., 2009)

		Age in years													
Dataset		10	11	12	13	14	15	16	17	18	19	20	21	22	23
This study	Iron Age														
	Roman							1 - 2		2 - 3					
	Anglo-Saxon					1 - 2									
	Mediaeval					1 - 2	1 - 2	1 - 3							
	Post-Mediaeval														
Published data	(a) 1826-1938AD, Coimbra														
	(b) 1887-1975AD, Lisbon		1 - 2		2 - 3	1 & 3									
	(c) 1995AD, Bosnia		1 - 2				2 - 3								
	(d) Reference sample														

Table 6. 47: Fusion of the distal epiphysis of the ulna split by primary data collected for this thesis and secondary data, which was taken from published literature. References are below. Light grey = unfused (Stage 1). Dark grey = partial fusion (Stage 2). Black = complete fusion (Stage 3). Sometimes stages of fusion overlap due to variation in individuals. To keep the table simple, overlap of fusion stages is denoted by the white text. The Reference Sample is shown in blue as partial fusion (Stage 2) and complete fusion (Stage 3) are not distinguished in the text. References: (a) Modern, Coimbra, Portugal, 1826-1938AD (births and deaths), dry bone (Coqueugniot and Weaver, 2007), (b) Modern, Lisbon, Portugal, 1887-1975AD (births and deaths), dry bone (Cardoso, 2008a), (c) Modern, Bosnia, 1995AD (war victims from the fall of Srebrenica), males only, dry bone (Schaefer, 2008b), (d) Modern, Chandigarh, India, living patients, radiographs\*, (Sahni et al., 1995), (e) Reference sample (Schaefer et al., 2009)

		Age in years										
Dataset		13	14	15	16	17	18	19	20	21	22	23
This study	Iron Age											
	Roman											
	Anglo-Saxon											
	Mediaeval						1 & 3	1 - 2	1 - 3	1 & 3	1 & 3	
Published data	(a) 1826-1938AD, Coimbra						1 - 2	1 - 2	1 - 2	2 - 3	2 - 3	
	(b) 1887-1975AD, Lisbon				1 - 2	1 - 2	2 - 3					
	(c) 1995AD, Bosnia				1 - 2	1 - 3	1 & 3	2 - 3	2 - 3			
	(d) 1995AD, Chandigarh*						1 - 3	1 - 3	1 - 3	1 - 3		
	(e) Reference sample											

### 6.4.3. The lower appendicular skeleton

#### A) *The Os coxae*

The Post-Mediaeval males, Lisbon and Modern Los Angeles groups entered partial fusion (Stage 2) of the **iliac crest** earlier, at ages 14 to 16 years, than the archaeological groups (**Table 6. 48**). The Mediaeval archaeological sample entered partial fusion at age 17 years, like that of the Post-Mediaeval Coimbra females and Modern Bosnian males. Between 22 to 25 years, many of the archaeological (Roman, Anglo-Saxon and Mediaeval), Post-Mediaeval and Modern groups completed fusion (Stage 3) for their entire sample. Only the 1826 to 1938 AD Coimbra females completed fusion for the entire sample much later at age 27 years.

Except for the Modern Lisbon females, who first entered partial fusion (Stage 2) of the **acetabulum** of the os coxae at 11 years of age, all other groups first entered partial fusion at age 14 years (**Table 6. 49**). Complete fusion (Stage 3) for the entire sample occurred at age 17 years for the archaeological Mediaeval sample and the Modern Lisbon females. All other groups completed fusion for their entire sample between 18 to 20 years.

#### B) *The Femur*

The Mediaeval and Post-Mediaeval archaeological samples, as well as the Post-Mediaeval and Modern groups first entered fusion (Stages 2 and 3) of the **femoral head** between 14 to 16 years, except for the Post-Mediaeval Coimbra females and the 2017 AD radiographic Western Australian population (**Table 6. 50**). Complete fusion (Stage 3) for the entire sample occurred between 19 to 21 years for the archaeological groups, the Modern Lisbon and Bosnian males. All other Modern groups completed fusion before this age range (17 to 18 years) and all other Post-Mediaeval groups completed fusion after this age range (23 to 25 years).

Fusion (Stages 2 and 3) of the **greater trochanter** occurred earlier for the Post-Mediaeval Coimbra females, Modern Lisbon and Western Australia groups compared to the archaeological samples, Post-Mediaeval Coimbra males and Modern Bosnian males (**Table 6. 51**). Complete fusion (Stage 3) occurred for the entire sample between 19 to 21 years for all groups except for the Modern Lisbon females and Western Australian data, which completed fusion earlier.

Except for the earlier fusion (Stages 2 and 3) of the **lesser trochanter** in the Modern Lisbon females and the radiographic Western Australian data, most groups first entered fusion between 14 to 16 years of age (**Table 6. 52**). The Mediaeval archaeological group completed

fusion (Stage 3) for the entire sample at age 17 years, the same age that the Modern Lisbon females completed fusion for their entire sample. The archaeological Roman and Anglo-Saxon groups completed fusion for their entire sample later, at age 20 years, the same age the Post-Mediaeval Coimbra females also completed fusion for their entire sample.

Many of the Post-Mediaeval and Modern groups began fusion (Stages 2 and 3) of the **distal femur** earlier than the archaeological groups (**Table 6. 53**). Only the archaeological Mediaeval sample, Post-Mediaeval Coimbra females and the 1950s AD USA data entered fusion at the later age of 17 years. Complete fusion (Stage 3) of the entire sample occurred between 20 to 22 years for all groups, except for the radiographic data and the Modern Lisbon males who all completed fusion earlier.

### *C) The Tibia*

Fusion (Stages 2 and 3) of the **proximal tibia** occurred much earlier in the Post-Mediaeval and Modern datasets compared to the archaeological samples (**Table 6. 54**). Only the 1950s AD USA dataset entered fusion at the same time as the archaeological Mediaeval sample entered fusion, at age 17 years. For the Post-Mediaeval and Modern groups that analysed dry bone, complete fusion (Stage 3) of the entire sample occurred between 20 to 23 years, and this included the archaeological samples too. Only the studies that analysed radiographs showed an earlier age of between 15 to 18 years for the entire sample to complete fusion.

The Post-Mediaeval Coimbra females and the Modern Lisbon data entered partial fusion (Stage 2) of the **distal tibia** earlier than the archaeological Mediaeval sample and the Post-mediaeval Coimbra and Modern Bosnian males (**Table 6. 55**). Complete fusion (Stage 3) of the entire sample occurred between 19 to 21 years for all groups, except for the Modern Lisbon females, which completed fusion for the entire sample earlier at age 17 years.

Table 6. 48: Fusion of the iliac crest of the os coxae split by primary data collected for this thesis and secondary data, which was taken from published literature. References are below. Light grey = unfused (Stage 1). Dark grey = partial fusion (Stage 2). Black = complete fusion (Stage 3). Sometimes stages of fusion overlap due to variation in individuals. To keep the table simple, overlap of fusion stages is denoted by the white text. The Reference Sample is shown in blue as partial fusion (Stage 2) and complete fusion (Stage 3) are not distinguished in the text. References: (a) Modern, Coimbra, Portugal, 1826-1938AD (births and deaths), dry bone (Coqueugniot and Weaver, 2007), (b) Modern, Lisbon, Portugal, 1930-1960AD (deaths), dry bone (Cardoso, 2008b), (c) Modern, Bosnia, 1995AD (war victims from the fall of Srebrenica), males only, dry bone (Schaefer, 2008b), (d) Modern, Los Angeles, USA, 1977-1979AD (autopsies), (Webb and Suchey, 1985), (e) Reference sample (Schaefer et al., 2009)

		Age in years																	
Dataset		13	14	15	16	17	18	19	20	21	22	23	24	25	26	27			
This study	Iron Age		Light grey							Black									
	Roman							Light grey	Black	Dark grey						Black			
	Anglo-Saxon									Light grey	Black	Dark grey							
	Mediaeval				Light grey	1-2	1-2	2-3	1&3	1-3	2-3	2-3				Black			
	Post-Mediaeval							Dark grey											
Iliac crest	Published data	(a) 1826-1938AD, Coimbra				Light grey	1-2	1-2	1-2			2-3	2-3	2-3	2-3	2-3	Black	♀	
		(b) 1930-1960AD, Lisbon		Light grey	1-2			1-2	1-2	1-2	1-3	2-3	2-3	2-3	2-3			♂	
		(c) 1995AD, Bosnia			Light grey	1-2	1-2	1-2	2-3	2-3	2-3			Black	♂				
	(d) 1977-1979AD, Los Angeles				Light grey	1-2			1-2	1-3	2-3	2-3	2-3	2-3	2-3			♀	
	(e) Reference sample		Light grey	1-2	1-2	1-2	1-3	1-3	1-3	2-3	2-3	2-3	2-3	2-3				♂	
			Blue																

Table 6. 49: Fusion of the acetabulum of the os coxae split by primary data collected for this thesis and secondary data, which was taken from published literature. References are below. Light grey = unfused (Stage 1). Dark grey = partial fusion (Stage 2). Black = complete fusion (Stage 3). Sometimes stages of fusion overlap due to variation in individuals. To keep the table simple, overlap of fusion stages is denoted by the white text. The Reference Sample is shown in blue as partial fusion (Stage 2) and complete fusion (Stage 3) are not distinguished in the text. References: (a) Modern, Lisbon, Portugal, 1930-1960AD (deaths), dry bone (Cardoso, 2008b), (b) Modern, Bosnia, 1995AD (war victims from the fall of Srebrenica), males only, dry bone (Schaefer, 2008b), (c) Reference sample (Schaefer et al., 2009)

		Age in years													
Dataset		9	10	11	12	13	14	15	16	17	18	19	20	21	
Acetabulum	This study	Roman													
		Anglo-Saxon													
		Mediaeval													
	Published data	(a) 1930-1960AD, Lisbon													
		(b) 1995AD, Bosnia													
		(c) Reference sample													

Table 6. 50: Fusion of the femoral head split by primary data collected for this thesis and secondary data, which was taken from published literature. References are below. Light grey = unfused (Stage 1). Dark grey = partial fusion (Stage 2). Black = complete fusion (Stage 3). Sometimes stages of fusion overlap due to variation in individuals. To keep the table simple, overlap of fusion stages is denoted by the white text. The Reference Sample is shown in blue as partial fusion (Stage 2) and complete fusion (Stage 3) are not distinguished in the text. References: (a) Modern, Coimbra, Portugal, 1826-1938AD (births and deaths), dry bone (Coqueugniot and Weaver, 2007), (b) Modern, Lisbon, Portugal, 1930-1960AD (deaths), dry bone (Cardoso, 2008b), (c) Modern, Bosnia, 1995AD (war victims from the fall of Srebrenica), males only, dry bone (Schaefer, 2008b), (d) Modern, Western Australia, living patients, MDCT scans\* (Sullivan et al., 2017), (e) Reference sample (Schaefer et al., 2009)

		Age in years																						
Dataset		3	4	5	6	7	8	9	10	11	12	13	14	15	16	17	18	19	20	21	22	23	24	25
This study	Iron Age																							
	Roman																							
	Anglo-Saxon																							
	Mediaeval																							
	Post-Mediaeval																							
Femoral head	(a) 1826-1938AD, Coimbra																							
	(b) 1930-1960AD, Lisbon																							
	(c) 1995AD, Bosnia																							
	(d) 2017AD, Western Australia*																							
	(e) Reference sample																							

Table 6. 51: Fusion of the greater trochanter of the femur split by primary data collected for this thesis and secondary data, which was taken from published literature. References are below. Light grey = unfused (Stage 1). Dark grey = partial fusion (Stage 2). Black = complete fusion (Stage 3). Sometimes stages of fusion overlap due to variation in individuals. To keep the table simple, overlap of fusion stages is denoted by the white text. The Reference Sample is shown in blue as partial fusion (Stage 2) and complete fusion (Stage 3) are not distinguished in the text. References: (a) Modern, Coimbra, Portugal, 1826-1938AD (births and deaths), dry bone (Coqueugniot and Weaver, 2007), (b) Modern, Lisbon, Portugal, 1930-1960AD (deaths), dry bone (Cardoso, 2008b), (c) Modern, Bosnia, 1995AD (war victims from the fall of Srebrenica), males only, dry bone (Schaefer, 2008b), (d) Modern, Western Australia, living patients, MDCT scans\* (Sullivan et al., 2017), (e) Reference sample

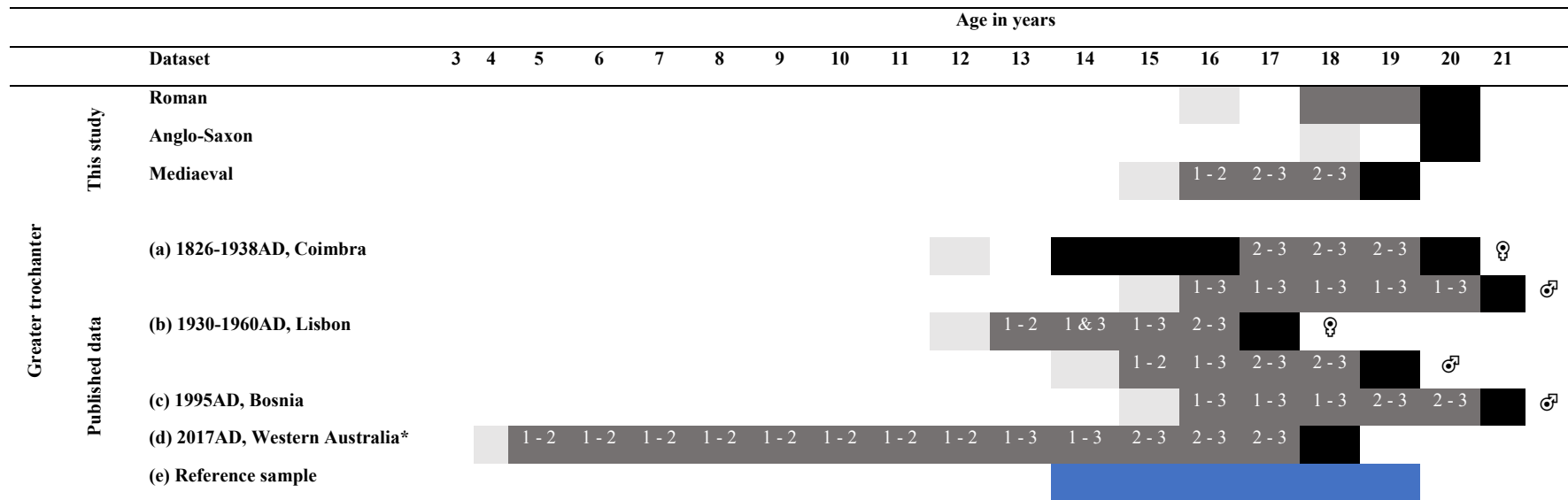


Table 6. 52: Fusion of the lesser trochanter of the femur split by primary data collected for this thesis and secondary data, which was taken from published literature. References are below. Light grey = unfused (Stage 1). Dark grey = partial fusion (Stage 2). Black = complete fusion (Stage 3). Sometimes stages of fusion overlap due to variation in individuals. To keep the table simple, overlap of fusion stages is denoted by the white text. The Reference Sample is shown in blue as partial fusion (Stage 2) and complete fusion (Stage 3) are not distinguished in the text. References: (a) Modern, Coimbra, Portugal, 1826-1938AD (births and deaths), dry bone (Coqueugniot and Weaver, 2007), (b) Modern, Lisbon, Portugal, 1930-1960AD (deaths), dry bone (Cardoso, 2008b), (c) Modern, Bosnia, 1995AD (war victims from the fall of Srebrenica), males only, dry bone (Schaefer, 2008b), (d) Modern, Western Australia, living patients, MDCT scans\* (Sullivan et al., 2017), (e) Reference sample (Schaefer et al., 2009)

		Age in years													
		9	10	11	12	13	14	15	16	17	18	19	20	21	22
<b>This study</b>	<b>Roman</b>										1 - 2				
	<b>Anglo-Saxon</b>														
	<b>Mediaeval</b>							1 & 3	1 - 2						
<b>Lesser trochanter</b>	<b>(a) 1826-1938AD, Coimbra</b>									2 - 3	2 - 3	2 - 3			♀
	<b>(b) 1930-1960AD, Lisbon</b>					1 - 2	1 & 3	1 - 3	2 - 3		♀				♂
	<b>(c) 1995AD, Bosnia</b>							1 - 2	1 - 3	2 - 3	2 - 3		♂		
	<b>(d) 2017AD, Western Australia*</b>	1 - 2	1 - 2	1 - 2	1 - 2	1 - 3	1 - 3	1 - 3	1 - 3	2 - 3					
	<b>(e) Reference sample</b>														

Table 6. 53: Fusion of the distal epiphysis of the femur split by primary data collected for this thesis and secondary data, which was taken from published literature. References are below. Light grey = unfused (Stage 1). Dark grey = partial fusion (Stage 2). Black = complete fusion (Stage 3), Sometimes stages of fusion overlap due to variation in individuals. To keep the table simple, overlap of fusion stages is denoted by the white text. The Reference Sample is shown in blue as partial fusion (Stage 2) and complete fusion (Stage 3) are not distinguished in the text. References: (a) Modern, Coimbra, Portugal, 1826-1938AD (births and deaths), dry bone (Coqueugniot and Weaver, 2007), (b) Modern, Lisbon, Portugal, 1930-1960AD (deaths), dry bone (Cardoso, 2008b), (c) Modern, USA, 1950-1952AD (war victims from the Korean war), males only, dry bone (McKern and Stewart, 1957), (d) Modern, Bosnia, 1995AD (war victims from the fall of Srebrenica), males only, dry bone (Schaefer, 2008b), (e) Modern, Cork, Ireland, living patients, radiographs\*, (O'Connor et al., 2008), (f) Modern, Delta state, Nigeria, living patients, radiographs\*, (Ebeye et al., 2016), (g) Reference sample (Schaefer et al., 2009)

		Age in years													
Dataset		9	10	11	12	13	14	15	16	17	18	19	20	21	22
This study	Iron Age									1					
	Roman										1				
	Anglo-Saxon														
	Mediaeval									1 & 3		2 - 3	2 - 3		
	Post-Mediaeval														
Distal femur	(a) 1826-1938AD, Coimbra									1 - 3	1 - 3	1 - 3			♀
	(b) 1930-1960AD, Lisbon					1 - 2	1 - 2	1 - 2	2 - 3	2 - 3	2 - 3			♀	♂
	(c) 1950-1952AD, USA								1 & 3	1 - 3	1 & 3		♂		
	(d) 1995AD, Bosnia								1 - 2	1 - 3	1 - 3	1 - 3	2 - 3		♂
	(e) 2008AD, Cork*		1 - 2		1 - 2	1 - 3	2 - 3	2 - 3				♀			
	(f) 2016AD, Delta state*		1 - 2		1 - 2	1 - 3	1 - 2	1 - 3	2 - 3	2 - 3			♂		
	(g) Reference sample														

Table 6. 54: Fusion of the proximal epiphysis of the tibia split by primary data collected for this thesis and secondary data, which was taken from published literature. References are below. Light grey = unfused (Stage 1). Dark grey = partial fusion (Stage 2). Black = complete fusion (Stage 3). Sometimes stages of fusion overlap due to variation in individuals. To keep the table simple, overlap of fusion stages is denoted by the white text. The Reference Sample is shown in blue as partial fusion (Stage 2) and complete fusion (Stage 3) are not distinguished in the text. References: (a) Modern, Coimbra, Portugal, 1826-1938AD (births and deaths), dry bone (Coqueugniot and Weaver, 2007), (b) Modern, Lisbon, Portugal, 1930-1960AD (deaths), dry bone (Cardoso, 2008b), (c) Modern, USA, 1950-1952AD (war victims from the Korean war), males only, dry bone (McKern and Stewart, 1957), (d) Modern, Bosnia, 1995AD (war victims from the fall of Srebrenica), males only, dry bone (Schaefer, 2008b), (e) Modern, Cork, Ireland, living patients, radiographs\*, (O'Connor et al., 2008), (f) Modern, Delta state, Nigeria, living patients, radiographs\*, (Ebeye et al., 2016), (g) Reference sample (Schaefer et al., 2009)

		Age in years														
Dataset		9	10	11	12	13	14	15	16	17	18	19	20	21	22	23
This study	Iron Age															
	Roman															
	Anglo-Saxon															
	Mediaeval															
	Post-Mediaeval															
Proximal tibia	(a) 1826-1938AD, Coimbra															
	(b) 1930-1960AD, Lisbon															
	(c) 1950-1952AD, USA															
	(d) 1995AD, Bosnia															
	(e) 2008AD, Cork*															
	(f) 2016AD, Delta state*															
	(g) Reference sample															

Table 6. 55: Fusion of the distal epiphysis of the tibia split by primary data collected for this thesis and secondary data, which was taken from published literature. References are below. Light grey = unfused (Stage 1). Dark grey = partial fusion (Stage 2). Black = complete fusion (Stage 3). Sometimes stages of fusion overlap due to variation in individuals. To keep the table simple, overlap of fusion stages is denoted by the white text. The Reference Sample is shown in blue as partial fusion (Stage 2) and complete fusion (Stage 3) are not distinguished in the text. References: (a) Modern, Coimbra, Portugal, 1826-1938AD (births and deaths), dry bone (Coqueugniot and Weaver, 2007), (b) Modern, Lisbon, Portugal, 1930-1960AD (deaths), dry bone (Cardoso, 2008b), (c) Modern, Bosnia, 1995AD (war victims from the fall of Srebrenica), males only, dry bone (Schaefer, 2008b), (d) Reference sample (Schaefer et al., 2009)

		Age in years									
Datasets		13	14	15	16	17	18	19	20	21	22
This study	Iron Age		Light grey								Black
	Roman						Light grey		Black		
	Anglo-Saxon						Light grey		Black		
	Mediaeval			Light grey	1 - 2	2 - 3			Black		
Distal tibia Published data	(a) 1826-1938AD, Coimbra	Light grey	1 - 2	1 - 2	1 - 2	1 - 3	2 - 3	2 - 3	Black		♀
	(b) 1930-1960AD, Lisbon	Light grey	1 - 2	1 - 3	1 - 3		♀			Black	♂
	(c) 1995AD, Bosnia			1 - 2	1 - 3	2 - 3	1 & 3	Black	♂		
	(d) Reference sample		Blue	Blue	Blue	Blue	Blue	Blue			

## **6.5. THE SEQUENCE OF FUSION AT BRITISH ARCHAEOLOGICAL PERIODS AND COMPARED TO POST-MEDIAEVAL AND MODERN (18<sup>TH</sup> – 20<sup>TH</sup> CENTURY AD) PUBLISHED DATA**

**Table 6. 56** presents the modal sequence – the most common sequence found – for complete fusion (Stage 3) for the Roman, Anglo-Saxon and Mediaeval groups. This archaeological data is compared to previously published literature. The Iron age and Post-Mediaeval data were not included due to low sample sizes.

### **6.5.1. Archaeological sites**

The occipital bones (lateral-squama and basilar-lateral) were always the first bones to fuse for the Roman, Anglo-Saxon and Mediaeval samples. The ischiopubic ramus, distal humerus and acetabulum were always the third, fourth and fifth bones to fuse within the sequence. The iliac crest, medial clavicle, and sacral bodies 1 to 2 were the last bones to fuse in the sequence, although not necessarily in that order. Usually, individuals were older when the knee, wrist and shoulder fused. The sequence in which other bones fused was more variable.

### **6.5.2. Archaeological sites compared to Post-Mediaeval and Modern (18<sup>th</sup> – 20<sup>th</sup> century) samples**

Like the archaeological samples, and when modal values were considered, the occipital bones fused first, and the ischiopubic ramus fused third for the European sample. The proximal humerus, iliac crest, and medial clavicle were the last to fuse in that order, for the European and Bosnian samples. The knee, wrist and shoulder were also found to fuse nearer the end of the modal sequence in the Post-Mediaeval and Modern published samples. Fusion sites in the middle of the sequence were more variable in the order in which they fused. The degree of variability differed between sites. For example, the proximal ulna, coracoid of the scapula, the medial humeral epicondyle and acetabulum of the os coxae tended to fuse early in the sequence but would differ in their order of fusion between groups. Whereas the fusion of the distal humerus was highly variable and did not have a specific place within the sequence.

Table 6. 56: The sequence of ossification sites completing fusion by period of Roman, Anglo-Saxon and Mediaeval samples compared to previous studies. The modal sequence is the most common order of fusion found in both the time period samples and the comparison studies. Outliers are ossification sites that completed fusion in a different sequence to the modal sequence of the samples and are listed below. The key is taken from Lenover and Šešelj, (2019), from the ossification sites that were used in both the partial and complete modal sequences of that study for their European samples. For the comparison studies, grouped ossification sites – shown via a collective colour – are ossification sites that completed fusion together. For the time period samples, grouped ossification sites either are ossification sites that completed fusion together or had a low sample size that the ossification sites could be properly placed between other sites, but could not be sorted individually e.g. the sequence of site A and site B may be found to sit between site C and D, but low sample sizes may not show whether site A or site B is first. Numbers with a line next to them e.g. “(1) –“ means that the site was not included in that sample. Names of ossification sites differ between studies based on what was written in the original study. References: (A) European sample includes skeletons from London, England (18<sup>th</sup>-19<sup>th</sup> century), Lisbon, Portugal (19<sup>th</sup>-20<sup>th</sup> century) and Cleveland, USA (early 20<sup>th</sup> century), age known (Lenover and Šešelj, 2019), (B) Bosnian sample includes skeletons who were Bosniak (Bosnian Muslim) males, age known (Schaefer and Black, 2007)

Key <sup>A</sup>	European modal sequence <sup>A</sup>	Bosnia modal sequence <sup>B</sup>	Roman modal sequence	Anglo-Saxon modal sequence	Mediaeval modal sequence
(1) Occipital lateral-squama	(1) Occipital lateral-squama	(1) -	(1) Occipital lateral-squama	(1) Occipital lateral-squama	(1) Occipital lateral-squama
(2) Occipital basilar-lateral	(2) Occipital basilar-lateral	(2) -	(2) Occipital basilar-lateral	(2) Occipital basilar-lateral	(2) Occipital basilar-lateral
(3) Ischiopubic ramus	(3) Ischiopubic ramus	(3) -	(3) Ischiopubic ramus	(3) -	(3) Ischiopubic ramus
(4) Ischium-pubis (acetabulum)	(5) Coracoid	(10) Distal humerus	(10) Distal humerus	(10) Distal humerus	(10) Distal humerus
(5) Coracoid	(4) Ischium-pubis (acetabulum)	(6) Proximal ulna	(4) Acetabulum	(4) -	(4) Acetabulum *
(6) Proximal ulna	(6) Proximal ulna	(5) Coracoid	(5) Coracoid	(5) -	(8) Proximal radius*
(7) Medial humeral epicondyle	(7) Medial humeral epicondyle	(7) Medial humerus	(6) Proximal ulna	(6) -	(5) Coracoid*
(8) Proximal radius	(8) Proximal radius	(8) Proximal radius	(7) Medial humeral epicondyle	(7) Medial humeral epicondyle	(6) Proximal ulna*
(9) Femoral head	(9) Femoral head	(4) Acetabulum	(8) Proximal radius	(11) Distal tibia	(7) Medial humeral epicondyle *
(10) Distal humerus	(12) Greater trochanter	(11) Distal tibia	(14) Sphenooccipital synchondrosis	(13) Lesser trochanter	(13) Lesser trochanter*
(11) Distal tibia	(11) Distal tibia	(13) Lesser trochanter	(11) -	(8) Proximal radius	(14) Sphenooccipital synchondrosis*
(12) Greater trochanter	(13) Lesser trochanter	(9) Proximal femur	(9) Femoral head	(9) Femoral head*	(12) Greater trochanter
(13) Lesser trochanter	(10) Distal humerus	(12) Greater trochanter	(12) Greater trochanter	(12) Greater trochanter	(11) Distal tibia
(14) Sphenooccipital synchondrosis	(14) -	(14) -	(13) Lesser trochanter	(14) Sphenooccipital synchondrosis	(16) Acromion
(15) Proximal tibia	(15) Proximal tibia	(16) Acromion	(15) Proximal tibia	(15) Proximal tibia*	(9) Femoral head*
(16) Acromion	(16) Acromion	(15) Proximal tibia	(16) Acromion	(16) Acromion*	(15) Proximal tibia*
(17) Distal femur	(18) Distal radius	(17) Distal femur	(17) Distal femur	(17) Distal femur	(17) Distal femur*
(18) Distal radius	(17) Distal femur	(19) Distal ulna	(18) Distal radius	(18) Distal radius	(18) Distal radius
(19) Distal ulna	(19) Distal ulna	(18) Distal radius	(19) Distal ulna	(19) Distal ulna	(19) Distal ulna
(20) Proximal humerus	(20) Proximal humerus	(20) Proximal humerus	(20) Proximal humerus	(20) Proximal humerus	(20) Proximal humerus
(21) Iliac crest	(21) Iliac crest	(21) Iliac crest	(21) Iliac crest	(21) Iliac crest	(21) Iliac crest
(22) Sacral 1-2	(22) -	(22) -	(22) Sacral 1-2	(21) Medial clavicle	(22) Sacral 1-2*
(23) Medial clavicle	(23) Medial clavicle	(23) Medial clavicle	(23) Medial clavicle	(22) Sacral 1-2	(23) Medial clavicle*

\*Outliers (n /total)

**Anglo-Saxon:** Proximal tibia **completes prior to** the femoral head (1/3)

**Anglo-Saxon:** Acromion **completes prior to** the femoral head (1/2 - femoral head was a later stage when acromion completed first)

**Mediaeval:** Proximal radius **completes prior to** the acetabulum (1/4)

**Mediaeval:** Coracoid **completes prior to** the proximal radius (1/3)

**Mediaeval:** Proximal ulna **completes prior to** the proximal radius (1/4)

**Mediaeval:** Lesser trochanter **completes prior to** the proximal ulna (1/3)

**Mediaeval:** Lesser trochanter **completes prior to** the medial humeral epicondyle (1/3)

**Mediaeval:** Sphenooccipital synchondrosis **completes prior to** the medial humeral epicondyle (1/3)

**Mediaeval:** Lesser trochanter **completes prior to** the proximal radius (1/5)

**Mediaeval:** Medial clavicle **completes prior to** the sacral bodies 1-2 (2/4 - sacral 1-2 was a later stage when medial clavicle completed first)

## CHAPTER 7

**RESULTS**AGE AT PUBERTY COMPARED AMONGST MEDIAEVAL SITES AND BETWEEN  
ARCHAEOLOGICAL PERIODS

This chapter compares age at puberty amongst Mediaeval sites and between different time periods. An additional exploration was conducted into the relationship between age at puberty, and fusion of skeletal elements that are not considered indicators of puberty. These additional explorations are undertaken for Mediaeval sites and compared between archaeological periods. These are presented separately in **Appendices 11 – 14**. Key findings from **Appendices 11 – 14** were that fusion of many of the epiphyses occurred at a similar pubertal phase throughout British history. Meaning that regardless of differences in the age-at-fusion, the epiphyses fuse at a similar pubertal phase. Although the dentocentral and neurocentral junctions of the axis was found to fuse (Stages 2 and 3) at a significantly later pubertal phase in the Mediaeval group (Acceleration) than in the Anglo-Saxon group (Pre-puberty). Secondly, the complete fusion (Stage 3) of the sacral bodies 1 and 2 signified that puberty had completed.

## 7.1. RESEARCH QUESTIONS

### **Question 1. Does age at puberty differ between Mediaeval Canterbury and Mediaeval York?**

In this section, the age at which the five pubertal phases (Pre-puberty, Acceleration, PHV, Deceleration, Maturation and Completion) occurred in Mediaeval Canterbury are compared to Mediaeval York. The Mediaeval Canterbury skeletons consisted of both high and low individuals from St Gregory's priory and cemetery. The Mediaeval York skeletons consisted of two York samples, All Saint's church and Fishergate House. Results are presented in **Section 7.2**.

### **Question 2. Does the age at which each pubertal phase is attained change when compared between archaeological periods?**

In this section, the age at which the five pubertal phases occurred is compared across archaeological periods. Results are presented in **Section 7.3**.

\*\*\*

**A note on statistics:** The statistical tests used in this chapter include a Mann Whitney U, a Kruskal Wallis test, and a multiple regression. The Mann Whitney U was used to look at the age at pubertal phase between Mediaeval Canterbury and Mediaeval York. The assumptions for a Mann-Whitney U test can be found in **Section 5.1**. The Kruskal Wallis was used to look at the age at pubertal phase between archaeological periods. The multiple regression was used to see if age at pubertal phase could predict which archaeological period the skeleton was attributed to. Assumptions for a multiple regression can be found in **Section 6.1**.

Assumptions for a Kruskal-Wallis test include (1) One dependent variable that is continuous or ordinal, (2) One independent variable that has two or more categorical, independent groups, and (3) There is independence of observations (Lund and Lund, 2013a). Assumptions for this test are met in that (1) Pubertal phase is ordinal data, (2) Archaeological periods have more than two categorical, independent groups, and (3) A skeleton can only be in one archaeological group and one pubertal phase.

As a final note on statistics, when comparing puberty data between Mediaeval Canterbury and Mediaeval York, as well as between the archaeological periods, the sample sizes for Mediaeval Canterbury and the Mediaeval archaeological period are far bigger than the other samples. This is especially true for the Iron Age and Post-Mediaeval data, which are extremely small in size. This may potentially be why no significant differences were found for the univariate tests. It is probable that the multiple regression between puberty and archaeological periods met statistical significance because of the disparity between samples.

## 7.2. AGE AT PUBERTY COMPARED BETWEEN MEDIAEVAL CANTERBURY AND YORK SAMPLES

**Table 7. 1** shows the pubertal phase and estimated age for Mediaeval Canterbury and York skeletons. Mediaeval Canterbury and Mediaeval York children remained in **Pre-puberty** until 8 years of age, with some remaining in this phase until age 12 years. No significant differences were found between Mediaeval Canterbury and York when the age at which the Pre-puberty phase occurred was compared ( $p = 1.000$ ,  $U = 375.000$ ). For both Mediaeval Canterbury and Mediaeval York, the **Acceleration** phase commenced at age 9 years for some juveniles, while others remained in this stage until age 16 years. No significant differences were found between Mediaeval Canterbury and York's Acceleration phase ( $p = 1.000$ ,  $U = 137.500$ ). Mediaeval Canterbury adolescents entered **PHV** at age 14 years, whereas Mediaeval York adolescents were slightly older aged 15 years. No significant differences were found when the PHV phase at Mediaeval Canterbury was compared to the age that the PHV phase occurred at York ( $p = 1.000$ ,  $U = 22.000$ ). The earliest age at which the **Deceleration** phase occurred was 16 years, which was the same age for both groups. No significant differences were found between Mediaeval Canterbury and York's Deceleration phase ( $p = 1.000$ ,  $U = 5.000$ ).

Table 7. 1: Age at puberty for Mediaeval Canterbury and Mediaeval York. The stages of union are recorded as percentages.

		Age at puberty for Mediaeval groups						
	Age	<i>n</i>	Pre-puberty	Acceleration	PHV	Deceleration	Maturation	Completion
<i>Canterbury</i>	5	6	100.0	-	-	-	-	-
	6	6	100.0	-	-	-	-	-
	7	5	100.0	-	-	-	-	-
	8	7	100.0	-	-	-	-	-
	9	5	40.0	60.0	-	-	-	-
	10	2	100.0	-	-	-	-	-
	11	5	20.0	80.0	-	-	-	-
	12	7	57.1	42.9	-	-	-	-
	13	3	-	100.0	-	-	-	-
	14	5	-	80.0	20.0	-	-	-
	15	10	-	50.0	50.0	-	-	-
	16	5	-	20.0	60.0	20.0	-	-
	17	2	-	-	50.0	-	50.0	-
	18	2	-	-	-	50.0	50.0	-
	19	6	-	-	-	16.7	50.0	33.3
	20	2	-	-	-	50.0	-	50.0
	21	8	-	-	12.5	12.5	25.0	50.0
	22	1	-	-	-	-	-	100.0
	23	3	-	-	-	-	-	100.0
	24	1	-	-	-	-	-	100.0
25	7	-	-	-	-	14.3	85.7	
28	2	-	-	-	-	-	100.0	
	Age	<i>n</i>	Pre-puberty	Acceleration	PHV	Deceleration		
<i>York</i>	5	4	100.0	-	-	-		
	6	2	100.0	-	-	-		
	7	2	100.0	-	-	-		
	8	1	100.0	-	-	-		
	9	1	-	100.0	-	-		
	10	3	66.7	33.3	-	-		
	11	2	100.0	-	-	-		
	12	3	66.7	33.4	-	-		
	13	5	-	100.0	-	-		
	14	1	-	100.0	-	-		
	15	2	-	50.0	50.0	-		
	16	5	-	20.0	60.0	20.0		
	18	1	-	-	-	100.0		

### 7.3. AGE AT PUBERTY COMPARED BETWEEN ARCHAEOLOGICAL PERIODS

Pubertal phase was estimated for all skeletons from each archaeological period and compared to their estimated ages (**Table 7. 2**). No individual remained in the **Pre-puberty** phase past the age of 12 years. No significant differences were found between the archaeological groups (Roman, Anglo-Saxon, Mediaeval and Post-Mediaeval) for the Pre-puberty phase ( $X^2 (3) = 0.000, p = 1.000$ ).

The age at which **Acceleration** commenced differed between the groups. This phase commenced for some individuals at 9 years of age for the Mediaeval sample and 11 years of age for  $n = 1$  Roman skeleton and  $n = 2$  Anglo-Saxons. Acceleration lasted until age 16 years for some Roman and Mediaeval individuals and age 18 years for one Anglo-Saxon adolescent. No significant differences were found between the archaeological groups (Iron Age, Roman, Anglo-Saxon and Mediaeval) for the Acceleration phase ( $X^2 (3) = 0.000, p = 1.000$ ).

**PHV** was recorded for Roman, Anglo-Saxon and Mediaeval skeletons only. This phase was present between 14 to 17 years of age for the Anglo-Saxon sample. The mean age at PHV was 15 years for the Anglo-Saxons (mean age = 15.29, s.d. = 1.11). PHV was recorded between 14 to 21 years for the Mediaeval sample. The mean age at PHV was also 15 years (s.d. = 0.76) for the Mediaeval sample. The Roman group showed a later age for PHV at 18 years. No statistically significant differences existed between these archaeological groups for the PHV phase ( $X^2 (2) = 0.000, p = 1.000$ ).

**Deceleration** was recorded between 17 to 21 years for the Anglo-Saxon sample and between 16 to 21 years for the Mediaeval sample. The mean age during Deceleration was 18 years for the Mediaeval group (mean age = 17.56, s.d. = 1.90). The Post-Mediaeval group had a limited sample size, but individuals were recorded in Deceleration between 17 to 19 years, close to the age range recorded in the Anglo-Saxon and Mediaeval samples. No significant differences were found between archaeological groups (Iron Age, Roman, Anglo-Saxon, Mediaeval and Post-Mediaeval) for the Deceleration phase ( $X^2 (4) = 0.000, p = 1.000$ ).

**Maturation** was recorded between 17 to 25 years for the Mediaeval group. The mean age at Maturation was 19 years for the Mediaeval sample (mean age = 19.15, s.d. = 1.28). Although sample sizes were low for all the other archaeological groups, these groups showed ages at Maturation within the age range of the Mediaeval group. The Iron Age sample had two individuals that had attained this phase aged 20 and 21 years. The Roman group had two individuals aged 21 years, and the Anglo-Saxon had one 23-year-old recorded in Maturation.

No significant differences were found between archaeological groups (Iron Age, Roman, Anglo-Saxon and Mediaeval) for the Maturation phase ( $\chi^2 (3) = 0.000, p = 1.000$ ).

The Iron Age ( $n = 2$ ) skeletons had reached the **Completion** phase of puberty by 21 years of age. The Romans ( $n = 1$ ) reached this phase at age 20 years and the Anglo-Saxons ( $n = 2$ ) reached this phase at age 22 years. Finally, the Mediaeval ( $n = 7$ ) sample reached Completion at the earliest age of 19 years. The mean age to complete puberty was 22 years (mean age = 22.08, s.d. 2.24) for the Mediaeval sample. No significant differences were found between the archaeological groups (Iron Age, Roman, Anglo-Saxon and Mediaeval) for the Completion phase ( $\chi^2 (3) = 0.000, p = 1.000$ ).

Table 7. 2: Age at puberty for all archaeological groups. The stages of union are recorded as percentages.

Age at puberty for all archaeological groups								
	Age	n	Acceleration	Deceleration	Maturation	Completion		
<i>Iron Age</i>	14	1	100.0	-	-	-	-	
	17	1	-	100.0	-	-	-	
	20	1	-	-	100.0	-	-	
	21	2	-	-	50.0	50.0	-	
	25	1	-	-	-	-	100.0	
	Age	n	Pre-puberty	Acceleration	PHV	Deceleration	Maturation	Completion
<i>Roman</i>	6	1	100.0	-	-	-	-	-
	9	1	100.0	-	-	-	-	-
	11	1	-	100.0	-	-	-	-
	12	3	100.0	-	-	-	-	-
	13	1	-	100.0	-	-	-	-
	15	2	-	100.0	-	-	-	-
	16	2	-	50.0	50.0	-	-	-
	18	2	-	-	100.0	-	-	-
	19	1	-	-	-	100.0	-	-
	20	1	-	-	-	-	-	100.0
	21	2	-	-	-	-	100.0	-
	24	1	-	-	-	-	-	100.0
	25	3	-	-	-	-	-	100.0
	Age	n	Pre-puberty	Acceleration	PHV	Deceleration	Maturation	Completion
<i>Anglo-Saxon</i>	6	3	100.0	-	-	-	-	-
	7	6	100.0	-	-	-	-	-
	8	3	100.0	-	-	-	-	-
	9	1	100.0	-	-	-	-	-
	10	2	100.0	-	-	-	-	-
	11	3	33.3	66.7	-	-	-	-
	12	3	33.3	66.7	-	-	-	-
	13	2	-	100.0	-	-	-	-
	14	2	-	50.0	50.0	-	-	-
	15	2	-	-	100.0	-	-	-
	16	2	-	50.0	50.0	-	-	-
	17	2	-	-	50.0	50.0	-	-
	18	1	-	100.0	-	-	-	-
	20	1	-	-	-	100.0	-	-
21	2	-	-	-	100.0	-	-	
22	2	-	-	-	-	-	100.0	
23	1	-	-	-	-	100.0	-	
	Age	n	Pre-puberty	Acceleration	PHV	Deceleration	Maturation	Completion
<i>Medieval</i>	6	10	100.0	-	-	-	-	-
	7	7	100.0	-	-	-	-	-
	8	9	100.0	-	-	-	-	-
	9	6	33.3	66.7	-	-	-	-
	10	5	80.0	20.0	-	-	-	-
	11	8	37.5	62.5	-	-	-	-
	12	10	60.0	40.0	-	-	-	-
	13	8	-	100.0	-	-	-	-
	14	8	-	62.5	37.5	-	-	-
	15	13	-	53.8	46.2	-	-	-
	16	10	-	20.0	60.0	20.0	-	-
	17	2	-	-	50.0	-	50.0	-
	18	3	-	-	-	66.7	33.3	-
	19	7	-	-	-	28.6	42.9	28.6
	20	2	-	-	-	50.0	-	50.0
	21	9	-	-	11.1	11.1	22.2	55.6
	22	2	-	-	-	-	-	100.0
23	3	-	-	-	-	-	100.0	
24	1	-	-	-	-	-	100.0	
25	7	-	-	-	-	14.3	85.7	
28	2	-	-	-	-	-	100.0	
	Age	n	Pre-puberty	Deceleration				
<i>Post Medieval</i>	7	2	100.0	-				
	8	1	100.0	-				
	17	1	-	-	100.0			
	19	1	-	-	-	100.0		

### 7.3.1. Summary of findings

There were no significant differences in the age at which the pubertal phases were attained when compared between the archaeological sites. A summary of the pubertal phases for each archaeological period is given in **Table 7.3**.

Table 7.3: Age-at-death per pubertal phase for the archaeological periods

	Rounded age-at-death estimation (years)													
	8	9	10	11	12	13	14	15	16	17	18	19	20	21-25
Iron Age							Acc.				Dec.			
													Maturation	Comp
Roman		Pre-puberty					Acceleration			PHV		Dec.		
														Mat.
													Completion	
Anglo-Saxon		Pre-puberty					Acceleration		PHV			Deceleration		
														Mat.
													Completion	
Mediaeval		Pre-puberty					Acceleration			PHV		Deceleration		
														Maturation
													Completion	
Post-Mediaeval											Deceleration			

### 7.3.2. Multivariate analysis

A multiple regression was carried out to see if the age at pubertal phase could be predicted from the archaeological group. Before carrying out the test, assumptions for the multiple regression were checked (**Table 7. 4**). The age range was set to between 9 to 25 years, which considers the earliest age of when skeletons entered the Acceleration phase and some of the last ages for individuals in the Maturation phase of puberty. See **Appendix 15** for additional information.

Table 7. 4: Assumptions carried out for the multiple regression.

Assumption	Test	Result	Pass or fail of test
Independence of observation	Durbin-Watson	2.282	✓
A linear relationship exists between the variables	Scatter plot between Studentised Deleted Residual and Studentised Residual	See <b>Appendix 15</b>	✓
The data must show homoscedasticity			✓
The data must not show multicollinearity	Collinearity Statistics	1.007	✓
Data should not have any significant outliers, high leverage points or highly influential points	Case wise diagnostics Leverage points Cook's Distance Values	There was only one case-wise diagnostic. It was decided to keep the diagnostic in.	✓
		See <b>Appendix 15</b>	✓
Errors are normally distributed	Histogram		✓

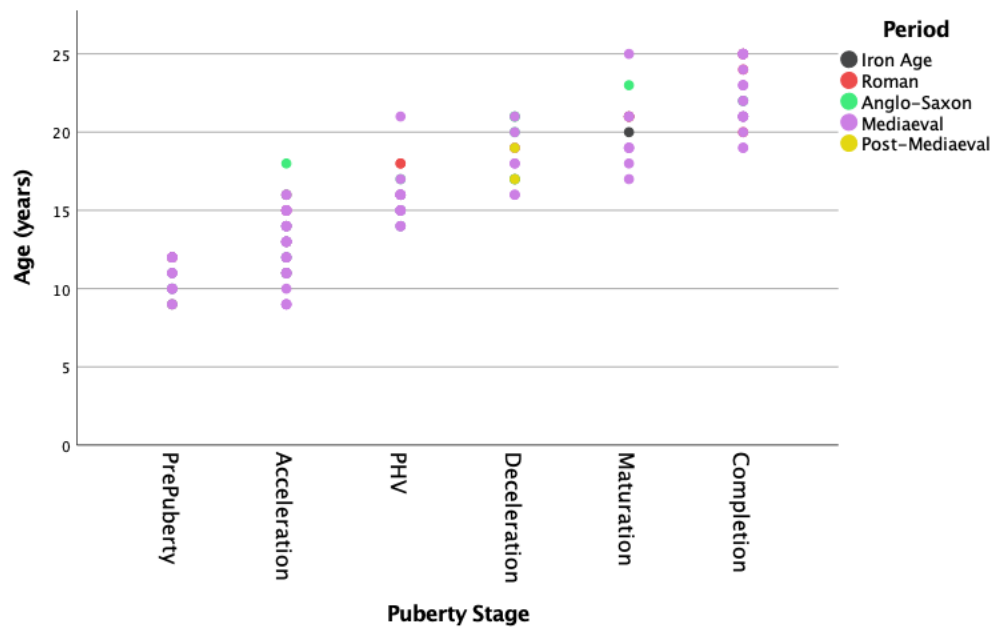
The multiple regression showed a strong linear relationship ( $r = 0.919$ ) between the dependent and independent variables (Lund and Lund, 2013b). This is presented in **Table 7. 5**. The multiple regression model statistically significantly predicted the archaeological period,  $F(2,155) 418.218, p < 0.001$ . Both variables added statistical significance to the prediction  $p < 0.001$ . The variables showed that as the archaeological periods moved towards the present day, the age of the skeletons decreased. At the same time, the puberty phase increased. However, **Figure 7. 1** shows that this result is most likely the case because the sample sizes for the archaeological periods were not even, with the Mediaeval sample being the most dominant

sample size. Thus, the significant relationship between the archaeological period and age may not necessarily reflect a true association.

Table 7. 5: Multiple regression to examine if age at pubertal phase could be predicted by archaeological period.

Independent variables	B	<i>p</i>	ANOVA	<i>r</i>	Adjusted <i>r</i> <sup>2</sup>
Period	-0.347	<b>0.039</b>	<i>F</i> (2,155)		
Puberty phase	2.406	<b>&lt;0.001</b>	418.218, <i>p</i> <0.001	0.919	0.842

Figure 7. 1: Scatterplot to show age correlated with pubertal phase filtered by archaeological period



## CHAPTER 8

# DISCUSSION

### 8.1. INTRODUCTION

Chapter Eight discusses the results from Chapters five to seven. This chapter is split into seven sections. Section 8.2. considers maturation of the Mediaeval skeleton, including age-at-fusion in Mediaeval St Gregory's, which is subdivided into socioeconomic environments. Section 8.3. discusses skeletal maturation through British archaeological periods. Age-at-fusion is compared between the Iron Age, Roman, Anglo-Saxon, Mediaeval and Post-Mediaeval groups, and significant differences found between the groups are discussed in-depth, alongside published literature. The sequence of fusion in St Gregory's compared to those from archaeological periods is discussed in Section 8.4. Puberty is examined in Section 8.5, including age at each pubertal phase in St Gregory's, when compared between Mediaeval sites, as well as archaeological periods. Finally, Section 8.6. looks at methodological constraints within this study. Highlights of Chapter eight are summarised in the final section.

## 8.2. MATURATION OF THE MEDIAEVAL SKELETON

This section discusses age-at-fusion within the Mediaeval skeleton, including St Gregory's skeletal collection from Canterbury (found in **Section 5.2. – 5.3.**) and the comparison of St Gregory's to Mediaeval York (found in **Section 6.2.**).

### 8.2.1. Age-at-fusion in St Gregory's

Out of all the bones tested, skeletal age-at-death (from dentition) was significantly associated with fusion stage of the epiphyses at only ten skeletal sites (**Table 8. 1**). These sites were the atlas (1. Anterior arch and 2. Posterior synchondrosis) and the axis (3. Ossiculum terminale, 4. Dentoneural synchondrosis, 5. Dentocentral and neurocentral junctions, 6. Posterior synchondrosis) of the cervical vertebrae, (7) the lateral clavicle, (8) the proximal ulna, (9) the proximal radius and (10) metacarpals 2 – 5, proximal and middle phalangeal epiphyses of the hand. Thus, age did not significantly associate with a specific fusion stage at other skeletal sites. When a Bonferroni test was conducted on the data, only four sites remained statistically significant. These were: (1) the anterior arch and (2) posterior synchondrosis of the atlas, (3) dentocentral and neurocentral junctions of the axis, and the (4) metacarpals of the hand.

#### *A) Summary of the significant associations*

**The Atlas:** The anterior arch was unfused (Stage 1) until 15 years of age and complete fusion (Stage 3) had occurred by  $\geq 8$  years. The posterior synchondrosis was unfused (Stage 1) until 15 years of age but completed fusion (Stage 3) by the age of 4 years. However, fusion (Stages 2 and 3) of the anterior arch should be considered to have occurred between 8 to 9 years of age, and between 4 to 8 years for the posterior synchondrosis.

**The Axis:** The ossiculum terminale fused (Stages 2 and 3) between 8 to 15 years and the dentoneural synchondrosis between 3 to 6 years of age. The dentoneural and neurocentral junctions fused between 3 to 16 years and the posterior synchondrosis between 3 to 5 years.

**The clavicle:** The lateral epiphysis of the clavicle fused (Stages 2 and 3) between 17 to 23 years of age.

**The ulna:** The proximal epiphysis of the ulna fused (Stages 2 and 3) between 14 to 16 years. The age-at-fusion of the distal epiphysis of the ulna approached significance and fused between 17 to 21 years of age.

**The radius:** The proximal epiphysis of the radius fused (Stages 2 and 3) between 15 to 16 years of age.

**The hand:** The metacarpals 2 – 5, proximal and middle phalangeal epiphyses fused (Stages 2 and 3) between 12 to 17 years of age.

Table 8. 1: Significant associations between age and Stages 1 – 3. \* = Anomalous individuals not included, \*\* = More likely to be under 8 years of age, \*\*\* = More likely to be between 8 – 10 years

Bone	Fusion site	Unfused age	Partially fused age	Completely fused age
Atlas	Anterior arch	≤7 years*	9 years	≥8 years
	Posterior synchondrosis	≤5 years*		≥4 years
Axis	Ossiculum terminale	≤14 years**	7 – 15 years***	≥11 years
	Dentoneural synchondrosis	≤6 years		≥3 years
	Dentocentral & neurocentral junctions	≤6 years	3 – 16 years	≥5 years
	Posterior synchondrosis	≤5 years		≥3 years
Clavicle	Lateral epiphysis	≤19 years	17 – 22 years	≥19 years
Ulna	Proximal epiphysis	≤16 years	14 – 15 years	≥17 years
Radius	Proximal epiphysis	≤15 years	15 – 16 years	≥15 years
Hand	Metacarpals 2 – 5, proximal and middle phalangeal epiphyses	≤16 years	12 – 16 years	≥17 years

Many studies that research age-at-fusion use documented collections where sex and age-at-death are known (Cardoso, 2007, 2008b, 2008a; Coqueugniot and Weaver, 2007; Schaefer and Black, 2007; Schaefer, 2008b; Cardoso et al., 2013a). This means that age does not have to be estimated or averaged. However, a caveat of only using documented collections means that other skeletal collections that are undocumented are not exploited. Most documented skeletal collections are Post-Mediaeval or Modern (Cardoso, 2007, 2008b, 2008a; Coqueugniot and

Weaver, 2007; Schaefer and Black, 2007; Schaefer, 2008b; Cardoso et al., 2013a), leaving more historical collections unexplored.

Estimating age-at-death from epiphyseal fusion in a British Mediaeval skeletal collection is helpful when the dentition is not available. Even when teeth are preserved in skeletons, estimating age from dental eruption becomes harder as age increases as the period of dental development is typically complete by early adulthood. Furthermore, the eruption of some tooth types, especially the third molar, is highly variable (Shapland and Lewis, 2014). **In this case, estimating age from later fusing epiphyses is particularly valuable** (Cardoso, 2008b). For this reason, this study has made an important contribution to the methods that are available for estimating age in Mediaeval skeletons. **Table 8. 1** shows that some skeletal elements are particularly useful for estimating age-at-death in adolescent skeletons from Mediaeval St Gregory's. Partially fused (Stage 2) bones from the hand indicate the skeletons are no less than 12 years of age, while partial fusion of the ulna and clavicle indicates a minimum age-at-death of 14 and 17 years, respectively.

### 8.2.2. Age-at-fusion between High and Low status

No significant differences were found between high and low-status groups. It was expected that there would be a difference, in which fusion would occur earlier for the high-status group compared to the low-status group, but this was not the case. Possible explanations for the lack of differences between the groups are detailed below.

The alternative hypothesis was that the high-status Mediaeval Canterbury group would fuse earlier than the low-status group, as it was expected that Mediaeval Canterbury high-status sub-adults would have access to better socioeconomic conditions (Low et al., 1964; So and Yen, 1990). The low-status group was expected to suffer from environmental stressors that may come with being in a lower social class. Poverty and its impact, such as poor nutrition, can have repercussions on growth (Gafni and Baron, 2000). For instance, previous research has found that the older children of the low-status Mediaeval Canterbury group had significantly different osteon circularity and diameters compared to the high-status children (Pitfield et al., 2019). This indicated that the low-status older children carried out more habitual loading than the high-status group (Pitfield et al., 2019). These differences were not found between the high

and low-status younger cohort (Pitfield et al., 2019). Bone microstructure of the Mediaeval Canterbury children, therefore, showed that the older children from the low-status group were taking on different responsibilities that involved more habitual loading than the high-status group (Pitfield et al., 2019).

While current research indicates that physical activity is more likely to damage the growth plate than affect linear growth, the child has to receive a sufficient diet not to be affected (Malina et al., 2004; Mirtz et al., 2011; Malina, 2012; Jazbinšek and Kotnik, 2020). Significant differences in femoral cortical microstructure between low and high-status adults of St Gregory's skeletal collection have alluded to poor health and malnutrition within the low-status group (Miszkiewicz and Mahoney, 2016). Yet evidence suggests that Mediaeval children received a similar diet regardless of status (Reitsema and Vercellotti, 2012; Dawson and Brown, 2013). This hypothesis was further supported through the analysis of dental microwear texture of the St Gregory's children that found no indication of differences in diet between the groups (Mahoney et al., 2016). Thus, even though status greatly affected the lives of Mediaeval adults, it did not affect the linear growth of the Mediaeval child, and this would most likely account for the lack of differences found in age-at-fusion between the low and high-status Mediaeval Canterbury children. Although the possibility that no statistical significance was found due to the small sample of the high-status group, the lack of differences found between Mediaeval children and their diet – a contributor to healthy, skeletal growth – shows value in this non-significant outcome.

### **8.2.3. Age-at-fusion compared between Mediaeval Canterbury and York**

Differences between the two sites were not expected. This is because Mediaeval Canterbury and Mediaeval York appeared to be socioeconomically similar during this period (Gillingham and Griffiths, 2000; Dobson, 2007; Burt, 2013; Lyle, 2013; see **Section 3.1.**). Equally, socioeconomic status is argued to have less of an impact on skeletal maturation during adolescence, than it does during childhood (Cardoso, 2008b). Out of all the sites tested, only the fusion age of the ossiculum terminale to the dens of the axis of the cervical vertebrae differed significantly between Mediaeval York and Canterbury. Potential reasons for this are discussed below.

The ossiculum terminale fused (Stages 2 and 3) at a significantly later age in the Canterbury sample when compared to York. Complete fusion (Stage 3) occurred by 12 years of age for the entire Mediaeval York sample. The entire Canterbury sample did not complete fusion until age 16 years. There can be considerable variation in the age that the ossiculum terminale fuses (Ogden, 1984), with some Modern human populations found to fuse between the ages of 12 to 15 years (Ogden, 1984; Akobo et al., 2015). Failure of the ossiculum terminale to fuse is also a fairly common occurrence in modern humans. The condition is known as Ossiculum Terminale Persistens Bergman and occurs in approximately one out of two hundred people (Todd and D'Errico, 1926; Cunningham et al., 2016). The condition can occur from either trauma or congenital deformity but is generally asymptomatic (Cunningham et al., 2016). Thus, the difference between York and Canterbury may relate to a fusion site that is highly variable in the age that it fuses.

When all the Mediaeval data were compared to published Mediaeval studies, the ages at fusion were similar. A study that looked at the pars lateralis to pars basilaris in a Mediaeval Balkans sample showed that complete fusion (Stage 3) occurred at age 7 years, the same age when this Mediaeval sample first completed fusion (Redfield, 1970). Published Mediaeval English data for the distal radius and iliac crest showed slightly earlier ages at partial fusion (Stage 2) compared to the Mediaeval data of this study, but complete fusion (Stage 3) of the distal radius occurred at the same age for all (Shapland and Lewis, 2013; Shapland et al., 2015). Only the iliac crest of the published data showed earlier ages at fusion (Stages 2 and 3) compared to this study by 1 to 2 years (Shapland and Lewis, 2013; Shapland et al., 2015). The compared data can be found in **Appendix 16**.

#### **8.2.4. Pathologies in the Mediaeval samples**

This section considers the pathologies that were observed in the cervical vertebrae, particularly for skeletons 364, 607 and 760 of St Gregory's. These are considered because pathology can affect fusion (Hochberg, 2002).

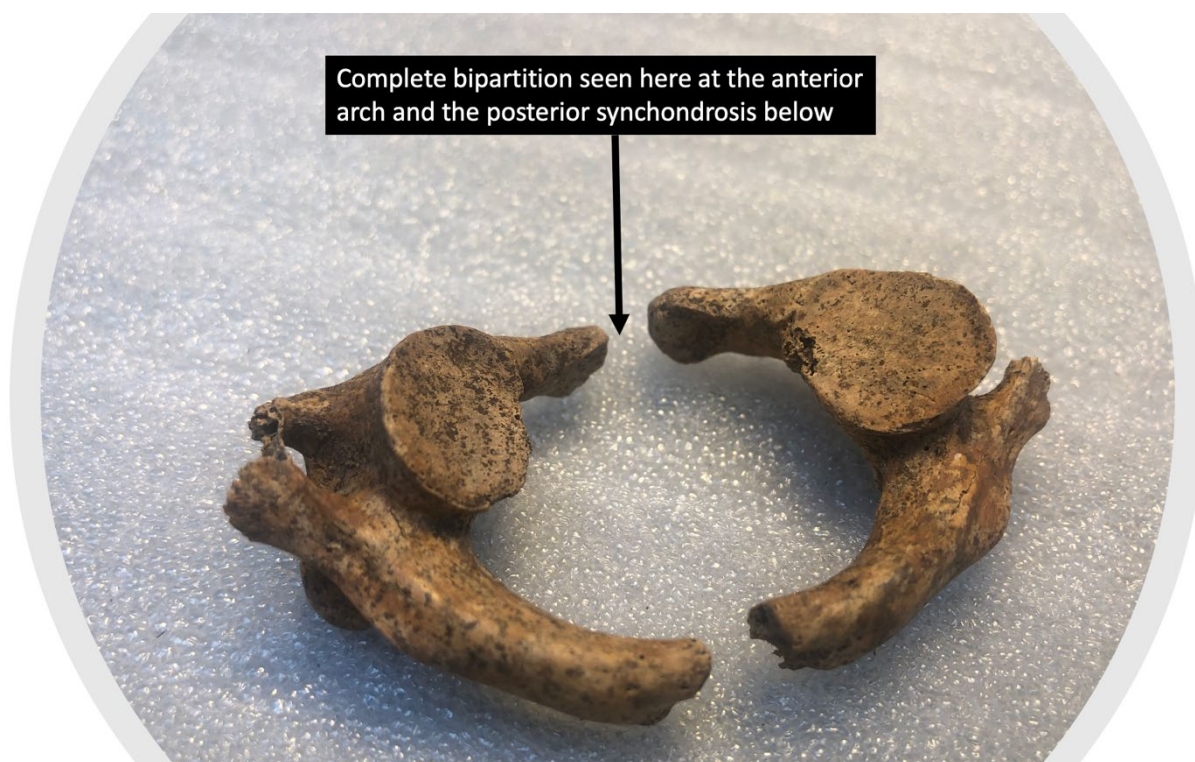
**Atlas:** In Modern populations, this site tends to fuse at approximately 4 to 5 years for the posterior synchondrosis and between 5 to 6 years for the anterior arch, although fusion can occur at a later age range of 8 to 12 years (Schaefer et al., 2009; Junewick et al., 2011; Karwacki

and Schneider, 2012; Cunningham et al., 2016). Only three skeletons in Mediaeval Canterbury were found to be unfused (Stage 1) past the age of 5 years for the posterior synchondrosis.

Defects at the posterior arch of the atlas are a common occurrence in modern humans. This is reflected in the many variations of defects that can occur in this area, including (1) no fusion down the middle of the posterior arch, (2) no fusion to one side, (3) a posterior arch that is unfused at two points, therefore appearing as an unfused anterior arch, (4) almost no posterior arch, and (5) no posterior arch development (Ramdhan et al., 2017). Spina bifida atlantis is a common posterior arch defect in which the posterior arch of the atlas does not close. Spina bifida atlantis is asymptomatic and occurs in approximately 1.5 to 5.0% of a modern human population (Cunningham et al., 2016; Ramdhan et al., 2017). Spina bifida atlantis occurs when a segment of cartilage does not form where the posterior arches of the atlas are supposed to form (Ramdhan et al., 2017). **Based on the evidence, it is possible that spina bifida atlantis occurred in St Gregory's skeletal collection and was present in the three individuals aged nine (sk. 607), twelve (sk. 364) and fifteen years (sk. 760).**

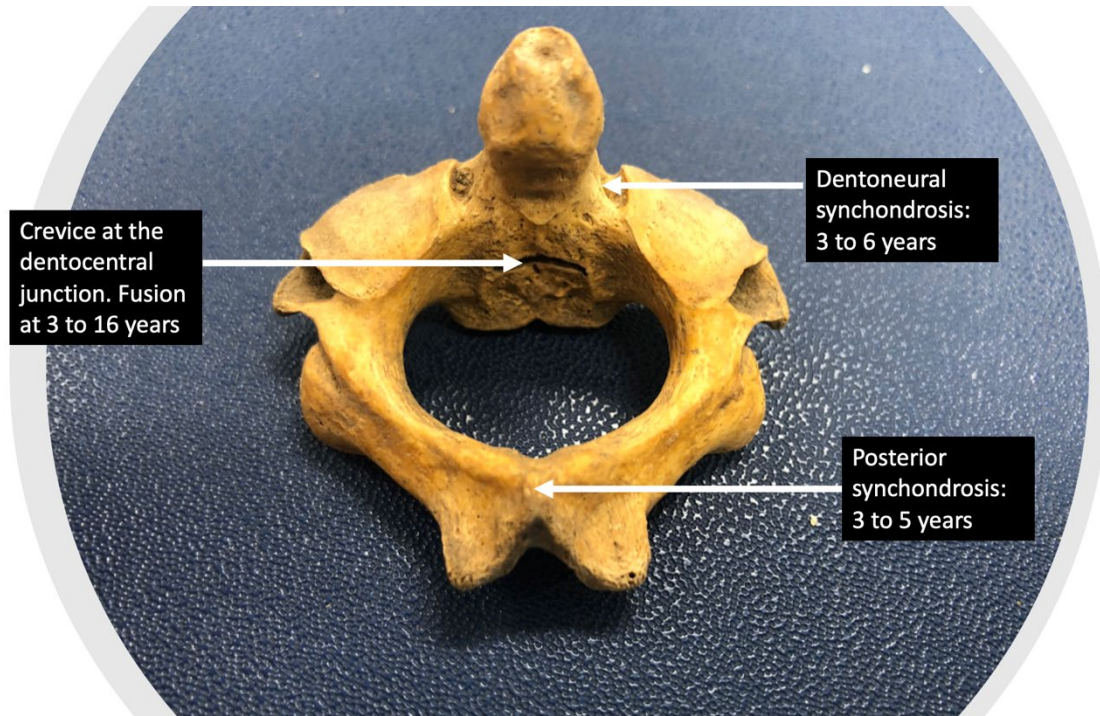
Aplasia (undeveloped) at the posterior arch of the atlas is the most common congenital anomaly that can occur at this vertebra. The atlas can have a wide variety of growth anomalies. Complete bipartition of the atlas occurs in approximately 0.1% of a population, and an isolated anterior arch cleft can occur in about 0.1 to 0.7% of a population (Hummel and De Groot, 2013; Ramdhan et al., 2017). Two individuals from St Gregory's were unfused at twelve and fifteen years for their anterior arch of the atlas. These individuals were the same skeletons (sk. 364 and sk. 760) found to have anomalies on the posterior arch of their atlases. It is believed that the two skeletons had the uncommon congenital anomaly of complete bipartition, where the anterior and posterior arches of the atlas remain unfused past the typical age of closure (**Figure 8. 1**). Complete bipartition is a rare condition but is often inherited (Motateanu et al., 1991; Ramdhan et al., 2017). This may, therefore, be an indication that these two individuals were related.

Figure 8. 1: The atlas of the cervical vertebrae with complete bipartition. Photograph was taken by J.A.M Dolding-Smith from the St Gregory's skeletal collection held at the University of Kent



**Axis:** This site in Modern populations tend to fuse between 4 to 6 years for the dentocentral and neurocentral junctions, but can fuse at a later age range of 7 to 9 years (Cunningham et al., 2016). Both Mediaeval Canterbury and Mediaeval York had much later ages when fusion was underway (Stage 2), and this might have been partly due to pathological conditions rather than a difference in ontogeny between Mediaeval and Modern populations. For some people, a crevice can remain at the posterior dentocentral junction and this may or may not fuse at a later age (Fullenlove, 1954; Cunningham et al., 2016). This is illustrated in **Figure 8. 2**. **Thus, rather than a later age at fusion for the Mediaeval samples, it might be that some of the population more likely had this crevice at the dentocentral junction, which would cause a higher age at partial fusion (Stage 2).**

Figure 8. 2: The axis of the cervical vertebrae with a crevice at the dentocentral junction. Ages at fusion that occurs during the childhood phase of modern human growth is given in the black boxes for St Gregory's skeletal collection. Photograph was taken by J.A.M Dolding-Smith from the Fishergate skeletal collection held at the University of Durham



### 8.3. MATURATION OF THE MODERN HUMAN SKELETON THROUGH BRITISH ARCHAEOLOGICAL PERIODS

This section discusses age-at-fusion between the archaeological periods. The results for this section can be found in **Chapter 6**. Comparisons are also undertaken with the published literature.

#### 8.3.1. Comparing age-at-fusion between Iron Age, Roman, Anglo-Saxon, Mediaeval and Post-Mediaeval sites

Significant differences were expected between archaeological periods (See **Section 2.4.1**). Specifically, it was expected that improvements in lifestyle through technological advancements, such as in food production and healthcare, would decrease the age-at-fusion from the Iron Age to the Anglo-Saxon period. It was then predicted that age-at-fusion would increase during the Mediaeval period before decreasing once more. This is because stature fell during the Mediaeval period and then increased after this period (Cole, 2003; Steckel, 2004; Lu et al., 2016). Epiphyseal fusion and stature can correlate through environmental influence (Prendiville et al., 1986; Nilsson et al., 2005; Ellison and Reiches, 2012; Hochberg and Belsky, 2013; Shim, 2015). These expectations are assessed against the results from **Section 6.3**.

##### *A) Iron Age*

The proximal tibia of the Iron Age group (21 years) fused (Stages 2 and 3) significantly later compared to the Roman (19 years) and Mediaeval (19 years) groups. The Iron Age saw the adoption of specialist trades and the expansion of a more dynamic society (Pryor, 2004; Schama, 2009). However, social classes existed and it is possible that the non-elite may have had more psychological stressors during childhood compared to the elite (Peck, 2013). **Although the Iron Age saw no major invasions or mass migrations** (Pryor, 2004; Schama, 2009), **the later ages at fusion compared to the Roman and Mediaeval samples may be due to advancing technology in the later periods** (see below for why the Anglo-Saxons would not be included). For example, the Roman invasion brought economic change, including an increase in domesticates and livestock development, as well as advancements in medical

care (Albarella et al., 2008; Redfern, 2010). Advancements in nutrition and/or healthcare can have far-reaching effects on growth (Gafni and Baron, 2000). Thus, the decrease in fusion age in the Roman and Mediaeval samples compared to the Iron Age group may be from innovations that helped to optimise growth.

### *B) Roman*

The greater and lesser trochanters of the Roman group (19 years) fused (Stages 2 and 3) significantly later than the Mediaeval (g.troch: 17 years, l.troch: 16 years) group. Except for the initial Roman invasion, the Roman era was fairly peaceful during the second and third centuries of Roman rule in Britain (Pryor, 2004; Schama, 2009). For some, Roman presence went largely unnoticed (Pryor, 2004; Schama, 2009). Places like Colchester became urban hubs, with many Romano-British settlements enjoying hydraulic and sanitary convenience that would not be seen again in Britain until the 19<sup>th</sup> century (Schama, 2009).

However, Romano-British life caused some deleterious effects. The marginalisation of the young and old, the introduction of new settlement types, new detrimental cultural practices and new diseases helped increase the risk of mortality (Redfern and Dewitte, 2011). Osteological studies from Roman cemeteries have shown high rates of skeletal stress markers caused by infectious and metabolic diseases, possibly resulting from urban Roman environments that were detrimental to people's health (Redfern and Roberts, 2005; Redfern et al., 2015; Arthur et al., 2016). While the Mediaeval period also had adverse urban environments (Burt, 2013), they may not have been as harmful compared to a possible fast implementation of urbanisation and culturalisation exacted by Roman influence.

The romanisation of Britain may have therefore had a dual effect, in which new technologies, such as a more efficient plough and livestock management, advancing medical technology, and an increase in diet variety may have contributed to optimal growth (Albarella et al., 2008; Redfern, 2010; Redfern and Dewitte, 2011). Although previous research suggests that the Roman diet may not have been greatly beneficial compared to the Iron Age diet (Redfern and Dewitte, 2011). Regardless, any benefits that may have come from the Roman conquest could have been offset by an increased disease burden from new settlement types and an influx of immigrants from abroad, as well as the marginalisation of children based on a new, cultural hierarchical system, which put children more at risk, along with other new cultural practices, such as the use of wet nurses and swaddling (Redfern, 2007; Redfern and Dewitte,

2011). **This could have all contributed to delayed fusion for some bones compared to the Mediaeval sample.**

*C) Anglo-Saxon: Axial skeleton*

For the axial skeleton, age-at-fusion occurred significantly later in the Mediaeval sample compared to the preceding Anglo-Saxon sample for the anterior arch of the atlas (AS: 9 years, M: 12 years), the ossiculum terminale (AS: 10 years, M: 13 years), and the dentocentral and neurocentral junctions (AS: 9 years, M: 11 years) of the axis. Diet may have been a factor. Mahoney et al., (2016) have shown that Mediaeval Canterbury children did not enter the adult dietary sphere until 6 to 8 years of age. At this age, Mediaeval children would be treated as young adults, who would take on employment and apprenticeships outside of the home (Bailey et al., 2015; Mahoney et al., 2016). Children can experience delayed or advanced growth and maturation based on independent environmental stressors (Klepinger, 2001). Growth and maturation may slow when the body experiences an adverse period, but can catch-up to its original growth trajectory if the onslaught is not too severe or long-lasting (Golden, 1994; Cameron and Demerath, 2002; Gosman, 2012; Hauspie and Roelants, 2012; Doe et al., 2017). In this respect, the introduction of new Mediaeval adulthood stressors at this age may have had an initial knock-on effect on skeletal maturation that could have briefly delayed growth until the body adjusted a few years later.

The environment may have contributed to earlier fusion in the Anglo-Saxon period. Anglo-Saxon settlements were most likely small (Wade, 2000), whereas Mediaeval towns suffered from poor sanitation, and were cramped and in close proximity to livestock (Burt, 2013). In Modern times, children tend to mature faster in urban settings compared to rural environments, as urban children have better access to socioeconomic benefits like better healthcare (Low et al., 1964; Takai and Akiyoshi, 1983; So and Yen, 1990). In contrast, historical populations tended to suffer more so in urban environments. A higher mortality rate was found in Mediaeval English women living in urban areas compared to rural (Walter and DeWitte, 2017). However, growth profiles between rural and urban Mediaeval children were non-significant (Lewis, 2002) and therefore the urban environment of Mediaeval Britain may not be to blame for the later maturation ages compared to the Anglo-Saxon children. An urban environment hypothesis may also not account for the later ages at fusion of the appendicular skeleton found in the Anglo-Saxons compared to the Mediaeval adolescents.

#### *D) Anglo-Saxon: Appendicular skeleton*

Overall, many fusion sites for the Anglo-Saxon sample fused at a significantly later age, compared to many of the other archaeological groups (see **Section 6.3.4.** for specifics). These sites were the spheno-occipital synchondrosis of the axial skeleton and the radius, distal ulna, metacarpals, iliac crest, acetabulum, femoral head, distal femoral epiphysis and the proximal tibia of the appendicular skeleton. The delayed appendicular skeletal maturation of the Anglo-Saxon sample may be due to how unsettled this period was in British history. The Anglo-Saxon period was an era of continual invasions (Jenkins, 2012). From 410 to 600 AD, a possible aggressive expansion occurred through Britain by the Saxons, with political unrest occurring from 600 to 800 AD (Jenkins, 2012). Viking raiding occurred in Britain between 800 to 1066 AD (Jenkins, 2012; Simpson, 2017). Finally, in 1066 AD, William I conquered England, with many natives dying from either slaughter or starvation brought about by the Norman conquest (Jenkins, 2012).

The possible unrest that individuals felt during the Anglo-Saxon period may have affected skeletal maturation. **War conditions can increase the rate of disease and decrease nutrition and hygiene, as well as cause psychological impacts, such as fear, anxiety, suffering, separation and loss, and these factors can influence growth and maturation** (Prebeg and Bralić, 2000). Usually, these factors cause growth and maturation to delay or slow (Prebeg and Bralić, 2000) but can sometimes accelerate development (Boynton-Jarrett and Harville, 2012; Dewitte and Lewis, 2020).

#### *E) Mediaeval*

Except for the axial skeleton, the Mediaeval sample continually fused (Stages 2 and 3) at an earlier age than the other archaeological samples (Iron Age, Roman, Anglo-Saxon). Improvements to nutrition tend to see an increase in stature and earlier maturation in the affected population (Matsuoka et al., 1999) and the events of the 12<sup>th</sup> century may have helped boost the health of the Mediaeval people. The English Mediaeval period began perilously, from Scottish and Danish raids, and the onslaught of William the Conqueror, who caused massive suffering, through starvation, murder and disease, of York in particular, when the city tried to rebel against him (Schama, 2009). However, during the 12<sup>th</sup> century, Mediaeval England saw abundant harvests from warmer climates, technological innovations, a boom in markets and

profitable connections from safer travel around the country (Schama, 2009). The population boomed and grew to its previous Romano-British numbers of around 2 to 6 million (Dyer, 1994), which had previously dwindled around 300 to 1000 AD (Dyer, 1994).

The population increase caused the inevitable, as bad harvests in 1257 AD and between 1315 to 1316 AD meant that not everyone could be fed (Schama, 2009). The successive famines and the civil war of 1264 AD caused animosity between the people and increased crime rates (Schama, 2009). Finally, in 1348 AD, the plague made it to English shores and killed half the population within 18 months (Schama, 2009). Population numbers would not recover until after 1520 AD (Dyer, 1994). Yet the drop in population allowed food quality, nutrition, peasant conditions and wages to rise after 1375 AD (Dyer, 1994). Through famine and pestilence, stature decreased, and menarcheal age increased, but with improved nutrition and reduced disease burdens through depopulation by the plague, menarcheal age decreased yet truncated growth, possibly through the biphasic effect of oestrogen (Dewitte and Lewis, 2020). Thus, the famine and plague caused the population to become healthier. These events could have decreased the age-at-fusion for the Mediaeval people after the Anglo-Saxon era.

### **8.3.2. Comparing skeletal maturation in the archaeological sample to Post-Mediaeval and Modern published data**

This section compares published age-at-fusion research from the Post-Mediaeval (1540 AD – 1901 AD) and Modern (1901 AD – present day, see **Section 1.4.**) era to the results of the archaeological samples presented in this study. Only the skeletal sites that differed between the archaeological periods and the Post-Mediaeval/Modern periods are presented here. **Appendix 17** shows the figures for comparisons of other fusion sites that are not presented here.

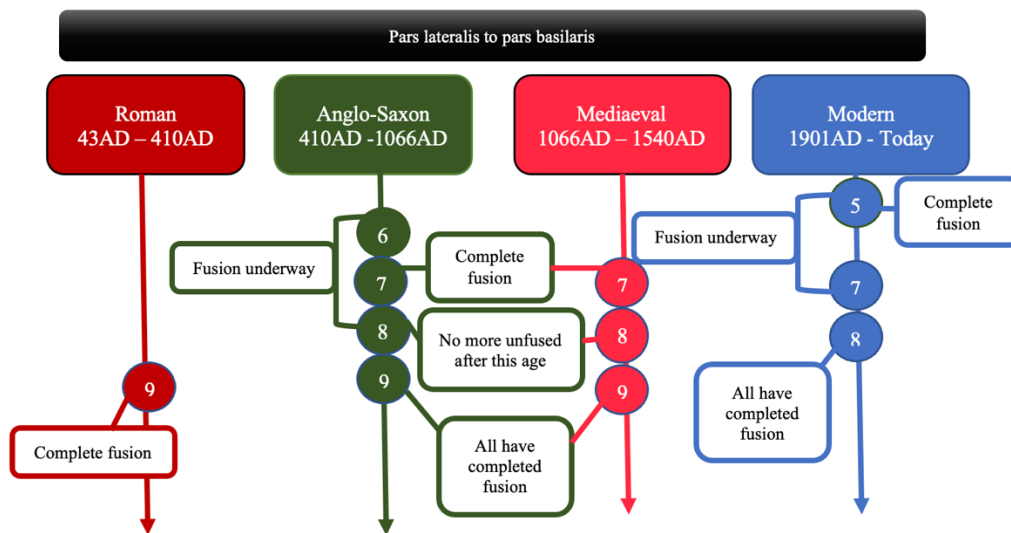
#### *A) The Skull*

*Summary finding from results:* **The archaeological samples entered fusion (Stages 2 and 3) at a later age compared to the Modern published data.** This was found for both the pars lateralis to pars basilaris and the spheno-occipital synchondrosis.

An earlier age at skeletal maturation would be expected in Modern populations as nutrition and healthcare have improved over time and a shortening of the growth period has occurred

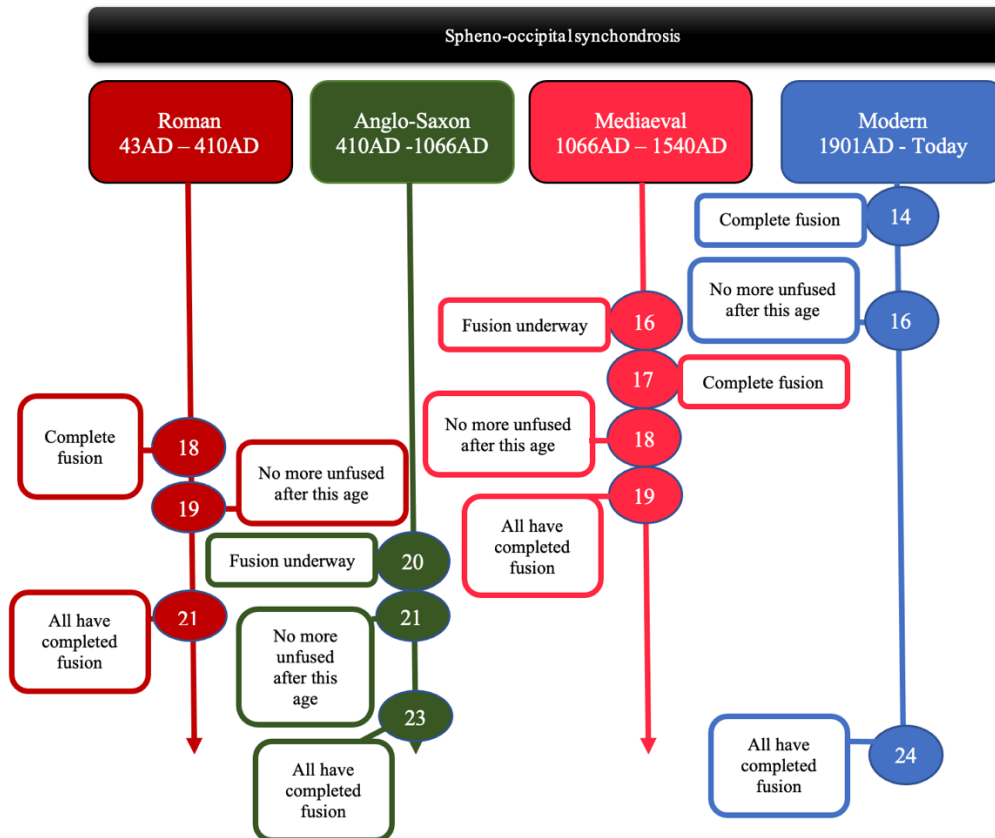
(Hauspie et al., 1997; Matsuoka et al., 1999). However, when all data is analysed together, as seen in **Figure 8. 3**, complete fusion (Stage 3) of the **pars lateralis to pars basilaris** for the entire sample appears similar for all periods. It has been reported previously that the fusion of the pars lateralis to pars basilaris is not greatly affected by environmental influence (Redfield, 1970) and this seems to be supported by the results presented here. Thus, while there is an earlier age-at-fusion for the Modern data, the difference may be considered more similar than different.

Figure 8. 3: Fusion of the pars lateralis to pars basilaris compared between archaeological groups. Age in years is given in coloured circles. Modern data is from Lisbon, Portugal, 1908-1984AD (births and deaths), dry bone (Cardoso et al., 2013b)



Complete fusion (Stage 3) of the **spheno-occipital synchondrosis** occurred at an earlier age in the Modern period compared to all the archaeological data (**Figure 8. 4**). However, the Modern Coimbra (Coqueugniot and Weaver, 2007) and USA (Shirley and Jantz, 2011) groups completed fusion for their entire sample at a similar age to the archaeological data. Meaning that while fusion (Stages 2 and 3) could begin earlier in Modern samples, later maturing individuals may have completed fusion (Stage 3) around a comparable age to historical populations.

Figure 8. 4: Fusion of the speno-occipital synchondrosis compared between archaeological groups. Age in years is given in coloured circles. Modern data is from Coimbra, Portugal, 1826-1938AD (births and deaths), dry bone (Coqueugniot and Weaver, 2007)



### B) The Sacrum

*Summary finding from results:* The archaeological and Post-Mediaeval and Modern published samples entered fusion (Stages 2 and 3) at a similar time for the sacral bodies 1 and 2. However, the Modern published data had some individuals remain unfused (Stage 1) or partially fused (Stage 2) into the fifth decade of life, whereas complete fusion (Stage 3) for the entire sample had occurred by the age of 25 years for most of the archaeological samples.

The archaeological data from this study had much earlier ages at complete fusion (Stage 3) for the entire sample compared to the published data. Coqueugniot and Weaver, (2007) reported individuals in partial fusion (Stage 2) until age 29 years. Belcastro et al., (2008) reported individuals in partial fusion between 20 to 59 years of age. In this study, individuals were

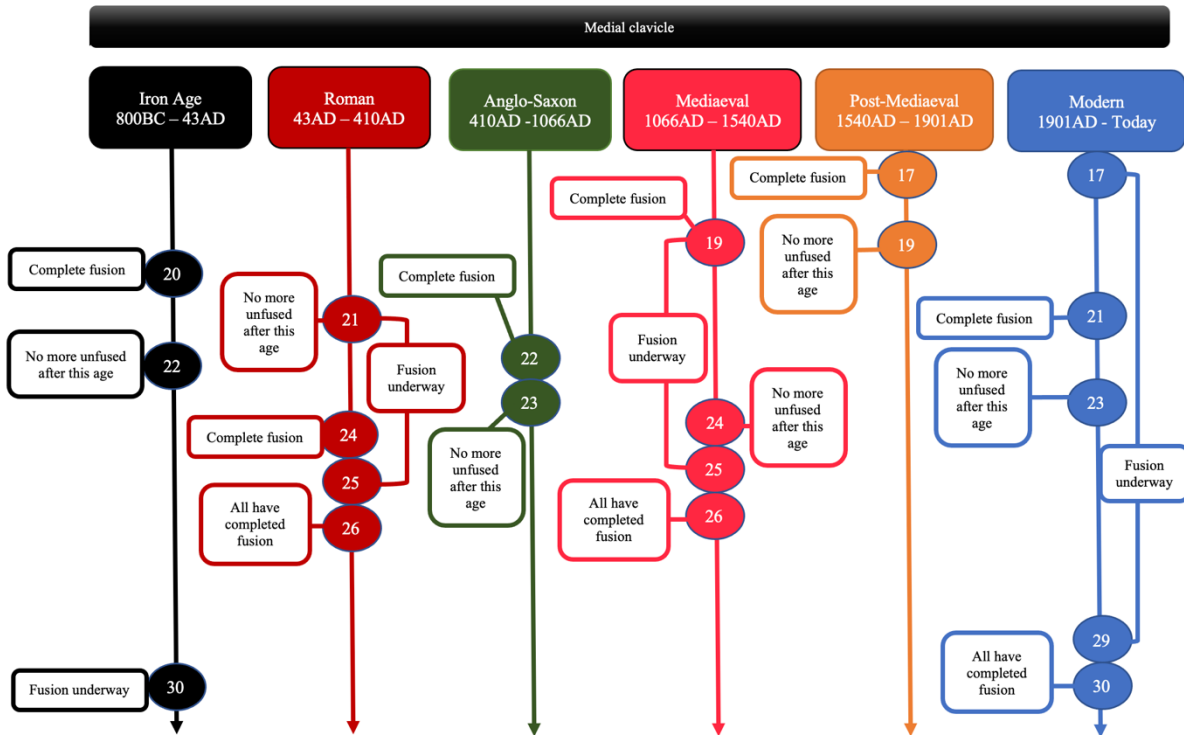
recorded in partial fusion up until age 25 years. Potentially then, the differences in the later ages could be methodological, but more research will need to be carried out to understand if this is the case.

### *C) The Clavicle*

*Summary finding from results:* The range of fusion ages for the medial clavicle was much greater for the later Post-Mediaeval and Modern datasets compared to the archaeological samples. In particular, partial fusion (Stage 2) continued into the third decade of life for some individuals in the Modern samples, whereas partial fusion did not continue past the age of 25 years for many of the archaeological samples.

The medial epiphysis of the clavicle proved of interest, as a clear pattern can be discerned from the data (**Figure 8. 5**). For example, the Iron Age sample had individuals' complete fusion (Stage 3) at the earliest age of 20 years, but some skeletons were still in partial fusion (Stage 2) at age 30 years, like that of the Modern data. However, none of the fusion data between archaeological groups was significant. This may be due to small sample sizes and future research should focus on the medial clavicle across archaeological periods. Additional information on the medial clavicle can be found in **Appendix 18**.

Figure 8. 5: Fusion of the medial clavicle compared between archaeological groups. Age in years is given in coloured circles. Modern data is from Bosnia, 1995AD (war victims from the fall of Srebrenica), males only, dry bone (Schaefer, 2008b)



#### D) The Scapula

*Summary finding from results:* Complete fusion (Stage 3) of the medial border of the scapula occurred at an earlier age in the Modern published samples compared to the archaeological samples. The Post-Mediaeval published data for the inferior angle completed fusion for the entire sample earlier than the archaeological or Modern data.

Data was limited for the medial border and inferior angle of the scapula. Complete fusion (Stage 3) of the **medial border** occurred at the earliest age range of 17 to 18 years for the Modern data and between 19 to 25 years for the archaeological data. Post-Mediaeval and Modern data for the **inferior angle** fused (Stages 2 and 3) between 16 to 17 years, whereas the archaeological data occurred between 18 to 22 years.

*E) Summary*

The Mediaeval group appears most similar to the Post-Mediaeval and Modern published data. This could be because the Mediaeval period overall saw a rise in technological innovation and nutrition. However, it could also be that the Mediaeval group had the largest sample size and therefore appeared healthier because it had a more extensive spread of data.

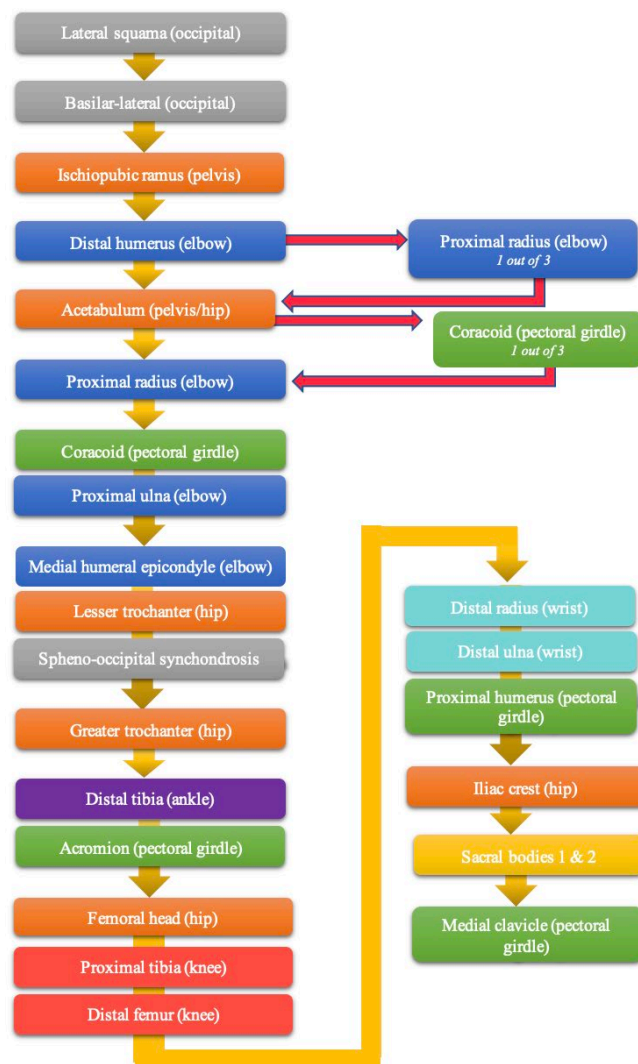
#### **8.4. THE SEQUENCE OF FUSION**

This section discusses the modal sequences – the most common fusion pattern – produced in **Sections 5.4.** and **6.5.** The first part discusses the sequence of fusion in Mediaeval Canterbury only, along with variations found. The second part looks at differences in the sequence of fusion between the archaeological groups and published modal sequences from a Modern Bosnian male sample and a collection of European skeletons. Finally, the findings of parts one and two are discussed in a wider context in the final segment.

### 8.4.1. The sequence of fusion in St Gregory's

The modal sequence of St Gregory's is given in **Figure 8. 6**. The pink arrows on the figure denote variations to the sequence e.g., one individual out of three fused their proximal radius after the distal humerus and before the acetabulum. Some earlier studies believed the sequence of epiphyseal fusion was fixed (Stevenson, 1924; Stewart, 1934; Shigehara, 1980; Schaefer and Black, 2007), but more recent research supports natural human variation within and between populations (Schaefer and Black, 2007; Schaefer, 2008a, 2014; Schaefer et al., 2009; Lenover and Šešelj, 2019). **Figure 8. 6** establishes the sequence of fusion in a Mediaeval English skeletal collection.

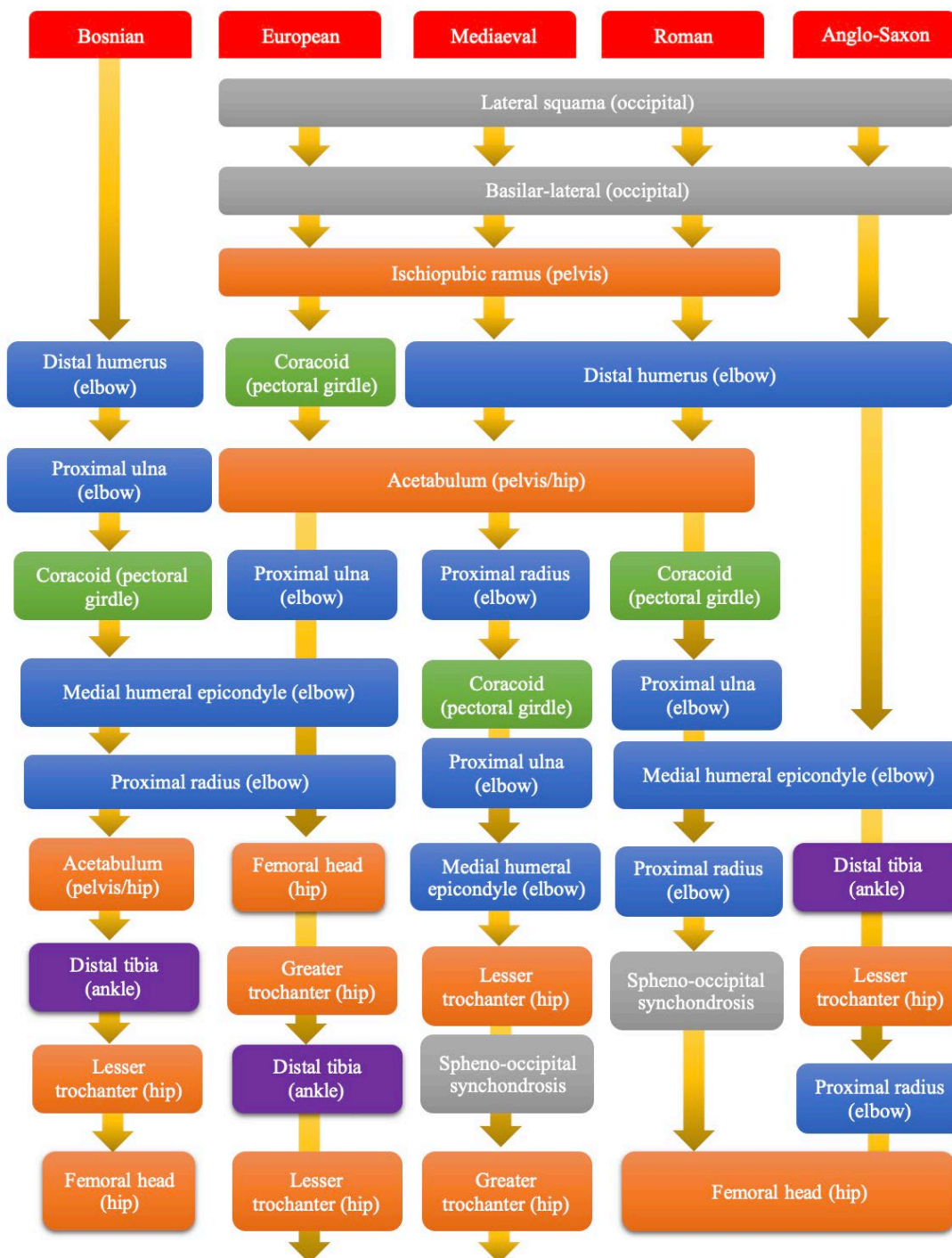
Figure 8. 6: Sequence of fusion for St Gregory's skeletal collection. The modal sequence is on the left, whereas outliers are denoted by pink arrows (n/ total) e.g., 1 out of 3 sequences, the proximal radius comes after the distal humerus and before the acetabulum

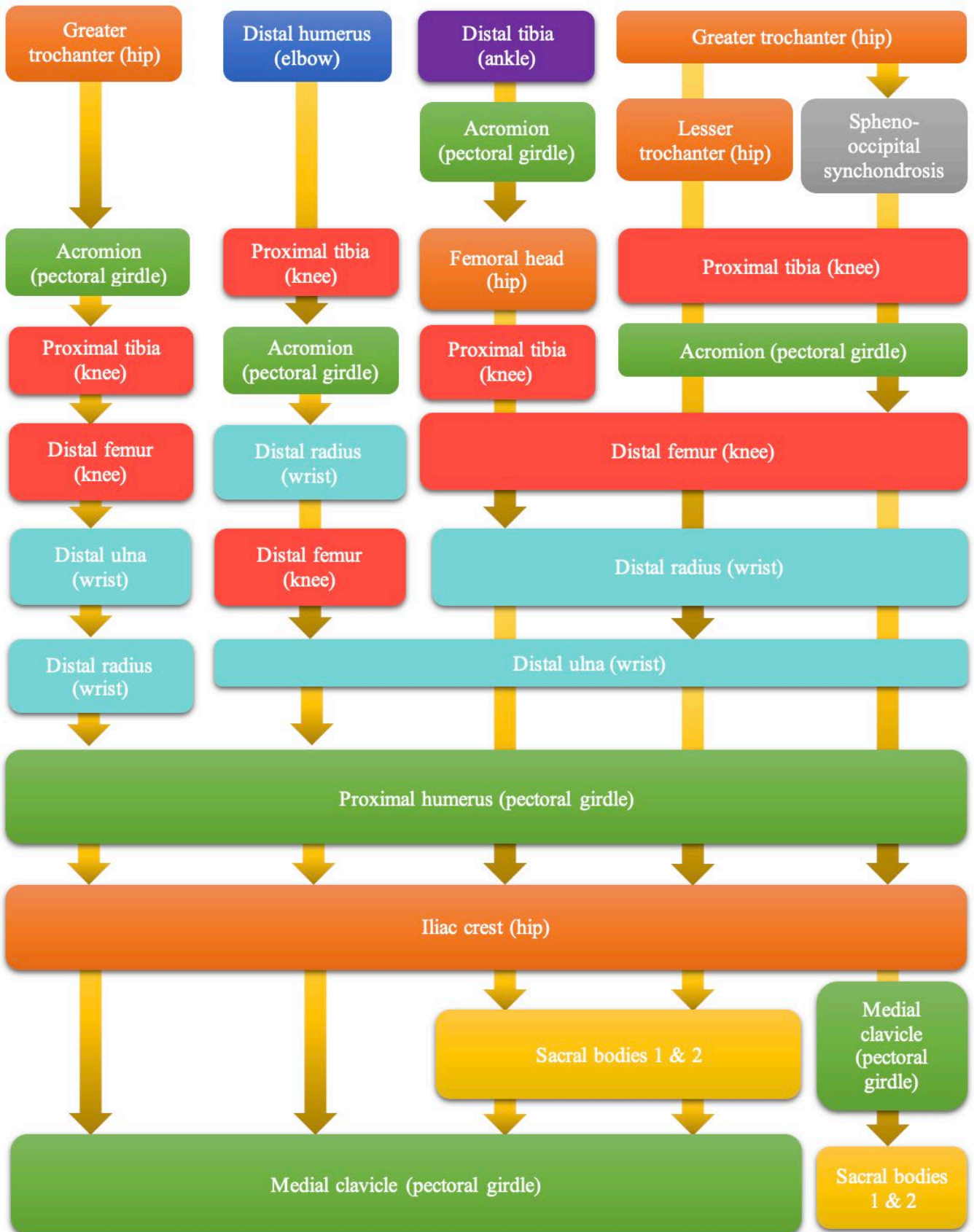


#### **8.4.2. The sequence of fusion in British archaeological periods and compared to Post-Mediaeval and Modern (18<sup>th</sup> – 20<sup>th</sup> century AD) published data**

A fusion sequence for a Modern Bosnian male sample was produced by Schaefer and colleagues to help with the sorting of commingled juvenile remains (Schaefer and Black, 2007; Schaefer, 2008a, 2014). From this, Lenover and Šešelj, (2019) examined the variation between the modal sequences of skeletal collections grouped by continent. The European modal sequence for complete fusion from the Lenover and Šešelj, (2019) study, along with the Bosnian sequence was compared against the modal sequences of complete fusion for the Roman, Anglo-Saxon and Mediaeval archaeological groups (**Figure 8. 7**). The Mediaeval group had the largest sample size and replicated St Gregory's modal sequence. The Anglo-Saxon group was the least varied from the Mediaeval group because of having the smallest sample size. Two points of interest were that (1) more variation was found towards the middle of the sequence, with the beginning and end sequences in a more fixed position, as found by Lenover and Šešelj, (2019) and (2) the published data appeared to deviate more from the archaeological groups' modal sequences than the archaeological groups deviated from one another, and this may reflect a methodological bias among the studies.

Figure 8. 7: Sequence of fusion for the Roman, Anglo-Saxon and Mediaeval archaeological groups, as well as the Bosnian (Schaefer and Black, 2007) and European (Lenover and Šešelj, 2019) modal sequences for complete fusion. Fusion sites with a yellow line and not an arrow dictate where the order in the sequence is unknown. Gaps represent no data. Colours underneath headers at the top are as follows: Grey = occipital bones, orange = bones/epiphyses that make up the pelvis and hip, dark blue = epiphyses that make up the elbow, green = epiphyses that make up the pectoral girdle, purple = epiphyses that make up the ankle, red = epiphyses that make up the knee, and light blue = epiphyses that make up the wrist.





### 8.4.3. The sequence of fusion in the modern human skeleton

Based on the fusion sequences analysed in this study, commonalities between the archaeological and published Post-Mediaeval/Modern modal sequences are reviewed here.

The bones of the occipital (the lateral-squama and basilar-lateral) were found to always fuse first. The brain grows rapidly during infancy and childhood, with the brain completing most of its growth at the end of childhood (Bogin, 2012, 2015). The skull will most likely fuse at the beginning of the sequence to protect the brain (Betts et al., 2016), with the skeleton growing in response to organ development (Humphrey, 1998; Schaefer and Black, 2007; Lenover and Šešelj, 2019). Lenover and Šešelj, (2019) noted that the vertebral and occipital sites tended to fuse at the beginning and were the least variable at this stage in the sequence.

The ischiopubic ramus is always the first to fuse in pelvic development in both modern humans and in non-human apes (Beasley, 2022). It was the third site to fuse in the archaeological and Post-Mediaeval/Modern sequences. The ischiopubic ramus is unusual as it is one of the few bone centres that fuse during the childhood period, whereas the rest of the pelvis fuses during adolescence (Cardoso et al., 2013a). It is believed to unite fairly quickly (Cardoso et al., 2013a). The ischiopubic ramus provides a base for the ilium to fuse to (Beasley, 2022).

After the fusion of the ischiopubic ramus, the fusion of the elbow (distal humerus, proximal radius, proximal ulna and medial humeral epicondyle), acetabulum and the coracoid come next. There is no set order as to which sites of the elbow, acetabulum and coracoid come first or last, and these vary between sequences. However, many sequences had the distal humerus come fourth and the acetabulum come fifth.

The acetabulum and coracoid may come earlier in the sequence compared to most of the other epiphyses for the hip and pectoral girdle because of their importance to other parts of the body. For example, the fusion of the acetabulum provides the socket for the femoral head to sit in and also brings together the ilium, ischium and pubis (known as the tri-radiate complex) to complete the pelvis (Schaefer, 2008b; Mansfield and Neumann, 2019). The coracoid process is an important attachment site for muscles that both stabilise the shoulder and allows for movement of the shoulders and arm at the shoulder joint (Mohammed et al., 2016).

In contrast, the distal humerus is considered to be a highly variable site, along with the speno-occipital synchondrosis and the acromion of the scapula, and this is thought to be due to functionality and constraint (Lenover and Šešelj, 2019). For example, while both the

acromion and coracoid process stabilise the shoulder, the coracoid process is under more constraint because it is an attachment for various muscles and ligaments, compared to the acromion (Lenover and Šešelj, 2019).

Within the sequences examined here, the spheno-occipital synchondrosis tended to fuse after the elbow and in tandem with the hip (femoral head, greater and lesser trochanters – excludes the acetabulum and iliac crest). The growth of the spheno-occipital synchondrosis affects the depth and height of the upper face, as well as the position of the upper teeth (Coben, 1998). The spheno-occipital synchondrosis closes at the onset of puberty, and in girls, the spheno-occipital synchondrosis closes before menarche (Alhazmi et al., 2017). Adolescence is also the time when the brain completes growth through remodelling (Herting and Sowell, 2017; Vijayakumar et al., 2018).

The knee tends to come after the fusion of the hip and ankle and before the wrist, with slight variations on individual epiphyses. The knee is the growing end of the leg and is, therefore, one of the later areas to fuse to allow for longitudinal growth to occur (Cunningham et al., 2016). The wrist is the growing end of the lower arm and the proximal epiphysis of the humerus is the growing end of the upper arm (Pritchett, 1991; Cunningham et al., 2016). All growing-end epiphyses fuse late in the sequence because of the growth required to elongate the skeleton to adult proportions.

The iliac crest fuses after the proximal humerus. Fusion of the iliac crest suggests that menarche has been achieved in girls (Lewis et al., 2016) and therefore, the iliac crest's correlation to puberty may be why it fuses so late in the sequence. Either the medial clavicle or sacral bodies 1 and 2 end the fusion sequence. Skeletal maturation is then achieved. A summary of the fusion sequence is presented in **Figure 8. 8**.

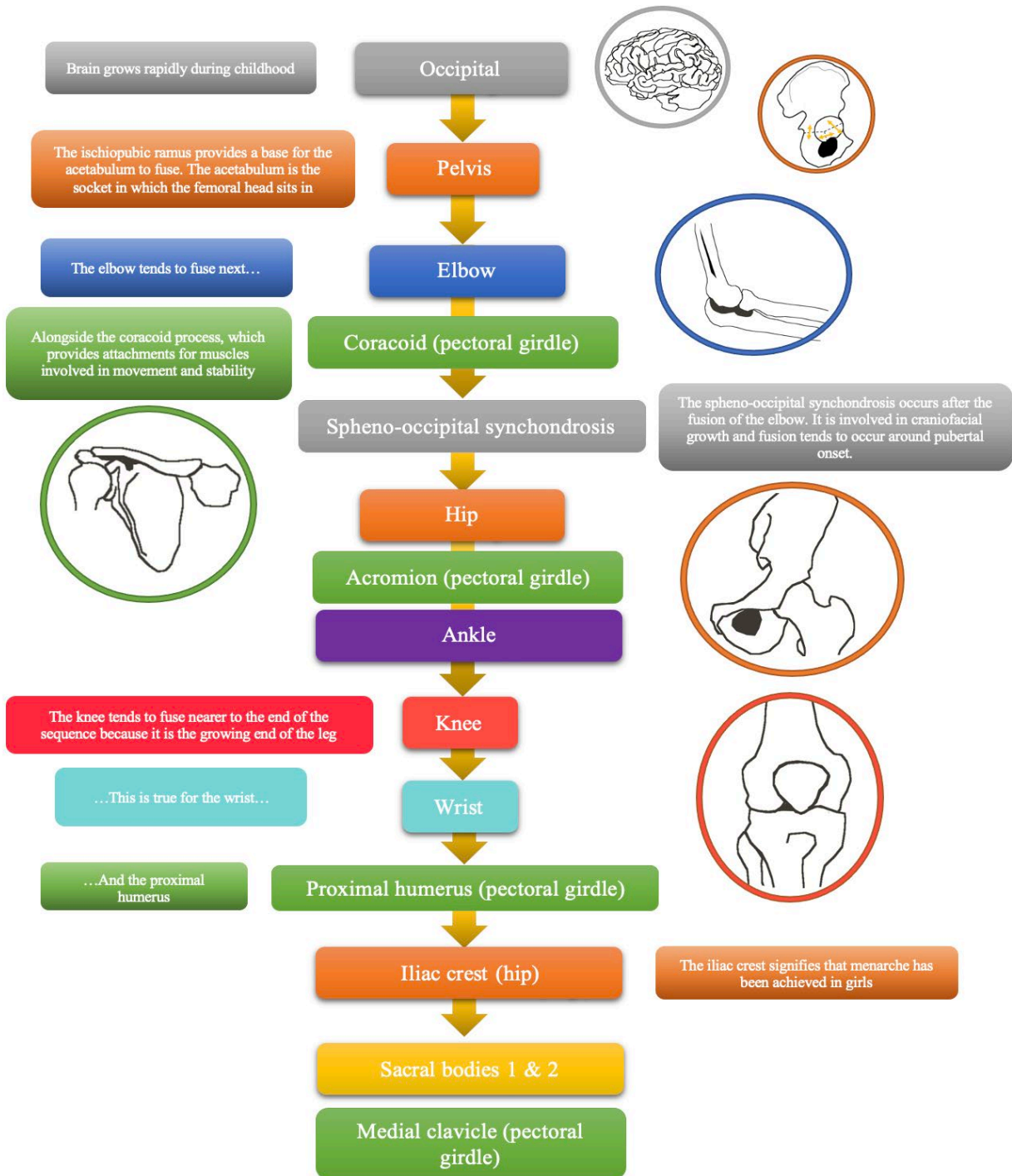
The function of the bones tends to dictate their placement within the sequence – growing ends fuse towards the end and bones under more pressure will more likely be less variable in when they fuse (Lenover and Šešelj, 2019). A study that looked at the sequence of epiphyseal fusion in chimpanzees found the sequence to be: Elbow, Hip, Ankle, Knee, Wrist and Shoulder (Zihlman et al., 2007). Apart from the shoulder, which had fusion sites spread throughout the sequence, the pattern for the archaeological and Post-Mediaeval/Modern samples followed the sequence found in chimpanzees.

Within the primate order, the sequence of fusion always starts with the elbow (Shigehara, 1980). The hip is often next, apart from in certain species, such as tamarins, in which the ankle comes next (Shigehara, 1980). Thirdly is the ankle, and the fourth in the

sequence is either the knee or the wrist (Shigehara, 1980). The shoulder and the wrist compete for last place between species, but the shoulder is usually last in the sequence (Shigehara, 1980). When the sequence of fusion is extended to the mammalian class, the elbow still comes first in the sequence.

Previous research has shown that the sequence of fusion is not fixed between species (Shigehara, 1980) or between geographical modern human populations (Lenover and Šešelj, 2019), and this research has shown how the sequence of fusion may change between archaeological modern human populations. Finally, previous research and this study (using St Gregory's) have shown how the sequence of fusion can vary within the same modern human population (Schaefer and Black, 2007; Schaefer, 2008a, 2014; Schaefer et al., 2009; Lenover and Šešelj, 2019).

Figure 8. 8: Summary of the sequence of fusion for the modern human skeleton



## 8.5. PUBERTY

This section discusses the age at each pubertal phase in St Gregory's (results found in **Section 5.5**). This is followed by a comparison between Mediaeval Canterbury and York, and then between archaeological groups (results found in **Chapter 7**). Puberty in St Gregory's focuses on how growth and maturation are structured in a Mediaeval Canterbury sample. Puberty between Mediaeval sites is explained briefly, which follows into a wider discussion.

### 8.5.1. Puberty in St Gregory's

Age at each pubertal phase was assessed for St Gregory's skeletal collection. Epiphyses not required to predict puberty were also examined to see the pubertal phase in which they fused in. Results can be found in **Section 5.5**. The ossiculum terminale was found to fuse at a significantly later pubertal phase (mean phase was PHV for the high-status group) in the high-status group compared to the low-status group (mean phase: Acceleration). This contrasts with age-at-fusion, which showed no differences between the two social classes of Mediaeval St Gregory's. It has been stated that the ossiculum terminale is a highly variable site and this could have contributed to the difference. It was unfortunate that preservation of the high-status skeletons was not as good as the low-status skeletons, as the inclusion of more high-status skeletons could help address this question.

It was also found that complete fusion (Stage 3) of sacral bodies 1 & 2 signalled the completion of puberty. This result was found for all archaeological groups. Although an individual could be in partial fusion (Stage 2) of sacral bodies 1 and 2 and have completed puberty, no individuals were found to have completed fusion (Stage 3) and not have completed puberty.

Sexual maturation is argued to occur before growth completes (Shigehara, 1980; Zihlman et al., 2007) and it is of interest that the complete fusion of sacral bodies 1 and 2 are correlated with the end of sexual maturation. However, the complete fusion of the sacrum is not required for the completion of puberty. Still, this result can be of help in age estimation, as a matured sacrum signifies the skeleton was beyond puberty at death. Through the collaboration of the age-at-fusion and puberty results, it can be stated that within St Gregory's skeletal collection:

- (1) An unfused sacral body 1 and 2 signifies that the individual was under the age of 17 years. The individual is within the following pubertal phases: Pre-puberty, Acceleration or PHV.
- (2) A partially fused sacral body 1 and 2 signifies an individual is over 16 years. The individual can be in any pubertal phase from PHV to Completion.
- (3) A completely fused sacral body 1 and 2 signifies the individual has completed puberty and is over the age of 19 years.

### 8.5.2. Puberty between Mediaeval Canterbury and York

No significant differences in the age at each pubertal phase existed between the two Mediaeval cities. Data was limited for York so that not all pubertal phases could be compared, but the little data that was available showed that York's pubertal phases fit within the age ranges given for Canterbury. Significant differences were not expected for similar reasons to **Section 8.2.3.**, but it was of interest that almost no variation existed between the two sites. For example, Pre-puberty did not go past age 12 years and Acceleration lasted between 9 to 16 years for both groups.

### 8.5.3. Puberty compared between archaeological groups

No significant differences in the age at each pubertal phase existed between the archaeological groups. This is in stark contrast to the significant differences found between age-at-fusion in the epiphyses between the groups in **Section 8.3.1.**

### 8.5.4. Puberty compared to published archaeological data

A) *Roman published data: 43 AD – 410 AD*

**Table 8. 2** illustrates age-at-death plotted against the pubertal phase for the Iron Age and Roman archaeological samples compared to Roman published data. The Anglo-Saxon (this study) and British Roman males (Arthur et al., 2016) recorded  $n = 1$  skeleton each aged eighteen years in Acceleration. The Anglo-Saxon eighteen-year-old was from Black Gate, Sheffield (Sk. 132). Arthur et al., (2016) described the Roman eighteen-year-old male as anomalous and pathological.

Abnormally delayed or absent puberty can arise when the hypothalamic-pituitary-gonadal axis is disturbed by situations of severe stress, anorexia nervosa, or the participation of intense physical activity (Brämswig and Dübbers, 2009). Developmental mutations to the pituitary gland or genes involved with pubertal onset, as well as diseases, such as tumours, can cause the absence of puberty altogether (Brämswig and Dübbers, 2009). Since both eighteen-year-olds were in the Acceleration phase when they died signifies an external stressor on the body, rather than a mutation. This is of interest as the Anglo-Saxon adolescents in this study were believed to be under a great amount of stress due to the period in which they lived.

Table 8. 2: Age-at-death per pubertal phase for the primary data of Iron Age and Roman groups with the Roman secondary data. Pubertal phases are named as found. Reference: (i) Roman, England, 1<sup>st</sup>-5<sup>th</sup> century, dry bone (Arthur et al., 2016)

	Rounded age-at-death estimation (years)													
	8	9	10	11	12	13	14	15	16	17	18	19	20	21-25
Iron Age (Primary data)							Acc.			Dec.				
Roman (Primary data)		Pre-puberty			Acceleration				PHV		Dec.		Maturation	Comp
Roman British females <sup>i</sup>	Pre-puberty		Acceleration		PHV			Menarche		Deceleration			Mat.	Completion
Roman British males <sup>i</sup>	Pre-puberty				Acceleration				PHV	Deceleration				

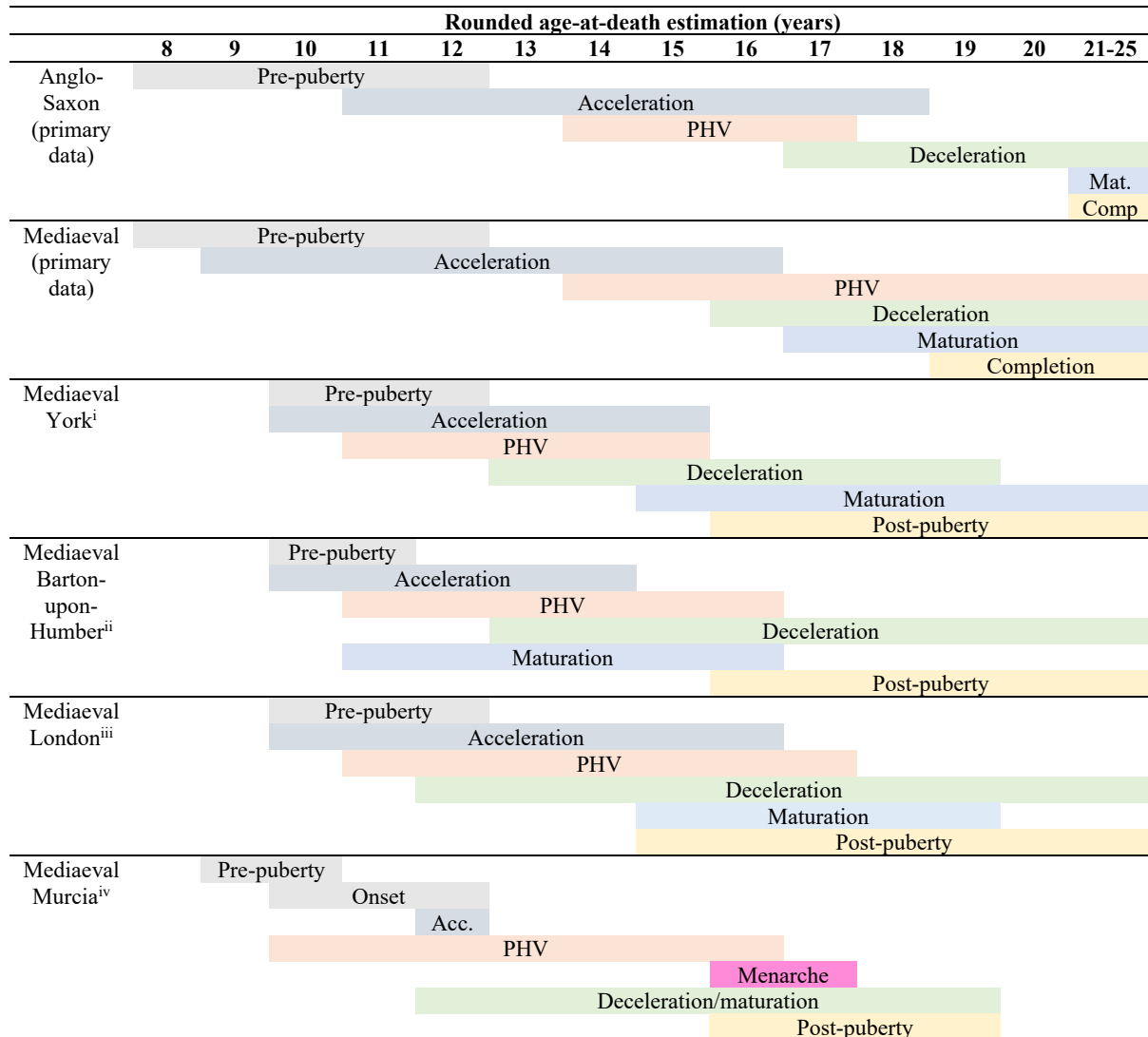
It was predicted that the Roman published data would resemble the ages at pubertal phases in the Roman archaeological group. This was predicted because the sites chosen were most likely environmentally comparable during this period. The Roman British data was recorded from the urban sites of Londinium and Queenford farm. Queenford farm was a small, nameless Roman town in Oxfordshire, with plenty of open spaces and surrounded by fertile agricultural land (Arthur et al., 2016). In contrast, Londinium (now known as London) was the principal point of contact between Rome and Britain (Arthur et al., 2016). It was one of the largest capitals in

the empire's western provinces (Arthur et al., 2016). Like Londinium, Corinium (now known as Cirencester and the area in which this study's Roman samples were taken) was a large Roman town, with Corinium being the second-largest Roman town after Londinium within the province (Holbrook, 2012). However, the ages at pubertal phase appeared to occur at a later age in the Corinium group compared to the combined Londinium/ Queenford farm group. Although the Corinium group could be considered more like the Roman males than females. When the published data was divided into Londinium and Queenford farm samples, the Corinium skeletons appeared closer to the Queenford farm sample than Londinium.

*B) Mediaeval published data: 1066 AD – 1540 AD*

**Table 8. 3** illustrates age-at-death plotted against pubertal phase for the Mediaeval primary data (and the Anglo-Saxon data) and the Mediaeval published data. The published data for York, Barton-upon-Humber and London were analysed by the same research group (Lewis et al., 2016) and all three sites appeared more similar to one another than when compared to the sites of this study. This may thus show a methodological bias, as both the Mediaeval sample of this study and the published York sample included skeletons from the Fishergate House skeletal collection, and it would be expected that these two groups would correlate the closest.

Table 8. 3: Age-at-death per pubertal phase for the primary data of Anglo-Saxon and Mediaeval groups with the Mediaeval secondary data. Pubertal phases are named as found. References: (i) Mediaeval, York, England, 950-1700AD, dry bone (Lewis et al., 2016), (ii) Mediaeval, Barton-upon-Humber, England, 950-1700AD, dry bone (Lewis et al., 2016), (iii) Mediaeval, St Mary Spital, London, England, 950-1500AD, dry bone (Lewis et al., 2016), (iv) Mediaeval, Murcia, Spain, 11<sup>th</sup>-13<sup>th</sup> centuries, dry bone (Doe et al., 2017)



C) Post-Mediaeval and Modern period: 1540 AD – present day

Table 8. 4 illustrates age-at-death plotted against pubertal phase for the Post-Mediaeval archaeological data and the Post-Mediaeval and Modern published data. All archaeological groups were found not to remain in Pre-puberty past the age of 12 years. This finding is consistent with previous research that suggests that the activation of puberty is not greatly affected by the environment, as both past and Modern children have been found to enter Acceleration between 9 to 12 years (Malina et al., 2004; Aksglaede et al., 2008; Hauspie and



suggests that PHV occurred at a later age in past populations compared to modern populations (Aksglaede et al., 2008; Hauspie and Roelants, 2012; Arthur et al., 2016; Lewis et al., 2016).

The Deceleration phase was recorded between 16 to 21 years for the Mediaeval sample. Many of the groups lacked data from PHV onwards, but the Anglo-Saxon sample had individuals in the Deceleration phase between 17 to 21 years. A Post-Mediaeval Dutch study found Deceleration to occur between 16 to 26 years and Maturation to occur between 15 to 25 years (Blom et al., 2021). The Deceleration phase, therefore, appeared similar between historical and Modern populations. Maturation in Modern Western populations occurs at approximately 16 to 17 years for girls and 18 to 19 years for boys, with additional minimal growth potentially carrying on into the late twenties (Hauspie and Roelants, 2012). The Middenbeemster Maturation phase occurred at a younger age in early maturers compared to the archaeological groups.

Overall, ages at pubertal onset, Acceleration, Deceleration and Completion appeared similar across historical and Post-Mediaeval/Modern populations. Differences occurred for PHV and the Maturation phase of puberty whereby the archaeological data appeared delayed compared to the published Post-Mediaeval data. While this is in line with current hypotheses that denote that puberty occurred later for past peoples, it was of interest that some of the published Mediaeval groups and the published Roman female group occurred at earlier ages for certain pubertal phases compared to the archaeological data, and sometimes occurred more in line with the published Post-Mediaeval ages at pubertal phase. Again, this may be due to potential methodological issues. To combat this, a larger Post-Mediaeval sample would be required to be collected to better compare to the data of this study.

Pubertal differences between populations, in particular, between past and Modern populations, have been questioned, with suggestions that the differences reside within the methodology (Doe et al., 2017). Although methodology appears to be an important factor in the variations viewed between populations, as seen in this study, puberty work from longitudinal studies on living patients (Aksglaede et al., 2008) and the examination of historical records (Blom et al., 2021) have alluded to historical populations as having experienced an extended puberty. In general, correlations can be made across all samples to see a broad analogous nature to pubertal timing, both Modern and in the past, but earlier timings within more Modern populations for particular pubertal phases and extended pubertal phases in historical populations can also be highlighted, both in this research and in published work. However, potential differences based on methodology are a hazardous factor and a future

direction would be to assess puberty in multiple archaeological periods, which this research has begun to do.

## **8.6. METHODOLOGICAL CONSIDERATIONS**

This section considers the methodological constraints, specifically the osteological paradox, sampling size, the use of undocumented collections and differences between this study and others.

### **8.6.1. Osteological Paradox**

The osteological paradox is when skeletons are used to make predictions about the past, but these skeletons are a sample of individuals who have died and therefore may not represent the actual population that was living at that point in time (Wood et al., 1992; Dewitte and Stojanowski, 2015). Problems arise from this, such as hidden frailty heterogeneity (individuals are susceptible to different environmental stressors and diseases and this increases or decreases an individual's mortality risk), biased samples (the skeletons are not healthy, living people) and demographic non-stationarity (skeletal collections may reflect brief periods in which changes have occurred, such as migrations, or changes in fertility and mortality and these will not necessarily be recorded, Wood et al., 1992; Redfern and Dewitte, 2011; Dewitte and Stojanowski, 2015; Zarulli, 2016).

The aim of this study was to research skeletal maturation and development across the archaeological periods of Britain, but this involved the use of juvenile remains. Although some skeletons within this study were known to have died through non-disease-related deaths, such as beheadings, most causes of death were unknown. The skeletons used in this study and other osteological studies are skeletons that were selected out of living populations and into skeletal collections (Wood et al., 1992; Dewitte and Stojanowski, 2015) and this is especially true of juvenile and young adult skeletons, who should have lived to old age. Thus, it is unknown whether the age-at-fusion represents a true analysis of past fusion or just those who have died. However, as many of the results can correlate well to previous studies, it is hopeful that this study represents a true analysis of growth and development of the past.

### 8.6.2. Sample size

Due to the constraints of accessing skeletal collections, coupled with the preservation of the skeletons, some sample sizes were small. These complicated comparisons, such as understanding general trends from the data. Small sample sizes made it difficult to understand which data was representative of the population and which information was skewed because of a lack of samples. St Gregory's skeletal collection had the largest sample size, making this the best group for understanding trends. However, as St Gregory's sample size was larger than the other datasets, it dominated the Mediaeval group, and therefore the Mediaeval group was more representative of Mediaeval Canterbury than Mediaeval Britain. A future consideration would be to add more skeletons to the analysis.

### 8.6.3. Undocumented collections

Many skeletal analyses that study epiphyseal fusion use documented collections and will therefore know the sex and age-at-death of each skeleton (Cardoso, 2007, 2008b, 2008a; Coqueugniot and Weaver, 2007; Schaefer and Black, 2007; Schaefer, 2008b; Cardoso et al., 2013a). This thesis used undocumented collections, and therefore, age had to be determined by the skeleton. Although most of the skeletons were aged by their dentition, a few had to be aged by epiphyseal fusion. To prevent a circular argument, the epiphyseal fusion used to determine age was not used in the analysis of the age-at-fusion. However, an average age at death had to be acquired, meaning that differences found between groups may be due to the average age selected and not the skeleton's actual chronological age. This is problematic but this type of methodology has been used in previous literature (Shapland and Lewis, 2013, 2014; Arthur et al., 2016; Lewis et al., 2016; Blom et al., 2021), in which dentition and epiphyseal fusion are used to give an average age to then study puberty from fusion. Equally, while the ages were averaged, much of the epiphyseal and puberty data generated within this thesis matched previous literature reviewed above.

The sex of the skeletons was not known. Females are found to mature earlier than boys (Topper and Mulier, 1932; Coqueugniot and Weaver, 2007) and this would have been helpful to the analysis. In particular, it was often found that the fusion of certain epiphyses was more similar to published male data than female data and it would have been of interest to know the ratio of males to females for this data. While methods are available for estimating sex in juveniles (Schutkowski, 1993; Bruzek, 2002; Bass, 2005; Rogers, 2009), it is often stated that

estimating sex in juveniles is imprecise, especially in prepubertal children (White et al., 2012; Doe et al., 2017; Nikita, 2017). This is due to the low levels of sex hormones circulating in pre-pubescent children, responsible for secondary sexual characteristics (White et al., 2012; Doe et al., 2017; Nikita, 2017). Future considerations could use sex chromosome-linked isoforms (proteins that are similar) from the enamel-forming protein – amelogenin – that is found in dental enamel to assign sex to each skeleton (Fincham et al., 1991; Stewart et al., 2017).

#### **8.6.4. Methodological differences**

Cardoso, (2008a) has previously stated the importance of methodological differences between studies when comparing and contrasting data. This is possibly why the Mediaeval puberty data performed by Lewis et al., (2016) appeared more similar to each other than the data of this study, and why the Medieval and Anglo-Saxon samples of this study appeared more similar to each other than the Mediaeval data was to that of Lewis et al., (2016). However, an advantage of the current study is that so many samples were analysed and analysed by the same researcher, which means that the primary archaeological data can be compared without the issue of analysis differences.

## 8.7. SUMMARY

- No differences were found between the high and low samples from Mediaeval Canterbury. This is believed to be because all Mediaeval children received a similar diet regardless of their parent's social class. The lack of differences continued when Mediaeval York was compared to Canterbury. Only the fusion of the ossiculum terminale showed any statistically significant differences.
- The Anglo-Saxon group had significantly later ages at fusion for many of their appendicular epiphyses compared to the other archaeological samples. It was thought that this could potentially be because of the unsettled period that people lived through during these times, which included multiple invaders to Britain.
- Some fusion sites, such as the medial clavicle, showed a different pattern, in which the Roman period had much later ages at complete fusion than the other archaeological periods, although this was not statistically significant. It was thought that the poor diet, urban living and cultural practices of the Roman era may have been detrimental to the growth of specific fusion sites.
- Mediaeval Canterbury had some individuals with defects on their atlas vertebrae. Two individuals specifically – aged 12 and 15 years – had both posterior and the rarer anterior defects on their atlases. As anterior atlas defects are primarily inherited, it is presumed these two are related.
- When looking at the sequence of fusion, early to middle fusion sites were found to be more variable between archaeological groups than the beginning and later sites in the sequence. This supported previous findings. While the fusion sites within the sequence could be variable, a common pattern was followed in the fusion of the elbow – (hip) – ankle – (shoulder) – knee – wrist.
- Overall, puberty was found to occur at similar ages among archaeological groups. When compared to published Mediaeval and Post-Mediaeval/Modern data, PHV and Maturation, in particular, were found to occur at a later age in the archaeological data.
- Complete fusion of sacral bodies 1 and 2 meant that the individual had also completed puberty.

## CHAPTER 9

# CONCLUSION

### 9.1. CONCLUSION OF RESEARCH

#### 9.1.1. Maturation of the Mediaeval Skeleton

The first research question was to determine if epiphyseal fusion could be used to estimate age-at-death for Mediaeval skeletons from Canterbury. It was found that nine fusion sites could be used because they either had always completed fusion (Stage 3) by a certain age (e.g., the posterior synchondrosis of the atlas usually completed fusion from 4 years and up), or they were in the process of fusion (Stage 2) between a specific age range. A significant association between ages 15 to 16 years and the fusion of the proximal radius was also found when a Fisher-Freeman-Halton Exact Test was run on the data ( $p = 0.041$ ). Although only four sites remained statistically significant when a Bonferroni correction was performed: the anterior arch and posterior synchondrosis of the atlas, the dentocentral and neurocentral junctions of the axis and metacarpals 2 – 5, as well as the proximal and middle phalangeal epiphyses of the hand.

No significant differences were found in fusion age between the high and low statuses of St Gregory's. It was inferred that the lack of significant differences was because the diet of Mediaeval children remained similar, regardless of social class. The similarity in growth profiles indicates that social status does not undermine the estimation of age from epiphyseal fusion in British Mediaeval juvenile skeletal collections.

Except for the age-at-fusion of the ossiculum terminale, no significant differences were found between Mediaeval Canterbury and York. It was predicted that no differences would arise between these two sites because they most likely had similar environments including their economy and broader diet. The age-at-fusion of the ossiculum terminale most likely differed between Canterbury and York because it is a highly variable fusion site. These findings mean

that age at death estimates from fusion of the skeleton is likely to produce a similar age range for either St Gregory's in Canterbury or York.

### **9.1.2. Maturation of the modern human skeleton through British Archaeological periods**

Skeletal fusion was compared between different periods of British history, including the Iron Age, Roman, Anglo-Saxon, Mediaeval and Post-Mediaeval periods. It was found that fusion was delayed in the Anglo-Saxons compared to other archaeological groups. It is likely that this may be due, in part, to significant political and economic unrest that occurred in the Anglo-Saxon era. Although only one site remained statistically significant (proximal radius between the Anglo-Saxon and Mediaeval groups) after the test was corrected for multiple comparisons. However, it may be likely that with larger sample sizes, these sites would reach significance.

These results were compared to published studies that examined age-at-fusion in Post-Mediaeval and Modern individuals. Seven fusion sites (pars lateralis to pars basilaris, sphenoccipital synchondrosis, sacral bodies 1 and 2, medial clavicle, medial border and inferior angle of the scapula, and the proximal tibia) were considered to differ between the archaeological groups and the Post-Mediaeval and Modern published studies. Although the pars lateralis to pars basilaris may be considered more similar than different. The archaeological groups tended to fuse at a later age for the skull, scapula and tibia compared to the Post-Mediaeval/Modern data. Whereas Post-Mediaeval and Modern individuals were found to be in partial fusion (Stage 2) much later than many of the archaeological groups for the sacrum and the clavicle. However, whether this is a true comparison or not would require statistical analysis through the collaboration of projects or the collection of more recently deceased human remains.

### **9.1.3. The sequence of fusion**

The order in which the epiphyses complete fusion (Stage 3) was determined for Mediaeval skeletons from Canterbury and compared to other archaeological periods and published data from Post-Mediaeval and Modern sample populations. It was found that subtle variations occurred between all the groups, but the overall sequence remained the same for all, in that epiphyseal sites tended to group by their function, such as epiphyses for the elbow or knee.

#### **9.1.4. Puberty**

Puberty was found to begin around the age of 12 years and end at the earliest age of 19 years in Mediaeval Canterbury. Most epiphyseal fusion occurred during Adolescence, which incorporated the pubertal phases of PHV, Deceleration and Maturation. Complete fusion (Stage 3) of sacral bodies 1 and 2 signalled that puberty had also been completed. Age-at-puberty did not differ significantly between Mediaeval sites, nor between any of the archaeological groups. This is an indication that puberty age has varied only slightly within British history.

## 9.2. FUTURE DIRECTION

Future studies could build on this research through the inclusion of more skeletons, especially skeletons from the collections already sampled. This would help to provide answers to whether the Mediaeval group were healthier compared to the Anglo-Saxon group, and whether the Roman group's growth was affected by the cultural changes and urbanisation of the times. Isotopic evidence may be of value here, as skeletal maturation can be compared to isotopic profiles. Microscopic analysis of the enamel (which has already been collected for all skeletons used in this study) could be used to determine if any environmental insults may have occurred during growth through the study of hypoplastic defects. Analysis of the teeth could also research into the sex of the skeleton through enamel peptides and retzius periodicity to study any trends within and between archaeological groups.

Sampling of more Mediaeval skeletal collections around Britain would be valuable in understanding more about how this period affected growth. As detailed in **Chapter 8**, the Middle Ages had advantageous years, in which warmer climates and technological innovations saw the rise in population, as well as disadvantageous years, in which famine and pestilence were rife (Dyer, 1994; Schama, 2009). Although this ultimately became beneficial for those who survived, as the dramatic drop in population allowed for better health and socioeconomic conditions overall (Dyer, 1994). Thus, through the inclusion of more Mediaeval skeletal collections, it is hopeful that skeletal maturation could be tracked through the period to see if these events had an impact on fusion. Dewitte and Lewis, (2020) tracked age-at-menarche over the course of the black death and thus a similar study tracking age-at-fusion would be of additional value to the further understanding of the growth and maturation of modern humans. It is hoped that the future direction of this research through the improvements given above will help to delve deeper into the understanding of modern human maturation in British history.

## CHAPTER 10

**BIBLIOGRAPHY**

- Abad, V., Meyers, J.L., Weise, M., Gafni, R.I., Barnes, K.M., Nilsson, O., Bacher, J.D., Baron, J., 2002. The Role of the Resting Zone in Growth Plate Chondrogenesis. *Endocrinology*. 143, 1851–1857.
- Abassi, V., 1998. Growth and Normal Puberty. *Pediatrics*. 102, 507–11.
- Addyman, P. V., 1980. Eburacum, Jorvik, York. *Scientific American*. 242, 76–87.
- Akobo, S., Rizk, E., Loukas, M., Chapman, J.R., Oskouian, R.J., Tubbs, R.S., 2015. The odontoid process : a comprehensive review of its anatomy, embryology, and variations. *Child’s Nervous System*. 31, 2025–34.
- Aksglaede, L., Olsen, L.W., Sørensen, T.I.A., Juul, A., 2008. Forty Years Trends in Timing of Pubertal Growth Spurt in 157, 000 Danish School Children. *PLoS ONE*. 3, 1–8.
- Albarella, U., Johnstone, C., Vickers, K., 2008. The development of animal husbandry from the Late Iron Age to the end of the Roman period: a case study from South-East Britain. *Journal of Archaeological Science*. 35, 1828–1848.
- Alhazmi, A., Vargas, E., Palomo, J.M., Hans, M., Latimer, B., Simpson, S., 2017. Timing and rate of spheno-occipital synchondrosis closure and its relationship to puberty. *PLoS ONE*. 12, 1–16.
- Alonso, L.C., Rosenfield, R.L., 2002. Oestrogens and puberty. *Best Practice & Research Clinical Endocrinology and Metabolism*. 16, 13–30.
- AlQahtani, S.J., Hector, M.P., Liversidge, H.M., 2010. Brief communication: The London atlas of human tooth development and eruption. *American Journal of Physical Anthropology*. 142, 481–490.
- Anderson, T., Andrews, J., 2001. The human remains. In: Hicks, M., Hicks, A. (Eds.), *St Gregory’s Priory, Northgate, Canterbury: Excavations 1988-1991*. Geerings, Ashford.
- Appleby, J., Stahl-Timmins, W., 2018. Consumption, flux, and dropsy: Counting deaths in 17th century London. *BMJ (Online)*. 363, 1–5.
- Arthur, N.A., Gowland, R.L., Redfern, R.C., 2016. Coming of age in Roman Britain: Osteological evidence for pubertal timing. *American Journal of Physical Anthropology*.

- 159, 698–713.
- Baer, H.J., Rich-Edwards, J.W., Colditz, G.A., Hunter, D.J., Willett, W.C., Michels, K.B., 2006. Adult height, age at attained height, and incidence of breast cancer in premenopausal women. *International Journal of Cancer*. 119, 2231–2235.
- Bailey, B.G., Bernard, M.E., Carrier, G., Elliott, C.L., Langdon, J., Leishman, N., Mlynarz, M., Mykhed, O., Sidders, L.C., 2015. Coming of Age and the Family in Medieval England. *Journal of Family History*. 33, 41–60.
- Ballock, R.T., O’Keefe, J.O., 2003. The Biology of the Growth Plate. *The Journal of Bone and Joint Surgery*. 85-A, 715–726.
- Barber, J., 2016. Chronology. In: *Living and Dying at Auldham, East Lothian: The Excavation of an Anglian Monastic Settlement and Medieval Parish Church*. The Society of Antiquaries of Scotland, Edinburgh.
- Barbier, P., 1998. *The World of the Castrati: The History of an Extraordinary Operatic Phenomenon*. Souvenir Press, London.
- Barker, J., De Villiers, C., Harper, T., 2021. Unit 12: The Skeletal System [WWW Document]. Douglas College Human Anatomy & Physiology I. URL <https://pressbooks.bccampus.ca/dcbiol110311092nded/chapter/unit-12-skeletal-system/>
- Barnes, M.E., 2018. Neural Crest. *The Embryo Project Encyclopedia*.
- Baron, J., Säwendahl, L., De Luca, F., Dauber, A., Phillip, M., Wit, J.M., Nilsson, O., 2015. Short and tall stature: a new paradigm emerges. *Nature Reviews Endocrinology*. 11, 1–12.
- Bass, W.M., 2005. *Human osteology: a laboratory and field manual*. Missouri Archaeology Society, Columbia.
- Beasley, M., 2022. Age of Pelvic Bone Fusion [WWW Document]. *Anatomy and Biomechanics*. URL <https://carta.anthropogeny.org/moca/topics/age-pelvic-bone-fusion>
- Belcastro, M.G., Pietrobelli, A., Rastelli, E., Iannuzzi, V., Toselli, S., Mariotti, V., 2019. Variations in epiphyseal fusion and persistence of the epiphyseal line in the appendicular skeleton of two identified modern (19th–20th c.) adult Portuguese and Italian samples. *American Journal of Physical Anthropology*. 169, 448–463.
- Belcastro, M.G., Rastelli, E., Mariotti, V., 2008. Variation of the Degree of Sacral Vertebral Body Fusion in Adulthood in Two European Modern Skeletal Collections. *American Journal of Physical Anthropology*. 160, 149–160.
- Berendsen, A.D., Olsen, B.R., 2015. Bone Development. *Bone*. 80, 14–18.

- Berkey, C.S., Wang, X., Dockery, D.W., Ferris Jr., B.G., 1994. Adolescent height growth of US children. *Annals of Human Biology*. 21, 435–442.
- Berkson, J., 1944. Application of the Logistic Function to Bio-Assay. *Journal of the American Statistical Association*. 39, 357–365.
- Betts, J.G., Young, K.A., Wise, J.A., Johnson, E., Poe, B., Kruse, D.H., Korol, O., Johnson, J.E., Womble, M., DeSaix, P., Blaker, W., Bowers, J., Barlow, M., Hortsch, M., Bradshaw, E., Tallman, K., Campbell, B., Tarapore, R., Jablanovic, B., Dobbins, P., Shmaefsky, B., Christie-Pope, B., Sizemore, D., Culver, M., McLaughlin, D., Maring, B., Dukehart, P., Dentel, S., Tattersall, E., Weck, M., Westergaard, N., Chapman, M., Kleinelp, W., Leady, B., Heinze, S., May, J., Caplea, A., Aaronson, K., Agarwal, L., Allen, G., Bryska, N., Opsal, S.C., Johnson, N., Leupen, S., Mallet, R., Crane, K., Cushman, H., Gopalan, C., Hubley, M., Horeth, D., Weiss, K., Ellerton, S., Thompson, J., Thrasher, R., Mitchell, N., Van Wylen, D., Martin, E., Paul, I., Liang, L., Wortham, D., Natarajan, S., Ott, B., Dubowsky, S., Niles, M.J., Thomas, M., Pyle, M., Yadav, U., Henninger, A., DuPriest, E., Ballard, T., Nicotera, P., Giangrande, M., Maxwell, N., Perkins, C., Rawding, R., Gargan, L., Keyte, J., Greco, V., Allison, R., Armbruster, H., Wandrey, L., Pfeiffer, D., Jonasson, M., Spencer, S., Kleinert, L., Schreer, J., Pilat, T., Nwosu, I., Dolan, P., DuPré, E., Lepri, J., Endres, C., Preston, E., Sun, E., Swenson, T., Yates, T., York, J., Zao, C., Zoubina, E., Cutter, N., Danzl-Tauer, L., Feldman, M., Davis, J., Hubbard, R., Payette, A., Fitch, G., Sullivan, R., DelliPizzi, A., Standley, C., Natarajan, S., Payne, S., Sheldahl, L., Elf, P., 2016. *Anatomy and Physiology*. Rice University, International.
- Beunen, G.P., Rogol, A.D., Malina, R.M., 2006. Indicators of biological maturation and secular changes in biological maturation. *Food and Nutrition Bulletin*. 27, 244–256.
- Bielicki, T., Hauspie, R., 1994. On the Independence of Adult Stature From the Timing of the Adolescent Growth Spurt. *American Journal of Human Biology*. 6, 245–247.
- Biro, F.M., McMahon, R.P., Striegel-Moore, R., Crawford, P., Obarzanek, E., Morrison, J.A., Barton, B.A., Falkner, F., 2001. Impact of timing of pubertal maturation on growth in black and white female adolescents: The National Heart, Lung, and Blood Institute Growth and Health Study. *The Journal of Paediatrics*. 138, 636–643.
- Black, S., Scheuer, L., 1996. Age Changes in the Clavicle: from the Early Neonatal Period to Skeletal Maturity. *International Journal of Osteoarchaeology*. 6, 425–434.
- Blom, A.A., Schats, R., Hoogland, M.L.P., Waters-Rist, A., 2021. Coming of age in the

- Netherlands: An osteological assessment of puberty in a rural Dutch post-medieval community. *American Journal of Physical Anthropology*. 174, 463–478.
- Blumsohn, A., Hannon, R.A., Wrattet, R., Bartont, J., 1994. Biochemical markers of bone turnover in girls during puberty. *Clinical Endocrinology*. 40, 663–670.
- Boeyer, M.E., Sherwood, R.J., Deroche, C.B., Duren, D.L., 2018. Early Maturity as the New Normal: A Century-long Study of Bone Age. *Clinical orthopaedics and related research*. 476, 2112–2122.
- Bogin, B., 1990. The Evolution of Human Childhood. *Bioscience*. 40, 16–25.
- Bogin, B., 1999a. *Patterns of Human Growth*. Cambridge University Press, Cambridge.
- Bogin, B., 1999b. Evolutionary Perspective on Human Growth. *Annual Review of Anthropology*. 28, 109–53.
- Bogin, B., 2003. The human pattern of growth and development in paleontological perspective. In: Thompson, J.L., Krovitz, G.E., Nelson, A.J. (Eds.), *Patterns of Growth and Development in the Genus Homo*. Cambridge University Press, Cambridge, pp. 15–44.
- Bogin, B., 2012. The Evolution of Human Growth. In: Cameron, N., Bogin, B. (Eds.), *Human Growth and Development*. Elsevier Inc., London.
- Bogin, B., 2015. Human Growth and Development. In: Meuhlenbein, M.P. (Ed.), *Basics in Human Evolution*. Academic, London, pp. 285–293.
- Bogin, B., Campbell, B., 2021. Adrenarche [WWW Document]. Centre for Academic Research & Training in Anthropogeny. URL <https://carta.anthropogeny.org/moca/topics/adrenarche>
- Bogin, B., Smith, B.H., 2000. Evolution of the Human Life Cycle. In: Stinson, S., Bogin, B., O'Rourke, D.H. (Eds.), *Human Biology: An Evolutionary and Biocultural Perspective*. John Wiley & Sons Ltd, New Jersey, pp. 377–424.
- Börjesson, A.E., Lagerquist, M.K., Liu, C., Shao, R., Windahl, S.H., Karlsson, C., Sjögren, K., Movérare-Skrtic, S., Antal, M.C., Krust, A., Mohan, S., Chambon, P., Ohlsson, C., 2010. The role of estrogen receptor  $\alpha$  in growth plate cartilage for longitudinal bone growth. *Journal of Bone and Mineral Research*. 25, 2690–2700.
- Boyle, A., 1998. Synopsis: the Anglo-Saxon cemetery and later activity. In: Boyle, A., Jennings, D., Miles, D., Palmer, S. (Eds.), *The Anglo-Saxon Cemetery at Butler's Field, Lechlade, Gloucestershire. Volume I: Prehistoric and Roman Activity and Anglo-Saxon Grave Catalogue*. Oxbow Books, Oxford.
- Boyle, A., Palmer, S., 1998. Introduction. In: Boyle, A., Jennings, D., Miles, D., Palmer, S.

- (Eds.), *The Anglo-Saxon Cemetery at Butler's Field, Lechlade, Gloucestershire. Volume I: Prehistoric and Roman Activity and Anglo-Saxon Grave Catalogue*. Oxbow Books, Oxford.
- Boynton-Jarrett, R., Harville, E.W., 2012. A prospective study of childhood social hardships and age at menarche. *Annals of Epidemiology*. 22, 731–737.
- Brämswig, J., Dübbers, A., 2009. Disorders of Pubertal Development. *Deutsches Arzteblatt*. 106, 295–304.
- Bravais, A., 1846. *Analyse Mathématique sur les Probabilités des Erreurs de Situation d'un Point*. *Memoires par divers Savans*. 9, 255–332.
- Brimacombe, C.S., 2017. The enigmatic relationship between epiphyseal fusion and bone development in primates. *Evolutionary Anthropology*. 26, 325–335.
- Brooks, S., Suchey, J.M., 1990. Skeletal Age Determination based on the os pubis: a Comparison of the Acsadi-Nemeskeri and Suchey-Brooks Methods. *Human Evolution*. 5, 227–238.
- Brothwell, D.R., 1981. *Digging up Bones*, Third. ed. Cornell University Press, Ithaca.
- Bruzek, J., 2002. A method for visual determination of sex, using the human hip bone. *American Journal of Physical Anthropology*. 117, 157–168.
- Bryant, R.M., Heighway, C.M., 1998. Historical and Topographical Background: The Topographical Development of the site. In: Wilkinson, D., McWhirr, A. (Eds.), *Cirencester Excavations IV: Cirencester Anglo-Saxon Church and Medieval Abbey*. Cotswold Archaeological Trust Ltd, Cirencester.
- Buck Louis, G.M., Gray, L.E., Marcus, M., Ojeda, S.R., Pescovitz, O.H., Witchel, S.F., Sippell, W., Abbott, D.H., Soto, A., Tyl, R.W., Bourguignon, J.-P., Skakkebaek, N.E., Swan, S.H., Golub, M.S., Wabitsch, M., Toppari, J., Euling, S.Y., 2008. Environmental Factors and Puberty Timing: Expert Panel Research Needs. *Pediatrics*. 121, S192–S207.
- Buckberry, J., Chamberlain, A., 2002. Age Estimation from the Auricular Surface of the Ilium: A Revised Method. *American Journal of Physical Anthropology*. 119, 231–239.
- Buckman, J., Newmarch, C.H., 1850. *Illustrations of the remains of Roman art in Cirencester, the site of Ancient Corinium*. G.Bell, Cirencester.
- Buikstra, J.E., Ubelaker, D.H., 1994. Standards for data collection from human skeletal remains. *Arkansas Archaeological Survey*, Arkansas.
- Burt, N.M., 2013. Stable isotope ratio analysis of breastfeeding and weaning practices of children from medieval Fishergate House York, UK. *American Journal of Physical*

- Anthropology. 152, 407–416.
- Calfee, R.P., Sutter, M., Steffen, J.A., Goldfarb, C.A., 2010. Skeletal and chronological ages in American adolescents: current findings in skeletal maturation. *Journal of Children's Orthopaedics*. 4, 467–470.
- Cameron, N., 2012a. The Human Growth Curve, Canalisation and Catch-up Growth. In: Cameron, N., Bogin, B. (Eds.), *Human Growth and Development*. Academic Press, Boston.
- Cameron, N., 2012b. Assessment of Maturation. In: Cameron, N., Bogin, B. (Eds.), *Human Growth & Development*. Academic Press, London, pp. 515–536.
- Cameron, N., Demerath, E.W., 2002. Critical periods in human growth and their relationship to diseases of aging. *Yearbook of Physical Anthropology*. 45, 159–184.
- Cardoso, H.F.V., Pereira, V., Rios, L., 2014. Chronology of Fusion of the Primary and Secondary Ossification Centers in the Human Sacrum and Age Estimation in Child and Adolescent Skeletons. *American Journal of Physical Anthropology*. 153, 214–225.
- Cardoso, H.F.V., Severino, R.S.S., 2010. The chronology of epiphyseal union in the hand and foot from dry bone observations. *International Journal of Osteoarchaeology*. 20, 737–746.
- Cardoso, H.F. V, 2007. Environmental Effects on Skeletal Versus Dental Development: Using a Documented Subadult Skeletal Sample to Test a Basic Assumption in Human Osteological Research. *American Journal of Physical Anthropology*. 132, 223–233.
- Cardoso, H.F. V, 2008a. Age Estimation of Adolescent and Young Adult Male and Female Skeletons II, Epiphyseal Union at the Upper Limb and Scapular Girdle in a Modern Portuguese Skeletal Sample. *American Journal of Physical Anthropology*. 137, 97–105.
- Cardoso, H.F. V, 2008b. Epiphyseal Union at the Innominate and Lower Limb in a Modern Portuguese Skeletal Sample, and Age Estimation in Adolescent and Young Adult Male and Female Skeletons. *American Journal of Physical Anthropology*. 135, 161–170.
- Cardoso, H.F. V, Campanacho, V., Gomes, J., Marinho, L., 2013a. Timing of fusion of the ischiopubic ramus from dry bone observations. *HOMO-Journal of Comparative Human Biology*. 1–9.
- Cardoso, H.F. V, Gomes, J., Campanacho, V., Marinho, L., 2013b. Age estimation of immature human skeletal remains using the post-natal development of the occipital bone. *International Journal of Legal Medicine*. 127, 997–1004.
- Carel, J., Lahlou, N., Roger, M., Chaussain, J.L., 2004. Precocious puberty and statural growth. *Human Reproduction Update*. 10, 135–147.

- Cavallo, F., Mohn, A., Chiarelli, F., Giannini, C., 2021. Evaluation of Bone Age in Children: A Mini-Review. *Frontiers in Pediatrics*. 9, 5–8.
- Cendekiawan, T., Wong, R.W.K., Rabie, A.B.M., 2010. Relationships Between Cranial Base Synchondroses and Craniofacial Development: A Review. *The Open Anatomy Journal*. 2, 67–75.
- Cheung, C., Schroeder, H., Hedges, R.E.M., 2012. Diet, social differentiation and cultural change in Roman Britain: New isotopic evidence from Gloucestershire. *Archaeological and Anthropological Sciences*. 4, 61–73.
- Chun, H., Shin, E., 2018. Secular Trends and Socioeconomic Differentials in Menarcheal Age for South Korean Women. *Iranian Journal of Public Health*. 47, 1254–1260.
- Clarke, B., 2008. Normal Bone Anatomy and Physiology. *American Society of Nephrology*. 3, 131–139.
- Clarke, B.L., Khosla, S., 2009. Androgens and bone. *Steroids*. 74, 296–305.
- Clegg, C.M., Mackean, D.G., 2000. *Biology: Principles & Applications*, Second. ed. John Murray Ltd, London.
- Coben, S.E., 1998. The sphenoid-occipital synchondrosis: the missing link between the profession's concept of craniofacial growth and orthodontic treatment. *American journal of orthodontics and dentofacial orthopedics: official publication of the American Association of Orthodontists, its constituent societies, and the American Board of Orthodontics*. 114, 709–712.
- Cole, T.J., 2003. The secular trend in human physical growth: a biological view. *Economics and Human Biology*. 1, 161–168.
- Conceição, E.L.N., Cardoso, H.F.V., 2011. Environmental effects on skeletal versus dental development II: Further testing of a basic assumption in human osteological research. *American Journal of Physical Anthropology*. 144, 463–470.
- Cooke, P.S., Nanjappa, M.K., Ko, C., Prins, G.S., Hess, R.A., 2017. Estrogens in male physiology. *Physiological Reviews*. 97, 995–1043.
- Cooper, C., Kuh, D., Egger, P., Wadsworth, M., Barker, D., 1996. Childhood growth and age at menarche. *British Journal of Obstetrics and Gynaecology*. 103, 814–817.
- Cope, Z., 1920. Fusion-Lines of Bones. *Journal of Anatomy*. 55, 36–37.
- Copeland, T., 2011. *Roman Gloucestershire*. The History Press, Stroud.
- Coqueugniot, H., Weaver, T.D., 2007. Brief Communication: Infracranial Maturation in the Skeletal Collection From Coimbra, Portugal: New Aging Standards for Epiphyseal Union.

- American Journal of Physical Anthropology. 134, 424–437.
- Coqueugniot, H., Weaver, T.D., Houët, F., 2010. Brief Communication: A Probabilistic Approach to Age Estimation From Infracranial Sequences. *American Journal of Physical Anthropology*. 142, 655–664.
- Corbett, M.E., Moore, W.J., 1976. Distribution of dental Caries in Ancient British Populations: IV. The 19th Century. *Caries Research*. 10, 401–414.
- Corron, L.K., Stock, M.K., Cole, S.J., Hulse, C.N., Garvin, H.M., Klales, A.R., Stull, K.E., 2021. Standardising ordinal subadult age indicators: Testing for observer agreement and consistency across modalities. *Forensic Science International*. 110687, 1–13.
- Coutinho, S., Buschang, P.H., Miranda, F., 1993. Relationships between mandibular canine calcification stages and skeletal maturity. *American Journal of Orthodontics and Dentofacial Orthopaedics*. 104, 262–268.
- Cox, D.R., 1966. Some Procedures Connected with the Logistic Qualitative Response Curve. In: David, F.N. (Ed.), *Research Papers in Statistics: Festschrift for J. Neyman*. Wiley, London.
- Creighton, C., 1981. *A History of Epidemics in Britain from AD 664 to the Extinction of Plague*. University Press, Cambridge.
- Crone, A., Hindmarch, E., 2016. *Living and dying at Auldhame, East Lothian: The excavation of an Anglian monastic settlement and medieval parish church*. The Society of Antiquaries of Scotland, Edinburgh.
- Crowder, C., Austin, D., 2005. Age Ranges of Epiphyseal Fusion in the Distal Tibia and Fibula of Contemporary Males and Females. *ASTM International*. 50, 1001–1007.
- Cunha, E., Baccino, E., Martrille, L., Ramsthaler, F., Prieto, J., Schuliar, Y., Lynnerup, N., Cattaneo, C., 2009. The problem of aging human remains and living individuals: A review. *Forensic Science International*. 193, 1–13.
- Cunningham, C., Scheuer, L., Black, S., Liversidge, H., 2016. *Developmental Juvenile Osteology*. Academic Press, London.
- Cutler, G.B., 1997. The Role of Estrogen in Bone Growth and Maturation During Childhood and Adolescence. *The Journal of Steroid Biochemistry and Molecular Biology*. 61, 141–144.
- Daniell, C., 2007. Early Medieval York. In: Nuttgens, P. (Ed.), *The History of York: From Earliest Times to the Year 2000*. Blackthorn Press, Pickering.
- Davies, C., Hackman, L., Black, S., 2013. The persistence of epiphyseal scars in the adult tibia.

- International Journal of Legal Medicine. 128, 335–343.
- Davies, C., Hackman, L., Black, S., 2015. The epiphyseal scar: changing perceptions in relation to skeletal age estimation. *Annals of Human Biology. Journal of the Society for the Study of Human Biology.* 42, 346–355.
- Dawson-Hobbs, H., 2016. Precious things: examining the status and care of children in late medieval England through the analysis of cultural and biological markers. In: Powell, L., Southwell-Wright, W., Gowland, R. (Eds.), *Care in the Past: Archaeological and Interdisciplinary.* Oxbow Books, Oxford, pp. 53–69.
- Dawson, H., Brown, K.R., 2013. Exploring the relationship between dental wear and status in late medieval subadults from England. *American Journal of Physical Anthropology.* 150, 433–441.
- de Muinck Keizer-Schrama, S.M.P.F., Mul, D., 2001. Trends in pubertal development in Europe. *Human Reproduction Update.* 7, 287–291.
- Delgado-Martos, M.J., Touza Fernández, A., Canillas, F., Quintana-Villamandos, B., Santos del Riego, S., Delgado-martos, E., Martos-Rodriguez, A., Delgado-Baeza, E., 2013. Does the epiphyseal cartilage of the long bones have one or two ossification fronts? *Medical Hypotheses.* 81, 695–700.
- Demerath, E.W., Jones, L.L., Hawley, N.L., Norris, S.A., Pettifor, J.M., Duren, D., Chumlea, W.C., Towne, B., Cameron, N.N., Chumlea, C., Towne, B., Cameron, N.N., 2009. Rapid Infant Weight Gain and Advanced Skeletal Maturation in Childhood. *The Journal of Paediatrics.* 155, 355–361.
- Demerath, E.W., Li, J., Sun, S.S., Chumlea, W.C., Remsberg, K.E., Czerwinski, S.A., Towne, B., Siervogel, R.M., 2004. Fifty-year trends in serial body mass index during adolescence in girls: the Fels Longitudinal Study. *The American Journal of Clinical Nutrition.* 80, 441–446.
- Dequéant, M.L., Pourquié, O., 2008. Segmental patterning of the vertebrate embryonic axis. *Nature Reviews Genetics.* 9, 370–382.
- DeRuiter, C., 2018. Somites: Formation and Role in Developing the Body Plan. *The Embryo Project Encyclopedia.*
- DeRuiter, C., Doty, M., 2011. Gastrulation in *Gallus gallus* (Domestic Chicken). *The Embryo Project Encyclopedia.*
- Dewitte, S.N., 2014. Health in Post-Black Death London ( 1350 – 1538 ): Age Patterns of Periosteal New Bone Formation in a Post-Epidemic Population. 267, 260–267.

- Dewitte, S.N., 2015. Setting the Stage for Medieval Plague : Pre-Black Death Trends in Survival and Mortality. 451, 441–451.
- Dewitte, S.N., 2018. Stress, sex, and plague: Patterns of developmental stress and survival in pre- and post-Black Death London. *American Journal of Human Biology*. 30, 1–15.
- Dewitte, S.N., Lewis, M., 2020. Medieval menarche: Changes in pubertal timing before and after the Black Death. *American Journal of Human Biology*. e23439, 1–15.
- Dewitte, S.N., Slavin, P., 2013. Between Famine and Death: England on the Eve of the Black Death — Evidence from Paleoepidemiology and Manorial Accounts. *Journal of Interdisciplinary History*. XLIV, 37–60.
- Dewitte, S.N., Stojanowski, C.M., 2015. The Osteological Paradox 20 Years Later : Past Perspectives , Future Directions. 397–450.
- Dobson, B., 2007. Later Medieval York. In: Nuttgens, P. (Ed.), *The History of York: From Earliest Times to the Year 2000*. Blackthorn Press, Pickering.
- Doe, D.M., Molina Moreno, M., Rascón Pérez, J., Candelas González, N., Cambra-Moo, O., Campo Martín, M., González Martín, A., 2019. Puberty in the Bronze Age: first application of a puberty estimation method to a prehistoric population. *International Journal of Osteoarchaeology*. 29, 1091–1099.
- Doe, D.M., Rascón Pérez, J., Cambra-Moo, O., Campo Martín, M., González Martín, A., Pérez, J.R., Cambra-Moo, O., Martín, M.C., Martín, A.G., 2017. Assessing pubertal stage in adolescent remains: an investigation of the San Nicolás Maqbara burial site (Murcia, Spain). *Archaeological and Anthropological Sciences*. 11, 541–554.
- Dorn, L.D., Biro, F.M., 2011. Puberty and Its Measurement: A Decade in Review. *Journal of Research on Adolescence*. 21, 180–195.
- Dossus, L., Kvaskoff, M., Bijon, A., Fervers, B., Boutron-Ruault, M.-C., Mesrine, S., Clavel-chapelon, F., 2012. Determinants of age at menarche and time to menstrual cycle regularity in the French E3N cohort. *Annals of Epidemiology*. 22, 723–730.
- Down, A., Welch, M., 1990. *Chichester Excavations: Apple Down & The Mardens*. Chichester District Council, Chichester.
- Dunsworth, H.M., 2020. Expanding the evolutionary explanations for sex differences in the human skeleton. *Evolutionary Anthropology*. 29, 108–116.
- Duren, D.L., Nahhas, R.W., Sherwood, R.J., 2015. Do Secular Trends in Skeletal Maturity Occur Equally in Both Sexes? *Clinical Orthopaedics and Related Research*. 473, 2559–2567.

- Dwyer, A., Quinton, R., 2019. Anatomy and Physiology of the Hypothalamic-Pituitary-Gonadal (HPG) Axis. In: Llahana, S., Follin, C., Yedinak, C., Grossman, A. (Eds.), *Advanced Practice in Endocrinology Nursing*. Springer, Switzerland, pp. 841–851.
- Dyer, C., 1994. *Everyday Life in Medieval England*. Cambridge University Press, Hambledon.
- Dyer, C., 2002. *Making a living in the Middle Ages: The People of Britain 850-1520*. Yale University Press, New Haven.
- Eastell, R., 2005. Role of oestrogen in the regulation of bone turnover at the menarche. *Journal of Endocrinology*. 185, 223–234.
- Ebeye, O.A., Eboh, D.E., Onyia, N.S., 2016. Radiological assessment of age from epiphyseal fusion at the knee joint. *Anatomy*. 10.
- Ebeye, O.A., Okoro, O.G., Ikubor, J.E., 2021. Radiological assessment of age from epiphyseal fusion at the wrist and ankle in Southern Nigeria. *Forensic Science International: Reports*. 3, 100164.
- Edens Hurst, A.C., 2019. Mucopolysaccharides [WWW Document]. Medline Plus: Trusted Health Information for You. URL <https://medlineplus.gov/ency/article/002263.htm>
- Eggington, J., 2020. Diet, skeletal stress and socioeconomic status in post-medieval Britain (1700-1850) [WWW Document]. The Post Hole. URL <https://www.theposthole.org/read/article/463>
- Ellison, P.T., Reiches, M.W., 2012. Puberty. In: Cameron, N., Bogin, B. (Eds.), *Human Growth & Development*. Academic Press, London, pp. 81–108.
- Emons, J., Chagin, A.S., Malmlöf, T., Lekman, M., Tivesten, Å., Ohlsson, C., Wit, J.M., Karperien, M., Sävendahl, L., 2010. Expression of vascular endothelial growth factor in the growth plate is stimulated by estradiol and increases during pubertal development. *Journal of Endocrinology*. 205, 61–68.
- Eng, J.T., Zhang, Q., Zhu, H., 2010. Skeletal effects of castration on two eunuchs of Ming China. *Anthropological Science*. 118, 107–116.
- English Heritage, 2022. An introduction to Stuart England (1603–1714) [WWW Document]. English Heritage. URL <https://www.english-heritage.org.uk/learn/story-of-england/stuarts/>
- englishmonarchs.co.uk, 2022. Egbert 827-839 [WWW Document]. English Monarchs. URL <https://www.englishmonarchs.co.uk/saxon.htm> (accessed 12.1.22).
- Ersoy, B., Balkan, C., Gunay, T., Onag, A., Egemen, A., 2004. Effects of different socioeconomic conditions on menarche in Turkish female students. *Early Human*

- Development. 76, 115–125.
- EuroStemCell, 2016. Mesenchymal stem cells: the “other” bone marrow stem cells [WWW Document]. EuroStemCell. URL <https://www.eurostemcell.org/mesenchymal-stem-cells-other-bone-marrow-stem-cells>
- Faisant, M., Rerolle, C., Faber, C., Dedouit, F., Telmon, N., Saint-martin, P., 2015. Is the persistence of an epiphyseal scar of the knee a reliable marker of biological age? *International Journal of Legal Medicine*. 129, 603–608.
- Fernández-Pérez, M.J., Alarcón, J.A., McNamara, J.A., Velasco-Torres, M., Benavides, E., Galindo-Moreno, P., Catena, A., 2016. Spheno-occipital synchondrosis fusion correlates with cervical vertebrae maturation. *PLoS ONE*. 11, 1–11.
- Fincham, A.G., Bessem, C.C., Lau, E.C., Pavlova, Z., Shuler, C., Slavkin, H.C., Snead, M.L., 1991. Human developing enamel proteins exhibit a sex-linked dimorphism. *Calcified Tissue International*. 48, 288–290.
- Fisher, R.A., 1934. *Statistical methods for research workers*, Fifth Edit. ed. Oliver & Boyd Ltd, Edinburgh.
- Fojas, C., Collins, S., Shirley, N., 2015. Radiographic Versus Dry Bone Assessment of Sacral Epiphyses. *Federation of American Societies for Experimental Biology*. 29.
- Forbes, A.P., Ronaghy, H.A., Majd, M., 1971. Skeletal Maturation of Children in Shiraz, Iran. *American Journal of Physical Anthropology*. 35, 449–454.
- Ford, P., Collins, D., Bailey, R., MacNamara, Á., Pearce, G., Toms, M., 2012. Participant development in sport and physical activity: The impact of biological maturation. *European Journal of Sport Science*. 12, 515–526.
- Franzen, L., Smith, C., 2009. Differences in stature, BMI, and dietary practices between US born and newly immigrated Hmong children. *Social Science & Medicine*. 69, 442–450.
- Freeman, G.H., Halton, J.H., 1951. Note on an exact treatment of contingency, goodness of fit and other problems of significance. *Biometrika*. 38, 141–149.
- Freitas, D., Maia, J., Beunen, G., Lefevre, J., Claessens, A., Marques, A., Rodrigues, A., Silva, C., Crespo, M., Thomis, M., Sousa, A., Malina, R., 2004. Skeletal maturity and socio-economic status in Portuguese children and youths: The Madeira Growth Study. *Annals of Human Biology*. 31, 408–420.
- Fudvoye, J., Parent, A.S., 2017. Secular trends in growth. *Annales d’Endocrinologie*. 78, 88–91.
- Fullenlove, T.M., 1954. Congenital absence of the odontoid process. *Radiology*. 63, 72–73.

- Gafni, R.I., Baron, J., 2000. Catch-up growth: possible mechanisms. *Paediatric Nephrology*. 14, 616–619.
- Galton, F., 1894. *Natural Inheritance*, Fifth Edit. ed. Macmillan and Company, New York.
- GARD, 2017. Achondroplasia [WWW Document]. Genetic and Rare Diseases Centre. URL <https://rarediseases.info.nih.gov/diseases/8173/achondroplasia#:~:text=Achondroplasia is a disorder of,small fingers%2C and normal intelligence>.
- GARD, 2018. Hypochondroplasia [WWW Document]. Genetic and Rare Diseases Centre. URL <https://rarediseases.info.nih.gov/diseases/6724/hypochondroplasia>
- GARD, 2021. Acrocapitofemoral dysplasia [WWW Document]. Genetic and Rare Diseases Centre. URL <https://rarediseases.info.nih.gov/diseases/10605/acrocapitofemoral-dysplasia>
- Garland, N., 2012. *Boundaries and Change: The Examination of the Late Iron Age-Roman Transition*. *Theoretical Roman Archaeology*. TRAC 2011, 91–104.
- Garn, S.M., Rohmann, C.G., 1960. Variability in the Order of Ossification of the Bony Centers of the Hand and Wrist. *American Journal of Physical Anthropology*. 18, 219–230.
- Garn, S.M., Rohmann, C.G., Wallace, D.K., 1961. Association Between Alternate Sequences of Hand- Wrist Ossification. *American Journal of Physical Anthropology*. 19, 361–364.
- Garn, S.M., Russell, A.L., 1971. The effect of nutritional extremes on dental development. *The American Journal of Clinical Nutrition*. 24, 285–286.
- Garvin, H.M., Passalacqua, N. V., Uhl, N.M., Gipson, D.R., Overbury, R.S., Cabo, L.L., 2012. *Developments in Forensic Anthropology: Age-at-Death Estimation*. In: Dirkmaat, D. (Ed.), *A Companion to Forensic Anthropology*. John Wiley & Sons Ltd, ProQuest Ebook.
- Gasser, T., Sheehy, A., Molinari, L., Largo, R.H., 2001. Growth processes leading to a large or small adult size. *Annals of Human Biology*. 28, 319–327.
- Gaur, A., 2017. York. *Encyclopaedia Britannica*.
- Genetic Home Reference, 2012. SHOX gene: Short Stature Homeobox [WWW Document]. Medline Plus: Trusted Health Information for You. URL <https://medlineplus.gov/genetics/gene/shox/>
- Gies, F., Gies, J., 1990. *Life in a Medieval Village*. Harper & Row, New York.
- Gilbert, S.F., 2000. *Developmental Biology*, Sixth. ed. Sinauer Associates.
- Gillingham, J., Griffiths, R., 2000. *Medieval Britain: A Very Short Introduction*. Oxford University Press, Oxford.
- Golden, M., 1994. Is complete catch-up possible for stunted malnourished children? *European*

- Journal of Clinical Nutrition. 48, 58–71.
- Goldsmith, M.I., Fisher, S., Waterman, R., Johnson, S.L., 2003. Saltatory control of isometric growth in the zebrafish caudal fin is disrupted in long fin and rapunzel mutants. *Developmental Biology*. 259, 303–317.
- Golub, M.S., Collman, G.W., Foster, P.M.D., Kimmel, C.A., Rajpert De Meyts, E., Reiter, E.O., Sharpe, R.M., Skakkebaek, N.E., Toppari, J., 2008. Public Health Implications of Altered Puberty Timing. *Paediatrics*. 121, 218–230.
- Goodenough, D.A., Paul, D.L., 2009. Gap Junctions. *Cold Spring Harbor Perspectives in Biology*. 1, 339–347.
- Gosman, J.H., 2012. Growth and Development: Morphology, Mechanisms, and Abnormalities. In: Crowder, C., Stout, S. (Eds.), *Bone Histology: An Anthropological Perspective*. CRC Press, Florida.
- Grave, K.C., Brown, T., 1976. Skeletal ossification and the adolescent growth spurt. *American Journal of Orthodontics*. 69, 611–619.
- Greulich, W.W., Pyle, S.I., 1950. *Radiographic Atlas of Skeletal Development of the Hand and Wrist*. Stanford University Press, California.
- Hägg, U., Taranger, J., 1982. Maturation indicators and the pubertal growth spurt. *American Journal of Orthodontics*. 82, 299–309.
- Hägg, U., Taranger, J., 1991. Height and height velocity in early, average and late maturers followed to the age of 25: a prospective longitudinal study of Swedish urban children from birth to adulthood. *Annals of Human Biology*. 18, 47–56.
- Halim, A., 2008. *Human Anatomy: Upper Limb and Thorax*. International Publishing House, New Dehli.
- Hall, B.K., 2015. *Bones and Cartilage: Developmental and Evolutionary Skeletal Biology*, Second. ed. Academic Press, London.
- Hamilton, W.J., Manton, S.M., 2019. Embryology of vertebrate skeletons. *Britannica*.
- Hanawalt, B.A., 1993. *Growing up in Medieval London: The experience of childhood in history*. Oxford University Press, New York.
- Harman, M., 1998. The human remains. In: Boyle, A., Jennings, D., Miles, D., Palmer, S. (Eds.), *The Anglo-Saxon Cemetery at Butler's Field, Lechlade, Gloucestershire. Volume I: Prehistoric and Roman Activity and Anglo-Saxon Grave Catalogue*. Oxbow Books, Oxford.
- Hassel, B., Farman, A.G., 1995. Skeletal maturation evaluation using cervical vertebrae.

- American Journal of Orthodontics and Dentofacial Orthopedics. 107, 58–66.
- Hauspie, R., Roelants, M., 2012. Adolescent Growth. In: Cameron, N., Bogin, B. (Eds.), Human Growth & Development. Academic Press, London, pp. 57–80.
- Hauspie, R., Susanne, C., Alexander, F., 1977. Maturational delay and temporal retardation in asthmatic boys. The Journal of allergy and clinical immunology. 59, 200–206.
- Hauspie, R.C., Vercauteren, M., Susanne, C., 1997. Secular changes in growth and maturation: An update. Acta Paediatrica, International Journal of Paediatrics, Supplement. 86, 20–27.
- Hawley, N.L., Rousham, E.K., Norris, S.A., Cameron, L., Pettifor, J.M., Cameron, N., 2009. Secular trends in skeletal maturity in South Africa: 1962-2001. Annals of Human Biology. 36, 584–594.
- Haydock, H., Clarke, L., Craig-Atkins, E., Howcroft, R., Buckberry, J., 2013. Weaning at Anglo-Saxon Raunds: Implications for changing breastfeeding in Britain over two millennia. American Journal of Physical Anthropology. 151, 604–612.
- Heighway, C.M., Harman, M., Viner, L., Wilkinson, D.J., 1998. The Burials. In: Wilkinson, D., McWhirr, A. (Eds.), Cirencester Excavations IV: Cirencester Anglo-Saxon Church and Medieval Abbey. Cotswolds Archaeological Trust Ltd, Cirencester.
- Hellemans, J., Coucke, P.J., Giedion, A., De Paepe, A., Kramer, P., Beemer, F., Mortier, G.R., 2003. Homozygous mutations in IHH cause acrocapitofemoral dysplasia, an autosomal recessive disorder with cone-shaped epiphyses in hands and hips. American Journal of Human Genetics. 72, 1040–1046.
- Henderson, C.Y., Padez, C., 2017. Testing times: identifying puberty in an identified skeletal sample. Annals of Human Biology. 44, 332–337.
- Hermanussen, M., 2016. Growth in Childhood and Puberty. In: Kumanov, P., Agarwal, A. (Eds.), Puberty: Physiology and Abnormalities. Springer International Publishing, Switzerland, pp. 65–76.
- Herting, M.M., Sowell, E.R., 2017. Puberty and structural brain development in humans. Frontiers in Neuroendocrinology. 44, 122–137.
- Hewitt, D., 1957. Some Familial Correlations in Height, Weight and Skeletal Maturity. Annals of Human Genetics. 22, 26–35.
- Hewitt, D., Acheson, R.M., 1961a. Some Aspects of Skeletal Development through Adolescence. II. The inter-relationship between skeletal maturation and growth at puberty. American Journal of Physical Anthropology. 19, 333–344.
- Hewitt, D., Acheson, R.M., 1961b. Some Aspects of Skeletal Development through

- Adolescence. I. Variations in the rate and pattern of skeletal maturation at puberty. *American Journal of Physical Anthropology*. 19, 321–331.
- Hicks, M., Hicks, A., 2001. St Gregory's Priory, Northgate, Canterbury: Excavations 1988-1991. Geerings, Ashford.
- Hirai, T., Chagin, A.S., Kobayashi, T., Mackem, S., Kronenberg, H.M., 2011. Parathyroid hormone/parathyroid hormone-related protein receptor signaling is required for maintenance of the growth plate in postnatal life. *Proceedings of the National Academy of Sciences of the United States of America*. 108, 191–196.
- History Extra, 2016. Stuart Britain: what was life like for ordinary people? [WWW Document]. History Extra. URL <https://www.historyextra.com/period/stuart/stuart-britain-what-was-life-like-for-ordinary-people/> (accessed 3.16.22).
- Hochberg, Z., 2002. Clinical physiology and pathology of the growth plate. *Best Practice and Research: Clinical Endocrinology and Metabolism*. 16, 399–419.
- Hochberg, Z., Belsky, J., 2013. Evo-devo of human adolescence : beyond disease models of early puberty. *BMC Medicine*. 11, 1–11.
- Hoddinott, J., Behrman, J.R., Maluccio, J.A., Melgar, P., Quisumbing, A.R., Ramirez-Zea, M., Stein, A.D., Yount, K.M., Martorell, R., 2013. Adult consequences of growth failure in early childhood. *American Society for Nutrition*. 98, 1170–1178.
- Holbrook, N., 2012. Corinium Dobunorum ( Cirencester ). In: Bagnall, R.S., Brodersen, K., Champion, C.B., Erskine, A., Huebner, S.R. (Eds.), *The Encyclopedia of Ancient History*. John Wiley & Sons Ltd, pp. 1783–1784.
- Holbrook, N., 2017a. Excavation Results. In: Holbrook, N., Wright, J., McSloy, E.R., Geber, J. (Eds.), *Cirencester Excavations VII: The Western Cemetery of Roman Cirencester. Excavations at the Former Bridges Garage, Tetbury Road, Cirencester, 2011-2015*. Cotswold Archaeology, Cirencester.
- Holbrook, N., 2017b. Discussion. In: Holbrook, N., Wright, J., McSloy, E.R., Geber, J. (Eds.), *Cirencester Excavations VII: The Western Cemetery of Roman Cirencester. Excavations at the Former Bridges Garage, Tetbury Road, Cirencester, 2011-2015*. Cotswold Archaeology, Cirencester.
- Holmes, M., 2016. “We’ll have what they’re having”, cultural identity through diet in the english saxon period. *Environmental Archaeology*. 21, 59–78.
- Hoogendam, J., Farih-Sips, H., Wynaendts, L.C., Löwik, C.W.G.M., Wit, J.M., Karperien, M., 2007. Novel mutations in the parathyroid hormone (PTH)/PTH-related peptide receptor

- type 1 causing blomstrand osteochondrodysplasia types I and II. *Journal of Clinical Endocrinology and Metabolism*. 92, 1088–1095.
- Houston, W.J.B., 1980. Relationships between skeletal maturity estimated from hand-wrist radiographs and the timing of the adolescent growth spurt. *European Journal of Orthodontics*. 2, 81–93.
- Hsieh, C.-W., Liu, T.-C., Jong, T.-L., Tiu, C.-M., 2013. Long-term secular trend of skeletal maturation of Taiwanese children between agricultural (1960s) and contemporary (after 2000s) generations using the Tanner-Whitehouse 3 (TW3) method. *Journal of Pediatric Endocrinology & Metabolism*. 26, 231–237.
- Hudson-Edwards, K.A., Macklin, M.G., Finlayson, R., Passmore, D.G., 1999. Mediaeval Lead Pollution in the River Ouse at York, England. *Journal of Archaeological Science*. 26, 809–819.
- Humanpath.com, 2007. Neural tube closure [WWW Document]. Human pathology. URL <https://www.humphath.com/spip.php?article12929>
- Hummel, E., De Groot, J.C., 2013. Three cases of bipartition of the atlas. *Spine Journal*. 13, e1–e5.
- Humphrey, L.T., 1998. Growth Patterns in the Modern Human Skeleton. *American Journal of Physical Anthropology*. 105, 57–72.
- Hunter, J., Cox, M., 2005. *Forensic Archaeology: Advances in theory and practice*. Routledge, Abingdon.
- Ibáñez, L., Ferrer, A., Marcos, M.V., Hierro, F.R., de Zegher, F., 2000. Early Puberty: Rapid Progression and Reduced Final Height in Girls With Low Birth Weight. *Paediatrics*. 106, 1–3.
- Introna, F., Campobasso, C.P., 2006. Biological vs legal age of living individuals. In: Schmitt, A., Cunha, E., Pinheiro, J. (Eds.), *Forensic Anthropology and Medicine: Complementary Sciences From Recovery to Cause of Death*. Humana Press, Totowa, pp. 57–82.
- Işcan, M.Y., 1981. Concepts in teaching forensic anthropology. *Medical Anthropology Newsletter*. 13, 10–12.
- Ito, Y., Fitzsimmons, J.S., Sanyal, A., Mello, M.A., Mukherjee, N., O’Driscoll, S.W., 2001. Localization of chondrocyte precursors in periosteum. *Osteoarthritis and Cartilage*. 9, 215–223.
- Janson, C.H., Van Schaik, C.P., 1993. Ecological risk aversion in juvenile primates: slow and steady wins the race. In: Pereira, M.E., Fairbanks, L.A. (Eds.), *Juvenile Primates*. Oxford

- University Press, New York, pp. 57–74.
- Jay, M., 2008. Iron Age Diet at Glastonbury Lake Village: The isotopic evidence for negligible aquatic resource consumption. *Oxford Journal of Archaeology*. 27, 201–216.
- Jay, M., Fuller, B.T., Richards, M.P., Knüsel, C.J., King, S.S., 2008. Iron age breastfeeding practices in Britain: Isotopic evidence from wetwang slack, east yorkshire. *American Journal of Physical Anthropology*. 136, 327–337.
- Jay, M., Richards, M.P., 2006. Diet in the Iron Age cemetery population at Wetwang Slack, East Yorkshire, UK: Carbon and nitrogen stable isotope evidence. *Journal of Archaeological Science*. 33, 653–662.
- Jazbinšek, S., Kotnik, P., 2020. Influence of physical activity on linear growth in children and adolescents. *Annales Kinesiologiae*. 29–42.
- Jenkins, S., 2012. *A Short History of England*. Profile Books Ltd, London.
- Jennings, R., Premanandan, C., 2018. *Veterinary Histology*. The Ohio State University, Ohio.
- Johnston, F.E., 1961. Sequence of epiphyseal union in a pre-historic Kentucky population from Indian Knoll. *Human Biology*. 33, 66–81.
- Jones, A.D., Rukobo, S., Chasekwa, B., Mutasa, K., Ntozini, R., Mbuya, M.N.N., Stoltzfus, R.J., Humphrey, J.H., Prendergast, A.J., 2015. Acute Illness Is Associated with Suppression of the Growth Hormone Axis in Zimbabwean Infants. *The American Journal of Tropical Medicine and Hygiene*. 92, 463–470.
- Jones, T., Ereira, A., 2004. *Terry Jones' Medieval Lives*. BBC Books, London.
- Jousilahti, P., Tuomilehto, J., Vartiainen, E., Eriksson, J., Puska, P., 2000. Relation of Adult Height to Cause-specific and Total Mortality: A Prospective Follow-up Study of 31,199 Middle-aged Men and Women in Finland. *American Journal of Epidemiology*. 151, 1112–1120.
- Junewick, J.J., Chin, M.S., Meesa, I.R., Ghorri, S., Boynton, S.J., Luttenton, C.R., 2011. Ossification patterns of the atlas vertebra. *American Journal of Roentgenology*. 197, 1229–1234.
- Juul, A., 2001. The effects of oestrogens on linear bone growth. *Human Reproduction Update*. 7, 303–313.
- Kang, S., Kim, Y.M., Lee, J.A., Kim, D.H., Lim, J.S., 2019. Early Menarche is a Risk Factor for Short Stature in Young Korean Females: An Epidemiologic Study. *The Journal of Clinical Research in Paediatric Endocrinology and Diabetes Society*. 11, 234–239.
- Kannian, V.G., Ryan, F.J., 2019. *Physiology of Growth Hormone in Fetus and Child*, 2nd ed, 319

- Encyclopedia of Endocrine Diseases, 2nd Edition. Elsevier Inc.
- Kaplowitz, P.B., 2008. Link Between Body Fat and the Timing of Puberty. *Paediatrics*. 121, 208–217.
- Kaprio, J., Rimpelä, A., Winter, T., Viken, R.J., Rimpelä, M., Rose, R.J., 1995. Common Genetic Influences on BMI and Age at Menarche. *Human Biology*. 67, 739–753.
- Karimian, E., Chagin, A.S., Sävendahl, L., 2012. Genetic regulation of the growth plate. *Frontiers in Endocrinology*. 3, 1–10.
- Karwacki, G.M., Schneider, J.F., 2012. Normal ossification patterns of atlas and axis: A CT study. *American Journal of Neuroradiology*. 33, 1882–1887.
- Kassab, C., Kerrigan, B.P., Caruso, H., Al Enazy, S., Heimberger, A.B., 2019. Immunomodulatory Methods. In: Lonser, R.R., Sarntinoranont, M., Bankiewicz, K. (Eds.), *Nervous System Drug Delivery: Principles and Practice*. Elsevier Inc., pp. 297–334.
- Kaushal, R.K., 2019. *Self Assessment and Review of Anatomy, Fourth ed.* ed. Jaypee Brothers Medical Publishers, UK.
- Kemkes-Grottenthaler, A., 2005. The Short Die Young: The Interrelationship Between Stature and Longevity - Evidence From Skeletal Remains. *American Journal of Physical Anthropology*. 128, 340–347.
- Kern, K.F., 2006. T.Wingate Todd: Pioneer of Modern American Physical Anthropology. *Kirtlandia*. 55, 1–42.
- Kessler, M.J., Wang, Q., Cerroni, A.M., Grynepas, M.D., Gonzalez Velez, O.D., Rawlins, R.G., Ethun, K.F., Wimsatt, J.H., Kensler, T.B., Pritzker, K.P.H., 2016. Long-Term Effects of Castration on the Skeleton of Male Rhesus Monkeys (*Macaca mulatta*). *American Journal of Primatology*. 78, 152–166.
- Kimura, K., 1981. Skeletal Maturity in Twins. *Journal of the Anthropological Society of Nippon*. 89, 457–477.
- Kindblom, J.M., Nilsson, O., Hurme, T., Ohlsson, C., Sävendahl, L., 2002. Expression and localization of Indian hedgehog (Ihh) and parathyroid hormone related protein (PTHrP) in the human growth plate during pubertal development. *Journal of Endocrinology*. 174.
- Klein, K.O., Larmore, K.A., De Lancey, E., Brown, J.M., Considine, R. V., Hassink, S.G., 1998. Effect of Obesity on Estradiol Level, and Its Relationship to Leptin, Bone Maturation, and Bone Mineral Density in Children. *Journal of Clinical Endocrinology and Metabolism*. 83, 3469–3475.

- Klepinger, L.L., 2001. Stature, Maturation Variation and Secular Trends in Forensic Anthropology \*. *Journal of Forensic Sciences*. 46, 788–790.
- Kronenberg, H.M., 2003. Developmental regulation of the growth plate. *Nature*. 423, 332–336.
- Kruskal, W.H., Wallis, W.A., 1952. Use of Ranks in One-Criterion Variance Analysis. *Journal of the American Statistical Association*. 47, 583–621.
- Kumar, R., Gupta, P., Grover, R., Goyal, J., Meena, N., Kumar, D., 2020. Age Determination by Radiological Epiphyseal Fusion of Elbow and Wrist in Adolescent Population in Malwa Region of Madhya Pradesh. *International Journal of Medical Science and Education*. 7, 43–50.
- L'Abbe, E.N., 2005. A case of commingled remains from rural South Africa. *Forensic Science International*. 151, 201–206.
- Lacoste Jeanson, A., Santos, F., Bruzek, J., Urzel, V., 2016. Detecting menarcheal status through dental mineralisation stages? *American Journal of Physical Anthropology*. 161, 367–373.
- Lai, E.H.-H., Chang, J.Z.-C., Yao, C.-C.J., Tsai, S., Liu, J.-P., Chen, Y.-J., Lin, C.-P., 2008. Relationship between age at menarche and skeletal maturation stages in Taiwanese female orthodontic patients. *Journal of the Formosan Medical Association*. 107, 527–532.
- Lampl, M., 2009. Human growth from the cell to the organism: Saltations and integrative physiology. *Annals of Human Biology*. 36, 478–495.
- Lampl, M., Schoen, M., 2017. How long bones grow children: Mechanistic paths to variation in human height growth. *American Journal of Human Biology*. 29.
- Lampl, M., Veldhuis, J.D., Johnson, M.L., 1992. Saltation and stasis: a model of human growth. *Science (New York, NY)*. 258, 801–803.
- Langley-Shirley, N., Jantz, R.L., 2010. A bayesian approach to age estimation in modern Americans from the clavicle. *Journal of Forensic Sciences*. 55, 571–583.
- Langley, N.R., 2016. The lateral clavicular epiphysis: fusion timing and age estimation. *International Journal of Legal Medicine*. 130, 511–517.
- Largo, R.H., Gasser, T., Prader, A., Stuetzle, W., Huber, P.J., 1978. Analysis of the adolescent growth spurt using smoothing spline functions. *Annals of Human Biology*. 5, 421–434.
- Lazarus, J.E., Hegde, A., Andrade, A.C., Nilsson, O., Baron, J., 2007. Fibroblast growth factor expression in the postnatal growth plate. *Bone*. 40, 577–586.
- Legge, S.S., 2005. Estimating puberty in a prehistoric skeletal collection. *Annals of Human Biology*. 32, 383–389.

- Lejarraga, H., 2012. Growth in Infancy and Childhood: A Paediatric Approach. In: Cameron, N., Bogin, B. (Eds.), *Human Growth and Development*. Elsevier Inc., London.
- Lenover, M.B., Šešelj, M., 2019. Variation in the fusion sequence of primary and secondary ossification centers in the human skeleton. *American Journal of Physical Anthropology*. 170, 373–392.
- LePace, D., 2016. Medical Embryology [WWW Document]. Drexel University College of Medicine. URL <https://webcampus.drexelmed.edu/neurobio/embryology/page9/page13/>
- Lewin, P., 1929. Epiphyses: Their Growth, Development, Injuries and Diseases. *Journal of Diseases of Children*. 37, 141–178.
- Lewis, M., 2002. Impact of Industrialisation: Comparative Study of Child Health in Four Sites From Medieval and Postmedieval England (A.D. 850-1859). *American Journal of Physical Anthropology*. 119, 211–223.
- Lewis, M., 2011. The osteology of infancy and childhood: misconceptions and potential. In: Lally, M., Moore, A. (Eds.), *(Re)Thinking the Little Ancestor: New Perspectives on the Archaeology of Infancy and Childhood*. BAR International Series 2271, Oxford, pp. 47–62.
- Lewis, M., Shapland, F., Watts, R., 2016. On the threshold of adulthood: A new approach for the use of maturation indicators to assess puberty in adolescents from medieval England. *American Journal of Human Biology*. 28, 48–56.
- Lewis, M.E., 1999. *The Impact Of Urbanisation And Industrialisation In Medieval And Post-Medieval Britain - An assessment of the morbidity and mortality of non-adult from the cemeteries of two urban and two rural sites in England (AD 850 - 1859)*. University of Bradford.
- Lewis, M.E., 2013. Children of the Golden Minster: St. Oswald's Priory and the Impact of Industrialisation on Child Health. *Journal of Anthropology*. 2013, 1–11.
- Little, N., Rogers, B., Flannery, M., 2011. Bone formation, remodelling and healing. *Surgery*. 29, 141–145.
- Livitt, P., 1990. The Origin of Villages Study and Gazetteer. In: *Chichester Excavations: Apple Down and the Mardens*. Chichester District Council, Chichester.
- Locker, A., 2007. In piscibus diversis ; the Bone Evidence for Fish Consumption in Roman Britain . *Britannia*. 38, 141–180.
- Loesch, D.Z., Huggins, R., Rogucka, E., Hoang, N.H., Hopper, J.L., 1995. Genetic correlates of menarcheal age: a multivariate twin study. *Annals of Human Biology*. 22, 476–490.

- Long, F., 2011. Prenatal Bone Development. In: Glorieux, F.H., Pettifor, J.M., Jüppner, H. (Eds.), *Paediatric Bone: Biology and Diseases*. Academic Press, London.
- Lotha, G., 2017. Sheffield. *Encyclopaedia Britannica*.
- Lotha, G., 2019a. Canterbury. *Encyclopaedia Britannica*.
- Lotha, G., 2019b. Newcastle upon Tyne. *Encyclopaedia Britannica*.
- Lovejoy, C.O., Meindl, R.S., Pryzbeck, T.R., Mensforth, R.P., 1985. Chronological metamorphosis of the auricular surface of the ilium: A new method for the determination of adult skeletal age at death. *American Journal of Physical Anthropology*. 68, 15–28.
- Low, W.D., Chan, S.T., Chang, K.S.F., Lee, M.M.C., 1964. Skeletal Maturation of Southern Chinese Children. *Child Development*. 35, 1313.
- Lu, R., Zeng, X., Duan, J., Gao, T., Huo, D., Zhou, T., Song, Y., Deng, Y., Guo, X., 2016. Secular growth trends among children in Beijing (1955-2010). *Economics and Human Biology*. 21, 210–220.
- Lukacs, Z., 2008. Mucopolysaccharides. In: Blau, N., Duran, M., Gibson, K.M. (Eds.), *Laboratory Guide to the Methods in Biochemical Genetics*. Springer Berlin Heidelberg, Berlin, Heidelberg, pp. 287–324.
- Lund, A., Lund, M., 2013a. Kruskal-Wallis H Test [WWW Document]. Laerd Statistics. URL <https://statistics.laerd.com/spss-tutorials/kruskal-wallis-h-test-using-spss-statistics.php>
- Lund, A., Lund, M., 2013b. Multiple Regression SPSS Statistics [WWW Document]. Laerd Statistics. URL <https://statistics.laerd.com/spss-tutorials/multiple-regression-using-spss-statistics.php>
- Lund, A., Lund, M., 2018a. Chi-Square Goodness-of-Fit Test in SPSS Statistics [WWW Document]. Laerd Statistics. URL <https://statistics.laerd.com/spss-tutorials/chi-square-goodness-of-fit-test-in-spss-statistics.php#:~:text=SPSS Statistics Output for Chi,variable is equal or unequal>.
- Lund, A., Lund, M., 2018b. Binomial Logistic Regression using SPSS Statistics [WWW Document]. Laerd Statistics. URL <https://statistics.laerd.com/spss-tutorials/binomial-logistic-regression-using-spss-statistics.php>
- Lund, A., Lund, M., 2020a. Wilcoxon Signed-Rank Test using SPSS Statistics [WWW Document]. Laerd Statistics. URL <https://statistics.laerd.com/spss-tutorials/wilcoxon-signed-rank-test-using-spss-statistics.php>
- Lund, A., Lund, M., 2020b. Dependent T-Test using SPSS Statistics [WWW Document]. Laerd Statistics. URL <https://statistics.laerd.com/spss-tutorials/dependent-t-test-using-spss-323>

statistics.php

- Lund, A., Lund, M., 2020c. Mann-Whitney U Test using SPSS Statistics [WWW Document]. Laerd Statistics. URL <https://statistics.laerd.com/spss-tutorials/mann-whitney-u-test-using-spss-statistics.php>
- Lund, M., Lund, A., 2018. Multinomial Logistic Regression [WWW Document]. Laerd Statistics. URL <https://statistics.laerd.com/spss-tutorials/multinomial-logistic-regression-using-spss-statistics.php>
- Luyer, M. Le, Mahoney, P., 2017. Biorhythm in deciduous molars from the Tooth Fairy collection: preliminary results Results & Discussion [Poster], 17th International Symposium on Dental Morphology & 2nd Congress of International Association for Palaeodontology. Bordeaux.
- Lyle, M., 2013. Canterbury: 2000 Years of History. The History Press, Gloucestershire.
- MacCord, K., 2013. Ectoderm. The Embryo Project Encyclopedia.
- MacLaughlin, S.M., 1990. Epiphyseal fusion at the sternal end of the clavicle in a modern portuguese skeletal sample. *Anthropologia Portuguesa*. 8, 59–68.
- Mader, S.S., 2008. Human Biology, 11th ed. McGraw Hill, New York.
- Maeda, Y., Nakamura, E., Nguyen, M.T., Suva, L.J., Swain, F.L., Razzaque, M.S., Mackem, S., Lanske, B., 2007. Indian Hedgehog produced by postnatal chondrocytes is essential for maintaining a growth plate and trabecular bone. *PNAS*. 104, 6382–6387.
- Maggiano, C.M., 2012. Making the Mould: A Microstructural Perspective on Bone Modelling during Growth and Mechanical Adaptation. In: Crowder, C., Stout, S.D. (Eds.), *Bone Histology: An Anthropological Perspective*. CRC Press, Florida.
- Mahoney, P., Miskiewicz, J.J., Chapple, S., Le Luyer, M., Schlecht, S.H., Stewart, T.J., Griffiths, R.A., Deter, C., Guatelli-Steinberg, D., 2018. The biorhythm of human skeletal growth. *Journal of Anatomy*. 232, 26–38.
- Mahoney, P., Schmidt, C.W., Deter, C., Remy, A., Slavin, P., Johns, S.E., Miskiewicz, J.J., Nystrom, P., 2016. Deciduous enamel 3D microwear texture analysis as an indicator of childhood diet in medieval Canterbury, England. *Journal of Archaeological Science*. 66, 128–136.
- Mainman, A., 2019. Anglian York. Blackthorn Press, Pickering.
- Malina, R.M., 1974. Adolescent Changes in Size, Build, Composition and Performance. *Human Biology*. 46, 117–131.
- Malina, R.M., 1990. Research on secular trends in auxology. *Anthropologischer Anzeiger*. 48,

209–227.

- Malina, R.M., 2012. Physical Activity as a Factor in Growth and Maturation. In: Cameron, N., Bogin, B. (Eds.), *Human Growth & Development*. Academic Press, London, pp. 375–396.
- Malina, R.M., Bouchard, C., Bar-Or, O., 2004. *Growth, Maturation, and Physical Activity*, Second Edi. ed. Human Kinetics, Leeds.
- Malina, R.M., Little, B.B., Buschang, P.H., DeMoss, J., Selby, H.A., 1985. Socioeconomic variation in the growth status of children in a subsistence agricultural community. *American Journal of Physical Anthropology*. 68, 385–391.
- Malkiewicz, A., Dziedzic, M., 2012. Bone marrow reconversion - Imaging of physiological changes in bone marrow. *Polish Journal of Radiology*. 77, 45–50.
- Mann, H.B., Whitney, D.R., 1947. On a Test of Whether one of Two Random Variables is Stochastically Larger than the Other. *The Annals of Mathematical Statistics*. 18, 50–60.
- Mansfield, P.J., Neumann, D.A., 2019. Structure and Function of the Hip. In: Mansfield, P.J., Neumann, D.A. (Eds.), *Essentials of Kinesiology for the Physical Therapist Assistant*. Elsevier, pp. 233–277.
- Mant, M., Roberts, C., 2015. Diet and Dental Caries in Post-Medieval London. *International Journal of Historical Archaeology*. 19, 188–207.
- Maqsood, A., Naumenko, D.J., Hermanussen, M., Scheffler, C., Groth, D., 2020. No correlation between short term weight gain and lower leg length gain in healthy German children. *Anthropologischer Anzeiger*. 77, 399–403.
- Marshall, W.A., 1978. Puberty. In: Falkner, F., Tanner, J.M. (Eds.), *Human Growth: Postnatal Growth*. Plenum Press, New York, pp. 141–167.
- Marshall, W.A., Tanner, James M., 1986. Puberty. In: Falkner, F.T., Tanner, J.M. (Eds.), *Human Growth. A Comprehensive Treatise. Volume 2. Postnatal Growth Neurobiology*. Springer, New York.
- Matson, R., 2021. Splanchnopleure vs. Somatopleure [WWW Document]. KennesawState University. URL <http://facultyweb.kennesaw.edu/rmatson/somatopleure.php>
- Matsuoka, H., Sato, K., Sugihara, S., Murata, M., 1999. Bone Maturation Reflects the Secular Trend in Growth. *Hormone Research*. 52, 125–130.
- Mauras, N., 2001. Growth Hormone and Sex Steroids. Interactions in Puberty. *Neuroendocrinology*. 30, 529–544.
- Mays, S., 2010. The Effects of Infant Feeding Practices on Infant and Maternal Health in a

- Medieval Community. *Childhood in the Past*. 3, 63–78.
- Mays, S., 2018. The study of growth in skeletal populations. In: Crawford, S.E.E., Hadley, D.M., Shepherd, G.B. (Eds.), *The Oxford Handbook of the Archaeology of Childhood*. Oxford University Press, Oxford, pp. 71–89.
- Mays, S., Beavan, N., 2012. An investigation of diet in early Anglo-Saxon England using carbon and nitrogen stable isotope analysis of human bone collagen. *Journal of Archaeological Science*. 39, 867–874.
- McDade, T.W., Ryan, C.P., Jones, M.J., Hoke, M.K., Borja, J., Miller, G.E., Kuzawa, C.W., Kobor, M.S., 2019. Genome-wide analysis of DNA methylation in relation to socioeconomic status during development and early adulthood. *American Journal of Physical Anthropology*. 1–9.
- McIntyre, L., Bruce, G., 2010. Excavating All Saint's: a Medieval church rediscovered. *Current Archaeology*. 245, 30–37.
- McIntyre, L.J., 2016. The York 113: osteological analysis of 10 mass graves from Fishergate, York. *Journal of Conflict Archaeology*. 11, 114–133.
- McIntyre, M.H., 2011. Adult stature, body proportions and age at menarche in the United States National Health and Nutrition Survey (NHANES) III. *Annals of Human Biology*. 38, 716–720.
- McKern, T., Stewart, T., 1957. Skeletal age changes in young American males. Analysed from the standpoint of age identification. Quatermaster Research and Development Centre, Environmental Protection Research Division, Massachusetts.
- McWhirr, A., Viner, L., Wells, C., 1982. *Cirencester Excavations II: Romano-British Cemeteries at Cirencester*. Cirencester Excavation Committee, Cirencester.
- McWhirr, A.D., 1998. Introduction. In: Wilkinson, D.J., McWhirr, Alan D. (Eds.), *Cirencester Excavations IV: Cirencester Anglo-Saxon Church and Medieval Abbey*. Cotswold Archaeological Trust Ltd, Cirencester.
- Miles, D., 2006. *The tribes of Britain*. Orion Books Ltd, London.
- Millán, M.S., Rissech, C., Turbón, D., 2013. A test of Suchey-Brooks (pubic symphysis) and Buckberry-Chamberlain (auricular surface) methods on an identified Spanish sample: paleodemographic implications. *Journal of Archaeological Science*. 40, 1743–1751.
- Mirtz, T., Chandler, J.P., Evers, C.M., 2011. The Effects of Physical Activity on the Epiphyseal Growth Plates: A Review of the Literature on Normal Physiology and Clinical Implications. *Journal of Clinical Medicine Research*. 3, 1–7.

- Miszkiwicz, J.J., Mahoney, P., 2016. Ancient Human Bone Microstructure in Medieval England: Comparisons between Two Socio-Economic Groups. *Anatomical Record*. 299, 42–59.
- Mitchell, B., Sharma, R., 2009. *Embryology. An illustrated Colour text*. Elsevier, Edinburgh.
- Mohammed, H., Skalski, M.R., Patel, D.B., Tomasian, A., Schein, A.J., White, E.A., Rick Hatch, G.F., Matcuk, G.R., 2016. Coracoid process: The lighthouse of the shoulder. *Radiographics*. 36, 2084–2101.
- Moody, G., 2008. *The Isle of Thanet: from prehistory to the Norman conquest*. History Press, Stroud.
- Moore, T., 2014. The birth of a capital? Bagendon “Oppidum” and the impact of Rome on the southern Cotswolds. In: Breeze, D. (Ed.), *The Impact of Rome on the British Countryside. A Conference Organised by the Royal Archaeological Institute*. Royal Archaeological Institute, London.
- Morrill, J.S., 2016. *Great Plague of London*. Britannica.
- Morris, D.H., Jones, M.E., Schoemaker, M.J., Ashworth, A., Swerdlow, A.J., 2010. Determinants of age at menarche in the UK: analyses from the Breakthrough Generations Study. *British Journal of Cancer*. 103, 1760–1764.
- Mortier, G.R., Vanden Berghe, W., 2012. Genomics, Epigenetics and Growth. In: *Human Growth and Development*. Academic Press, London, pp. 153–172.
- Motateanu, M., Gudinchet, F., Sarraj, H., Schnyder, P., 1991. Case report 665. *Skeletal Radiology*. 20, 231–232.
- Mount, T., 2016. *A Year in the Life of Medieval England*. Amberley Publishing, Gloucestershire.
- Muhr, J., Ackerman, K.M., 2022. *Embryology, Gastrulation* [WWW Document]. StatPearls [Internet]. URL <https://www.ncbi.nlm.nih.gov/books/NBK554394/>
- Müldner, G., Richards, M.P., 2005. Fast or feast: Reconstructing diet in later medieval England by stable isotope analysis. *Journal of Archaeological Science*. 32, 39–48.
- Müldner, G., Richards, M.P., 2006. Diet in Medieval England: The Evidence from Stable Isotopes. In: Woolgar, C.M., Serjeantson, D., Waldron, T. (Eds.), *Food in Medieval England: Diet and Nutrition*. Oxford University Press, Oxford.
- Müldner, G., Richards, M.P., 2007. Stable Isotope Evidence for 1500 Years of Human Diet at the City of York, UK. *American journal of physical anthropology*. 133, 682–697.
- Murel, J., 2021. Print, authority, and the bills of mortality in seventeenth-century London.

- Seventeenth Century. 36, 935–959.
- Nakashima, T., Furukawa, H., 1997. A rare case of complete proximal epiphyses (so-called pseudoepiphyses) of the metacarpal and metatarsal bones in the human. *Annals of Anatomy*. 179, 549–551.
- Nanci, A., 2008. *Ten Cate's Oral Histology*, Seventh. ed. Mosby Elsevier, China.
- Naski, M.C., Colvin, J.S., Douglas Coffin, J., Ornitz, D.M., 1998. Repression of hedgehog signaling and BMP4 expression in growth plate cartilage by fibroblast growth factor receptor 3. *Development*. 125, 4977–4988.
- Newman, S.L., Gowland, R.L., 2017. Dedicated Followers of Fashion? Bioarchaeological Perspectives on Socio-Economic Status, Inequality, and Health in Urban Children from the Industrial Revolution (18th–19th C), England. *International Journal of Osteoarchaeology*. 27, 217–229.
- Newman, S.L., Gowland, R.L., Caffell, A.C., 2019. North and south : A comprehensive analysis of non-adult growth and health in the industrial revolution. *American Journal of Physical Anthropology*. 1–18.
- Nicholson, J.T., Nixon, J.E., 1961. Epiphyseal fractures. *The Journal of Paediatrics*. 59, 939–950.
- Nikita, E., 2017. *Osteoarchaeology*. Academic Press, London.
- Nilsson, O., Baron, J., 2004. Fundamental limits on longitudinal bone growth: growth plate senescence and epiphyseal fusion. *Trends in Endocrinology and Metabolism*. 15, 4–8.
- Nilsson, O., Chrysis, D., Pajulo, O., Boman, A., Holst, M., Rubinstein, J., Ritzén, E.M., Sävendahl, L., 2003. Localization of estrogen receptors- $\alpha$  and - $\beta$  and androgen receptor in the human growth plate at different pubertal stages. *Journal of Endocrinology*. 177, 319–326.
- Nilsson, O., Marino, R., De Luca, F., Phillip, M., Baron, J., 2005. Endocrine Regulation of the Growth Plate. *Hormone Research*. 64, 157–165.
- Nitsch, E.K., Humphrey, L.T., Hedges, R.E.M., 2011. Using stable isotope analysis to examine the effect of economic change on breastfeeding practices in Spitalfields, London, UK. *American Journal of Physical Anthropology*. 146, 619–628.
- Nolan, J., Harbottle, B., Vaughan, J., 2010. The Early Medieval cemetery at the Castle, Newcastle upon Tyne. *Archaeologia Aeliana*. 39, 147–287.
- Noonan, K.J., Farnum, C.E., Leiferman, E.M., Lampl, M., Markel, M.D., Wilsman, N.J., 2004. Growing pains: Are they due to increased growth during recumbency as documented in a

- lamb model? *Journal of Pediatric Orthopaedics*. 24, 726–731.
- Nyström, A.M., Vågerö, D.H., 1989. Adult body height, self perceived health and mortality in the Swedish population. *Journal of Epidemiology and Community Health*. 43, 380–384.
- O'Connor, J.E.O.J.E., Bogue, C., Spence, L.D.D., Last, J., 2008. A method to establish the relationship between chronological age and stage of union from radiographic assessment of epiphyseal fusion at the knee: An Irish population study. *Journal of Anatomy*. 212, 198–209.
- O'Driscoll, S.W.M., Saris, D.B.F., Ito, Y., Fitzimmons, J.S., 2001. The chondrogenic potential of periosteum decreases with age. *Journal of Orthopaedic Research*. 19, 95–103.
- Oddy, D.J., 2003. *From Plain Fare to Fusion Food: British Diet from the 1890s to the 1990s*. Boydell Press, Suffolk.
- Ogden, J.A., 1984. Radiology of postnatal skeletal development. *Skeletal Radiology*. 12, 12–20.
- Okamoto, K., Ito, J., Tokiguchi, S., Furusawa, T., 1996. High-resolution CT findings in the development of the sphenoccipital synchondrosis. *American Journal of Neuroradiology*. 17, 117–120.
- Oliver, N., 2012. *A History of Ancient Britain*. Orion Books Ltd, London.
- Onland-Moret, N.C., Peeters, P.H.M., van Gils, C.H., Clavel-Chapelon, F., Key, T., Tjønneland, A., Trichopoulou, A., Kaaks, R., Manjer, J., Panico, S., Palli, D., Tehard, B., Stoikidou, M., Bueno-De-Mesquita, H.B., Boeing, H., Overvad, K., Lenner, P., Quirós, J.R., Chirlaque, M.D., Miller, A.B., Khaw, K.T., Riboli, E., 2005. Age at Menarche in Relation to Adult Height: The EPIC Study. *American Journal of Epidemiology*. 162, 623–632.
- Opdahl, S., Nilsen, T.I.L., Romundstad, P.R., Vanky, E., Carlsen, S.M., Vatten, L.J., 2008. Association of size at birth with adolescent hormone levels, body size and age at menarche: relevance for breast cancer risk. *British Journal of Cancer*. 99, 201–206.
- Ottaway, P., 2004. Roman York. In: Nuttgens, P. (Ed.), *The History of York: From Earliest Times to the Year 2000*. The History Press, Gloucestershire.
- Öz, O.K., Millsaps, R., Welch, R., Birch, J., Zerwekh, J.E., 2001. Expression of aromatase in the human growth plate. *Journal of Molecular Endocrinology*. 27, 249–253.
- Palliser, D.M., 2014. *Medieval York*. OUP Oxford, Oxford.
- Parfitt, A.M., 2002. Misconceptions (1): Epiphyseal Fusion Causes Cessation of Growth. *Bone*. 30, 337–339.

- Parsons, F.G., 1904. Observations on Traction Epiphyses. *Journal of Anatomy*. 38, 248–258.
- Parsons, F.G., 1908. Further Remarks on Traction Epiphyses. *Journal of Anatomy*. 42, 388–396.
- Paterson, R.S., 1929. A Radiological Investigation of Epiphyses of the Long Bones. *Journal of Anatomy*. 64, 28–46.
- Patil, S.T., Parchand, M.P., Meshram, M.M., Kamdi, N.Y., 2012. Applicability of Greulich and Pyle skeletal age standards to Indian children. *Forensic Science International*. 216, 200.e1-200.e4.
- Pearson, E.S., 1938. *Mathematical Statistics and Data Analysis*. Duxbury, Belmont.
- Pearson, K., 1900. X. On the criterion that a given system of deviations from the probable in the case of a correlated system of variables is such that it can be reasonably supposed to have arisen from random sampling. *The London, Edinburgh, and Dublin Philosophical Magazine and Journal of Science*. 50, 157–175.
- Pechey, R., Monsivais, P., 2016. Socioeconomic inequalities in the healthiness of food choices: Exploring the contributions of food expenditures. *Preventive Medicine*. 88, 203–209.
- Peck, J.J., 2013. Status, health, and lifestyle in Middle Iron Age Britain: A bioarcheological study of elites and non-elites from East Yorkshire, Northern England. *International Journal of Paleopathology*. 3, 83–94.
- Perkins, D., 1995. *Researches and Discoveries in Kent: Report on work by the Thames Trust for Archaeology*. *Archaeologia Cantiana*. 115.
- Perry, R., Farquharson, C., Ahmed, F., 2008. The role of sex steroids in controlling pubertal growth. *Clinical Endocrinology*. 68, 4–15.
- Peschel, E.R., Peschel, R.E., 1987. Medical Insights into the Castrati in Opera. *American Scientist*. 75, 578–583.
- Phenice, T.W., 1967. A Newly Developed Visual Method of Sexing the Os Pubis. *American Journal of Physical Anthropology*. 30, 297–302.
- Pinhasi, R., Shaw, P., White, B., Ogden, A.R., 2006. Morbidity, rickets and long-bone growth in post-medieval Britain - A cross-population analysis. *Annals of Human Biology*. 33, 372–389.
- Pitfield, R., 2019. *The biorhythm of human juvenile skeletal growth*. University of Kent.
- Pitfield, R., Deter, C., Mahoney, P., 2019. Bone histomorphometric measures of physical activity in children from medieval England. *American Journal of Physical Anthropology*. 169, 730–746.

- Pope, R.E., Ralston, I.B.M., 2011. Approaching sex and status in Iron Age Britain with reference to the nearer continent. In: Armada, L., Moore, T. (Eds.), *Atlantic Europe in the First Millennium BC: Crossing the Divide*. Oxford University Press, Oxford.
- Poulton-Smith, A., 2013. *East Kent Place Names*. DB Publishing, Great Britain.
- Powell, M.L., Collins Cook, D., Bogdan, G., Buikstra, J.E., Castro, M.M., Horne, P.D., Hunt, D.R., Koritzer, R.T., Mendonça de Souza, S.F., Sandford, M.K., Saunders, L., Sene, G.A.M., Sullivan, L., Swetnam, J.J., 2006. *Invisible Hands: Women in Bioarchaeology*. In: Buikstra, J.E., Beck, L.A. (Eds.), *Bioarchaeology: The Contextual Analysis of Human Remains*. Academic Press, Burlington, pp. 131–193.
- Prader, A., 1982. Biomedical and Endocrinological Aspects of Normal Growth and Development. In: Borms, J., Hauspie, R., Sand, A., Susanne, C., Hebbelinck, M. (Eds.), *Human Growth and Development*. Springer Science, New York, pp. 1–22.
- Prader, A., Tanner, J.M., von Harnack, G.A., 1963. Catch-up growth following illness or starvation: An example of developmental canalisation in man. *The Journal of Paediatrics*. 62, 646–659.
- Prebeg, Ž., Bralić, I., 2000. Changes in menarcheal age in girls exposed to war conditions. *American Journal of Human Biology*. 12, 503–508.
- Prendiville, J., Bingham, E.A., Burrows, D., 1986. Premature epiphyseal closure - a complication of etretinate therapy in children. *Journal of the American Academy of Dermatology*. 15, 1259–1262.
- Pritchett, J.W., 1991. Growth Plate Activity in the Upper Extremity. *Clinical Orthopaedics and Related Research*. 268, 235–242.
- Privat, K.L., O'connell, T.C., Richards, M.P., 2002. Stable isotope analysis of human and faunal remains from the Anglo-Saxon Cemetery and Berinsfield, Oxfordshire: Dietary and social implications. *Journal of Archaeological Science*. 29, 779–790.
- Pryor, F., 2004. *Britain BC: Life in Britain and Ireland before the Romans*, 9th ed. Harper Perennial, London.
- Ramadhan, R.C., Palakunnel, J.J., Saker, E., Araujo, M.R., Johal, J., Loukas, M., Tubbs, R.S., 2017. The Split Atlas Anomaly: A Comprehensive Review. *The Spine Scholar*. 1, 37–44.
- Rando, C., Hillson, S., Antoine, D., 2014. Changes in mandibular dimensions during the mediaeval to post-mediaeval transition in London: A possible response to decreased masticatory load. *Archives of Oral Biology*. 59, 73–81.
- Redfern, R., 2007. *The influence of culture upon childhood: as osteological study of Iron Age*

- and Romano-British Dorset. In: Harlow, M., Laurence, R. (Eds.), *Age and Ageing in the Roman Empire*. *Journal of Roman Archaeology Supplementary Series*.
- Redfern, R., 2008. A Bioarchaeological Investigation of Cultural Change in Dorset, England (Mid-to-Late Fourth Century B.C. to the End of the Fourth Century A.D. *Britannia*. 39, 161–191.
- Redfern, R., 2010. A regional examination of surgery and fracture treatment in Iron Age and Roman Britain. *International Journal of Osteoarchaeology*. 20, 443–471.
- Redfern, R., Roberts, C., 2005. Health in Romano-British Urban Communities: Reflections from the Cemeteries. In: *Fertile Ground: Papers in Honour of Susan Limbrey*. Oxbow Books, Oxford.
- Redfern, R.C., Dewitte, S.N., 2011. A new approach to the study of Romanization in Britain: A regional perspective of cultural change in late Iron Age and Roman Dorset using the Siler and Gompertz-Makeham models of mortality. *American Journal of Physical Anthropology*. 144, 269–285.
- Redfern, R.C., Dewitte, S.N., Pearce, J., Hamlin, C., Dinwiddy, K.E., 2015. Urban-rural differences in Roman Dorset, England: A bioarchaeological perspective on Roman settlements. *American Journal of Physical Anthropology*. 157, 107–120.
- Redfern, R.C., Hamlin, C., Athfield, N.B., 2010. Temporal changes in diet: A stable isotope analysis of late Iron Age and Roman Dorset, Britain. *Journal of Archaeological Science*. 37, 1149–1160.
- Redfern, R.C., Millard, A.R., Hamlin, C., 2012. A regional investigation of subadult dietary patterns and health in late Iron Age and Roman Dorset, England. *Journal of Archaeological Science*. 39, 1249–1259.
- Redfield, A., 1970. A new aid to aging immature skeletons: Development of the occipital bone. *American Journal of Physical Anthropology*. 33, 207–220.
- Reid, D.J., Dean, M.C., 2006. Variation in modern human enamel formation times. *Journal of Human Evolution*. 50, 329–346.
- Reitsemá, L.J., Vercellotti, G., 2012. Stable isotope evidence for sex- and status-based variations in diet and life history at medieval Trino Vercellese, Italy. *American Journal of Physical Anthropology*. 148, 589–600.
- Resnick, D., Kransdorf, M.J., 1996. *Bone and Joint Imaging*. Elsevier Saunders, Philadelphia.
- Ribot, I., Roberts, C., 1996. A study of non-specific stress indicators and skeletal growth in two mediaeval subadult populations. *Journal of Archaeological Science*. 23, 67–79.

- Riis, B.J., Krabbe, S., Christiansen, C., Catherwood, B.D., Deftos, L.J., 1985. Bone Turnover in Male Puberty: A Lonitudinal Study. *Calcified Tissue International*. 37, 213–217.
- Rios, L., Weisensee, K., Rissech, C., 2008. Sacral fusion as an aid in Age Estimation. *Forensic Science International*. 180.
- Roberts, C.A., 2009. Health and welfare in mediaeval England: the human skeletal remains contextualised. In: Gilchrist, R. (Ed.), *Reflections: 50 Years of Mediaeval Archaeology*. Routledge, London, pp. 307–325.
- Roche, A.F., 1978. Bone Growth and Maturation. In: Falkner, F., Tanner, J.M. (Eds.), *Human Growth: Postnatal Growth*. Plenum Press, New York, pp. 317–349.
- Roche, A.F., 1992. *Growth, Maturation and Body Composition: The Fels Longitudinal Study 1929-1991*. University Press, Cambridge.
- Rodriguez, E., 2017. Isle of Thanet. *Encyclopaedia Britannica*.
- Rogers, T.L., 2009. Sex determination of adolescent skeletons using the distal humerus. *American Journal of Physical Anthropology*. 140, 143–148.
- Rogol, A.D., Roemmich, J.N., Clark, P.A., 2002. Growth at Puberty. *Journal of Adolescent Health*. 31, 192–200.
- Romundstad, P.R., Vatten, L.J., Lund Nilsen, T.I., Holmen, T.L., Hsieh, C., Trichopoulos, D., Stuver, S.O., 2003. Birth size in relation to age at menarche and adolescent body size: Implications for breast cancer risk. *International Journal of Cancer*. 105, 400–403.
- Roskams, S., Neal, C., 2020. Landscape and settlement in the Vale of York: archaeological investigations at Heslington East, York, 2003-13. The Society of Antiquaries of London, London.
- Rowing, E.H., 2011. *Diet in the Past: An Isotopic Investigation into Dietary trends during the Iron Age and Anglo-Saxon periods in Kent*. University of Kent.
- Saggese, G., Baroncelli, G.I., Bertelloni, S., 2002. Puberty and bone development. *Best Practice & Research Clinical Endocrinology and Metabolism*. 16, 53–64.
- Sahni, D., Jit, I., Sanjeev, 1995. Time of fusion of epiphyses at the elbow and wrist joints in girls of Northwest India. *Forensic Science International*. 74, 47–55.
- Sakai, Y., 2017. *Transition from the Late Roman period to the Early Anglo-Saxon period in the Upper Thames Valley based on stable isotopes*. University of Oxford.
- Schaefer, M., 2008a. Patterns of Epiphyseal Union and Their Use in the Detection and Sorting of Commingled Remains. In: Adams, B.J., Byrd, J.E. (Eds.), *Recovery, Analysis, and Identification of Commingled Human Remains*. Humana Press, New York.

- Schaefer, M., 2008b. A Summary of Epiphyseal Union Timings in Bosnian Males. *International Journal of Osteoarchaeology*. 18, 536–545.
- Schaefer, M., 2014. A Practical Method for Detecting Commingled Remains Using Epiphyseal Union. In: Adams, B.J., Byrd, J.E. (Eds.), *Commingled Human Remains: Methods in Recovery, Analysis, and Identification*. Elsevier, Boston, pp. 123–144.
- Schaefer, M., Aben, G., Vogelsberg, C., 2015. A demonstration of appearance and union times of three shoulder ossification centers in adolescent and post-adolescent children. *Journal of Forensic Radiology and Imaging*. 3, 49–56.
- Schaefer, M., Black, S., Scheuer, L., 2009. *Juvenile Osteology: A Laboratory and Field Manual*. Elsevier, London.
- Schaefer, M., Black, S.M., 2005. Comparison of Ages of Epiphyseal Union in North American and Bosnian Skeletal Material. *Journal of Forensic Sciences*. 50, 1–8.
- Schaefer, M.C., Black, S.M., 2007. Epiphyseal Union Sequencing: Aiding in the Recognition and Sorting of Commingled Remains. *Journal of Forensic Sciences*. 52.
- Schama, S., 2009. *A History of Britain. At the edge of the world? 3000BC - AD1603*. The Bodley Head, London.
- Schmeling, A., Reisinger, W., Loreck, D., Vendura, K., Markus, W., Geserick, G., 2000. Effects of ethnicity on skeletal maturation: consequences for forensic age estimations. *International Journal of Legal Medicine*. 113, 253–258.
- Schmeling, A., Schulz, R., Reisinger, W., Wernecke, M.M.K., 2004. Studies on the time frame for ossification of the medial clavicular epiphyseal cartilage in conventional radiography. *International Journal of Legal Medicine*. 118, 5–8.
- Schooling, C.M., Jiang, C.Q., Lam, T.H., Zhang, W.S., Adab, P., Cheng, K.K., Leung, G.M., 2010. Leg Length and Age of Puberty Among Men and Women from a Developing Population: The Guangzhou Biobank Cohort Study. *American Journal of Human Biology*. 22, 683–687.
- Schuenke, M., Schulte, E., Schmacher, U., 2020. *General Anatomy and Musculoskeletal System*. Thieme Medical Publishers Inc, New York.
- Schutkowski, H., 1993. Sex determination of infant and juvenile skeletons: I. Morphognostic features. *American Journal of Physical Anthropology*. 90, 199–205.
- Seeman, E., 1998. Editorial: Growth in Bone Mass and Size — Are Racial and Gender Differences in Bone Mineral Density More Apparent than Real? *Journal of Clinical Endocrinology and Metabolism*. 83, 1414–1419.

- Shapland, B.F., Lewis, M., Watts, R., 2015. The Lives and Deaths of Young Medieval Women : The Osteological Evidence. *Medieval Archaeology*. 59, 272–289.
- Shapland, F., Lewis, M., 2013. Brief communication: A proposed osteological method for the estimation of pubertal stage in human skeletal remains. *American Journal of Physical Anthropology*. 151, 302–310.
- Shapland, F., Lewis, M., 2014. Brief communication: A proposed method for the assessment of pubertal stage in human skeletal remains using cervical vertebrae maturation. *American Journal of Physical Anthropology*. 153, 144–153.
- Shedge, R., Kanchan, T., Garg, P.K., Dixit, S.G., Warriar, V., Khera, P., Krishan, K., 2020. Computed tomographic analysis of medial clavicular epiphyseal fusion for age estimation in Indian population. *Legal Medicine*. 46, 1–7.
- Shigehara, N., 1980. Epiphyseal union, tooth eruption, and sexual maturation in the common tree shrew, with reference to its systematic problem. *Primates*. 21, 1–19.
- Shim, K.S., 2015. Pubertal growth and epiphyseal fusion. *Annals of Pediatric Endocrinology & Metabolism*. 20, 8–12.
- Shirley, N.R., Jantz, R.L., 2011. Spheno-Occipital Synchronosis Fusion in Modern Americans. *Journal of Forensic Sciences*. 56, 580–585.
- Silventoinen, K., 2003. Determinants of Variation in Adult Body Height. *Journal of Biosocial Science*. 35, 263–285.
- Silventoinen, K., Rahkonen, O., 1999. Social background, adult body-height and health. *International Journal of Epidemiology*. 28, 911–918.
- Simpson, D., 2017. Newcastle Upon Tyne in Roman and Saxon times [WWW Document]. England’s North East. URL <https://englandsnortheast.co.uk/roman-newcastle/>
- Simpson, D., 2022. King Aethelfrith and King Edwin [WWW Document]. England’s North East. URL <https://englandsnortheast.co.uk/northumbria-aethelfrith-edwin/> (accessed 12.1.22).
- Singh, D., Sanyal, S., Chattopadhyay, N., 2011. The role of estrogen in bone growth and formation: changes at puberty. *Cell Health and Cytoskeleton*. 3, 1–12.
- Sisk, C.L., Foster, D.L., 2004. The neural basis of puberty and adolescence. *Nature Neuroscience*. 7, 1040–1047.
- So, L.L.Y., Yen, P.K.J., 1990. Secular trend in skeletal maturation in Southern Chinese girls in Hong Kong. *Zeitschrift für Morphologie und Anthropologie*. 78, 145–153.
- Spall, C.A., Toop, N., 2005. Blue Bridge Lane & Fishergate House, York. Report on

- Excavations: July 2000 to July 2002 [WWW Document]. Archaeological Planning Consultancy Ltd. URL <http://www.mgassocs.com/mono/001/index.html>
- Spatola, G.F., Uzzo, M.L., Lanzarone, A., Piscionieri, D., Daricello, D., Zerbo, S., 2020. The Essential of Bone Histology for Forensic Applications. In: Lo Re, G., Argo, A., Midiri, M., Cattaneo, C. (Eds.), *Radiology in Forensic Medicine*. Springer, Switzerland, pp. 87–92.
- Steckel, R.H., 2004. New Light on the “Dark Ages”: The Remarkably Tall Stature of Northern European Men during the Medieval Era. *Social Science History*. 28, 211–229.
- Steckel, R.H., 2012. Social and Economic Effects on Growth. In: Cameron, N., Bogin, B. (Eds.), *Human Growth & Development*. Academic Press, London.
- Stemple, D.L., 2005. Structure and function of the notochord: An essential organ for chordate development. *Development*. 132, 2503–2512.
- Stevenson, P.H., 1924. Age order of epiphyseal union in man. *American Journal of Physical Anthropology*. 7, 53–93.
- Stewart, N.A., Gerlach, R.F., Gowland, R.L., Gron, K.J., Montgomery, J., 2017. Sex determination of human remains from peptides in tooth enamel. *Proceedings of the National Academy of Sciences*. 201714926.
- Stewart, T.D.D., 1934. Sequence of epiphyseal union, third molar eruption and suture closure in Eskimos and American Indians. *American Journal of Physical Anthropology*. 19, 433–452.
- Stone, A.I., 2007. Ecological Risk Aversion and Foraging Behaviors of Juvenile Squirrel Monkeys (*Saimiri sciureus*). *Ethology*. 113, 782–792.
- Stout, S.A.M.D., Lueck, R., 1995. Bone Remodeling Rates and Skeletal Maturation in Three Archaeological Skeletal Populations. *American Journal of Physical Anthropology*. 98, 161–171.
- Sullivan, S., Flavel, A., Franklin, D., 2017. Age estimation in a sub-adult Western Australian population based on the analysis of the pelvic girdle and proximal femur. *Forensic Science International*. 281, 185.e1-185.e10.
- Swerdloff, R.S., Wang, C., Sinha Hikim, A.P., 2009. Hypothalamic – Pituitary – Gonadal Axis in Men. *Hormones, Brain and Behaviour*. 2357–2395.
- Sylvia, V.L., Gay, I., Hardin, R., Dean, D.D., Boyan, B.D., Schwartz, Z., 2002. Rat Costochondral Chondrocytes Produce  $17\beta$ -Estradiol and Regulate Its Production by  $1\alpha,25(\text{OH})_2\text{D}_3$ . *Bone*. 30, 57–63.

- Szilvássy, J., 1968. Eine Methode zur Altersbestimmung mit Hilfe der sternalen Gelenksflächen der Schlüsselbeine. *Mitteilungen der Anthropologischen Gesellschaft in Wien*. 108, 166–168.
- Szilvássy, J., 1980. Age determination on the sternal articular faces of the clavícula. *Journal of Human Evolution*. 9, 609–610.
- Takai, S., Akiyoshi, T., 1983. Skeletal Maturity of Japanese Children in Western Kyushu. *American Journal of Physical Anthropology*. 62, 199–204.
- Tamura, N., Doolittle, L.K., Hammer, R.E., Shelton, J.M., Richardson, J.A., Garbers, D.L., 2004. Critical roles of the guanylyl cyclase B receptor in endochondral ossification and development of female reproductive organs. *Proceedings of the National Academy of Sciences of the United States of America*. 101, 17300–17305.
- Tanner, J., Oshman, D., Babbage, F., Healy, M., 1997. Tanner-Whitehouse bone age reference values for North American children. *The Journal of Paediatrics*. 131, 34–40.
- Tanner, J.M., 1962. *Growth at Adolescence*. Lowe and Brydone Ltd, London.
- The Editors of Encyclopaedia Britannica, 2022. Endoderm. Britannica.
- The University of Sheffield, 2003. Human Skeletal Collection [WWW Document]. McIntyre, L. and Willmott, H. 2003. Excavations at the Methodist Chapel, Carver Street, Sheffield. Unpublished report for ARCUS. URL <https://www.sheffield.ac.uk/archaeology/research/human-osteo-lab/human-skeletal-collection>
- Tikkanen, A., 2022. Blastula. Britannica.
- Tillmann, B., Lorenz, R., 1978. The stress at the Human Atlanto-Occipital Joint. *Anatomy and Embryology*. 153, 269–277.
- Tirpude, B.H., Surwade, V.B., Murkey, P.N., Wankhade, P.A., Meena, S.K., 2014. Age Determination from Epiphyseal Union of Bones at Shoulder Joint in Girls of Central India. *Journal of Forensic Medicine, Science and Law*. 23, 1–8.
- Todd, T.W., 1920. Age changes in the pubic bone.: I. The male white pubis. *American Journal of Physical Anthropology*. 3, 285–334.
- Todd, T Wingate, 1921a. Age Changes In the Pubic Bone II. The Pubis Of The Male Negro-White Hybrid, III. The Pubis Of The White Female, IV. The Pubis Of The Female Negro-White Hybrid. *American Journal of Physical Anthropology*. 4, 1–77.
- Todd, T. Wingate, 1921. Age changes in the public bone. VI. The interpretation of variations in the symphyseal area. *American Journal of Physical Anthropology*. 4, 407–424.

- Todd, T Wingate, 1921b. Age changes in the pubic bone. V. Mammalian Pubic Metamorphosis. *American Journal of Physical Anthropology*. 4.
- Todd, T.W., 1930a. The Anatomical Features of Epiphysial Union. *Child Development*. 1, 186.
- Todd, T.W., 1930b. Comparative Youth: The Physical Aspect. *Child Development*. 1, 79.
- Todd, T.W., D'Errico, J., 1926. The Odontoid Ossicle of the Second Cervical Vertebra. *Annals of surgery*. 83, 20–31.
- Todd, T.W., D'Errico, J., 1928. The clavicular epiphyses. *American Journal of Anatomy*. 41, 25–50.
- Topper, A., Mulier, H., 1932. Basal Metabolism of Normal Children: The Puberty Reaction. *The American Journal of Diseases of Children*. 43, 327–336.
- Towne, B., Demerath, E.W., Czerwinski, S.A., 2012. The Genetic Epidemiology of Growth and Development. In: Cameron, N., Bogin, B. (Eds.), *Human Growth and Development*. Elsevier, London, pp. 173–224.
- Tremblay, L., Larivière, M., 2020. Predictors of Puberty Onset. In: Hupp, S., Jewell, J. (Eds.), *The Encyclopaedia of Child and Adolescent Development*. Wiley - Blackwell, Illinois, pp. 1–10.
- Turner, R.T., Riggs, B.L., Spelsberg, T.C., 1994. Skeletal Effects of Estrogen. *Endocrine Reviews*. 15, 275–300.
- Tuvemo, T., Cnattingius, S., Jonsson, B., 1999. Prediction of Male Adult Stature Using Anthropometric Data at Birth: A Nationwide Population-Based Study. *Pediatric Research*. 46.
- Ubelaker, D.H., 1984. *Human Skeletal Remains: Excavation, Analysis, Interpretation*. Taraxacum, Washington.
- Ubelaker, D.H., 1987. Estimating Age at Death from Immature Human Skeletons: An Overview. *Journal of Forensic Sciences*. 32, 11176J.
- University of Bradford, 2022. Archaeological periods of time [WWW Document]. Glossary. URL <https://www.bradford.ac.uk/archaeomagnetism/glossary/>
- Vaiserman, A.M., Grigoryev, P.E., Belaya, I.I., Voitenko, V.P., 2003. Variation of mortality rate during the individual annual cycle. *Biogerontology*. 4, 221–225.
- van Coeverden, S.C.C.M., Netelenbos, J.C., de Ridder, C.M., Roos, J.C., Popp-Snijders, C., Delemarre van de Waal, H.A., 2002. Bone metabolism markers and bone mass in healthy pubertal boys and girls. *Clinical Endocrinology*. 57, 107–116.
- Van der Veen, M., 2014. Arable Farming, Horticulture, and Food. In: Millett, M., Revell, L., 338

- Moore, A. (Eds.), *The Oxford Handbook of Roman Britain*. Oxford Handbooks Online, Oxford, pp. 1–20.
- van Lenthe, F.J., Kemper, H.C.G., van Mechelen, W., 1996. Rapid maturation in adolescence results in greater obesity in adulthood: The Amsterdam Growth and Health Study. *American Journal of Clinical Nutrition*. 64, 18–24.
- van Wieringen, J.C., 1978. Secular Growth Changes. In: Falkner, F., Tanner, J.M. (Eds.), *Human Growth: Postnatal Growth*. Plenum Press, New York, pp. 445–470.
- Vanderschueren, D., Vandenput, L., Boonen, S., 2005. Reversing Sex Steroid Deficiency and Optimizing Skeletal Development in the Adolescent with Gonadal Failure. *Endocrine Development*. 8, 150–165.
- Vanderschueren, D., Vandenput, L., Boonen, S., Lindberg, M.K., Bouillon, R., Ohlsson, C., 2004. Androgens and bone. *Endocrine Reviews*. 25, 389–425.
- Verhulst, P.F., 1838. Notice sur la loi que la population suit dans son accroissement. In: Quetelet, A. (Ed.), *Correspondence Mathématique et Physique*. Société Belge de Librairie, Bruxelles, pp. 113–121.
- Verhulst, P.F., 1845. Recherches mathématiques sur la loi d'accroissement de la population. *Nouveaux Mémoires de l'Académie Royale des Sciences, des Lettres et des Beaux-Arts de Belgique*. 18, 1–38.
- Vijayakumar, N., Op de Macks, Z., Shirtcliff, E.A., Pfeifer, J.H., 2018. Puberty and the human brain: Insights into adolescent development. *Neuroscience and Biobehavioral Reviews*. 92, 417–436.
- Viner, Linda, Leech, R., 1982. Bath Gate Cemetery, 1969-1976. In: McWhirr, A., Viner, L., Wells, C. (Eds.), *Romano-British Cemeteries at Cirencester*. Cirencester Excavation Committee, Cirencester.
- Wacher, J.S., 1982. Chronological summary. In: Wacher, J.S., McWhirr, A.D. (Eds.), *Early Roman Occupation at Cirencester*. Cirencester Excavation Committee, Cirencester.
- Wade, K., 2000. Anglo-Saxon and Medieval (Rural). In: Brown, N., Glazebrook, J. (Eds.), *Research and Archaeology: A Framework for the Eastern Counties 2 - Research Agenda and Strategy*. East Anglian Archaeology, Norwich.
- Waldron, T., 2006. Nutrition and the Skeleton. In: Woolgar, C.M., Serjeantson, D., Waldron, T. (Eds.), *Food in Medieval England: Diet and Nutrition*. Oxford University Press, Oxford.
- Walker, R., Burger, O., Wagner, J., Rueden, C.R. Von, 2006a. Evolution of brain size and

- juvenile periods in primates. *Journal of Human Evolution*. 51, 480–489.
- Walker, R., Gurven, M., Hill, K., Migliano, A., Chagnon, N., De Souza, R., Djurovic, G., Hames, R., Hurtado, A.M., Kaplan, H., Kramer, K., Oliver, W.J., Valeggia, C., Yamauchi, T., 2006b. Growth Rates and Life Histories in Twenty-Two Small-Scale Societies. *American Journal of Human Biology*. 18, 295–311.
- Wallenfeldt, J., 2014. Cirencester. *Encyclopaedia Britannica*.
- Wallenfeldt, J., 2018. East Lothian. *Encyclopaedia Britannica*.
- Walter, B.S., DeWitte, S.N., 2017. Urban and rural mortality and survival in Medieval England. *Annals of Human Biology*. 44, 338–348.
- Walter, B.S., Dewitte, S.N., Redfern, R.C., 2016. Archives of Oral Biology Sex differentials in caries frequencies in Medieval London. *Archives of Oral Biology*. 63, 32–39.
- Wang, Y., 2002. Is Obesity Associated With Early Sexual Maturation? A Comparison of the Association in American Boys Versus Girls. *Paediatrics*. 110, 903–910.
- Ward, J., 2006. *Women in England in the Middle Ages*. Hambledon Continuum, New York.
- Watts, R., 2015. The long-term impact of developmental stress. Evidence from later medieval and post-medieval London (AD1117-1853). *American Journal of Physical Anthropology*. 158, 569–580.
- Weale, M.E., Weiss, D.A., Jager, R.F., Bradman, N., Thomas, M.G., 2002. Y chromosome evidence for Anglo-Saxon mass migration. *Molecular Biology and Evolution*. 19, 1008–1021.
- Weaver, C.M., Fuchs, R.K., 2013. Skeletal Growth and Development. In: Burr, D.B., Allen, M.R. (Eds.), *Basic and Applied Bone Biology*. Academic Press, London.
- Webb, P.A.O., Suchey, J.M., 1985. Epiphyseal Union of the Anterior Iliac Crest and Medial Clavicle in a Modern Multiracial Sample of American Males and Females. *American Journal of Physical Anthropology*. 68, 457–466.
- Weise, M., De-levi, S., Barnes, K.M., Gafni, R.I., Abad, V., Baron, J., 2001. Effects of estrogen on growth plate senescence and epiphyseal fusion. *PNAS*. 98, 6871–6876.
- Weiss, E., Desilva, J., Zipfel, B., 2012. Brief Communication: Radiographic Study of Metatarsal One Basal Epiphyseal Fusion: A Note of Caution on Age Determination. *American Journal of Physical Anthropology*. 147, 489–492.
- White, T.D., Black, M.T., Folkens, P.A., 2012. *Human Osteology*, Third. ed. Elsevier Academic Press, Amsterdam.
- Wigley, C., Adams, M.A., Black, S.M., Dolan, P., Partridge, T.A., 2008. *Functional anatomy*

- of the musculoskeletal system. In: Standring, S. (Ed.), *Gray's Anatomy: The Anatomical Basis of Clinical Practice*. Elsevier.
- Wilcoxon, F., 1945. Individual Comparisons By Ranking Methods. *Biometrics Bulletin*. 1, 80–83.
- Willacy, H., 2016. Adrenarche [WWW Document]. Patient Info. URL <https://patient.info/childrens-health/adrenarche>
- Wilson, E.B., Worcester, J., 1943. The Determination of L.D. 50 and Its Sampling Error in Bio-assay. *Proceedings of the National Academy of Sciences*. 29, 79–85.
- Wilson, J.D., Roehrborn, C., 1999. Long-Term Consequences of Castration in Men: Lessons from the Skoptzy and the Eunuchs of the Chinese and Ottoman Courts. *The Journal of Clinical Endocrinology & Metabolism*. 84, 4324–4331.
- Witte, R.S., Witte, J.S., 2017. *Statistics*, 11th ed. Wiley, Danvers.
- Wittschieber, D., Vieth, V., Domnick, C., Pfeiffer, H., Schmeling, A., 2013. The iliac crest in forensic age diagnostics: evaluation of the apophyseal ossification in conventional radiography. *International Journal of Legal Medicine*. 127, 473–479.
- Wood, J.W., Milner, G.R., Harpending, H.C., Weiss, K.M., Cohen, M.N., Eisenbergh, L.E., Hutchinson, D.L., Jankauskas, R., Cesnys, G., M, A.K., Lukas, J.R., McGrath, J.W., Abella Roth, E., Ubelaker, D.H., Wilkinson, R.G., 1992. The Osteological Paradox: Problems of Inferring Prehistoric Health from Skeletal Samples. *Current Anthropology*.
- Woolgar, C.M., Serjeantson, D., Waldron, T., 2006. Conclusion. In: Woolgar, C.M., Serjeantson, D., Waldron, T. (Eds.), *Food in Medieval England: Diet and Nutrition*. Oxford University Press, Oxford.
- Wray, N.R., Visscher, P., 2008. Estimating Trait Heritability. *Nature Education*. 1, 29.
- Wright, J., Bateman, C., Holbrook, N., 2017. Introduction and Background. In: Holbrook, N., Wright, J., McSloy, E.R., Geber, J. (Eds.), *Cirencester Excavations VII: The Western Cemetery of Roman Cirencester. Excavations at the Former Bridges Garage, Tetbury Road, Cirencester, 2011-2015*. Cotswold Archaeology, Cirencester.
- Yaşar İşcan, M., Steyn, M., 2013. *The Human Skeleton in Forensic Medicine*, Third. ed. Charles C Thomas Publisher Ltd, Illinois.
- Yaussy, S.L., Dewitte, S.N., 2018. Patterns of frailty in non-adults from medieval London. *International Journal of Paleopathology*. 22, 1–7.
- York Museums Trust, 2022. Viking Timeline [WWW Document]. History of York. URL <http://www.historyofyork.org.uk/themes/viking-timeline> (accessed 12.1.22).

- Zarulli, V., 2016. Unobserved Heterogeneity of Frailty in the Analysis of Socioeconomic Differences in Health and Mortality. *European Journal of Population*. 32, 55–72.
- Zhang, P., Jobert, A.-S., Couvineau, A., Silve, C., 1998. A Homozygous Inactivating Mutation in the Parathyroid Hormone/Parathyroid Hormone-Related Peptide Receptor Causing Blomstrand Chondroplasia. *The Journal of Clinical Endocrinology & Metabolism*. 83, 3373–3376.
- Zihlman, A.L., Bolter, D.R., Boesch, C., 2007. Skeletal and dental growth and development in chimpanzees of the Taï National Park, Côte D'Ivoire. *Journal of Zoology*. 273, 63–73.
- Zuvich, A., 2016. *A Year in the Life of Stuart Britain*. Amberley Publishing, Gloucestershire.

## CHAPTER 11

## APPENDICES

## APPENDIX 1: PREVIOUS LITERATURE

A list of some of the previous literature on epiphyseal fusion is given below, including studies that have looked at dry bone and through medical imaging technology. The studies have been sorted by date of publication.

Date	Name	Type	Description	Findings
1924	Stevenson	Dry bone, Stages 1-4	Looked at sequence and timing of epiphyseal fusion for various fusion sites of known age skeletons.	The age at which skeletons had reached each stage was recorded.
1926	Paterson	Radiographs	Looked at the appearance and fusion of the diaphysis and epiphyses of various bones.	Found differences in the fusion of the epiphyses between the sexes.
1928	Todd and D'Errico	Dry bone, Stages 1-4	Studied the epiphyses of the <b>clavicle</b> .	Found that the medial epiphysis completed around 25 years of age for almost all skeletons analysed. The lateral epiphysis was examined, as prior to this the lateral epiphysis was rarely analysed or accepted.

1930	Todd	Radiographs and dry bone, Stages 1-9	Summary of findings made so far on epiphyseal fusion since Stevenson, (1924).	Created a nine-stage system of analysing epiphyseal fusion.
1957	McKern and Stewart	Dry bone, Stages 0-4	Epiphyseal fusion of various bones was analysed for male <b>American</b> soldiers that were killed in the Korean war.	Fusion age was recorded for American soldiers.
1960	Johnston	Dry bone, Stages 1-3	Looked at epiphyseal fusion in a Native American sample excavated from the Indian Knoll archaeological site.	He compared his findings to other studies charting epiphyseal fusion. He also looked at sex differences within the Indian Knoll sample.
1970	Redfield	Dry bone	Looked at the development of the <b>occipital</b> bone, including fusion in skeletons excavated at the <b>Yugoslavian-Albanian</b> border.	The percentage of individuals that reached fusion at various age ranges were recorded.
1980	Szilvássy	Dry bone, Stages 1-3	Adapted into English from an earlier paper - (Szilvássy, 1968) - <b>clavicles</b> were removed from autopsied individuals and recorded.	A three-phase system was developed and changes charted with corresponding age ranges.
1985	Webb and Suchey	Dry bone, Stages 1-4	Looked at epiphyseal fusion in the medial	Skeletons are separated by sex and ancestry.

			<b>clavicle</b> and the anterior iliac crest of the <b>pelvis</b> in autopsied <b>Americans</b> .	Epiphyseal fusion may vary by sex, but not always. Epiphyseal fusion did not appear to vary much by ancestry.
1990	So and Yen	Radiographic, Greulich & Pyle method	The <b>hand and wrist</b> were assessed in Southern <b>Chinese</b> girls from Hong Kong from 1961-1963 and 1986-1987.	Earlier maturation was found in the later cohort and is thought to be due to improved socioeconomic conditions.
1990	MacLaughlin	Dry bone, Stages 1-5	Studied the medial <b>clavicle</b> in a known aged skeletal sample from Lisbon, Portugal.	Discusses the changes of the medial clavicle with chronological age.
1994	Buikstra and Ubelaker	N/A	Gives a three-stage system in which to record epiphyseal fusion.	N/A
1995	Sahni et al.	Radiographic, Stages 0-3	Epiphyseal fusion of the <b>upper limb</b> are studied in girls from <b>Chandigarh</b> , Northwest India.	Age at fusion is recorded and compared to previous studies.
1995	Stout and Lueck	Histological sample	Cortical bone remodelling rates of <b>rib</b> samples were analysed from <b>Native American</b> population samples. The first sample was radiocarbon dated to between 6,900-8,120 BC, the second between	Earlier populations were found to reach skeletal maturity at an older age than Modern American populations.

			50BC-400AD, the third dated at 1,000AD. The last sample was from contemporary <b>Americans</b> of black and white ethnicities.	
1996	Black and Scheuer	Dry bone, phases 1-5	Growth of the clavicle and epiphyseal fusion of the medial epiphysis of the <b>clavicle</b> were recorded in skeletons from three different samples of different periods.	Age at fusion was similar for all three samples.
1996	Okamoto et al.	CT scans	CT scans were performed on living patients in Niigata, <b>Japan</b> to look at fusion of the <b>spheno-occipital synchondrosis</b> .	Ossification and fusion were recorded at different ages.
1997	Tanner et al.	Radiographic, Tanner-Whitehouse method	Looked at x-rays of the <b>hand and wrist</b> of <b>American</b> children of European origin and a good socioeconomic background.	The children in this study were found to mature earlier than UK children tested in the 1960s. The children were also found to be 3 months ahead of contemporary Spanish children.
2000	Matsuoka et al.	Radiographic, Tanner-Whitehouse 2- RUS (radius-ulna-	X-rays were compared of the <b>hand and wrist</b> between a mid-1980s cohort and a mid-1990s	Bone maturity remained largely the same between the two cohorts. It is thought because the secular trend plateaued.

		short bones) method	cohort of children living in Tokyo, <b>Japan</b> .	
2003	Schmelting et al.	Radiographic, Stages 1-5	Ossification and epiphyseal fusion of the medial epiphysis of the <b>clavicle</b> is recorded for living patients that were x-rayed between 1995- 2000 in Berlin, <b>Germany</b> .	Age at fusion was recorded and differences in sex were recorded.
2005	Crowder and Austin	Radiographic, Stages 1-4	Epiphyseal fusion of the distal <b>tibia</b> and <b>fibula</b> is looked at in living patients from <b>America</b> .	Females fused before males. Males of African and Mexican descent completed fusion significantly earlier than males of European descent.
2005	Schaefer and Black	Dry bone, Stages 0-4	Data from McKern and Stewart, (1957) was compared with <b>Bosnian</b> male soldiers who died in the fall of Srebrenica.	The Bosnian sample was found to be more skeletally advanced than the American soldiers. This is thought to be due to genetic differences.
2007	Coqueugniot and Weaver	Dry bone, Stages a-c	Epiphyseal fusion was reviewed on a variety of bones from the skeleton in a sample of individuals from Coimbra, <b>Portugal</b> .	Stage of fusion was recorded in 137 skeletons between 7-29 years of age. Females were found to fuse earlier on average. The data was compared to previous studies.
2008	Belcastro et al.	Dry bone, Stages 0-3	Fusion of the <b>sacrum</b> was looked at in a Sardinian, <b>Italian</b>	Females fused earlier than males. Italian men were

			sample and a Coimbra, <b>Portuguese</b> sample.	found to fuse later than Portuguese men.
2008b	Schaefer	Dry bone, Stages 0-2	Epiphyseal fusion is recorded in various bones of Bosniak ( <b>Bosnian</b> Muslim) males who died during the fall of Srebrenica.	Stage of fusion is recorded for ages.
2008	O'Connor et al.	Radiographic, Stages 0-4	Epiphyseal fusion within an <b>Irish</b> population of the <b>knee</b> .	Females develop quicker than males. Strongest relationship between chronological age and epiphyseal fusion on certain bones and differ between the sexes. Potential positive secular trend.
2008	Rios et al.	Dry bone, Stages 0-4	<b>Sacral</b> fusion in a skeletal sample from Lisbon, <b>Portuguese</b> .	Females develop quicker than males in the earlier stages of fusion. Earlier fusion was found to be the best for age estimation.
2008a	Cardoso	Dry bone, Stages 1-3	Epiphyseal fusion is looked at in the upper skeleton in a Lisbon, <b>Portuguese</b> sample.	Fusion sequence is recorded, and females are found to fuse earlier than males. Age ranges for fusion are found to be similar to previous studies.
2008b	Cardoso	Dry bone, Stages 1-3	Epiphyseal fusion is looked at in the lower	Females fuse earlier than males. Age of fusion

			skeleton in a Lisbon, <b>Portuguese</b> sample.	similar to previous studies.
2009	Schaefer et al.	N/A	Gives average ages at fusion for various bones based off of previous studies.	N/A
2009	Hawley et al.	Radiographic, Greulich & Pyle atlas	The <b>hand and wrist</b> were assessed in <b>South Africans</b> from 1962 and 2001.	White children from the later cohort were found to be skeletally more advanced than the earlier children, but this was non-significant. The same was found for black children, but the results were significant. This may be due to racism, in which the black population were given access to similar circumstances as whites.
2010	Langley-Shirley and Jantz	Dry bone, various	<b>American</b> samples were used to look at epiphyseal union of the <b>medial clavicle</b> . The results were then compared to the study by McKern and Stewart, (1957).	Out of the various methods used, the three-phase system was found to be the least subjective. Females were found to fuse earlier than men. Modern Americans were found to fuse earlier than both 20 <sup>th</sup> century Americans and the American males who died in the Korean war.
2010	Calfee et al.	Radiograph, Greulich & Pyle atlas	Wanted to test whether skeletal and chronological age matched in the left	Skeletal age was found to be greater than chronological age.

			<b>hand and wrist</b> of contemporary <b>American</b> children.	
2010	Coqueugniot et al.	Dry bone, Stages a-c	Epiphyseal fusion on multiple sites of the skeleton from a skeletal sample from <b>Coimbra, Portugal.</b>	The more fusion sites used, the more accurate age estimation becomes for sub-adults, but only to a certain point. Some fusion sites, such as the pelvis provide more accurate age estimates because the pelvis has multiple fusion sites that cover a wide range of ages.
2010	Cardoso and Severino	Dry bone, Stages 1-3	Studied epiphyseal fusion in the <b>hands</b> and <b>feet</b> of the <b>Lisbon, Portuguese</b> skeletal sample.	Sex differences and age range were charted.
2011	Shirley and Jantz	Dry bone, Stages 1-3	Fusion of the <b>spheno-occipital synchondrosis</b> in a <b>Modern American</b> sample.	Females fused earlier than males. Fusion tended to reflect the age at puberty onset.
2012	Weiss et al.	Radiographic	The first metatarsal should fuse at the basal end between 14-16 years, but can epiphyseal scar remain after this age.	The epiphyseal scar was visible in decreased adults aged at 80 years.

2013	Wittschieber et al.	Radiographic, Various stages	Ossification and fusion of the <b>iliac crest</b> is examined in Münster, <b>Germany</b> .	Age at ossification and fusion was recorded.
2013	Hsieh et al.	Radiographic, Tanner-Whitehouse 3 method	<b>Carpal</b> bones were analysed in <b>Taiwanese</b> children from two generations. The first generation was the agricultural generation from 1966-1967, whereas the second generation was from after the year 2000.	Children from the mid-2000s were found to mature skeletally faster than children from the mid-1960s.
2013a	Cardoso et al.	Dry bone, Stages I-III	Fusion of the <b>ischio-pubic ramus</b> of a Lisbon, <b>Portuguese</b> sample.	Females fused between 5 – 11 years, and males fused between 7-8 years.
2013b	Cardoso et al.	Dry bone, Stages I-III	Fusion within the <b>occipital</b> bone of a Lisbon, <b>Portuguese</b> sample.	Sequence of fusion is documented. No sex differences are found.
2014	Cardoso et al.	Dry bone, Stages 1-3	Fusion of the <b>sacrum</b> in a Lisbon, <b>Portuguese</b> sample.	Sequence of fusion is documented for primary and secondary ossification centres. No sex differences found in pre-puberty fusion, but females found to fuse earlier in post-puberty.

2014	Tirpude et al.	Radiographic, Stages 1-3	Epiphyseal fusion in the bones of the <b>shoulder</b> in <b>Central Indian</b> girls.	Central Indian girls were delayed by 1-3 years compared to East India.
2015	Duren et al.	Radiographic, Fels methods	X-rays of the <b>hand and wrist</b> were looked at for <b>American</b> children between 1930-1964 and 1965-2001.	Skeletal maturity was found to be more advanced in the later cohort. Sex differences were found for certain bones, in that the later cohort for girls were found to be more advanced than the earlier cohort for the density of long bones and projection of the carpals. The later cohort of boys were found to be less advanced than the earlier cohort for long bone shape.
2015	Schaefer et al.	Radiographs, Various phases used	Appearance and fusion of the <b>shoulder</b> in <b>American</b> children.	Threshold ages were implemented in which to provide an ageing technique in Forensic research e.g., females tend to be <16 years if they display an unfused proximal humerus, no secondary centres for the acromion and an unfused or fusing coracoid angle.
2016	Ebeye et al.	Radiographic, Stages 0-4	Epiphyseal fusion of the <b>knee</b> was documented in living	Females fused earlier than males. Age at fusion was documented.

			patients from Delta State, <b>Nigeria</b> .	
2016	Fernández-Pérez et al.	Cone Beam Computed Tomography (CBCT), Various stages	Correlating the fusion of the <b>spheno-occipital</b> synchondrosis with the maturation of the <b>cervical vertebrae</b> in <b>American</b> children.	A correlation was found between the two.
2016	Cunningham et al.	N/A	Gives average ages at fusion for various bones based off of previous studies.	N/A
2016	Langley	Dry bone, Stages 1-3	Epiphyseal fusion of the <b>lateral clavicle</b> in autopsied <b>American</b> whites.	Females fused earlier than males. Ages were recorded. The epiphysis either fuses as a separate flake or a smoothing over of the diaphysis.
2017	Sullivan et al.	Multi Detector computer tomography scans, Stages 1-3	Fusion timing in the <b>pelvic girdle</b> and <b>proximal femur</b> in a <b>Western Australian</b> population.	Females were found to fuse earlier than males. Ages were found similar to previous research.
2018	Boeyer et al.	Radiographic, Fels method	Examined the left <b>hand and wrist</b> of <b>American</b> children between the years of 1915 to 2006.	A positive secular trend was noted with children born in 1995 maturing earlier than children born in 1935.
2019	Belcastro et al.	Dry bone, Stages 1-5	Examined stages of epiphyseal fusion, including the	Found that the epiphyseal scar was more likely to be found in skeletons whose

			epiphyseal scar in two identified skeletal collections from <b>Portugal and Italy.</b>	age-at-death was 35 years or younger.
2020	Kumar et al.	Radiographic	Epiphyseal fusion was examined in the <b>elbow</b> and <b>wrist</b> of adolescents from the Malwa region of Madhya Pradesh in central <b>India.</b>	No differences were found between the left and right side. No differences were found between groups from different religions of the Malwa region. This sample population fused later than previous studies that looked at Western populations. This is a common finding in Indian studies and could be due to a number of factors.
2020	Shedge et al.	CT (Computed tomography) scans, Stages 1-5	Ossification and epiphyseal fusion is recorded for the medial epiphysis of the <b>clavicle</b> for Jodhpur, <b>India.</b>	Fusion stages of the medial clavicle are correlated with chronological age.
2021	Ebeye et al.	Radiographic, Stages 0-3	Epiphyseal fusion in the distal ends of the <b>radius, ulna, tibia</b> and <b>fibula</b> of children and adolescents in <b>Nigeria.</b>	Females fused earlier than males.

## APPENDIX 2: EPIPHYSEAL FUSION SITES

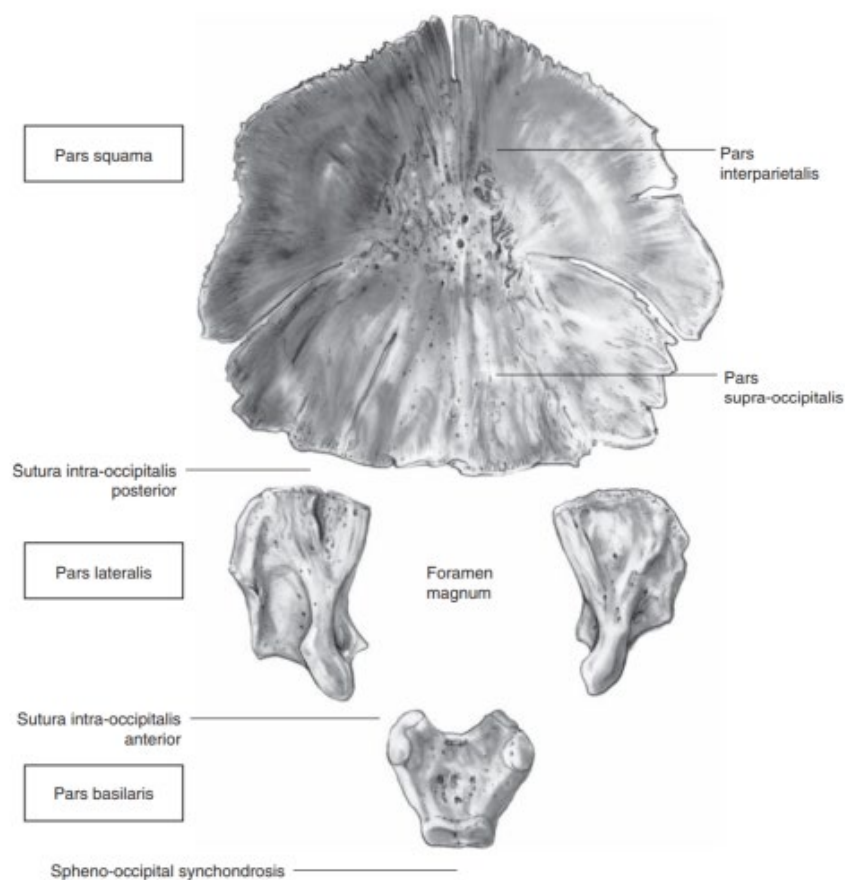
Schaefer et al., (2009) was an essential text for assessing which fusion sites to use within this thesis. Thirty-four fusion sites were chosen to represent skeletal maturation throughout the modern human growth period and are listed below.

Bone	Fusion site
Occipital	Pars lateralis to squama Pars lateralis to pars basilaris Spheno-occipital synchondrosis
Cervical vertebrae	Anterior arch of C1 Posterior synchondrosis of C1 Ossiculum terminale of the C2 Dentoneural synchondrosis of C2 Dentocentral & neurocentral junctions of C2 Posterior synchondrosis of C2
Sacrum	Sacral bodies 1 – 2
Clavicle	Medial epiphysis Lateral epiphysis
Scapula	Coracoid Acromial epiphysis Medial border Inferior angle epiphysis
Humerus	Medial humeral epicondyle Distal composite epiphysis Humeral head
Radius	Proximal epiphysis Distal epiphysis
Ulna	Proximal epiphysis Distal epiphysis
Hand	Heads of metacarpals 2 - 5, proximal and middle phalangeal epiphyses Distal phalanges
Os coxae	Ischiopubic ramus Iliac crest Acetabulum
Femur	Femoral head Greater trochanter Lesser trochanter Distal epiphysis
Tibia	Proximal epiphysis Distal epiphysis

### A2.1. The Axial skeleton

Ten sites were chosen from the axial skeleton. The below pictures are taken from Schaefer et al., (2009) and illustrate each fusion site that was examined on each skeleton used within this study. The data underneath each figure simply reiterates the fusion sites used in this study that are found in the above table.

The figure below shows the intercranial view of the perinatal **occipital bone** of the skull, as found in Schaefer et al., (2009) on page 4 of *Juvenile Osteology: A Laboratory and Field Manual*.



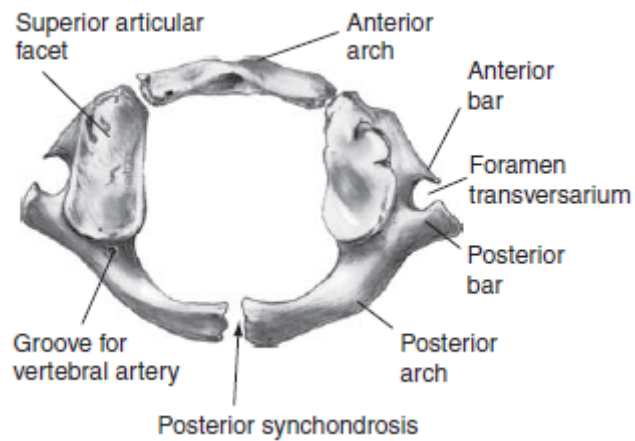
#### *Occipital of the Skull:*

Pars lateralis to squama

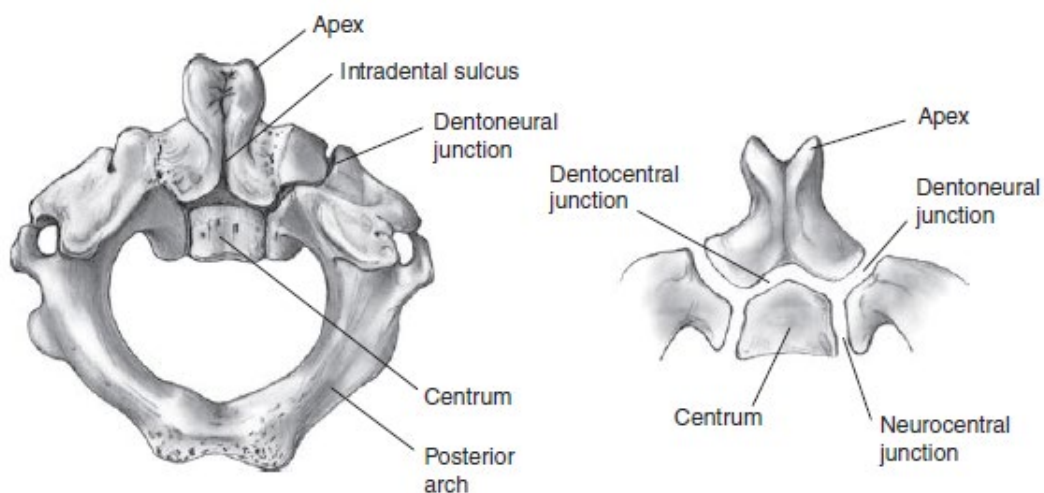
Pars lateralis to pars basilaris

Spheno-occipital synchondrosis

The figure below shows the superior view of the **atlas** (C1) at 2 to 3 years of age, as found in Schaefer et al., (2009) on page 106 of *Juvenile Osteology: A Laboratory and Field Manual*.



The figure below shows the posteriorsuperior view of the **axis** (C2) at 3 years of age, as found in Schaefer et al., (2009) on page 108 of *Juvenile Osteology: A Laboratory and Field Manual*.



***Cervical vertebrae:***

Atlas: Anterior arch

Atlas: Posterior synchondrosis

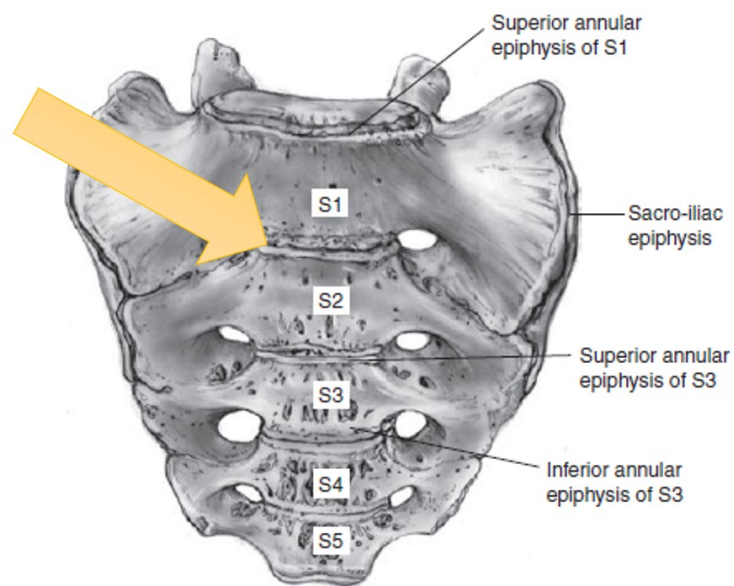
Axis: Ossiculum terminale to the dens

Axis: Dentoneural synchondrosis

Axis: Dentocentral and neurocentral junctions

Axis: Posterior synchondrosis

The figure below shows the anterior view of the **sacrum** of a 16 to 18-year-old female, as found in Schaefer et al., (2009) on page 112 of *Juvenile Osteology: A Laboratory and Field Manual*. The arrow has been added to show the area of fusion studied.



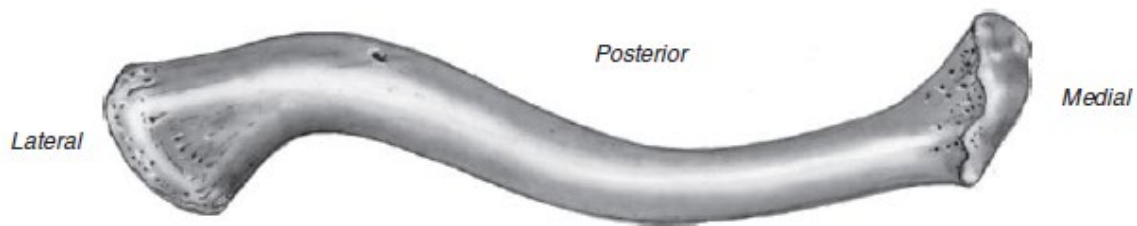
***Sacrum:***

Bodies 1 and 2

## A2.2. The Appendicular skeleton

Twenty-four sites were chosen from the appendicular skeleton. The pictures below are taken from Schaefer et al., (2009) and illustrate each fusion site that was examined on each skeleton used within this study.

The picture below shows the superior view of the right perinatal **clavicle**, as found in Schaefer et al., (2009) on page 140 of *Juvenile Osteology: A Laboratory and Field Manual*.

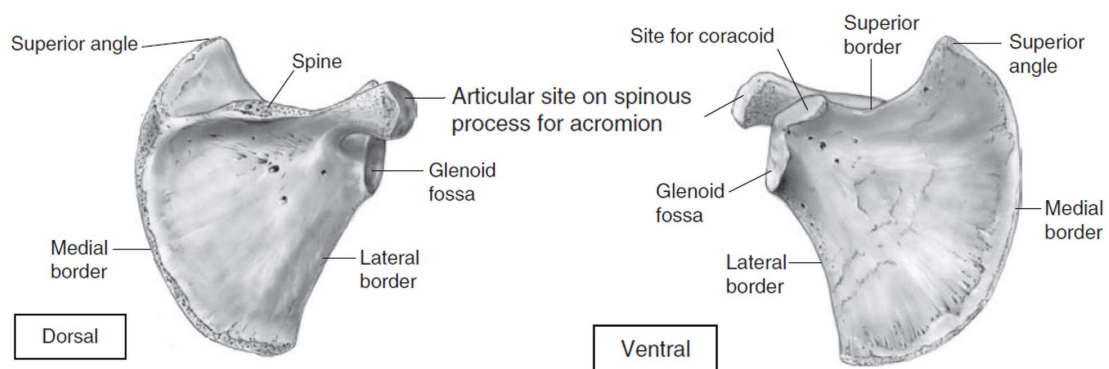


### **Clavicle:**

Medial epiphysis

Lateral epiphysis

The picture below shows the dorsal and ventral view of a right perinatal **scapula**, as found in Schaefer et al., (2009) on page 151 of *Juvenile Osteology: A Laboratory and Field Manual*.



### **Scapula:**

Coracoid

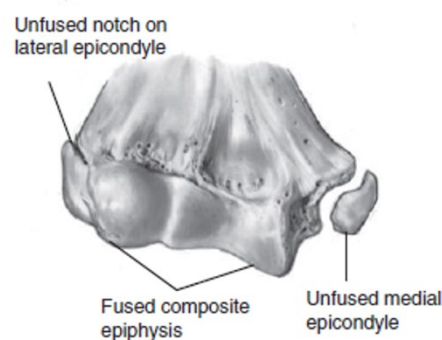
Acromial epiphysis

Epiphyseal islands along the medial border

Inferior angle epiphysis

The fusion of the coracoid can be split into two phases: (1) the fusion of the subcoracoid and coracoid secondary centres, and (2) the coracoid as a unit fusing onto the body of the scapula (Coqueugniot and Weaver, 2007; Schaefer, 2008b). Only the coracoid as a whole, which fuses onto the body of the scapula is considered in this study and the fusion of the subcoracoid centre is ignored, as found in the Coqueugniot and Weaver, (2007) study.

The picture below shows the anterior view of the distal epiphyses of the **humerus** in an adolescent, as found in Schaefer et al., (2009) on page 170 of *Juvenile Osteology: A Laboratory and Field Manual*.



***Humerus:***

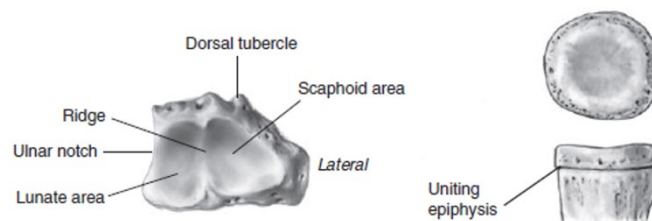
Medial epicondyle

Distal composite epiphysis

Proximal epiphysis

Only the entire proximal and distal epiphyses to the shaft of the humerus were considered in this study and not the individual centres.

The picture below shows a right distal **radial** epiphysis of a late adolescent on the left-hand side of the image and a right proximal radial epiphysis of a late adolescent on the right-hand side of the image, as found in Schaefer et al., (2009) on pages 186 - 187 of *Juvenile Osteology: A Laboratory and Field Manual*.

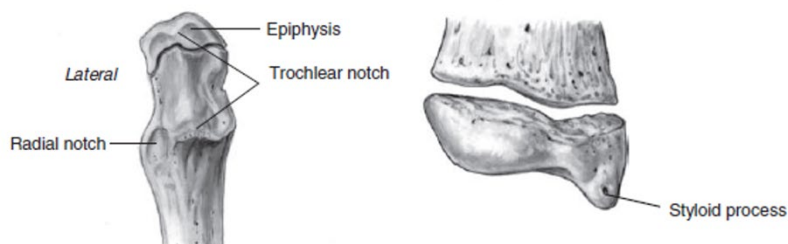


***Radius:***

Proximal epiphysis

Distal epiphysis

The picture below shows a right proximal **ulna** epiphysis of an early adolescent on the left-hand image and a right distal ulna epiphysis of a later stage adolescent on the right-hand image, as found in Schaefer et al., (2009) on pages 202 - 203 of *Juvenile Osteology: A Laboratory and Field Manual*.

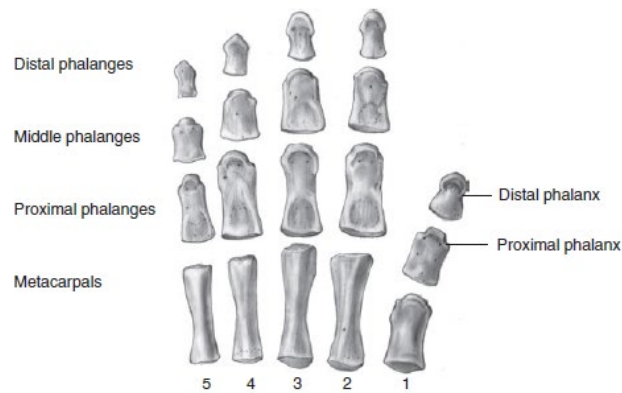


***Ulna:***

Proximal epiphysis

Distal epiphysis

The picture below shows the palmar view of a right perinatal **hand**, as found in Schaefer et al., (2009) on page 214 of *Juvenile Osteology: A Laboratory and Field Manual*.

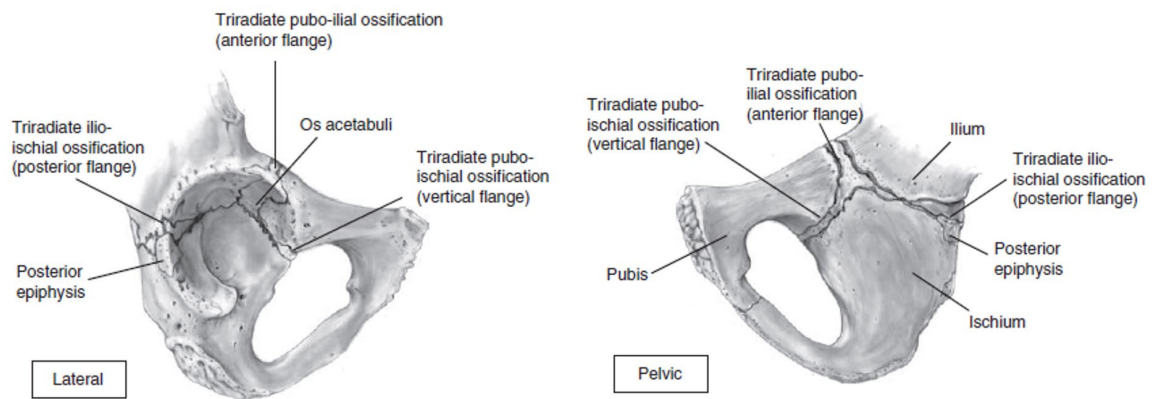


***Hand:***

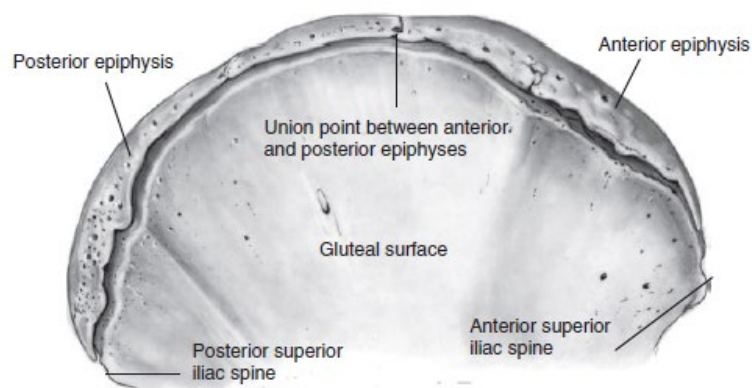
Heads of metacarpals 2 – 5 and the proximal and middle phalangeal epiphyses

Distal phalanges

The picture below shows the lateral and **pelvic** view of the ossification of a right tri-radiate and the acetabular epiphyses of an approximate 15-year-old individual, as found in Schaefer et al., (2009) on page 236 of *Juvenile Osteology: A Laboratory and Field Manual*.



The picture below shows the lateral view of a right ilium and an isolated iliac crest of an approximately 17-year-old individual, as found in Schaefer et al., (2009) on page 238 of *Juvenile Osteology: A Laboratory and Field Manual*.



***Os coxae:***

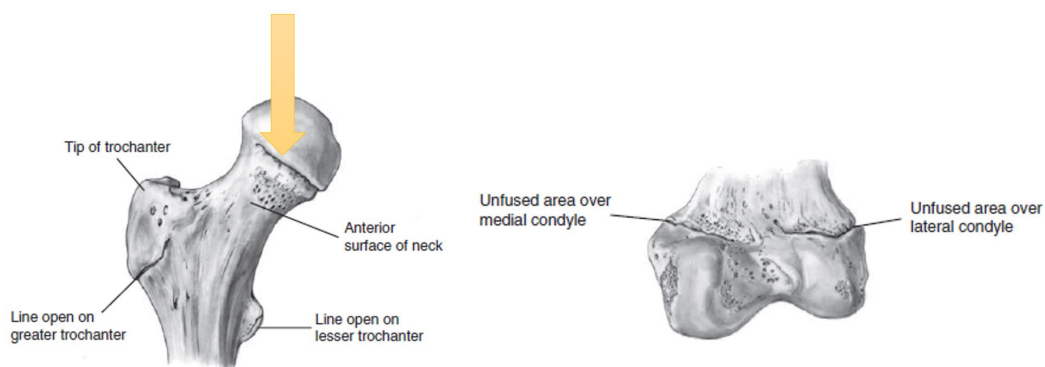
Ischiopubic ramus

Acetabulum

Iliac crest

In some studies, the triradiate unit-acetabulum may be considered separate fusion sites (Cardoso, 2008b; Schaefer, 2008b), whereas other studies may consider the site one functional unit (Schaefer, 2008b; Schaefer et al., 2009). This study agrees with the latter.

The picture below shows the anterior view of the proximal **femur** of a late adolescent on the left-hand side of the image and a posterior view of the distal femur of an adolescent on the right side of the image, as found in Schaefer et al., (2009) on pages 260 - 262 of *Juvenile Osteology: A Laboratory and Field Manual*. The arrow points to a partially fusing femoral head.



***Femur:***

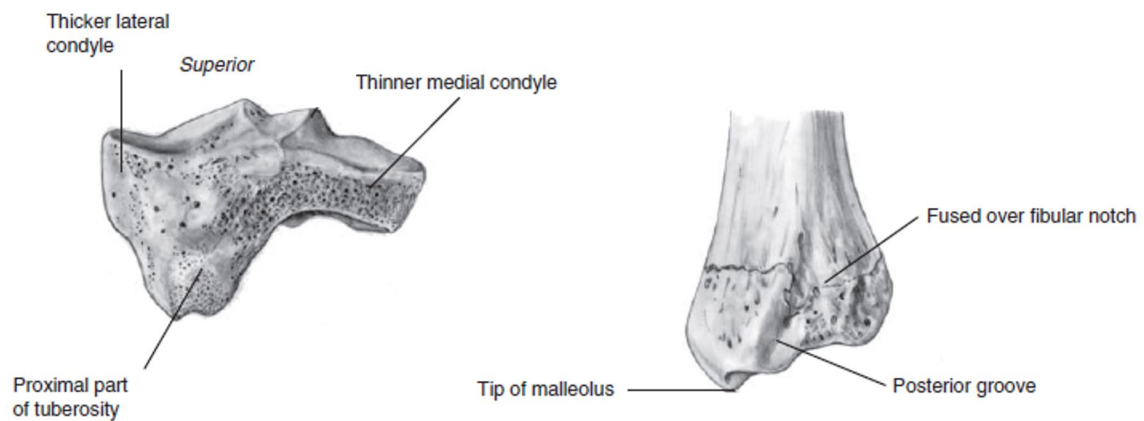
Femoral head

Greater trochanter

Lesser trochanter

Distal epiphysis

The picture below shows the anterior view of a right proximal epiphysis of the tibia of a female aged 14 years old on the left of the image, and the posterior view of a right distal tibia showing the development of the distal tibial epiphysis of an adolescent is on the right of the image, as found in Schaefer et al., (2009) on pages 280 - 282 of *Juvenile Osteology: A Laboratory and Field Manual*.



***Tibia:***

Proximal epiphysis

Distal epiphysis

### APPENDIX 3: CORRECTIONS FOR MULTIPLE COMPARISONS

#### A3.1 Age-at-fusion in St Gregory's

The table below gives a Bonferroni correction to all goodness-of-fit chi-square tests performed on the St Gregory's skeletal data. \*\* = statistically significant.

Fusion sites tested	Chi-square $p$ value	Bonferroni test	Pass or fail of test
Pars lateralis to pars basilaris	0.096		
Spheno-occipital synchondrosis	0.223		
Anterior arch C1	<b>0.001**</b>		✓
Posterior synchondrosis C1	<b>0.001**</b>		✓
Ossiculum terminale	<b>0.015**</b>		X
Dentoneural synchondrosis	<b>0.006**</b>		X
Dentocentral & neurocentral junctions	<b>&lt;0.001**</b>		✓
Posterior synchondrosis C2	<b>0.008**</b>		X
Sacral bodies 1 & 2	0.251		
Medial clavicle	0.179		
Lateral clavicle	<b>0.004**</b>		X
Medial border (Scapula)	0.564		
Acromial border	1.000		
Inferior angle	1.000		
Medial epicondyle (humerus)	0.819	0.05/31 = 0.0016	
Distal composite epiphysis (humerus)	0.074		
Proximal humerus	0.193		
Proximal radius	0.292		
Distal radius	0.115		
Proximal ulna	<b>0.007**</b>		X
Distal ulna	0.056		
Metacarpals	<b>&lt;0.001**</b>		✓
Distal phalanges (hand)	0.180		
Ischiopubic ramus	0.564		
Iliac crest	0.072		
Acetabulum	0.247		
Femoral head	0.196		
Greater & lesser trochanters	0.819		
Distal femur	0.202		
Proximal tibia	0.417		
Distal tibia	0.564		

The table below gives a Bonferroni correction to the Fisher's Exact Test and Fisher-Freeman-Halton Exact tests performed on the St Gregory's skeletal data. \*\* = statistically significant.

<b>Fusion site</b>	<b>p value</b>	<b>Bonferroni correction</b>
Pars lateralis to pars basilaris	1.000	
Spheno-occipital synchondrosis	0.333	
Medial border of scapula	1.000	
Acromial border	1.000	
Inferior angle	1.000	
Medial humeral epicondyle	0.200	
Proximal radius	<b>0.041**</b>	0.05/12 = 0.0042
Distal phalanges of the hand	0.200	
Ischiopubic ramus	1.000	
Distal femur	0.367	
Proximal tibia	0.536	
Distal tibia	1.000	

### A3.2 Puberty in Mediaeval Canterbury

The table below gives a Bonferroni correction for the Mann Whitney U tests performed on puberty data from St Gregory's skeletal collection. \*\* = statistically significant.

<b>Fusion sites tested</b>	<b>p value</b>	<b>Bonferroni correction</b>
Anterior arch C1	0.787	
Posterior synchondrosis C1	0.556	
Ossiculum terminale	<b>0.047**</b>	
Dentocentral & neurocentral junctions	0.162	0.05/8 = 0.0063
Medial clavicle	0.422	
Lateral clavicle	0.460	
Proximal humerus	0.843	
Distal ulna	0.339	

### A3.3 Mediaeval Canterbury compared to other British Mediaeval sites

The table below gives a Bonferroni correction for the Mann Whitney U tests performed on Canterbury compared to other British Mediaeval sites. \*\* = statistically significant.

Fusion sites tested	<i>p</i> value	Bonferroni correction
Ossiculum terminale	<b>0.005**</b>	
Dentoneural synchondrosis	0.251	
Dentocentral and neurocentral junctions	0.602	
Medial epicondyle of the humerus	0.814	0.05/9 = 0.0056
Proximal radius	0.761	
Proximal ulna	0.076	
Iliac crest	0.586	
Greater trochanter	0.683	
Lesser trochanter	0.099	

The table below shows the age groups tested for the multiple regression that looked at the association between age-at-fusion and Mediaeval British sites with a Bonferroni corrections test.

Age groups tested (years)	Significant variables	<i>p</i> value	Bonferroni test
3 – 10	Posterior synchondrosis C1	0.016	
3 - 15	Mediaeval site	0.034	
13 - 20	Ossiculum terminale	<0.001	0.05/6 = 0.0083
13 - 20	Greater trochanter	0.022	
13 - 20	Lesser trochanter	<0.001	
16 – 23	Distal femur	0.011	
16 - 30	No significant results		

### A3.4 Comparing age-at-fusion between Iron age, Roman, Anglo-Saxon, Mediaeval and Post-Mediaeval sites

The table on the next page gives a Bonferroni correction for the Mann Whitney U tests performed on the archaeological data. The grey box shows the only significant *p* value when the Bonferroni test was performed. \*\* = statistically significant

Fusion site	Archaeological groups tested	<i>p</i> value	Bonferroni test
Spheno-occipital synchondrosis	AS. vs. Med.	0.032**	
Anterior arch C1	AS. vs. Med.	0.037**	
Ossiculum terminale	AS. vs. Med.	0.009**	
Dentocentral & neurocentral junctions	AS. vs. Med.	0.037**	
	AS. vs. Med (Stage 2 only)	0.822	
	AS. vs. PM.	0.304	
	AS. vs. PM (Stage 2 only)	0.502	
	Med. vs. PM.	0.062	
Sacral bodies 1 & 2	Med. vs. PM (Stage 2 only)	0.445	
	AS. vs. Med (Stage 2 only)	1.000	
Medial clavicle	Rom. vs. Med.	0.259	
Lateral clavicle	AS. vs. Med.	0.442	
Medial humeral epicondyle	AS. vs. Med.	0.068	
Proximal humerus	AS. vs. Med.	0.688	
Proximal radius	AS. vs. Rom.	0.047**	
	AS. vs. Med.	0.001**	
	Rom. vs. Med.	0.067	
Distal radius	IA. vs. AS.	0.099	
	IA. vs. Med.	0.371	
	AS. vs. Med.	0.019**	
Proximal ulna	AS. vs. Rom. (Stage 2 only)	0.159	
	Rom. vs. Med. (Stage 2 only)	0.055	
	AS. vs. Med. (Stage 2 only)	0.855	0.05/46 =0.0012
Distal ulna	AS. vs. Rom.	0.099	
	Rom. vs. Med.	0.310	
	AS. vs. Med.	0.019**	
Metacarpals	AS. vs. Med.	0.024**	
	AS. vs. PM.	0.046**	
	Med. vs. PM.	0.649	
Iliac crest	AS. vs. Med.	-0.036**	
	AS. vs. Rom.	0.280	
	Rom. vs. Med.	0.263	
Acetabulum	AS. vs. Med.	0.025**	
Proximal femur	AS. vs. Rom.	0.046**	
	AS. vs. Med.	0.007**	
	Rom. vs. Med.	0.371	
Greater trochanter	Rom. vs. Med.	0.027**	
Lesser trochanter	Rom. vs. Med.	0.018**	
	AS. vs. Rom.	0.767	
	AS. vs. Med.	1.000	
Distal femur	AS. vs. Med.	0.005**	
Proximal tibia	IA. vs. Rom.	0.046**	
	IA. vs. Med.	0.007**	
	IA. vs. AS.	0.197	
	AS. vs. Rom.	0.072	
	Rom. vs. Med.	0.477	

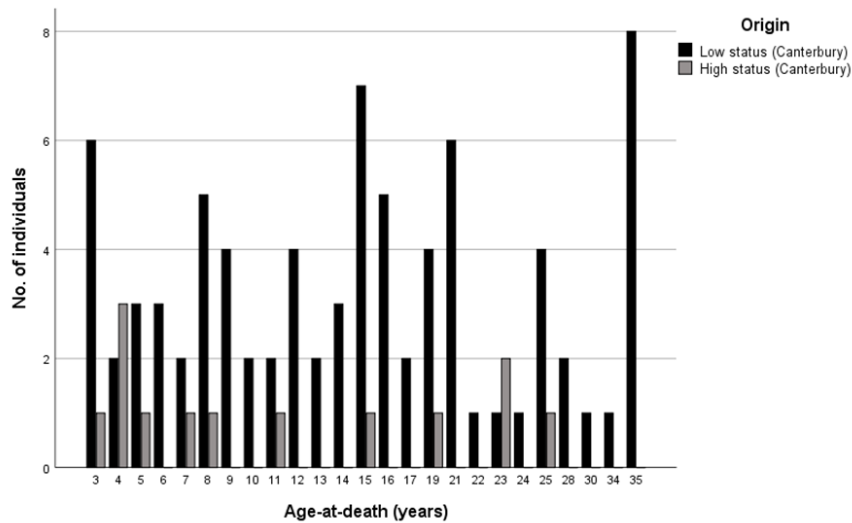
The table below shows the age groups tested for the multiple regression that looked at the association between age-at-fusion and archaeological sites with a Bonferroni corrections test.

Age groups tested (years)	Significant variables	<i>p</i> value	Bonferroni test
3 - 10	Pars lateralis to pars basilaris	<0.001	0.05/7 = 0.0071
	Dentoneural synchondrosis	0.027	
3 - 15	Ossiculum terminale	<0.001	
	Dentocentral & neurocentral junctions	0.031	
12 - 19	Medial humeral epicondyle	<0.001	
13 - 20	Greater trochanter	<0.001	
13 - 20	Period	0.021	
	Lesser trochanter	<0.001	
	Distal femur	0.015	
16 - 23	No significant results		
16 - 30	Sacral bodies 1 & 2	0.018	

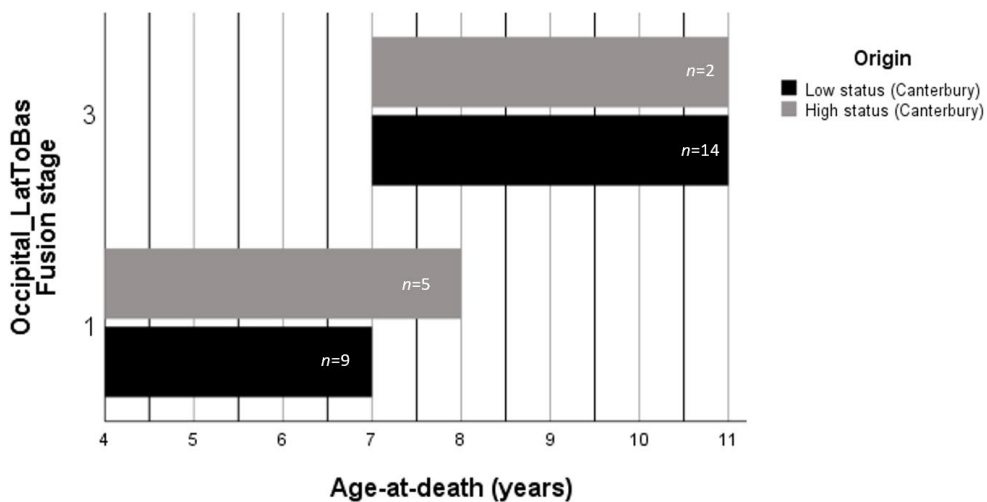
**APPENDIX 4: AGE-AT-FUSION BETWEEN HIGH AND LOW STATUS ST  
GREGORY'S SKELETAL COLLECTION**

**A4.1 The Skull**

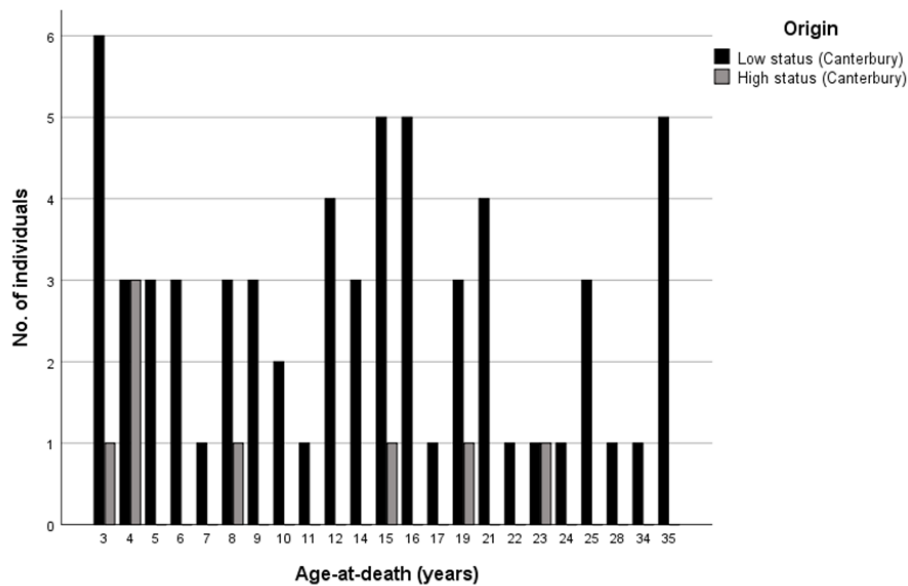
The figure below shows the age distribution for low-status and high-status individuals from Canterbury for the fusion of the **pars lateralis to pars basilaris** of the occipital bone. This shows the entire sub-sample that had these bones present.



The figure below shows the timing of fusion for low-status and high-status individuals from Mediaeval Canterbury for the **pars lateralis to pars basilaris**. Stage 1 (unfused), Stage 3 (fused).



The below figure shows the age distribution for low-status and high-status individuals from Canterbury for the fusion of the **spheno-occipital synchondrosis** of the occipital bone. This shows the entire sub-sample that had these bones present.

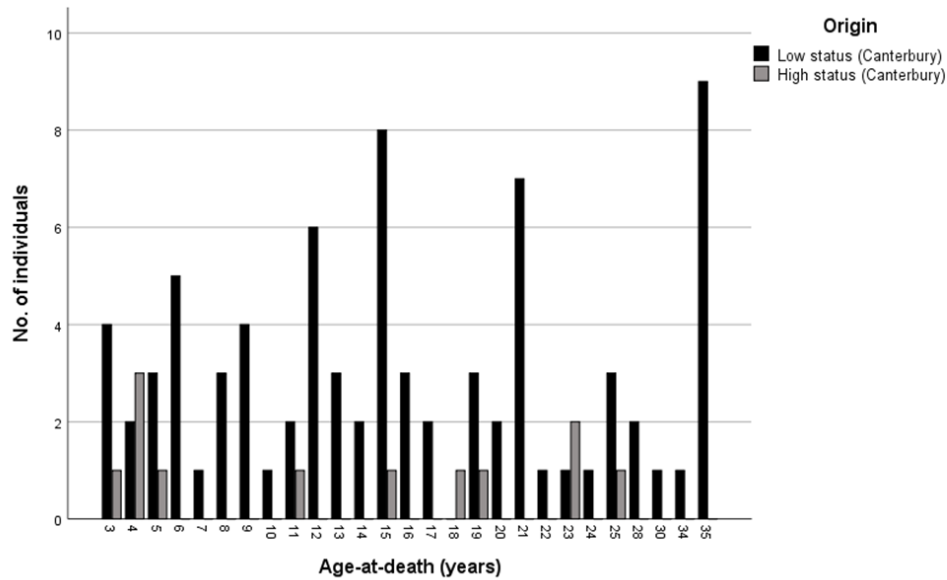


The table below gives the age-at-fusion for St Gregory’s skeletal collection divided by high and low status and compared to the entire sample for the pars lateralis to the pars basilaris and the spheno-occipital synchondrosis of the occipital bone of the skull.

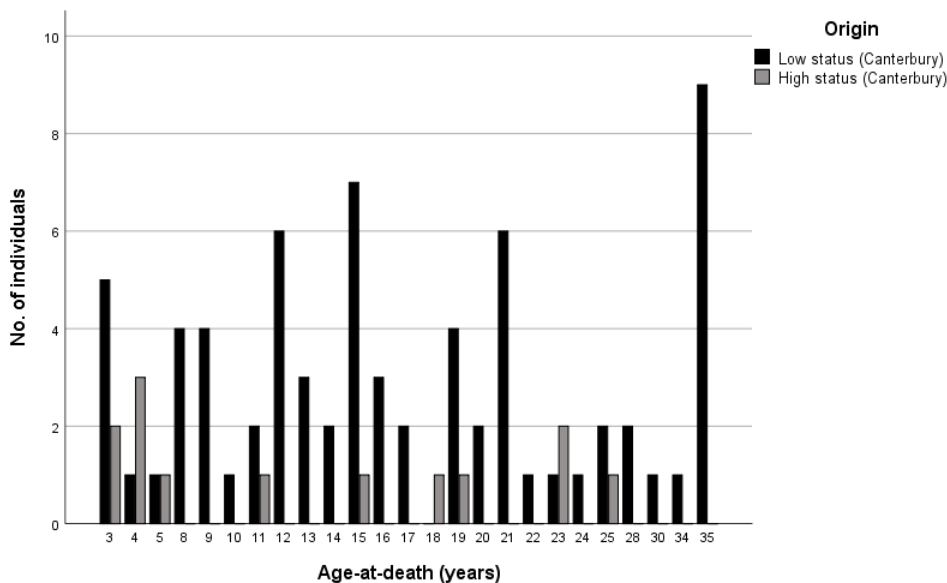
		Entire Sample				Low status				High-status						
		Stage of union				Stage of union				Stage of union						
		Age	<i>n</i>	1	3	Age	<i>n</i>	1	3	Age	<i>n</i>	1	3			
<i>The Occipital of the skull</i>	<i>Pars lateralis to pars basilaris</i>	4	5	100.0	–	4	2	100.0	–	4	3	100.0	–			
		5	4	100.0	–	5	3	100.0	–	5	1	100.0	–			
		6	3	100.0	–	6	3	100.0	–	7	1	–	100.0			
		7	3	33.3	66.7	7	2	50.0	50.0	8	1	100.0	–			
		8	6	16.7	83.3	8	5	–	100.0	11	1	–	100.0			
		9	4	–	100.0	9	4	–	100.0							
		10	2	–	100.0	10	2	–	100.0							
		11	3	–	100.0	11	2	–	100.0							
<i>Spheno-occipital synchondrosis</i>		Age	<i>n</i>	1	2	3	Age	<i>n</i>	1	2	3	Age	<i>n</i>	1	2	3
		14	3	100.0	–	–	14	3	100.0	–	–	15	1	100.0	–	–
		15	6	100.0	–	–	15	5	100.0	–	–	19	1	–	–	100.0
		16	5	80.0	20.0	–	16	5	80.0	20.0	–					
		17	1	–	–	100.0	17	1	–	–	100.0					
	19	4	–	–	100.0	19	3	–	–	100.0						

### A4.2. The Cervical vertebrae

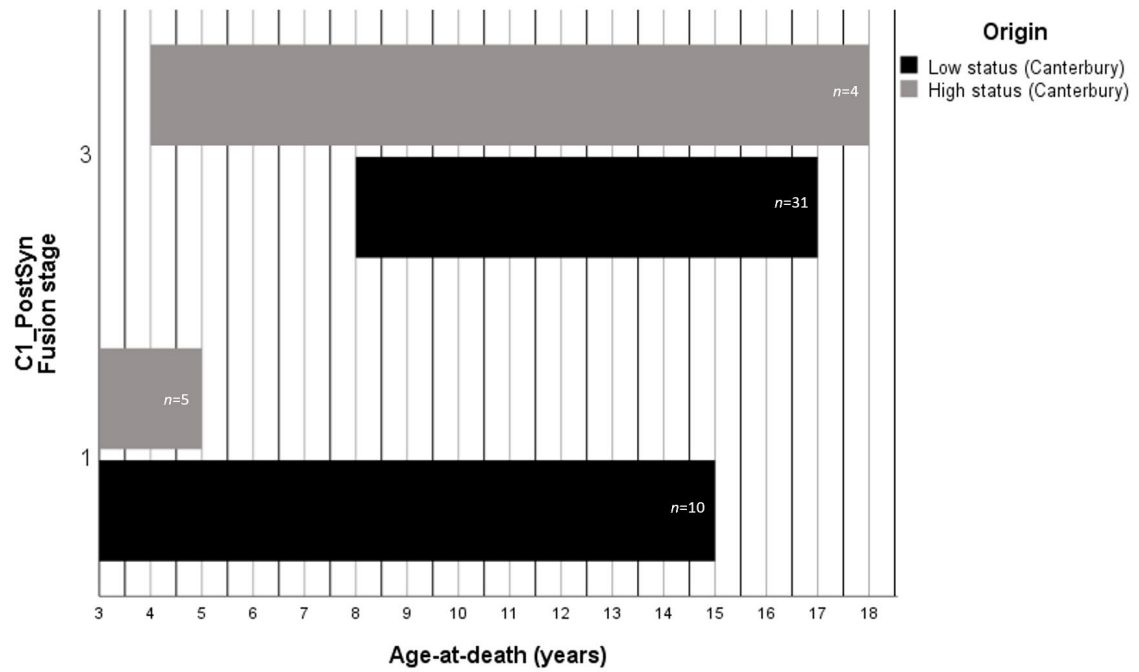
The figure below shows the age distribution for low-status and high-status individuals from Canterbury for the **anterior arch of the atlas (C1)** of the cervical vertebrae column. This shows the entire sub-sample that had these bones present.



The figure below shows the age distribution for low-status and high-status individuals from Canterbury for the fusion of the **posterior synchondrosis of the atlas (C1)**. This shows the entire sub-sample that had these bones present.



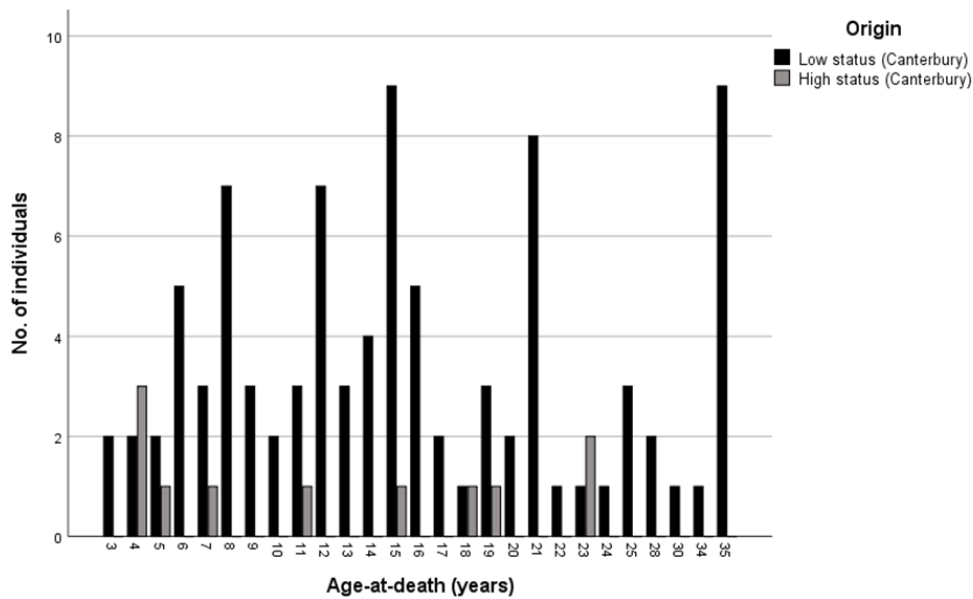
The figure below shows the timing of fusion for low-status and high-status individuals from Mediaeval Canterbury for the fusion of the **posterior synchondrosis of the atlas (C1)**. Stage 1 (unfused), Stage 3 (fused).



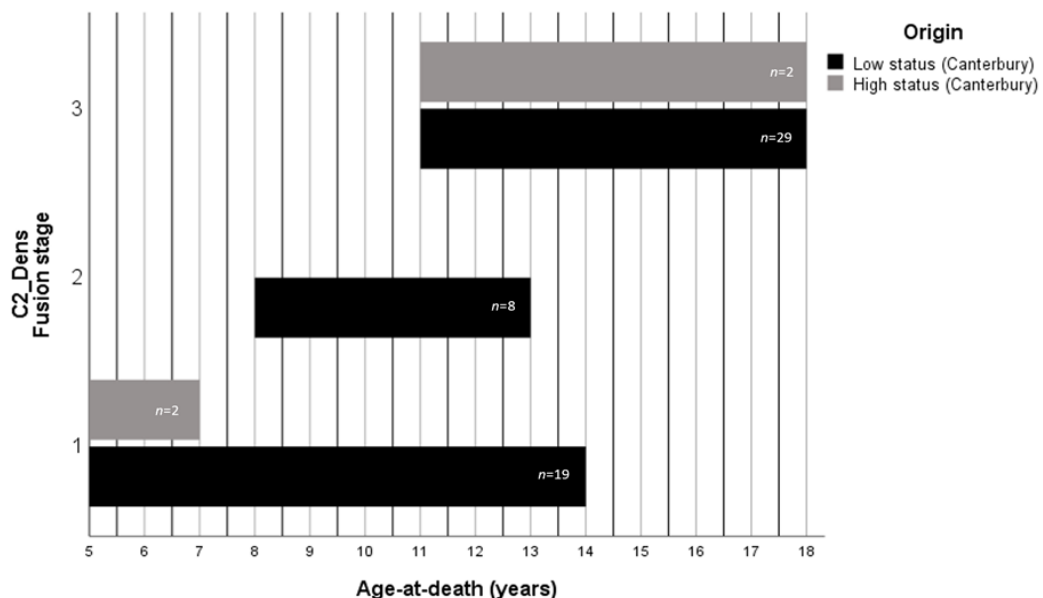
The table below gives the age-at-fusion for St Gregory's skeletal collection divided by high and low status and compared to the entire sample for the anterior arch and posterior synchondrosis of the **atlas of the cervical vertebrae**.

		Entire sample					Low status					High status					
		Stage of union					Stage of union					Stage of union					
		Age	<i>n</i>	1	2	3	Age	<i>n</i>	1	2	3	Age	<i>n</i>	1	2	3	
<i>The atlas</i>	Anterior arch	5	4	100.0	–	–	5	3	100.0	–	–	5	1	100.0	–	–	
		6	5	100.0	–	–	6	5	100.0	–	–	11	1	–	–	100.0	
		7	1	100.0	–	–	7	1	100.0	–	–	15	1	–	–	100.0	
		8	3	–	–	100.0	8	3	–	–	100.0	18	1	–	–	100.0	
		9	4	–	25.0	75.0	9	4	–	25.0	75.0	19	1	–	–	100.0	
		10	1	–	–	100.0	10	1	–	–	100.0						
		11	3	–	–	100.0	11	2	–	–	100.0						
		12	6	16.7	–	83.3	12	6	16.7	–	83.3						
		13	3	–	–	100.0	13	3	–	–	100.0						
		14	2	–	–	100.0	14	2	–	–	100.0						
		15	9	11.1	–	88.9	15	8	12.5	–	87.5						
		16	3	–	–	100.0	16	3	–	–	100.0						
		17	2	–	–	100.0	17	2	–	–	100.0						
		18	1	–	–	100.0											
				Age	<i>n</i>	1	3	Age	<i>n</i>	1	3	Age	<i>n</i>	1	3		
				3	7	100.0	–	3	5	100.0	–	3	2	100.0	–		
				4	4	75.0	25.0	4	1	100.0	–	4	3	66.7	33.3		
				5	2	100.0	–	5	1	100.0	–	5	1	100.0	–		
		8	4	–	100.0	8	4	–	100.0	11	1	–	100.0				
		9	4	25.0	75.0	9	4	25.0	75.0	15	1	–	100.0				
		10	1	–	100.0	10	1	–	100.0	18	1	–	100.0				
		11	3	–	100.0	11	2	–	100.0								
		12	6	16.7	83.3	12	6	16.7	83.3								
		13	3	–	100.0	13	3	–	100.0								
		14	2	–	100.0	14	2	–	100.0								
		15	8	12.5	87.5	15	7	14.3	85.7								
		16	3	–	100.0	16	3	–	100.0								
		17	2	–	100.0	17	2	–	100.0								

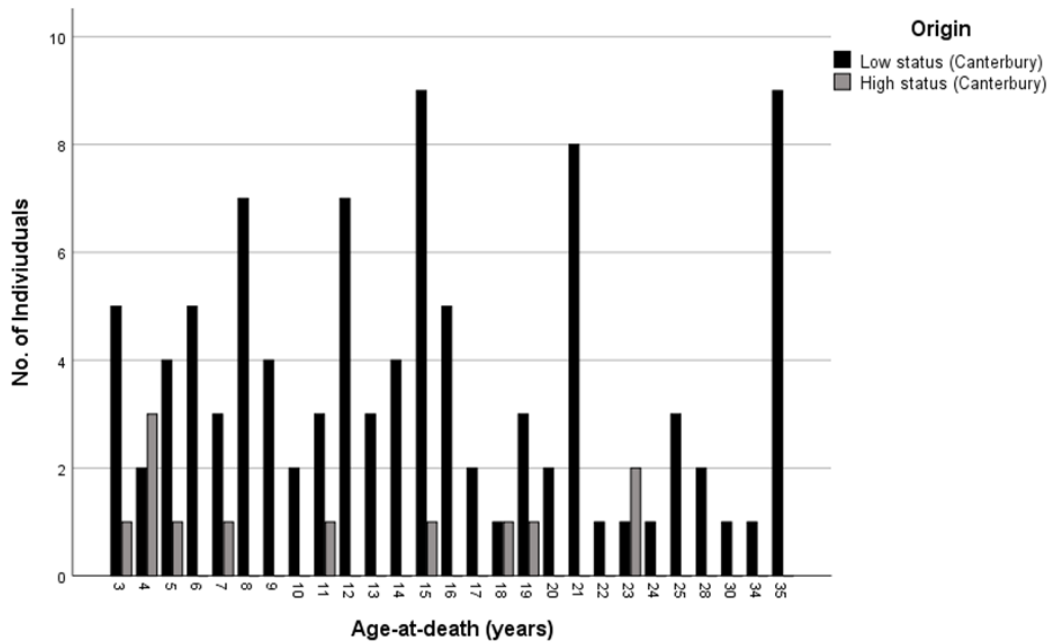
The figure below shows the age distribution for low-status and high-status individuals from Canterbury for the fusion of the **ossiculum terminale to the dens of the axis (C2)**. This shows the entire sub-sample that had these bones present.



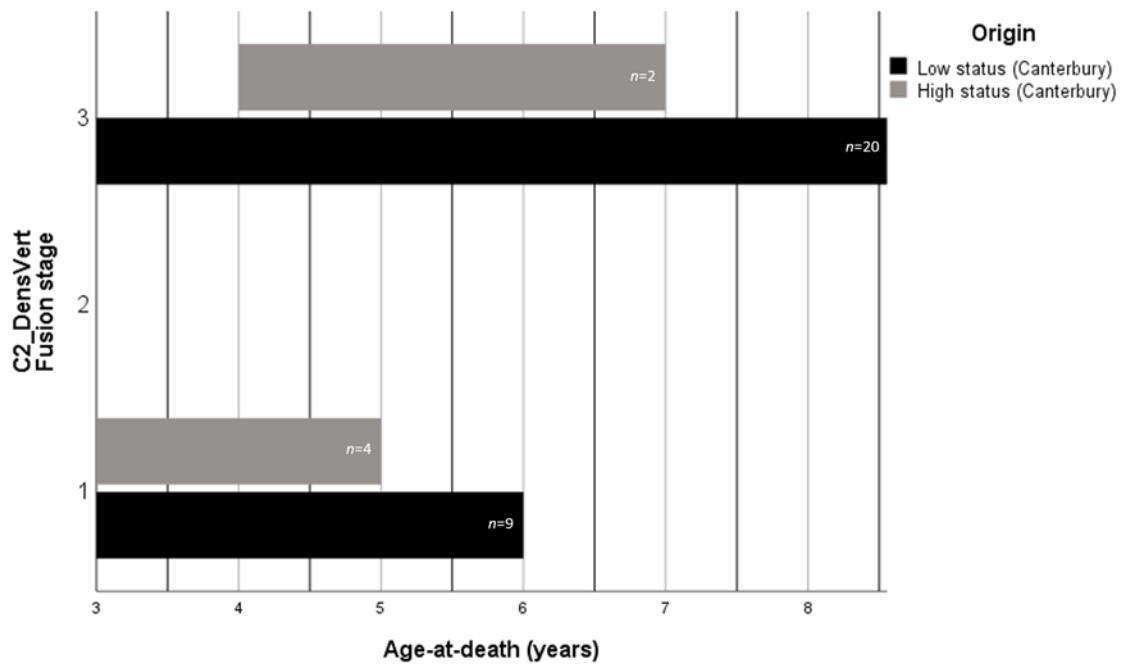
The figure below shows the timing of fusion for low-status and high-status individuals from Mediaeval Canterbury for the fusion of the **ossiculum terminale to the dens of the axis (C2)**. Stage 1 (unfused), Stage 2 (fusing), Stage 3 (fused). No Stage 2 is presented on the figure for the high-status group due to only one data point.



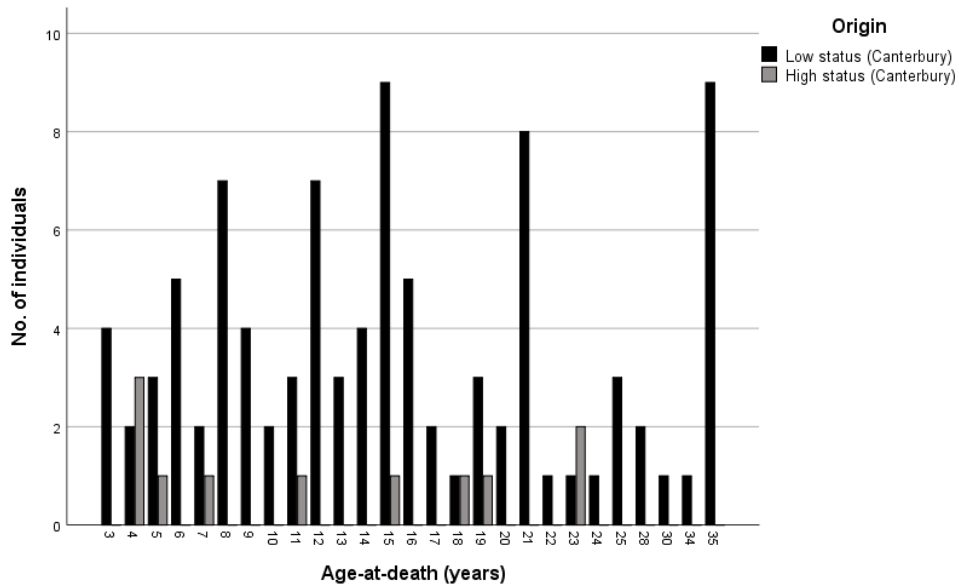
The below figure shows the age distribution for low-status and high-status individuals from Canterbury for the fusion of the **dentoneural synchondrosis of the axis (C2)**. This shows the entire sub-sample that had these bones present.



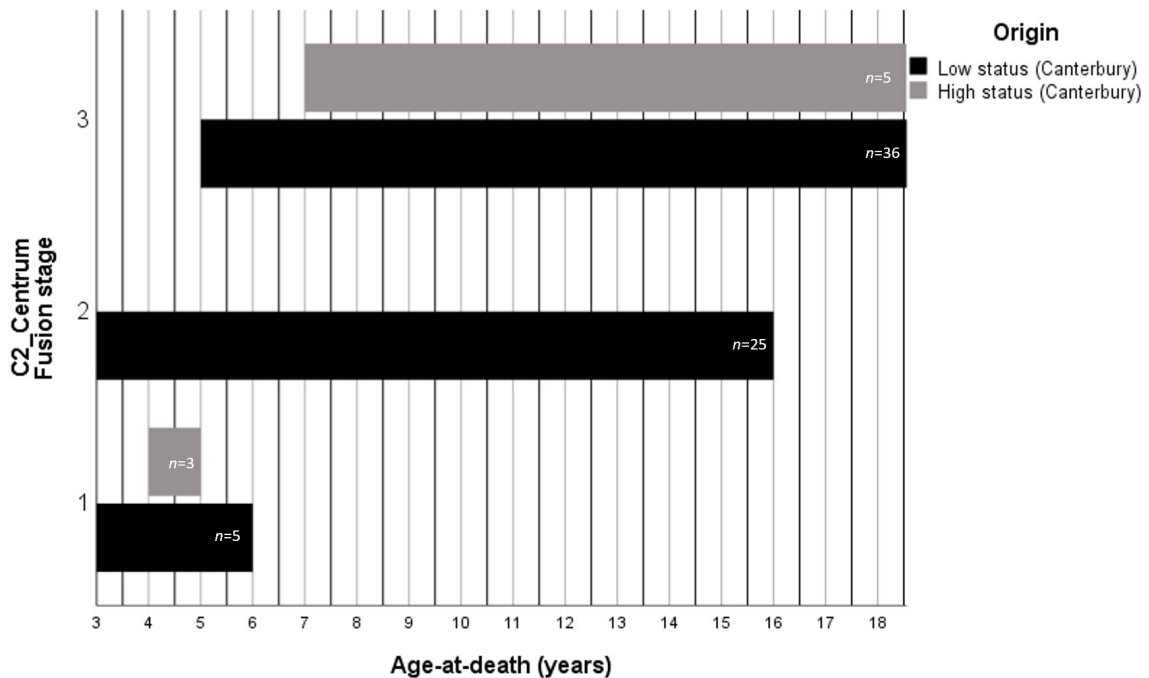
The figure below shows the timing of fusion for low-status and high-status individuals from Mediaeval Canterbury for the fusion of the **dentoneural synchondrosis of the axis (C2)**. Stage 1 (unfused), Stage 2 (fusing), Stage 3 (fused).



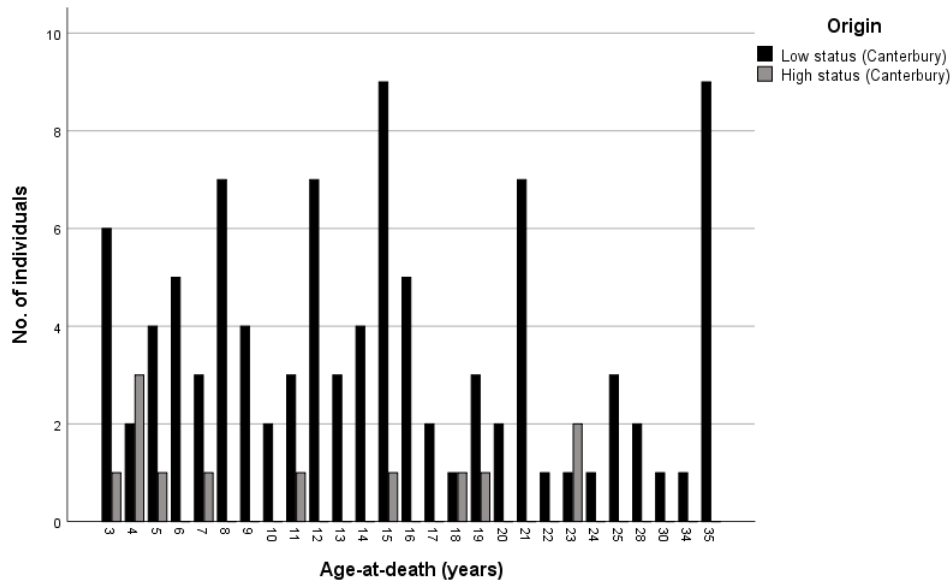
The figure below shows the age distribution for low-status and high-status individuals from Canterbury for the fusion of the **dentocentral and neurocentral junctions of the axis (C2)**. This shows the entire sub-sample that had these bones present.



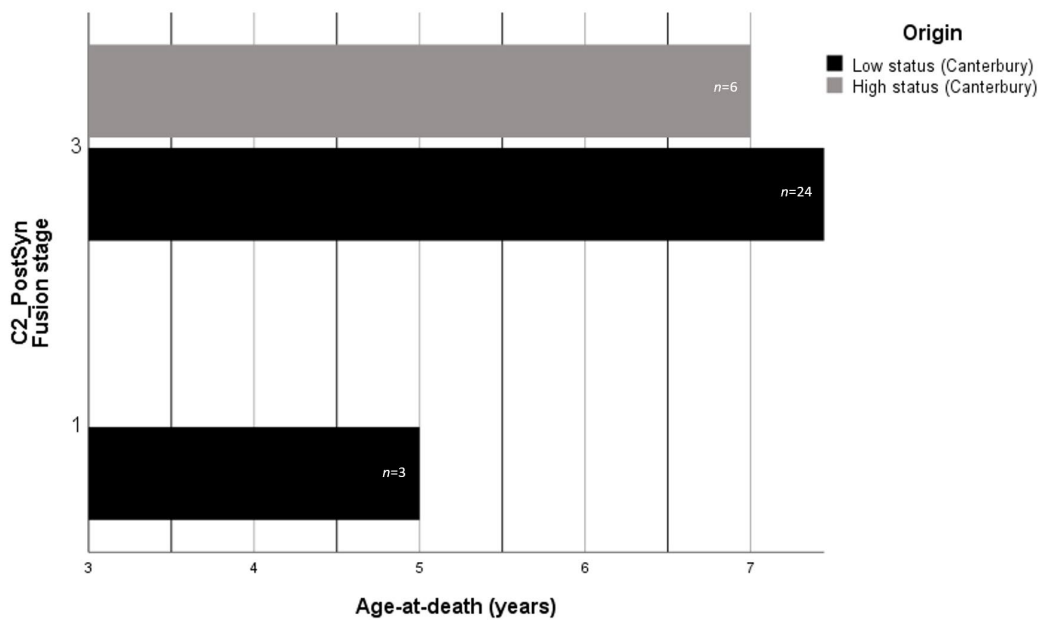
The figure below shows the timing of fusion for low-status and high-status individuals from Mediaeval Canterbury for the fusion of the **neurocentral and dentocentral junction of the axis (C2)**. Stage 1 (unfused), Stage 2 (fusing), Stage 3 (fused). Stage 2 for the high-status group is not shown on the figure as it is a singular data point.



The figure below shows the age distribution for low-status and high-status individuals from Canterbury for the fusion of the **posterior synchondrosis of the axis (C2)**. This shows the entire sub-sample that had these bones present.



The figure below shows the timing of fusion for low-status and high-status individuals from Mediaeval Canterbury for the fusion of the **posterior synchondrosis of the axis (C2)**. Stage 1 (unfused), Stage 3 (fused).



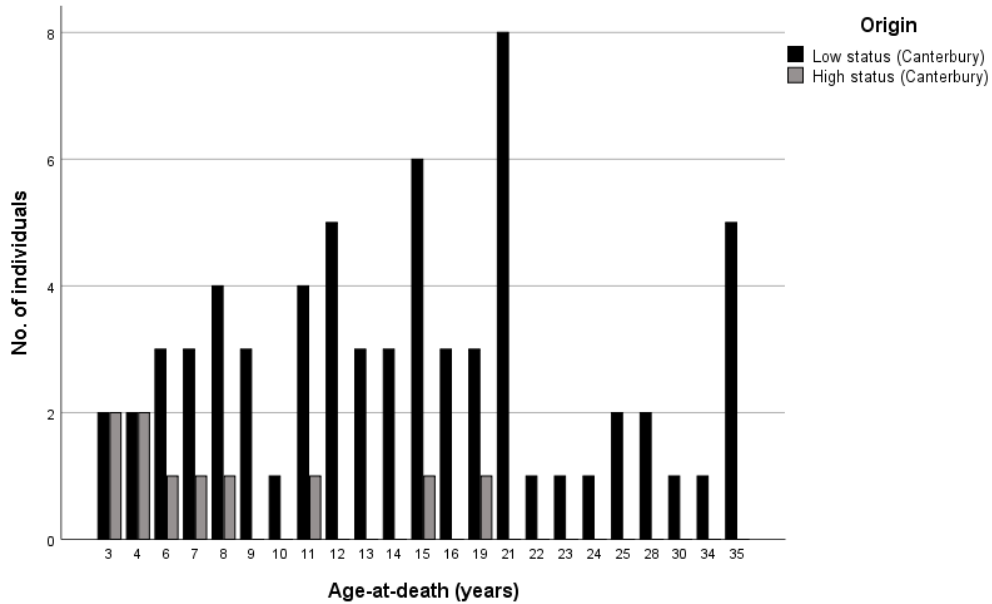
The tables below give the age-at-fusion for St Gregory's skeletal collection divided by high and low status and compared to the entire sample for the ossiculum terminale, the dentoneural synchondrosis, the dentocentral and neurocentral junctions and the posterior synchondrosis of the axis of the cervical vertebrae.

		Entire sample					Low status					High sample						
		Stage of union					Stage of union					Stage of union						
		Age	n	1	2	3	Age	n	1	2	3	Age	n	1	2	3		
<i>The axis</i>	<i>Ossiculum terminale to the dens</i>	5	3	100.0	–	–	5	2	100.0	–	–	5	1	100.0	–	–		
		6	5	100.0	–	–	6	5	100.0	–	–	7	1	100.0	–	–		
		7	4	100.0	–	–	7	3	100.0	–	–	11	1	–	–	100.0		
		8	7	85.7	14.3	–	8	7	85.7	14.3	–	15	1	–	100.0	–		
		9	3	33.3	66.7	–	9	3	33.3	66.7	–	18	1	–	–	100.0		
		10	2	–	100.0	–	10	2	–	100.0	–							
		11	4	25.0	–	75.0	11	3	33.3	–	66.7							
		12	7	–	28.6	71.4	12	7	–	28.6	71.4							
		13	3	–	33.3	66.7	13	3	–	33.3	66.7							
		14	4	25.0	–	75.0	14	4	25.0	–	75.0							
		15	10	–	10.0	90.0	15	9	–	–	100.0							
		16	5	–	–	100.0	16	5	–	–	100.0							
		17	2	–	–	100.0	17	2	–	–	100.0							
		18	2	–	–	100.0	18	1	–	–	100.0							
		<i>Dentoneural synchondrosis</i>		3	6	83.3	–	16.7	3	5	80.0	–	20.0	3	1	100.0	–	–
				4	5	60.0	–	40.0	4	2	50.0	–	50.0	4	3	66.7	–	33.3
				5	5	60.0	–	40.0	5	4	50.0	–	50.0	5	1	100.0	–	–
				6	5	40.0	20.0	40.0	6	5	40.0	20.0	40.0	7	1	–	–	100.0
7	4			–	–	100.0	7	3	–	–	100.0							
8	7			–	–	100.0	8	7	–	–	100.0							
9	4			–	–	100.0	9	4	–	–	100.0							

		Entire sample					Low status					High status						
		Stage of union					Stage of union					Stage of union						
		Age	<i>n</i>	1	2	3	Age	<i>n</i>	1	2	3	Age	<i>n</i>	1	2	3		
<i>The axis</i>	<i>Dentocentral &amp; neurocentral junctions</i>	3	4	75.0	25.0	–	3	4	75.0	25.0	–	4	3	66.7	33.3	–		
		4	5	60.0	40.0	–	4	2	50.0	50.0	–	5	1	100.0	–	–		
		5	4	25.0	50.0	25.0	5	3	–	66.7	33.3	7	1	–	–	100.0		
		6	5	20.0	80.0	–	6	5	20.0	80.0	–	11	1	–	–	100.0		
		7	3	–	66.7	33.3	7	2	–	100.0	–	15	1	–	–	100.0		
		8	7	–	57.1	42.9	8	7	–	57.1	42.9	18	1	–	–	100.0		
		9	4	–	50.0	50.0	9	4	–	50.0	50.0	19	1	–	–	100.0		
		10	2	–	50.0	50.0	10	2	–	50.0	50.0							
		11	4	–	–	100.0	11	3	–	–	100.0							
		12	7	–	71.4	28.6	12	7	–	71.4	28.6							
		13	3	–	33.3	66.7	13	3	–	33.3	66.7							
		14	4	–	25.0	75.0	14	4	–	25.0	75.0							
		15	10	–	–	100.0	15	9	–	–	100.0							
		16	5	–	20.0	80.0	16	5	–	20.0	80.0							
		17	2	–	–	100.0	17	2	–	–	100.0							
		18	2	–	–	100.0	18	1	–	–	100.0							
		19	4	–	–	100.0	19	3	–	–	100.0							
				Age	<i>n</i>	1	2	3	Age	<i>n</i>	1	2	3	Age	<i>n</i>	1	2	3
		<i>Posterior synchondrosis</i>	3	7	28.6	–	71.4	3	6	33.3	–	66.7	3	1	–	–	100.0	
4	5		–	–	100.0	4	2	–	–	100.0	4	3	–	–	100.0			
5	5		20.0	–	80.0	5	4	25.0	–	75.0	5	1	–	–	100.0			
6	5		–	–	100.0	6	5	–	–	100.0	7	1	–	–	100.0			
7	4		–	–	100.0	7	3	–	–	100.0								
8	7		–	–	100.0	8	7	–	–	100.0								

### A4.3. The Sacrum

The figure below shows the age distribution for low-status and high-status individuals from Canterbury for the fusion of **sacral bodies 1 and 2** of the sacrum. This shows the entire sub-sample that had these bones present.

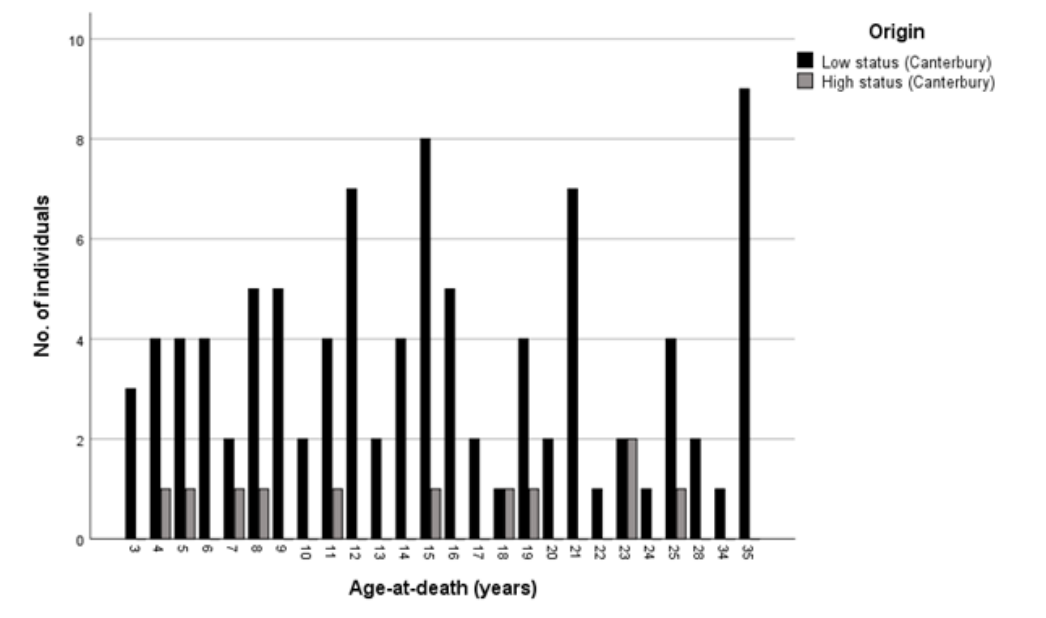


The table below gives the age-at-fusion for St Gregory's skeletal collection divided by high and low status and compared to the entire sample for **bodies 1 and 2** of the sacrum.

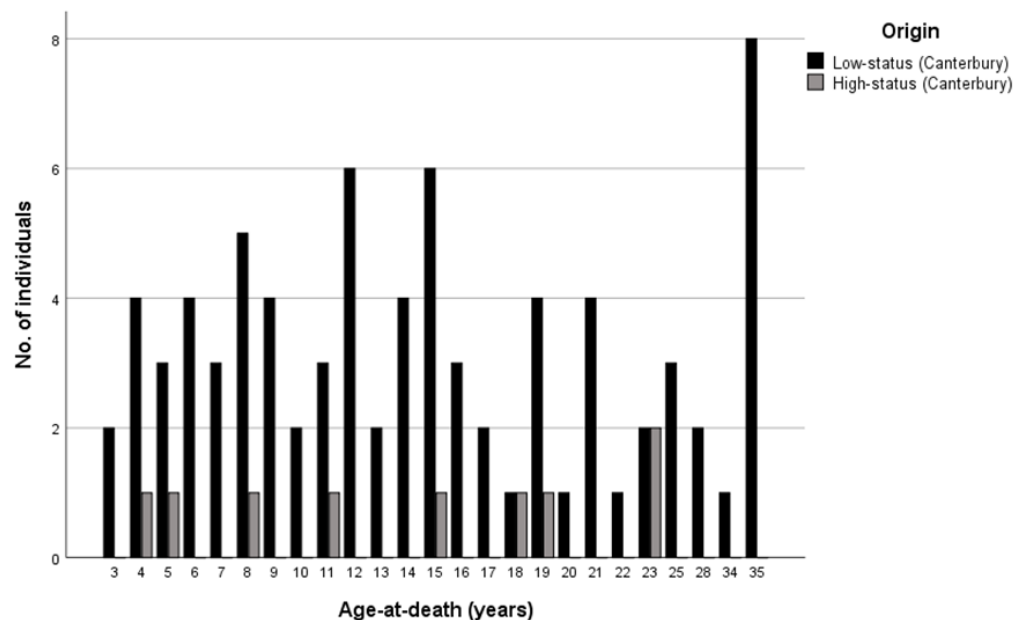
	Entire sample						Low status					High status			
			Stage of union					Stage of union					Stage of union		
	Age	n	1	2	3	Age	n	1	2	3	Age	n	1	2	3
<i>The sacrum</i> <i>Bodies 1 &amp; 2</i>	16	3	100.0	–	–	16	3	100.0	–	–	19	1	–	100.0	–
	19	4	–	75.0	25.0	19	3	–	66.7	33.3					
	21	8	–	75.0	25.0	21	8	–	75.0	25.0					
	22	1	–	100.0	–	22	1	–	100.0	–					
	23	1	–	–	100.0	23	1	–	–	100.0					
	24	1	–	–	100.0	24	1	–	–	100.0					
	25	2	–	100.0	–	25	2	–	100.0	–					
	28	2	–	–	100.0	28	2	–	–	100.0					

#### A4.4. The Clavicle

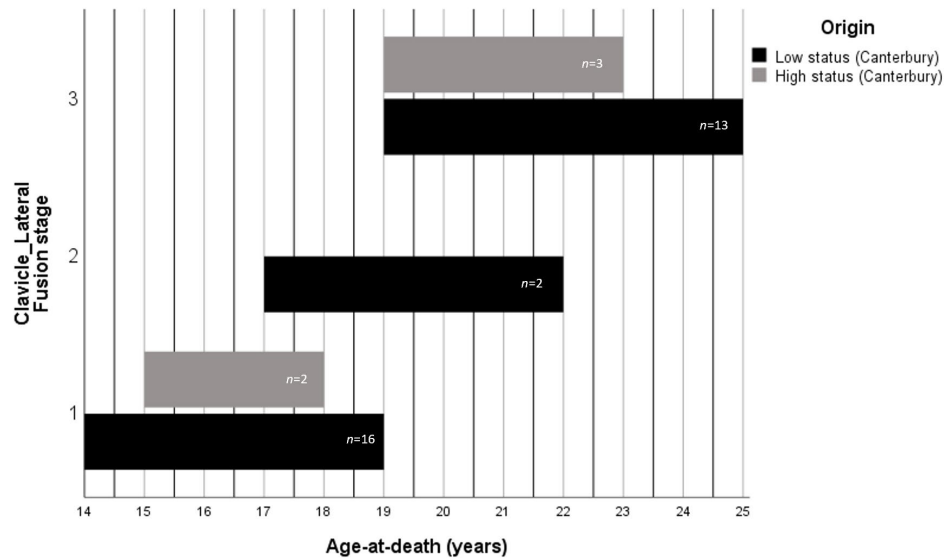
The figure below gives the age distribution for low-status and high-status individuals from Canterbury for the **medial epiphysis of the clavicle**. This shows the entire sub-sample that had these bones present.



The figure below gives the age distribution for low-status and high-status individuals from Canterbury for the **lateral epiphysis of the clavicle**. This shows the entire sub-sample that had these bones present.



The figure below shows the timing of fusion for low-status and high-status individuals from Mediaeval Canterbury for the **lateral clavicle**. Stage 1 (unfused), Stage 2 (fusing), Stage 3 (fused).

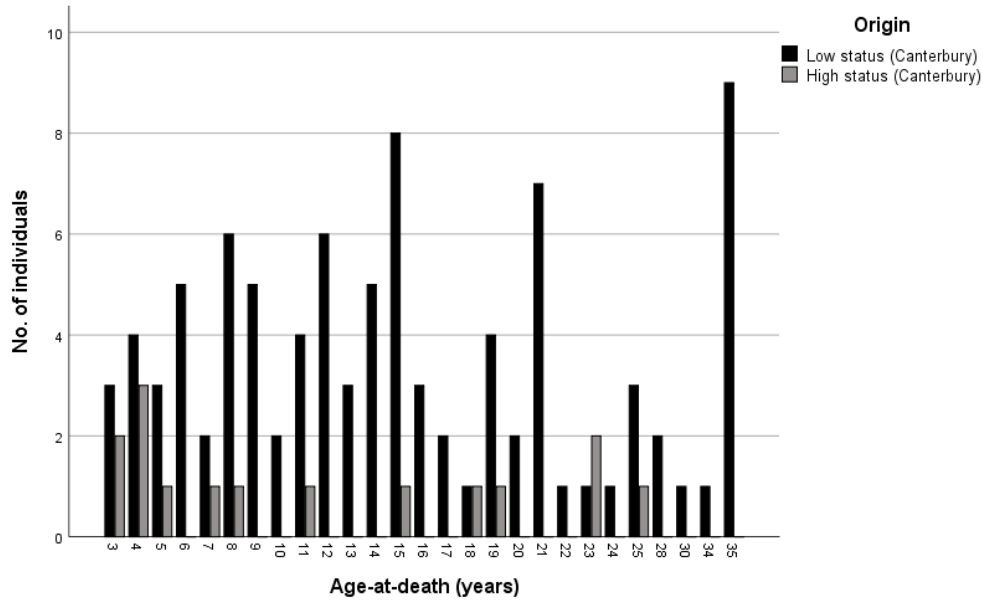


The table below gives the age-at-fusion for St Gregory's skeletal collection divided by high and low status and compared to the entire sample for the medial and lateral epiphyses of the clavicle. When the skeletal samples were subdivided into lower and higher-status groups, fusion commenced at a similar age for both groups, but the high-status individuals finished fusion earlier. However, this could be a product of a small sample size.

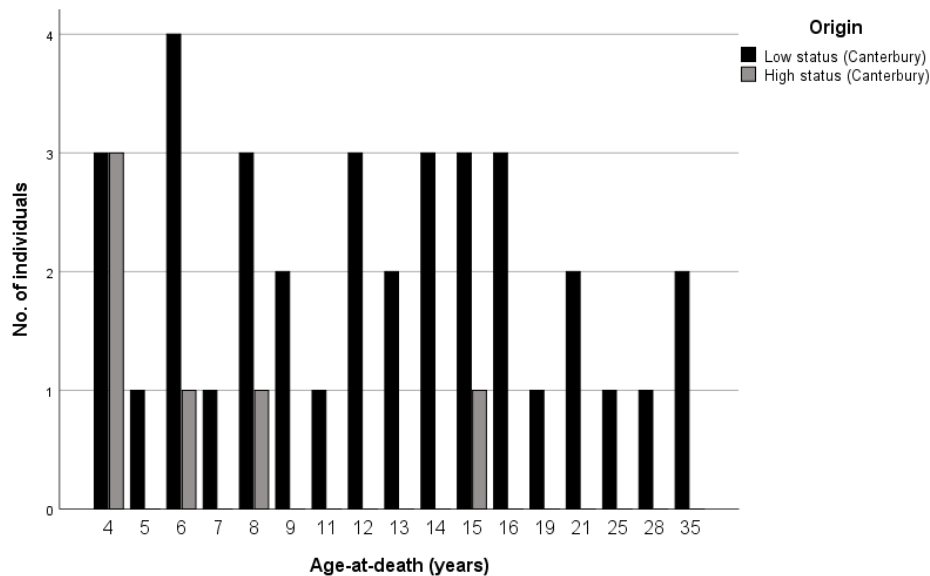
		Entire Sample					Low status					High-status				
		Stage of union					Stage of union					Stage of union				
		Age	<i>n</i>	1	2	3	Age	<i>n</i>	1	2	3	Age	<i>n</i>	1	2	3
<i>Medial epiphysis</i>	<i>The clavicle</i>	16	5	100.0	–	–	16	5	100.0	–	–	18	1	100.0	–	–
		17	2	100.0	–	–	17	2	100.0	–	–	19	1	–	100.0	–
		18	2	100.0	–	–	18	1	100.0	–	–	23	2	–	–	100.0
		19	5	60.0	20.0	20.0	19	4	75.0	–	25.0	25	1	–	–	100.0
		20	2	50.0	–	50.0	20	2	50.0	–	50.0					
		21	7	42.9	28.6	28.6	21	7	42.9	28.6	28.6					
		22	1	100.0	–	–	22	1	100.0	–	–					
		23	4	25.0	–	75.0	23	2	50.0	–	50.0					
		24	1	100.0	–	–	24	1	100.0	–	–					
		25	5	–	20.0	80.0	25	4	–	25.0	75.0					
		28	2	–	–	100.0	28	2	–	–	100.0					
<i>Lateral epiphysis</i>	<i>The clavicle</i>	14	4	100.0	–	–	14	4	100.0	–	–	15	1	100.0	–	–
		15	7	100.0	–	–	15	6	100.0	–	–	18	1	100.0	–	–
		16	3	100.0	–	–	16	3	100.0	–	–	19	1	–	–	100.0
		17	2	50.0	50.0	–	17	2	50.0	50.0	–	23	2	–	–	100.0
		18	2	100.0	–	–	18	1	100.0	–	–					
		19	5	20.0	–	80.0	19	4	25.0	–	75.0					
		20	1	–	–	100.0	20	1	–	–	100.0					
		21	4	–	–	100.0	21	4	–	–	100.0					
		22	1	–	100.0	–	22	1	–	100.0	–					
		23	4	–	–	100.0	23	2	–	–	100.0					
		25	3	–	–	100.0	25	3	–	–	100.0					

### A4.5. The Scapula

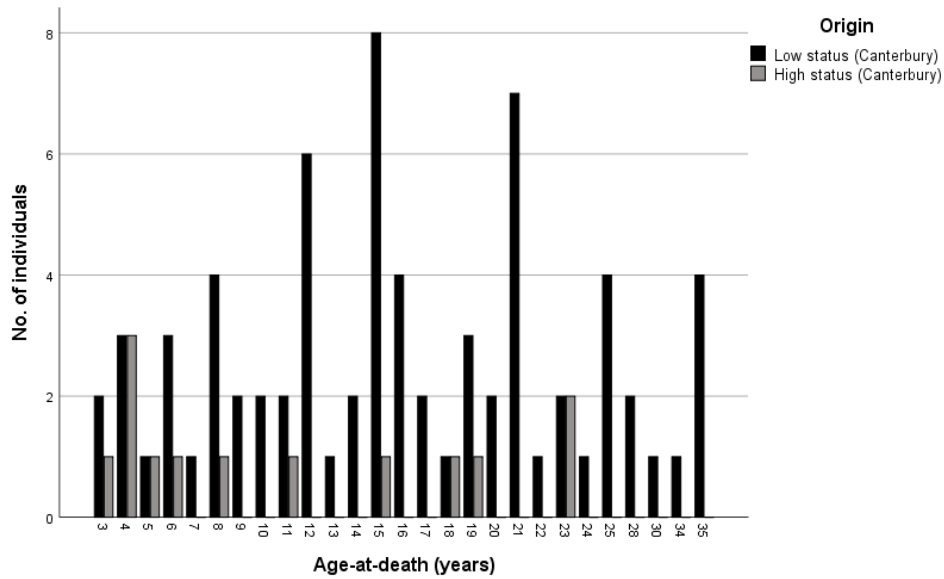
The figure below gives the age distribution for low-status and high-status individuals from Canterbury for the fusion of the **coracoid to the body of the scapula**. This shows the entire sub-sample that had these bones present.



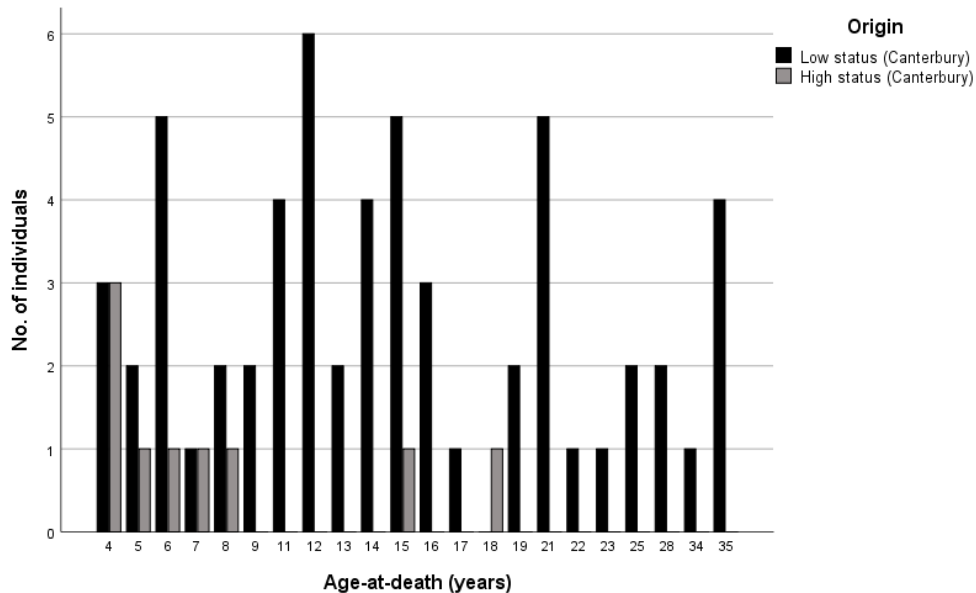
The figure below gives the age distribution for low-status and high-status individuals from Canterbury for the fusion of **medial border of the scapula**. This shows the entire sub-sample that had these bones present.



The figure below gives the age distribution for low-status and high-status individuals from Canterbury for the fusion of the **acromial epiphysis to the scapula**. This shows the entire sub-sample that had these bones present.



The figure below gives the age distribution of low-status and high-status individuals from Canterbury for the fusion of the **inferior angle epiphysis to the scapula**. This shows the entire sub-sample that had these bones present.

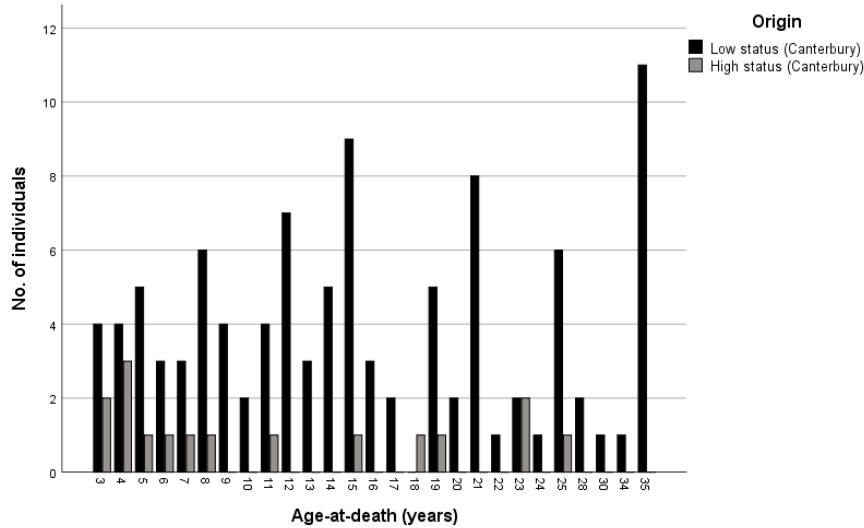


The table below gives the age-at-fusion for St Gregory's skeletal collection divided by high and low status and compared to the entire sample for the coracoid, medial border, acromial epiphysis and the inferior angle epiphysis of the scapula.

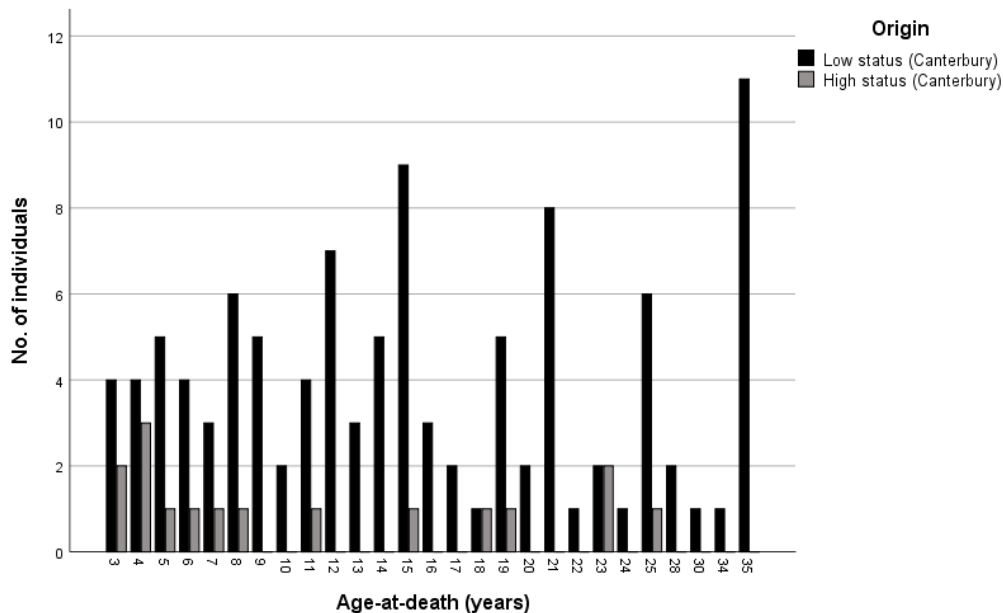
		Entire sample				Low status				High status						
		Stage of union				Stage of union				Stage of union						
		Age	<i>n</i>	1	2	3	Age	<i>n</i>	1	2	3	Age	<i>n</i>	1	2	3
<i>Coracoid</i>		13	3	100.0	–	–	13	3	100.0	–	–	15	1	100.0	–	–
		14	5	100.0	–	–	14	5	100.0	–	–	18	1	–	–	100.0
		15	9	100.0	–	–	15	8	100.0	–	–	19	1	–	–	100.0
		16	3	–	33.3	66.7	16	3	–	33.3	66.7					
		17	2	–	–	100.0	17	2	–	–	100.0					
		18	2	–	–	100.0	18	1	–	–	100.0					
		19	5	–	–	100.0	19	4	–	–	100.0					
<i>Medial border</i>		Age	<i>n</i>	1	3	Age	<i>n</i>	1	3	Age	<i>n</i>	1	3			
		16	3	100.0	–	16	3	100.0	–	15	1	100.0	–			
		19	1	–	100.0	19	1	–	100.0							
		21	2	50.0	50.0	21	2	50.0	50.0							
	25	1	–	100.0	25	1	–	100.0								
<i>The scapula</i> <i>Acromial epiphysis</i>		Age	<i>n</i>	1	3	Age	<i>n</i>	1	3	Age	<i>n</i>	1	3			
		14	2	100.0	–	14	2	100.0	–	15	1	100.0	–			
		15	9	100.0	–	15	8	100.0	–	18	1	–	100.0			
		16	4	100.0	–	16	4	100.0	–	19	1	–	100.0			
		17	2	50.0	50.0	17	2	50.0	50.0							
		18	2	50.0	50.0	18	1	100.0	–							
		19	4	–	100.0	19	3	–	100.0							
		20	2	–	100.0	20	2	–	100.0							
	21	7	–	100.0	21	7	–	100.0								
<i>Inferior angle epiphysis</i>		Age	<i>n</i>	1	3	Age	<i>n</i>	1	3	Age	<i>n</i>	1	3			
		15	6	100.0	–	15	5	100.0	–	15	1	100.0	–			
		16	3	100.0	–	16	3	100.0	–	18	1	–	100.0			
		17	1	100.0	–	17	1	100.0	–							
		18	1	–	100.0	19	2	50.0	50.0							
		19	2	50.0	50.0	21	5	60.0	40.0							
		21	5	60.0	40.0	22	1	–	100.0							
		22	1	–	100.0	23	1	–	100.0							
	23	1	–	100.0												

#### A4.6. The Humerus

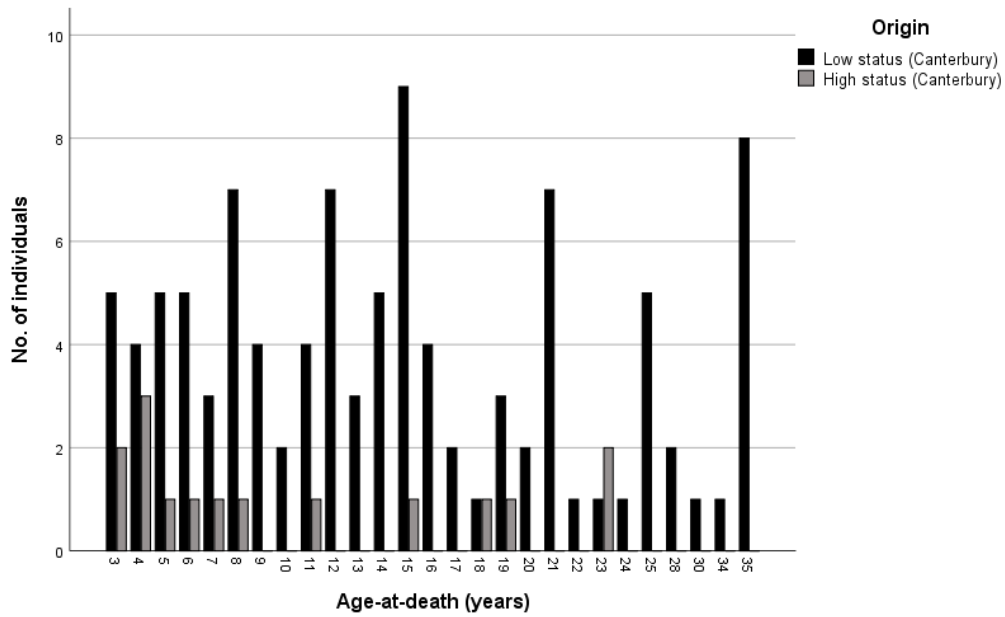
The figure below gives the age distribution for low-status and high-status individuals from Canterbury for the fusion of the **medial epicondyle to the shaft of the humerus**. This shows the entire sub-sample that had these bones present.



The figure below gives the age distribution for low-status and high-status individuals from Canterbury for the **distal composite epiphysis of the humerus**. This shows the entire sub-sample that had these bones present.



The figure below gives the age distribution for low-status and high-status individuals from Canterbury for the fusion of the **proximal epiphysis to the shaft of the humerus**. This shows the entire sub-sample that had these bones present.

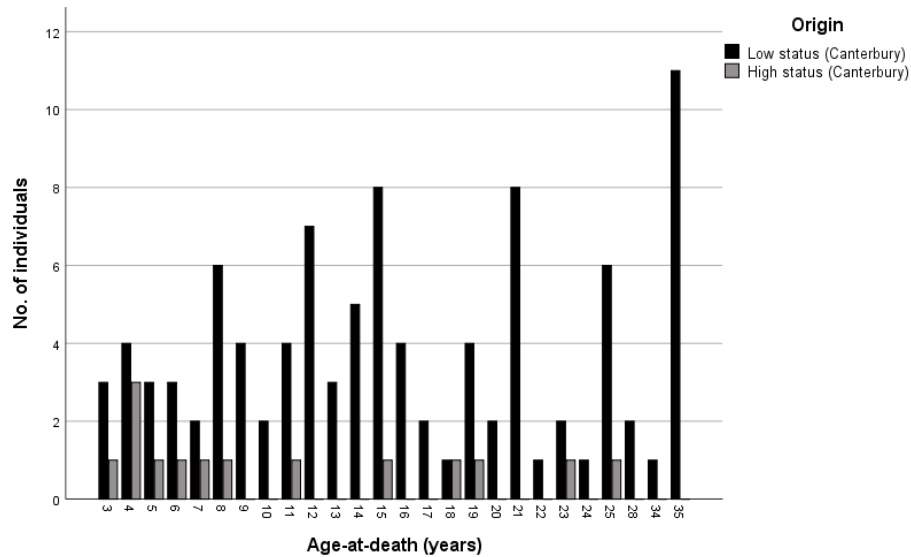


The table below gives the age-at-fusion for St Gregory's skeletal collection divided by high and low status and compared to the entire sample for the medial epicondyle, the distal composite epiphysis to the shaft and the proximal epiphysis of the humerus.

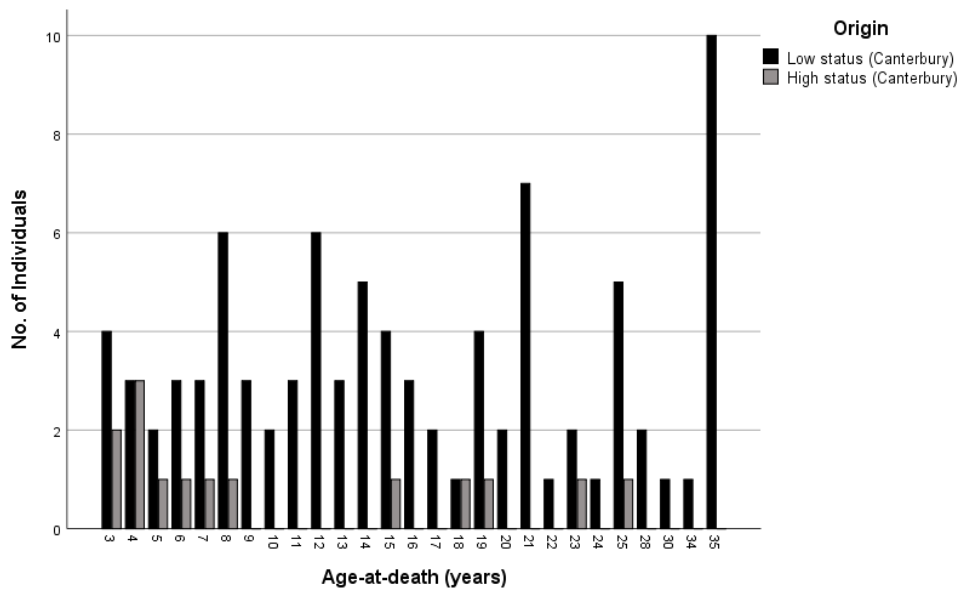
	Entire sample					Low status					High status				
	Stage of union					Stage of union					Stage of union				
	Age	<i>n</i>	1	2	3	Age	<i>n</i>	1	2	3	Age	<i>n</i>	1	2	3
<i>Medial epicondyle</i>	13	3	100.0	–	–	13	3	100.0	–	–	15	1	100.0	–	–
	14	5	100.0	–	–	14	5	100.0	–	–	18	1	–	–	100.0
	15	10	100.0	–	–	15	9	100.0	–	–	19	1	–	–	100.0
	16	3	66.7	33.3	–	16	3	66.7	33.3	–					
	17	2	–	–	100.0	17	2	–	–	100.0					
	18	1	–	–	100.0	19	5	–	–	100.0					
	19	6	–	–	100.0	20	2	–	–	100.0					
	20	2	–	–	100.0										
<i>The humerus</i> <i>Distal composite epiphysis to shaft</i>	11	5	100.0	–	–	11	4	100.0	–	–	11	1	100.0	–	–
	12	7	100.0	–	–	12	7	100.0	–	–	15	1	100.0	–	–
	13	3	100.0	–	–	13	3	100.0	–	–	18	1	–	–	100.0
	14	5	80.0	–	20.0	14	5	80.0	–	20.0					
	15	10	40.0	10.0	50.0	15	9	33.3	11.1	55.6					
	16	3	–	–	100.0	16	3	–	–	100.0					
	17	2	–	–	100.0	17	2	–	–	100.0					
	18	2	–	–	100.0	18	1	–	–	100.0					
<i>Proximal epiphysis</i>	14	5	100.0	–	–	14	5	100.0	–	–	15	1	100.0	–	–
	15	10	100.0	–	–	15	9	100.0	–	–	18	1	–	100.0	–
	16	4	100.0	–	–	16	4	100.0	–	–	19	1	–	–	100.0
	17	2	50.0	–	50.0	17	2	50.0	–	50.0	23	2	–	–	100.0
	18	2	50.0	50.0	–	18	1	100.0	–	–					
	19	4	25.0	25.0	50.0	19	3	33.3	33.3	33.3					
	20	2	–	50.0	50.0	20	2	–	50.0	50.0					
	21	7	–	28.6	71.4	21	7	–	28.6	71.4					
	22	1	–	–	100.0	22	1	–	–	100.0					
	23	3	–	–	100.0	23	1	–	–	100.0					
24	1	–	–	100.0	24	1	–	–	100.0						

### A4.7. The Radius

The figure below gives the age distribution for low-status and high-status individuals from Canterbury for the **proximal epiphysis of the radius**. This shows the entire sub-sample that had these bones present.



The figure below gives the age distribution for low-status and high-status individuals from Canterbury for the fusion of the **distal epiphysis to the radius**. This shows the entire sub-sample that had these bones present.

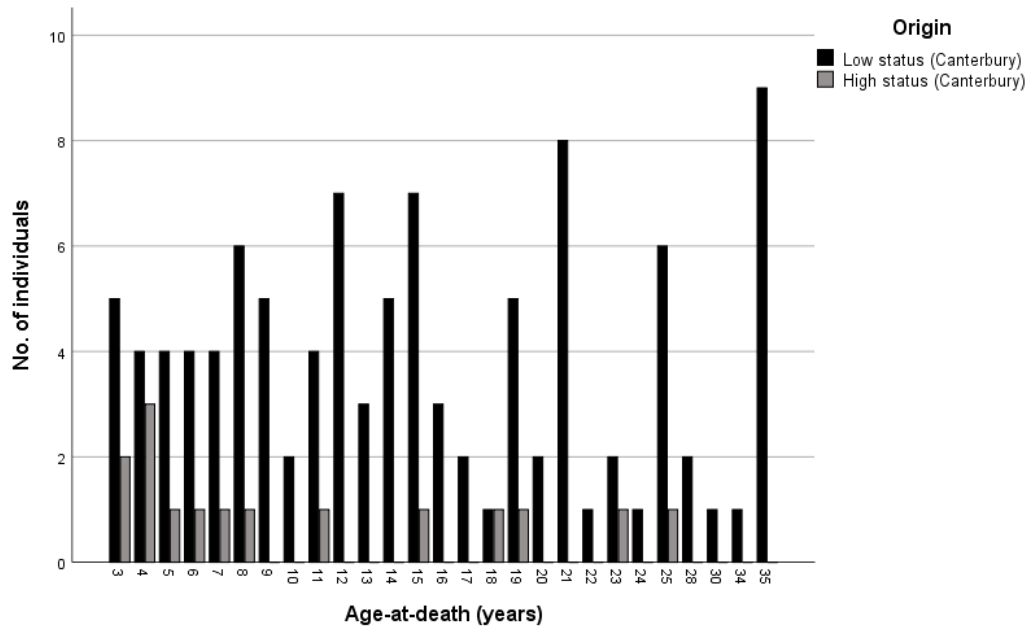


The table below gives the age-at-fusion for St Gregory's skeletal collection divided by high and low status and compared to the entire sample for the proximal and distal epiphyses of the radius.

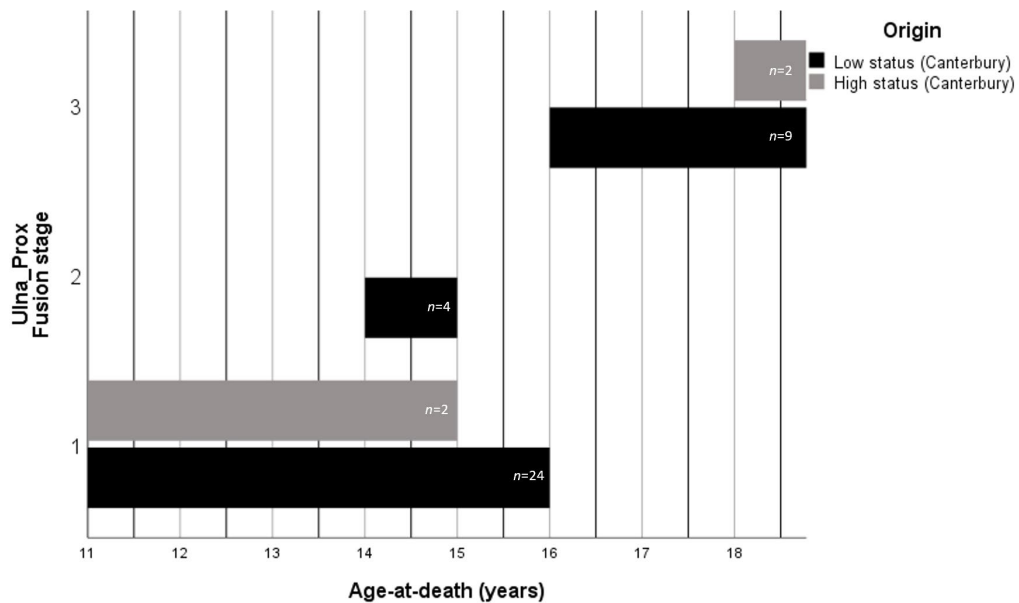
	Entire sample					Low status					High status				
			Stage of union					Stage of union					Stage of union		
	Age	<i>n</i>	1	2	3	Age	<i>n</i>	1	2	3	Age	<i>n</i>	1	2	3
<i>Proximal epiphysis</i>	12	7	100.0	–	–	12	7	100.0	–	–	15	1	100.0	–	–
	13	3	100.0	–	–	13	3	100.0	–	–	18	1	–	–	100.0
	14	5	100.0	–	–	14	5	100.0	–	–	19	1	–	–	100.0
	15	9	77.8	11.1	11.1	15	8	75.0	12.5	12.5					
	16	4	–	50.0	50.0	16	4	–	50.0	50.0					
	17	2	–	–	100.0	17	2	–	–	100.0					
	18	2	–	–	100.0	18	1	–	–	100.0					
	19	5	–	–	100.0	19	4	–	–	100.0					
<i>Radius</i> <i>Distal epiphysis</i>	14	5	100.0	–	–	14	5	100.0	–	–	15	1	100.0	–	–
	15	5	100.0	–	–	15	4	100.0	–	–	18	1	–	100.0	–
	16	3	100.0	–	–	16	3	100.0	–	–	19	1	–	–	100.0
	17	2	50.0	–	50.0	17	2	50.0	–	50.0	23	1	–	–	100.0
	18	2	50.0	50.0	–	18	1	100.0	–	–					
	19	5	20.0	20.0	60.0	19	4	25.0	25.0	50.0					
	20	2	50.0	–	50.0	20	2	50.0	–	50.0					
	21	7	14.3	14.3	71.4	21	7	14.3	14.3	71.4					
	22	1	–	–	100.0	22	1	–	–	100.0					
	23	3	–	–	100.0	23	2	–	–	100.0					
	24	1	–	–	100.0	24	1	–	–	100.0					

#### A4.8. The Ulna

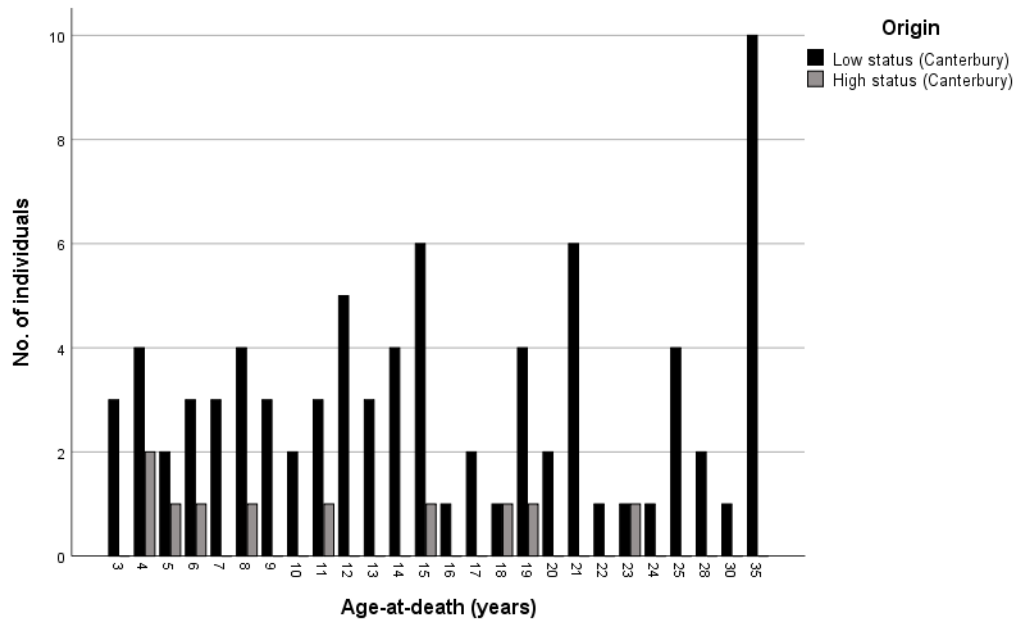
The figure below gives the age distribution for low-status and high-status individuals from Canterbury for the **proximal epiphysis of the ulna**. This shows the entire sub-sample that had these bones present.



The figure below shows the timing of fusion for low-status and high-status individuals from Mediaeval Canterbury for the **proximal epiphysis to the ulna**. Stage 1 (unfused), Stage 2 (fusing), Stage 3 (fused).



The figure below gives the age distribution for low-status and high-status individuals from Canterbury for the **distal epiphysis of the ulna**. This shows the entire sub-sample that had these bones present.

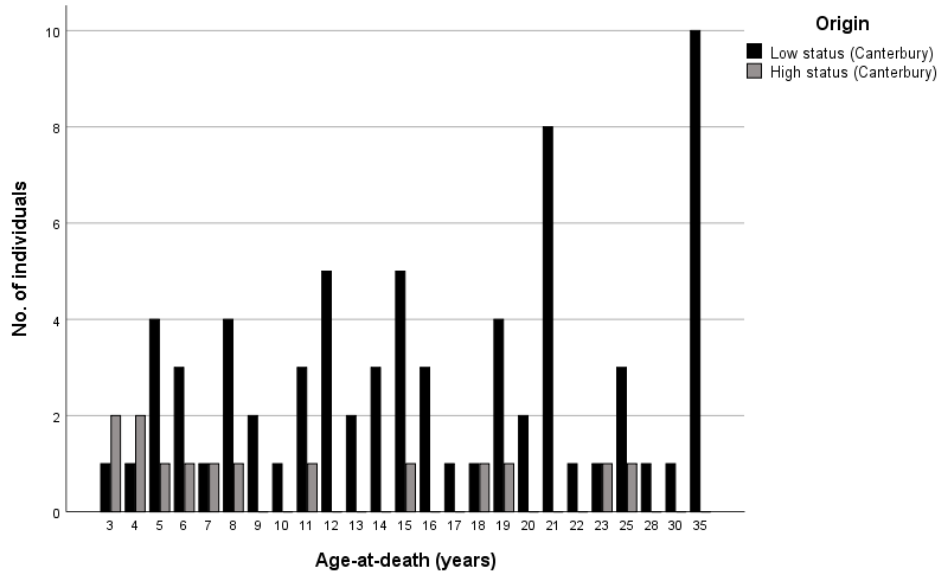


The table below gives the age-at-fusion for St Gregory’s skeletal collection divided by high and low status and compared to the entire sample for the proximal and distal epiphyses of the ulna.

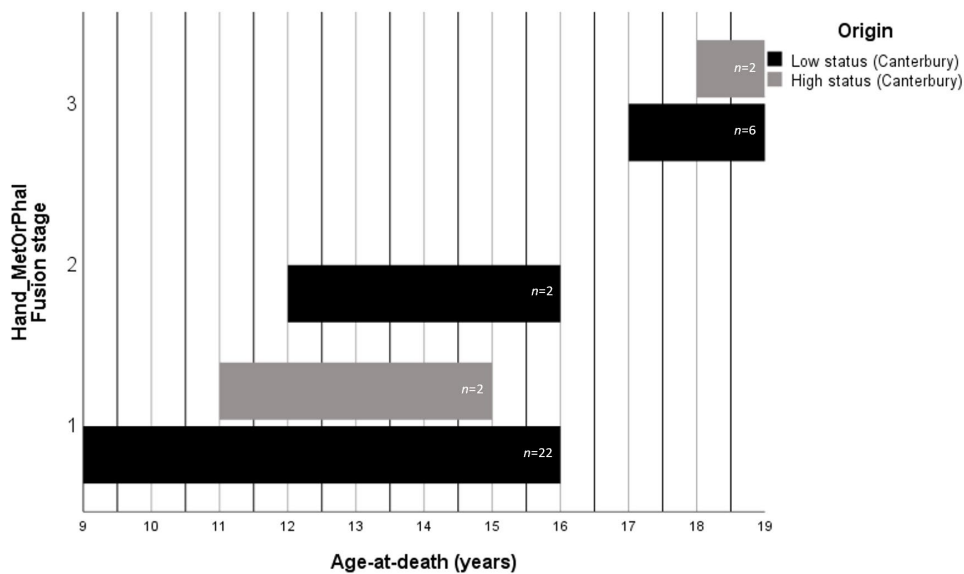
		Entire sample			Low status			High status									
		Stage of union			Stage of union			Stage of union									
		Age	n	1	2	3	Age	n	1	2	3	Age	n	1	2	3	
<i>Proximal epiphysis</i>		11	5	100.0	–	–	11	2	100.0	–	–	11	1	100.0	–	–	
		12	7	100.0	–	–	12	7	100.0	–	–	15	1	100.0	–	–	
		13	3	100.0	–	–	13	3	100.0	–	–	18	1	–	–	100.0	
		14	5	80.0	20.0	–	14	5	80.0	20.0	–	19	1	–	–	100.0	
		15	8	62.5	37.5	–	15	7	57.1	42.9	–						
		16	3	66.7	–	33.3	16	3	66.7	–	33.3						
		17	2	–	–	100.0	17	2	–	–	100.0						
		18	2	–	–	100.0	18	1	–	–	100.0						
		19	6	–	–	100.0	19	5	–	–	100.0						
<i>The ulna</i>		Age	n	1	2	3	Age	n	1	2	3	Age	n	1	2	3	
	<i>Distal epiphysis</i>		14	4	100.0	–	–	14	4	100.0	–	–	15	1	100.0	–	–
			15	7	100.0	–	–	15	6	100.0	–	–	18	1	–	100.0	–
			16	1	100.0	–	–	17	2	50.0	–	50.0	19	1	–	–	100.0
			17	2	50.0	–	50.0	18	1	100.0	–	–	23	1	–	–	100.0
			18	2	50.0	50.0	–	19	4	25.0	25.0	50.0					
			19	5	20.0	20.0	60.0	20	2	50.0	–	50.0					
			20	2	50.0	–	50.0	21	6	16.7	–	83.3					
			21	2	16.7	–	83.3	22	1	–	–	100.0					
			22	1	–	–	100.0	23	1	–	–	100.0					
		23	2	–	–	100.0	24	1	–	–	100.0						
	24	1	–	–	100.0												

### A4.9. The Hand

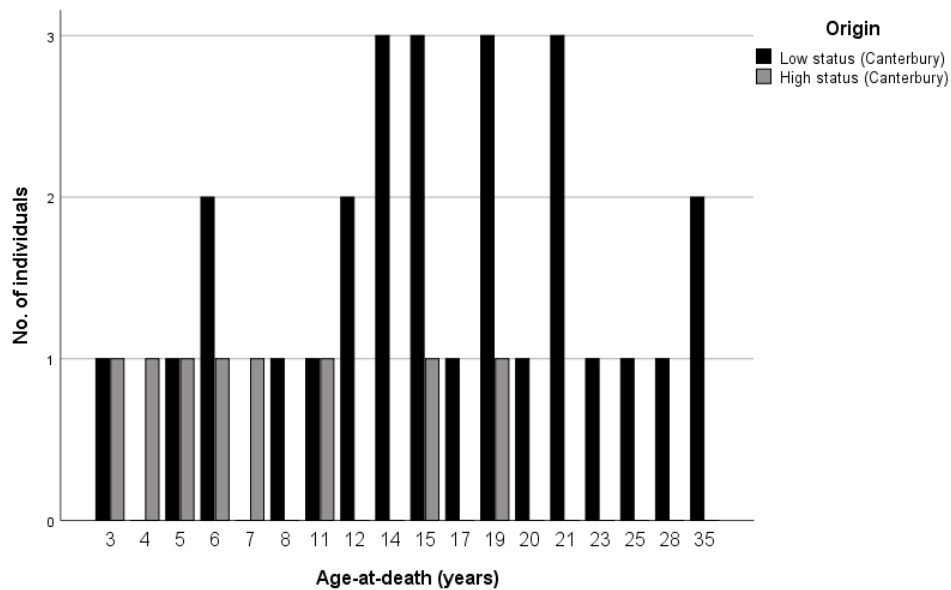
The figure below gives the age distribution for low-status and high-status individuals from Canterbury for the fusion of the heads of the **metacarpals 2-5 and the epiphyses of the proximal and middle phalanges of the hand**. This shows the entire sub-sample that had these bones present.



The figure below shows the timing of fusion for low-status and high-status individuals from Mediaeval Canterbury for the fusion of the **heads of the metacarpals 2-5, proximal and middle phalangeal epiphyses of the hand**. Stage 1 (unfused), Stage 2 (fusing), Stage 3 (fused).



The figure below gives the age distribution for low-status and high-status individuals from Canterbury for the epiphysis to the **distal phalanges of the hand**. This shows the entire sub-sample that had these bones present.

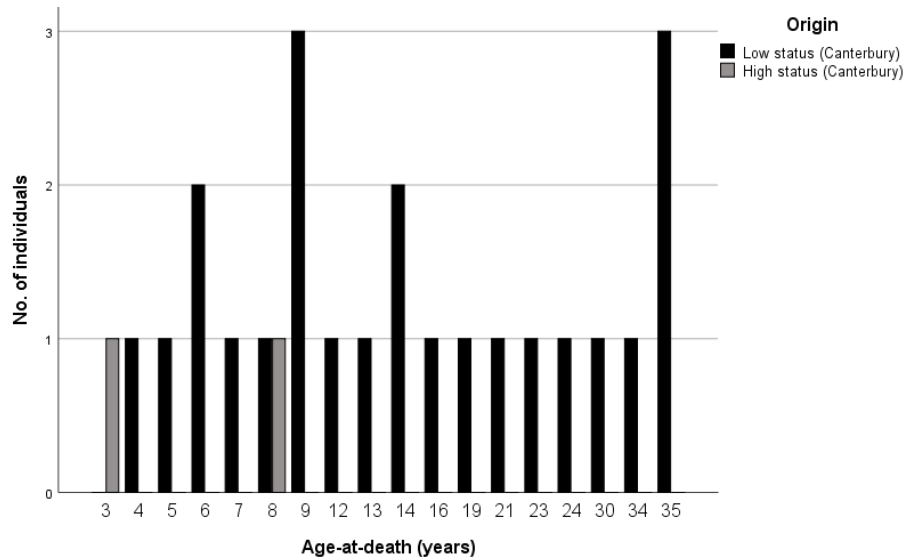


The table below gives the age-at-fusion for St Gregory’s skeletal collection divided by high and low status and compared to the entire sample for the heads of the metacarpals 2-5, the proximal and middle phalangeal epiphyses and the distal phalangeal epiphyses of the hand.

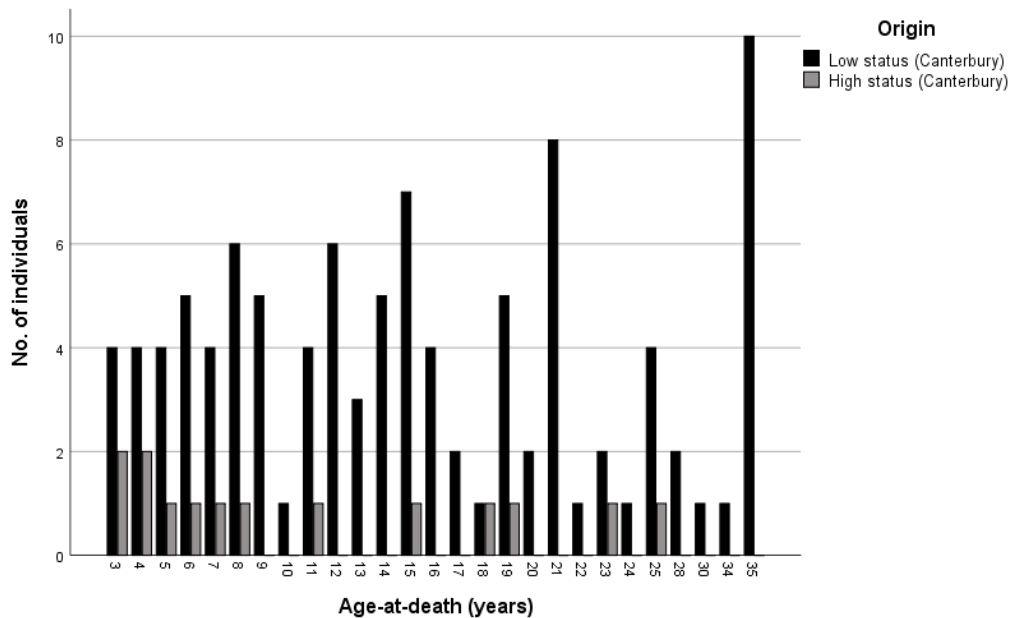
		Entire sample			Low status			High status								
		Stage of union			Stage of union			Stage of union								
		Age	n	1	2	3	Age	n	1	2	3	Age	n	1	2	3
<i>The hand</i>	<i>Metacarpals 2-5, proximal and middle phalangeal epiphyses</i>	9	2	100.0	-	-	9	2	100.0	-	-	11	1	100.0	-	-
		10	1	100.0	-	-	10	1	100.0	-	-	15	1	100.0	-	-
		11	4	100.0	-	-	11	3	100.0	-	-	18	1	-	-	100.0
		12	5	80.0	20.0	-	12	5	80.0	20.0	-	19	1	-	-	100.0
		13	2	100.0	-	-	13	2	100.0	-	-					
		14	3	100.0	-	-	14	3	100.0	-	-					
		15	6	100.0	-	-	15	5	100.0	-	-					
		16	3	66.7	33.3	-	16	3	66.7	33.3	-					
		17	1	-	-	100.0	17	2	-	-	100.0					
		18	2	-	-	100.0	18	1	-	-	100.0					
		19	5	-	-	100.0	19	4	-	-	100.0					
		<i>Distal phalanges</i>	14	3	100.0	-	14	3	100.0	-	15	1	100.0	-		
			15	4	100.0	-	15	3	100.0	-	19	1	-	100.0		
			17	1	-	100.0	17	1	-	100.0						
			19	4	-	100.0	19	3	-	100.0						
			20	1	-	100.0	20	1	-	100.0						
			21	3	-	100.0	21	3	-	100.0						

#### A4.10. The Os coxae

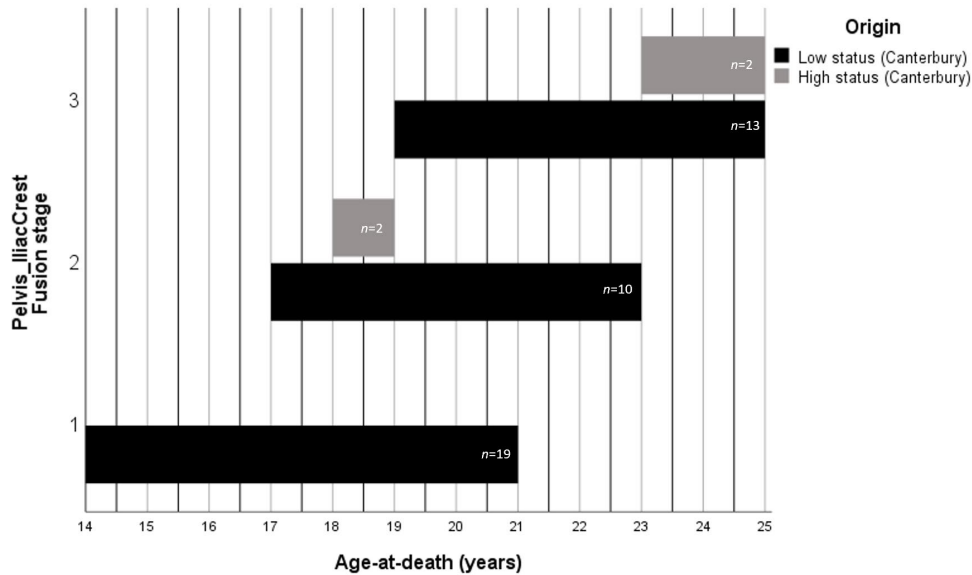
The figure below gives the age distribution for low-status and high-status individuals from Canterbury for the fusion of the **ischiopubic ramus of the os coxae**. This shows the entire sub-sample that had these bones present.



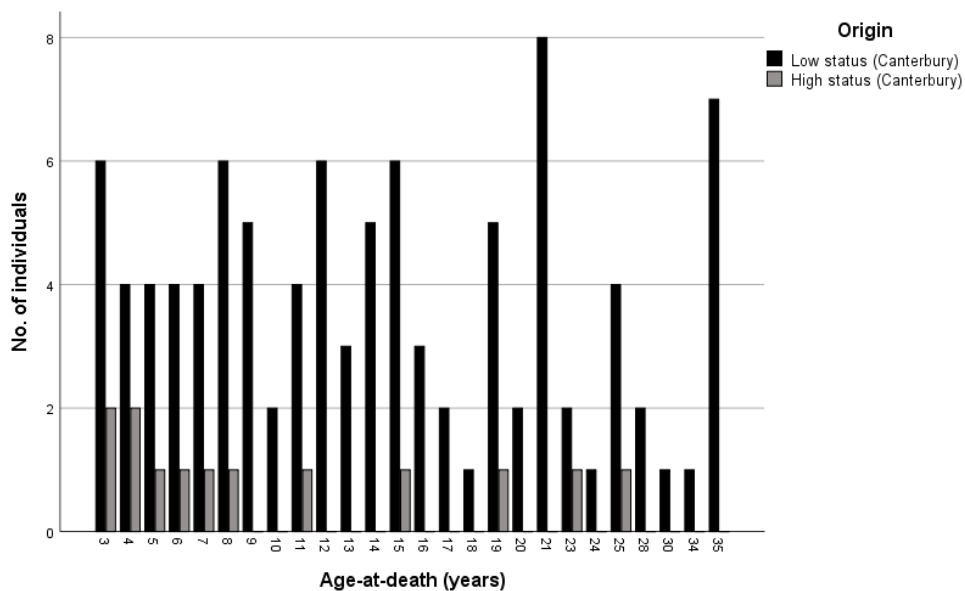
The figure below gives the age distribution for low-status and high-status individuals from Canterbury for the fusion of the **iliac crest of the os coxae**. This shows the entire sub-sample that had these bones present.



The figure below shows the timing of fusion for low-status and high-status individuals from Mediaeval Canterbury for the fusion of the **iliac crest of the os coxae**. Data is not represented on the figure if the sample is lower than two. Stage 1 (unfused), Stage 2 (fusing), Stage 3 (fused).



The figure below gives the age distribution for low-status and high-status individuals from Canterbury for the fusion of the **acetabulum of the os coxae**. This shows the entire sub-sample that had these bones present.

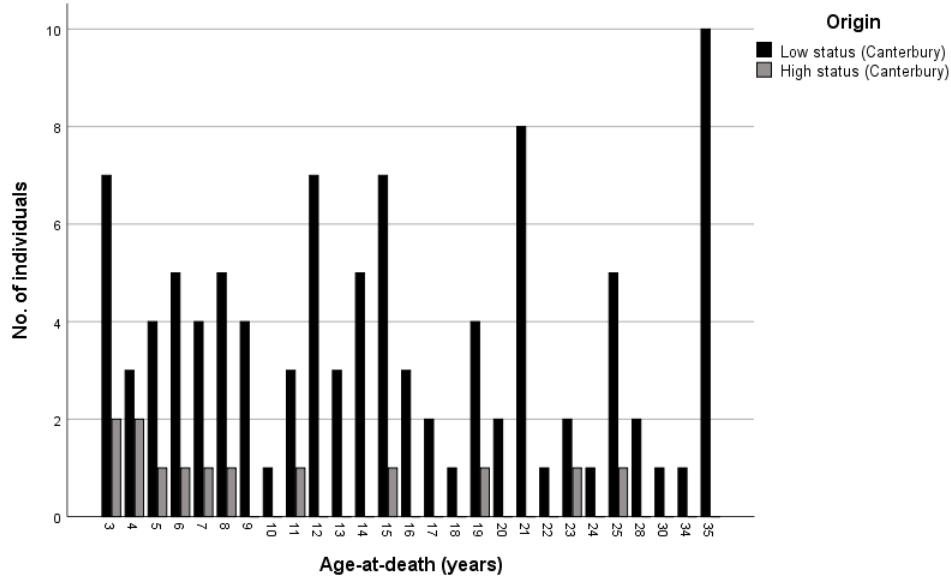


The table below gives the age-at-fusion for St Gregory's skeletal collection divided by high and low status and compared to the entire sample for the ischiopubic ramus, the iliac crest and the acetabulum of the os coxae.

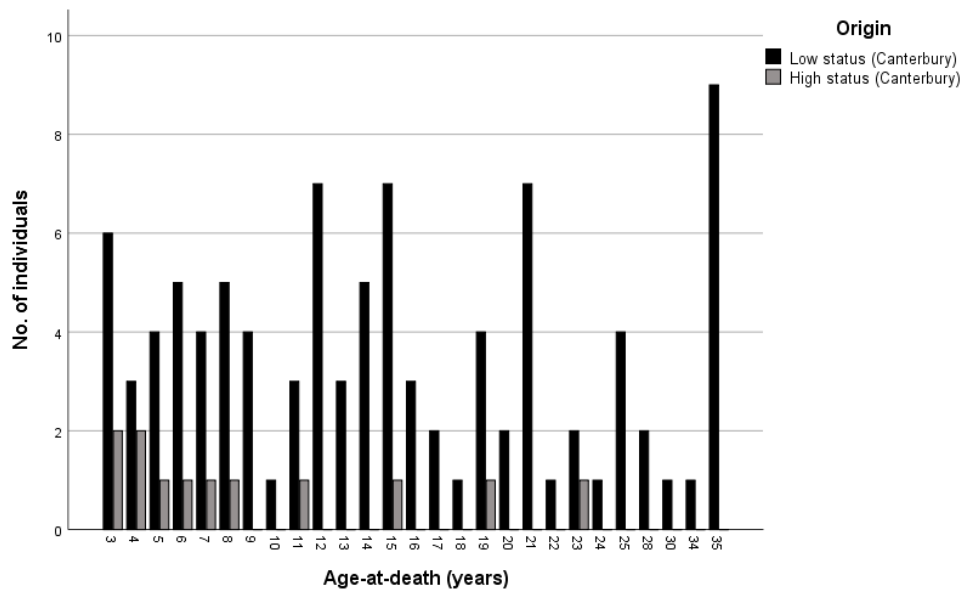
		Entire Sample					Low status					High-status					
		Stage of union					Stage of union					Stage of union					
		Age	<i>n</i>	1	2	3	Age	<i>n</i>	1	2	3	Age	<i>n</i>	1	2	3	
<i>Os coxae</i>	<i>Ischiopubic ramus</i>	12	1	100.0	–	–											
		13	1	–	–	100.0											
		14	2	50.0	–	50.0											
		16	1	–	–	100.0											
			Age	<i>n</i>	1	2	3	Age	<i>n</i>	1	2	3	Age	<i>n</i>	1	2	3
			14	5	100.0	–	–	14	5	100.0	–	–	15	1	100.0	–	–
			15	8	100.0	–	–	15	7	100.0	–	–	18	1	–	100.0	–
			16	4	100.0	–	–	16	4	100.0	–	–	19	1	–	100.0	–
			17	2	50.0	50.0	–	17	2	50.0	50.0	–	23	1	–	–	100.0
			18	2	–	100.0	–	18	1	–	100.0	–	25	1	–	–	100.0
		<i>Iliac crest</i>	19	6	–	66.7	33.3	19	5	–	60.0	40.0					
			20	2	50.0	–	50.0	20	2	50.0	–	50.0					
			21	8	12.5	37.5	50.0	21	8	12.5	37.5	50.0					
			22	1	–	100.0	–	22	1	–	100.0	–					
			23	3	–	33.3	66.7	23	2	–	50.0	50.0					
			24	1	–	–	100.0	24	1	–	–	100.0					
	25		5	–	–	100.0	25	4	–	–	100.0						
			Age	<i>n</i>	1	2	3	Age	<i>n</i>	1	2	3	Age	<i>n</i>	1	2	3
		11	5	100.0	–	–	11	4	100.0	–	–	11	1	100.0	–	–	
		12	6	100.0	–	–	12	6	100.0	–	–	15	1	100.0	–	–	
		13	3	100.0	–	–	13	3	100.0	–	–	19	1	–	–	100.0	
	<i>Acetabulum</i>	14	5	80.0	20.0	–	14	5	80.0	20.0	–						
		15	7	57.1	28.6	14.3	15	6	50.0	33.3	16.7						
		16	3	–	33.3	66.7	16	3	–	33.3	66.7						
		17	2	–	–	100.0	17	2	–	–	100.0						
		18	1	–	–	100.0	18	1	–	–	100.0						
		19	6	–	–	100.0	19	5	–	–	100.0						

### A4.11. The Femur

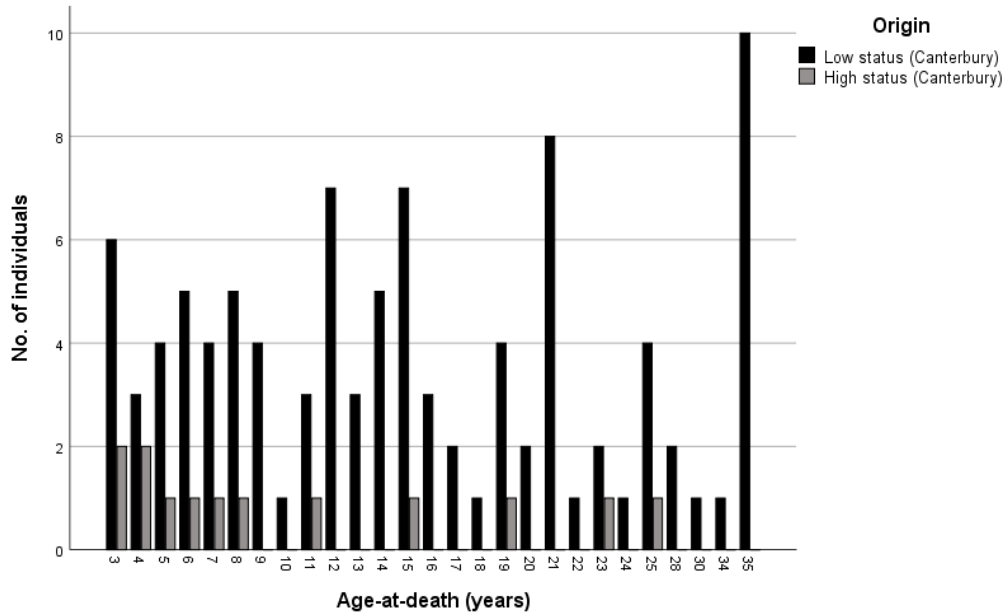
The figure below gives the age distribution for low-status and high-status individuals from Canterbury for the fusion of the **femoral head of the femur**. This shows the entire sub-sample that had these bones present.



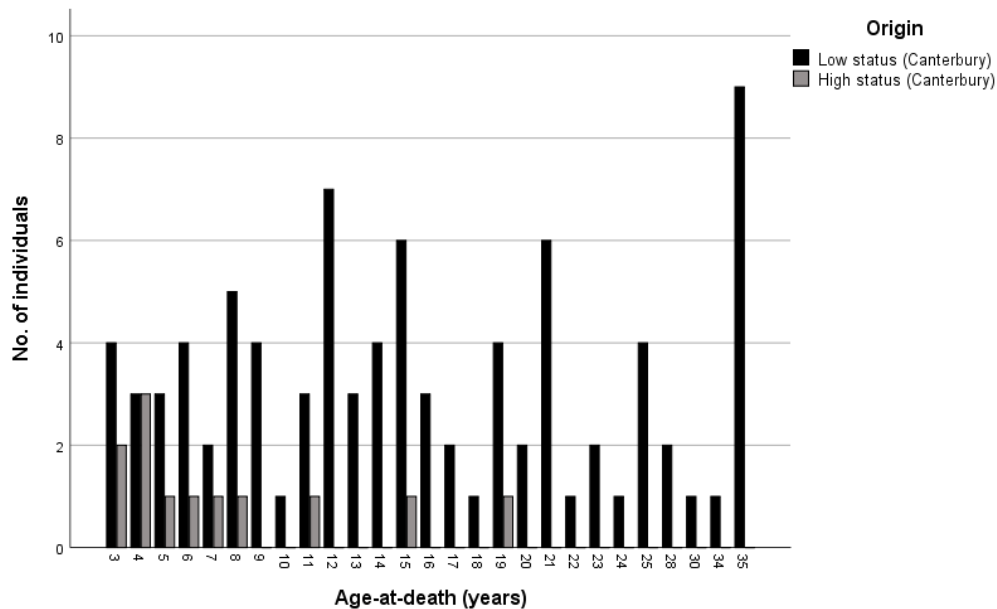
The figure below gives the age distribution for low-status and high-status individuals from Canterbury for the fusion of the **greater trochanter to the femur**. This shows the entire sub-sample that had these bones present.



The figure below gives the age distribution for low-status and high-status individuals from Canterbury for the **lesser trochanter to the femur**. This shows the entire sub-sample that had these bones present.



The figure below gives the age distribution for low-status and high-status individuals from Canterbury for the fusion of the **distal femoral epiphysis to the shaft of the femur**. This shows the entire sub-sample that had these bones present.

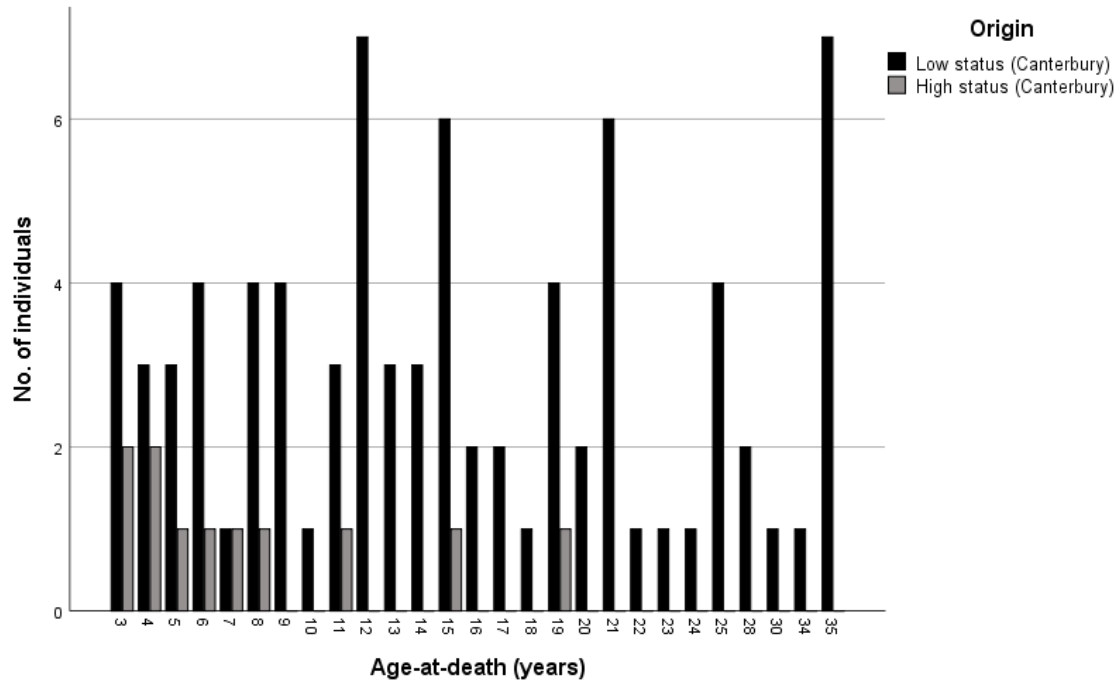


The tables below give the age-at-fusion for St Gregory's skeletal collection divided by high and low status and compared to the entire sample for the femoral head, the greater and lesser trochanters and the distal femoral epiphysis of the femur.

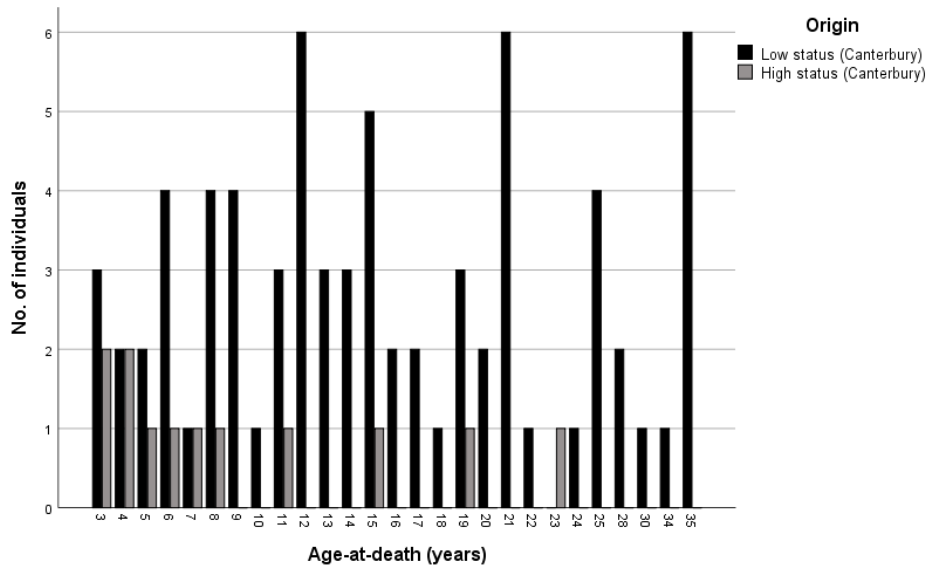
		Entire sample					Low status					High status				
		Stage of union					Stage of union					Stage of union				
		Age	<i>n</i>	1	2	3	Age	<i>n</i>	1	2	3	Age	<i>n</i>	1	2	3
<i>Femur</i>	<i>Femoral head</i>	12	7	100.0	–	–	12	7	100.0	–	–	15	1	100.0	–	–
		13	3	100.0	–	–	13	3	100.0	–	–	19	1	–	–	100.0
		14	5	100.0	–	–	14	5	100.0	–	–					
		15	8	87.5	12.5	–	15	7	85.7	14.3	–					
		16	3	100.0	–	–	16	3	100.0	–	–					
		17	2	–	50.0	50.0	17	2	–	50.0	50.0					
		18	1	–	100.0	–	18	1	–	100.0	–					
		19	5	–	20.0	80.0	19	4	–	25.0	75.0					
		20	2	–	–	100.0	20	2	–	–	100.0					
		21	8	–	–	100.0	21	8	–	–	100.0					
22	1	–	–	100.0	22	1	–	–	100.0							
		Age	<i>n</i>	1	2	3	Age	<i>n</i>	1	2	3	Age	<i>n</i>	1	2	3
	<i>Greater trochanter</i>	13	3	100.0	–	–	13	3	100.0	–	–	15	1	100.0	–	–
14		5	100.0	–	–	14	5	100.0	–	–	19	1	–	–	100.0	
15		8	100.0	–	–	15	7	100.0	–	–						
16		3	66.7	33.3	–	16	3	66.7	33.3	–						
17		2	–	50.0	50.0	17	2	–	50.0	50.0						
18		1	–	–	100.0	18	1	–	–	100.0						
19		5	–	–	100.0	19	4	–	–	100.0						
20	2	–	–	100.0	20	2	–	–	100.0							
		Age	<i>n</i>	1	2	3	Age	<i>n</i>	1	2	3	Age	<i>n</i>	1	2	3
	<i>Lesser trochanter</i>	13	3	100.0	–	–	13	3	100.0	–	–	15	1	100.0	–	–
14		5	100.0	–	–	14	5	100.0	–	–	19	1	–	–	100.0	
15		8	100.0	–	–	15	7	100.0	–	–						
16		3	66.7	33.3	–	16	3	66.7	33.3	–						
17		2	–	–	100.0	17	2	–	–	100.0						
18		1	–	–	100.0	18	1	–	–	100.0						
19		5	–	–	100.0	19	4	–	–	100.0						
		Age	<i>n</i>	1	2	3	Age	<i>n</i>	1	2	3	Age	<i>n</i>	1	2	3
	<i>Femur</i>	14	4	100.0	–	–	14	4	100.0	–	–	15	1	100.0	–	–
15		7	100.0	–	–	15	6	100.0	–	–	19	1	–	–	100.0	
16		3	100.0	–	–	16	3	100.0	–	–						
17		2	50.0	–	50.0	17	2	50.0	–	50.0						
18		1	100.0	–	–	18	1	100.0	–	–						
19		5	–	20.0	80.0	19	4	–	25.0	75.0						
20		2	–	50.0	50.0	20	2	–	50.0	50.0						
21		6	–	–	100.0	21	6	–	–	100.0						
22		1	–	–	100.0	22	1	–	–	100.0						
23		2	–	–	100.0	23	2	–	–	100.0						
		Age	<i>n</i>	1	2	3	Age	<i>n</i>	1	2	3	Age	<i>n</i>	1	2	3
	<i>Distal epiphysis</i>	14	4	100.0	–	–	14	4	100.0	–	–	15	1	100.0	–	–
15		7	100.0	–	–	15	6	100.0	–	–	19	1	–	–	100.0	
16		3	100.0	–	–	16	3	100.0	–	–						
17		2	50.0	–	50.0	17	2	50.0	–	50.0						
18		1	100.0	–	–	18	1	100.0	–	–						
19		5	–	20.0	80.0	19	4	–	25.0	75.0						
20		2	–	50.0	50.0	20	2	–	50.0	50.0						
21		6	–	–	100.0	21	6	–	–	100.0						
22		1	–	–	100.0	22	1	–	–	100.0						
23		2	–	–	100.0	23	2	–	–	100.0						

### A4.12. The Tibia

The figure below gives the age distribution for low-status and high-status from Canterbury for the **proximal epiphysis of the tibia**. This shows the entire sub-sample that had these bones present.



The figure below gives the age distribution for low-status and high-status individuals from Canterbury for the fusion of **distal epiphysis of the tibia**. This shows the entire sub-sample that had these bones present.



The table below gives the age-at-fusion for St Gregory's skeletal collection divided by high and low status and compared to the entire sample for the proximal and distal epiphyses of the tibia.

		Entire sample					Low status					High status					
		Stage of union					Stage of union					Stage of union					
		Age	<i>n</i>	1	2	3	Age	<i>n</i>	1	2	3	Age	<i>n</i>	1	2	3	
<i>Tibia</i>	<i>Proximal epiphysis</i>	14	3	100.0	–	–	14	3	100.0	–	–	15	1	100.0	–	–	
		15	7	100.0	–	–	15	6	100.0	–	–	19	1	–	–	100.0	
		16	2	100.0	–	–	16	2	100.0	–	–						
		17	2	–	50.0	50.0	17	2	–	50.0	50.0						
		18	1	100.0	–	–	18	1	100.0	–	–						
		19	5	–	40.0	60.0	19	4	–	50.0	50.0						
		20	2	–	–	100.0	20	2	–	–	100.0						
	21	6	–	–	100.0	21	6	–	–	100.0							
	22	1	–	–	100.0	22	1	–	–	100.0							
			Age	<i>n</i>	1	2	3	Age	<i>n</i>	1	2	3	Age	<i>n</i>	1	2	3
		<i>Distal epiphysis</i>	14	3	100.0	–	–	14	3	100.0	–	–	15	1	100.0	–	–
	15		6	100.0	–	–	15	5	100.0	–	–	19	1	–	–	100.0	
	16		2	100.0	–	–	16	2	100.0	–	–						
	17		2	–	50.0	50.0	17	2	–	50.0	50.0						
18	1		–	100.0	–	18	1	–	100.0	–							
19	4		–	–	100.0	19	3	–	–	100.0							
20	2		–	–	100.0	20	2	–	–	100.0							
21	6	–	–	100.0	21	6	–	–	100.0								

## APPENDIX 5: PUBERTY IN MEDIAEVAL CANTERBURY

*Pars lateralis to pars basilaris:* The pars lateralis fused to the pars basilaris before puberty began in low-status individuals. The same is true for high-status individuals.

*Spheno-occipital synchondrosis:* One low-status individual in partial fusion was recorded in Deceleration, whereas one completely fused low-status individual was in PHV. Data was limited for the high-status group. However, it appears that the spheno-occipital synchondrosis fusion occurs during the PHV and Deceleration phases.

*Anterior arch of the atlas:* Unfused low-status children were only found in Pre-puberty (88.2%) and Acceleration (11.8%). One partially fused low-status child was found in Pre-puberty, and 12.9% of completely fused low-status children were still in Pre-puberty. The mean pubertal phase that fusion (Stages 2 & 3) occurred was the Acceleration phase (mean phase = 1.85, s.d. = 0.72) for low-status children. All high-status children that were fused were found in Acceleration and above. No significant differences in the pubertal phase at fusion were found between the two groups ( $p = 0.787$ ,  $U = 11.500$ ).

*Posterior synchondrosis of the atlas:* No unfused low-status children were in any pubertal phase past Acceleration, but 14.8% of completely fused low-status children were still in Pre-puberty. The mean pubertal phase that low-status children were in at the time of fusion (Stages 2 and 3) was Acceleration (mean phase = 1.81, s.d. = 0.69). No unfused high-status children were past the Pre-puberty phase, but 12.5% of high-status children who had completed fusion were still in Pre-puberty. The mean pubertal phase that high-status children were in at fusion (Stages 2 and 3) was Acceleration (mean phase = 1.50, s.d. = 0.71). No significant differences were found between the two groups in the mean pubertal phase at fusion ( $p = 0.556$ ,  $U = 20.000$ ).

*Ossiculum terminale to the dens:* No low-status juvenile skeletons that were unfused at the time of their death were in any phase past Acceleration. Partially fused low-status skeletons also only remained in the first two phases of puberty. Two low-status individuals who were in pre-puberty had also completely fused. The mean pubertal phase low-status individuals were in at fusion (Stages 2 and 3) was Acceleration (mean phase = 1.55, s.d. = 0.51). No unfused high-status individuals went past the Pre-puberty phase. All partially fused high-status skeletons

were in the Acceleration phase. All completely fused high-status individuals were in the Acceleration phase and above. The pubertal phase at fusion (Stages 2 and 3) for the high-status juveniles was PHV (s.d. = 1.73). The high-status group, therefore, fused at a later pubertal phase when compared to the low-status group. **This was statistically significantly different** ( $p = 0.047$ ,  $U = 11.000$ ).

*Dentoneural synchondrosis*: Fusion occurs before puberty begins.

*Dentocentral and neurocentral junctions*: No unfused low-status individuals had entered puberty. Partially fused low-status individuals were recorded 72.0% in Pre-puberty, 24.0% in Acceleration and 4.0% in PHV. However, 10.9% of completely fused low-status individuals were still in Pre-puberty. The mean pubertal phase for fusion (Stages 2 and 3) of the dentocentral and neurocentral junctions is Acceleration (mean phase = 1.72, s.d. = 0.79). Unfused and partially fused high-status skeletons were recorded in Pre-puberty only. Fourteen-point three per cent of high-status individuals who had completed fusion were also in Pre-puberty. Mean pubertal phase for high-status individuals was Pre-puberty (s.d. = 0.000). No significant differences were found in the mean pubertal phase at fusion between the two groups ( $p = 0.162$ ,  $U = 25.000$ ).

*Posterior synchondrosis of the axis*: Fusion occurs before the onset of puberty.

*Sacral bodies 1 & 2:* The table below shows skeletons recorded for the age at fusion of sacral bodies 1 and 2 cross-tabulated with the pubertal stage reached at the time of death. This table is for low-status Mediaeval Canterbury skeletons only. Frequencies are recorded as percentages.

<i>Fusion stage</i>	<i>Age</i>	<i>n</i>	<i>Pre-puberty</i>	<i>Acceleration</i>	<i>PHV</i>	<i>Deceleration</i>	<i>Maturation</i>	<i>Completion</i>	
<b>1</b>	<b>3</b>	2	100.0	-	-	-	-	-	
	<b>4</b>	2	100.0	-	-	-	-	-	
	<b>6</b>	3	100.0	-	-	-	-	-	
	<b>7</b>	3	100.0	-	-	-	-	-	
	<b>8</b>	4	100.0	-	-	-	-	-	
	<b>9</b>	3	66.7	33.3	-	-	-	-	
	<b>10</b>	1	100.0	-	-	-	-	-	
	<b>11</b>	4	25.0	75.0	-	-	-	-	
	<b>12</b>	5	80.0	20.0	-	-	-	-	
	<b>13</b>	3	-	100.0	-	-	-	-	
	<b>14</b>	3	-	100.0	-	-	-	-	
	<b>15</b>	6	-	66.7	33.3	-	-	-	
	<b>16</b>	3	-	33.3	66.7	-	-	-	
	<b>2</b>	<b>19</b>	2	-	-	-	-	100.0	-
		<b>21</b>	6	-	-	16.7	16.7	33.3	33.3
		<b>22</b>	1	-	-	-	-	-	100.0
<b>25</b>		2	-	-	-	-	-	100.0	
<b>3</b>	<b>19</b>	1	-	-	-	-	-	100.0	
	<b>21</b>	2	-	-	-	-	-	100.0	
	<b>23</b>	1	-	-	-	-	-	100.0	
	<b>24</b>	1	-	-	-	-	-	100.0	
	<b>28</b>	2	-	-	-	-	-	100.0	

*Medial clavicle:* The table below shows skeletons recorded for the age at fusion of the medial epiphysis of the clavicle cross-tabulated with the pubertal stage reached at the time of death. This table is for low-status Mediaeval Canterbury skeletons only. Frequencies are recorded as percentages.

<i>Fusion stage</i>	<i>Age</i>	<i>n</i>	<i>PHV</i>	<i>Deceleration</i>	<i>Maturation</i>	<i>Completion</i>
1	19	3	-	33.3	66.7	-
	20	1	-	100.0	-	-
	21	3	33.3	-	66.7	-
	22	1	-	-	-	100.0
	23	1	-	-	-	100.0
	24	1	-	-	-	100.0
2	21	2	-	50.0	-	50.0
	25	1	-	-	-	100.0
3	19	1	-	-	-	100.0
	20	1	-	-	-	100.0
	21	2	-	-	-	100.0
	23	1	-	-	-	100.0
	25	3	-	-	33.3	66.7

Low-status individuals who had an unfused medial epiphysis spanned all pubertal phases. Partially fused low-status individuals were only in Deceleration and Completion, whereas completely fused low-status skeletons were recorded in Maturation and beyond. Fusion (Stages 2 and 3) was found to take place once puberty had ended for most low-status skeletons (mean phase = 5.73, s.d. = 0.65). Unfused high-status skeletons were found in pubertal phases, Pre-puberty, Acceleration and Maturation. One partially fused high-status skeleton was recorded in Maturation, and all completely fused high-status individuals had also completed fusion. Fusion (Stages 2 and 3) was found to occur at the end of puberty for high-status individuals (mean phase = 5.50, s.d. = 0.71). No statistically significant differences were found between the groups in the mean pubertal phase ( $p = 0.422$ ,  $U = 8.000$ ).

*Lateral clavicle:* Unfused low-status individuals were found to be in all pubertal phases apart from Completion. Partially fused low-status individuals were only found in Maturation and Completion. However, one completely fused individual was in PHV. The mean phase for fusion (Stages 2 and 3) of the lateral epiphysis of the clavicle occurred in the Maturation phase (mean phase = 5.33, s.d. = 0.99). Like the low-status group, unfused high-status individuals were in every pubertal phase except for Completion. However, phases PHV and Deceleration were missing. Those who had completed fusion ( $n = 2$ ) were recorded in Maturation and Completion. No significant differences in the mean phase at fusion between the groups were found ( $p = 0.460$ ,  $U = 3.500$ ).

*Coracoid of scapula:* Unfused low-status skeletons were found in Pre-puberty (55.4%), Acceleration (33.9%) and PHV (10.7%). One individual was recorded in partial fusion and was in PHV. This was the mean pubertal phase for fusion (Stages 2 and 3) of the coracoid to the body of the scapula (mean phase = 3.33, s.d. = 0.58). Completely fused low-status individuals were recorded from PHV onwards. Unfused high-status skeletons were recorded in Pre-puberty (75.0%) and Acceleration (25.0%). Completely fused high-status individuals were found to be 50.0% in Maturation and 50.0% in Completion.

*Medial border of scapula:* Unfused low-status individuals were recorded in Pre-puberty until PHV, whereas completely fused individuals were recorded from Maturation onwards. Although the mean puberty phase at fusion was Completion (mean phase = 5.50, s.d. = 0.71), no data was available for partial fusion. Due to how the data was spread, fusion is more likely to have occurred during the Deceleration phase. Data was limited for the high-status group.

*Acromial epiphysis of scapula:* Unfused low-status individuals were recorded from Pre-puberty until Deceleration, whereas completely fused individuals were recorded from PHV onwards. Complete fusion was found to occur in the Maturation phase of puberty (mean phase = 4.75, s.d. = 0.50), but this does not consider partial fusion, which was missing from the data. PHV and Deceleration were missing in the high-status group. However, unfused high-status individuals were recorded in Pre-puberty and Acceleration, whereas completely fused individuals were recorded in Maturation and Completion.

*Inferior angle of the scapula:* Unfused low-status individuals were in every puberty phase except for Completion, whereas completely fused individuals were in Maturation and Completion only. Based only on complete fusion, the mean pubertal phase for fusion for the low-status group was once puberty had completed (mean phase = 5.67, s.d. = 0.58), but it is more likely that fusion occurred during Maturation. Data was limited for the high-status group.

*Medial humeral epicondyle:* Unfused low-status individuals were in pubertal phases, Pre-puberty to PHV. One partially fused individual was recorded in PHV, whereas completely fused low-status individuals were recorded in PHV and beyond. The mean pubertal phase for fusion (Stages 2 and 3) of the medial epicondyle of the humerus was Deceleration (mean phase = 3.67, s.d. = 1.16). PHV and Deceleration were missing for the high-status group. However,

unfused high-status individuals were recorded in Pre-puberty and Acceleration, and completely fused individuals were recorded in Maturation and Completion.

*Distal composite epiphysis to the shaft of the humerus:* Unfused low-status individuals were in the pubertal phases, Pre-puberty to PHV. One individual was recorded in partial fusion in Acceleration. Completely fused low-status individuals were recorded in Acceleration and beyond. The mean pubertal phase low-status individuals fused (Stages 2 and 3) in was PHV (mean phase = 2.71, s.d. = 0.49). PHV and Deceleration were missing in the high-status group, but unfused individuals were recorded in Pre-puberty and Acceleration, whereas completely fused individuals were recorded in Maturation and Completion.

*Proximal epiphysis of the humerus:* Unfused low-status individuals were recorded in Pre-puberty to Deceleration. Those in partial fusion were found in PHV to Maturation. Completely fused low-status individuals were recorded in Deceleration and beyond. The mean phase at fusion (Stages 2 and 3) for low-status individuals was Maturation (s.d. = 0.95). PHV and Deceleration were missing for the high-status group, but unfused high-status individuals were found in Pre-puberty and Acceleration. One partially fused individual was found in Maturation, whereas completely fused individuals were recorded in Maturation and beyond. The mean pubertal phase at fusion (Stages 2 and 3) for high-status individuals was Maturation (s.d. = 0.000). No significant differences were found between the groups for the mean pubertal phase at fusion ( $p = 0.843$ ,  $U = 11.000$ ).

*Proximal epiphysis of the radius:* Unfused low-status individuals were recorded in Pre-puberty to PHV, whereas 66.7% of partially fused low-status individuals were found in PHV and 33.3% in Deceleration. Those who had completed fusion were found from PHV onwards. The mean phase low-status individuals were in at fusion (Stages 2 and 3) was PHV (mean phase = 3.17, s.d. = 0.41). PHV and Deceleration were missing for the high-status group, but unfused high-status individuals were found in Pre-puberty and Acceleration. Fused high-status skeletons were in Maturation and Completion.

*Distal epiphysis of the ulna:* Unfused low-status individuals were recorded in Pre-puberty to Deceleration. One partially fused skeleton was recorded in Maturation, whereas those completely fused were recorded from Deceleration onwards. The mean pubertal phase recorded for low-status individuals for the fusion of the distal epiphysis of the ulna was Maturation

(mean phase = 5.40, s.d. = 0.70). PHV and Deceleration were missing for the high-status group, but unfused high-status individuals were found in Pre-puberty and Acceleration. One partially fused individual was recorded in Maturation, whereas completely fused high-status individuals were recorded from Maturation onwards. The mean pubertal phase for the fusion of the distal epiphysis of the ulna for the high-status group was Maturation (s.d. = 0.000). No significant differences were found in the mean pubertal phase at fusion between the two groups ( $p = 0.339$ ,  $U = 6.000$ ).

*Metacarpals 2-5, proximal and middle phalangeal epiphyses of the hand:* Unfused low-status individuals were recorded in Pre-puberty to PHV. One partially fused skeleton was found in Pre-puberty, whereas another was found in Deceleration. Completely fused low-status skeletons were recorded from Deceleration onwards. The mean pubertal phase low-status individuals were found in during the fusion (Stages 2 and 3) of their metacarpals 2 – 5, as well as the proximal and middle phalangeal epiphyses was PHV (mean phase = 3.33, s.d. = 2.08). PHV and Deceleration were missing for the high-status group, but unfused high-status individuals were found in Pre-puberty and Acceleration. Completely fused high-status individuals were recorded in Maturation onwards.

*Acetabulum of the os coxae:* Unfused low-status individuals remained in Pre-puberty and Acceleration. Twenty-five per cent of partially fused individuals were in Acceleration, and 75.0% were in PHV. Low-status skeletons that had completely fused were found in PHV and beyond. The mean pubertal phase low-status individuals were in when fusion (Stages 2 and 3) occurred for the acetabulum was PHV (s.d. = 0.58). PHV and Deceleration were missing for the high-status group, but unfused high-status individuals were found in Pre-puberty and Acceleration. Completely fused high-status individuals were recorded in Maturation onwards.

*Femoral head:* Unfused low-status individuals were found in Pre-puberty to PHV. Fifty per cent of partially fused individuals were recorded in PHV, and 25.0% in Deceleration and Maturation. Low-status individuals who had completed fusion were in PHV and beyond. The mean pubertal phase for the fusion (Stages 2 and 3) of the femoral head for low-status individuals was Maturation (mean phase = 4.50, s.d. = 1.20). PHV and Deceleration were missing for the high-status group, but unfused high-status individuals were found in Pre-puberty and Acceleration. Completely fused high-status individuals were recorded in Maturation onwards.

*Greater and lesser trochanters of the femur:* Unfused low-status individuals were recorded in Pre-puberty to PHV for both trochanters. Partially fused individuals were recorded in PHV. Low-status individuals who had completed fusion were in PHV and beyond. The mean pubertal phase that fusion of both trochanters occurred for the low-status group was Deceleration (mean phase = 3.67, s.d. = 1.16). PHV and Deceleration were missing for the high-status group, but unfused high-status individuals were found in Pre-puberty and Acceleration. Completely fused high-status individuals were recorded in Maturation onwards.

*Distal epiphysis of the femur:* Unfused low-status individuals were recorded from Pre-puberty to Deceleration. Partially fused individuals were recorded in Deceleration and Maturation. Completely fused low-status individuals were in PHV onwards. The mean pubertal phase for the fusion of the distal epiphysis for the low-status group was Maturation (mean phase = 5.14, s.d. = 0.90). Data was limited for the high-status group.

*Proximal epiphysis of the tibia:* Unfused low-status individuals were recorded from Pre-puberty to Deceleration. Partially fused individuals were recorded in PHV to Maturation, whereas completely fused low-status individuals were in PHV onwards. The mean pubertal phase for the fusion (Stages 2 and 3) of the proximal epiphysis of the tibia for the low-status group was Maturation (mean phase = 4.83, s.d. = 1.17). Data was limited for the high-status group.

*Distal epiphysis of the tibia:* Unfused low-status individuals were recorded from Pre-puberty to PHV. Partially fused individuals were found in PHV and Deceleration, whereas those completely fused were in PHV and beyond. The mean pubertal phase for the fusion (Stages 2 and 3) of the distal epiphysis of the tibia for the low-status group was Maturation (mean phase = 4.67, s.d. = 1.21). Data was limited for the high-status group.

## APPENDIX 6: SUMMARY OF CHAPTER 5

Bone	Fusion site	Summary
Occipital	Pars basilaris to the pars lateralis	<ul style="list-style-type: none"> <li>• Fusion occurred between the ages of 7 to 8 years for Mediaeval Canterbury.</li> <li>• Fusion occurred prior to puberty.</li> </ul>
	Spheno-occipital synchondrosis	<ul style="list-style-type: none"> <li>• Fusion occurred between the ages of 16 to 17 years in Mediaeval Canterbury.</li> <li>• Fusion occurred during PHV.</li> </ul>
Atlas (C1)	Anterior arch	<ul style="list-style-type: none"> <li>• The majority of fusion occurred at 8 years of age for Mediaeval Canterbury.</li> <li>• Fusion occurs around the onset of puberty.</li> </ul>
	Posterior synchondrosis	<ul style="list-style-type: none"> <li>• Fusion occurred between the ages of 4 to 8 years for the majority of children from Mediaeval Canterbury.</li> <li>• Fusion occurs around the onset of puberty.</li> </ul>
Axis (C2)	Ossiculum terminale to the dens	<ul style="list-style-type: none"> <li>• Fusion occurred between the ages of 8 to 15 years for Mediaeval Canterbury.</li> <li>• Fusion occurs in early puberty.</li> <li>• The pubertal phase in which low-status (Acceleration) and high-status (PHV) fused at was statistically significantly different.</li> </ul>
	Dentoneural synchondrosis	<ul style="list-style-type: none"> <li>• Fusion occurred between the ages of 3 to 6 years for Mediaeval Canterbury.</li> <li>• Fusion occurs before pubertal onset.</li> </ul>
	Dentocentral and neurocentral junctions	<ul style="list-style-type: none"> <li>• Fusion occurred between the ages of 3 to 16 years old for Mediaeval Canterbury.</li> <li>• Fusion occurred before puberty for the high-status group only and at the onset of puberty for the low-status group, but no significant differences existed between the groups.</li> </ul>
	Posterior synchondrosis	<ul style="list-style-type: none"> <li>• Fusion occurred between the ages of 3 to 5 years old for Mediaeval Canterbury.</li> <li>• Fusion occurs before the onset of puberty.</li> </ul>
Sacrum	Bodies 1 & 2	<ul style="list-style-type: none"> <li>• Fusion occurred between the ages of 19 to 28 years for Mediaeval Canterbury.</li> </ul>

		<ul style="list-style-type: none"> <li>• Fusion is found to begin in the later stages of puberty, but complete fusion is associated with completion of puberty.</li> </ul>
Clavicle	Medial epiphysis	<ul style="list-style-type: none"> <li>• Fusion occurred between 19 to 25 years of age for Mediaeval Canterbury.</li> <li>• Fusion occurs near the end of puberty or once puberty has completed.</li> </ul>
	Lateral epiphysis	<ul style="list-style-type: none"> <li>• Fusion occurred between the ages of 17 to 23 years old for Mediaeval Canterbury. No individuals remained unfused after the age of 19 years old. Complete fusion first occurred in the sample at 19 years.</li> <li>• Fusion occurs near the end of puberty.</li> </ul>
Scapula	Coracoid	<ul style="list-style-type: none"> <li>• Fusion occurred at age 16 years.</li> <li>• Fusion occurred in PHV.</li> </ul>
	Medial border	<ul style="list-style-type: none"> <li>• Fusion occurred between the ages of 19 to 21 years for Mediaeval Canterbury.</li> <li>• Fusion occurs around the Deceleration phase.</li> </ul>
	Acromial epiphysis	<ul style="list-style-type: none"> <li>• Fusion occurred between the ages of 17 to 18 years for Mediaeval Canterbury.</li> </ul>
	Inferior angle epiphysis	<ul style="list-style-type: none"> <li>• Fusion occurred between the ages of 18 to 21 years for Mediaeval Canterbury.</li> </ul>
Humerus	Medial epicondyle	<ul style="list-style-type: none"> <li>• Fusion occurred between the ages of 16 to 17 years.</li> <li>• Fusion occurs during Deceleration.</li> </ul>
	Distal composite epiphysis	<ul style="list-style-type: none"> <li>• Fusion occurred between the ages of 14 to 15 years.</li> <li>• Fusion occurs during PHV.</li> </ul>
	Proximal epiphysis	<ul style="list-style-type: none"> <li>• Fusion occurred between the ages of 17 to 21 years.</li> <li>• Fusion occurs at the tail end of puberty but fuses before puberty ends.</li> </ul>
Radius	Proximal epiphysis	<ul style="list-style-type: none"> <li>• Fusion occurred between the ages of 15 to 16 years.</li> <li>• Fusion occurs during PHV.</li> </ul>
	Distal epiphysis	<ul style="list-style-type: none"> <li>• Fusion occurred between the ages of 17 to 21 years.</li> </ul>
Ulna	Proximal epiphysis	<ul style="list-style-type: none"> <li>• Fusion occurred between the ages of 14 to 16 years.</li> </ul>
	Distal epiphysis	<ul style="list-style-type: none"> <li>• Fusion occurred between the ages of 17 to 21 years.</li> <li>• Fusion occurs near the end of puberty.</li> </ul>
Hand	Metacarpals 2-5, proximal and middle phalangeal epiphyses	<ul style="list-style-type: none"> <li>• Fusion occurred between the ages of 12 to 17 years.</li> <li>• Fusion occurs during PHV.</li> </ul>
	Distal phalanges	<ul style="list-style-type: none"> <li>• Complete fusion occurred at age 17 years.</li> </ul>

Os coxae	Ischiopubic ramus	<ul style="list-style-type: none"> <li>No statistical significant differences in mean age at partial fusion were found between high and low-status groups.</li> </ul>
	Acetabulum	<ul style="list-style-type: none"> <li>Fusion occurred between the ages of 14 to 16 years.</li> <li>Fusion occurs during PHV.</li> </ul>
Femur	Femoral head	<ul style="list-style-type: none"> <li>Fusion occurred between the ages of 15 to 19 years.</li> <li>Fuses near the end of puberty.</li> </ul>
	Greater and lesser trochanters	<ul style="list-style-type: none"> <li>Fusion occurred between the ages of 16 to 17 years.</li> <li>Fuses during Deceleration.</li> </ul>
	Distal epiphysis	<ul style="list-style-type: none"> <li>Fusion occurred between the ages of 17 to 20 years.</li> <li>Fuses near to the end of puberty.</li> </ul>
Tibia	Proximal epiphysis	<ul style="list-style-type: none"> <li>Fusion occurs between the ages of 17 to 19 years.</li> <li>Fuses near to the end of puberty, but before Completion.</li> </ul>
	Distal epiphysis	<ul style="list-style-type: none"> <li>Fusion occurs between the ages of 17 to 19 years.</li> <li>Fuses near to the end of puberty, but before Completion.</li> </ul>

## APPENDIX 7: MEDIAEVAL CANTERBURY COMPARED TO OTHER BRITISH MEDIAEVAL SITES

### A7. 1. The Skull

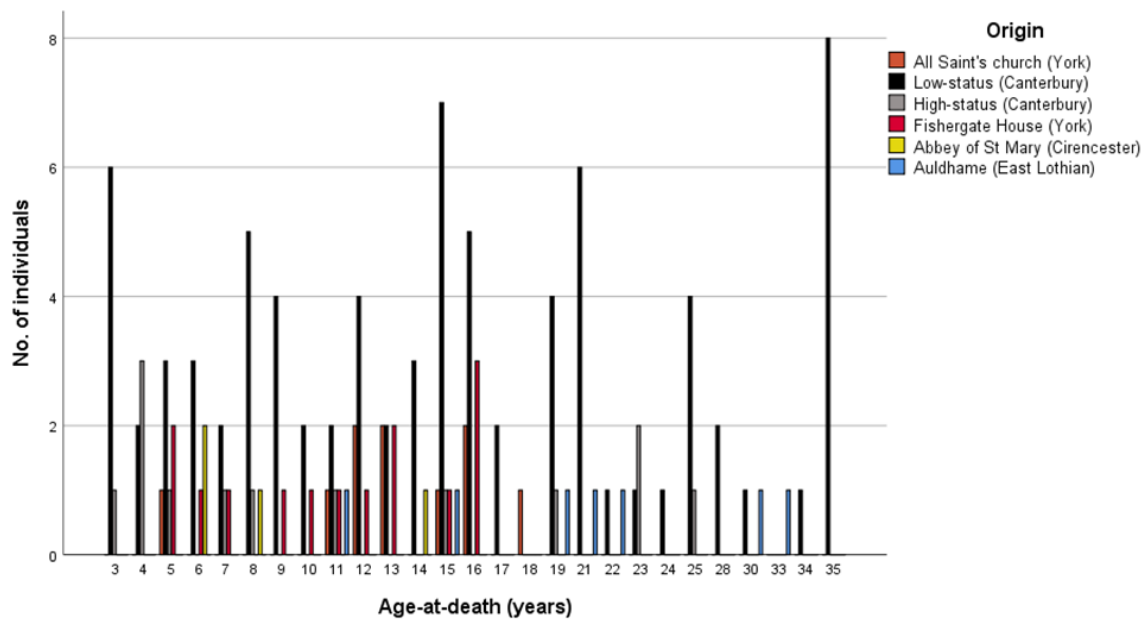
The table below shows the age at death/phase for the fusion of the **pars lateralis to pars basilaris** for all archaeological Mediaeval sites sampled. Frequencies are recorded as percentages.

Pars lateralis to pars basilaris												
All Saint's church (York)				Low-status (Canterbury)				High-status (Canterbury)				
		Stage of union				Stage of union				Stage of union		
Age	n	1	3	Age	n	1	3	Age	n	1	3	
5	1	100.0	-	4	2	100.0	-	4	3	100.0	-	
11	1	-	100.0	5	3	100.0	-	5	1	100.0	-	
				6	3	100.0	-	7	1	-	100.0	
				7	2	50.0	50.0	8	1	100.0	-	
				8	5	-	100.0	11	1	-	100.0	
				9	4	-	100.0					
				10	2	-	100.0					
				11	2	-	100.0					

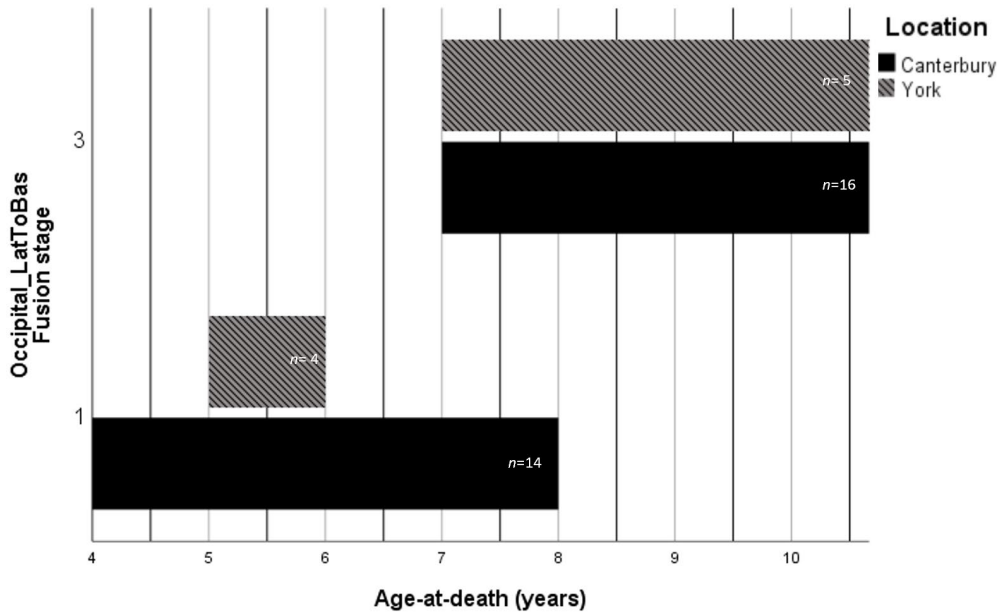
  

Fishergate House (York)				Abbey of St Mary (Cirencester)				Auldham (East Lothian)			
		Stage of union				Stage of union				Stage of union	
Age	n	1	3	Age	n	1	3	Age	n	1	3
5	2	100.0	-	6	2	100.0	-	11	1	-	100.0
6	1	100.0	-	8	1	100.0	-				
7	1	-	100.0								
9	1	-	100.0								
10	1	-	100.0								
11	1	-	100.0								

The figure below shows the age distribution of individuals from various Mediaeval sites for the **pars lateralis to pars basilaris** of the occipital bone. This shows the entire sub-sample that had these bones present.



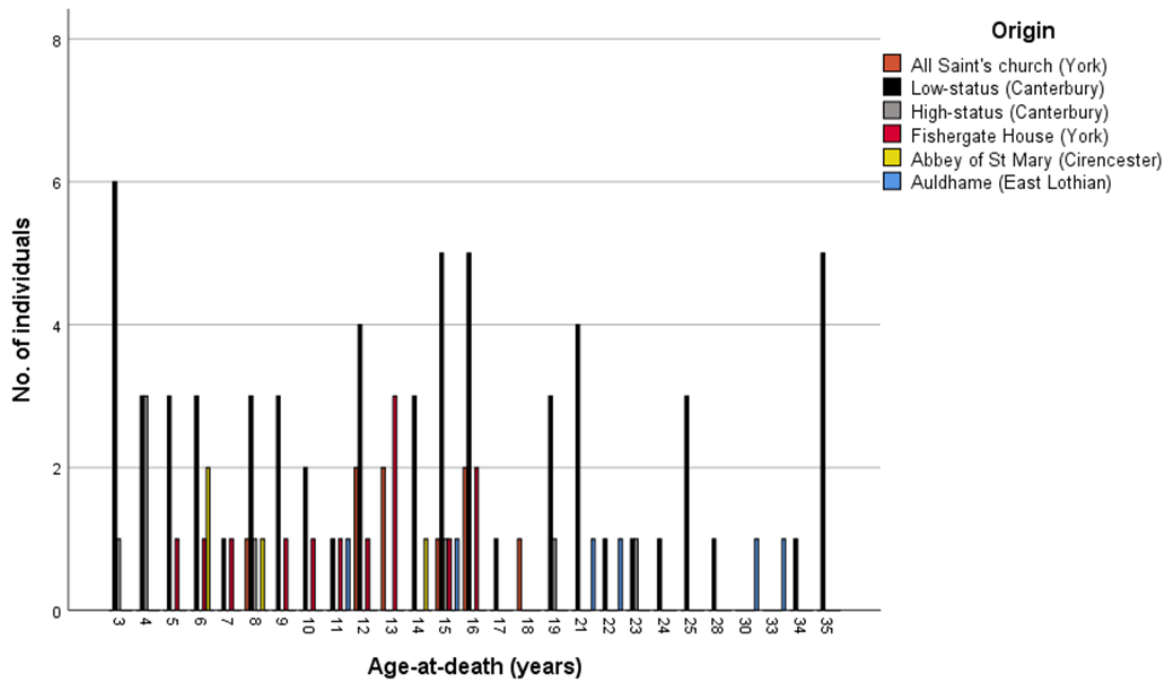
The figure below shows the timing of fusion for individuals from various Mediaeval archaeological sites grouped under Canterbury and York for the **pars lateralis to pars basilaris**. Stage 1 (unfused), Stage 3 (fused).



The table below shows age at death/phase for the fusion of the **spheno-occipital synchondrosis** for all archaeological Mediaeval sites sampled. Frequencies are recorded as percentages.

Spheno-occipital synchondrosis														
All Saint's church (York)				Low-status				High-status						
Stage of union				Stage of union				Stage of union						
Age	n	1	2	3	Age	n	1	2	3	Age	n	1	2	3
13	2	100.0	-	-	14	3	100.0	-	-	15	1	100.0	-	-
15	1	100.0	-	-	15	5	100.0	-	-	19	1	-	-	100.0
16	2	50.0	-	50.0	16	5	80.0	20.0	-					
18	1	100.0	-	-	17	1	-	-	100.0					
					19	3	-	-	100.0					
Fishergate House (York)				Abbey of St Mary (Cirencester)				Auldham (East Lothian)						
Stage of union				Stage of union				Stage of union						
Age	n	1	2	3	Age	n	1	2	3	Age	n	1	2	3
13	3	100.0	-	-	14	1	100.0	-	-	15	1	100.0	-	-
15	1	100.0	-	-						21	1	-	-	100.0
16	2	100.0	-	-										

The figure below shows age distribution of individuals from various Mediaeval sites for the fusion of the **spheno-occipital synchondrosis**. This shows the entire sub-sample that had these bones present.



The table below shows the age in years/ phase for the fusion of the occipital bone of the skull, including the (1) pars lateralis to pars basilaris and (2) the spheno-occipital synchondrosis for the Mediaeval Canterbury and York samples. Frequencies are recorded as percentages.

		Mediaeval York					Mediaeval Canterbury					
		Stage of union					Stage of union					
		Age	<i>n</i>	1	2	3	Age	<i>n</i>	1	2	3	
The Occipital	Pars lateralis to pars basilaris	5	3	100.0		–	4	5	100.0		–	
		6	1	100.0		–	5	4	100.0		–	
		7	1	–		100.0	6	3	100.0		–	
		9	1	–		100.0	7	3	33.3		66.7	
		10	1	–		100.0	8	6	16.7		83.3	
		11	2	–		100.0	9	4	–		100.0	
	Spheno-occipital synchondrosis											
		13	5	100.0	–	–	14	3	100.0	–	–	
		15	2	100.0	–	–	15	6	100.0	–	–	
		16	4	75.0	–	25.0	16	5	80.0	20.0	–	
		18	1	100.0	–	–	17	1	–	–	100.0	
						19	4	–	–	100.0		

### A7. 2. The Cervical vertebrae

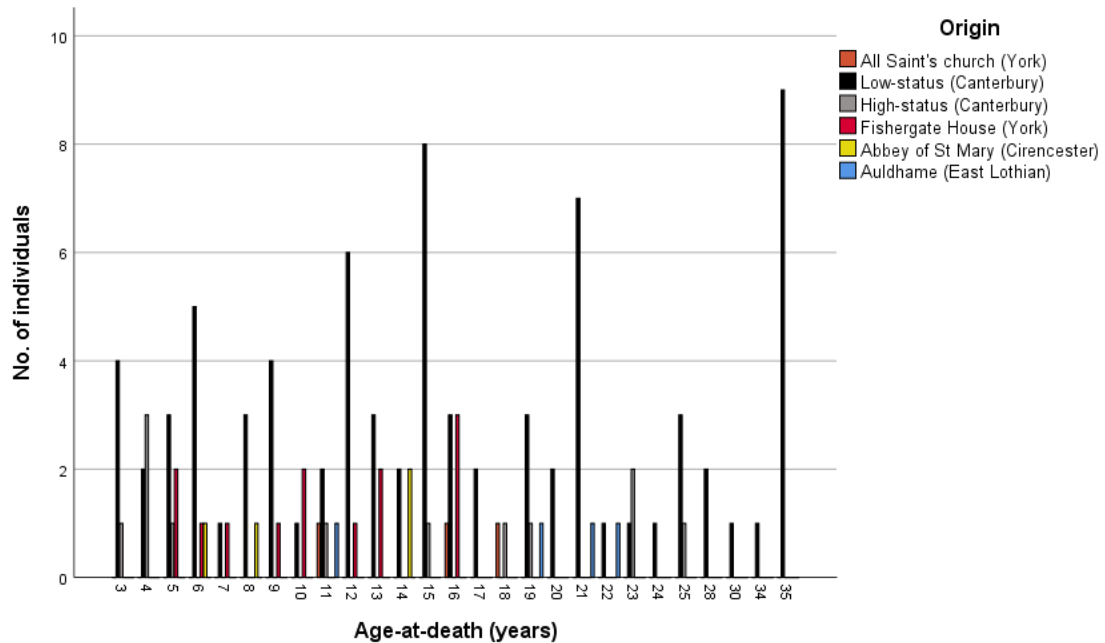
The table below shows age at death/phase for the fusion of the **anterior arch** of the atlas (C1) for all archaeological Mediaeval sites sampled. Frequencies are recorded as percentages.

Fusion of the anterior arch of the atlas (C1)														
All Saint's church (York)				Low-status				High-status						
Age	n	Stage of union			Age	n	Stage of union			Age	n	Stage of union		
		1	2	3			1	2	3			1	2	3
11	1	-	-	100.0	5	3	100.0	-	-	5	1	100.0	-	-
16	1	-	-	100.0	6	5	100.0	-	-	11	1	-	-	100.0
18	1	-	-	100.0	7	1	100.0	-	-	15	1	-	-	100.0
					8	3	-	-	100.0	18	1	-	-	100.0
					9	4	-	25.0	75.0	19	1	-	-	100.0
					10	1	-	-	100.0					
					11	2	-	-	100.0					
					12	6	16.7	-	83.3					
					13	3	-	-	100.0					
					14	2	-	-	100.0					
					15	8	12.5	-	87.5					
					16	3	-	-	100.0					
					17	2	-	-	100.0					

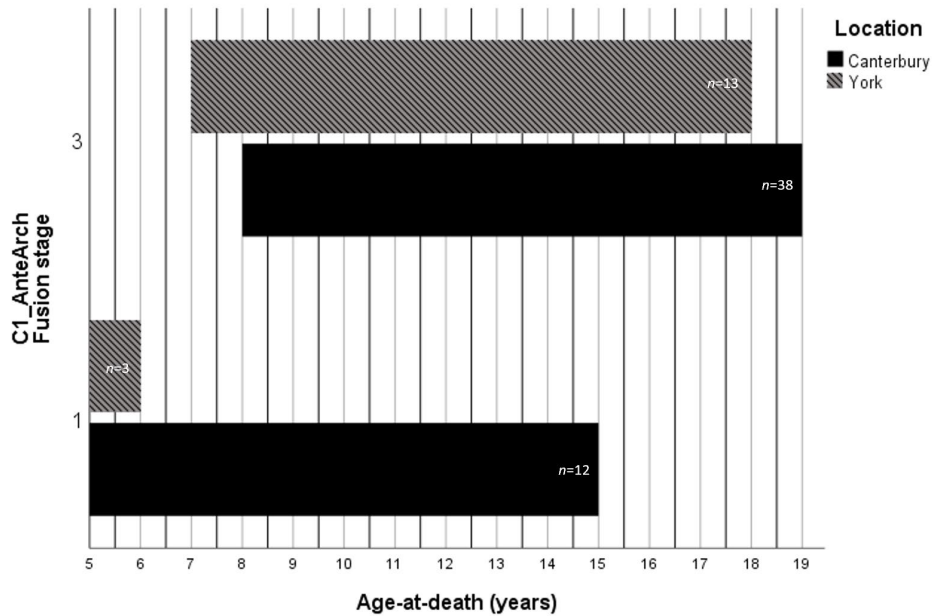
  

Fishergate House (York)				Abbey of St Mary (Cirencester)				Auldham (East Lothian)						
Age	n	Stage of union			Age	n	Stage of union			Age	n	Stage of union		
		1	2	3			1	2	3			1	2	3
5	2	100.0	-	-	6	1	100.0	-	-	11	1	-	-	100.0
6	1	100.0	-	-	8	1	-	100.0	-	19	1	-	-	100.0
7	1	-	-	100.0	14	2	-	-	100.0					
9	1	-	-	100.0										
10	2	-	-	100.0										
12	1	-	-	100.0										
13	2	-	-	100.0										
16	3	-	-	100.0										

The figure below shows the age distribution of individuals from various Mediaeval sites for the fusion of the **anterior arch** of the atlas (C1). This shows the entire sub-sample that had these bones present.



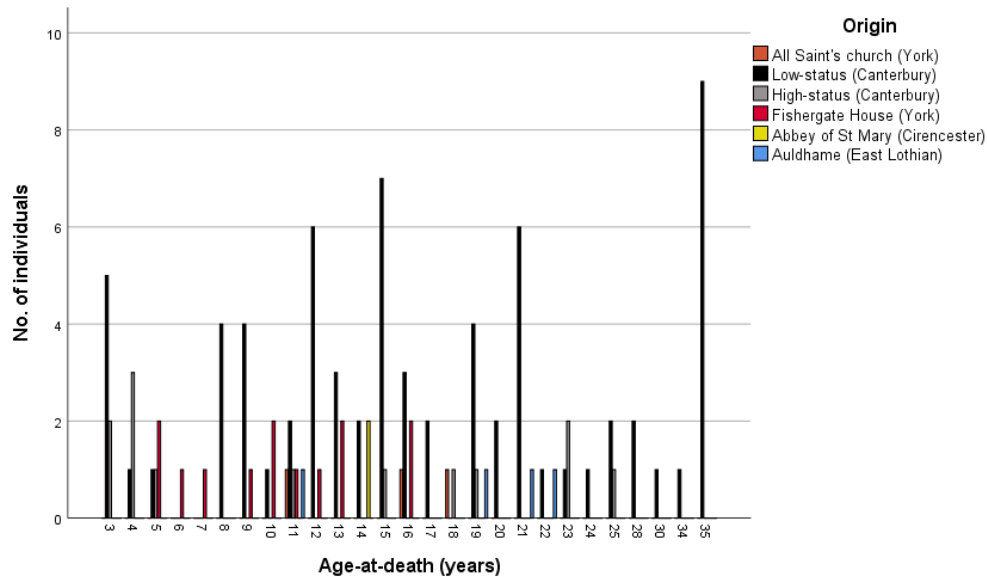
The figure below shows the timing of fusion for individuals from various Mediaeval archaeological sites grouped under Canterbury and York for the **anterior arch** of the atlas (C1). Stage 2 is not represented in the figure due to having only one data point. Stage 1 (unfused), Stage 3 (fused).



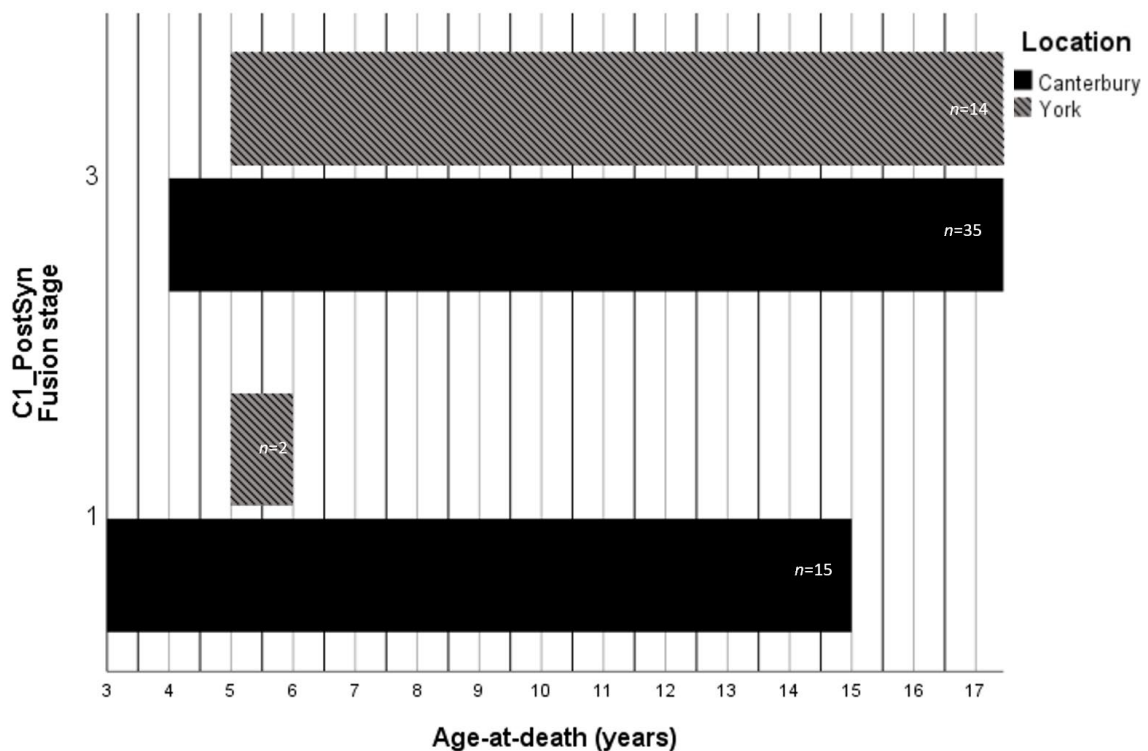
The table below gives the age at death/phase for the fusion of the **posterior synchondrosis** of the atlas (C1) for all archaeological Mediaeval sites sampled. Frequencies are recorded as percentages.

Fusion of the posterior synchondrosis of the atlas (C1)												
All Saint's church (York)				Low-status				High-status				
Stage of union		Stage of union		Stage of union		Stage of union		Stage of union		Stage of union		
Age	n	1	3	Age	n	1	3	Age	n	1	3	
11	1	-	100.0	3	5	100.0	-	3	2	100.0	-	
16	1	-	100.0	4	1	100.0	-	4	3	66.7	33.3	
18	1	-	100.0	5	1	100.0	-	5	1	100.0	-	
				8	4	-	100.0	11	1	-	100.0	
				9	4	25.0	75.0	15	1	-	100.0	
				10	1	-	100.0	18	1	-	100.0	
				11	2	-	100.0					
				12	6	16.7	83.3					
				13	3	-	100.0					
				14	2	-	100.0					
				15	7	14.3	85.7					
				16	3	-	100.0					
				17	2	-	100.0					
Fishergate House (York)				Abbey of St Mary (Cirencester)				Auldham (East Lothian)				
Stage of union		Stage of union		Stage of union		Stage of union		Stage of union		Stage of union		
Age	n	1	3	Age	n	1	3	Age	n	1	3	
5	2	50.0	50.0	14	2	-	100.0	11	1	-	100.0	
6	1	100.0	-									
7	1	-	100.0									
9	1	-	100.0									
10	2	-	100.0									
11	1	-	100.0									
12	1	-	100.0									
13	2	-	100.0									
16	2	-	100.0									

The figure below gives the age distribution of individuals from various Mediaeval sites for the fusion of the **posterior synchondrosis** of the atlas (C1). This shows the entire sub-sample that had these bones present.

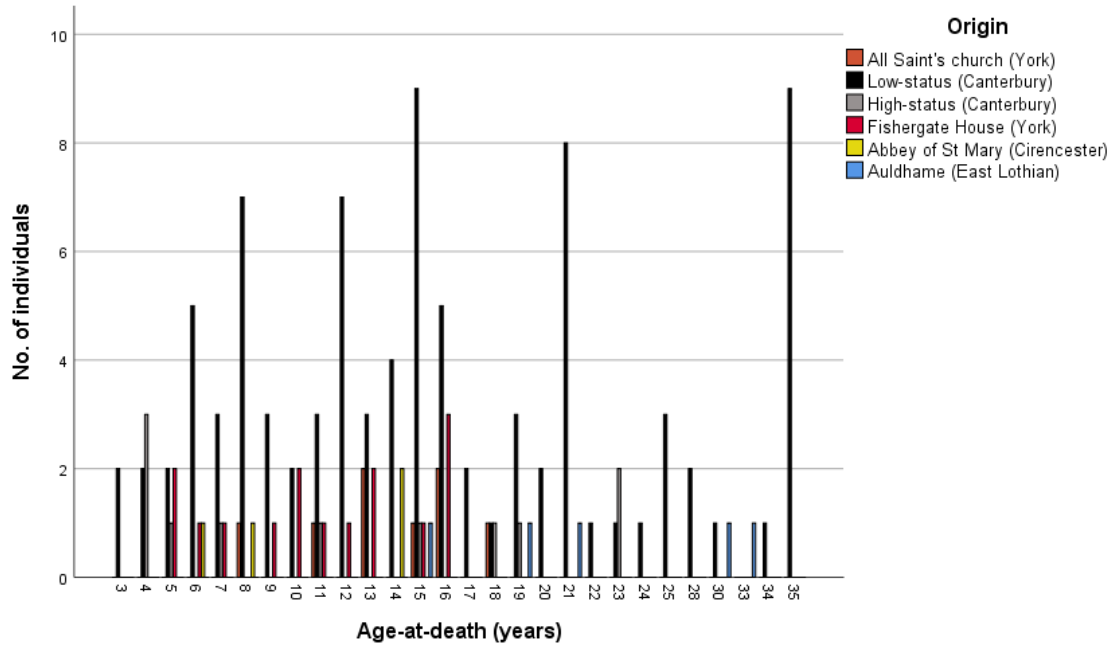


The figure below shows the timing of fusion for individuals from various Mediaeval archaeological sites grouped under Canterbury and York for the fusion of the **posterior synchondrosis** of the atlas (C1). Stage 1 (unfused), Stage 3 (fused).





The below table shows age distribution of individuals from various Mediaeval sites for the fusion of the **ossiculum terminale to the dens of the axis (C2)**. This shows the entire sub-sample that had these bones present.

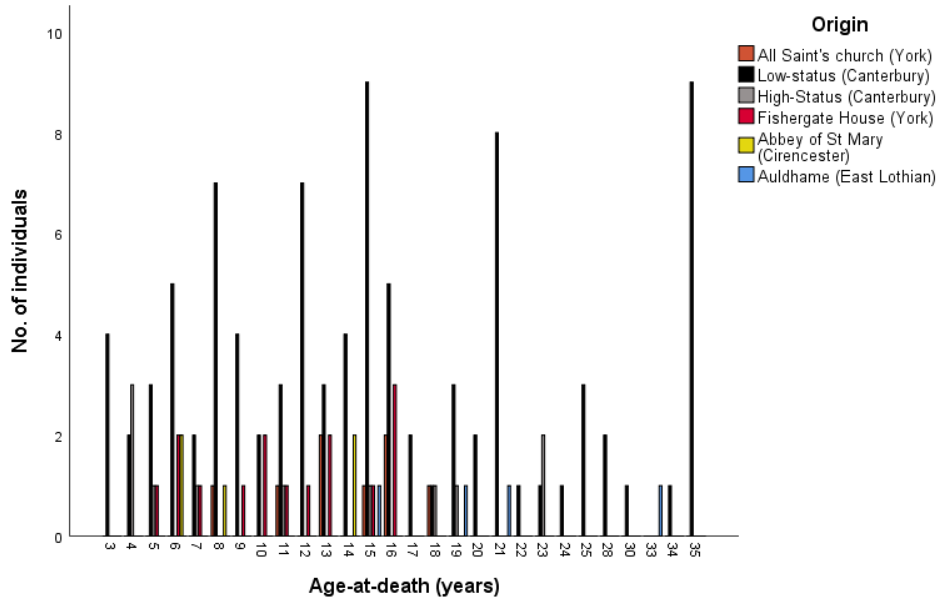


The table below shows the age at death/phase for the fusion of the **dentoneural synchondrosis** of the axis (C2) for all archaeological Mediaeval sites sampled. Frequencies are recorded as percentages.

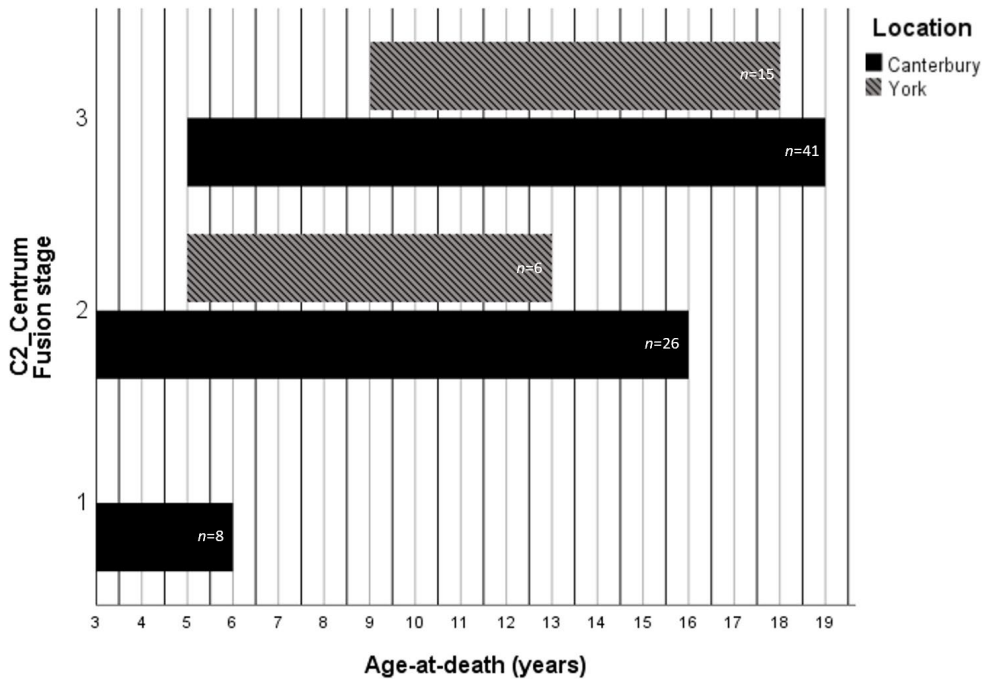
Fusion of the dentoneural synchondrosis of the axis vertebrae (C2)														
All Saint's church (York)					Low-status					High-status				
Stage of union					Stage of union					Stage of union				
Age	n	1	2	3	Age	n	1	2	3	Age	n	1	2	3
5	1	-	-	100.0	3	5	80.0	-	20.0	3	1	100.0	-	-
8	1	-	-	100.0	4	2	50.0	-	50.0	4	3	66.7	-	33.3
					5	4	50.0	-	50.0	5	1	100.0	-	-
					6	5	40.0	20.0	40.0	7	1	-	-	100.0
					7	3	-	-	100.0					
					8	7	-	-	100.0					
					9	4	-	-	100.0					
Fishergate House (York)					Abbey of St Mary (Cirencester)									
Stage of union					Stage of union									
Age	n	1	2	3	Age	n	1	2	3					
5	2	50.0	-	50.0	6	2	100.0	-	-					
6	1	-	100.0	-	8	1	-	-	100.0					
7	1	-	-	100.0										
9	1	-	-	100.0										



The figure below shows the age distribution of individuals from various Mediaeval sites for the fusion of the **dentocentral and neurocentral junctions** of the axis (C2). This shows the entire sub-sample that had these bones present.



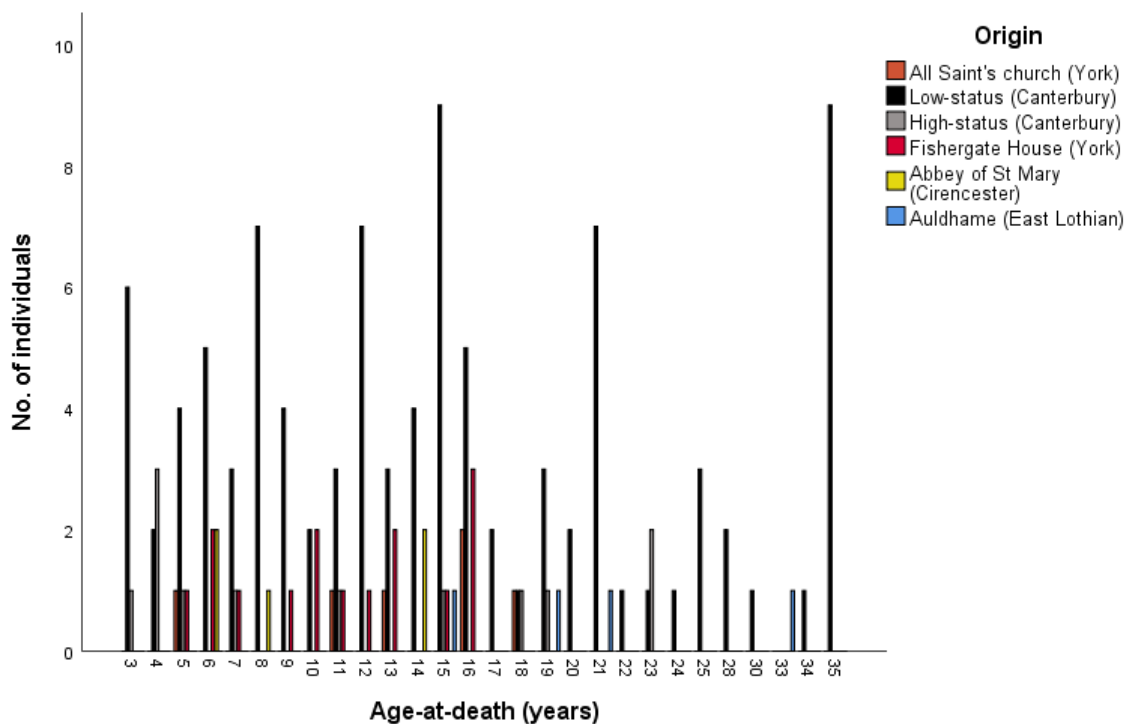
The figure below shows the timing of fusion for individuals from various Mediaeval archaeological sites grouped under Canterbury and York for the **dentocentral and neurocentral junctions** of the axis. Stage 1 of York is not represented on the figure due to being a singular data point. Stage 1 (unfused), Stage 2 (fusing), Stage 3 (fused).



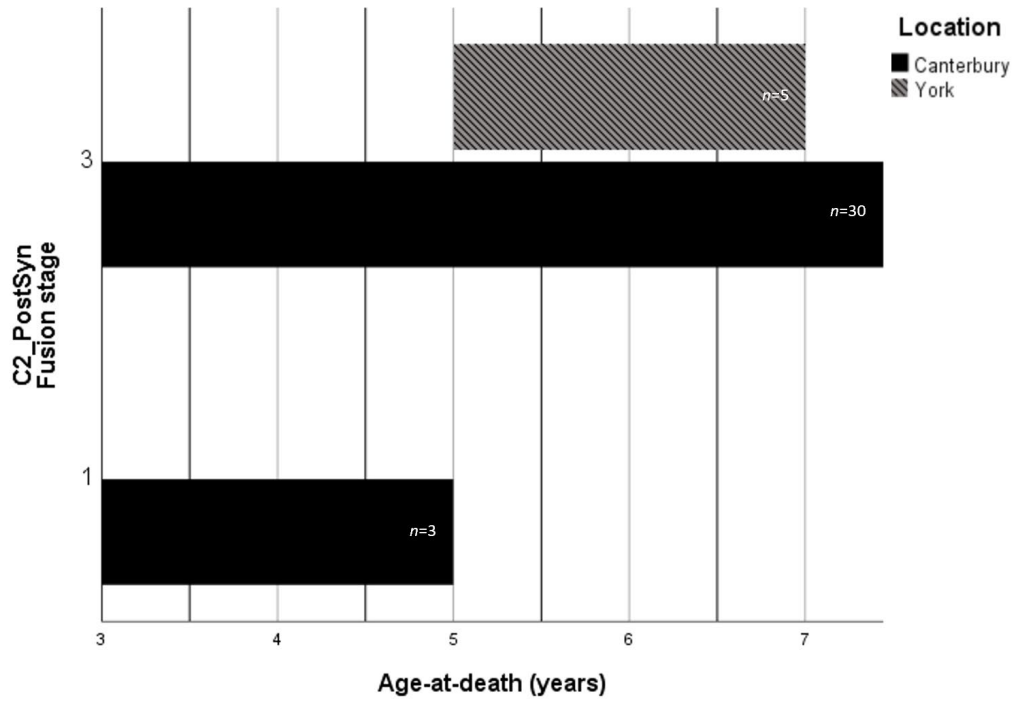
The table below shows the age at death/phase for the fusion of the **posterior synchondrosis** of the axis (C2) for all archaeological Mediaeval sites sampled. Frequencies are recorded as percentages.

Fusion of the posterior synchondrosis of the axis (C2)											
All Saint's church (York)				Low-status				High-status			
		Stage of union				Stage of union				Stage of union	
Age	n	1	3	Age	n	1	3	Age	n	1	3
5	1	-	100.0	3	6	33.3	66.7	3	1	-	100.0
				4	2	-	100.0	4	3	-	100.0
				5	4	25.0	75.0	5	1	-	100.0
				6	5	-	100.0	7	1	-	100.0
				7	3	-	100.0				
				8	7	-	100.0				
Fishergate House (York)				Abbey of St Mary (Cirencester)							
		Stage of union				Stage of union					
Age	n	1	3	Age	n	1	3				
5	1	-	100.0	6	2	-	100.0				
6	2	-	100.0	8	1	-	100.0				
7	1	-	100.0								

The figure below gives the age distribution of individuals from various Mediaeval sites for the fusion of the **posterior synchondrosis** of the axis (C2). This shows the entire sub-sample that had these bones present.



The figure shows the timing of fusion for individuals from various Mediaeval archaeological sites grouped under Canterbury and York for the **posterior synchondrosis** of the axis. Stage 1 (unfused), Stage 3 (fused).



The table below gives the age in years/phase for the fusion of the **axis of the cervical vertebrae**, including (1) the ossiculum terminale to the dens, (2) the dentoneural synchondrosis, (3) the dentocentral and neurocentral junctions, and (4) the posterior synchondrosis for the Mediaeval Canterbury and York samples. Frequencies are recorded as percentages.

		Mediaeval York				Mediaeval Canterbury							
		Stage of union			Stage of union								
		Age	n	1	2	3	Age	n	1	2	3		
The axis	Ossiculum terminale to the dens	5	2	100.0	-	-	5	3	100.0	-	-		
		6	1	100.0	-	-	6	5	100.0	-	-		
		7	1	100.0	-	-	7	4	100.0	-	-		
		8	1	-	100.0	-	8	7	85.7	14.3	-		
		9	1	-	-	100.0	9	3	33.3	66.7	-		
		10	2	-	-	100.0	10	2	-	100.0	-		
		11	2	50.0	-	50.0	11	4	25.0	-	75.0		
		12	1	-	-	100.0	12	7	-	28.6	71.4		
		13	4	-	-	100.0	13	3	-	33.3	66.7		
		15	2	-	-	100.0	14	4	25.0	-	75.0		
		16	5	-	-	100.0	15	10	-	10.0	90.0		
		18	1	-	-	100.0	16	5	-	-	100.0		
							17	2	-	-	100.0		
							18	2	-	-	100.0		
				Age	n	1	2	3	Age	n	1	2	3
			Dentoneural synchondrosis	5	3	33.3	-	66.7	3	6	83.3	-	16.7
				6	1	-	100.0	-	4	5	60.0	-	40.0
				7	1	-	-	100.0	5	5	60.0	-	40.0
	8	1		-	-	100.0	6	5	40.0	20.0	40.0		
	9	1		-	-	100.0	7	4	-	-	100.0		
		Age	n	1	2	3	Age	n	1	2	3		
	Dentocentral & neurocentral junctions	5	1	-	100.0	-	3	4	75.0	25.0	-		
		6	2	100.0	-	-	4	5	60.0	40.0	-		
		7	1	-	100.0	-	5	4	25.0	50.0	25.0		
		8	1	-	100.0	-	6	5	20.0	80.0	-		
		9	1	-	-	100.0	7	3	-	66.7	33.3		
		10	2	-	50.0	50.0	8	7	-	57.1	42.9		
		11	2	-	50.0	50.0	9	4	-	50.0	50.0		
		12	1	-	-	100.0	10	2	-	50.0	50.0		
		13	4	-	25.0	75.0	11	4	-	-	100.0		
		15	2	-	-	100.0	12	7	-	71.4	28.6		
		16	5	-	-	100.0	13	3	-	33.3	66.7		
		18	1	-	-	100.0	14	4	-	25.0	75.0		
							15	10	-	-	100.0		
							16	5	-	20.0	80.0		
						17	2	-	-	100.0			
						18	2	-	-	100.0			
						19	4	-	-	100.0			
		Age	n	1		3	Age	n	1		3		
	Posterior synchondrosis	5	2	-		100.0	3	7	28.6		71.4		
		6	2	-		100.0	4	5	-		100.0		
		7	1	-		100.0	5	5	20.0		80.0		
							6	5	-		100.0		
							7	4	-		100.0		
						8	7	-		100.0			

### A7.3. The Sacrum

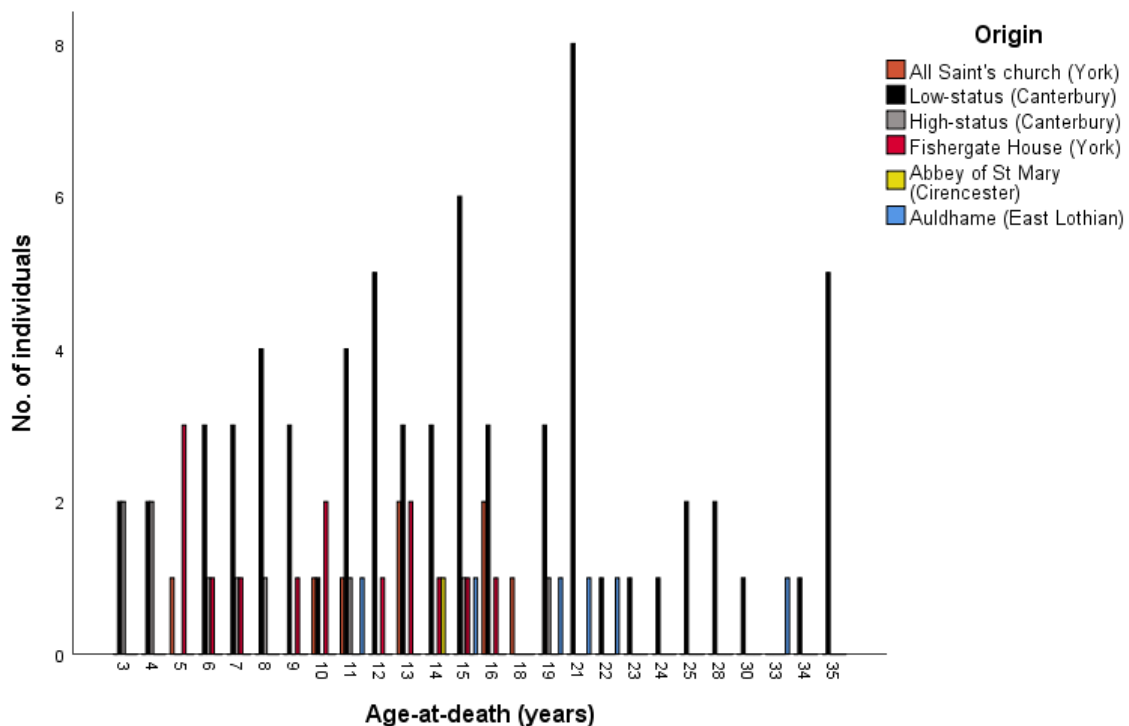
The table below shows the age at death/phase for the fusion of **sacral bodies 1 and 2** of the sacrum for all archaeological Mediaeval sites sampled. Frequencies are recorded as percentages.

Fusion of sacral bodies 1 & 2 of the sacrum														
All Saint's church (York)				Low-status				High-status						
Stage of union				Stage of union				Stage of union						
Age	n	1	2	3	Age	n	1	2	3	Age	n	1	2	3
16	2	100.0	-	-	16	3	100.0	-	-	19	1	-	100.0	-
18	1	100.0	-	-	19	3	-	66.7	33.3					
					21	8	-	75.0	25.0					
					22	1	-	100.0	-					
					23	1	-	-	100.0					
					24	1	-	-	100.0					
					25	2	-	100.0	-					
					28	2	-	-	100.0					

Fishergate House (York)				Auldham (East Lothian)					
Stage of union				Stage of union					
Age	n	1	2	3	Age	n	1	2	3
16	1	-	100.0	-	19	1	-	100.0	-
					21	1	-	-	100.0
					22	1	-	100.0	-

The figure below shows the age distribution of individuals from various Mediaeval sites for the fusion of **sacral bodies 1 and 2** of the sacrum. This shows the entire sub-sample that had these bones present.



The table below shows the age in years/ phase for the fusion of the sacrum for **bodies 1 and 2** for the Mediaeval Canterbury and York samples, Frequencies are recorded as percentages.

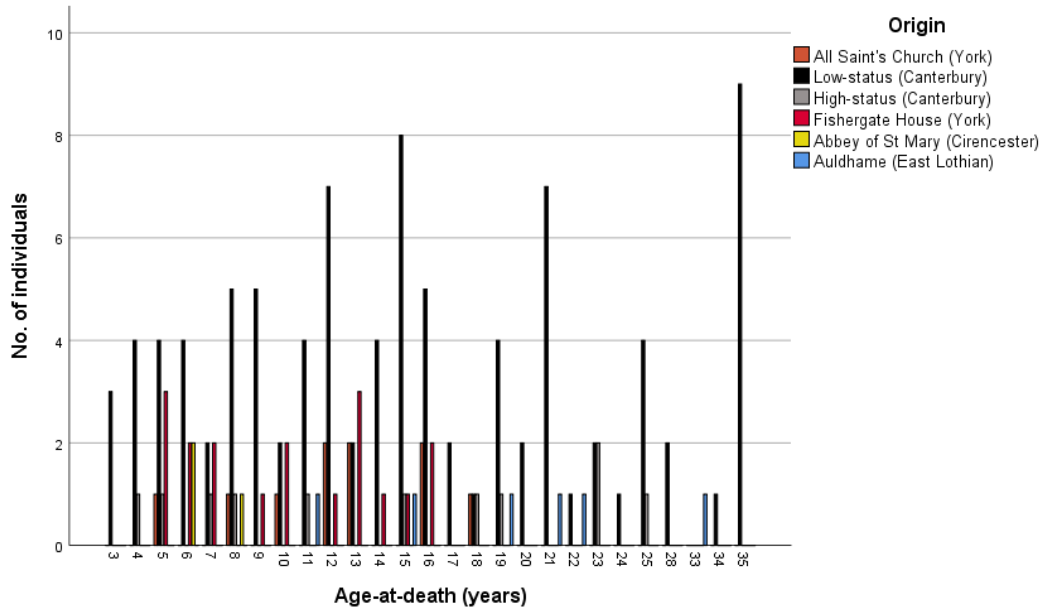
		Mediaeval York					Mediaeval Canterbury				
		Stage of union					Stage of union				
		Age	<i>n</i>	1	2	3	Age	<i>n</i>	1	2	3
The sacrum	Bodies 1 & 2	16	3	66.7	33.3	-	16	3	100.0	-	-
		18	1	100.0	-	-	19	4	-	75.0	25.0
							21	8	-	75.0	25.0
							22	1	-	100.0	-
							23	1	-	-	100.0
							24	1	-	-	100.0
							25	2	-	100.0	-
							28	2	-	-	100.0

#### A7. 4. The Clavicle

The table below shows the age at death/phase for the fusion of the **medial epiphysis** of the clavicle for all archaeological Mediaeval sites sampled. Frequencies are recorded as percentages.

Medial epiphysis of the clavicle														
All Saint's church (York)					Low-status					High-status				
Stage of union					Stage of union					Stage of union				
Age	<i>n</i>	1	2	3	Age	<i>n</i>	1	2	3	Age	<i>n</i>	1	2	3
16	2	100.0	-	-	16	5	100.0	-	-	18	1	100.0	-	-
18	1	100.0	-	-	17	2	100.0	-	-	19	1	-	100.0	-
					18	1	100.0	-	-	23	2	-	-	100.0
					19	4	75.0	-	25.0	25	1	-	-	100.0
					20	2	50.0	-	50.0					
					21	7	42.9	28.6	28.6					
					22	1	100.0	-	-					
					23	2	50.0	-	50.0					
					24	1	100.0	-	-					
					25	4	-	25.0	75.0					
					28	2	-	-	100.0					
Fishergate House (York)					Auldham (East Lothian)									
Stage of union					Stage of union									
Age	<i>n</i>	1	2	3	Age	<i>n</i>	1	2	3					
16	2	100.0	-	-	19	1	100.0	-	-					
					21	1	-	100.0	-					
					22	1	100.0	-	-					

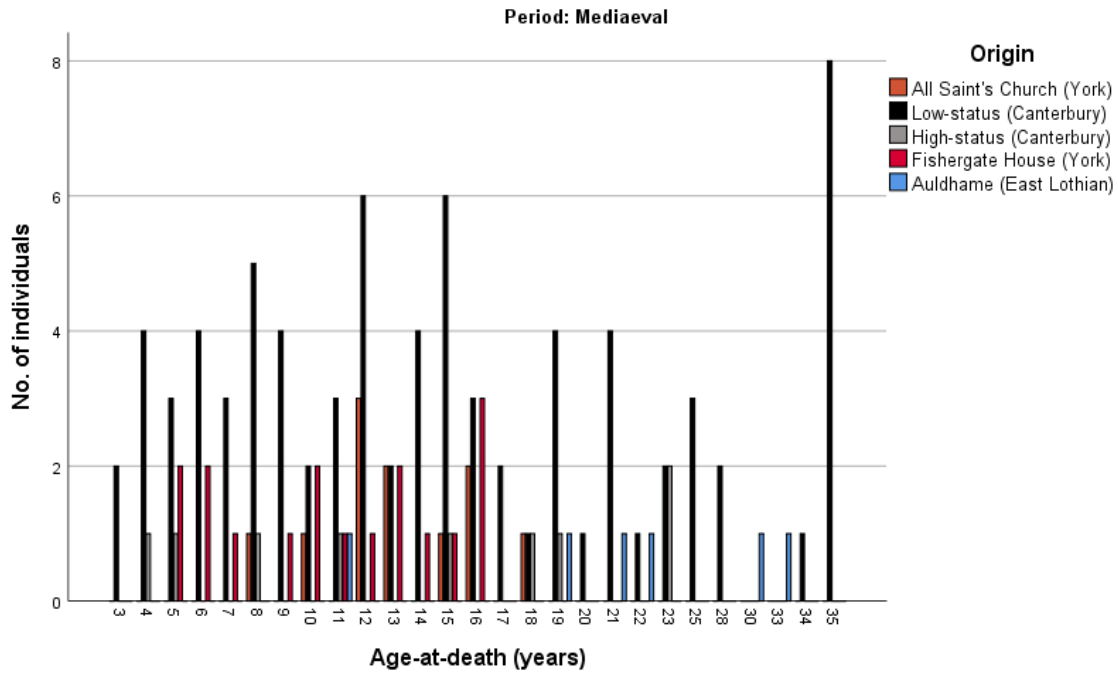
The figure below shows the age distribution of individuals from various Mediaeval sites for the fusion of the **medial epiphysis** of the clavicle. This shows the entire sub-sample that had these bones present.



The table below shows the age at death/phase for the fusion of the **lateral epiphysis** of the clavicle for all archaeological Mediaeval sites sampled. Frequencies are recorded as percentages.

Lateral epiphysis of the clavicle														
All Saint's church (York)					Low-status					High-status				
Age	n	1	2	3	Age	n	1	2	3	Age	n	1	2	3
15	1	100.0	-	-	14	4	100.0	-	-	15	1	100.0	-	-
16	2	100.0	-	-	15	6	100.0	-	-	18	1	100.0	-	-
18	1	100.0	-	-	16	3	100.0	-	-	19	1	-	-	100.0
					17	2	50.0	50.0	-	23	2	-	-	100.0
					18	1	100.0	-	-					
					19	4	25.0	-	75.0					
					20	1	-	-	100.0					
					21	4	-	-	100.0					
					22	1	-	100.0	-					
					23	2	-	-	100.0					
					25	3	-	-	100.0					
Fishergate House (York)					Auldhame (East Lothian)									
Age	n	1	2	3	Age	n	1	2	3					
14	1	100.0	-	-	19	1	100.0	-	-					
15	1	100.0	-	-	21	1	-	-	100.0					
16	3	100.0	-	-	22	1	100.0	-	-					

The figure below shows the age distribution of individuals from various Mediaeval sites for the fusion of the **lateral epiphysis** of the clavicle. This shows the entire sub-sample that had these bones present.



The table below gives the age in years/ phase for the fusion of the clavicle, including the (1) medial and (2) lateral epiphyses for the Mediaeval Canterbury and York samples. Frequencies are recorded as percentages.

		Mediaeval York					Mediaeval Canterbury					
		Stage of union					Stage of union					
		Age	<i>n</i>	1	2	3	Age	<i>n</i>	1	2	3	
The clavicle	Medial epiphysis	16	4	100.0	-	-	16	5	100.0	-	-	
		18	1	100.0	-	-	17	2	100.0	-	-	
							18	2	100.0	-	-	
							19	5	60.0	20.0	20.0	
							20	2	50.0	-	50.0	
							21	7	42.9	28.6	28.6	
							22	1	100.0	-	-	
						23	4	25.0	-	75.0		
						24	1	100.0	-	-		
						25	5	-	20.0	80.0		
						28	2	-	-	100.0		
		Lateral epiphysis	14	1	100.0	-	-	14	4	100.0	-	-
			15	2	100.0	-	-	15	7	100.0	-	-
		16	5	100.0	-	-	16	3	100.0	-	-	
		18	1	100.0	-	-	17	2	50.0	50.0	-	
							18	2	100.0	-	-	
							19	5	20.0	-	80.0	
							20	1	-	-	100.0	
							21	4	-	-	100.0	
							22	1	-	100.0	-	
							23	4	-	-	100.0	
							25	3	-	-	100.0	

### A7.5. The Scapula

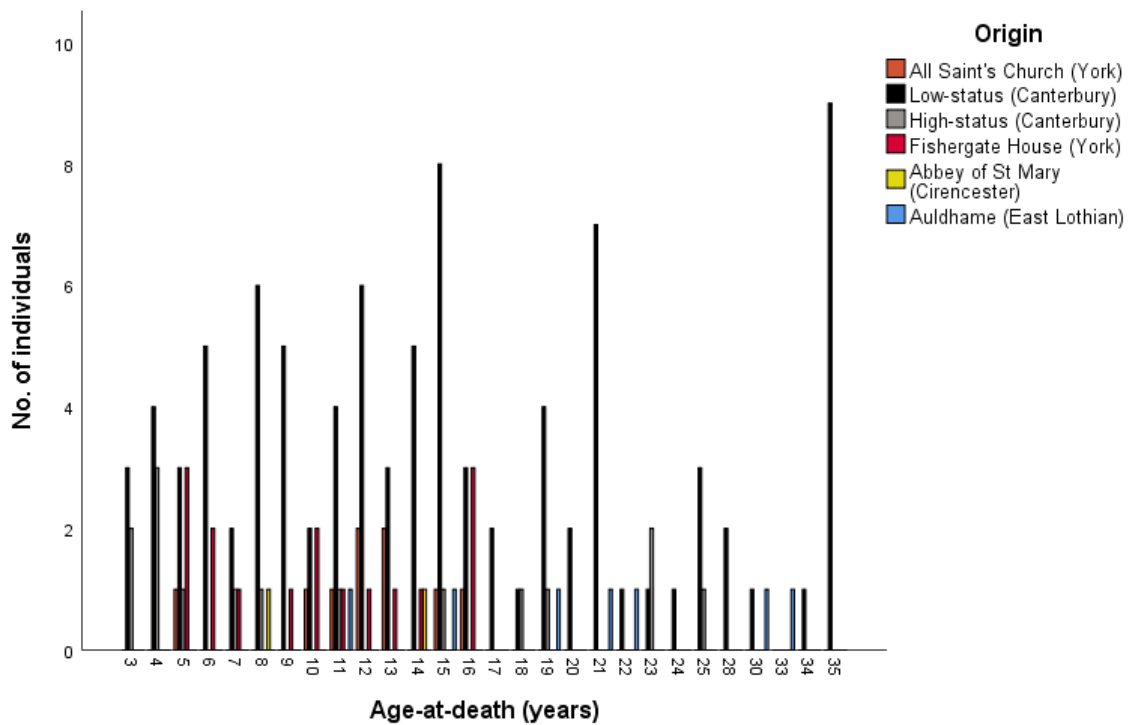
The table below shows the age at death/phase for the fusion of the **coracoid** to the body of the scapula for all archaeological Mediaeval sites sampled. Frequencies are recorded as percentages.

Coracoid process to body of the scapula														
All Saint's church (York)					Low-status					High-status				
Age	n	1	2	3	Age	n	1	2	3	Age	n	1	2	3
Stage of union					Stage of union					Stage of union				
13	2	100.0	-	-	13	3	100.0	-	-	15	1	100.0	-	-
15	1	100.0	-	-	14	5	100.0	-	-	18	1	-	-	100.0
16	1	100.0	-	-	15	8	100.0	-	-	19	1	-	-	100.0
					16	3	-	33.3	66.7					
					17	2	-	-	100.0					
					18	1	-	-	100.0					
					19	4	-	-	100.0					

Fishergate House (York)					Abbey of St Mary (Cirencester)					Auldham (East Lothian)				
Age	n	1	2	3	Age	n	1	2	3	Age	n	1	2	3
Stage of union					Stage of union					Stage of union				
13	1	100.0	-	-	14	1	100.0	-	-	15	1	100.0	-	-
14	1	100.0	-	-						19	1	-	-	100.0
16	3	33.3	-	66.7										

The figure shows the age distribution of individuals from various Mediaeval sites for the fusion of the **coracoid** to the body of the scapula. This shows the entire sub-sample that had these bones present.



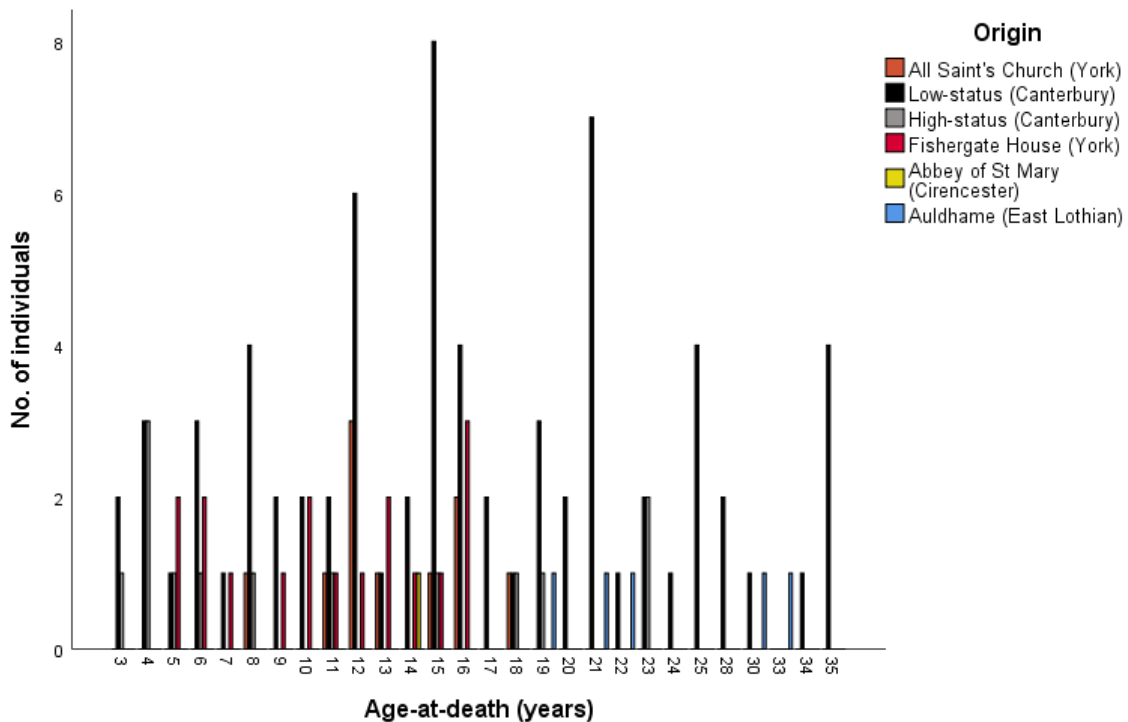
The table below shows the age at death/phase for the fusion of the **acromial epiphysis** to the scapula for all archaeological Mediaeval sites sampled. Frequencies are recorded as percentages.

Acromial epiphysis to the scapula											
All Saint's church (York)				Low-status				High-status			
Age	Stage of union			Age	Stage of union			Age	Stage of union		
	n	1	3		n	1	3		n	1	3
15	1	100.0	-	14	2	100.0	-	15	1	100.0	-
16	2	100.0	-	15	8	100.0	-	18	1	-	100.0
18	1	100.0	-	16	4	100.0	-	19	1	-	100.0
				17	2	50.0	50.0				
				18	1	100.0	-				
				19	3	-	100.0				
				20	2	-	100.0				
				21	7	-	100.0				

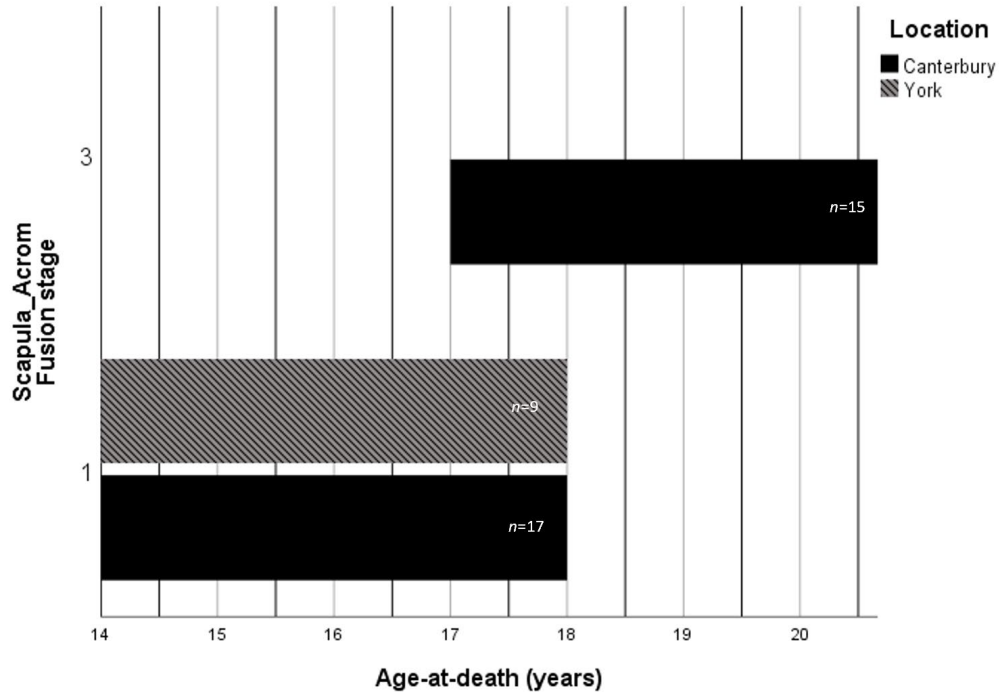
  

Fishergate House (York)				Abbey of St Mary (Cirencester)			
Age	Stage of union			Age	Stage of union		
	n	1	3		n	1	3
14	1	100.0	-	14	1	100.0	-
15	1	100.0	-				
16	3	100.0	-				

The figure below shows the age distribution of individuals from various Mediaeval sites for the fusion of the **acromial epiphysis** to the scapula. This shows the entire sub-sample that had these bones present.



The figure below shows the timing of fusion for individuals from various Mediaeval archaeological sites grouped under Canterbury and York for the **acromial epiphysis** of the scapula. Stage 1 (unfused), Stage 3 (fused).



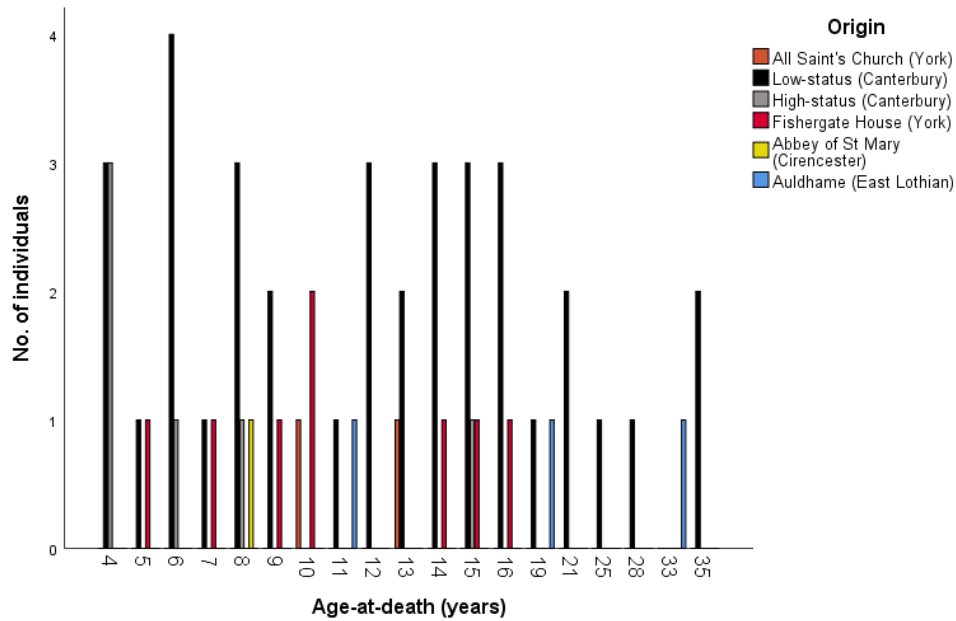
The table below shows the age at death/phase for the fusion of the **medial border** to the scapula for all archaeological Mediaeval sites sampled. Frequencies are recorded as percentages.

Medial border of the scapula												
Low-status				High-status					Fishergate House (York)			
Age	n	1	3	Age	n	1	3	Age	n	1	3	
16	3	100.0	-	15	1	100.0	-	15	1	100.0	-	
19	1	-	100.0					16	1	100.0	-	
21	2	50.0	50.0									
25	1	-	100.0									

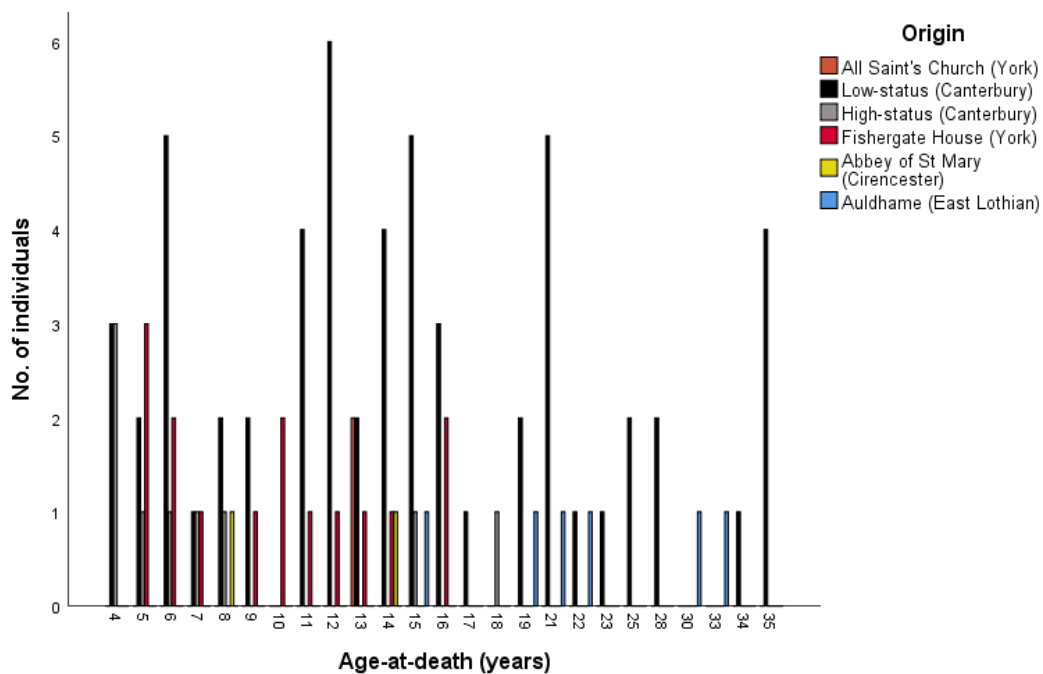
  

Auldham			
Age	n	1	3
19	1	-	100.0

The figure below shows the age distribution of individuals from various Mediaeval sites for the fusion of the **medial border** to the scapula. This shows the entire sub-sample that had these bones present.

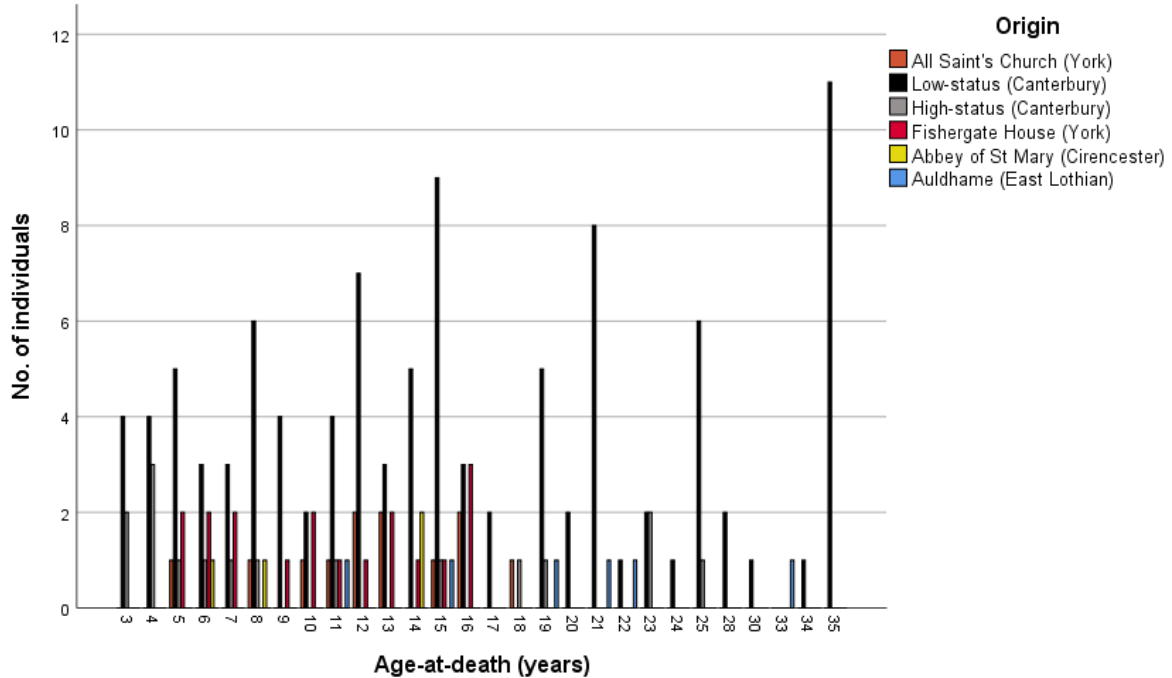


The figure below shows the age distribution of individuals from various Mediaeval sites for the fusion of the **inferior angle epiphysis** to the scapula. This shows the entire sub-sample that had these bones present.





The figure below shows the age distribution of individuals from various Mediaeval sites for the fusion of the **medial epicondyle** to the shaft of the humerus. This shows the entire sub-sample that had these bones present.



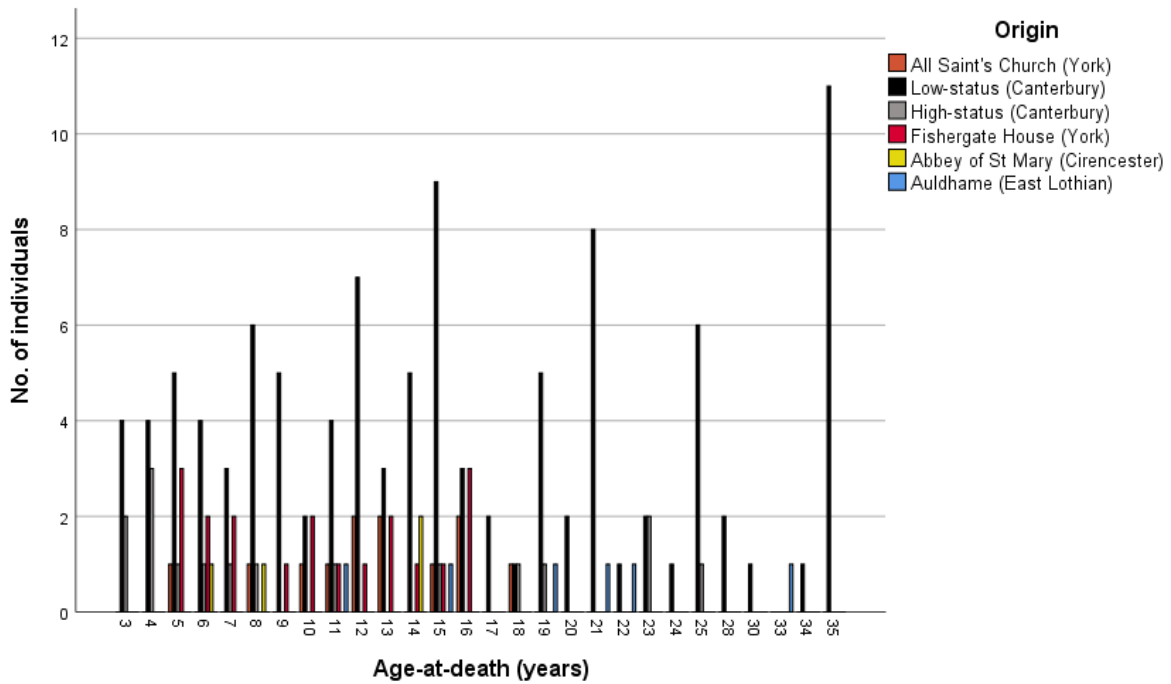
The table below shows the age at death/phase for the fusion of the **distal composite epiphysis** to the shaft of the humerus for all archaeological Mediaeval sites sampled. Frequencies are recorded as percentages.

Distal composite epiphysis to the shaft of the humerus														
All Saint's church (York)				Low-status				High-status						
Age	n	1	2	3	Age	n	1	2	3	Age	n	1	2	3
11	1	100.0	-	-	11	4	100.0	-	-	11	1	100.0	-	-
12	2	100.0	-	-	12	7	100.0	-	-	15	1	100.0	-	-
13	2	100.0	-	-	13	3	100.0	-	-	18	1	-	-	100.0
15	1	100.0	-	-	14	5	80.0	-	20.0					
16	2	100.0	-	-	15	9	33.3	11.1	55.6					
18	1	-	-	100.0	16	3	-	-	100.0					
					17	2	-	-	100.0					
					18	1	-	-	100.0					

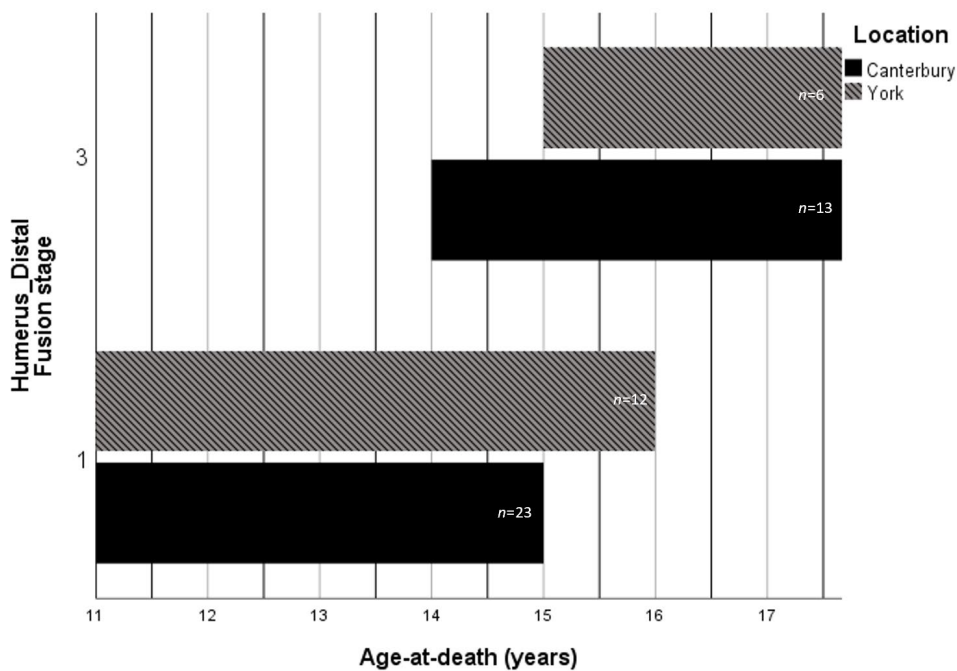
  

Fishergate House (York)				Abbey of St Mary (Cirencester)				Auldhame (East Lothian)						
Age	n	1	2	3	Age	n	1	2	3	Age	n	1	2	3
11	1	100.0	-	-	14	2	-	50.0	50.0	11	1	100.0	-	-
12	1	100.0	-	-						15	1	100.0	-	-
13	2	100.0	-	-										
14	1	100.0	-	-										
15	1	-	-	100.0										
16	3	-	-	100.0										

The figure below shows the age distribution of individuals from various Mediaeval sites for the fusion of the **distal composite epiphysis** to the shaft of the humerus. This shows the entire sub-sample that had these bones present.



The figure below shows the timing of the **distal composite epiphysis** to the shaft of the humerus. Stage 2 is not represented on the figure due to low sample size. Stage 1 (unfused), Stage 3 (fused).



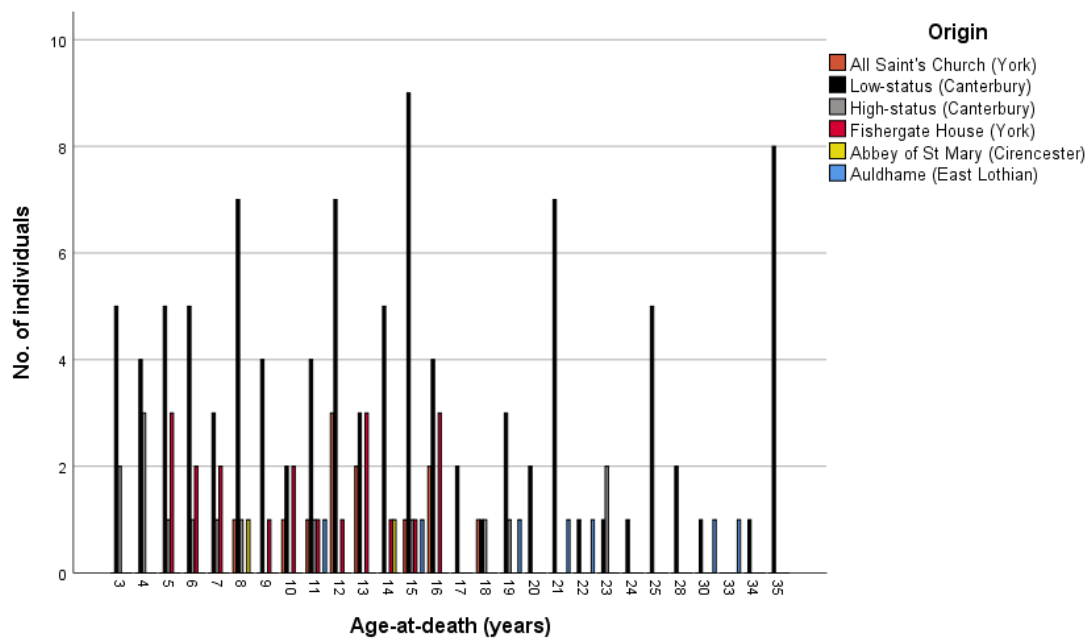
The table below shows the age at death/phase for the fusion of the **proximal epiphysis** to the shaft of the humerus for all archaeological Mediaeval sites sampled. Frequencies are recorded as percentages.

Proximal epiphysis to the shaft of the humerus														
All Saint's church (York)					Low-status					High-status				
Age	n	1	2	3	Age	n	1	2	3	Age	n	1	2	3
15	1	100.0	-	-	14	5	100.0	-	-	15	1	100.0	-	-
16	2	100.0	-	-	15	9	100.0	-	-	18	1	-	100.0	-
18	1	100.0	-	-	16	4	100.0	-	-	19	1	-	-	100.0
					17	2	50.0	-	50.0	23	2	-	-	100.0
					18	1	100.0	-	-					
					19	3	33.3	33.3	33.3					
					20	2	-	50.0	50.0					
					21	7	-	28.6	71.4					
					22	1	-	-	100.0					
					23	1	-	-	100.0					
					24	1	-	-	100.0					

Fishergate House (York)					Abbey of St Mary (Cirencester)					Auldham (East Lothian)				
Age	n	1	2	3	Age	n	1	2	3	Age	n	1	2	3
14	1	100.0	-	-	14	1	100.0	-	-	15	1	100.0	-	-
15	1	100.0	-	-						19	1	100.0	-	-
16	3	100.0	-	-						21	1	-	-	100.0
										22	1	-	-	100.0

The figure below shows the age distribution of individuals from various Mediaeval sites for the fusion of the **proximal epiphysis** to the shaft of the humerus. This shows the entire sub-sample that had these bones present.





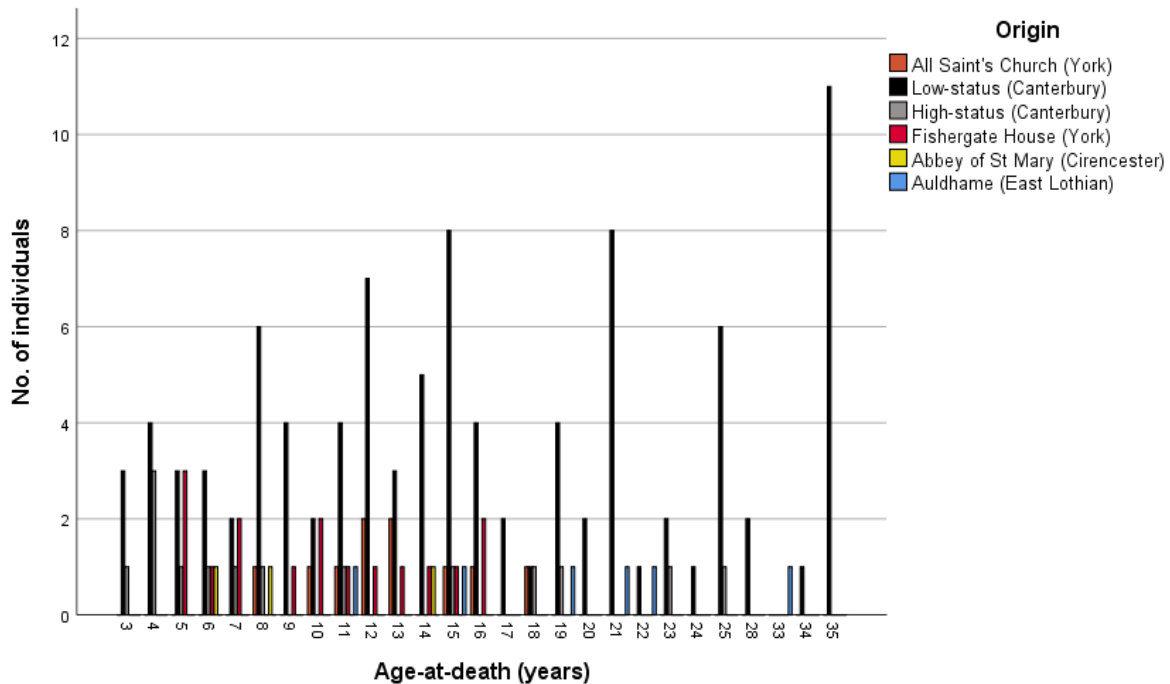
### A7. 7. The Radius

The table below shows the age at death/phase for the fusion of the **proximal epiphysis** to the radius for all archaeological Mediaeval sites sampled. Frequencies are recorded as percentages.

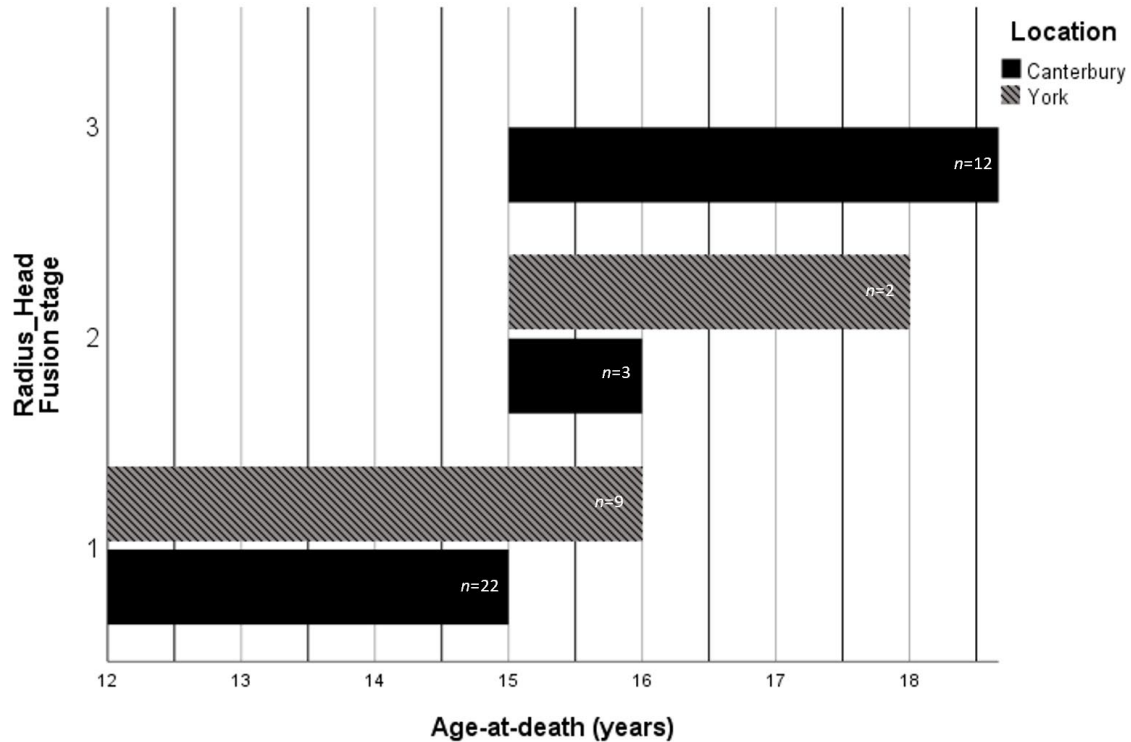
Proximal epiphysis to the radius														
All Saint's church (York)				Low-status				High-status						
Age	n	1	2	3	Age	n	1	2	3	Age	n	1	2	3
12	2	100.0	-	-	12	7	100.0	-	-	15	1	100.0	-	-
13	2	100.0	-	-	13	3	100.0	-	-	18	1	-	-	100.0
15	1	100.0	-	-	14	5	100.0	-	-	19	1	-	-	100.0
16	1	-	-	100.0	15	8	75.0	12.5	12.5					
18	1	-	100.0	-	16	4	-	50.0	50.0					
					17	2	-	-	100.0					
					18	1	-	-	100.0					
					19	4	-	-	100.0					

Fishergate House (York)				Abbey of St Mary (Cirencester)				Auldham (East Lothian)						
Age	n	1	2	3	Age	n	1	2	3	Age	n	1	2	3
12	1	100.0	-	-	14	1	100.0	-	-	15	1	100.0	-	-
13	1	100.0	-	-						19	1	-	-	100.0
14	1	100.0	-	-										
15	1	-	100.0	-										
16	2	50.0	-	50.0										

The figure shows the age distribution of individuals from various Mediaeval sites for the fusion of the **proximal epiphysis** to the radius. This shows the entire sub-sample that had these bones present.



The figure below shows the timing of fusion for individuals from various Mediaeval archaeological sites grouped under Canterbury and York for the fusion of the **proximal epiphysis** to the radius. Single data points are not represented on the figure, such as York Stage three. Stage 1 (unfused), Stage 2 (fusing), Stage 3 (fused).



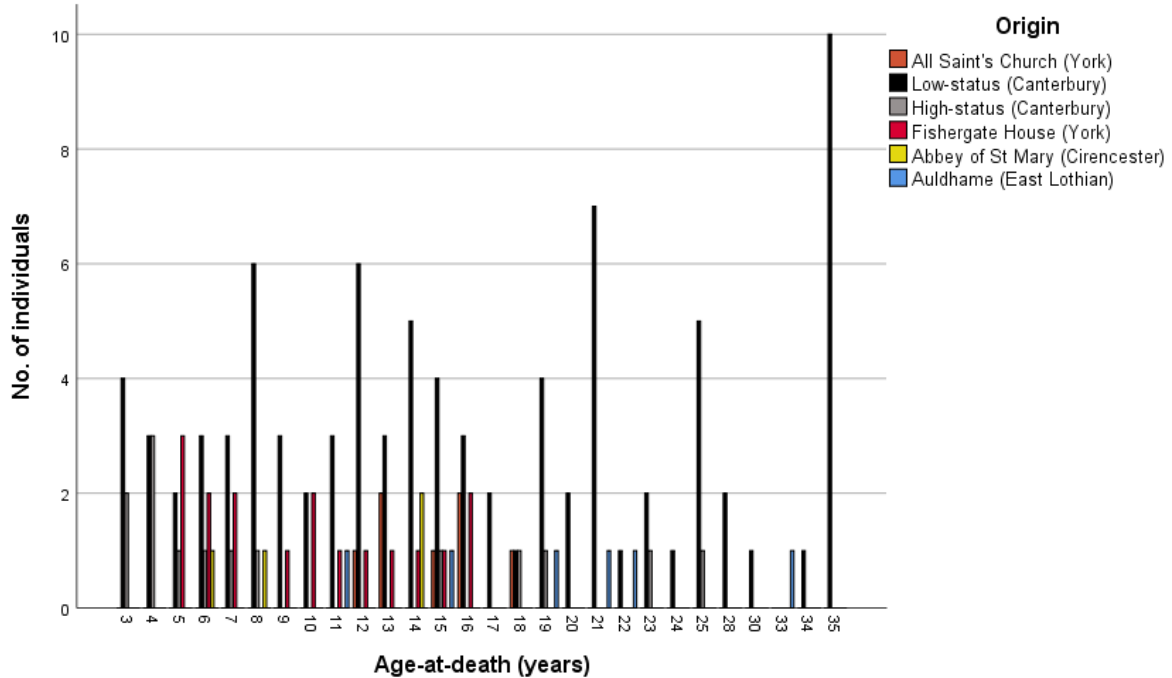
The table below shows the age at death/phase for the fusion of the **distal epiphysis** to the radius for all archaeological Mediaeval sites sampled. Frequencies are recorded as percentages.

Distal epiphysis to the radius														
All Saint's church (York)				Low-status				High-status						
Age	n	1	2	3	Age	n	1	2	3	Age	n	1	2	3
15	1	100.0	-	-	14	5	100.0	-	-	15	1	100.0	-	-
16	2	100.0	-	-	15	4	100.0	-	-	18	1	-	100.0	-
18	1	100.0	-	-	16	3	100.0	-	-	19	1	-	-	100.0
					17	2	50.0	-	50.0	23	1	-	-	100.0
					18	1	100.0	-	-					
					19	4	25.0	25.0	50.0					
					20	2	50.0	-	50.0					
					21	7	14.3	14.3	71.4					
					22	1	-	-	100.0					
					23	2	-	-	100.0					
					24	1	-	-	100.0					

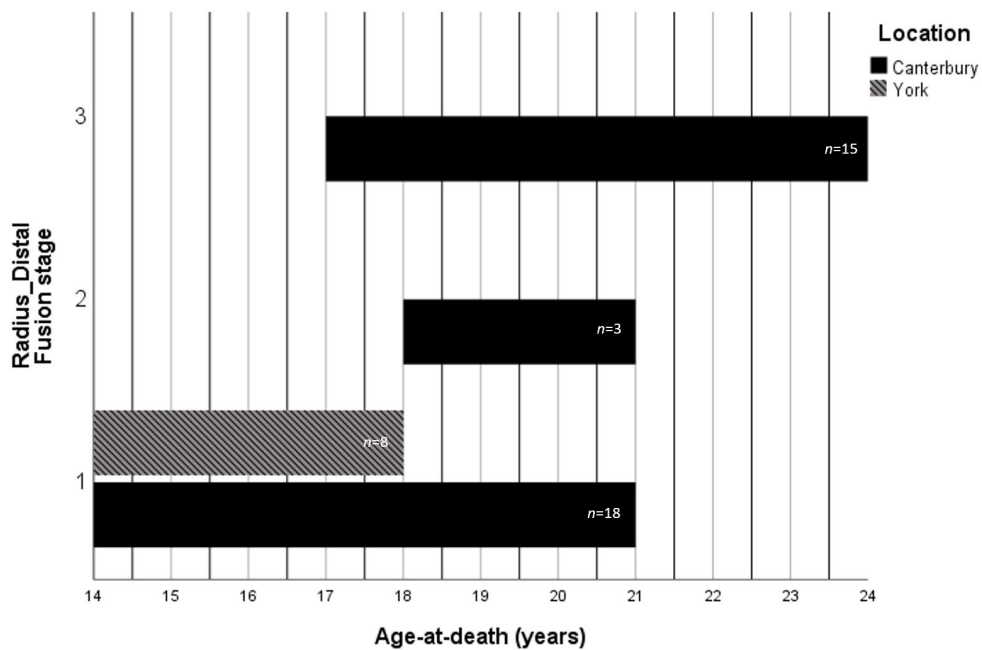
  

Fishergate House (York)				Abbey of St Mary (Cirencester)				Auldham (East Lothian)						
Age	n	1	2	3	Age	n	1	2	3	Age	n	1	2	3
15	1	100.0	-	-	14	2	100.0	-	-	15	1	100.0	-	-
16	2	100.0	-	-						19	1	100.0	-	-
										21	1	100.0	-	-
										22	1	-	-	100.0

The figure shows the age distribution of individuals from various Mediaeval sites for the fusion of the **distal epiphysis** to the radius. This shows the entire sub-sample that had these bones present.



The figure below shows the timing of fusion for individuals from various Mediaeval archaeological sites grouped under Canterbury and York for the **distal epiphysis** to the radius. Stage 1 (unfused), Stage 2 (fusing), Stage 3 (fused).



The table below shows the age in years/phase for the fusion of the radius, including the (1) proximal and (2) distal epiphyses for the Mediaeval Canterbury and York samples. Frequencies are recorded as percentages.

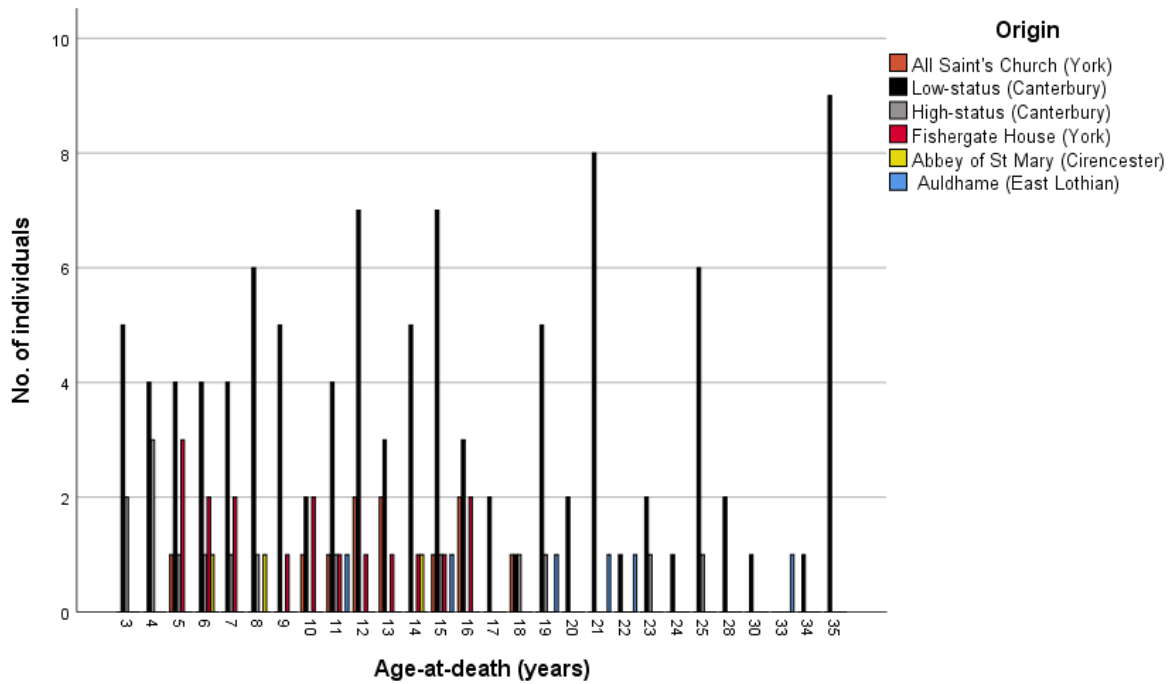
		Mediaeval York					Mediaeval Canterbury					
		Stage of union					Stage of union					
		Age	<i>n</i>	1	2	3	Age	<i>n</i>	1	2	3	
The radius	Proximal epiphysis	12	3	100.0	-	-	12	7	100.0	-	-	
		13	3	100.0	-	-	13	3	100.0	-	-	
		14	1	100.0	-	-	14	5	100.0	-	-	
		15	2	50.0	50.0	-	15	9	77.8	11.1	11.1	
		16	3	33.3	-	66.7	16	4	-	50.0	50.0	
		18	1	-	100.0	-	17	2	-	-	100.0	
		18	2	-	-	-	18	2	-	-	100.0	
						19	5	-	-	100.0		
			Age	<i>n</i>	1	2	3	Age	<i>n</i>	1	2	3
		Distal epiphysis	14	1	100.0	-	-	14	5	100.0	-	-
			15	2	100.0	-	-	15	5	100.0	-	-
			16	4	100.0	-	-	16	3	100.0	-	-
			18	1	100.0	-	-	17	2	50.0	-	50.0
								18	2	50.0	50.0	-
							19	5	20.0	20.0	60.0	
							20	2	50.0	-	50.0	
							21	7	14.3	14.3	71.4	
						22	1	-	-	100.0		
						23	3	-	-	100.0		
						24	1	-	-	100.0		

## A7. 8. The Ulna

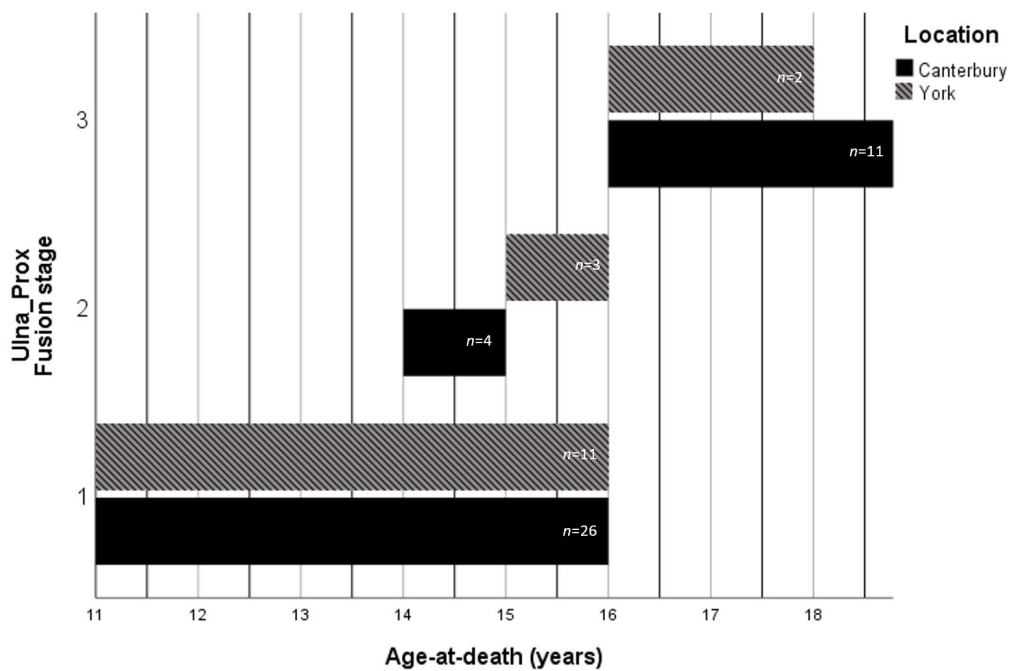
The table below shows the age at death/phase for the fusion of the proximal epiphysis to the ulna for all archaeological Mediaeval sites sampled. Frequencies are recorded as percentages.

Proximal epiphysis to the ulna														
All Saint's church (York)					Low-status					High-status				
		Stage of union					Stage of union					Stage of union		
Age	<i>n</i>	1	2	3	Age	<i>n</i>	1	2	3	Age	<i>n</i>	1	2	3
11	1	100.0	-	-	11	2	100.0	-	-	11	1	100.0	-	-
12	2	100.0	-	-	12	7	100.0	-	-	15	1	100.0	-	-
13	2	100.0	-	-	13	3	100.0	-	-	18	1	-	-	100.0
15	1	100.0	-	-	14	5	80.0	20.0	-	19	1	-	-	100.0
16	2	50.0	50.0	-	15	7	57.1	42.9	-					
18	1	-	-	100.0	16	3	66.7	-	33.3					
					17	2	-	-	100.0					
					18	1	-	-	100.0					
					19	5	-	-	100.0					
Fishergate House (York)					Abbey of St Mary (Cirencester)					Auldham (East Lothian)				
		Stage of union					Stage of union					Stage of union		
Age	<i>n</i>	1	2	3	Age	<i>n</i>	1	2	3	Age	<i>n</i>	1	2	3
11	1	100.0	-	-	14	1	-	100.0	-	11	1	100.0	-	-
12	1	100.0	-	-						15	1	100.0	-	-
13	1	100.0	-	-						19	1	-	-	100.0
14	1	100.0	-	-										
15	1	-	100.0	-										
16	2	-	50.0	50.0										

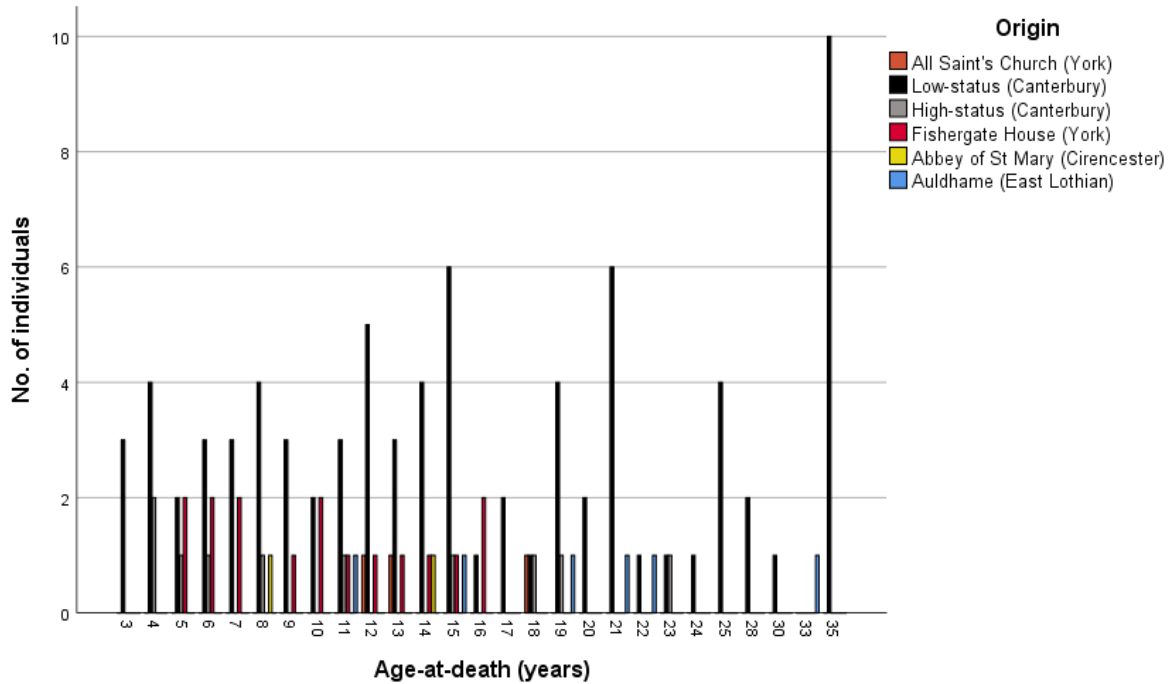
The figure shows the age distribution of individuals from various Mediaeval sites for the fusion of the **proximal epiphysis** of the ulna. This shows the entire sub-sample that had these bones present.



The figure below shows the timing of fusion for individuals from various Mediaeval archaeological sites grouped under Canterbury and York for the fusion of the **proximal epiphysis** to the ulna. Stage 1 (unfused), Stage 2 (fusing), Stage 3 (fused).



The figure below shows the age distribution of individuals from various Mediaeval sites for the fusion of the **distal epiphysis** of the ulna. This shows the entire sub-sample that had these bones present.



Age in years/ phase for the fusion of the ulna, including the (1) proximal and (2) distal epiphyses for the Mediaeval Canterbury, Auldham and York samples. Frequencies are recorded as percentages.

		Mediaeval York			Mediaeval Canterbury					Mediaeval Auldham						
		Stage of union			Stage of union					Stage of union						
		Age	n	1	2	3	Age	n	1	2	3	Age	n	1	2	3
The ulna	Proximal epiphysis	11	2	100.0	-	-	11	5	100.0	-	-	11	1	100.0	-	-
		12	3	100.0	-	-	12	7	100.0	-	-	12	1	100.0	-	-
		13	3	100.0	-	-	13	3	100.0	-	-	13	1	100.0	-	-
		14	1	100.0	-	-	14	5	80.0	20.0	-	14	1	100.0	-	-
		15	2	50.0	50.0	-	15	8	62.5	37.5	-	15	1	100.0	-	-
		16	4	25.0	50.0	25.0	16	3	66.7	-	33.3	16	1	100.0	-	-
		18	1	-	-	100.0	17	2	-	-	100.0	17	1	100.0	-	-
		18	1	-	-	100.0	18	2	-	-	100.0	18	1	100.0	-	-
The ulna	Distal epiphysis	14	1	100.0	-	-	14	4	100.0	-	-	14	1	100.0	-	-
		15	1	100.0	-	-	15	7	100.0	-	-	15	1	100.0	-	-
		16	2	100.0	-	-	16	1	100.0	-	-	16	1	100.0	-	-
		18	1	100.0	-	-	17	2	50.0	-	50.0	17	1	100.0	-	-
		18	1	100.0	-	-	18	2	50.0	50.0	-	18	1	100.0	-	-
		19	5	20.0	20.0	60.0	19	5	20.0	20.0	60.0	19	1	100.0	-	-
		20	2	50.0	-	50.0	20	2	50.0	-	50.0	20	1	100.0	-	-
		21	2	16.7	-	83.3	21	2	16.7	-	83.3	21	1	100.0	-	-
		22	1	-	-	100.0	22	1	-	-	100.0	22	1	100.0	-	-
		23	2	-	-	100.0	23	2	-	-	100.0	23	1	100.0	-	-
		24	1	-	-	100.0	24	1	-	-	100.0	24	1	100.0	-	-

### A7.9. The Hand

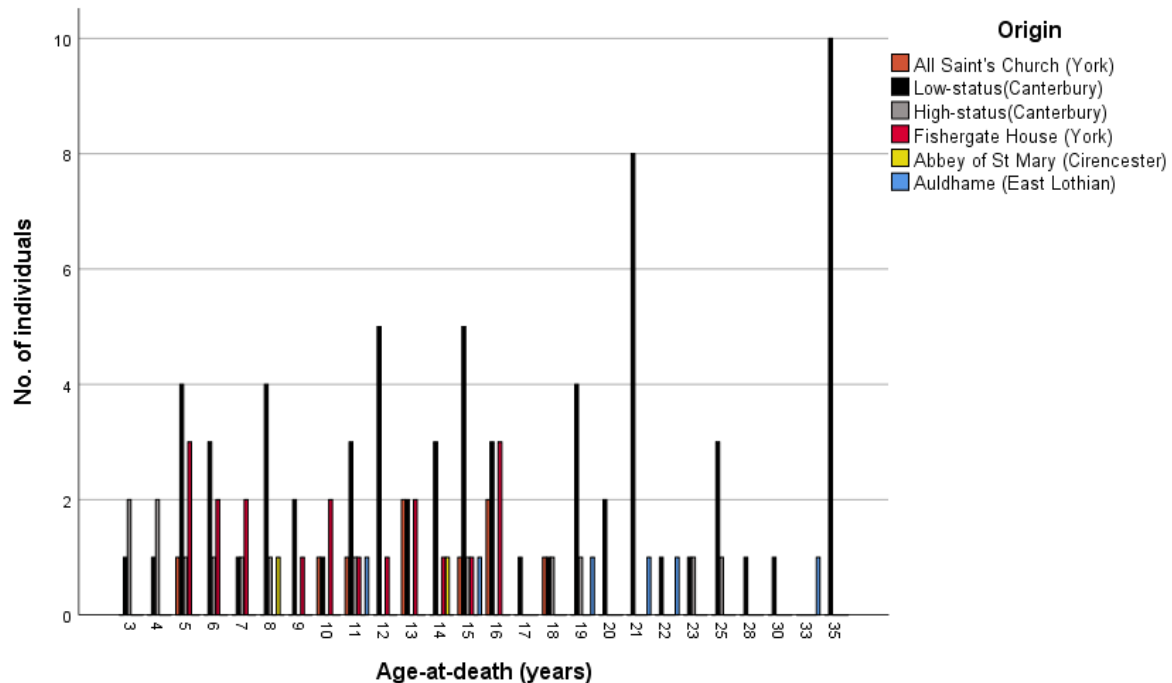
The table below shows the age at death/phase for the fusion of the **heads of the metacarpals 2-5, proximal and middle phalangeal epiphyses** of the hand for all archaeological Mediaeval sites sampled. Frequencies are recorded as percentages.

Heads of metacarpals 2-5 and epiphyses to the proximal and middle phalanges														
All Saint's church (York)				Low-status				High-status						
Age	n	1	2	3	Age	n	1	2	3	Age	n	1	2	3
10	1	100.0	-	-	9	2	100.0	-	-	11	1	100.0	-	-
11	1	100.0	-	-	10	1	100.0	-	-	15	1	100.0	-	-
13	2	100.0	-	-	11	3	100.0	-	-	18	1	-	-	100.0
15	1	100.0	-	-	12	5	80.0	20.0	-	19	1	-	-	100.0
16	2	100.0	-	-	13	2	100.0	-	-					
18	1	100.0	-	-	14	3	100.0	-	-					
					15	5	100.0	-	-					
					16	3	66.7	33.3	-					
					17	2	-	-	100.0					
					18	1	-	-	100.0					
					19	4	-	-	100.0					

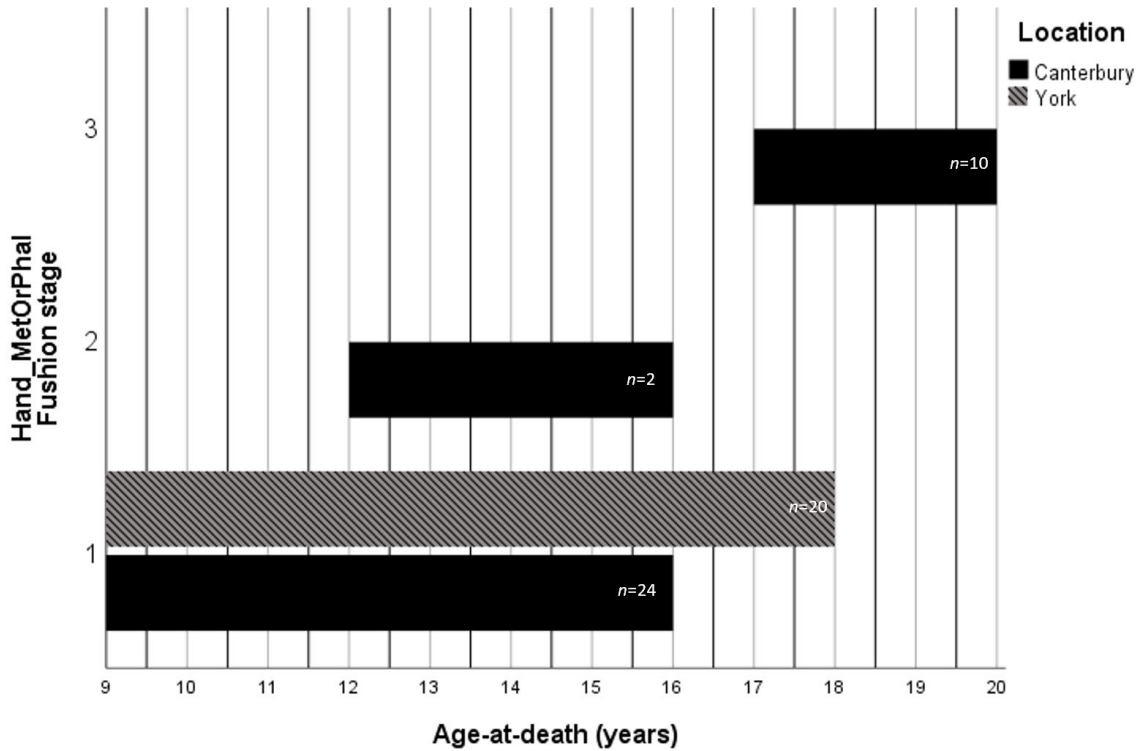
  

Fishergate House (York)				Abbey of St Mary (Cirencester)				Auldham (East Lothian)						
Age	n	1	2	3	Age	n	1	2	3	Age	n	1	2	3
9	1	100.0	-	-	14	1	100.0	-	-	11	1	100.0	-	-
10	2	100.0	-	-						15	1	100.0	-	-
11	1	100.0	-	-						19	1	-	-	100.0
12	1	100.0	-	-										
13	2	100.0	-	-										
14	1	100.0	-	-										
15	1	100.0	-	-										
16	3	100.0	-	-										

The figure below shows the age distribution of individuals from various Mediaeval sites for the fusion of the **metacarpals 2-5, proximal and middle phalangeal epiphyses** of the hand. This shows the entire sub-sample that had these bones present.



The figure below shows the timing of fusion for individuals from various Mediaeval archaeological sites grouped under Canterbury and York for the fusion of the **heads of the metacarpals 2-5, proximal and middle phalangeal epiphyses** of the hand. Stage 1 (unfused), Stage 2 (fusing), Stage 3 (fused).



The table below shows the age at death/phase for the fusion of the **distal phalangeal epiphyses** of the hand for all archaeological Mediaeval sites sampled. Frequencies are recorded as percentages.

Epiphyses to the distal phalanges of the hand														
All Saint's church (York)					Low-status					High-status				
Age	n	1	2	3	Age	n	1	2	3	Age	n	1	2	3
13	1	100.0	-	-	14	3	100.0	-	-	15	1	100.0	-	-
					15	3	100.0	-	-	19	1	-	-	100.0
					17	1	-	-	100.0					
					19	3	-	-	100.0					
					20	1	-	-	100.0					
					21	3	-	-	100.0					

Fishergate House (York)				Abbey of St Mary (Cirencester)				Auldham (East Lothian)						
Age	n	1	2	3	Age	n	1	2	3	Age	n	1	2	3
12	1	100.0	-	-	14	1	100.0	-	-	19	1	-	-	100.0
13	2	100.0	-	-						21	1	-	-	100.0
15	1	100.0	-	-										
16	2	50.0	50.0	-										



### A7. 10. The Os coxae

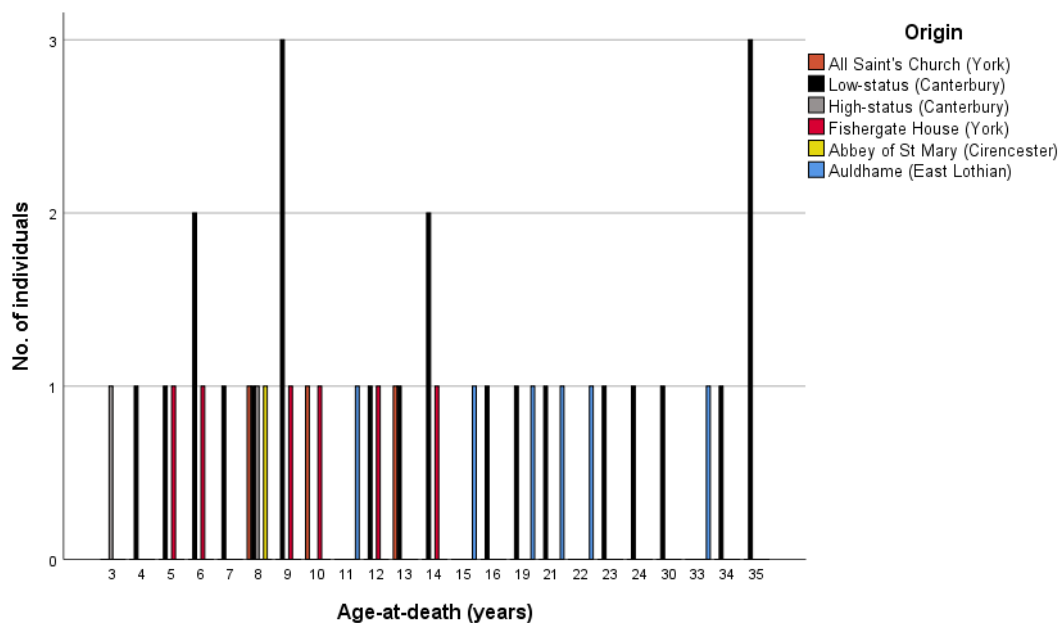
The table below shows the age at death/phase for the fusion of the **ischiopubic ramus** of the os coxae for all archaeological Mediaeval sites sampled. Frequencies are recorded as percentages.

Fusion of the ischopubic ramus of the os coxae							
All Saint's church (York)				Canterbury			
Stage of union				Stage of union			
Age	n	1	3	Age	n	1	3
10	1	100.0	-	9	3	100.0	-
13	1	-	100.0	12	1	100.0	-
				13	1	-	100.0
				14	2	50.0	50.0
				16	1	-	100.0

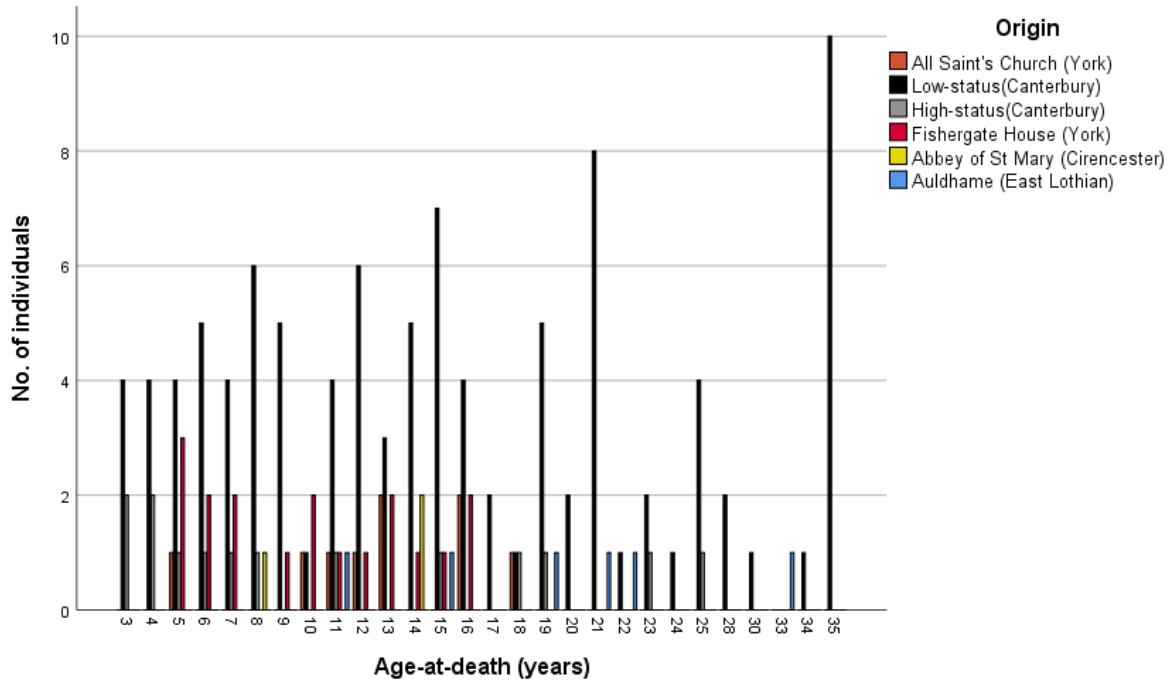
  

Fishergate House (York)				Auldhame (East Lothian)			
Stage of union				Stage of union			
Age	n	1	3	Age	n	1	3
9	1	-	100.0	11	1	100.0	-
10	1	-	100.0	15	1	100.0	-
12	1	-	100.0				
14	1	-	100.0				

The figure below shows the age distribution of individuals from various Mediaeval sites for the fusion of the **ischiopubic ramus** of the os coxae. This shows the entire sub-sample that had these bones present.



The figure below shows the age distribution of individuals from various Mediaeval sites for the fusion of the **iliac crest** of the os coxae. This shows the entire sub-sample that had these bones present.



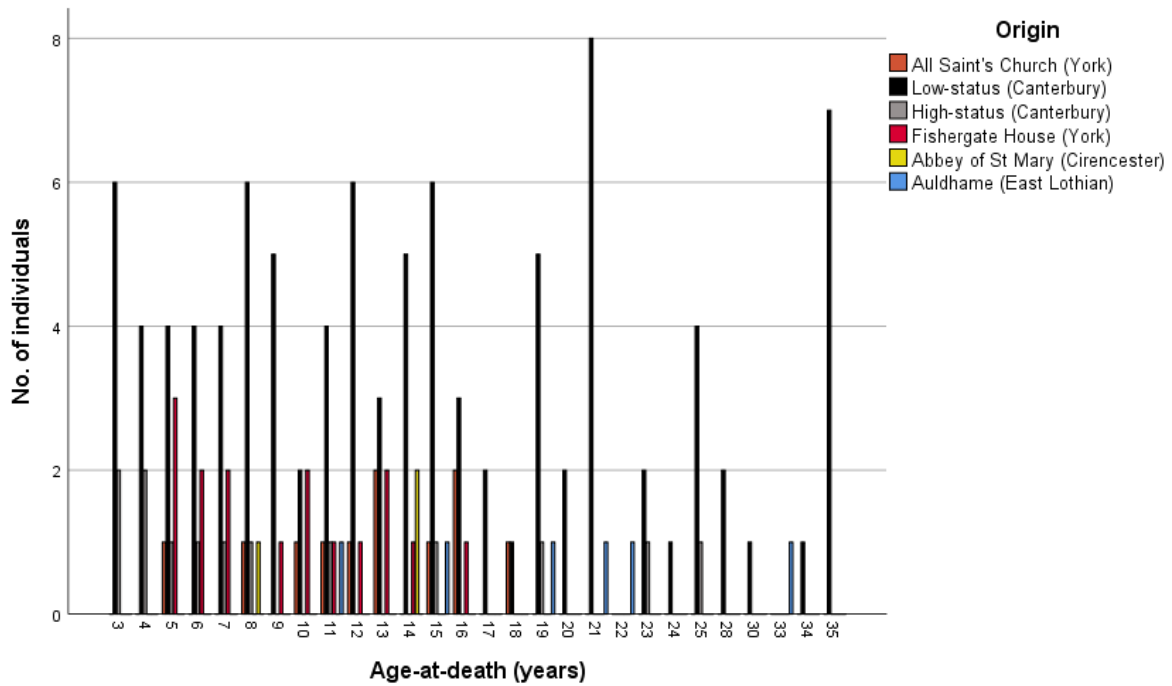
The table below shows the age at death/phase for the fusion of the **acetabulum** of the os coxae for all archaeological Mediaeval sites sampled. Frequencies are recorded as percentages.

Fusion of the acetabulum of the os coxae														
All Saint's church (York)				Low-status				High-status						
Age	n	Stage of union			Age	n	Stage of union			Age	n	Stage of union		
		1	2	3			1	2	3			1	2	3
11	1	100.0	-	-	11	4	100.0	-	-	11	1	100.0	-	-
12	1	100.0	-	-	12	6	100.0	-	-	15	1	100.0	-	-
13	2	100.0	-	-	13	3	100.0	-	-	19	1	-	-	100.0
15	1	100.0	-	-	14	5	80.0	20.0	-					
16	2	50.0	-	50.0	15	6	50.0	33.3	16.7					
18	1	-	-	100.0	16	3	-	33.3	66.7					
					17	2	-	-	100.0					
					18	1	-	-	100.0					
					19	5	-	-	100.0					

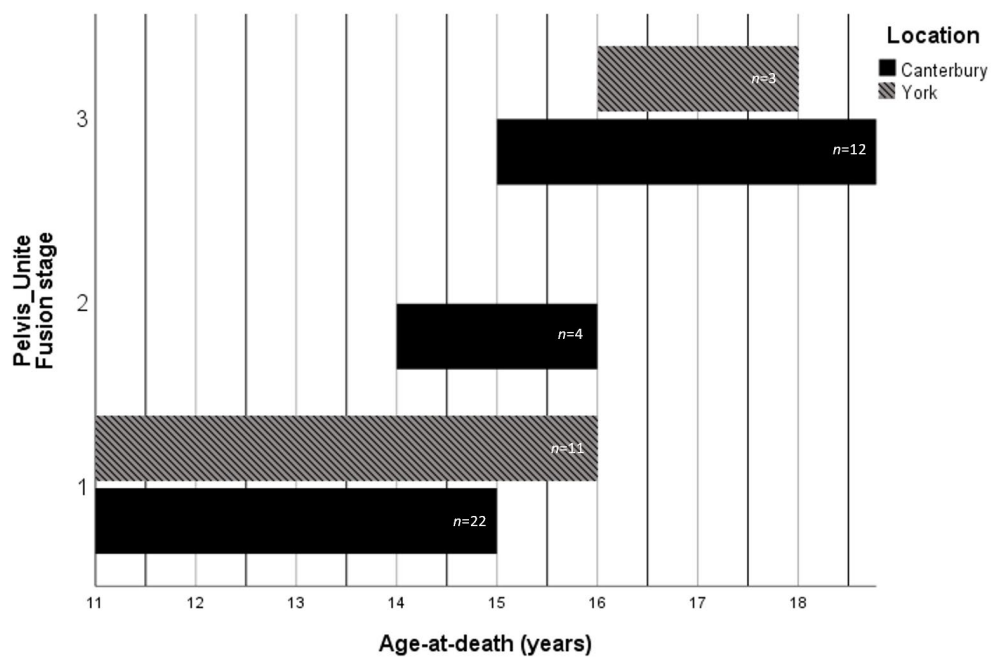
  

Fishergate House (York)				Abbey of St Mary (Cirencester)				Auldhame (East Lothian)						
Age	n	Stage of union			Age	n	Stage of union			Age	n	Stage of union		
		1	2	3			1	2	3			1	2	3
11	1	100.0	-	-	14	2	100.0	-	-	11	1	100.0	-	-
12	1	100.0	-	-						15	1	100.0	-	-
13	2	100.0	-	-						19	1	-	-	100.0
14	1	100.0	-	-										
16	1	-	-	100.0										

The figure below shows the age distribution of individuals from various Mediaeval sites for the fusion of the **acetabulum** of the os coxae. This shows the entire sub-sample that had these bones present.



The figure below shows the timing of fusion for individuals from various Mediaeval archaeological sites grouped under Canterbury and York for the **acetabulum** of the os coxae. Stage 1 (unfused), Stage 2 (fusing), Stage 3 (fused).



The table below gives the age in years/phase for the fusion of the os coxae, including the (1) ischiopubic ramus, (2) iliac crest and the (3) acetabulum for the Mediaeval Canterbury, Auldham and York samples. Frequencies are recorded as percentages.

		Mediaeval York					Mediaeval Canterbury						
		Stage of union					Stage of union						
	Age	<i>n</i>	1	2	3	Age	<i>n</i>	1	2	3			
Ischiopubic ramus	9	1	-	-	100.0	9	3	100.0	-	-			
	10	2	50.0	-	50.0	12	1	100.0	-	-			
	12	1	-	-	100.0	13	1	-	-	100.0			
	13	1	-	-	100.0	14	2	50.0	-	50.0			
	14	1	-	-	100.0	16	1	-	-	100.0			
The os coxae			Mediaeval York					Mediaeval Canterbury					
			Stage of union					Stage of union					
	Iliac crest	14	1	100.0	-	-	14	5	100.0	-	-		
		15	1	100.0	-	-	15	8	100.0	-	-		
		16	4	100.0	-	-	16	4	100.0	-	-		
		18	1	100.0	-	-	17	2	50.0	50.0	-		
							18	2	-	100.0	-		
							19	6	-	66.7	33.3		
							20	2	50.0	-	50.0		
							21	8	12.5	37.5	50.0		
							22	1	-	100.0	-		
							23	3	-	33.3	66.7		
						24	1	-	-	100.0			
						25	5	-	-	100.0			
			Mediaeval Auldham					Mediaeval Cirencester					
			Stage of union					Stage of union					
		Age	<i>n</i>	1	2	3	Age	<i>n</i>	1	2	3		
		15	1	100.0	-	-	14	2	100.0	-	-		
		19	2	-	100.0	-							
		21	1	-	-	100.0							
		22	1	-	-	100.0							
	Acetabulum			Mediaeval York					Mediaeval Canterbury				
				Stage of union					Stage of union				
			Age	<i>n</i>	1	2	3	Age	<i>n</i>	1	2	3	
			11	2	100.0	-	-	11	5	100.0	-	-	
		12	2	100.0	-	-	12	6	100.0	-	-		
		13	4	100.0	-	-	13	3	100.0	-	-		
		14	1	100.0	-	-	14	5	80.0	20.0	-		
		15	1	100.0	-	-	15	7	57.1	28.6	14.3		
		16	3	33.3	-	66.7	16	3	-	33.3	66.7		
		18	1	-	-	100.0	17	2	-	-	100.0		
						18	1	-	-	100.0			
						19	6	-	-	100.0			

### A7. 11. The Femur

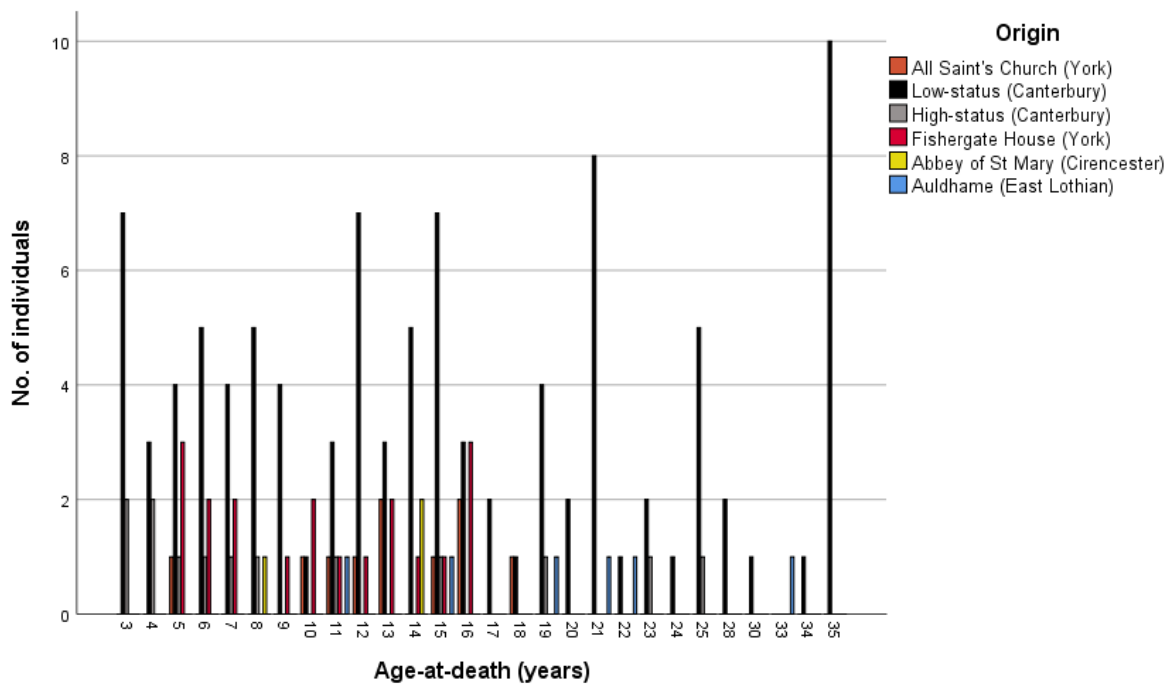
The table below shows the age at death/phase for the fusion of the **femoral head** of the femur for all archaeological Mediaeval sites sampled. Frequencies are recorded as percentages.

Fusion of the femoral head to the femur														
All Saint's church (York)				Low-status				High-status						
Age	n	1	2	3	Age	n	1	2	3	Age	n	1	2	3
12	1	100.0	-	-	12	7	100.0	-	-	15	1	100.0	-	-
13	2	100.0	-	-	13	3	100.0	-	-	19	1	-	-	100.0
15	1	100.0	-	-	14	5	100.0	-	-					
16	2	100.0	-	-	15	7	85.7	14.3	-					
18	1	-	-	100.0	16	3	100.0	-	-					
					17	2	-	50.0	50.0					
					18	1	-	100.0	-					
					19	4	-	25.0	75.0					
					20	2	-	-	100.0					
					21	8	-	-	100.0					
					22	1	-	-	100.0					

Fishergate House (York)				Abbey of St Mary (Cirencester)				Auldham (East Lothian)						
Age	n	1	2	3	Age	n	1	2	3	Age	n	1	2	3
12	1	100.0	-	-	14	2	100.0	-	-	15	1	100.0	-	-
13	2	100.0	-	-						19	1	-	100.0	-
14	1	100.0	-	-						21	1	-	-	100.0
15	1	100.0	-	-						22	1	-	-	100.0
16	3	66.7	33.3	-										

The figure below shows the age distribution of individuals from various Mediaeval sites for the fusion of the **femoral head** of the femur. This shows the entire sub-sample that had these bones present.



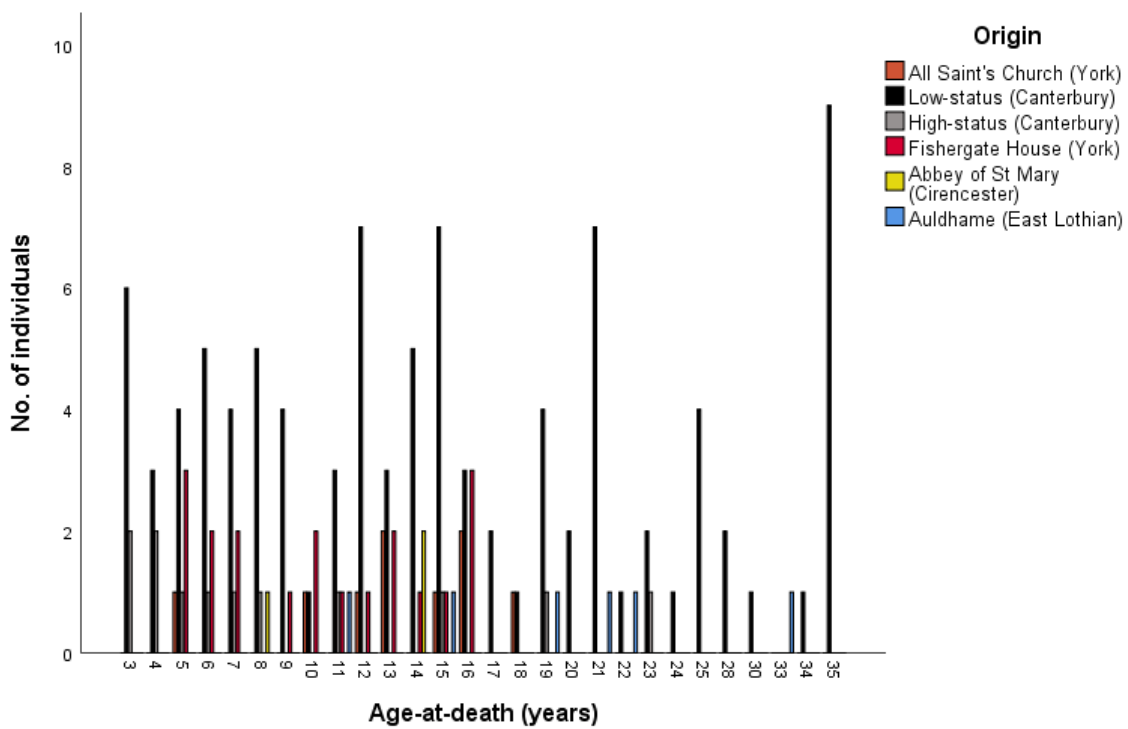
The table below shows the age at death/phase for the fusion of the **greater trochanter** of the femur for all archaeological Mediaeval sites sampled. Frequencies are recorded as percentages.

Fusion of the greater trochanter to the femur														
All Saint's church (York)				Low-status				High-status						
Age	n	1	2	3	Age	n	1	2	3	Age	n	1	2	3
13	2	100.0	-	-	13	3	100.0	-	-	15	1	100.0	-	-
15	1	100.0	-	-	14	5	100.0	-	-	19	1	-	-	100.0
16	2	100.0	-	-	15	7	100.0	-	-	16	3	66.7	33.3	-
18	1	-	100.0	-	17	2	-	50.0	50.0	17	2	-	-	100.0
					18	1	-	-	100.0	18	1	-	-	100.0
					19	4	-	-	100.0	19	4	-	-	100.0
					20	2	-	-	100.0					

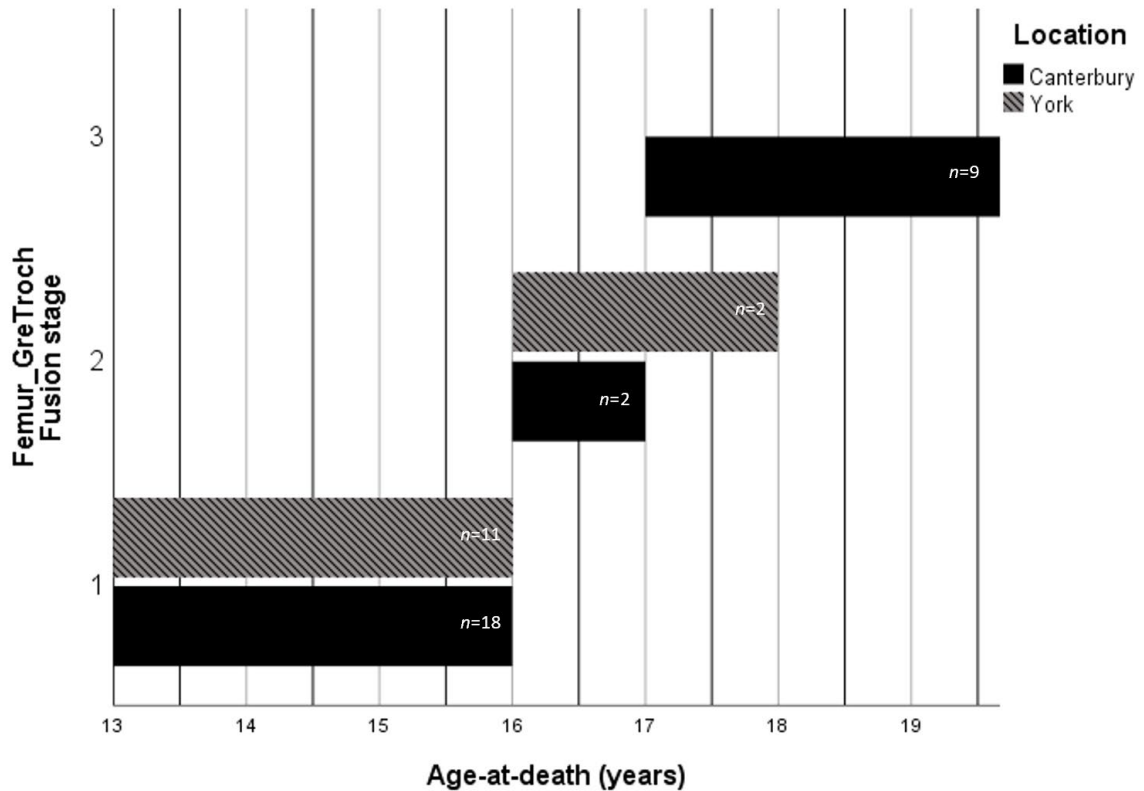
  

Fishergate House (York)				Abbey of St Mary (Cirencester)				Auldham (East Lothian)						
Age	n	1	2	3	Age	n	1	2	3	Age	n	1	2	3
13	2	100.0	-	-	14	2	100.0	-	-	15	1	100.0	-	-
14	1	100.0	-	-						19	1	-	-	100.0
15	1	100.0	-	-										
16	3	66.7	33.3	-										

The figure below shows the age distribution of individuals from different time periods for the fusion of the **greater trochanter** of the femur. This shows the entire sub-sample that had these bones present.



The figure below shows the timing of fusion for individuals from various Mediaeval archaeological sites grouped under Canterbury and York for the **greater trochanter** of the femur. Data was missing for age 17 years for the York sample. Stage 1 (unfused), Stage 2 (fusing), Stage 3 (fused).



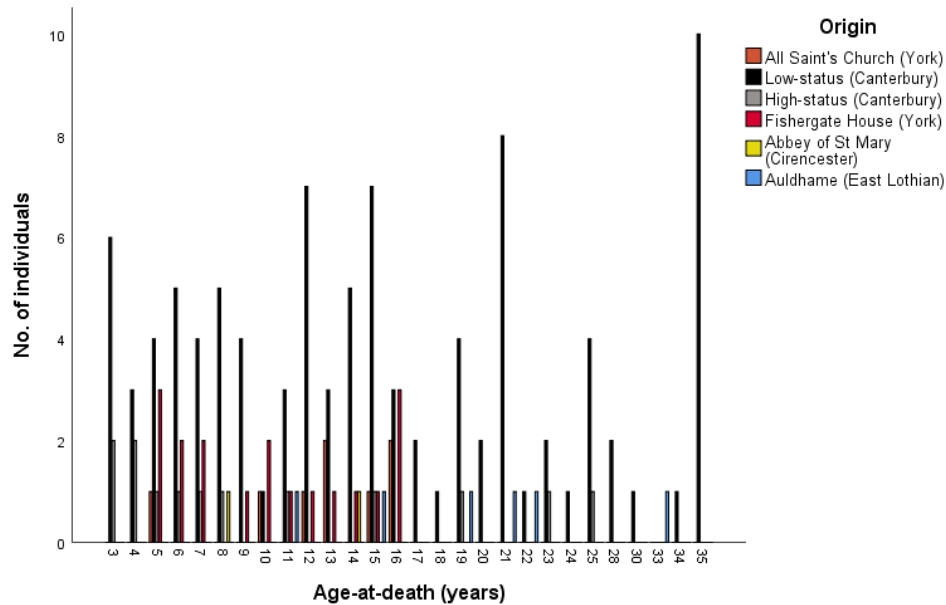
The table below shows the age at death/phase for the fusion of the **lesser trochanter** of the femur for all archaeological Mediaeval sites sampled. Frequencies are recorded as percentages.

Fusion of the lesser trochanter to the femur														
All Saint's church (York)				Low-status				High-status						
Age	n	Stage of union			Age	n	Stage of union			Age	n	Stage of union		
		1	2	3			1	2	3			1	2	3
13	2	100.0	-	-	13	3	100.0	-	-	15	1	100.0	-	-
15	1	100.0	-	-	14	5	100.0	-	-	19	1	-	-	100.0
16	2	100.0	-	-	15	7	100.0	-	-					
					16	3	66.7	33.3	-					
					17	2	-	-	100.0					
					18	1	-	-	100.0					
					19	4	-	-	100.0					

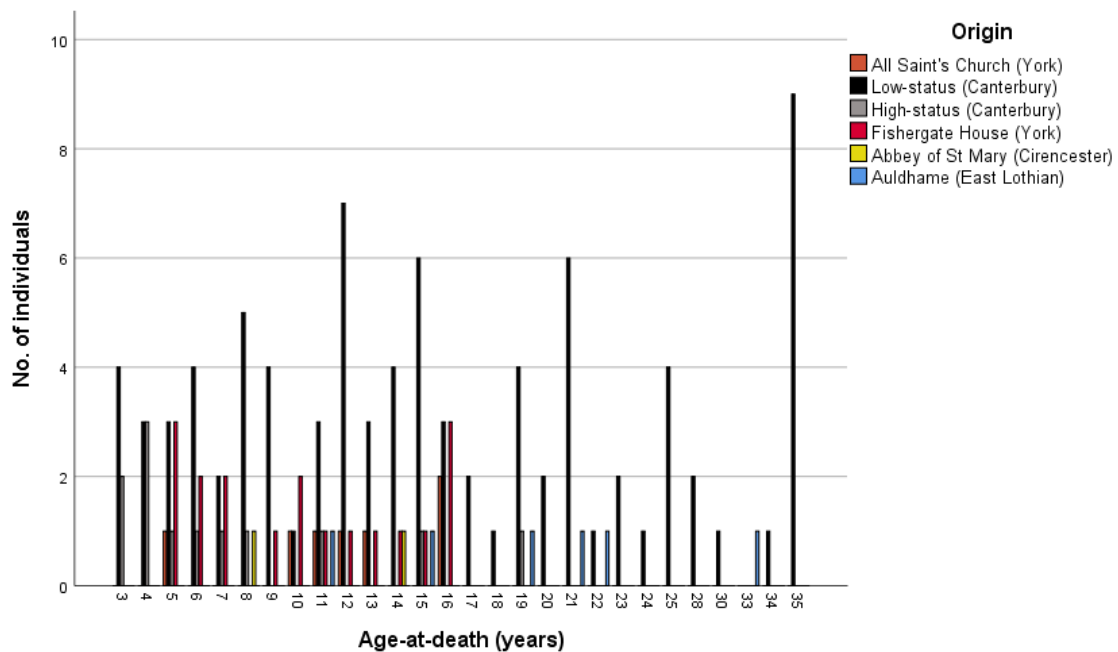
  

Fishergate House (York)				Abbey of St Mary (Cirencester)				Auldham (East Lothian)						
Age	n	Stage of union			Age	n	Stage of union			Age	n	Stage of union		
		1	2	3			1	2	3			1	2	3
13	1	100.0	-	-	14	1	100.0	-	-	15	1	100.0	-	-
14	1	100.0	-	-						19	1	-	-	100.0
15	1	-	-	100.0										
16	3	33.3	66.7	-										

The figure below shows the age distribution of individuals from different time periods for the fusion of the **lesser trochanter** of the femur. This shows the entire sub-sample that had these bones present.



The figure below shows the age distribution of individuals from different time periods for the fusion of the **distal epiphysis** to the femur. This shows the entire sub-sample that had these bones present.

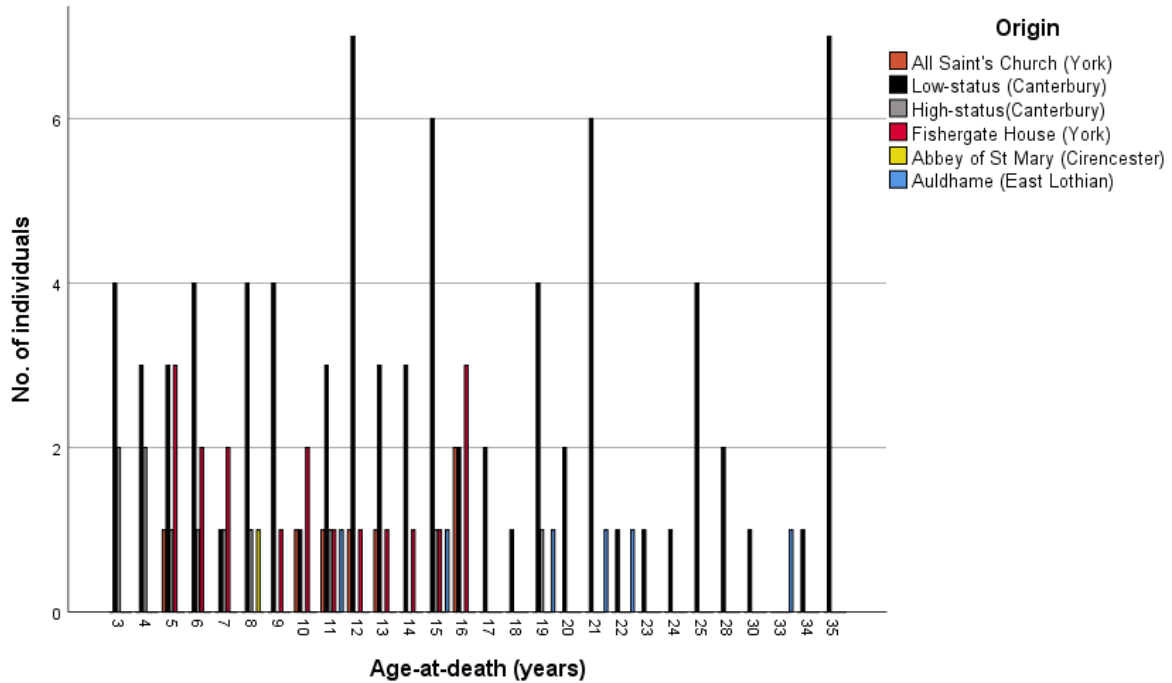


The table below shows the age in years/phase for the femur, including the (1) femoral head, (2) greater and (3) lesser trochanters and the (4) distal epiphysis for the Mediaeval Canterbury, Auldham and York samples. Frequencies are recorded as percentages.

		Mediaeval York			Mediaeval Canterbury					Mediaeval Auldham							
		Stage of union			Stage of union					Stage of union							
		Age	n	1	2	3	Age	n	1	2	3	Age	n	1	2	3	
The femur	Femoral head	12	2	100.0	-	-	12	7	100.0	-	-	11	1	100.0	-	-	
		13	4	100.0	-	-	13	3	100.0	-	-	15	1	100.0	-	-	
		14	1	100.0	-	-	14	5	100.0	-	-	19	1	-	100.0	-	
		15	2	100.0	-	-	15	8	87.5	12.5	-	21	1	-	-	100.0	
		16	5	80.0	20.0	-	16	3	100.0	-	-	22	1	-	-	100.0	
		18	1	-	-	-	17	2	-	50.0	50.0	33	1	-	-	100.0	
							18	1	-	100.0	-						
							19	5	-	20.0	80.0						
							20	2	-	-	100.0						
							21	8	-	-	100.0						
					22	1	-	-	100.0								
The femur	Greater trochanter	13	4	100.0	-	-	13	3	100.0	-	-						
		14	1	100.0	-	-	14	5	100.0	-	-						
		15	2	100.0	-	-	15	8	100.0	-	-						
		16	5	80.0	20.0	-	16	3	66.7	33.3	-						
		18	1	-	100.0	-	17	2	-	50.0	50.0						
							18	1	-	-	100.0						
							19	5	-	-	100.0						
							20	2	-	-	100.0						
The femur	Lesser trochanter	13	3	100.0	-	-	13	3	100.0	-	-						
		14	1	100.0	-	-	14	5	100.0	-	-						
		15	2	50.0	-	50.0	15	8	100.0	-	-						
		16	5	60.0	40.0	-	16	3	66.7	33.3	-						
							17	2	-	-	100.0						
							18	1	-	-	100.0						
							19	5	-	-	100.0						
The femur	Distal epiphysis	14	1	100.0	-	-	14	4	100.0	-	-	15	1	100.0	-	-	
		15	1	100.0	-	-	15	7	100.0	-	-	19	1	-	-	100.0	
		16	5	100.0	-	-	16	3	100.0	-	-	21	1	-	-	100.0	
							17	2	50.0	-	50.0	22	1	-	-	100.0	
							18	1	100.0	-	-						
							19	5	-	20.0	80.0						
							20	2	-	50.0	50.0						
							21	6	-	-	100.0						
							22	1	-	-	100.0						
							23	2	-	-	100.0						

### A7. 12. The Tibia

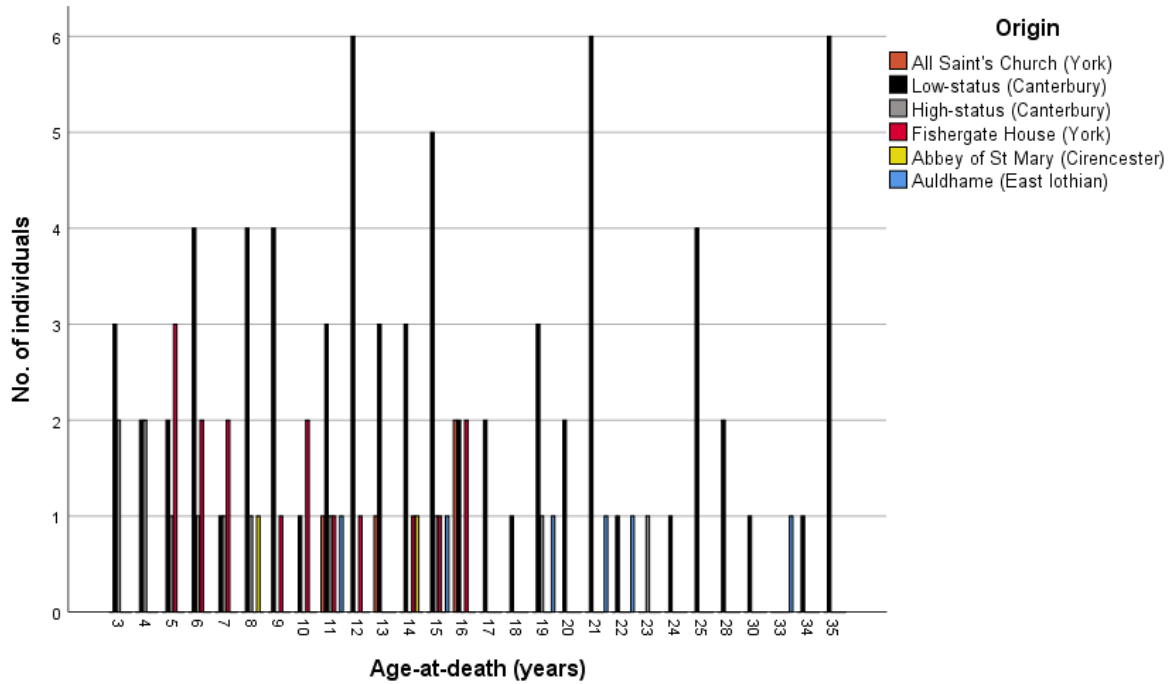
The figure below shows the age distribution of individuals from different time periods for the fusion of the **proximal epiphysis** to the tibia. This shows the entire sub-sample that had these bones present.



The table below shows the age at death/phase for the fusion of the **distal epiphysis** of the tibia for all archaeological Mediaeval sites sampled. Frequencies are recorded as percentages.

Fusion of the distal epiphysis of the tibia														
All Saint's church (York)					Low-status					High-status				
Age	n	Stage of union			Age	n	Stage of union			Age	n	Stage of union		
		1	2	3			1	2	3			1	2	3
16	2	100.0	-	-	14	3	100.0	-	-	15	1	100.0	-	-
					15	5	100.0	-	-	19	1	-	-	100.0
					16	2	100.0	-	-					
					17	2	-	50.0	50.0					
					18	1	-	100.0	-					
					19	3	-	-	100.0					
					20	2	-	-	100.0					
					21	6	-	-	100.0					
Fishergate House (York)					Abbey of St Mary (Cirencester)					Auldham (East Lothian)				
Age	n	Stage of union			Age	n	Stage of union			Age	n	Stage of union		
		1	2	3			1	2	3			1	2	3
14	1	100.0	-	-	14	1	100.0	-	-	15	1	100.0	-	-
15	1	100.0	-	-						19	1	-	-	100.0
16	2	-	100.0	-						21	1	-	-	100.0
										22	1	-	-	100.0

The figure below shows the age distribution of individuals from different time periods for the fusion of the **distal epiphysis** to the tibia. This shows the entire sub-sample that had these bones present.



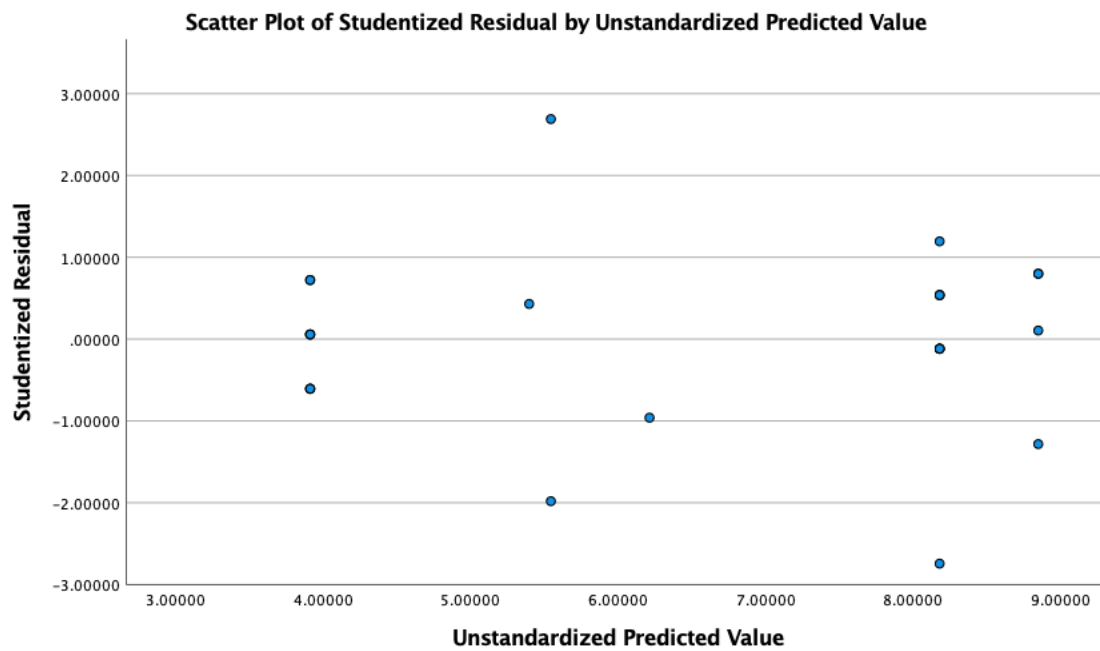
The table below shows age in years/ phase for the fusion of the tibia, including (1) the proximal and (2) distal epiphyses of the tibia for Mediaeval Canterbury, Auldhame, and York samples, Frequencies are recorded as percentages.

	Mediaeval York						Mediaeval Canterbury					Mediaeval Auldhame				
			Stage of union					Stage of union					Stage of union			
	Age	n	1	2	3	Age	n	1	2	3	Age	n	1	2	3	
The tibia	Proximal epiphysis	14	1	100.0	-	-	14	3	100.0	-	-	15	1	100.0	-	-
		15	1	100.0	-	-	15	7	100.0	-	-	19	1	-	-	100.0
		16	5	100.0	-	-	16	2	100.0	-	-	21	1	-	-	100.0
							17	2	-	50.0	50.0	22	1	-	-	100.0
							18	1	100.0	-	-					
							19	5	-	40.0	60.0					
							20	2	-	-	100.0					
							21	6	-	-	100.0					
							22	1	-	-	100.0					
The tibia	Distal epiphysis	14	1	100.0	-	-	14	3	100.0	-	-					
		15	1	100.0	-	-	15	6	100.0	-	-					
		16	2	-	100.0	-	16	2	100.0	-	-					
							17	2	-	50.0	50.0					
							18	1	-	100.0	-					
							19	4	-	-	100.0					
							20	2	-	-	100.0					
					21	6	-	-	100.0							

## APPENDIX 8: MULTIPLE REGRESSION OF MEDIAEVAL SITES

### A8. 1. Age Range 3 to 10 years

The figure below shows the scatter plot for the Studentised Residual and Unstandardised Predicted Value for the age range: 3 to 10 years to test for a linear relationship and homoscedasticity.



The table below gives the VIF statistics used to look at the multicollinearity of the test.

**Coefficients<sup>a</sup>**

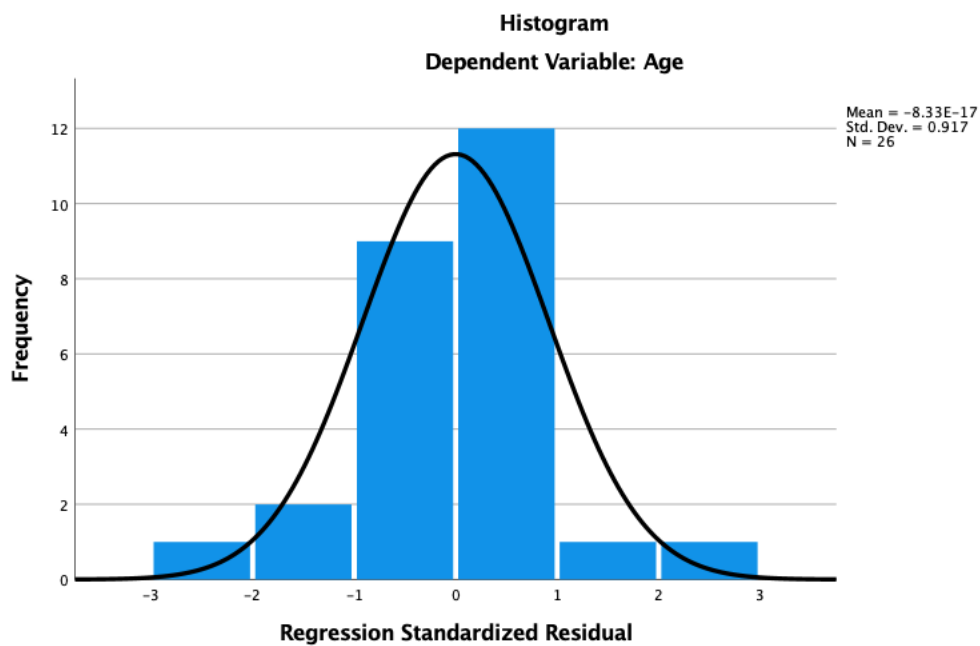
Model		Unstandardized Coefficients		Standardized Coefficients		Correlations			Collinearity Statistics		
		B	Std. Error	Beta	t	Sig.	Zero-order	Partial	Part	Tolerance	VIF
1	(Constant)	-.258	2.511		-.103	.919					
	Location	.669	.797	.110	.839	.411	.310	.180	.103	.879	1.137
	C2_DensVert	.816	.562	.301	1.451	.162	.754	.302	.179	.353	2.833
	C1_PostSyn	1.317	.502	.515	2.624	.016	.782	.497	.323	.394	2.541
	C2_PostSyn	.456	.851	.069	.537	.597	.265	.116	.066	.927	1.079

a. Dependent Variable: Age

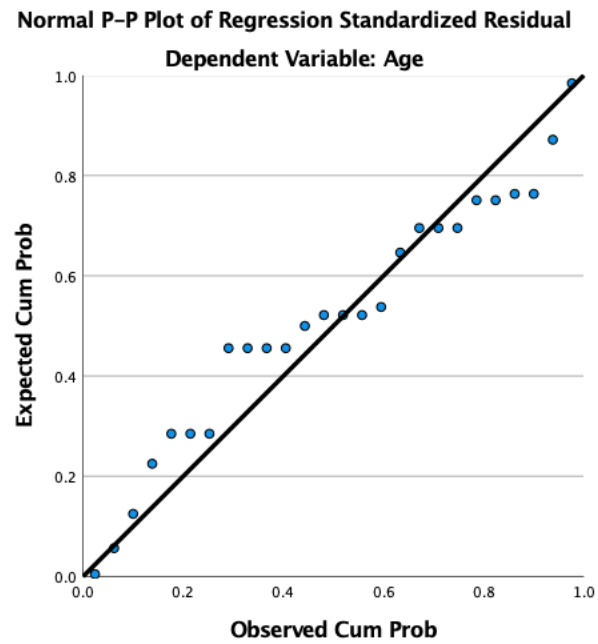
The table below shows the Leverage Regression and Cook's Distance Values to test for leverage points and influential points.

<b>COO 1</b>	<b>LEV 1</b>
.24216	.10055
.00277	.07536
.00716	.07536
.00716	.07536
.00429	.23103
.00429	.23103
.01502	.25982
.10026	.23103
.15789	.25982
.00143	.33420
.04923	.07536
.01245	.09215
.03488	.09215
.00141	.09215
.01646	.10055
.01646	.10055
.46867	.22173
.04923	.07536
.00716	.07536
.08032	.10055
.01646	.10055

The figure below shows a histogram used to test for normality.

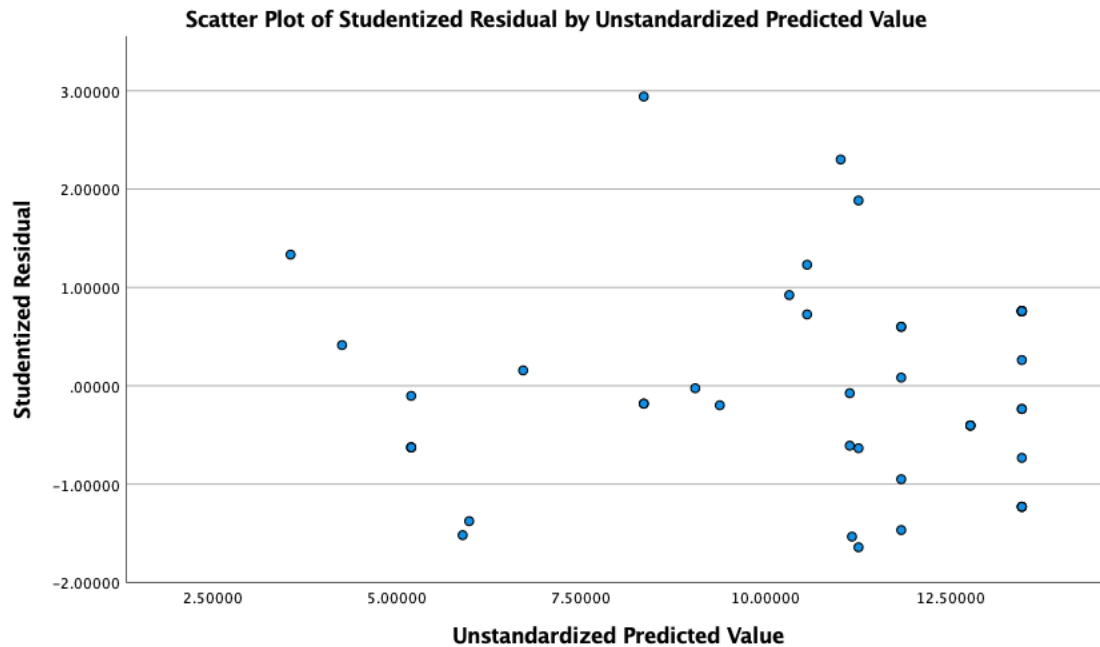


The figure below shows a normal P-P plot of regression standardised residual used to test for normality.



## A8.2 Age Range 3 to 15 years

The figure below shows the scatter plot for the Studentised Residual and Unstandardised Predicted Value for the age range: 3 to 15 years to test for a linear relationship and homoscedasticity.



The table below gives the VIF statistics used to look at the multicollinearity of the test.

**Coefficients<sup>a</sup>**

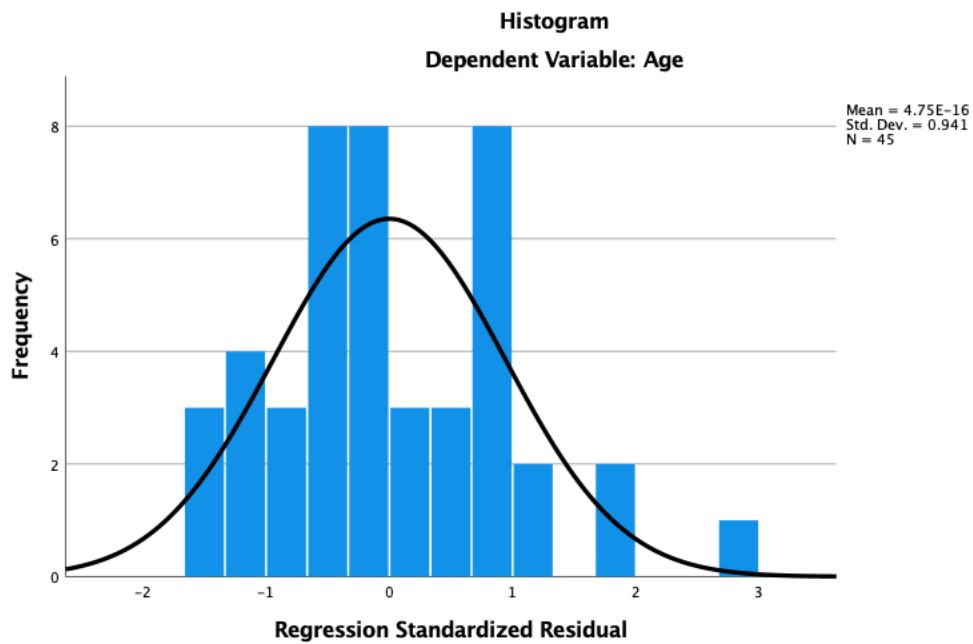
Model		Unstandardized Coefficients		Standardized Coefficients	t	Sig.	Correlations			Collinearity Statistics	
		B	Std. Error	Beta			Zero-order	Partial	Part	Tolerance	VIF
1	(Constant)	2.692	1.507		1.786	.082					
	C1_AnteArch	1.183	.787	.274	1.504	.141	.651	.234	.129	.220	4.549
	Location	-1.635	.746	-.189	-2.192	.034	-.136	-.331	-.187	.981	1.019
	C2_Dens	2.214	.477	.542	4.637	<.001	.765	.596	.396	.536	1.867
	C2_Centrum	.697	.691	.132	1.010	.319	.682	.160	.086	.424	2.356
	C1_PostSyn	.044	.715	.010	.062	.951	.567	.010	.005	.267	3.743

a. Dependent Variable: Age

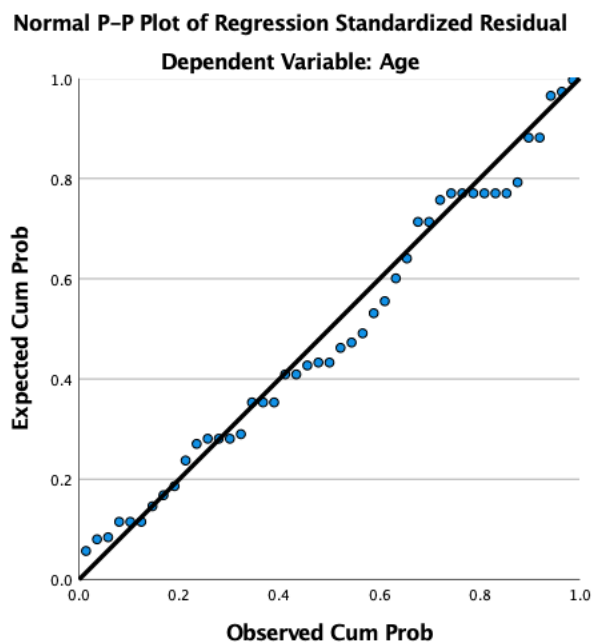
The table below shows the Leverage Regression and Cook's Distance Values to test for leverage points and influential points.

<b>COO 1</b>	<b>LEV 1</b>
.00000	.14036
.00053	.02689
.19901	.07819
.00552	.02689
.00017	.08571
.00552	.02689
.01452	.02689
.02738	.04166
.00053	.02689
.00552	.02689
.01452	.02689
.00017	.08571
.00000	.07819
.01185	.04166
.00076	.12799
.03345	.15200
.00451	.10124
.06896	.10180
.00413	.20301
.00017	.08571
.00552	.02689
.01534	.12799
.21035	.21409
.00000	.07819
.00552	.02689
.00515	.02689
.00371	.04166
.00561	.03715
.03366	.03715
.00066	.02689
.02300	.10124
.00552	.02689
.03857	.03715
.08723	.07819
.00030	.10124
.00451	.10124
.00451	.10124
.01452	.02689
.01032	.14036
.03225	.08661
.00007	.18133
.06634	.08661
.00056	.08661
.00295	.08661
.07741	.17569
.00037	.14270
.00295	.08661
.13394	.19758

The figure below shows a histogram used to test for normality.

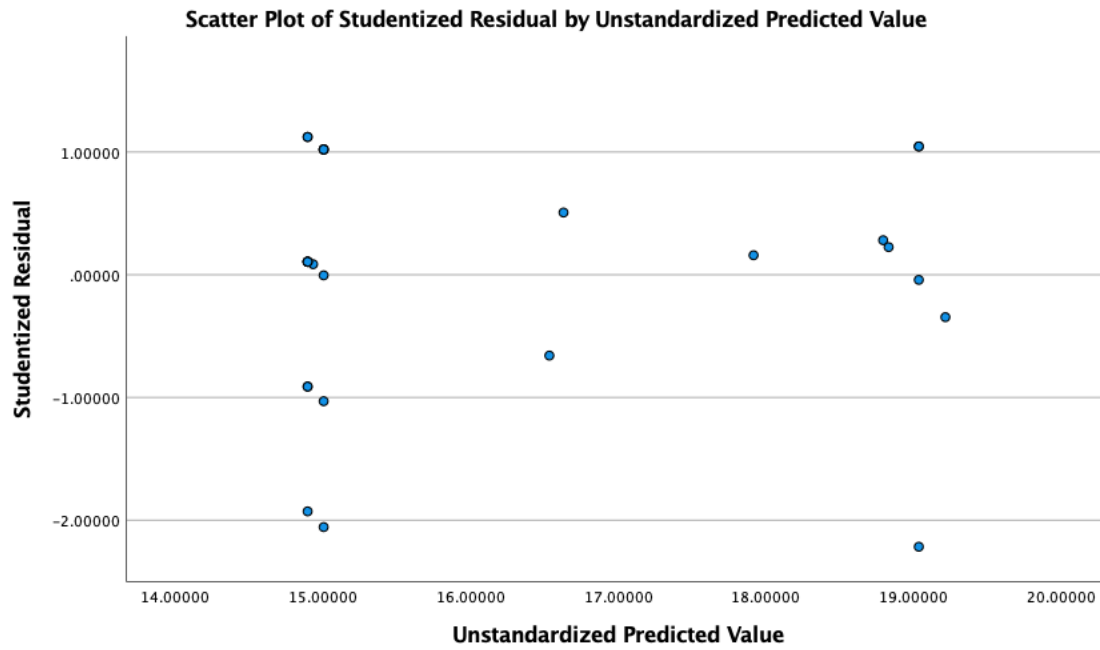


The figure below shows a normal P-P plot of regression standardised residual used to test for normality.



### A8.3 Age Range 13 to 20 years for the acromial border of the scapula, the femoral head, greater trochanter and the proximal tibia

The figure below shows the scatter plot for the Studentised Residual and Unstandardised Predicted Value for the age range: 13 to 20 years to test for a linear relationship and homoscedasticity.



The table below gives the VIF statistics used to look at the multicollinearity of the test.

**Coefficients<sup>a</sup>**

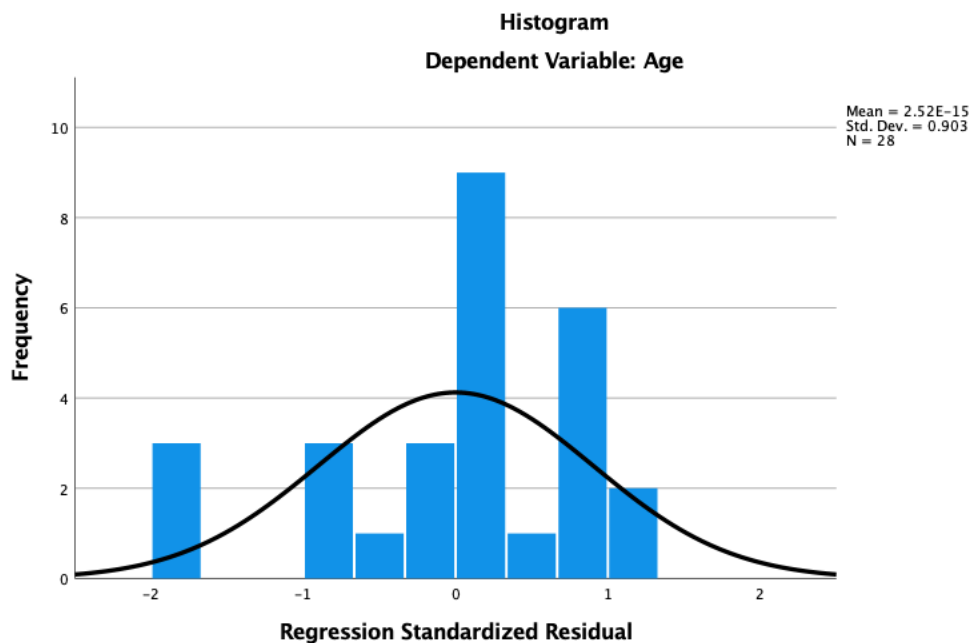
Model	Unstandardized Coefficients		Standardized Coefficients		Sig.	Correlations			Collinearity Statistics		
	B	Std. Error	Beta	t		Zero-order	Partial	Part	Tolerance	VIF	
1	(Constant)	12.716	.754		16.869	<.001					
	Location	.109	.386	.030	.281	.781	-.059	.060	.028	.840	1.191
	Scapula_Acrom	.337	.664	.147	.507	.617	.821	.107	.050	.114	8.774
	Tibia_Prox	.205	.730	.080	.280	.782	.802	.060	.027	.117	8.566
	Femur_Head	.037	.715	.015	.052	.959	.816	.011	.005	.123	8.151
	Femur_GreTroch	1.493	.604	.674	2.470	.022	.881	.466	.242	.129	7.756

a. Dependent Variable: Age

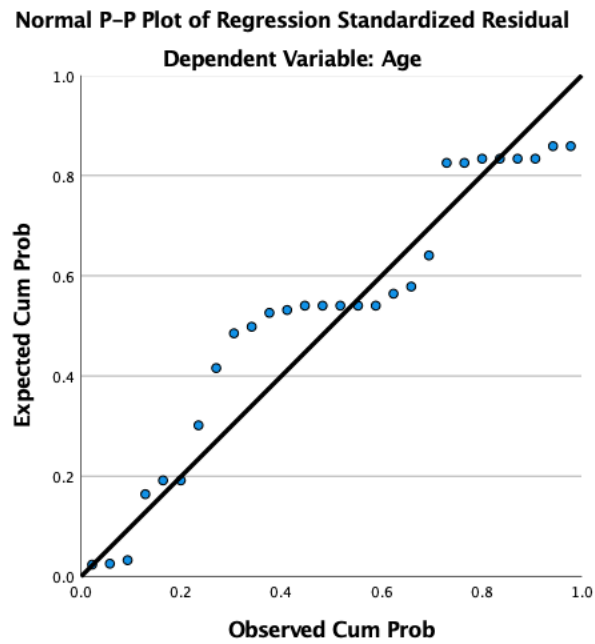
The table below shows the Leverage Regression and Cook's Distance Values to test for leverage points and influential points.

<b>COO 1</b>	<b>LEV 1</b>
.01932	.06431
.01932	.06431
.07827	.06431
.01276	.04881
.00017	.04881
.01353	.46991
.05718	.04881
.00017	.04881
.20337	.16336
.00091	.38810
.01941	.04881
.04532	.16336
.01272	.71438
.01941	.04481
.00797	.44857
.00017	.04881
.04228	.46058
.00017	.04881
.01276	.04881
.04532	.16336
.00017	.04881
.00007	.06431
.01932	.34099
.04363	.06431
.01965	.06431
.00000	.06431
.03259	.58580

The figure below shows a histogram used to test for normality.

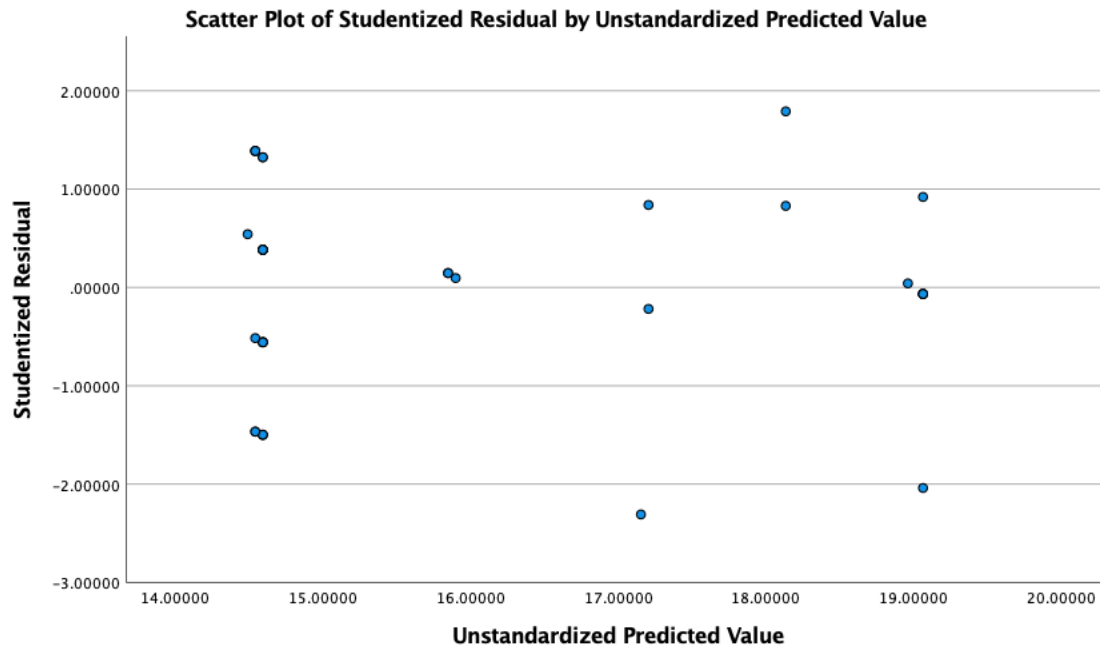


The figure below shows a normal P-P plot of regression standardised residual used to test for normality.



#### A8.4 Age Range 13 to 20 years for the lesser trochanter and the distal femur

The figure below shows the scatter plot for the Studentised Residual and Unstandardised Predicted Value for the age range: 13 to 20 years to test for a linear relationship and homoscedasticity.



The table below gives the VIF statistics used to look at the multicollinearity of the test

**Coefficients<sup>a</sup>**

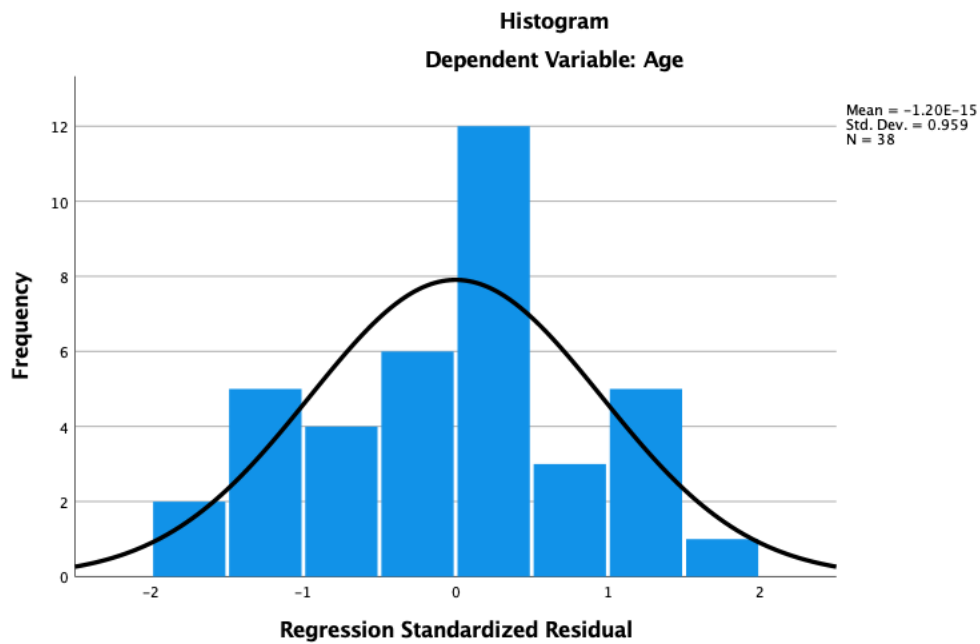
Model		Unstandardized Coefficients		Standardized Coefficients	t	Sig.	Correlations			Collinearity Statistics	
		B	Std. Error	Beta			Zero-order	Partial	Part	Tolerance	VIF
1	(Constant)	12.406	.591		21.008	<.001					
	Location	-.051	.310	-.014	-.166	.869	-.080	-.028	-.014	.993	1.008
	Femur_LessTroch	1.307	.297	.573	4.399	<.001	.838	.602	.373	.425	2.354
	Femur_Distal	.930	.348	.349	2.672	.011	.784	.417	.227	.423	2.362

a. Dependent Variable: Age

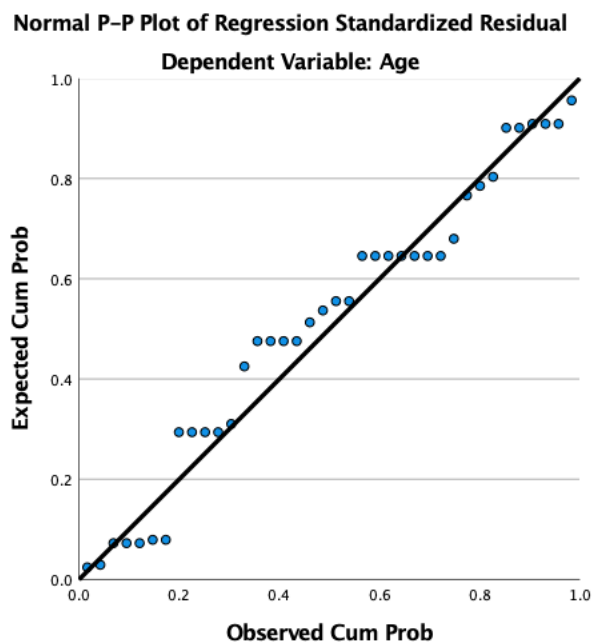
The table below shows the Leverage Regression and Cook's Distance Values to test for leverage points and influential points.

<b>COO 1</b>	<b>LEV 1</b>
.03881	.04819
.03881	.04819
.04324	.04819
.03147	.02684
.00435	.02684
.00207	.02684
.01766	.06664
.03147	.02684
.00207	.02684
.16787	.11276
.03147	.02684
.00207	.02684
.00435	.02684
.02463	.02684
.03424	.11276
.00020	.05125
.05867	.22361
.02463	.02684
.00017	.11276
.00207	.02684
.00017	.11276
.00207	.02684
.00395	.22361
.00435	.02684
.00017	.11276
.00207	.02684
.00435	.02684
.08221	.06664
.00207	.02684
.00017	.11276
.00059	.07176
.04324	.04819
.00059	.07176
.00532	.04819
.03881	.04819
.49149	.24329
.02533	.23006
.00027	.35628

The figure below shows a histogram used to test for normality.

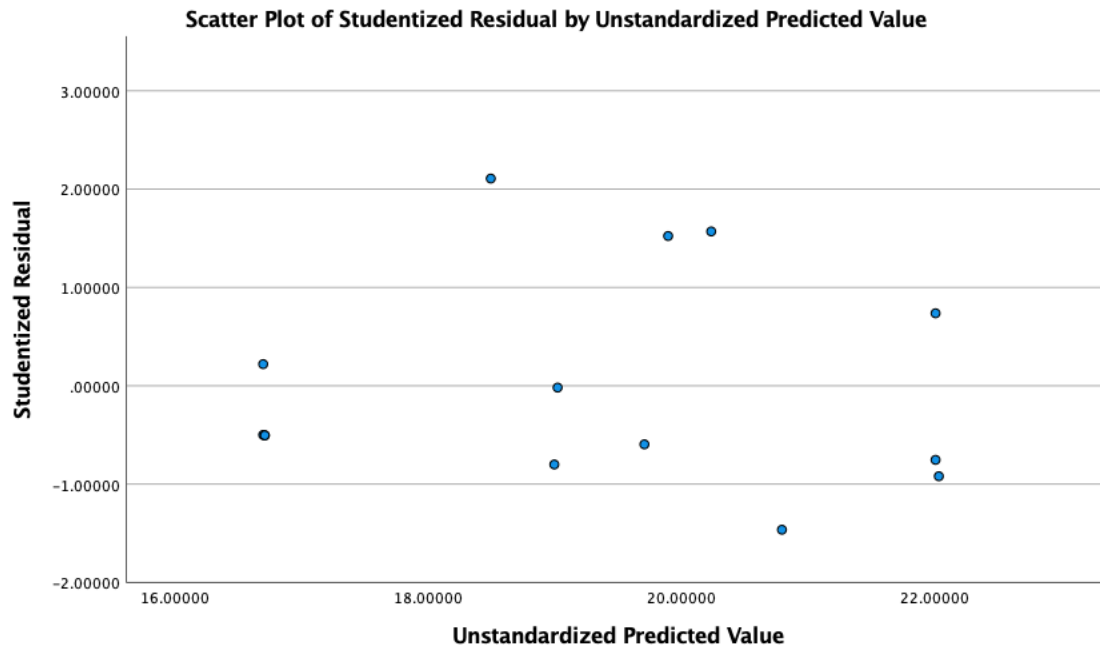


The figure below shows a normal P-P plot of regression standardised residual used to test for normality.



### A8.5 Age Range 16 to 23 years

The figure below shows the scatter plot for the Studentised Residual and Unstandardised Predicted Value for the age range: 16 to 23 years to test for a linear relationship and homoscedasticity.



The table below gives the VIF statistics used to look at the multicollinearity of the test

**Coefficients<sup>a</sup>**

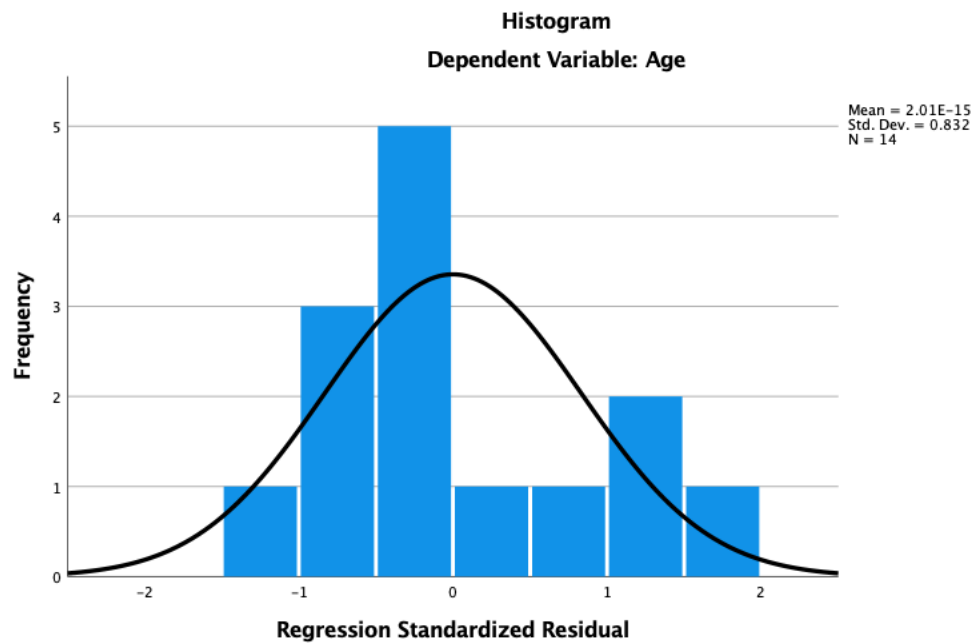
Model		Unstandardized Coefficients		Standardized Coefficients	t	Sig.	Correlations			Collinearity Statistics		
		B	Std. Error	Beta			Zero-order	Partial	Part	Tolerance	VIF	
1	(Constant)	14.022	1.555		9.017	<.001						
	Location	.013	.641	.005	.020	.984	.064	.007	.004	.665	1.504	
	Pelvis_IliacCrest	1.215	1.188	.414	1.023	.333	.774	.323	.187	.205	4.888	
	Clavicle_Lateral	.900	.617	.369	1.459	.178	.612	.437	.267	.524	1.908	
	Scapula_InfAngle	.544	.810	.230	.671	.519	.660	.218	.123	.286	3.495	

a. Dependent Variable: Age

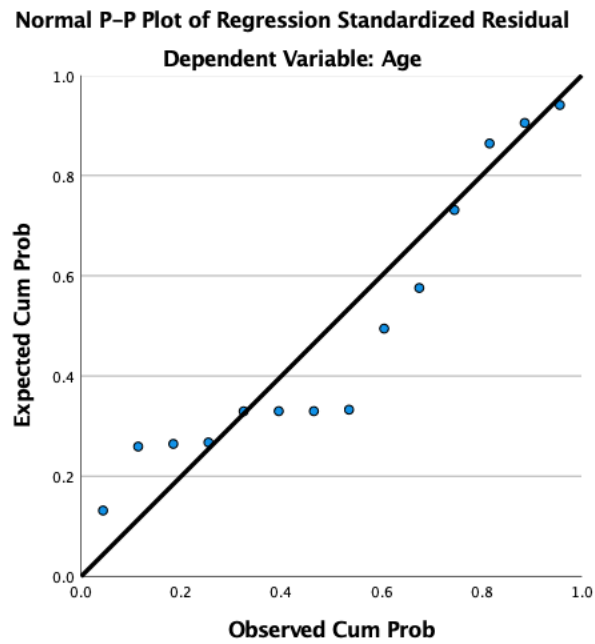
The table below shows the Leverage Regression and Cook's Distance Values to test for leverage points and influential points.

<b>COO 1</b>	<b>LEV 1</b>
.04893	.23005
.01669	.17951
.05805	.37916
.04701	.23005
.00327	.17951
.16267	.18802
.30443	.34413
.73040	.37966
.08476	.32712
.01564	.16437
.01564	.16437
.51342	.43870
.00005	.35964
.17396	.43570

The figure below shows a histogram used to test for normality.

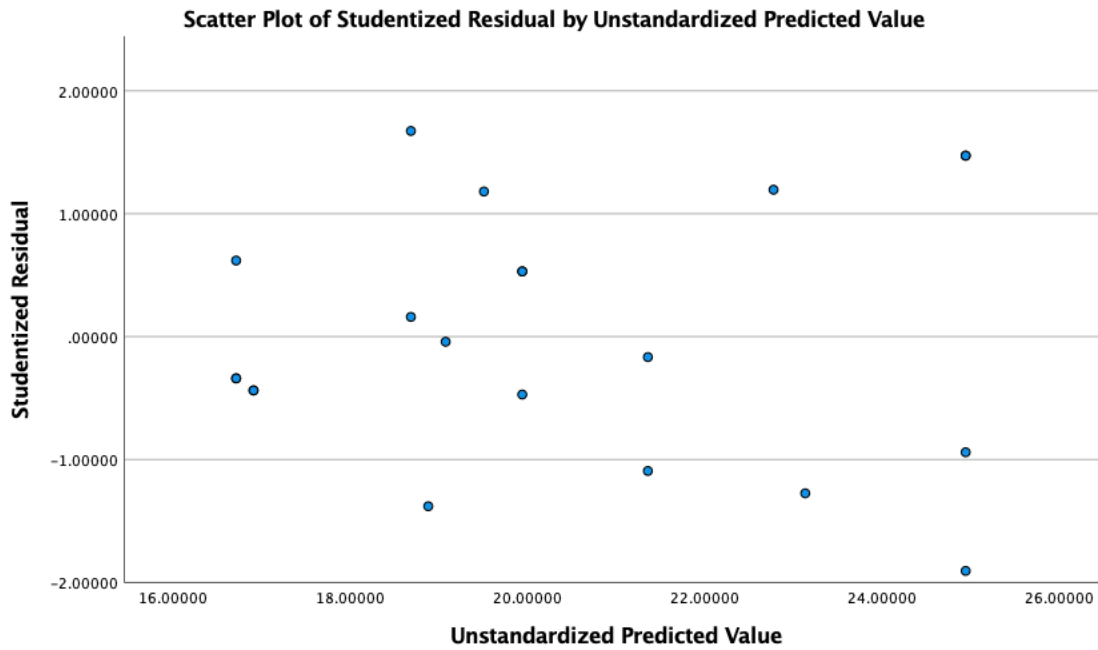


The figure below shows a normal P-P plot of regression standardised residual used to test for normality.



### A8.6 Age Range 16 to 30 years

The figure below shows the scatter plot for the Studentised Residual and Unstandardised Predicted Value for the age range: 16 to 30 years to test for a linear relationship and homoscedasticity.



The table below gives the VIF statistics used to look at the multicollinearity of the test

**Coefficients<sup>a</sup>**

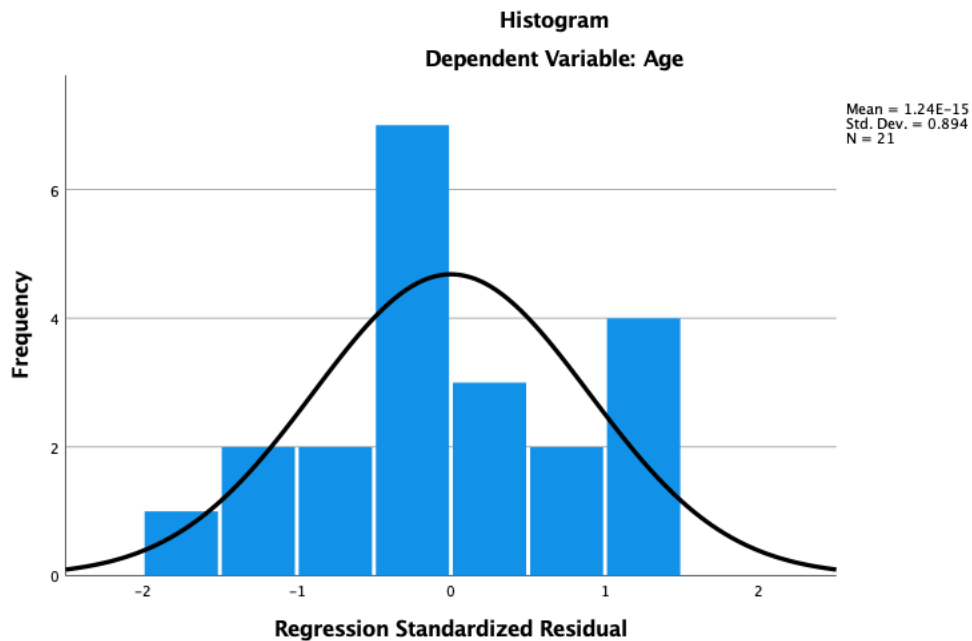
Model		Unstandardized Coefficients		Standardized Coefficients	t	Sig.	Correlations			Collinearity Statistics	
		B	Std. Error	Beta			Zero-order	Partial	Part	Tolerance	VIF
1	(Constant)	13.078	2.144		6.100	<.001					
	Clavicle_Lateral	.433	.914	.119	.474	.642	.673	.118	.068	.326	3.068
	Clavicle_Medial	1.419	.970	.340	1.463	.163	.747	.343	.210	.383	2.610
	Sacrum	2.170	1.331	.425	1.631	.122	.764	.378	.235	.305	3.284
	Location	-.196	.872	-.041	-.225	.825	-.246	-.056	-.032	.632	1.583

a. Dependent Variable: Age

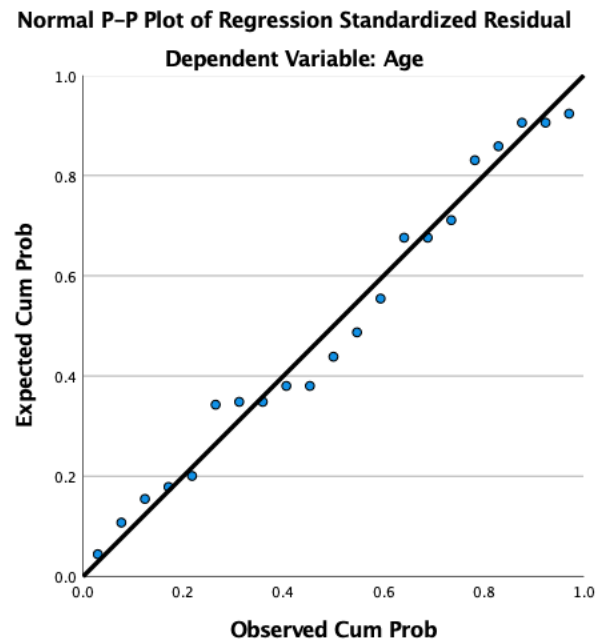
The table below shows the Leverage Regression and Cook's Distance Values to test for leverage points and influential points.

<b>COO 1</b>	<b>LEV 1</b>
.01828	.14477
.00548	.14477
.00548	.14477
.00022	.34905
.00087	.08767
.00999	.15948
.00999	.15948
.04521	.15597
.11087	.15597
.05862	.12602
.11087	.15597
.01559	.21271
.18565	.15597
.01984	.21271
.01984	.21271
.16035	.31175
.03735	.08767
.09094	.14520
.20803	.22316
.00192	.22316
.29821	.43104

The figure below shows a histogram used to test for normality.



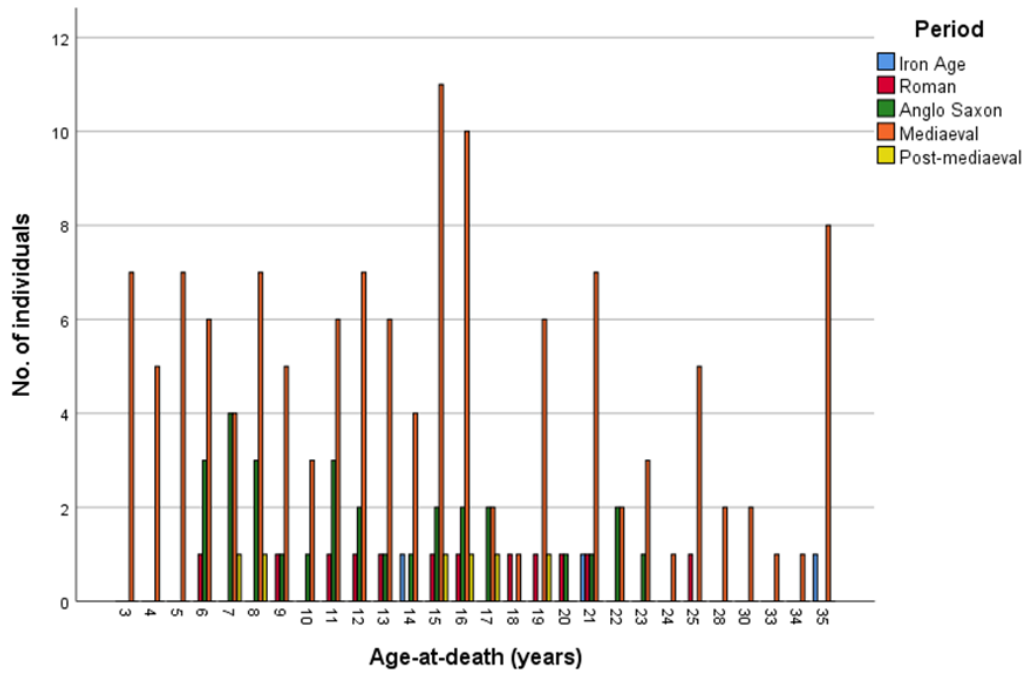
The figure below shows a normal P-P plot of regression standardised residual used to test for normality.



## APPENDIX 9: COMPARING AGE-AT-FUSION THROUGH TIME

### A9. 1. The Skull

The figure below shows the age distribution of individuals from different time periods for the **pars lateralis to pars basilaris** of the occipital bone. This shows the entire sub-sample that had these bones present.



The table below shows the fusion stages for the **pars lateralis to pars basilaris** for each period, broken down by archaeological site. Max. age Stage 1 refers to the oldest individuals in the samples who had an unfused pars lateralis to pars basilaris. Min-max age Stage 2 refers to the youngest and oldest individuals for which fusion was underway. Min. age Stage 3 refers to the minimum age of the youngest individual or individuals in those samples who were found to have fused pars lateralis to pars basilaris.

Period	Stage 1 (unfused)		Period	Stage 1 (unfused)						
Roman	Former Bridges Garage Cirencester		Mediaeval	Low-status	High-status	All Saint's church	Fisher gate House	Abbey of St Mary		
				Canterbury	Canterbury	York	York	Cirencester		
	Max. age 6			7	8	5	6	8		
Stage 3 (fused)			Stage 3 (fused)							
Former Bridges Garage		Bath Gate Cemetery	Low-status	High-status	All Saint's church	Fisher gate House	Abbey of St Mary	Auldham		
Cirencester		Cirencester	Canterbury	Canterbury	York	York	Cirencester	East Lothian		
Min. age 19*		9	7	7	11*	7	14*	11*		
Stage 1 (unfused)			Stage 1 (unfused)							
Anglo-Saxon	The Black Gate cemetery	Butler's Field cemetery	Post-mediaeval	Carvert Street						
	Newcastle-upon-Tyne	Lechlade		Sheffield						
	Max. age 7			8	Max. age N.D.					
Stage 2 (fusing)			Stage 2 (fusing)							
The Black Gate cemetery			Carvert Street							
Newcastle-upon-Tyne			Sheffield							
Min.- Max. age 6-8			Min.- Max. age 7-8							
Stage 3 (fused)			Stage 3 (fused)							
The Black Gate cemetery		Butler's Field cemetery	Apple Down cemetery							
Newcastle-upon-Tyne		Lechlade	Up Marden							
Min. age 10		7	8		Min. age 15*					

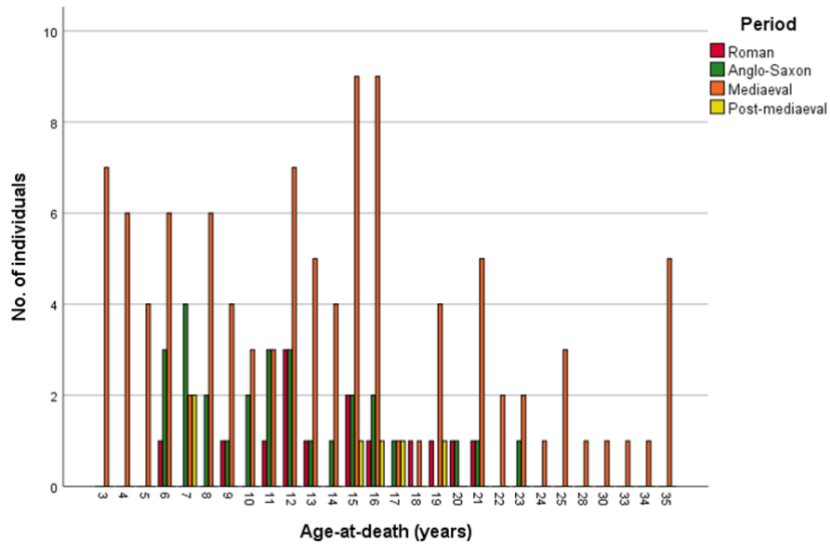
\* Large gaps in data between ages

The table below shows the fusion stages for the fusion of the **spheno-occipital synchondrosis**. Max. age Stage 1 refers to the oldest individual or individuals in the samples who had an unfused spheno-occipital synchondrosis. Min-max age Stage 2 refers to the youngest and oldest individuals for which fusion was underway. Min. age Stage 3 refers to the minimum age of the youngest individual or individuals in those samples who were found to have a fused spheno-occipital synchondrosis.

Period	Stage 1 (unfused)			Period	Stage 1 (unfused)						
Roman	Former Bridges Garage	Bath Gate Cemetery	St James' Place	Mediaeval	Low-status	High-status	All Saint's church	Fishergate House	Abbey of St Mary	Auldham	
	Cirencester	Cirencester	Cirencester		Canterbury	Canterbury	York	York	Cirencester	East Lothian	
	Max. age				Max. age						
	19	16	12		16	15	18	16	14	15*	
	Stage 2 (fusing)				Stage 2 (fusing)						
					Low-status						
					Canterbury						
					Min.- Max. age						
					16						
	Stage 3 (fused)				Stage 3 (fused)						
	Former Bridges Garage	Bath Gate Cemetery			Low-status	High-status	All Saint's church			Auldham	
	Cirencester	Cirencester			Canterbury	Canterbury	York			East Lothian	
	Min. age				Min. age						
	20	18			17	19	16			21*	
Anglo-Saxon	Stage 1 (unfused)			Post-mediaeval	Stage 1 (unfused)						
	The Black Gate cemetery	Butler's Field cemetery	Auldham		Apple Down cemetery	Carvert Street	Auldham				
	Newcastle-upon-Tyne	Lechlade	East Lothian		Up Marden	Sheffield	East Lothian				
	Max. age				Max. age						
	17	14*	21*	15*	17	19*					
	Stage 2 (fusing)				Stage 2 (fusing)						
					Apple Down cemetery						
					Up Marden						
					Min.- Max. age						
					20						
	Stage 3 (fused)				Stage 3 (fused)						
		Butler's Field cemetery			Carvert Street						
		Lechlade			Sheffield						
		Min. age			Min. age						
		23*			15						

\* Large gaps in data between ages

The figure below shows the age distribution of individuals from different time periods for the fusion of the **spheno-occipital synchondrosis** of the skull. This shows the entire sub-sample that had these bones present.



Age at death/ phase for the fusion of the occipital, including the (1) pars lateralis to pars basilaris and (2) the spheno-occipital synchondrosis for the skeletal samples collated by archaeological period. Frequencies are recorded as percentages.

		Roman			Anglo-Saxon						
		Stage of union			Stage of union						
	Age	<i>n</i>	1	2	3	Age	<i>n</i>	1	2	3	
Pars lateralis to pars basilaris	6	1	100.0	-	-	6	3	66.7	33.3	-	
	9	1	-	-	100.0	7	4	50.0	25.0	25.0	
	11	1	-	-	100.0	8	3	33.3	33.3	33.3	
		9	1	-	-	100.0					
		10	1	-	-	100.0					
		11	3	-	-	100.0					
The occipital											
Spheno-occipital synchondrosis											

## A9. 2. The Cervical vertebrae

The figure below shows the age distribution of individuals from different time periods for the fusion of the **anterior arch** of the atlas (C1). This shows the entire sub-sample that had these bones present.

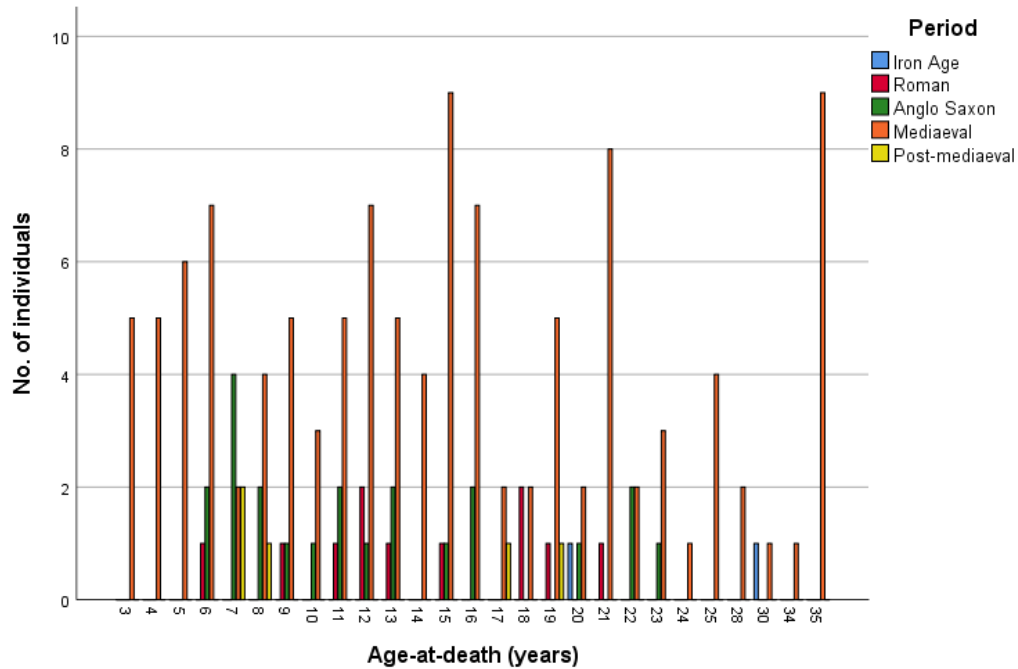


Table below shows the fusion stages for the fusion of the **anterior arch** of the atlas (C1). Max. age Stage 1 refers to the oldest individual or individuals in the samples who had an unfused anterior arch. Min-max age Stage 2 refers to the youngest and oldest individuals for which fusion was underway. Min. age Stage 3 refers to the minimum age of the youngest individual or individuals in those samples who were found to have a fused anterior arch of the atlas (C1).

Period	Stage 1 (unfused)			Period	Stage 1 (unfused)					
Roman	Former Bridges Garage Cirencester			Mediaeval	Low-status Canterbury	High-status Canterbury	All Saint's church York	Fishergate House York	Abbey of St Mary Cirencester	
	Max. age	6*			Max. age	15	5*	11*	6	6*
	Stage 2 (fusing)				Stage 2 (fusing)					
	Bath Gate Cemetery Cirencester				Low-status Canterbury				Abbey of St Mary Cirencester	
	Min. age	9			Min.- Max. age	9				
	Stage 3 (fused)				Stage 3 (fused)					
	Bath Gate Cemetery Cirencester	Former Bridges Garage Cirencester	St James' Place Cirencester		Low-status Canterbury	High-status Canterbury		Fishergate House York	Abbey of St Mary Cirencester	Auldham East Lothian
	Min. age	9	12*	12*	Min. age	8	11*	7	14*	11*
Period	Stage 1 (unfused)			Period	Stage 1 (unfused)					
Anglo-Saxon	The Black Gate cemetery Newcastle-upon-Tyne	Butler's Field cemetery Lechlade	Apple Down cemetery Up Marden	Post-Mediaeval	Carver Street Sheffield					
	Max. age	7	9*	11	Max. age	8*				
	Stage 2 (fusing)				Stage 2 (fusing)					
	The Black Gate cemetery Newcastle-upon-Tyne				The Black Gate cemetery Newcastle-upon-Tyne					
	Min.- Max. age	6			Min.- Max. age					
	Stage 3 (fused)				Stage 3 (fused)					
	The Black Gate cemetery Newcastle-upon-Tyne	Apple Down cemetery Up Marden			Carver Street Sheffield	Auldham East Lothian				
	Min. age	11*		8	Min. age	7* 19*				

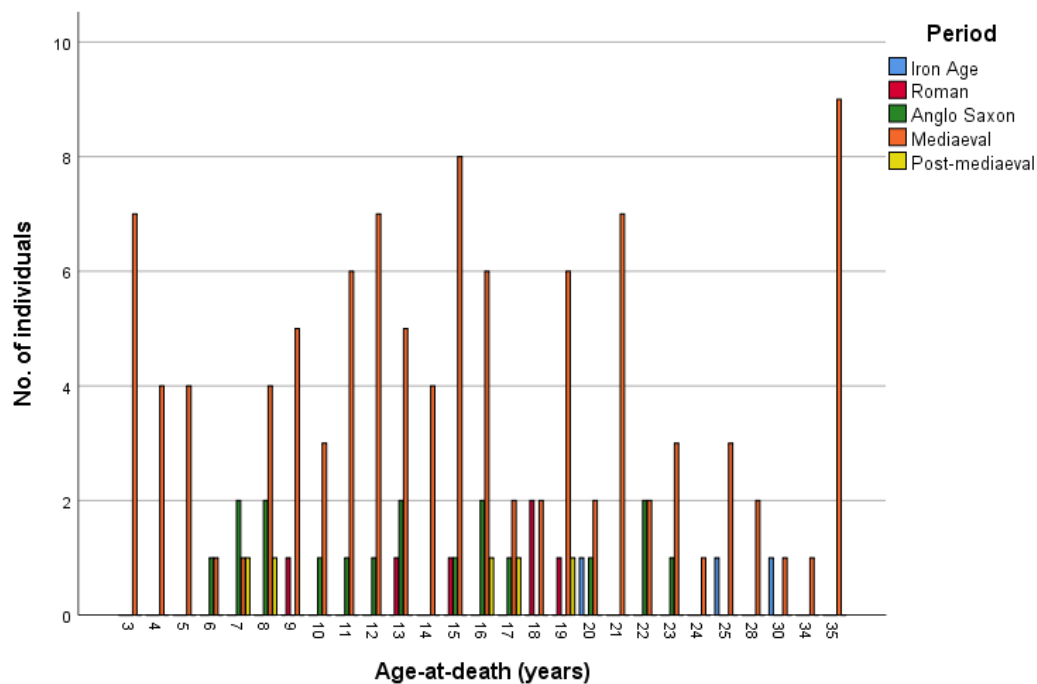
\* Large gaps in data between ages

The table below shows the fusion stages for the fusion of the **posterior synchondrosis** of the atlas (C1). Max. age Stage 1 refers to the oldest individual or individuals in the samples who had an unfused posterior synchondrosis. Min-max age Stage 2 refers to the youngest and oldest individuals for which fusion was underway. Min. age Stage 3 refers to the minimum age of the youngest individual or individuals in those samples who were found to have a fused posterior synchondrosis of the atlas (C1).

Period	Stage 1 (unfused)		Period	Stage 1 (unfused)						
Roman			Mediaeval	Low-status Canterbury	High-status Canterbury		Fishergate House York			
				Max. age 15	5		6			
	Stage 3 (fused)			Stage 3 (fused)						
	Bath Gate Cemetery	Former Bridges Garage		Low-status Canterbury	High-status Canterbury	All Saint's church York	Fishergate House York	Abbey of St Mary Cirencester	Auldham East Lothian	
	Cirencester	Cirencester		Min. age 9*	8	4	11*	5	14*	11*
Period	Stage 1 (unfused)		Period	Stage 1 (unfused)						
Anglo-Saxon		Butler's Field cemetery Lechlade	Apple Down cemetery Up Marden	Post-Mediaeval						
		Max. age 7*	7*							
	Stage 3 (fused)			Stage 3 (fused)						
	The Black Gate cemetery Newcastle-upon-Tyne	Butler's Field cemetery Lechlade	Apple Down cemetery Up Marden	Carver Street Sheffield	Auldham East Lothian					
	Min. age 6*	8*	8*	7*	19*					

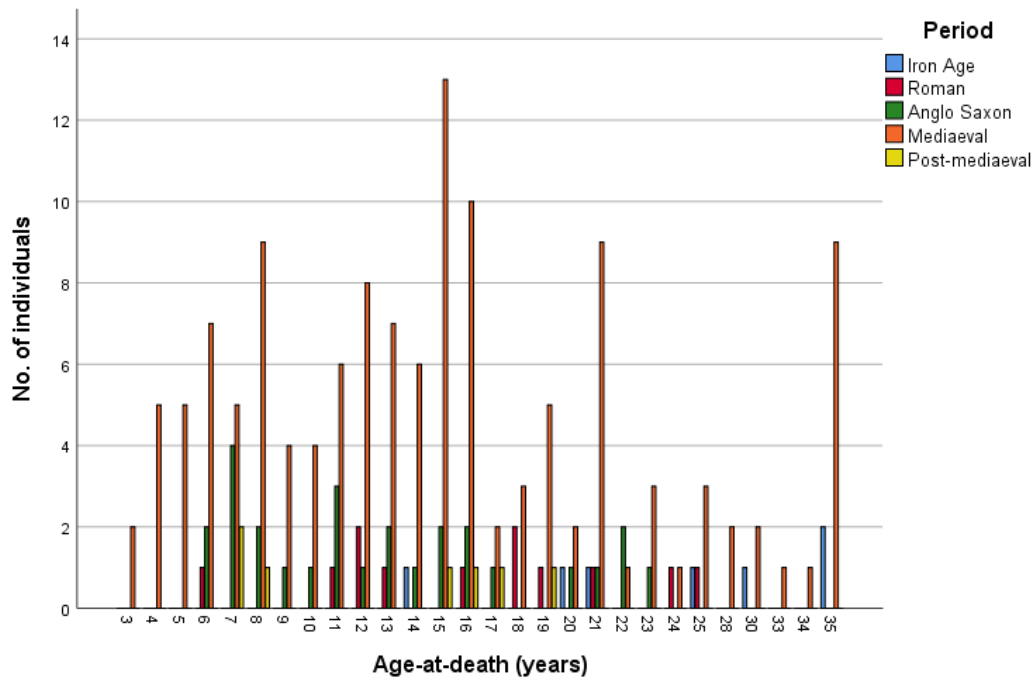
\* Large gaps in data between ages

The figure below shows the age distribution of individuals from different time periods for the fusion of the **posterior synchondrosis** of the atlas (C1). This shows the entire sub-sample that had these bones present.





The figure below shows the age distribution of individuals from different time periods for the fusion of the **ossiculum terminale** to the dens of the axis (C2). This shows the entire sub-sample that had these bones present.



The table below shows the fusion stages for the fusion of the **ossiculum terminale** to the dens of the axis (C2). Max. age Stage 1 refers to the oldest individual or individuals in the samples who had an unfused dens. Min-max age Stage 2 refers to the youngest and oldest individuals for which fusion was underway. Min. age Stage 3 refers to the minimum age of the youngest individual or individuals in those samples who were found to have a fused dens.

Period	Stage 1 (unfused)	Period	Stage 1 (unfused)	Period	Stage 1 (unfused)
Iron Age		Anglo-Saxon	The Black Gate cemetery Newcastle-upon-Tyne Max. age 7	Butler's Field cemetery Lechlade 8	Apple Down cemetery Up Marden 11*
			Stage 2 (fusing)		
				Butler's Field cemetery Lechlade 9	Apple Down cemetery Up Marden 8*
			Stage 3 (fused)		
	South Dumpton Down Broadstairs Min. age 14*		The Black Gate cemetery Newcastle-upon-Tyne Min. age 10	Butler's Field cemetery Lechlade 14*	Apple Down cemetery Up Marden 15*
					Carver Street Sheffield Min. age 15*
					Auldham East Lothian 19*
Roman	Former Bridges Garage Cirencester Max. age 6*	Mediaeval	Low-status Canterbury Max. age 14	High-status Canterbury 7	Fishergate House York 11
					Abbey of St Mary Cirencester 8*
			Stage 2 (fusing)		
			Low-status Canterbury Min.- Max. age 8-13	High-status Canterbury 15	All Saint's church York 8*
			Stage 3 (fused)		
	Bath Gate Cemetery Cirencester Min. age 11*	Former Bridges Garage Cirencester 12*	Low-status Canterbury Min. age 11	High-status Canterbury 11	All Saint's church York 11*
					Fishergate House York 9
					Abbey of St Mary Cirencester 14*
					Auldham East Lothian 15*

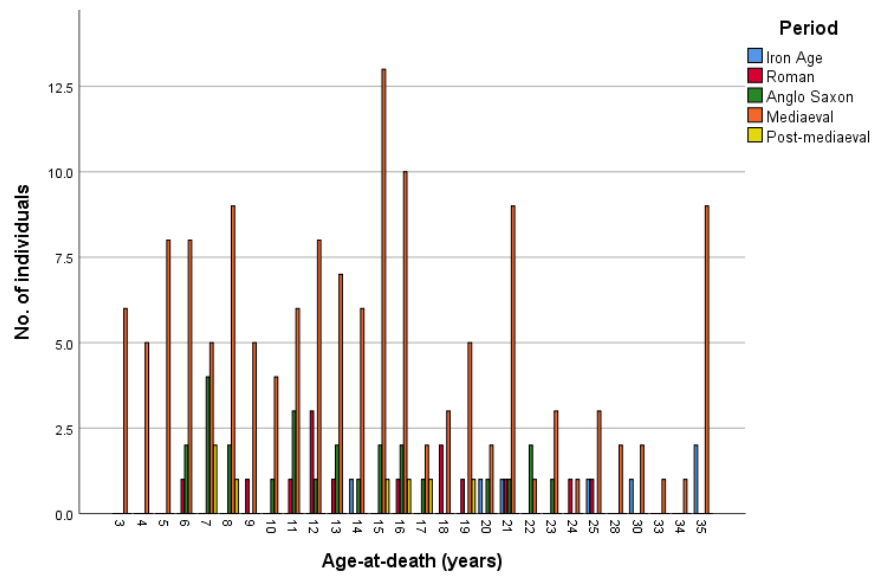
\* Large gaps in data between ages

The table below shows the fusion stages for the fusion of the **dentoneural synchondrosis** of the axis (C2). Max. age Stage 1 refers to the oldest individual or individuals in the samples who had an unfused dentoneural synchondrosis. Min-max age Stage 2 refers to the youngest and oldest individuals for which fusion was underway. Min. age Stage 3 refers to the minimum age of the youngest individual or individuals in those samples who were found to have a fused dentoneural synchondrosis of the axis (C2).

Period	Stage 1 (unfused)		Period	Stage 1 (unfused)				
Roman			Mediaeval	Low-status Canterbury	High-status Canterbury	Fishergate House York	Abbey of St Mary Cirencester	
				Max. age 6	4	5*	6*	
				<b>Stage 2 (fusing)</b>				
				Low-status Canterbury		Fishergate House York		
				Min.- Max. age 6		6*		
	<b>Stage 3 (fused)</b>			<b>Stage 3 (fused)</b>				
	Bath Gate Cemetery Cirencester	Former Bridges Garage Cirencester		Low-status Canterbury	High-status Canterbury	All Saint's church York	Fishergate House York	Abbey of St Mary Cirencester
	Min. age 9*	6*		Min. age 3	5	5*	5*	8*
Period	Stage 1 (unfused)		Period	Stage 1 (unfused)				
Anglo-Saxon	The Black Gate cemetery Newcastle-upon-Tyne	Butler's Field cemetery Lechlade	Post-Mediaeval					
	Max. age 7	8		<b>Stage 2 (fusing)</b>				
				Carver Street Sheffield				
				Min.- Max. age 8*				
	<b>Stage 3 (fused)</b>			<b>Stage 3 (fused)</b>				
	The Black Gate cemetery Newcastle-upon-Tyne	Butler's Field cemetery Lechlade		Carver Street Sheffield				
	Min. age 6*	7*		Min. age 7*				

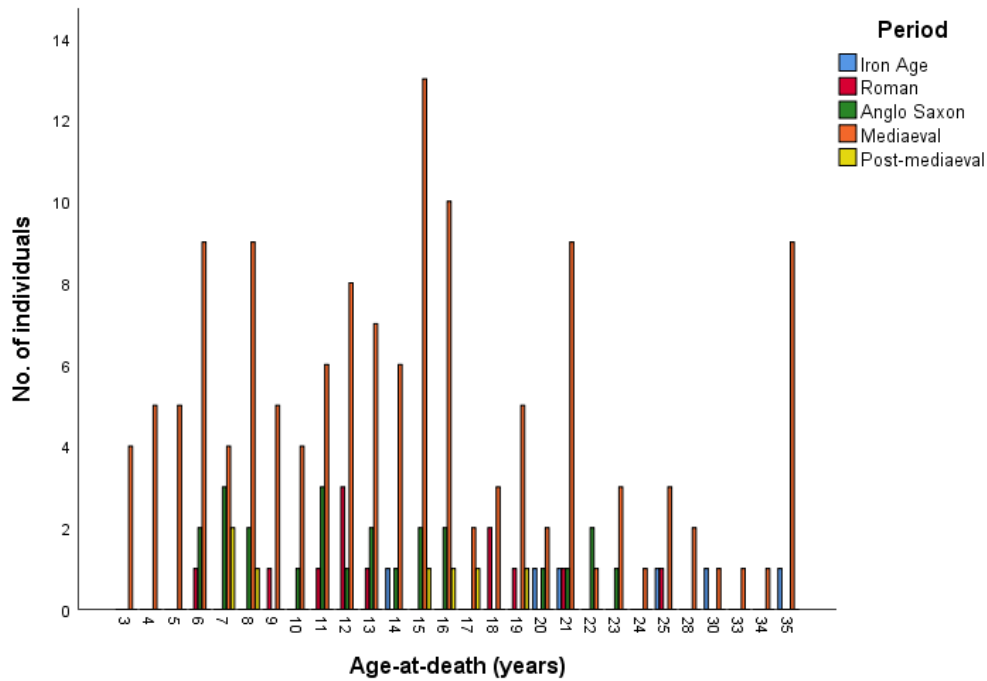
\* Large gaps in data between ages

The figure below shows the age distribution of individuals from different time periods for the fusion of the **dentoneural synchondrosis** of the axis (C2). This shows the entire sub-sample that had these bones present.





The figure below shows the age distribution of individuals from different time periods for the fusion of the **dentocentral and neurocentral junctions** of the axis (C2). This shows the entire sub-sample that had these bones present.



The table below shows the fusion stages for the fusion of the **dentocentral and neurocentral junctions** of the axis (C2). Max. age Stage 1 refers to the oldest individual or individuals in the samples who had unfused dentocentral and neurocentral junctions. Min-max age Stage 2 refers to the youngest and oldest individuals for which fusion was underway. Min. age Stage 3 refers to the minimum age of the youngest individual or individuals in those samples who were found to have fused dentocentral and neurocentral junctions of the axis (C2).

Period	Stage 1 (unfused)	Period	Stage 1 (unfused)	Period	Stage 1 (unfused)
Iron Age		Anglo-Saxon		Post-Medieval	
			<b>Stage 2 (fusing)</b>		<b>Stage 2 (fusing)</b>
			The Black Gate cemetery Newcastle-upon-Tyne Min.- Max. age 6-12	Butler's Field cemetery Lechlade 7*	Apple Down cemetery Up Marden 8-11*
					Carver Street Sheffield Min.- Max. age 7*
	<b>Stage 3 (fused)</b>		<b>Stage 3 (fused)</b>		<b>Stage 3 (fused)</b>
	South Dumpton Down Broadstairs Min. age 14*		The Black Gate cemetery Newcastle-upon-Tyne Min. age 11*	Butler's Field cemetery Lechlade 8*	Apple Down cemetery Up Marden 15*
					Carver Street Sheffield Min. age 8*
					Auldham East Lothian 19*
Period	Stage 1 (unfused)	Period	Stage 1 (unfused)	Period	Stage 1 (unfused)
Roman	Former Bridges Garage Cirencester Max. age 6*	Mediaeval	Low-status Canterbury Max. age 6	High-status Canterbury 5	Fishergate House York 6
					Abbey of St Mary Cirencester 6*
	<b>Stage 2 (fusing)</b>		<b>Stage 2 (fusing)</b>		<b>Stage 2 (fusing)</b>
	Bath Gate Cemetery Cirencester Min.- Max. age 9*		Low-status Canterbury Min.- Max. age 3-16	High-status Canterbury 4	All Saint's church York 8-13*
					Fishergate House York 5-10
					Abbey of St Mary Cirencester 8*
					Auldham East Lothian 15*
	<b>Stage 3 (fused)</b>		<b>Stage 3 (fused)</b>		<b>Stage 3 (fused)</b>
	Bath Gate Cemetery Cirencester Min. age 11*	Former Bridges Garage Cirencester 12*	Low-status Canterbury Min. age 5	High-status Canterbury 7	All Saint's church York 15*
		St James' Place Cirencester 12*			Fishergate House York 9
					Abbey of St Mary Cirencester 14*
					Auldham East Lothian 19*

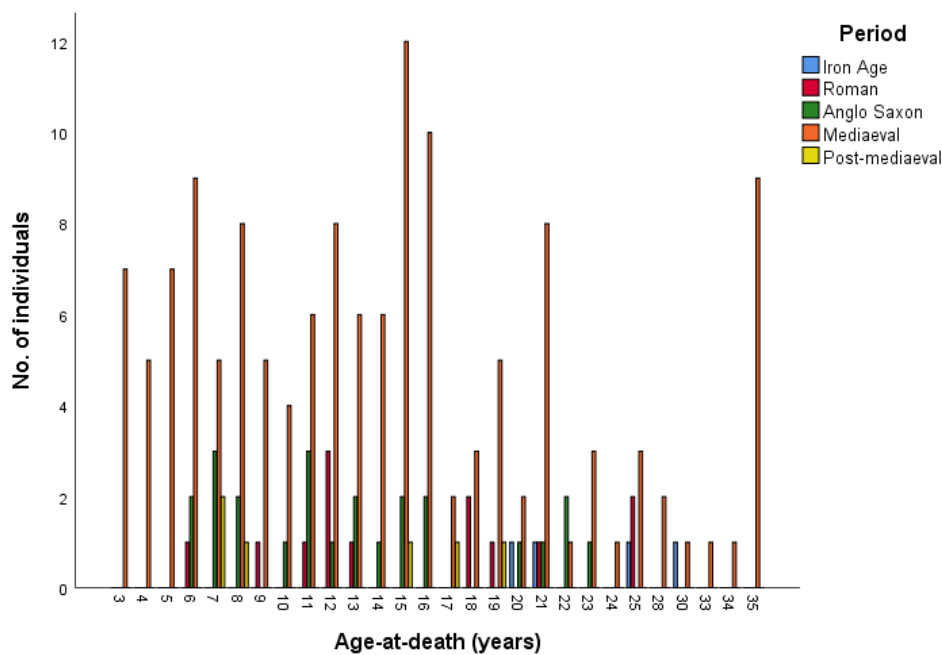
\* Large gaps in data between ages

The table below shows the fusion stages for the fusion of the **posterior synchondrosis of the axis (C2)**. Max. age Stage 1 refers to the oldest individual or individuals in the samples who had an unfused posterior synchondrosis. Min-max age Stage 2 refers to the youngest and oldest individuals for which fusion was underway. Min. age Stage 3 refers to the minimum age of the youngest individual or individuals in those samples who were found to have a fused posterior synchondrosis of the axis (C2).

Period	Stage 1 (unfused)	Period	Stage 1 (unfused)
Roman		Mediaeval	Low-status Canterbury Max. age 5
	<b>Stage 3 (fused)</b> Former Bridges Garage Cirencester Min. age 6*		<b>Stage 3 (fused)</b> Low-status Canterbury Min. age 3
		High-status Canterbury Min. age 3	All Saint's church York Min. age 5*
			Fishergate House York Min. age 5*
			Abbey of St Mary Cirencester Min. age 6*
Period	Stage 1 (unfused)	Period	Stage 1 (unfused)
Anglo-Saxon		Post-Mediaeval	
	<b>Stage 2 (fusing)</b> The Black Gate cemetery Newcastle-upon-Tyne Min.- Max. age 7*		<b>Stage 3 (fused)</b> Carver Street Sheffield Min. age 7*
	<b>Stage 3 (fused)</b> The Black Gate cemetery Newcastle-upon-Tyne Min. age 6*	Butler's Field cemetery Lechlade Min. age 7*	Apple Down cemetery Up Marden Min. age 8*

\* Large gaps in data between ages

The figure below shows the age distribution of individuals from different time periods for the fusion of the **posterior synchondrosis of the axis (C2)**. This shows the entire sub-sample that had these bones present.



Age at death/phase for the fusion of the axis, including the (1) dentocentral and neurocentral junctions and the (2) posterior synchondrosis of the axis for the skeletal samples collated by archaeological period. Frequencies are recorded as percentages.

		Roman			Anglo-Saxon											
		Stage of union			Stage of union											
	Age	<i>n</i>	1	2	3	Age	<i>n</i>	1	2	3						
The axis	Dentocentral & neurocentral junctions	6	1	100.0	-	-	6	2	-	100.0	-					
		9	1	-	100.0	-	7	3	-	100.0	-					
		11	1	-	-	100.0	8	2	-	50.0	50.0					
		12	3	-	-	100.0	10	1	-	100.0	-					
		13	1	-	-	100.0	11	3	-	66.7	33.3					
		18	2	-	-	100.0	12	1	-	100.0	-					
		19	1	-	-	100.0	13	2	-	-	100.0					
							14	1	-	-	100.0					
							15	2	-	-	100.0					
							16	2	-	-	100.0					
							Mediaeval			Post-Mediaeval						
							Stage of union			Stage of union						
							Age	<i>n</i>	1	2	3	Age	<i>n</i>	1	2	3
							3	4	75.0	25.0	-	7	2	-	100.0	-
							4	5	60.0	40.0	-	8	1	-	-	100.0
							5	5	20.0	60.0	20.0	15	1	-	-	100.0
							6	9	55.6	44.4	-	16	1	-	-	100.0
							7	4	-	75.0	25.0	17	1	-	-	100.0
							8	9	-	66.7	33.3	19	1	-	-	100.0
					9	5	-	40.0	60.0							
					10	4	-	50.0	50.0							
					11	6	-	16.7	83.3							
					12	8	-	62.5	37.5							
					13	7	-	28.6	71.4							
					14	6	-	16.7	83.3							
					15	13	-	7.7	92.3							
					16	10	-	10.0	90.0							
					17	2	-	-	100.0							
					18	3	-	-	100.0							
					19	5	-	-	100.0							
Posterior synchondrosis					Anglo-Saxon			Mediaeval								
					Stage of union			Stage of union								
					Age	<i>n</i>	1	2	3	Age	<i>n</i>	1	2	3		
					6	2	-	-	100.0	3	7	28.6	-	71.4		
					7	3	-	33.3	66.7	4	5	-	-	100.0		
					8	2	-	-	100.0	5	7	14.3	-	85.7		
										6	9	-	-	100.0		
										7	5	-	-	100.0		
										8	8	-	-	100.0		
										Post-Mediaeval						
									Stage of union							
					Age	<i>n</i>	1	2	3							
					7	2	-	-	100.0							
					8	1	-	-	100.0							

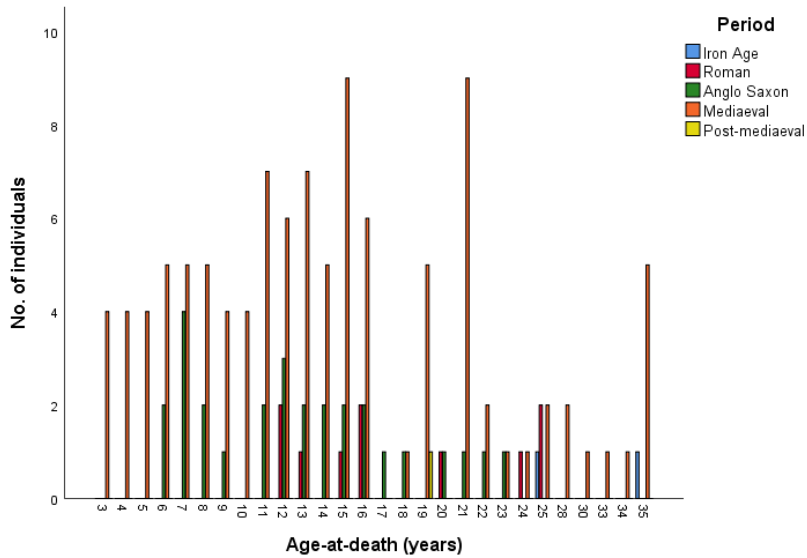
### A9.3. The Sacrum

The table below shows the fusion stages for the fusion of the **sacral bodies 1 and 2** of the sacrum. Max. age Stage 1 refers to the oldest individual or individuals in the samples who had unfused sacral bodies. Min-max age Stage 2 refers to the youngest and oldest individuals for which fusion was underway. Min. age Stage 3 refers to the minimum age of the youngest individual or individuals in those samples who were found to have fused sacral bodies 1 and 2 of the sacrum.

Period	Stage 1 (unfused)	Period	Stage 1 (unfused)	Period	Stage 1 (unfused)
Iron Age		Anglo-Saxon	The Black Gate cemetery Newcastle-upon-Tyne Max. age 18*	Butler's Field cemetery Lechlade 17*	Auldhame East Lothian 21*
					Apple Down cemetery Up Marden 20*
					Post-Mediaeval
					Stage 2 (fusing)
					Auldhame East Lothian Min.- Max. age 19*
					Stage 2 (fusing)
					Butler's Field cemetery Lechlade 23*
					Apple Down cemetery Up Marden 22*
					Stage 3 (fused)
					South Dumpton Down Broadstairs Min. age 25*
Period	Stage 1 (unfused)	Period	Stage 1 (unfused)	Period	Stage 1 (unfused)
	Bath Gate Cemetery Cirencester Max. age 16*	St James' Place Cirencester 16*	Mediaeval	Low-status Canterbury Max. age 16	All Saint's church York 18*
					Stage 2 (fusing)
					Low-status Canterbury Min.- Max. age 19-25
					High-status Canterbury 19*
					Fisergate House York 16*
					Auldhame East Lothian 19-22
					Stage 3 (fused)
					Low-status Canterbury Min. age 19
					Auldhame East Lothian 21

\* Large gaps in data between ages

The figure below shows the age distribution of individuals from different time periods for the fusion of the **sacral bodies 1 and 2** of the sacrum. This shows the entire sub-sample that had these bones present.

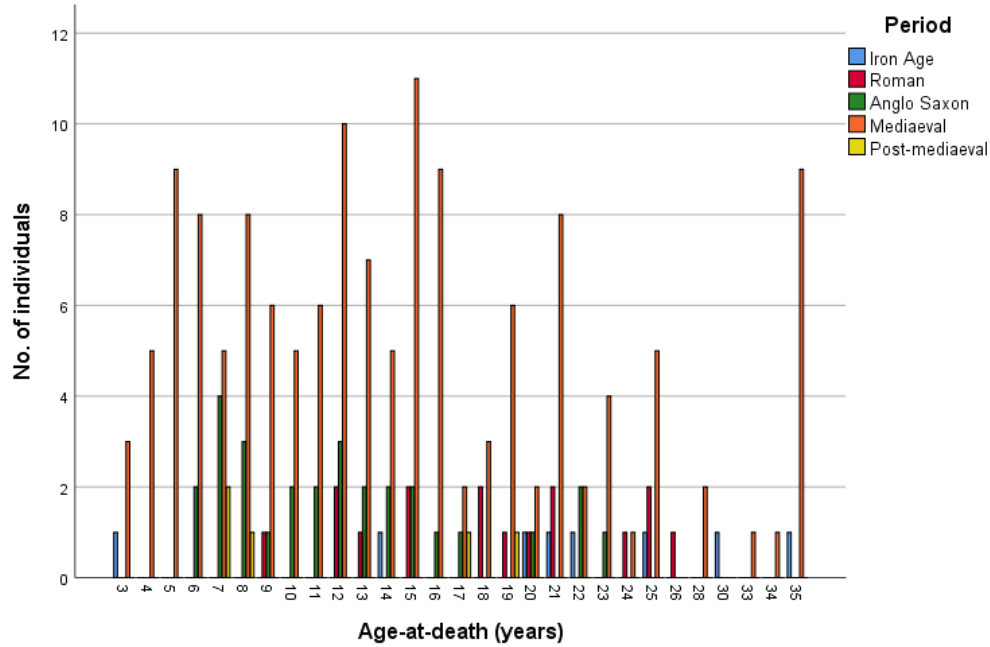


Age at death/phase for the fusion of **sacral bodies 1 & 2** for the skeletal samples collated by archaeological period. Frequencies are recorded as percentages.

		Roman			Anglo-Saxon						
		Stage of union			Stage of union						
		Age	n	1	2	3	Age	n	1	2	3
The sacrum	Bodies 1 & 2	16	2	100.0	-	-	16	2	100.0	-	-
		20	1	-	100.0	-	17	1	100.0	-	-
		24	1	-	-	100.0	18	1	100.0	-	-
		25	2	-	-	100.0	20	1	100.0	-	-
							21	1	100.0	-	-
							22	1	-	100.0	-
							23	1	-	100.0	-
		Mediaeval			Post-Mediaeval						
		Stage of union			Stage of union						
		Age	n	1	2	3	Age	n	1	2	3
		16	6	83.3	16.7	-	19	1	-	100.0	-
		18	1	100.0	-	-					
		19	5	-	80.0	20.0					
		21	9	-	66.7	33.3					
		22	2	-	100.0	-					
		23	1	-	-	100.0					
		24	1	-	-	100.0					
		25	2	-	100.0	-					
		28	2	-	-	100.0					

#### A9. 4. The Clavicle

The figure below shows the age distribution of individuals from different time periods for the fusion of the **medial epiphysis** of the clavicle. This shows the entire sub-sample that had these bones present.



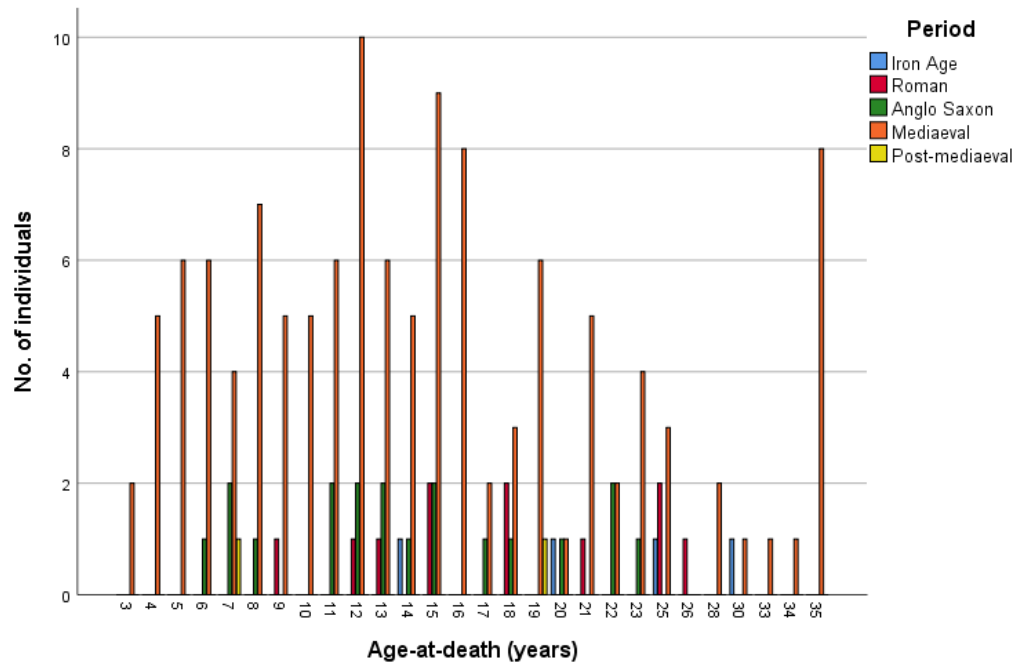
The table below shows the fusion stages for the fusion of the **medial epiphysis** of the clavicle. Max. age Stage 1 refers to the oldest individual or individuals in the samples who had an unfused medial clavicle. Min-max age Stage 2 refers to the youngest and oldest individuals for which fusion was underway. Min. age Stage 3 refers to the minimum age of the youngest individual or individuals in those samples who were found to have a fused medial clavicle.

Period	Stage 1 (unfused)		Period	Stage 1 (unfused)			Period	Stage 1 (unfused)	
Iron-Age	South Dumpton Down		Anglo-Saxon	The Black Gate cemetery	Butler's Field cemetery	Apple Down cemetery	Post-Mediaeval	Auldhame	
	Broadtairs			Newcastle-upon-Tyne	Lechlade	Up Marden		East Lothian	
	Max. age			Max. age				Max. age	
	22		16*	23	20		19*		
	<b>Stage 3 (fused)</b>			<b>Stage 3 (fused)</b>				<b>Stage 3 (fused)</b>	
	South Dumpton Down			Apple Down cemetery				Carvert Street	
	Broadtairs			Up Marden				Sheffield	
	Min. age			Min. age				Min. age	
	20				22			17*	
Period	Stage 1 (unfused)		Period	Stage 1 (unfused)					
Roman	Bath Gate Cemetery	Former Bridges Garage	Mediaeval	Low-status	High-status	All Saint's church	Fishegate House	Auldhame	
	Cirencester	Cirencester		Canterbury	Canterbury	York	York	East Lothian	
	Max. age			Max. age					
	21	20	24	18	18*	16*	22		
	<b>Stage 2 (fusing)</b>			<b>Stage 2 (fusing)</b>					
	Bath Gate Cemetery	Former Bridges Garage		Low-status	High-status	Auldhame			
	Cirencester	Cirencester		Canterbury	Canterbury	East Lothian			
	Min.- Max. age			Min.- Max. age					
	25	21		25	19		21		
	<b>Stage 3 (fused)</b>			<b>Stage 3 (fused)</b>					
	Bath Gate Cemetery	St James' Place		Low-status	High-status				
	Cirencester	Cirencester		Canterbury	Canterbury				
	Min. age			Min. age					
	25	24*		19	23				

\* Large gaps in data between ages



The figure below shows the age distribution of individuals from different time periods for the fusion of the **lateral epiphysis** of the clavicle. This shows the entire sub-sample that had these bones present.



Age at death/phase for the fusion of the clavicle, including the (1) medial and (2) lateral clavicle for skeletal samples collated by archaeological period. Frequencies are recorded as percentages.

		Iron Age			Roman			Anglo-Saxon								
		Stage of union			Stage of union			Stage of union								
		Age	n	1	2	3	Age	n	1	2	3					
The clavicle	Medial epiphysis	20	1	-	-	100.0	18	2	100.0	-	-	16	1	100.0	-	-
		21	1	100.0	-	-	19	1	100.0	-	-	17	1	100.0	-	-
		22	1	100.0	-	-	20	1	100.0	-	-	20	1	100.0	-	-
		25	1	-	-	100.0	21	2	50.0	50.0	-	22	2	-	-	100.0
							24	1	-	-	100.0	23	1	100.0	-	-
							25	2	-	50.0	50.0					
							26	1	-	-	100.0					
							<b>Mediaeval</b>			<b>Post-Mediaeval</b>						
							Stage of union			Stage of union						
							Age	n	1	2	3	Age	n	1	2	3
							16	9	100.0	-	-	17	1	-	-	100.0
							17	2	100.0	-	-	19	1	100.0	-	-
							18	3	100.0	-	-					
						19	6	66.7	16.7	16.7						
						20	2	50.0	-	50.0						
						21	8	37.5	37.5	25.0						
						22	2	100.0	-	-						
						23	4	25.0	-	75.0						
						24	1	100.0	-	-						
						25	5	-	20.0	80.0						
						28	2	-	-	100.0						
		Lateral epiphysis	<b>Iron age</b>			<b>Roman</b>			<b>Anglo-Saxon</b>							
			Stage of union			Stage of union			Stage of union							
							Age	n	1	2	3	Age	n	1	2	3
							14	1	100.0	-	-	14	1	-	-	100.0
						20	1	-	-	100.0	18	2	100.0	-	-	
						25	1	-	-	100.0	21	1	100.0	-	-	
											25	2	50.0	-	50.0	
											26	1	-	-	100.0	
											17	1	100.0	-	-	
											18	1	-	100.0	-	
											20	1	100.0	-	-	
										22	2	-	-	100.0		
										23	1	100.0	-	-		
					<b>Mediaeval</b>			<b>Stage of union</b>								
					Age	n	1	2	3							
					14	5	100.0	-	-							
					15	9	100.0	-	-							
					16	8	100.0	-	-							
					17	2	50.0	50.0	-							
					18	3	100.0	-	-							
					19	6	33.3	-	66.7							
					20	1	-	-	100.0							
					21	5	-	-	100.0							
					22	2	50.0	50.0	-							
					23	4	-	-	100.0							
					25	3	-	-	100.0							

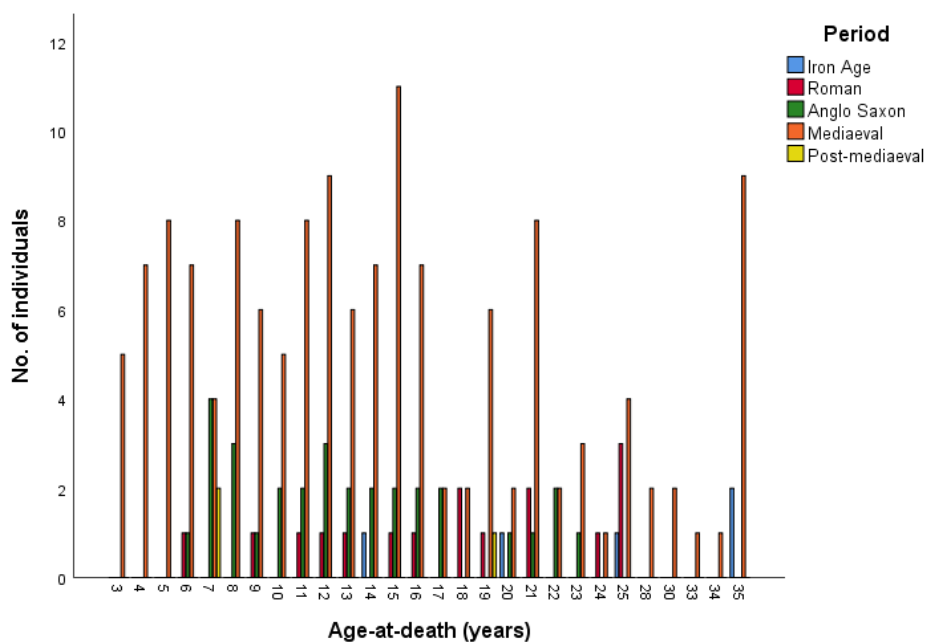
### A9. 5. The Scapula

The table below shows the fusion stages for the fusion of the **coracoid** to the scapula. Max. age Stage 1 refers to the oldest individual or individuals in the samples who had an unfused coracoid. Min-max age Stage 2 refers to the youngest and oldest individuals for which fusion was underway. Min. age Stage 3 refers to the minimum age of the youngest individual or individuals in those samples who were found to have a fused coracoid to the body of the scapula.

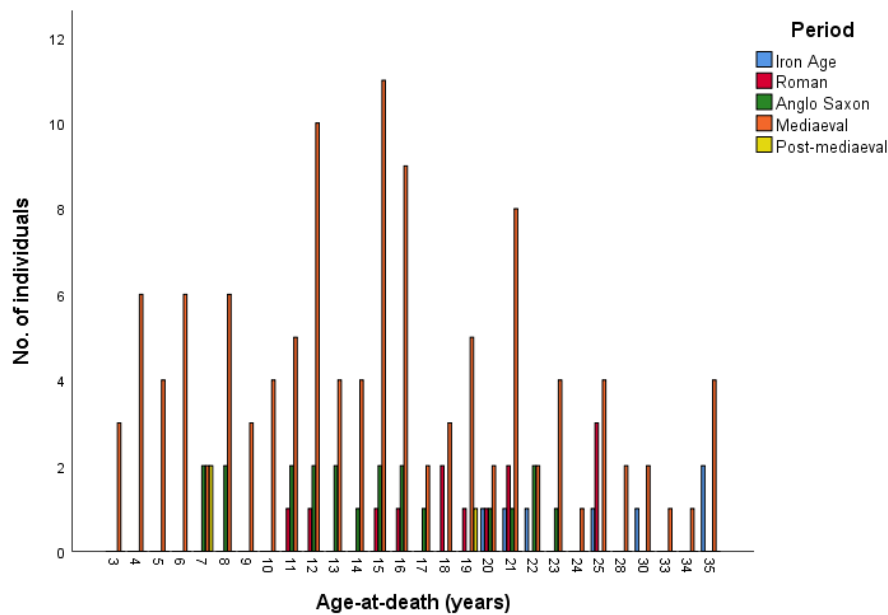
Period	Stage 1 (unfused)	Period	Stage 1 (unfused)	Period	Stage 1 (unfused)
Iron Age	South Dumpton Down Broadstairs Max. age 14*	Anglo-Saxon	The Black Gate cemetery Newcastle-upon-Tyne Max. age 16  Butler's Field cemetery Lechlade 17  Apple Down cemetery Up Marden 15*	Post-Medieval	
			Stage 3 (fused) The Black Gate cemetery Newcastle-upon-Tyne Min. age 17		Stage 3 (fused) Auldham East Lothian Min. age 19*
Period	Stage 1 (unfused)	Period	Stage 1 (unfused)	Period	Stage 1 (unfused)
Roman	Bath Gate Cemetery Cirencester Max. age 15	Medieval	Low-status Canterbury Max. age 15  High-status Canterbury 15  All Saint's chu York 16  Fishergate House York 16  Abbey of St Mary Cirencester 14*  Auldham East Lothian 15*		
			Stage 2 (fusing) Low-status Canterbury Min.- Max. age 16		
			Stage 3 (fused) Low-status Canterbury Min. age 16		Stage 3 (fused) Fishergate House York 16  Auldham East Lothian 19*

\* Large gaps in data between ages

The figure below shows the age distribution of individuals from different time periods for the fusion of the **coracoid** to the body of the scapula. This shows the entire sub-sample that had these bones present.



The figure below shows the age distribution of individuals from different time periods for the fusion of the **acromial epiphysis** to the scapula. This shows the entire sub-sample that had these bones present.



The table below shows the fusion stages for the fusion of the **acromial epiphysis** to the scapula. Max. age Stage 1 refers to the oldest individual or individuals in the samples who had an unfused acromial epiphysis. Min. age Stage 3 refers to the minimum age of the youngest individual or individuals in those samples who were found to have a fused acromial epiphysis to the scapula.

Period	Stage 1 (unfused)			Period	Stage 1 (unfused)				
Roman	Bath Gate Cemetery	Former Bridges Garage		Mediaeval	Low-status	High-status	All Saint's church	Fishergate House	Abbey of St Mary
	Cirencester	Cirencester			Canterbury	Canterbury	York	York	Cirencester
	Max. age				Max. age		15	18*	16*
	Stage 3 (fused)				Stage 3 (fused)				
	Bath Gate Cemetery	Former Bridges Garage			Low-status	High-status			Auldham
	Cirencester	Cirencester			Canterbury	Canterbury			East Lothian
	Min. age				Min. age				
	21*	20			17	18*			19*
Period	Stage 1 (unfused)			Period	Stage 1 (unfused)				
Anglo-Saxon	The Black Gate cemetery	Butler's Field cemetery	Apple Down cemetery	Post-Mediaeval	Auldham				
	Newcastle-upon-Tyne	Lechlade	Up Marden		East Lothian				
	Max. age				Max. age				
	16*	17*	20		19*				
	Stage 3 (fused)								
			Apple Down cemetery	Auldham					
			Up Marden	East Lothian					
			22	21*					

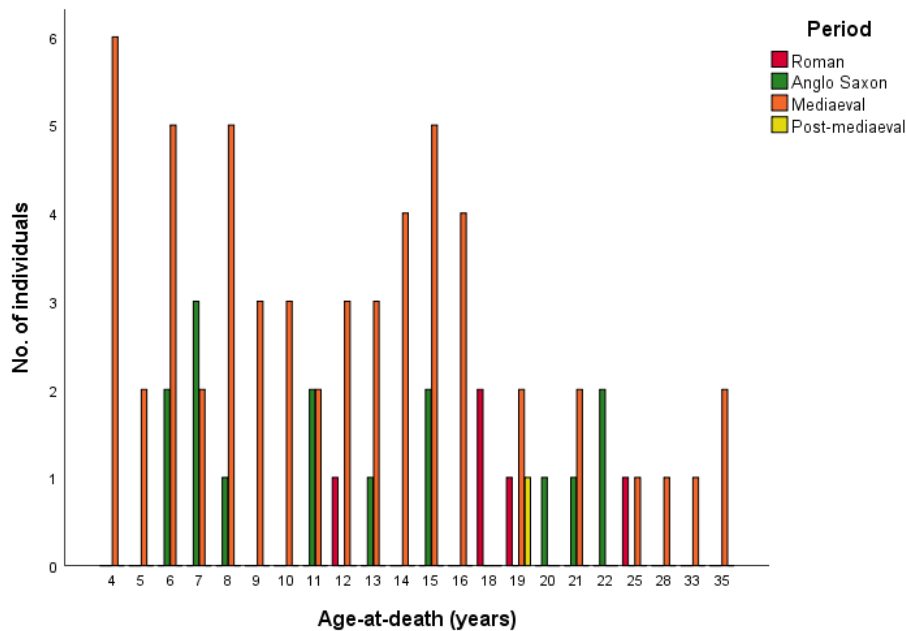
\* Large gaps in data between ages

The table below shows the fusion stages for the fusion of the **medial border** of the scapula. Max. age Stage 1 refers to the oldest individual or individuals in the samples who had an unfused medial border. Min. age Stage 3 refers to the minimum age of the youngest individual or individuals in those samples who were found to have a fused medial border of the scapula.

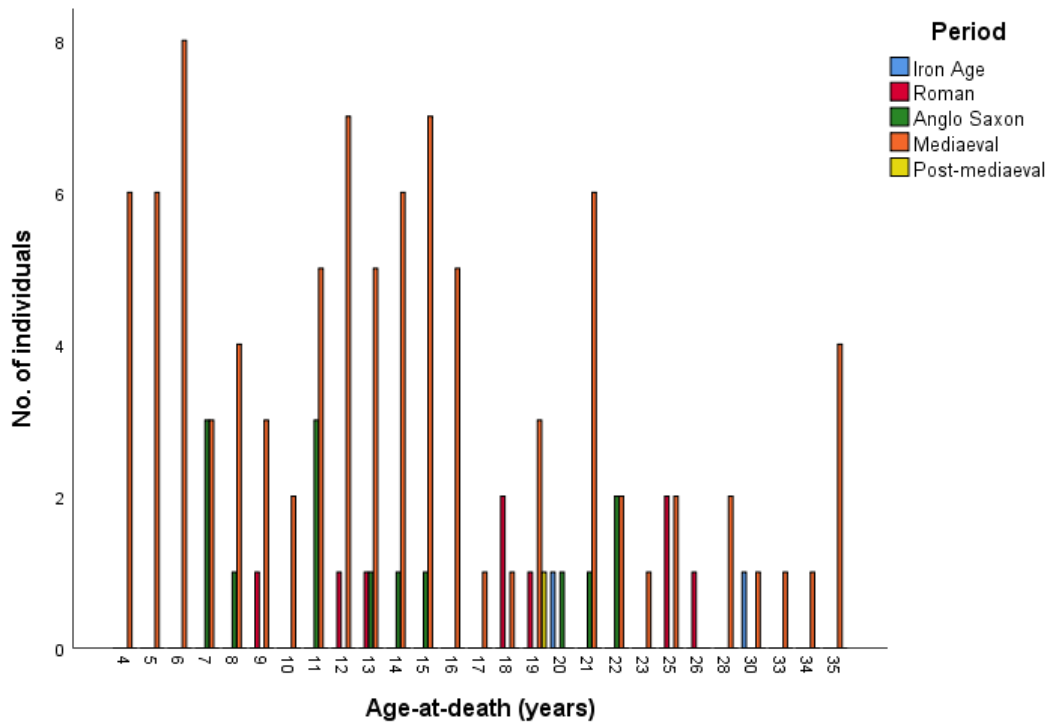
Period	Stage 1 (unfused)	Period	Stage 1 (unfused)
Roman	Former Bridges Garage Cirencester	Mediaeval	Low-status Canterbury High-status Canterbury Fishergate House York
	Max. age 19*		Max. age 21      15*      16*
	<b>Stage 3 (fused)</b> Bath Gate Cemetery Cirencester		<b>Stage 3 (fused)</b> Low-status Canterbury Auldhame East Lothian
	Min. age 25*		Min. age 19      19*
Period	Stage 1 (unfused)	Period	Stage 1 (unfused)
Anglo-Saxon	Apple Down cemetery Up Marden	Post-Mediaeval	Auldhame East Lothian
	Max. age 20*		Max. age 19*
	<b>Stage 3 (fused)</b> Apple Down cemetery Up Marden		Auldhame East Lothian
	Min. age 22*		Min. age 21*

\* Large gaps in data between ages

The figure below shows the age distribution of individuals from different time periods for the fusion of the **medial border** to the scapula. This shows the entire sub-sample that had these bones present.



The figure below shows the age distribution of individuals from different time periods for the fusion of the **inferior angle epiphysis** to the scapula. This shows the entire sub-sample that had these bones present.



The table below shows the fusion stages for the fusion of the **inferior angle epiphysis** of the scapula. Max. age Stage 1 refers to the oldest individual or individuals in the samples who had an unfused inferior angle epiphysis. Min. age Stage 3 refers to the minimum age of the youngest individual or individuals in those samples who were found to have a fused inferior angle epiphysis of the scapula.

Period	Stage 1 (unfused)	Period	Stage 1 (unfused)	Period	Stage 1 (unfused)
Iron Age		Anglo-Saxon	Apple Down cemetery Up Marden Max. age 20*	Post-Mediaeval	Auldhame East Lothian Max. age 19*
	<b>Stage 3 (fused)</b> South Dumpton Down Broadtairs Min. age 20*		<b>Stage 3 (fused)</b> Apple Down cemetery Up Marden Min. age 22*		
Period	Stage 1 (unfused)	Period	Stage 1 (unfused)	Period	Stage 1 (unfused)
Roman	Bath Gate Cemetery Cirencester Max. age 18*	Mediaeval	Low-status Canterbury Max. age 21	High-status Canterbury 15	Fishergate House York 16* Auldhame East Lothian 15
			<b>Stage 3 (fused)</b> Low-status Canterbury Min. age 19		<b>Stage 3 (fused)</b> High-status Canterbury 18 Auldhame East Lothian 19

\* Large gaps in data between ages

Age at death/phase for the fusion of the scapula, including the (1) coracoid and the (2) acromial epiphysis for the skeletal samples collated by archaeological period. Frequencies are recorded as percentages.

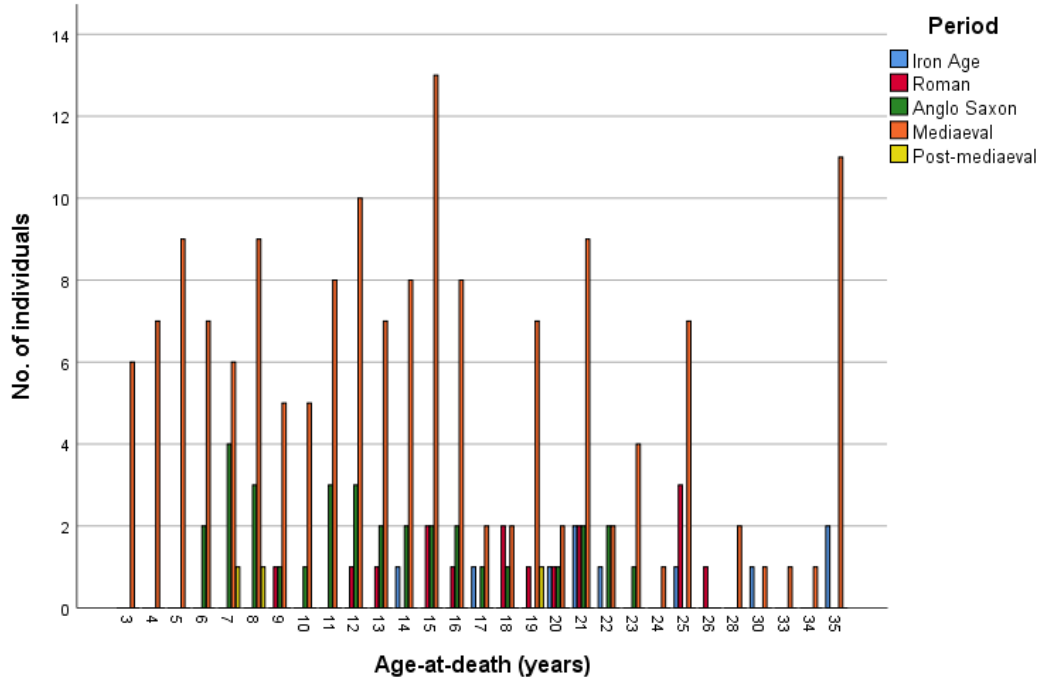
		Roman			Anglo-Saxon						
		Stage of union			Stage of union						
	Age	<i>n</i>	1	2	3	Age	<i>n</i>	1	2	3	
Coracoid	13	1	100.0	-	-	13	2	100.0	-	-	
	15	1	100.0	-	-	14	2	100.0	-	-	
	16	1	100.0	-	-	15	2	100.0	-	-	
	18	2	-	-	100.0	16	2	100.0	-	-	
	19	1	-	-	100.0	17	2	50.0	-	50.0	
			Mediaeval								
			Stage of union								
		Age	<i>n</i>	1	2	3					
		13	6	100.0	-	-					
		14	7	100.0	-	-					
	15	11	100.0	-	-						
	16	7	28.6	14.3	57.1						
	17	2	-	-	100.0						
	18	2	-	-	100.0						
	19	6	-	-	100.0						
The scapula			Roman			Anglo-Saxon					
			Stage of union			Stage of union					
		Age	<i>n</i>	1	2	3	Age	<i>n</i>	1	2	3
		15	1	100.0	-	-	14	1	100.0	-	-
		16	1	100.0	-	-	15	2	100.0	-	-
		18	2	100.0	-	-	16	2	100.0	-	-
		19	1	100.0	-	-	17	1	100.0	-	-
		20	1	-	-	100.0	20	1	100.0	-	-
		21	2	-	-	100.0	21	1	-	-	100.0
			Mediaeval								
		Stage of union									
	Age	<i>n</i>	1	2	3						
	14	4	100.0	-	-						
	15	11	100.0	-	-						
	16	9	100.0	-	-						
	17	2	50.0	-	50.0						
	18	3	66.7	-	33.3						
	19	5	-	-	100.0						
	20	2	-	-	100.0						
	21	8	-	-	100.0						

Age at death/ phase for the fusion of the scapula, including the (1) medial border and the (2) inferior angle for the skeletal samples collated by archaeological period. Frequencies are recorded as percentages.

		Roman				Anglo-Saxon				
		Stage of union				Stage of union				
	Age	<i>n</i>	1	3	Age	<i>n</i>	1	3		
Medial border	18	2	100.0	-	15	2	100.0	-		
	19	1	100.0	-	20	1	100.0	-		
	25	1	-	100.0	21	1	100.0	-		
					22	2	-	100.0		
			Mediaeval							
			Stage of union							
		Age	<i>n</i>	1	3					
		15	5	100.0	-					
		16	4	100.0	-					
		19	2	-	100.0					
	21	2	50.0	50.0						
	25	1	-	100.0						
The scapula			Roman				Anglo-Saxon			
			Stage of union				Stage of union			
		Age	<i>n</i>	1	3	Age	<i>n</i>	1	3	
		18	2	100.0	-	15	1	100.0	-	
		19	1	100.0	-	20	1	100.0	-	
						21	1	100.0	-	
						22	2	-	100.0	
			Mediaeval							
			Stage of union							
		Age	<i>n</i>	1	3					
	15	7	100.0	-						
	16	5	100.0	-						
	17	1	100.0	-						
	18	1	-	100.0						
	19	3	33.3	66.7						
	21	6	50.0	50.0						
	22	2	-	100.0						
	23	1	-	100.0						

### A9. 6. The Humerus

The figure below shows the age distribution of individuals from different time periods for the fusion of the **medial epicondyle** to the shaft of the humerus. This shows the entire sub-sample that had these bones present.



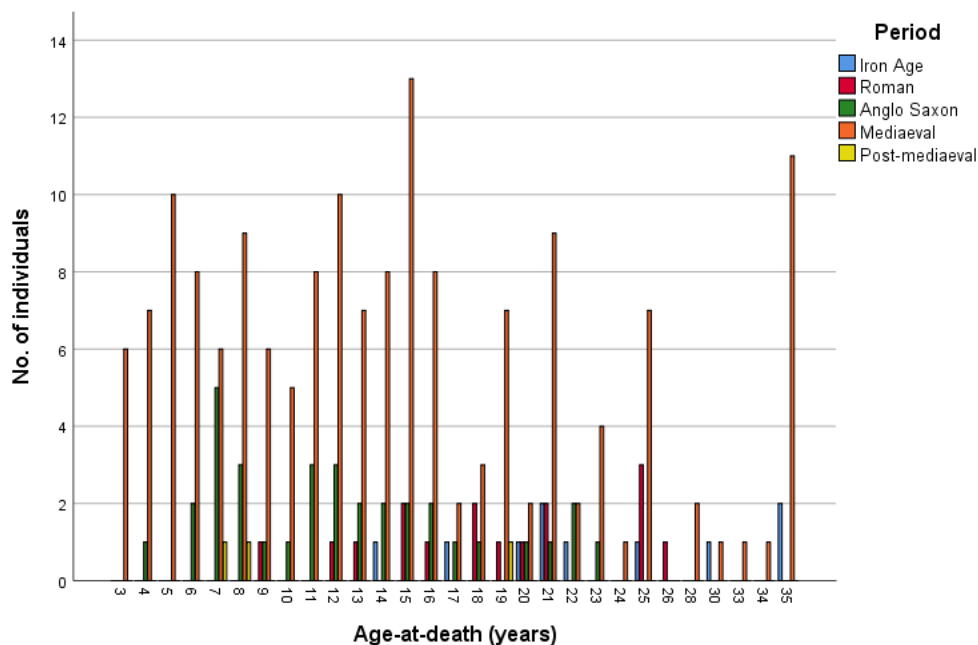


The table below shows the fusion stages for the fusion of the **distal composite epiphysis** to the shaft of the humerus. Max. age Stage 1 refers to the oldest individual or individuals in the samples who had an unfused distal composite epiphysis. Min-max age Stage 2 refers to the youngest and oldest individuals for which fusion was underway. Min. age Stage 3 refers to the minimum age of the youngest individual or individuals in those samples who were found to have a fused distal composite epiphysis to the shaft of the humerus.

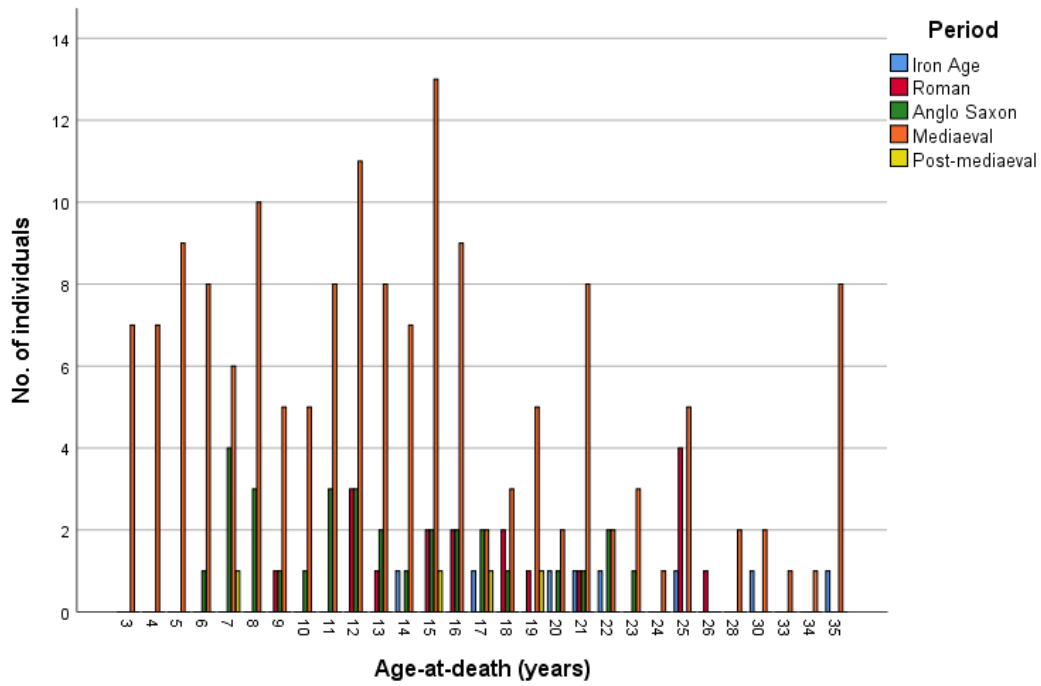
Period	Stage 1 (unfused)	Period	Stage 1 (unfused)	Period	Stage 1 (unfused)
Iron Age	South Dumpton Down Broadstairs Max. age 14*	Anglo-Saxon	The Black Gate cemetery Newcastle-upon-Tyne Max. age 16	Butler's Field cemetery Lechlade 14	Apple Down cemetery Up Marden 15
			<b>Stage 2 (fusing)</b>		
			The Black Gate cemetery Newcastle-upon-Tyne Min.- Max. age 18	Butler's Field cemetery Lechlade 14	Apple Down cemetery Up Marden 15
			<b>Stage 3 (fused)</b>		
	South Dumpton Down Broadstairs Min. age 17*			Butler's Field cemetery Lechlade 17	Apple Down cemetery Up Marden 20
					<b>Stage 3 (fused)</b> Auldhame East Lothian Min. age 19*
Period	Stage 1 (unfused)	Period	Stage 1 (unfused)	Period	Stage 1 (unfused)
Roman	Bath Gate Cemetery Cirencester Max. age 15*	Mediaeval	Low-status Canterbury Max. age 15	High-status Canterbury 15	All Saint's church York 16
					Fishergate House York 14
					Auldhame East Lothian 15
			<b>Stage 2 (fusing)</b>		
			Low-status Canterbury Min.- Max. age 15		Abbey of St Mary Cirencester 14
			<b>Stage 3 (fused)</b>		
	Bath Gate Cemetery Cirencester Min. age 18*	St James' Place Cirencester 16*	Low-status Canterbury Min. age 14	High-status Canterbury 18	All Saint's church York 16
					Fishergate House York 15
					Abbey of St Mary Cirencester 14
					Auldhame East Lothian 19

\* Large gaps in data between ages

The figure below shows the age distribution of individuals from different time periods for the fusion of the **distal composite epiphysis** to the shaft of the humerus. This shows the entire sub-sample that had these bones present.



The figure below shows the age distribution of individuals from different time periods for the fusion of the **proximal epiphysis** to the shaft of the humerus. This shows the entire sub-sample that had these bones present.



The table below shows the fusion stages for the fusion of the **proximal epiphysis** to the shaft of the humerus. Max. age Stage 1 refers to the oldest individual or individuals in the samples who had an unfused proximal epiphysis. Min-max age Stage 2 refers to the youngest and oldest individuals for which fusion was underway. Min. age Stage 3 refers to the minimum age of the youngest individual or individuals in those samples who were found to have a fused proximal epiphysis to the shaft of the humerus.

Period	Stage 1 (unfused)			Period	Stage 1 (unfused)			Period	Stage 1 (unfused)		
Iron Age	South Dumpton Down Broadstairs Max. age 17			Anglo-Saxon	The Black Gate cemetery Newcastle-upon-Tyne Max. age 18*	Butler's Field cemetery Lechlade 14	Apple Down cemetery Up Marden 20	Post-Medieval	Carver Street Sheffield Max. age 17*	Auldham East Lothian 19*	
	<b>Stage 2 (fusing)</b>				<b>Stage 2 (fusing)</b>						
	South Dumpton Down Broadstairs Min.- Max. age 22				Min.- Max. age	Butler's Field cemetery Lechlade 17	Auldham East Lothian 21*				
	<b>Stage 3 (fused)</b>				<b>Stage 3 (fused)</b>						
					Min. age	Butler's Field cemetery Lechlade 23	Apple Down cemetery Up Marden 22				
Period	Stage 1 (unfused)			Period	Stage 1 (unfused)						
Roman	Bath Gate Cemetery Cirencester Max. age 18	Former Bridges Garage Cirencester 19	St James' Place Cirencester 16*	Mediaeval	Low-status Canterbury Max. age 19	High-status Canterbury 15	All Saint's church York 18*	Fishergate House York 16*	Auldham East Lothian 19		
	<b>Stage 2 (fusing)</b>				<b>Stage 2 (fusing)</b>						
					Low-status Canterbury Min.- Max. age 19-21	High-status Canterbury 18					
	<b>Stage 3 (fused)</b>				<b>Stage 3 (fused)</b>						
	Min. age 21				Low-status Canterbury Min. age 17	High-status Canterbury 19	Abbey of St Mary Cirencester 14*	Auldham East Lothian 21			

\* Large gaps in data between ages

Age at death/phase for the fusion of the humerus, including the (1) medial epicondyle and the (2) distal composite epiphysis for the skeletal samples collated by archaeological period. Frequencies are recorded as percentages.

		Iron Age			Roman					Anglo-Saxon							
		Stage of union			Stage of union					Stage of union							
	Age	n	1	2	3	Age	n	1	2	3	Age	n	1	2	3		
The humerus	Medial epicondyle	14	1	100.0	-	-	13	1	100.0	-	-	13	2	100.0	-	-	
		17	1	100.0	-	-	15	2	100.0	-	-	14	2	100.0	-	-	
		20	1	-	-	100.0	16	1	100.0	-	-	15	2	100.0	-	-	
							18	2	50.0	-	50.0	16	2	100.0	-	-	
							19	1	-	-	100.0	17	1	100.0	-	-	
							20	1	-	-	100.0	18	1	-	100.0	-	
												20	1	-	-	100.0	
		Mediaeval															
		Stage of union															
	Age	n	1	2	3												
	13	7	100.0	-	-												
	14	8	100.0	-	-												
	15	13	100.0	-	-												
	16	8	62.5	12.5	25.0												
	17	2	-	-	100.0												
	18	2	-	50.0	50.0												
	19	7	-	-	100.0												
	20	2	-	-	100.0												
		Iron age			Roman					Anglo-Saxon							
		Stage of union			Stage of union					Stage of union							
	Age	n	1	2	3	Age	n	1	2	3	Age	n	1	2	3		
The humerus	Distal composite epiphysis	14	1	100.0	-	-	12	1	100.0	-	-	11	3	100.0	-	-	
		17	1	-	-	100.0	13	1	100.0	-	-	12	3	100.0	-	-	
							15	2	100.0	-	-	13	2	100.0	-	-	
							16	1	-	-	100.0	14	2	50.0	50.0	-	
							18	2	-	-	100.0	15	2	50.0	50.0	-	
												16	2	100.0	-	-	
												17	1	-	-	100.0	
												18	1	-	100.0	-	
		Mediaeval															
		Stage of union															
	Age	n	1	2	3												
	11	8	100.0	-	-												
	12	10	100.0	-	-												
	13	7	100.0	-	-												
	14	8	62.5	12.5	25.0												
	15	13	46.2	7.7	46.2												
	16	8	12.5	-	87.5												
	17	2	-	-	100.0												
	18	3	-	-	100.0												

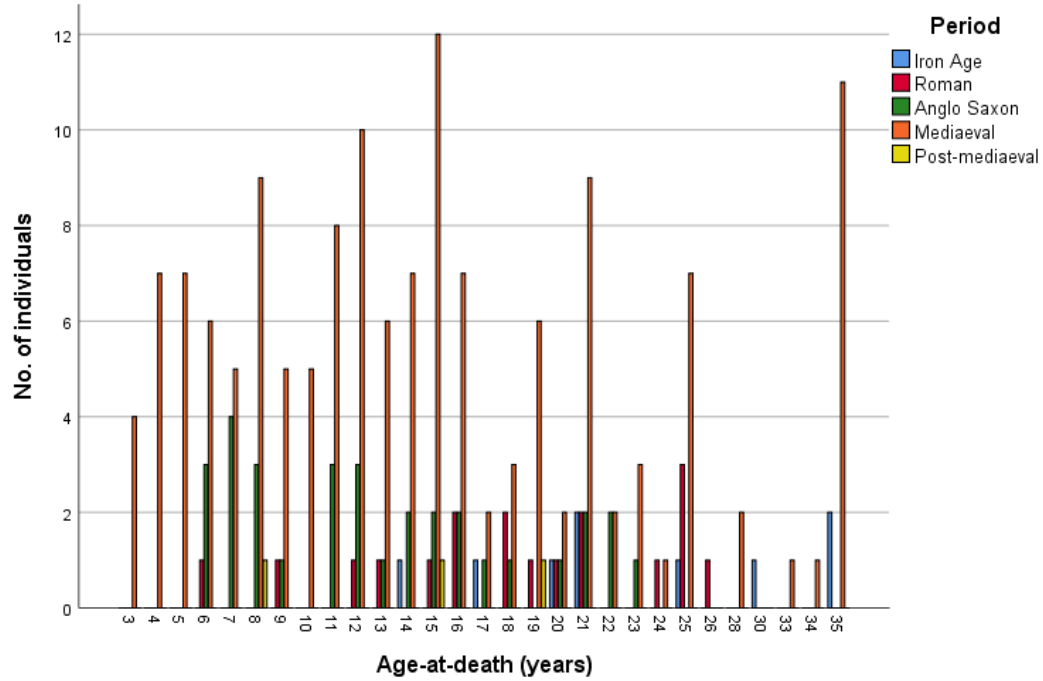
Age at death/ phase for the fusion of the proximal epiphysis of the humerus for the skeletal samples collated by archaeological period. Frequencies are recorded as percentages.

		<b>Iron Age</b>			<b>Roman</b>				<b>Anglo-Saxon</b>					
		<b>Stage of union</b>			<b>Stage of union</b>				<b>Stage of union</b>					
<b>Age</b>	<b>n</b>	<b>1</b>	<b>2</b>	<b>3</b>	<b>Age</b>	<b>n</b>	<b>1</b>	<b>2</b>	<b>3</b>	<b>Age</b>	<b>n</b>	<b>1</b>	<b>2</b>	<b>3</b>
14	1	100.0	-	-	15	2	100.0	-	-	14	1	100.0	-	-
17	1	100.0	-	-	16	2	100.0	-	-	15	2	100.0	-	-
20	1	-	-	100.0	18	2	100.0	-	-	16	2	100.0	-	-
21	1	-	-	100.0	19	1	100.0	-	-	17	2	50.0	50.0	-
22	1	-	100.0	-	21	1	-	-	100.0	18	1	100.0	-	-
										20	1	100.0	-	-
										21	1	-	100.0	-
										22	2	-	-	100.0
										23	1	-	-	100.0
		<b>Mediaeval</b>			<b>Post-Mediaeval</b>									
		<b>Stage of union</b>			<b>Stage of union</b>									
<b>Age</b>	<b>n</b>	<b>1</b>	<b>2</b>	<b>3</b>	<b>Age</b>	<b>n</b>	<b>1</b>	<b>2</b>	<b>3</b>					
15	13	100.0	-	-	15	1	100.0	-	-					
16	9	100.0	-	-	17	1	100.0	-	-					
17	2	50.0	-	50.0	19	1	100.0	-	-					
18	3	66.7	33.3	-										
19	5	40.0	20.0	40.0										
20	2	-	50.0	50.0										
21	8	-	25.0	75.0										
22	2	-	-	100.0										
23	3	-	-	100.0										
24	1	-	-	100.0										

The humerus  
Proximal epiphysis

### A9. 7. The Radius

The figure below shows the age distribution of individuals from different time periods for the fusion of the **proximal epiphysis** to the radius. This shows the entire sub-sample that had these bones present.



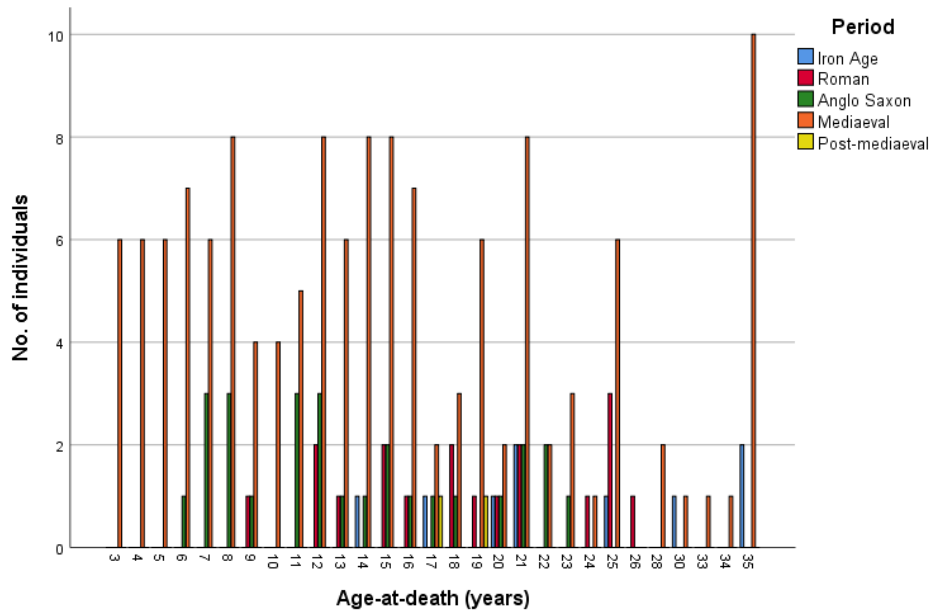


The table below shows the fusion stages for the fusion of the **distal epiphysis** to the radius. Max. age Stage 1 refers to the oldest individual or individuals in the samples who had an unfused distal epiphysis. Min-max age Stage 2 refers to the youngest and oldest individuals for which fusion was underway. Min. age Stage 3 refers to the minimum age of the youngest individual or individuals in those samples who were found to have a fused distal epiphysis to the radius.

Period	Stage 1 (unfused)		Period	Stage 1 (unfused)				Period	Stage 1 (unfused)	
Iron Age	South Dumpton Down		Anglo-Saxon	The Black Gate cemetery	Butler's Field cemetery	Auldhame	Apple Down cemetery	Post-Mediaeval	Carver Street	Auldhame
	Broadstairs			Newcastle-upon-Tyne	Lechlade	East Lothian	Up Marden		Sheffield	East Lothian
	Max. age			Max. age		Max. age			Max. age	
	17			18*	17*	21*	20*		17*	19*
	<b>Stage 2 (fusing)</b>			<b>Stage 2 (fusing)</b>						
	South Dumpton Down									
	Broadstairs									
	Min.-Max. age			Min.-Max. age						
	21								21*	
	<b>Stage 3 (fused)</b>			<b>Stage 3 (fused)</b>						
	South Dumpton Down									
	Broadstairs			Butler's Field cemetery		Apple Down cemetery				
	Min. age			Lechlade		Up Marden				
	20			23*		22*				
Period	Stage 1 (unfused)			Period	Stage 1 (unfused)					
Roman	Bath Gate Cemetery	Former Bridges Garage		Mediaeval	Low-status	High-status	All Saint's church	Fisergate House	Abbey of St Mary	Auldhame
	Cirencester	Cirencester			Canterbury	Canterbury	York	York	Cirencester	East Lothian
	Max. age				Max. age		Max. age		Max. age	
	18*	19*		21	15*	18*	16*	14*	19*	
	<b>Stage 2 (fusing)</b>				<b>Stage 2 (fusing)</b>					
					Low-status	High-status				
					Canterbury	Canterbury				
					Min.-Max. age					
					19-21		18			
	<b>Stage 3 (fused)</b>				<b>Stage 3 (fused)</b>					
	Bath Gate Cemetery	Former Bridges Garage	St James' Place		Low-status	High-status			Auldhame	
	Cirencester	Cirencester	Cirencester		Canterbury	Canterbury			East Lothian	
	Min. age				Min. age					
	21*	20*	24*		17	19			21*	

\* Large gaps in data between ages

The figure below shows the age distribution of individuals from different time periods for the fusion of the **distal epiphysis** to the radius. This shows the entire sub-sample that had these bones present.

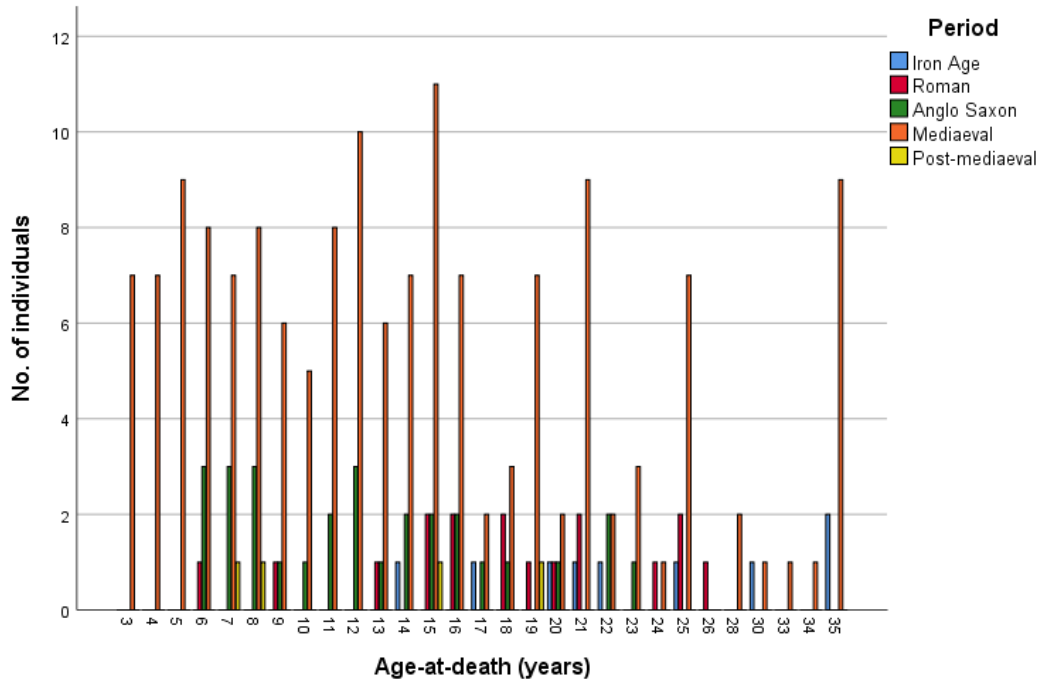


Age at death/phase for the fusion of the radius, including the (1) proximal and (2) distal epiphyses for the skeletal samples collated by archaeological period. Frequencies are recorded as percentages.

		Iron Age			Roman					Anglo-Saxon						
		Stage of union			Stage of union					Stage of union						
		Age	<i>n</i>	1	2	3	Age	<i>n</i>	1	2	3	Age	<i>n</i>	1	2	3
Proximal epiphysis		14	1	100.0	-	-	12	1	100.0	-	-	12	3	100.0	-	-
		17	1	-	100.0	-	13	1	100.0	-	-	13	1	100.0	-	-
		20	1	-	-	100.0	15	1	100.0	-	-	14	2	50.0	50.0	-
							16	2	100.0	-	-	15	2	100.0	-	-
							18	2	-	50.0	50.0	16	2	100.0	-	-
							19	1	-	-	100.0	17	1	100.0	-	-
												18	1	100.0	-	-
												20	1	-	-	100.0
												21	2	-	50.0	50.0
												22	2	-	-	100.0
The radius																
Distal epiphysis																

### A9. 8. The Ulna

The figure below shows the age distribution of individuals from different time periods for the fusion of the **proximal epiphysis** of the ulna. This shows the entire sub-sample that had these bones present.



The table below shows the fusion stages for the fusion of the **proximal epiphysis** of the ulna. Max. age Stage 1 refers to the oldest individual or individuals in the samples who had an unfused proximal epiphysis. Min-max age Stage 2 refers to the youngest and oldest individuals for which fusion was underway. Min. age Stage 3 refers to the minimum age of the youngest individual or individuals in those samples who were found to have a fused proximal epiphysis of the ulna.

Period	Stage 1 (unfused)	Period	Stage 1 (unfused)	Period	Stage 1 (unfused)				
Iron Age	South Dumpton Down Broadstairs Max. age 14*	Anglo-Saxon	The Black Gate cemetery Newcastle-upon-Tyne Max. age 18*	Butler's Field cemetery Lechlade 14	Apple Down cemetery Up Marden 12*				
	Stage 2 (fusing)		Stage 2 (fusing)	Butler's Field cemetery Lechlade 14-17	Apple Down cemetery Up Marden 15*				
Roman	Bath Gate Cemetery Cirencester Max. age 16	Mediaeval	Low-status Canterbury Max. age 16	High-status Canterbury 15	All Saint's church York 16*	Fishergate House York 14	Auldham East Lothian 15*	Post-Mediaeval	
	Stage 2 (fusing)		Stage 2 (fusing)	Low-status Canterbury Min.-Max. age 14-15	High-status Canterbury 18	All Saint's church York 16*	Fishergate House York 15-16	Abbey of St Mary Cirencester 14*	Stage 3 (fused)
	Bath Gate Cemetery Cirencester Min.-Max. age 18		Former Bridges Garage Cirencester 19*	Low-status Canterbury Min. age 16	High-status Canterbury 18	All Saint's church York 18*	Fishergate House York 16	Auldham East Lothian 19*	Carver Street Sheffield Min. age 15*

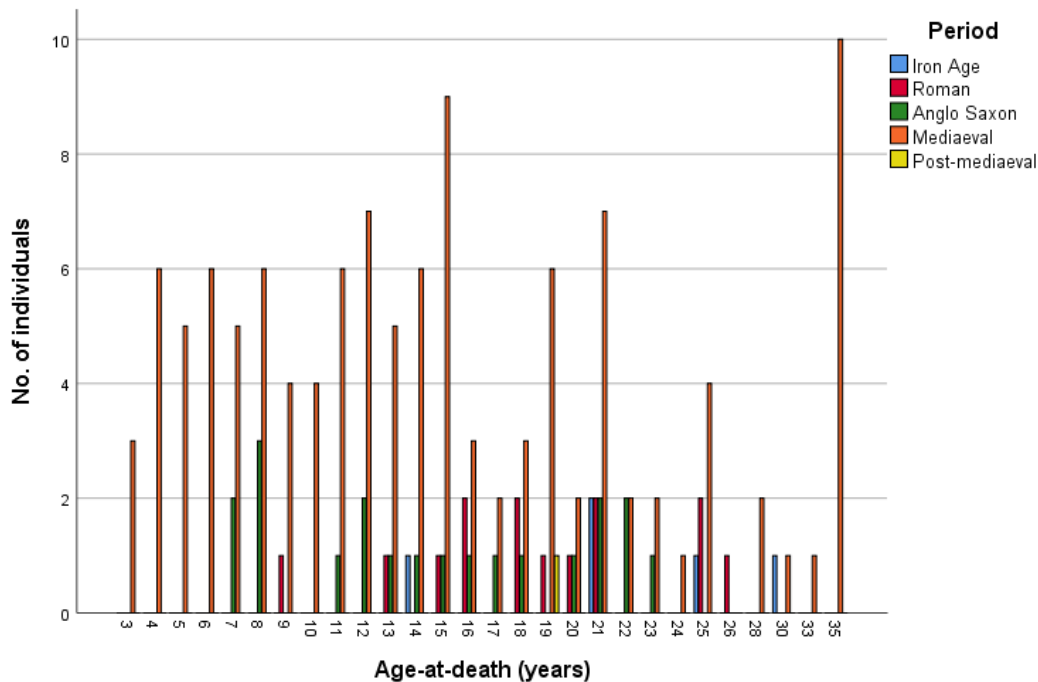
\* Large gaps in data between ages

The table below shows the fusion stages for the fusion of the **distal epiphysis** of the ulna. Max. age Stage 1 refers to the oldest individual or individuals in the samples who had an unfused distal epiphysis. Min-max age Stage 2 refers to the youngest and oldest individuals for which fusion was underway. Min. age Stage 3 refers to the minimum age of the youngest individual or individuals in those samples who were found to have a fused distal epiphysis of the ulna.

Period	Stage 1 (unfused)	Period	Stage 1 (unfused)	Period	Stage 1 (unfused)
Iron Age	South Dumpton Down Broadstairs Max. age 14*	Anglo-Saxon	The Black Gate cemetery Newcastle-upon-Tyne Max. age 18*	Butler's Field cemetery Lechlade Max. age 17*	Auldham East Lothian Max. age 21*
				Apple Down cemetery Up Marden Max. age 20	Post-Mediaeval Auldham East Lothian Max. age 19*
	Stage 2 (fusing) South Dumpton Down Broadstairs Min.- Max. age 21*		Stage 2 (fusing)		
			Min.- Max. age	Auldham East Lothian Min.- Max. age 21*	
			Stage 3 (fused)		
			Min. age	Butler's Field cemetery Lechlade Min. age 23*	Apple Down cemetery Up Marden Min. age 22
Roman	Bath Gate Cemetery Cirencester Max. age 18	Former Bridges Garage Cirencester Max. age 19*	St James' Place Cirencester Max. age 16*	Mediaeval	Low-status Canterbury Max. age 21
				High-status Canterbury Max. age 15	All Saint's church York Max. age 18*
					Fisergate House York Max. age 16*
					Abbey of St Mary Cirencester Max. age 14*
					Auldham East Lothian Max. age 19*
	Stage 2 (fusing) Bath Gate Cemetery Cirencester Min.- Max. age 21		Stage 2 (fusing)		
			Min.- Max. age	Low-status Canterbury Min.- Max. age 19	High-status Canterbury Min.- Max. age 18
	Stage 3 (fused)		Stage 3 (fused)		
	Min. age	Former Bridges Garage Cirencester Min. age 20*	Min. age	Low-status Canterbury Min. age 17	High-status Canterbury Min. age 19
					Auldham East Lothian Min. age 21*

\* Large gaps in data between ages

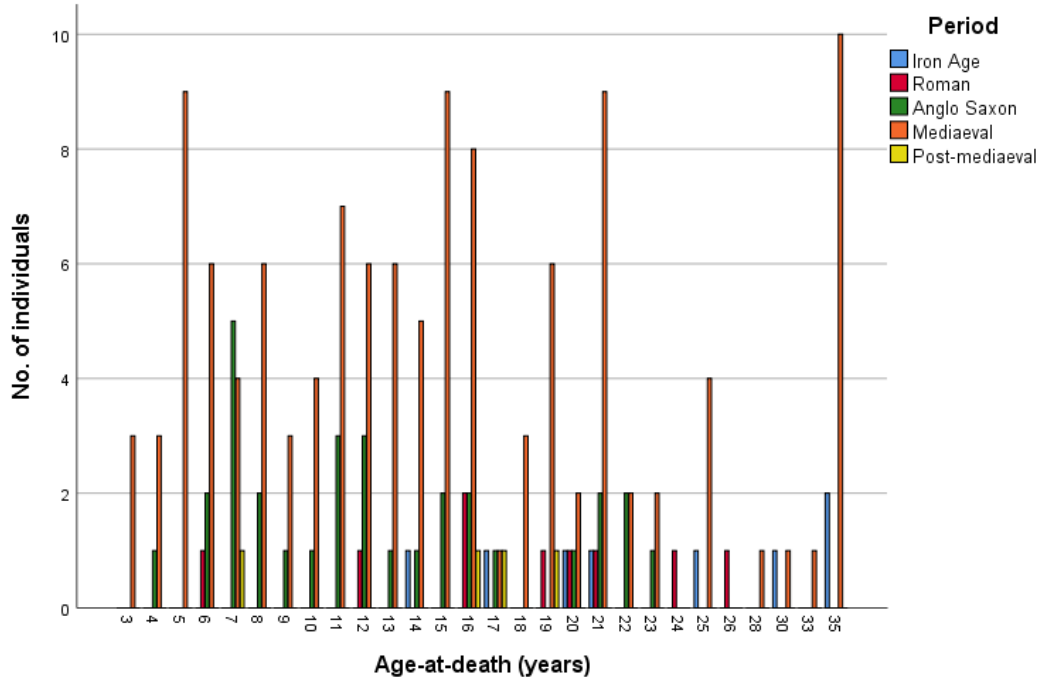
The figure below shows the age distribution of individuals from different time periods for the fusion of the **distal epiphysis** of the ulna. This shows the entire sub-sample that had these bones present.





### A9. 9. The Hand

The figure below shows the age distribution of individuals from different time periods for the fusion of the heads of the **metacarpals 2-5, proximal and middle phalangeal epiphyses** of the hand. This shows the entire sub-sample that had these bones present.



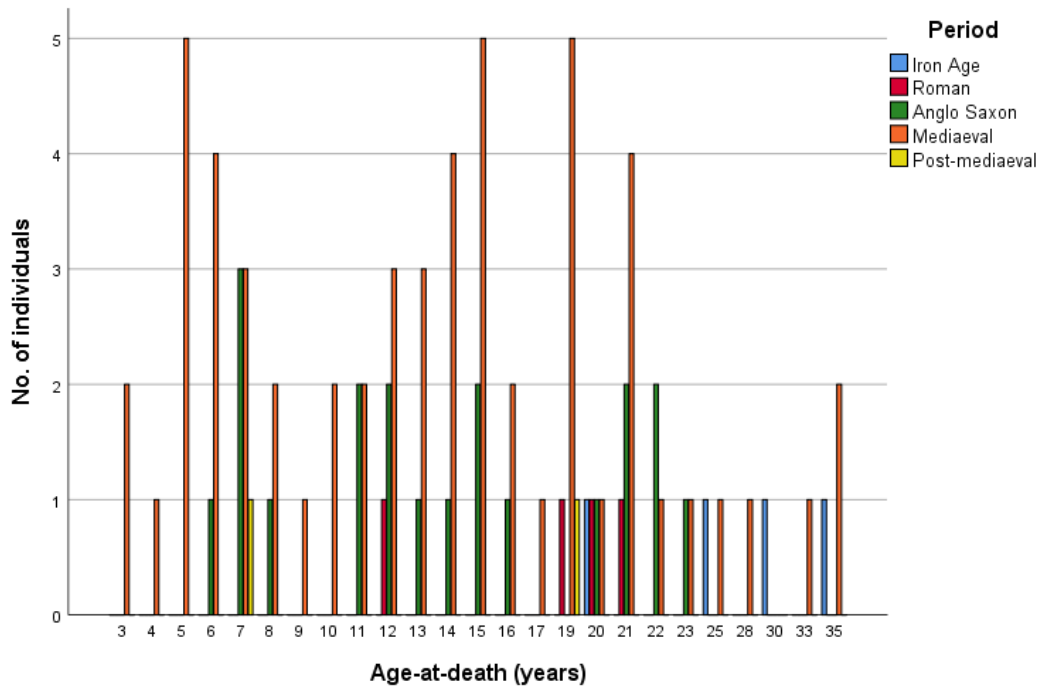
The table below shows the fusion stages for the fusion of the heads of the **metacarpals 2-5, proximal and middle phalangeal epiphyses** of the hand. Max. age Stage 1 refers to the oldest individual or individuals in the samples who had unfused heads of the metacarpals 2-5, proximal and middle phalangeal epiphyses. Min-max age Stage 2 refers to the youngest and oldest individuals for which fusion was underway. Min. age Stage 3 refers to the minimum age of the youngest individual or individuals in those samples who were found to have fused heads of the metacarpals 2-5, proximal and middle phalangeal epiphyses of the hand.

Period	Stage 1 (unfused)			Period	Stage 1 (unfused)						Period	Stage 1 (unfused)
Iron Age	South Dumpton Down Broadstairs			Anglo-Saxon	The Black Gate cemetery Newcastle-upon-Tyne	Butler's Field cemetery Lechlade	Apple Down cemetery Up Marden					
	Max. age				Max. age							
	17				16*	17*	15*					
	Stage 3 (fused)				Stage 3 (fused)							
	South Dumpton Down Broadstairs							Apple Down cemetery Up Marden				
	Min. age											
	20							20*				
Period	Stage 1 (unfused)			Period	Stage 1 (unfused)					Period	Stage 1 (unfused)	
Roman	Bath Gate Cemetery Cirencester	Former Bridges Garage Cirencester	St James' Place Cirencester	Medieval	Low-status Canterbury	High-status Canterbury	All Saint's church York	Fisergate House York	Abbey of St Mary Cirencester	Auldham East Lothian	Post-Medieval	
	Max. age				Max. age							
	16*	19	16*		16	15	18*	16*	14*	15*		
	Stage 2 (fusing)				Stage 2 (fusing)					Stage 2 (fusing)		
	Min.- Max. age				Low-status Canterbury	Min.- Max. age				Carver Street Sheffield		
					12-16					Min.- Max. age 17*		
	Stage 3 (fused)				Stage 3 (fused)					Stage 3 (fused)		
	Former Bridges Garage Cirencester				Low-status Canterbury	High-status Canterbury				Auldham East Lothian	Carver Street Sheffield	Auldham East Lothian
	Min. age				Min. age						Min. age	
	20				17	18				19*	16*	19*

\* Large gaps in data between ages



The figure below shows the age distribution of individuals from different time periods for the fusion of the **distal epiphyses** of the hand. This shows the entire sub-sample that had these bones present.



Age at death/phase for the fusion of the hand, including the (1) heads of the metacarpals 2-5, proximal and middle phalanges and (2) distal phalanges for the skeletal samples collated by archaeological period. Frequencies are recorded as percentages.

		Iron Age			Roman					Anglo-Saxon						
		Stage of union			Stage of union					Stage of union						
		Age	n	1	2	3	Age	n	1	2	3	Age	n	1	2	3
The hand	Heads of metacarpals 2-5, proximal and middle phalanges	14	1	100.0	-	-	12	1	100.0	-	-	9	1	100.0	-	-
		17	1	100.0	-	-	16	2	100.0	-	-	10	1	100.0	-	-
		20	1	-	-	100.0	19	1	100.0	-	-	11	3	100.0	-	-
							20	1	-	-	100.0	12	3	100.0	-	-
												13	1	100.0	-	-
												14	1	100.0	-	-
												15	2	100.0	-	-
												16	2	100.0	-	-
												17	1	100.0	-	-
												20	1	-	-	100.0
												21	2	-	50.0	50.0
												22	2	-	-	100.0
				Mediaeval			Post-Mediaeval									
				Stage of union			Stage of union									
				Age	n	1	2	3	Age	n	1	2	3			
				9	3	100.0	-	-	16	1	-	-	100.0			
				10	4	100.0	-	-	17	1	-	100.0	-			
				11	7	100.0	-	-	19	1	-	-	100.0			
				12	6	83.3	16.7	-								
				13	6	100.0	-	-								
				14	5	100.0	-	-								
				15	9	100.0	-	-								
		16	8	87.5	12.5	-										
		17	1	-	-	100.0										
		18	3	33.3	-	66.7										
		19	6	-	-	100.0										
		20	2	-	-	100.0										
		Roman			Anglo-Saxon					Mediaeval						
		Stage of union			Stage of union					Stage of union						
		Age	n	1	2	3	Age	n	1	2	3	Age	n	1	2	3
Distal phalanges		12	1	100.0	-	-	12	2	100.0	-	-	12	3	100.0	-	-
		19	1	-	-	100.0	13	1	100.0	-	-	13	3	100.0	-	-
		20	1	-	-	100.0	14	1	100.0	-	-	14	4	100.0	-	-
		21	1	-	-	100.0	15	2	100.0	-	-	15	5	100.0	-	-
												16	2	50.0	50.0	-
												17	1	-	-	100.0
												20	1	-	-	100.0
												21	4	-	-	100.0

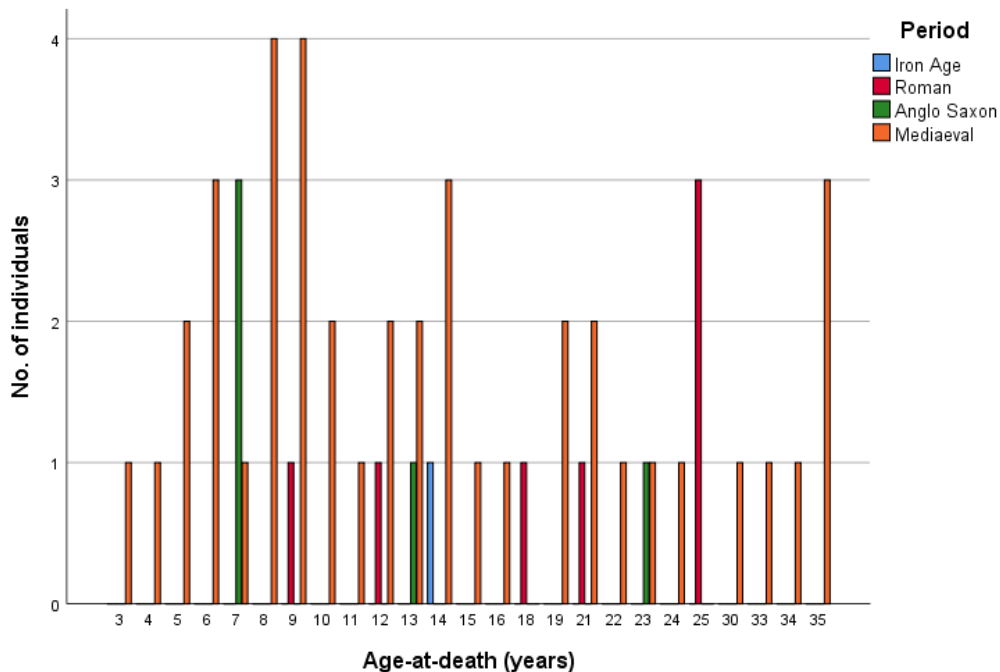
### A9. 10. The Os coxae

The table below shows the fusion stages for the fusion of the **ischiopubic ramus** of the os coxae. Max. age Stage 1 refers to the oldest individual or individuals in the samples who had unfused an ischiopubic ramus. Min. age Stage 3 refers to the minimum age of the youngest individual or individuals in those samples who were found to have a fused ischiopubic ramus of the os coxae.

Period	Stage 1 (unfused)	Period	Stage 1 (unfused)
Iron Age		Anglo-Saxon	The Black Gate cemetery Newcastle-upon-Tyne Max. age 13*
	<b>Stage 3 (fused)</b> South Dumpton Down Broadstairs Min. age 14*		
Period	Stage 1 (unfused)	Period	Stage 1 (unfused)
Roman		Mediaeval	Low-status Canterbury Max. age 14
			All Saint's church York 10*
			Auldhame East Lothian 15*
	<b>Stage 3 (fused)</b> Bath Gate Cemetery Cirencester Min. age 12*		<b>Stage 3 (fused)</b> Low-status Canterbury Min. age 13
			All Saint's church York 13*
			Fishergate House York 9*

\* Large gaps in data between ages

The figure below shows the age distribution of individuals from different time periods for the fusion of the **ischiopubic ramus** of the os coxae. This shows the entire sub-sample that had these bones present.



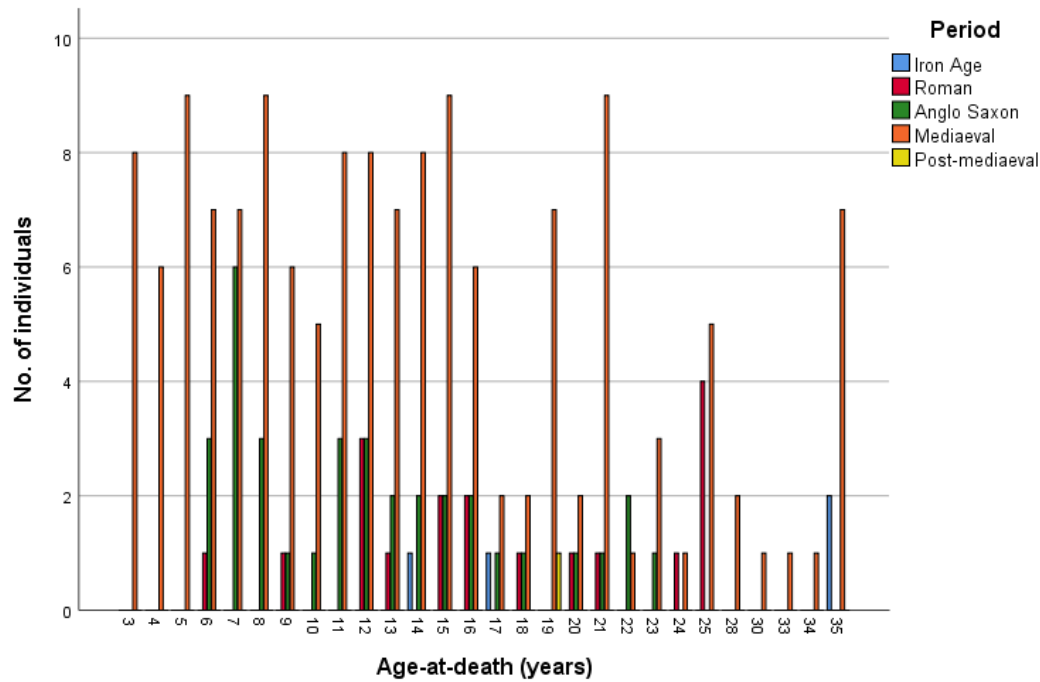


The table below shows the fusion stages for the fusion of the **acetabulum** of the os coxae. Max. age Stage 1 refers to the oldest individual or individuals in the samples who had an unfused acetabulum. Min-max age Stage 2 refers to the youngest and oldest individuals for which fusion was underway. Min. age Stage 3 refers to the minimum age of the youngest individual or individuals in those samples who were found to have a fused acetabulum of the os coxae.

Period	Stage 1 (unfused)			Period	Stage 1 (unfused)						
Iron Age	South Dumps-ton Down			Anglo-Saxon	The Black Gate cemetery	Butler's Field cemetery	Apple Down cemetery				
	Broadstairs				Newcastle-upon-Tyne	Lechlade	Up Marden				
	Max. age				Max. age						
	17*				16*	17*	15*				
					<b>Stage 2 (fusing)</b>						
					The Black Gate cemetery						
					Newcastle-upon-Tyne						
					Min.- Max. age						
					18*						
Period	Stage 1 (unfused)			Period	Stage 1 (unfused)			Period	Stage 1 (unfused)		
Roman	Bath Gate Cemetery	Former Bridges Garage	St James' Place	Mediaeval	Low-status	High-status	All Saint's church	Fishergate House	Abbey of St Mary	Auldham	Post-Mediaeval
	Cirencester	Cirencester	Cirencester		Canterbury	Canterbury	York	York	Cirencester	East Lothian	
	Max. age				Max. age						
	16	12*	16*		15	15	16	14	14*	15*	
					<b>Stage 2 (fusing)</b>						
					Low-status						
					Canterbury						
					Min.- Max. age						
					14-16						
	<b>Stage 3 (fused)</b>				<b>Stage 3 (fused)</b>				<b>Stage 3 (fused)</b>		
	Bath Gate Cemetery				Low-status	High-status	All Saint's church	Fishergate House		Auldham	
	Cirencester				Canterbury	Canterbury	York	York		East Lothian	
	Min. age				Min. age					Min. age	
	18				15	19	16	16		19*	19*

\* Large gaps in data between ages

The figure below shows the age distribution of individuals from different time periods for the fusion of the **acetabulum** of the os coxae. This shows the entire sub-sample that had these bones present.

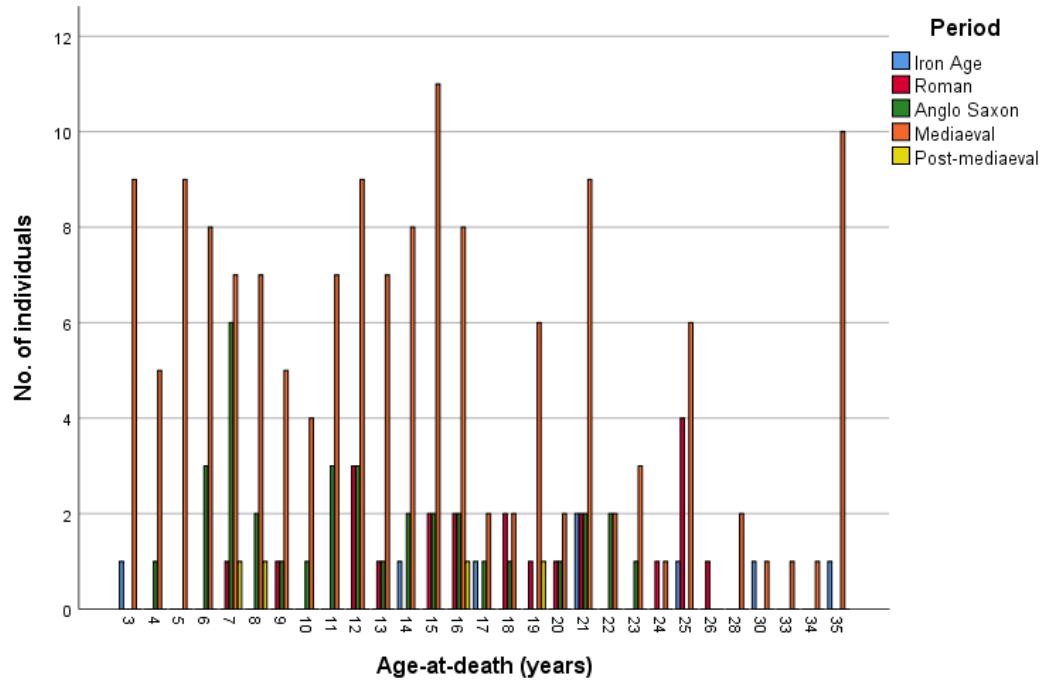


Age at death/phase for the fusion of the os coxae, including the (1) ischiopubic ramus, (2) iliac crest and the (3) acetabulum for the skeletal samples collated by archaeological period. Frequencies are recorded as percentages.

		Roman			Mediaeval										
		Stage of union			Stage of union										
	Age	n	1	2	3	Age	n	1	2	3					
Ischiopubic ramus	9	1	100.0	-	-	9	4	75.0	-	25.0					
	12	1	-	-	100.0	10	2	50.0	-	50.0					
						11	1	100.0	-	-					
						12	2	50.0	-	50.0					
						13	2	-	-	100.0					
		Iron Age			Roman			Anglo-Saxon							
		Stage of union			Stage of union			Stage of union							
	Age	n	1	2	3	Age	n	1	2	3	Age	n	1	2	3
The os coxae	14	1	100.0	-	-	15	2	100.0	-	-	14	2	100.0	-	-
	21	1	-	-	100.0	16	2	100.0	-	-	15	2	100.0	-	-
	25	1	-	-	100.0	18	2	100.0	-	-	16	2	100.0	-	-
						19	1	100.0	-	-	17	1	100.0	-	-
						20	1	-	-	100.0	18	1	100.0	-	-
						21	2	-	100.0	-	20	1	100.0	-	-
						24	1	-	-	100.0	21	2	100.0	-	-
						25	3	-	-	100.0	22	2	-	-	100.0
						26	1	-	-	100.0	23	1	-	100.0	-
			Mediaeval			Post-Mediaeval									
			Stage of union			Stage of union									
		Age	n	1	2	3	Age	n	1	2	3				
Iliac crest	14	8	100.0	-	-	19	1	-	100.0	-					
	15	10	100.0	-	-										
	16	8	100.0	-	-										
	17	2	50.0	50.0	-										
	18	3	33.3	66.7	-										
	19	7	-	71.4	28.6										
	20	2	50.0	-	50.0										
	21	9	11.1	33.3	55.6										
	22	2	-	50.0	50.0										
	23	3	-	33.3	66.7										
	24	1	-	-	100.0										
	25	5	-	-	100.0										
		Iron age			Roman			Anglo-Saxon							
		Stage of union			Stage of union			Stage of union							
	Age	n	1	2	3	Age	n	1	2	3	Age	n	1	2	3
Acetabulum	14	1	100.0	-	-	12	3	100.0	-	-	11	3	100.0	-	-
	17	1	100.0	-	-	13	1	100.0	-	-	12	3	100.0	-	-
						15	2	100.0	-	-	13	2	100.0	-	-
						16	2	100.0	-	-	14	2	100.0	-	-
						18	1	-	-	100.0	15	2	100.0	-	-
											16	2	100.0	-	-
											17	1	100.0	-	-
											18	1	-	100.0	-
											20	1	-	-	100.0
			Mediaeval												
			Stage of union												
		Age	n	1	2	3									
	11	8	100.0	-	-										
	12	8	100.0	-	-										
	13	7	100.0	-	-										
	14	8	87.5	12.5	-										
	15	9	66.7	22.2	11.1										
	16	6	16.7	16.7	66.7										
	17	2	-	-	100.0										
	18	2	-	-	100.0										
	19	7	-	-	100.0										

### A9. 11. The Femur

The figure below shows the age distribution of individuals from different time periods for the fusion of the **femoral head** to the femur. This shows the entire sub-sample that had these bones present.



The table below shows the fusion stages for the fusion of the **femoral head** to the femur. Max. age Stage 1 refers to the oldest individual or individuals in the samples who had an unfused femoral head. Min-max age Stage 2 refers to the youngest and oldest individuals for which fusion was underway. Min. age Stage 3 refers to the minimum age of the youngest individual or individuals in those samples who were found to have a fused femoral head of the femur.

Period	Stage 1 (unfused)			Period	Stage 1 (unfused)			Period	Stage 1 (unfused)	
Iron Age	South Dumpton Down Broadstairs Max. age 17*			Anglo-Saxon	The Black Gate cemetery Newcastle-upon-Tyne Max. age 18*	Butler's Field cemetery Lechlade 17*		Apple Down cemetery Up Marden 15*		Post-Mediaeval
					Stage 2 (fusing)				Stage 2 (fusing)	
								Auldhame East Lothian 21*		Auldhame East Lothian 19*
					Min.- Max. age					Min.- Max. age
	Stage 3 (fused)				Stage 3 (fused)				Stage 3 (fused)	
	South Dumpton Down Broadstairs Min. age 21*							Auldhame East Lothian 21*	Apple Down cemetery Up Marden 20*	Carver street Sheffield Min. age 16*
					Min. age					
Period	Stage 1 (unfused)			Period	Stage 1 (unfused)					
Roman	Bath Gate Cemetery Cirencester Max. age 16	Former Bridges Garage Cirencester 12	St James' Place Cirencester 16*	Mediaeval	Low-status Canterbury Max. age 16	High-status Canterbury 15	All Saint's church York 16	Fishergate House York 16*	Auldhame East Lothian 14*	Abbey of St Mary Cirencester 15*
	Stage 2 (fusing)				Stage 2 (fusing)					
	Bath Gate Cemetery Cirencester Min.- Max. age 18	Former Bridges Garage Cirencester 19			Low-status Canterbury Min.- Max. age 15-19		All Saint's church York 18	Fishergate House York 16*		Abbey of St Mary Cirencester 19*
	Stage 3 (fused)				Stage 3 (fused)					
	Bath Gate Cemetery Cirencester Min. age 21	Former Bridges Garage Cirencester 20			Low-status Canterbury Min. age 17	High-status Canterbury 19				Abbey of St Mary Cirencester 21*

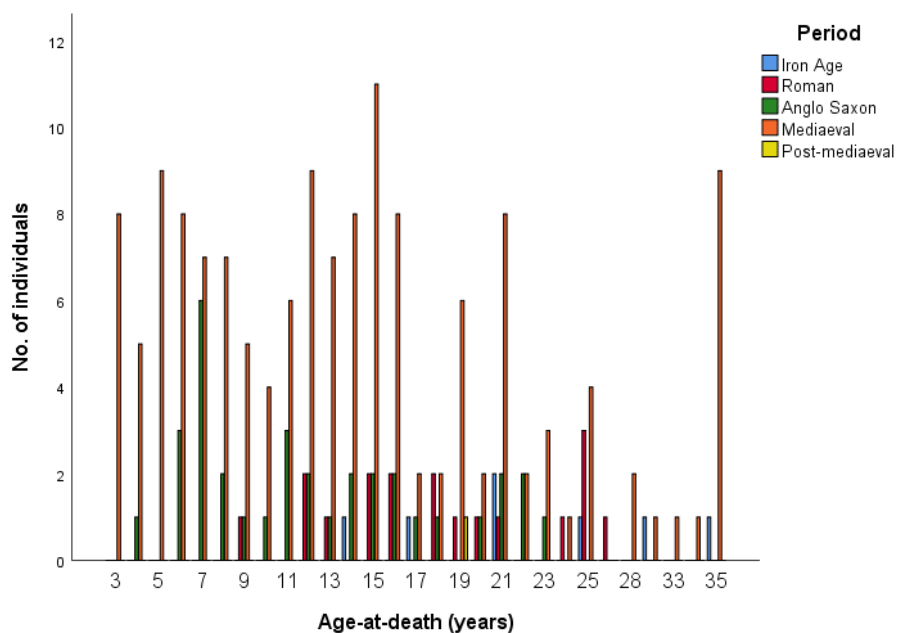
\* Large gaps in data between ages

The table below shows the fusion stages for the fusion of the **greater trochanter** to the femur. Max. age Stage 1 refers to the oldest individual or individuals in the samples who had an unfused greater trochanter. Min-max age Stage 2 refers to the youngest and oldest individuals for which fusion was underway. Min. age Stage 3 refers to the minimum age of the youngest individual or individuals in those samples who were found to have a fused greater trochanter of the femur.

Period	Stage 1 (unfused)	Period	Stage 1 (unfused)	Period	Stage 1 (unfused)
Iron Age	South Dumpton Down Broadstairs Max. age 17*	Anglo-Saxon	The Black Gate cemetery Newcastle-upon-Tyne Max. age 18*	Butler's Field cemetery Lechlade Max. age 17*	Apple Down cemetery Up Marden Max. age 15*
			Stage 3 (fused)		Stage 3 (fused)
				Apple Down cemetery Up Marden Min. age 20*	Auldham East Lothian Min. age 19*
Period	Stage 1 (unfused)	Period	Stage 1 (unfused)	Period	Stage 1 (unfused)
Roman	Bath Gate Cemetery Cirencester Max. age 16	St James' Place Cirencester	Mediaeval	Low-status Canterbury Max. age 16	High-status Canterbury Max. age 15
				All Saint's church York Max. age 16*	Fishergate House York Max. age 16*
				Abbey of St Mary Cirencester Max. age 14*	Auldham East Lothian Max. age 15*
	Stage 2 (fusing)		Stage 2 (fusing)		
	Bath Gate Cemetery Cirencester Min.- Max. age 18	Former Bridges Garage Cirencester Min.- Max. age 19*		Low-status Canterbury Min.- Max. age 16-17	All Saint's church York Min.- Max. age 18*
					Fishergate House York Min.- Max. age 16*
	Stage 3 (fused)		Stage 3 (fused)		
		Former Bridges Garage Cirencester Min. age 20*	Low-status Canterbury Min. age 17	High-status Canterbury Min. age 19	Auldham East Lothian Min. age 19*

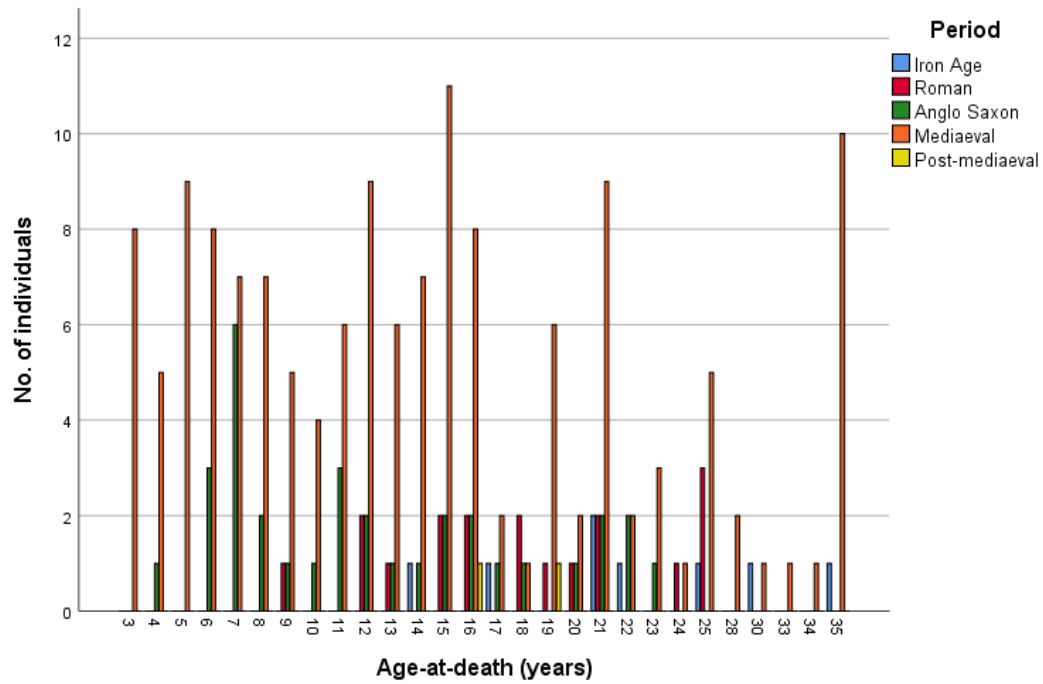
\* Large gaps in data between ages

The figure below shows the age distribution of individuals from different time periods for the fusion of the **greater trochanter** to the femur. This shows the entire sub-sample that had these bones present.





The figure shows the age distribution of individuals from different time periods for the fusion of the **lesser trochanter** to the femur. This shows the entire sub-sample that had these bones present.



The table shows the fusion stages for the fusion of the **lesser trochanter** to the femur. Max. age Stage 1 refers to the oldest individual or individuals in the samples who had an unfused lesser trochanter. Min-max age Stage 2 refers to the youngest and oldest individuals for which fusion was underway. Min. age Stage 3 refers to the minimum age of the youngest individual or individuals in those samples who were found to have a fused lesser trochanter of the femur.

Period	Stage 1 (unfused)		Period	Stage 1 (unfused)			Period	Stage 1 (unfused)	
Iron Age	South Dumpton Down Broadstairs Max. age 17*		Anglo-Saxon	The Black Gate cemetery Newcastle-upon-Tyne Max. age 18*	Butler's Field cemetery Lechlade 17*	Apple Down cemetery Up Marden 15*	Post-Mediaeval		
				<b>Stage 2 (fusing)</b>					
					Butler's Field cemetery Lechlade Min.-Max. age 14*				
				<b>Stage 3 (fused)</b>					
						Apple Down cemetery Up Marden Min. age 20*		<b>Stage 3 (fused)</b> Carver street Sheffield Min. age 16*	Auldham East Lothian 19*
<b>Roman</b>	<b>Bath Gate Cemetery Cirencester Max. age 18</b>	<b>St James' Place Cirencester 16*</b>	<b>Mediaeval</b>	<b>Low-status Canterbury Max. age 16</b>	<b>High-status Canterbury 15</b>	<b>All Saint's church York 16*</b>	<b>Fisergate House York 16*</b>	<b>Abbey of St Mary Cirencester 14*</b>	<b>Auldham East Lothian 15*</b>
	<b>Stage 2 (fusing)</b>			<b>Stage 2 (fusing)</b>					
	Bath Gate Cemetery Cirencester Min.-Max. age 18	Former Bridges Garage Cirencester 19*		Low-status Canterbury Min.-Max. age 16			Fisergate House York 16*		
	<b>Stage 3 (fused)</b>			<b>Stage 3 (fused)</b>					
	Bath Gate Cemetery Cirencester Min. age 21*	Former Bridges Garage Cirencester 20*		Low-status Canterbury Min. age 17	High-status Canterbury 19		Fisergate House York 15*		Auldham East Lothian 19*

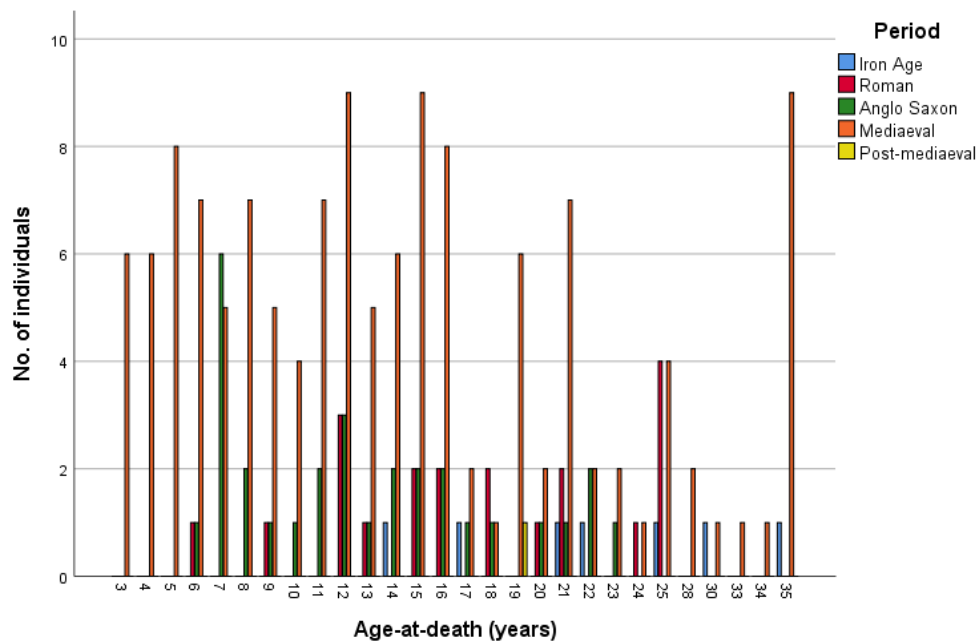
\* Large gaps in data between ages

The table below shows the fusion stages for the fusion of the **distal epiphysis** to the femur. Max. age Stage 1 refers to the oldest individual or individuals in the samples who had an unfused distal femur. Min-max age Stage 2 refers to the youngest and oldest individuals for which fusion was underway. Min. age Stage 3 refers to the minimum age of the youngest individual or individuals in those samples who were found to have a fused distal femur.

Period	Stage 1 (unfused)	Period	Stage 1 (unfused)	Period	Stage 1 (unfused)				
Iron Age	South Dumpton Down Broadstairs Max. age 17*	Anglo-Saxon	The Black Gate cemetery Newcastle-upon-Tyne Max. age 18*	Butler's Field cemetery Lechlade 17*	Apple Down cemetery Up Marden 15*				
			Stage 2 (fusing)		Stage 2 (fusing)				
			Min.-Max. age	Auldhame East Lothian 21*	Apple Down cemetery Up Marden 20*				
	Stage 3 (fused)		Stage 3 (fused)		Stage 3 (fused)				
	South Dumpton Down Broadstairs Min. age 21*		Butler's Field cemetery Lechlade Min. age 23*		Apple Down cemetery Up Marden 22*				
Roman	Bath Gate Cemetery Cirencester Max. age 18*	St James' Place Cirencester 16*	Mediaeval	Low-status Canterbury Max. age 18	High-status Canterbury 15*	All Saint's church York 16*	Fisergate House York 16*	Abbey of St Mary Cirencester 15*	Auldhame East Lothian 14*
			Stage 2 (fusing)						
			Low-status Canterbury Min.-Max. age 19-20						
	Stage 3 (fused)		Stage 3 (fused)						
	Bath Gate Cemetery Cirencester Min. age 21*	Former Bridges Garage Cirencester 20*	Low-status Canterbury Min. age 17	High-status Canterbury 19*				Abbey of St Mary Cirencester 19*	

\* Large gaps in data between ages

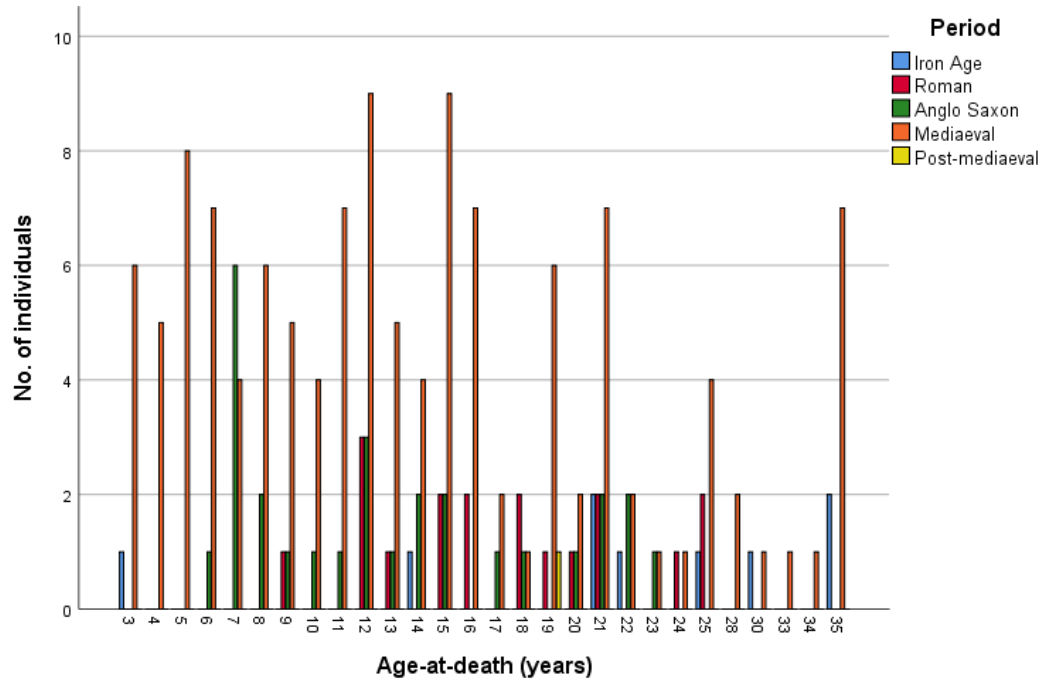
The figure shows the age distribution of individuals from different time periods for the fusion of the **distal epiphysis** to the femur. This shows the entire sub-sample that had these bones present.





### A9. 12. The Tibia

The figure below shows the age distribution of individuals from different time periods for the fusion of the **proximal epiphysis** to the tibia. This shows the entire sub-sample that had these bones present.



The table below shows the fusion stages for the fusion of the **proximal epiphysis** to the tibia. Max. age Stage 1 refers to the oldest individual or individuals in the samples who had an unfused proximal tibia. Min-max age Stage 2 refers to the youngest and oldest individuals for which fusion was underway. Min. age Stage 3 refers to the minimum age of the youngest individual or individuals in those samples who were found to have a fused proximal epiphysis to the tibia.

Period	Stage 1 (unfused)	Period	Stage 1 (unfused)	Period	Stage 1 (unfused)			
Iron Age	South Dumpton Down Broadstairs Max. age 14*	Anglo-Saxon	The Black Gate cemetery Newcastle-upon-Tyne Max. age 18*	Post-Medieval	Butler's Field cemetery Lechlade 17*			
			Apple Down cemetery Up Marden 15*					
	Stage 2 (fusing)		Stage 2 (fusing)		Stage 2 (fusing)			
	South Dumpton Down Broadstairs Min.- Max. age 22*		Min.- Max. age	Auldhame East Lothian 21*	Apple Down cemetery Up Marden 20*	Auldhame East Lothian Min.- Max. age 19*		
	Stage 3 (fused)		Min. age	Auldhame East Lothian 21*	Apple Down cemetery Up Marden 22*			
Roman	Bath Gate Cemetery Cirencester Max. age 18*	St James' Place Cirencester 16*	Mediaeval	Low-status Canterbury Max. age 18	High-status Canterbury 15*	All Saint's church York 16*	Fishergate House York 16*	Auldhame East Lothian 15*
	Stage 2 (fusing)			Stage 2 (fusing)	Stage 2 (fusing)	Stage 2 (fusing)	Stage 2 (fusing)	
	Bath Gate Cemetery Cirencester Min.- Max. age 18*			Former Bridges Garage Cirencester 19*	Low-status Canterbury Min.- Max. age 17-19	High-status Canterbury 19*		Auldhame East Lothian 19*
	Stage 3 (fused)		Min. age	Low-status Canterbury 17	High-status Canterbury 19*		Auldhame East Lothian 19*	

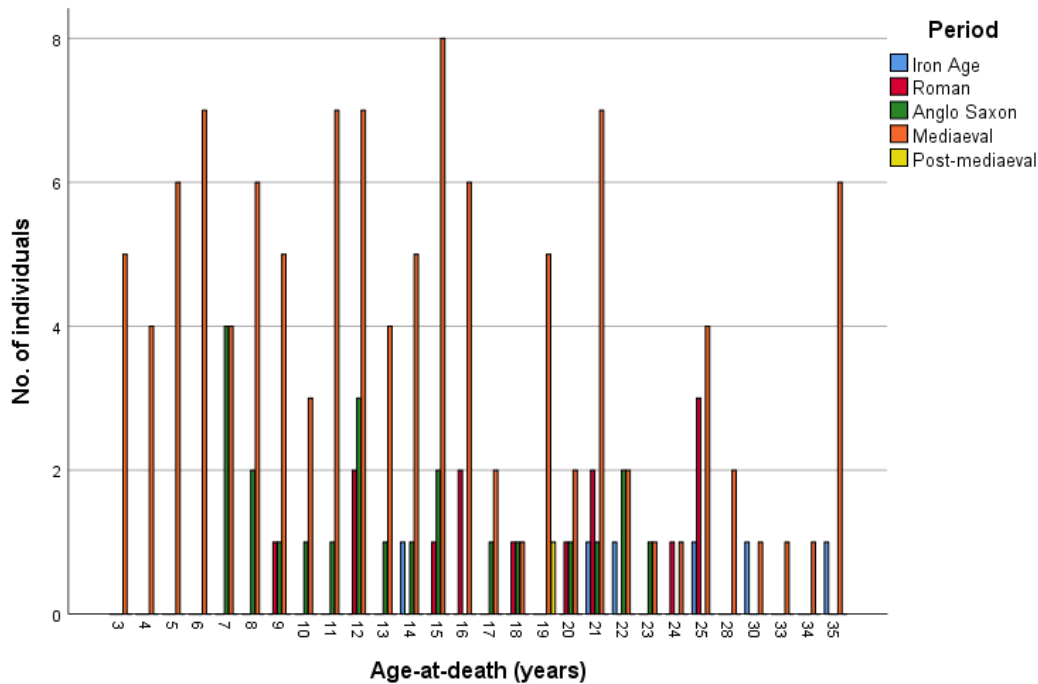
\* Large gaps in data between ages

The table below shows the fusion stages for the fusion of the **distal epiphysis** to the tibia. Max. age Stage 1 refers to the oldest individual or individuals in the samples who had an unfused distal tibia. Min-max age Stage 2 refers to the youngest and oldest individuals for which fusion was underway. Min. age Stage 3 refers to the minimum age of the youngest individual or individuals in those samples who were found to have a fused distal epiphysis to the tibia.

Period	Stage 1 (unfused)	Period	Stage 1 (unfused)	Period	Stage 1 (unfused)
Iron Age	South Dumpton Down Broadstairs Max. age 14*	Anglo-Saxon	The Black Gate cemetery Newcastle-upon-Tyne Max. age 18*	Butler's Field cemetery Lechlade Max. age 17*	Apple Down cemetery Up Marden Max. age 15*
	Stage 3 (fused)		Stage 3 (fused)		Stage 3 (fused)
	South Dumpton Down Broadstairs Min. age 21*		Min. age	Auldhame East Lothian Min. age 21*	Apple Down cemetery Up Marden Min. age 20*
					Auldhame East Lothian Min. age 19*
Period	Stage 1 (unfused)	Period	Stage 1 (unfused)	Period	Stage 1 (unfused)
Roman	Bath Gate Cemetery Cirencester Max. age 18	St James' Place Cirencester Max. age 16*	Mediaeval	Low-status Canterbury Max. age 16	High-status Canterbury Max. age 15
				All Saint's church York Max. age 16*	Fishergate House York Max. age 15
				Abbey of St Mary Cirencester Max. age 14*	Auldhame East Lothian Max. age 15*
			Stage 2 (fusing)		
			Low-status Canterbury Min.- Max. age 17-18		Fishergate House York Min. age 16
	Stage 3 (fused)		Stage 3 (fused)		
	Bath Gate Cemetery Cirencester Min. age 21	Former Bridges Garage Cirencester Min. age 20*	Low-status Canterbury Min. age 17	High-status Canterbury Min. age 19	Auldhame East Lothian Min. age 19*

\* Large gaps in data between ages

The figure below shows the age distribution of individuals from different time periods for the fusion of the **distal epiphysis** to the tibia. This shows the entire sub-sample that had these bones present.



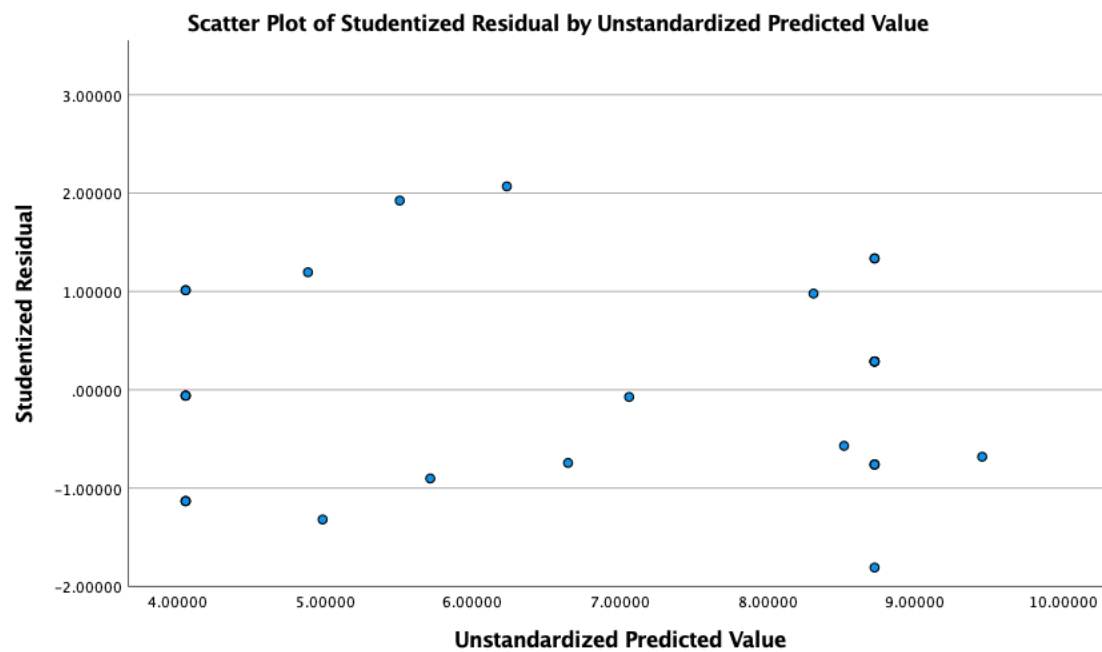
Age at death/phase for the fusion of the tibia, including the (1) proximal and (2) distal epiphyses for the skeletal samples collated by archaeological period. Frequencies are recorded as percentages.

		Iron Age			Roman					Anglo-Saxon						
		Stage of union			Stage of union					Stage of union						
	Age	n	1	2	3	Age	n	1	2	3	Age	n	1	2	3	
Proximal epiphysis	14	1	100.0	-	-	15	2	100.0	-	-	14	2	100.0	-	-	
	21	2	-	-	100.0	16	2	100.0	-	-	15	2	100.0	-	-	
	22	1	-	100.0	-	18	2	50.0	50.0	-	17	1	100.0	-	-	
						19	1	-	100.0	-	18	1	100.0	-	-	
						20	1	-	-	100.0	20	1	-	100.0	-	
						21	2	-	-	100.0	21	2	-	50.0	50.0	
											22	2	-	-	100.0	
						Mediaeval			Post-Mediaeval							
						Stage of union			Stage of union							
		Age	n	1	2	3	Age	n	1	2	3					
		14	4	100.0	-	-	19	1	-	100.0	-					
		15	9	100.0	-	-										
	16	7	100.0	-	-											
	17	2	-	50.0	50.0											
	18	1	100.0	-	-											
	19	6	-	33.3	66.7											
	20	2	-	-	100.0											
	21	7	-	-	100.0											
	22	2	-	-	100.0											
The tibia			Iron Age			Roman					Anglo-Saxon					
			Stage of union			Stage of union					Stage of union					
		Age	n	1	2	3	Age	n	1	2	3	Age	n	1	2	3
		14	1	100.0	-	-	15	1	100.0	-	-	14	1	100.0	-	-
		21	1	-	-	100.0	16	2	100.0	-	-	15	2	100.0	-	-
		22	1	-	-	100.0	18	1	100.0	-	-	17	1	100.0	-	-
							20	1	-	-	100.0	18	1	100.0	-	-
							21	2	-	-	100.0	20	1	-	-	100.0
												21	1	-	-	100.0
												22	2	-	-	100.0
							Mediaeval									
							Stage of union									
	Age	n	1	2	3											
	14	5	100.0	-	-											
	15	8	100.0	-	-											
	16	6	66.7	33.3	-											
	17	2	-	50.0	50.0											
	18	1	-	100.0	-											
	19	5	-	-	100.0											
	20	2	-	-	100.0											
	21	7	-	-	100.0											
	22	2	-	-	100.0											

**APPENDIX 10: MULTIVARIATE ANALYSIS OF MULTIPLE FUSION SITES  
FOUND SIGNIFICANT FROM UNIVARIATE ANALYSIS ON THE  
ARCHAEOLOGICAL DATA**

### A10.1 Age Range 3 to 10 years

The figure below shows the scatter plot for the Studentised Residual and Unstandardised Predicted Value for the age range: 3 to 10 years to test for a linear relationship and homoscedasticity.



The table below gives the VIF statistics used to look at the multicollinearity of the test.

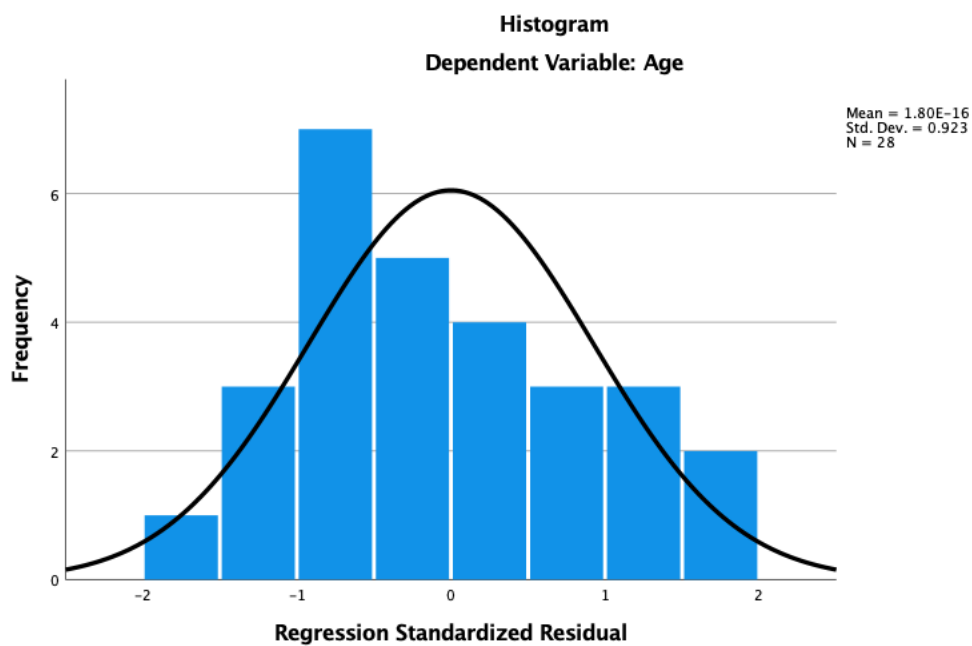
Coefficients <sup>a</sup>											
Model	Unstandardized Coefficients		Standardized Coefficients	t	Sig.	Correlations			Collinearity Statistics		
	B	Std. Error	Beta			Zero-order	Partial	Part	Tolerance	VIF	
1	(Constant)	.893	1.563		.571	.573					
	Period	.207	.352	.051	.588	.562	-.113	.122	.049	.919	1.089
	Occipital_LatToBas	1.870	.355	.784	5.262	<.001	.895	.739	.438	.313	3.197
	C2_DensVert	.829	.351	.329	2.365	.027	.783	.442	.197	.358	2.794
	C1_PostSyn	-.365	.347	-.160	-1.052	.304	.709	-.214	-.088	.299	3.340

a. Dependent Variable: Age

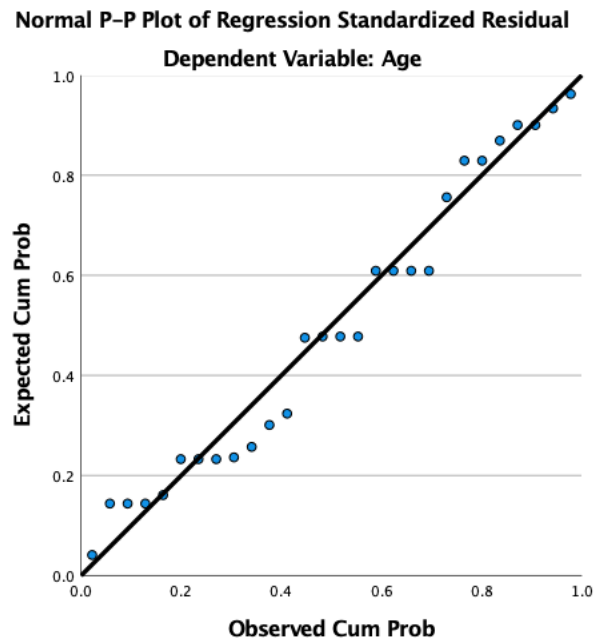
The table below shows the Leverage Regression and Cook's Distance Values to test for leverage points and influential points.

COO 1	LEV 1
.03311	.19496
.00961	.04118
.00139	.04118
.02763	.08289
.00009	.08289
.03446	.08289
.11238	.51259
.00961	.04118
.00139	.04118
.00139	.04118
.02975	.04118
.00961	.04118
.03446	.08289
.26827	.39984
.02763	.08289
.00009	.08289
.00009	.08289
.03446	.08289
.02975	.04118
.09333	.32921
.00139	.04118
.03795	.08150
.05442	.04118
.18981	.46189
.47293	.35390
.30077	.22426
.00040	.24079
.01252	.12611

The figure below shows a histogram used to test for normality.

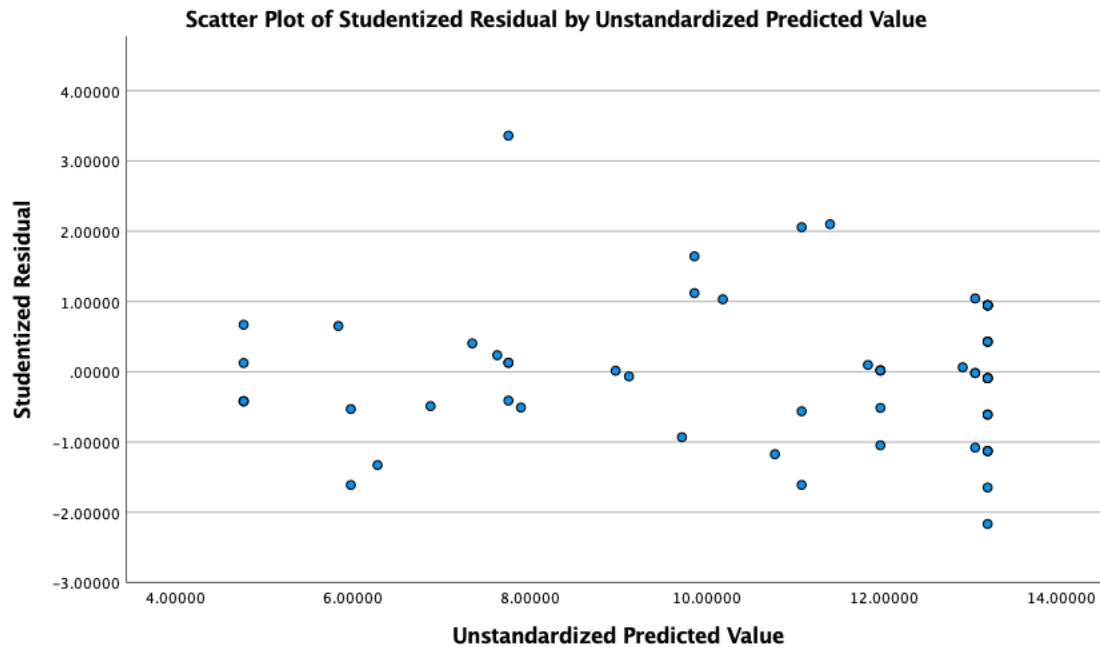


The figure below shows a normal P-P plot of regression standardised residual used to test for normality.



### A10.2 Age Range 3 to 15 years

The figure below shows the scatter plot for the Studentised Residual and Unstandardised Predicted Value for the age range: 3 to 15 years to test for a linear relationship and homoscedasticity.



The table below gives the VIF statistics used to look at the multicollinearity of the test.

**Coefficients<sup>a</sup>**

Model	Unstandardized Coefficients		Standardized Coefficients	t	Sig.	Correlations			Collinearity Statistics		
	B	Std. Error	Beta			Zero-order	Partial	Part	Tolerance	VIF	
1	(Constant)	.005	2.420		.002	.998					
	Period	.141	.538	.019	.262	.795	-.093	.036	.019	.975	1.025
	C1_AnteArch	.739	.549	.177	1.347	.184	.648	.182	.099	.314	3.188
	C1_PostSyn	.151	.545	.034	.277	.783	.526	.038	.020	.361	2.767
	C2_Dens	2.101	.404	.541	5.204	<.001	.797	.581	.383	.500	2.000
	C2_Centrum	1.211	.546	.226	2.219	.031	.670	.292	.163	.522	1.915

a. Dependent Variable: Age

The table below gives the case-wise diagnostics.

**Casewise Diagnostics<sup>a</sup>**

Case Number	Std. Residual	Age	Predicted Value	Residual
33	3.182	14	7.76	6.239

a. Dependent Variable: Age

The tables below show the Leverage Regression and Cook's Distance Values to test for leverage points and influential points.

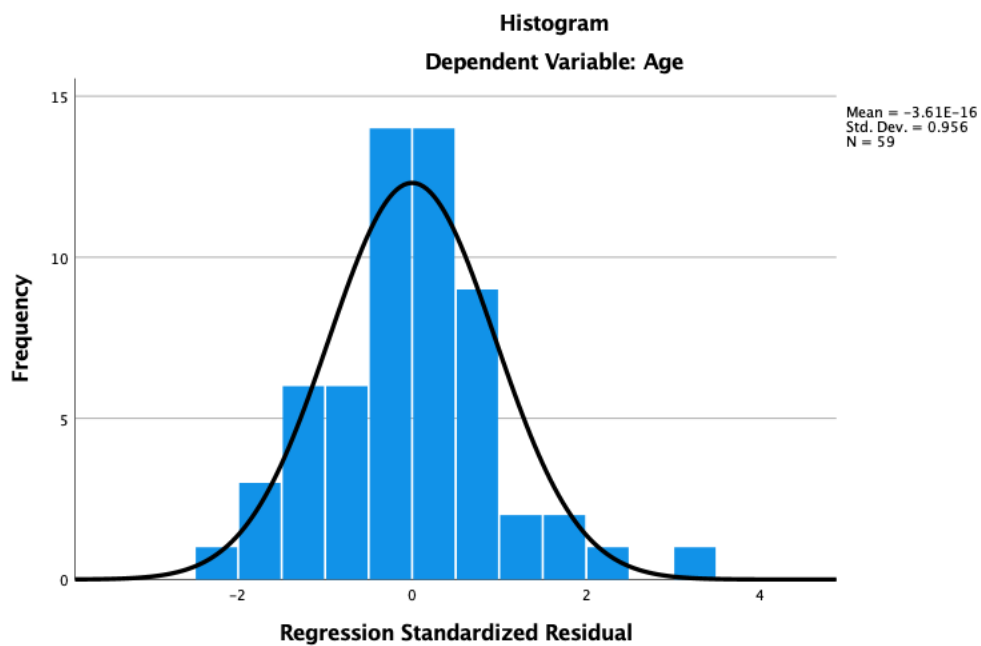
<b>COO 1</b>	<b>LEV 1</b>
.00000	.06094
.00000	.06094
.00721	.13663
.00024	.11329
.01642	.06094
.00414	.06900
.00005	.01766
.21984	.08755
.00537	.01766
.00001	.06900
.00537	.01766
.00761	.01766
.02513	.03588
.00005	.01766
.00537	.01766
.00761	.01766
.00001	.06900
.00032	.08755
.01167	.03588
.00001	.13995
.04305	.17800
.00408	.10547
.05384	.09363
.15796	.39064
.00001	.06900
.00537	.01766
.22528	.21737
.00032	.08755
.00537	.01766
.00222	.01766
.00007	.06946
.00297	.03641
.02437	.03641
.00110	.01766
.00537	.01766
.03980	.03641
.08856	.21463
.00036	.10547
.00408	.10547
.00408	.10547
.00761	.01766
.01718	.06900
.01621	.01766
.00583	.09363
.02804	.01766
.00222	.01766
.00005	.01766
.01042	.10547
.00327	.08755
.00005	.01766
.00110	.01766

---

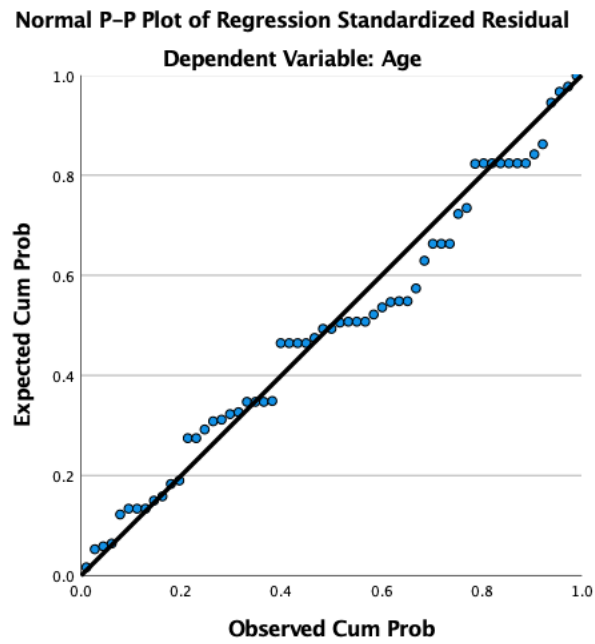
<b>COO_1</b>	<b>LEV_1</b>
.00110	.01766
.00026	.25473
.01372	.31769
.01520	.15978
.00565	.36046
.00960	.16525
.01811	.09443
.01536	.06094

---

The figure below shows a histogram used to test for normality.

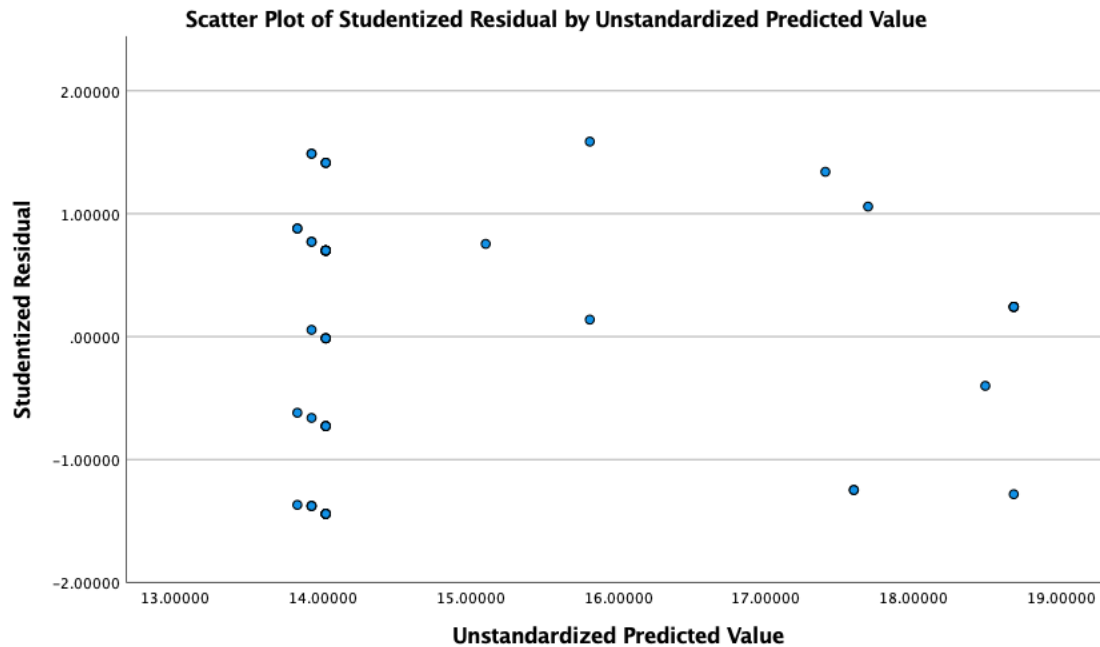


The figure below shows a normal P-P plot of regression standardised residual used to test for normality.



### A10.3 Age Range 12 to 19 years

The figure below shows the scatter plot for the Studentised Residual and Unstandardised Predicted Value for the age range: 12 to 19 years to test for a linear relationship and homoscedasticity.



The table below gives the VIF statistics used to look at the multicollinearity of the test.

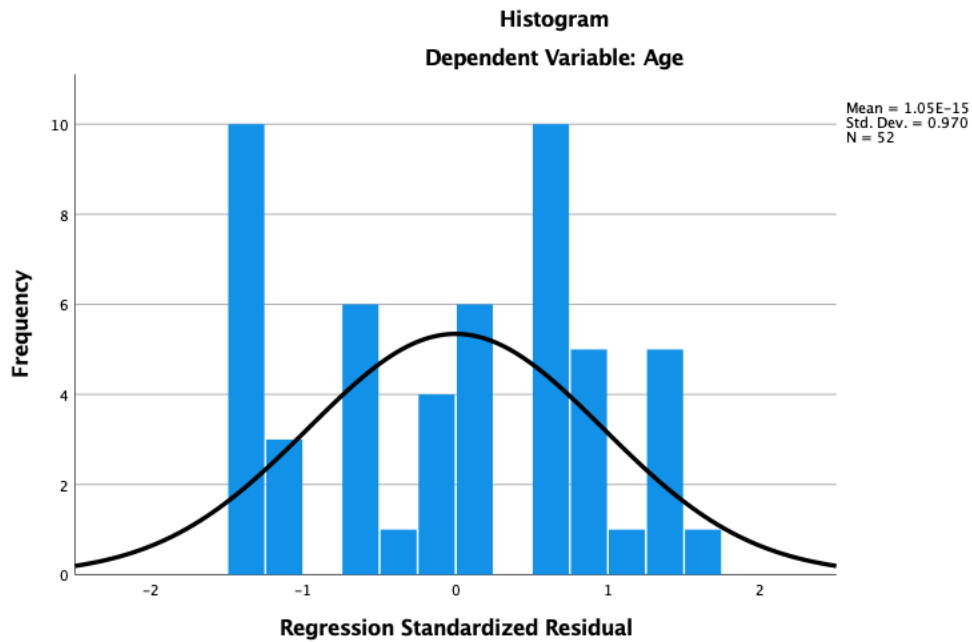
Coefficients <sup>a</sup>											
Model		Unstandardized Coefficients		Standardized Coefficients	t	Sig.	Correlations			Collinearity Statistics	
		B	Std. Error	Beta			Zero-order	Partial	Part	Tolerance	VIF
1	(Constant)	11.301	1.073		10.534	<.001					
	Period	.096	.278	.032	.346	.731	.096	.050	.031	.993	1.007
	Humerus_MedEp	1.790	.325	.653	5.500	<.001	.765	.622	.500	.585	1.709
	Occipital_SphenOcc	.542	.377	.170	1.437	.157	.592	.203	.131	.587	1.702

a. Dependent Variable: Age

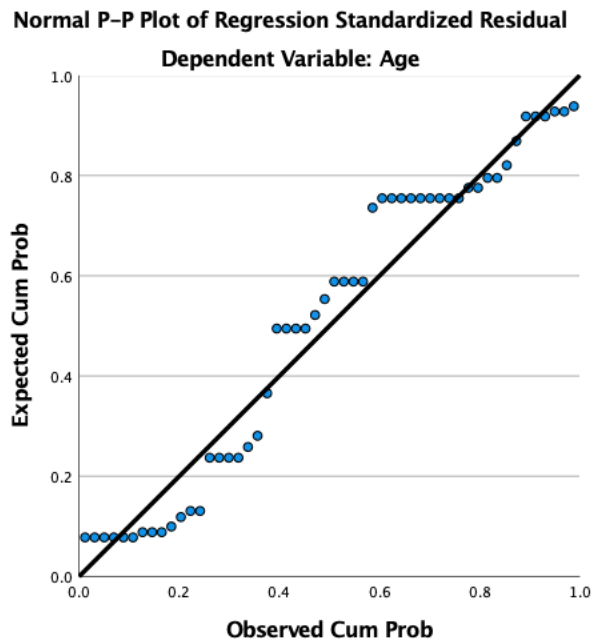
The table below shows the Leverage Regression and Cook's Distance Values to test for leverage points and influential points.

<b>COO 1</b>	<b>LEV 1</b>
.00429	.01860
.02178	.01860
.01864	.01860
.02178	.01860
.00398	.01220
.03892	.03897
.01686	.01220
.06178	.28317
.00429	.01220
.01624	.01220
.00429	.01220
.01624	.01220
.00398	.01220
.00000	.01220
.01624	.01220
.01686	.01220
.00030	.03897
.01686	.01220
.01686	.01220
.01686	.01220
.00259	.13055
.00398	.01220
.00259	.13055
.00398	.01220
.07235	.13055
.00000	.01220
.00259	.13055
.00398	.01220
.00000	.01220
.00398	.01220
.00398	.01220
.00259	.13055
.09093	.17029
.00429	.01220
.01686	.01220
.00429	.01220
.09093	.17029
.00398	.01220
.00000	.01220
.02660	.10155
.01316	.10155
.02660	.10155
.06431	.10155
.01423	.24318
.01864	.01860
.00003	.01860
.19431	.28241
.00398	.01220
.09252	.22907
.00586	.01860
.01864	.01860
.00586	.01860

The figure below shows a histogram used to test for normality.

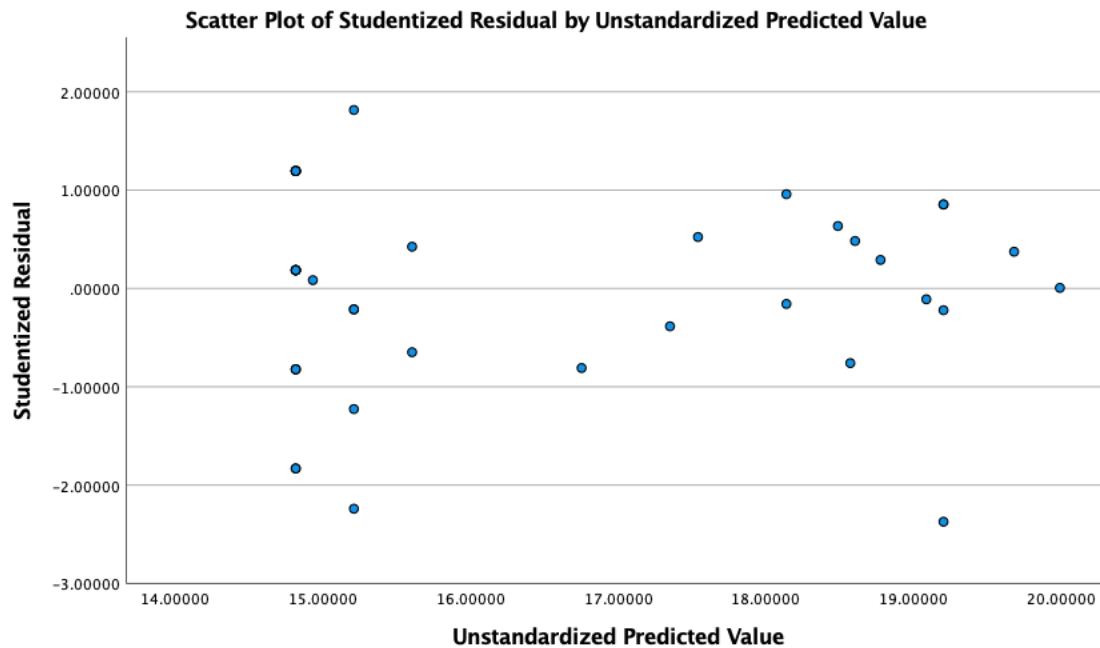


The figure below shows a normal P-P plot of regression standardised residual used to test for normality.



### A10.4 Age Range 13 to 20 years for the acromial border of the scapula, the femoral head, greater trochanter and the proximal tibia

The figure below shows the scatter plot for the Studentised Residual and Unstandardised Predicted Value for the age range: 13 to 20 years to test for a linear relationship and homoscedasticity.



The table below gives the VIF statistics used to look at the multicollinearity of the test.

**Coefficients<sup>a</sup>**

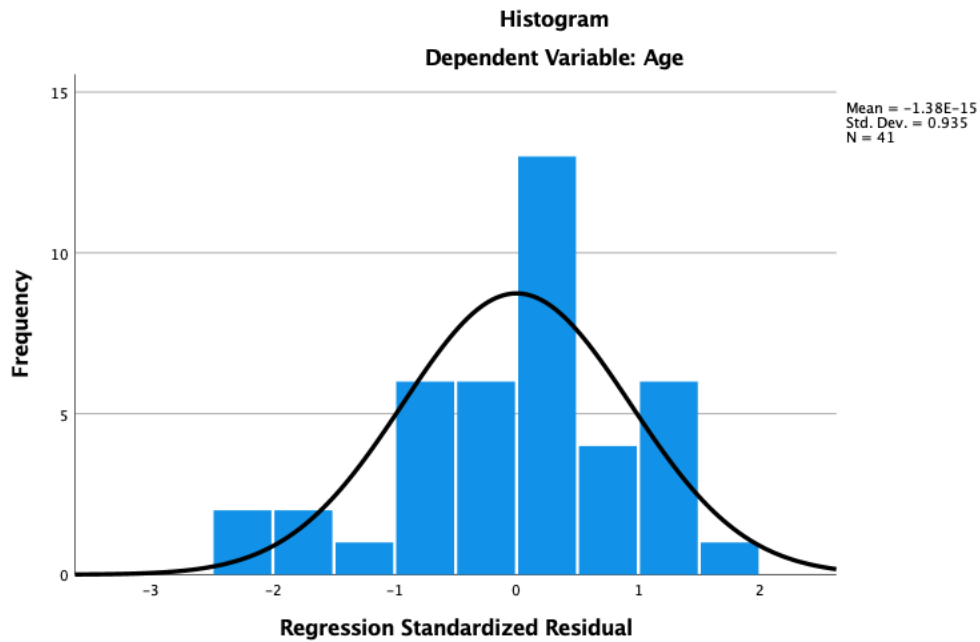
Model		Unstandardized Coefficients		Standardized Coefficients	t	Sig.	Correlations			Collinearity Statistics		
		B	Std. Error	Beta			Zero-order	Partial	Part	Tolerance	VIF	
1	(Constant)	14.197	.876		16.198	<.001						
	Period	-.394	.218	-.144	-1.813	.078	-.127	-.293	-.137	.910	1.099	
	Scapula_Acrom	-.342	.404	-.129	-.846	.403	.643	-.142	-.064	.246	4.073	
	Femur_Head	.116	.587	.042	.198	.844	.833	.033	.015	.125	8.003	
	Femur_GreTroch	1.821	.502	.759	3.626	<.001	.874	.523	.275	.131	7.635	
	Tibia_Prox	.599	.568	.211	1.054	.299	.785	.175	.080	.144	6.952	

a. Dependent Variable: Age

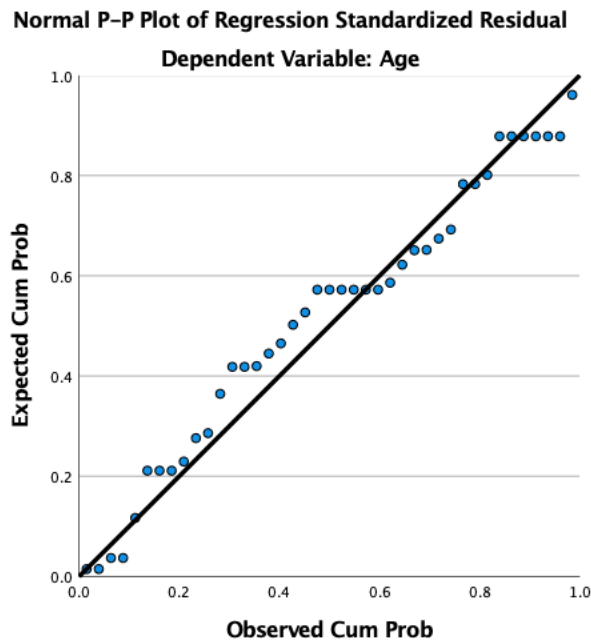
The table below shows the Leverage Regression and Cook's Distance Values to test for leverage points and influential points.

<b>COO 1</b>	<b>LEV 1</b>
.05031	.03238
.01167	.02233
.01167	.02233
.02736	.02233
.00552	.02233
.00028	.02233
.04026	.35005
.02736	.02233
.00028	.02233
.18119	.13757
.00069	.33981
.01167	.02233
.02353	.13757
.07709	.42111
.01167	.02233
.02156	.33191
.00028	.02233
.00572	.16402
.00028	.02233
.00552	.02233
.02353	.13757
.00028	.02233
.00157	.13757
.01167	.02233
.02080	.13591
.00552	.02233
.01167	.02233
.00028	.02233
.01319	.13419
.01576	.23207
.00568	.13419
.00117	.19762
.03306	.03238
.01507	.03238
.00000	.23508
.04376	.19762
.00114	.33793
.01092	.41279
.01040	.28384
.00045	.03238
.00045	.03238

The figure below shows a histogram used to test for normality.

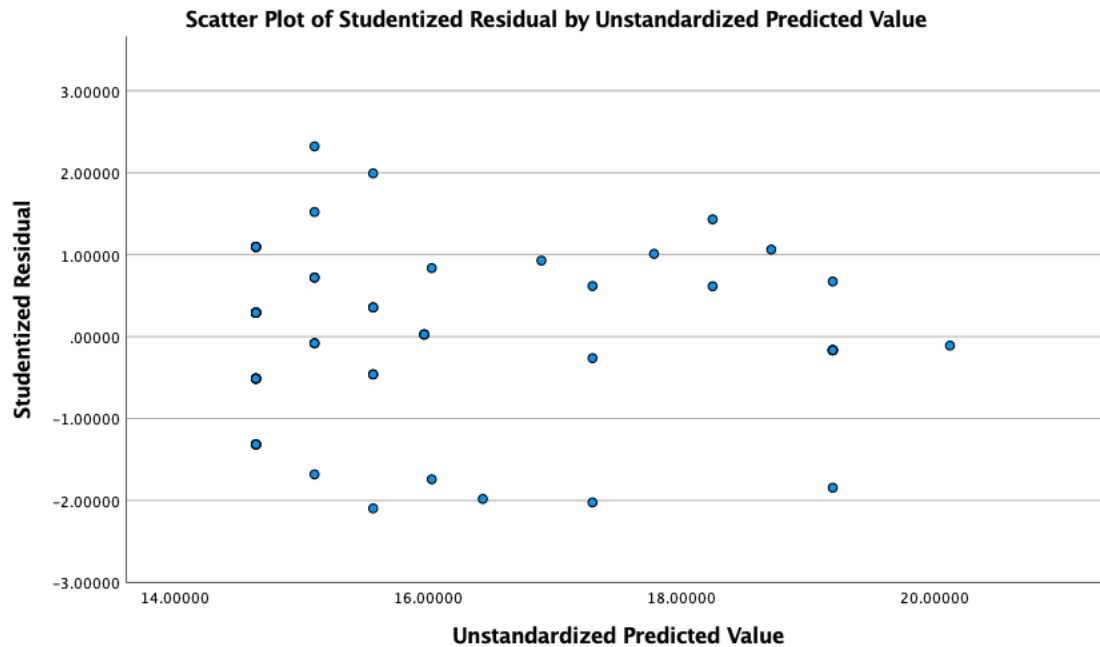


The figure below shows a normal P-P plot of regression standardised residual used to test for normality.



### A10.5 Age Range 13 to 20 years for the lesser trochanter and the distal femur

The figure below shows the scatter plot for the Studentised Residual and Unstandardised Predicted Value for the age range: 13 to 20 years to test for a linear relationship and homoscedasticity



The table below gives the VIF statistics used to look at the multicollinearity of the test.

**Coefficients<sup>a</sup>**

Model	Unstandardized Coefficients		Standardized Coefficients	t	Sig.	Correlations			Collinearity Statistics		
	B	Std. Error	Beta			Zero-order	Partial	Part	Tolerance	VIF	
1	(Constant)	14.209	.712		19.967	<.001					
	Period	-.463	.195	-.194	-2.373	.021	-.005	-.305	-.188	.940	1.064
	Femur_LessTroch	1.331	.311	.554	4.280	<.001	.759	.500	.340	.375	2.664
	Femur_Distal	.950	.377	.322	2.522	.015	.722	.322	.200	.387	2.583

a. Dependent Variable: Age

The tables below show the Leverage Regression and Cook's Distance Values to test for leverage points and influential points.

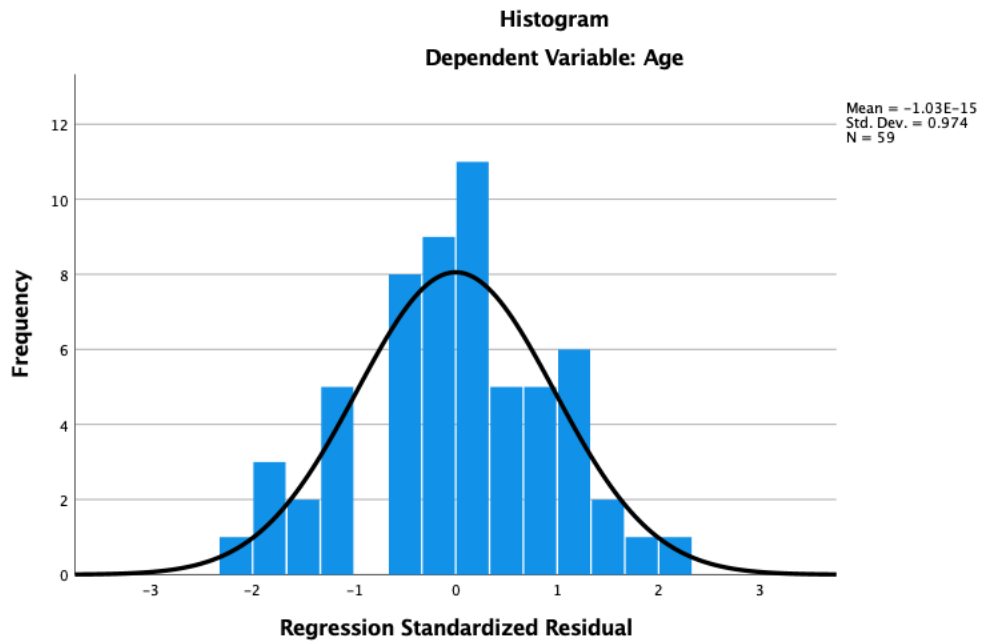
<b>COO 1</b>	<b>LEV 1</b>
.03862	.01090
.02023	.01090
.00372	.01090
.00372	.01090
.01098	.01830
.01098	.01830
.01579	.01830
.01579	.01830
.00239	.01830
.00078	.01830
.00679	.05010
.01579	.01830
.00078	.01830
.10993	.09765
.01579	.01830
.00078	.01830
.00239	.01830
.01098	.01830
.01467	.09765
.00001	.03858
.02334	.17932
.01098	.01830
.00089	.09765
.00078	.01830
.00089	.09765
.00078	.01830
.00419	.17932
.00239	.01830
.00089	.09765
.00078	.01830
.00239	.01830
.03685	.05010
.00078	.01830
.00089	.09765
.00001	.03858
.01579	.01830
.00001	.03858
.00239	.01830
.01098	.01830
.24982	.17932
.00239	.01830
.00386	.05105
.08008	.05105
.00386	.05105
.07242	.05105
.00233	.05105
.02805	.09826
.01658	.01090
.06434	.04465
.00069	.17255
.00233	.05105
.00078	.01830
.00089	.09765

---

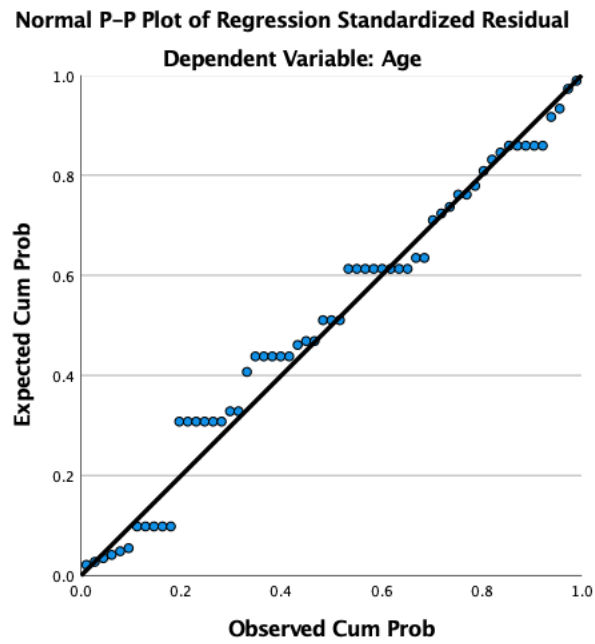
<b>COO_1</b>	<b>LEV_1</b>
.02774	.08104
.13966	.13873
.03225	.13873
.02579	.06670
.00005	.01090
.00005	.01090

---

The figure below shows a histogram used to test for normality.

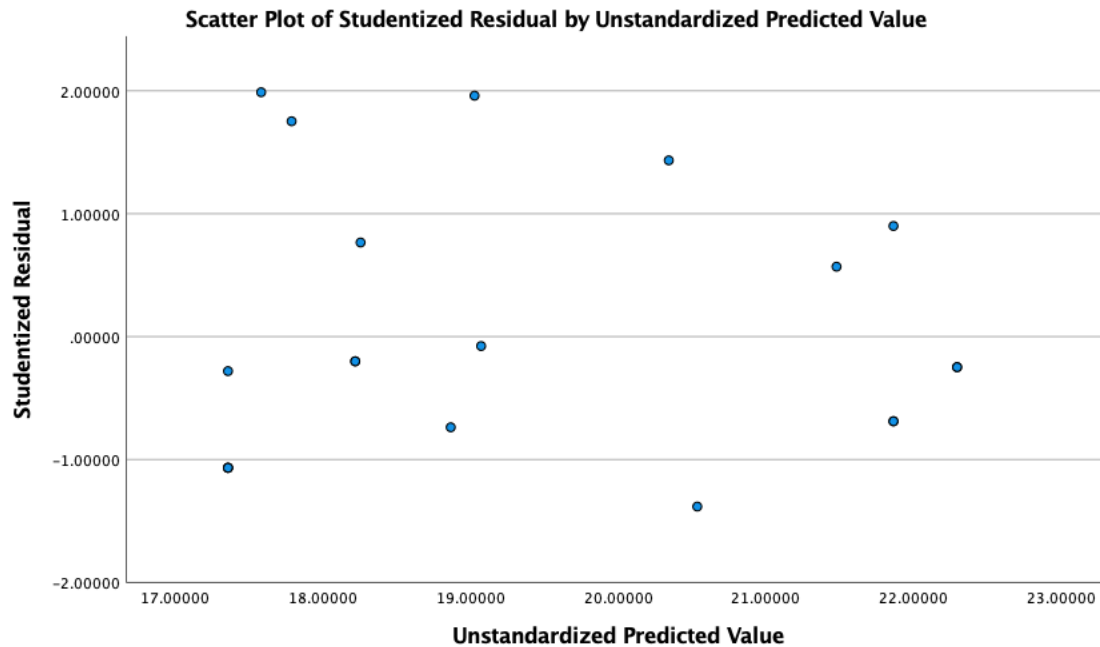


The figure below shows a normal P-P plot of regression standardised residual used to test for normality.



### A10.6 Age Range 16 to 23 years

The figure below shows the scatter plot for the Studentised Residual and Unstandardised Predicted Value for the age range: 16 to 23 years to test for a linear relationship and homoscedasticity



The table below gives the VIF statistics used to look at the multicollinearity of the test.

**Coefficients<sup>a</sup>**

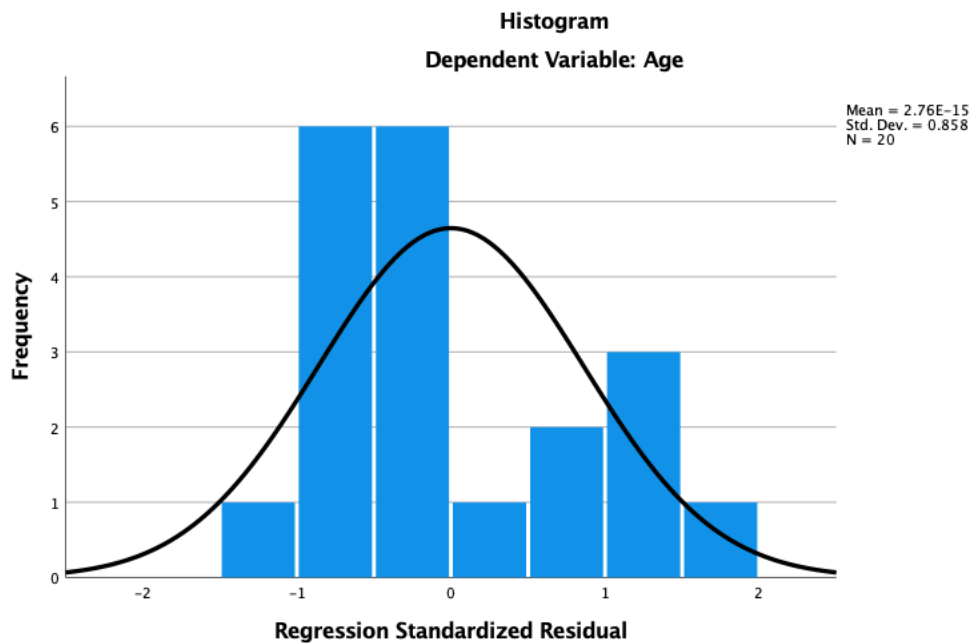
Model		Unstandardized Coefficients		Standardized Coefficients	t	Sig.	Correlations			Collinearity Statistics	
		B	Std. Error	Beta			Zero-order	Partial	Part	Tolerance	VIF
1	(Constant)	16.825	1.692		9.945	<.001					
	Period	-.431	.440	-.141	-.980	.344	-.010	-.253	-.138	.948	1.055
	Humerus_Head	1.285	.807	.556	1.592	.134	.800	.391	.223	.161	6.203
	Clavicle_Lateral	.193	.494	.085	.391	.702	.652	.104	.055	.414	2.416
	Scapula_InfAngle	-.553	.734	-.254	-.753	.464	.665	-.197	-.106	.174	5.753
	Pelvis_IliacCrest	1.330	.780	.507	1.704	.110	.771	.415	.239	.223	4.491

a. Dependent Variable: Age

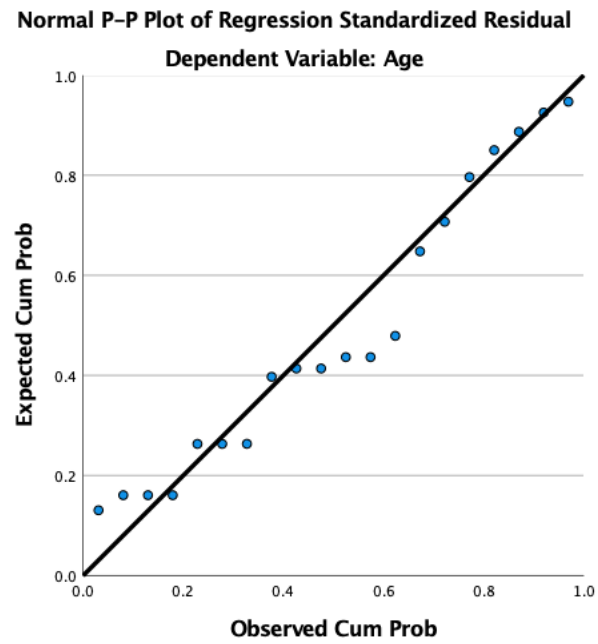
The table below shows the Leverage Regression and Cook's Distance Values to test for leverage points and influential points.

COO 1	LEV 1
.01422	.10274
.02995	.08638
.00109	.47947
.02437	.10274
.00206	.08638
.13815	.23717
.16363	.28946
.54241	.40850
.03233	.21306
.02995	.08638
.02995	.08638
.00386	.31602
.00386	.31602
.06737	.50489
1.76167	.67770
.09561	.44417
.01422	.10274
.00308	.18102
.00308	.18102
.08875	.09775

The figure below shows a histogram used to test for normality.

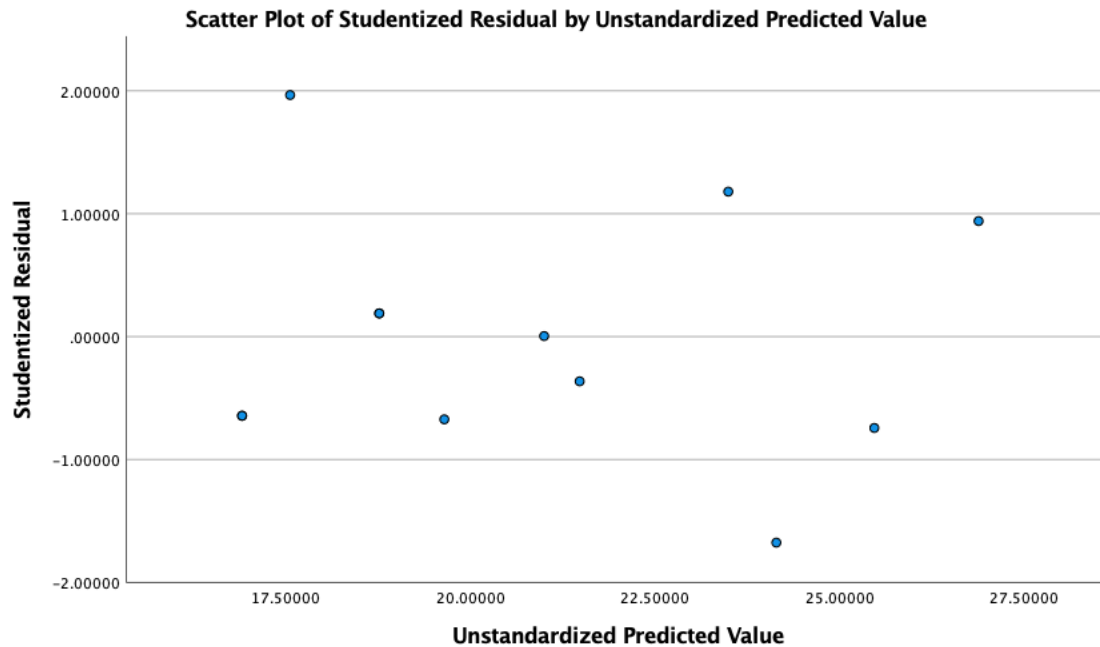


The figure below shows a normal P-P plot of regression standardised residual used to test for normality.



### A10.7 Age Range 16 to 30 years

The figure below shows the scatter plot for the Studentised Residual and Unstandardised Predicted Value for the age range: 16 to 30 years to test for a linear relationship and homoscedasticity.



The table below gives the VIF statistics used to look at the multicollinearity of the test.

**Coefficients<sup>a</sup>**

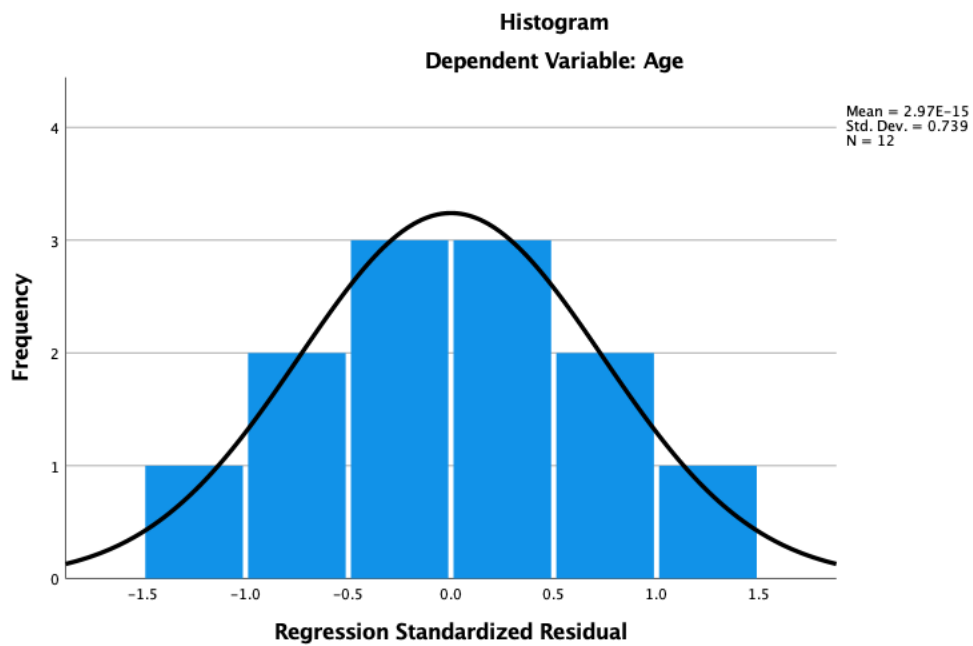
Model	Unstandardized Coefficients		Standardized Coefficients	t	Sig.	Correlations			Collinearity Statistics		
	B	Std. Error	Beta			Zero-order	Partial	Part	Tolerance	VIF	
1	(Constant)	14.516	3.465		4.189	.006					
	Clavicle_Medial	2.015	1.124	.493	1.793	.123	.809	.591	.249	.254	3.930
	Clavicle_Lateral	.351	.789	.100	.445	.672	.604	.179	.062	.383	2.609
	Period	-.651	.756	-.135	-.862	.422	-.341	-.332	-.119	.779	1.283
	Scapula_MedBord	-.767	.773	-.218	-.992	.360	.612	-.375	-.137	.400	2.503
	Sacrum	3.393	1.053	.625	3.223	.018	.821	.796	.447	.511	1.957

a. Dependent Variable: Age

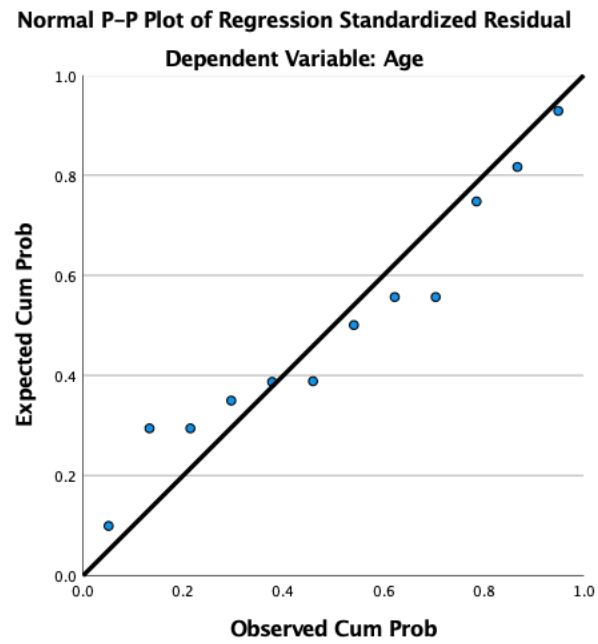
The table below shows the Leverage Regression and Cook's Distance Values to test for leverage points and influential points.

<b>COO 1</b>	<b>LEV 1</b>
.00459	.35094
.01324	.29259
.02862	.20987
.02862	.20987
.14527	.41297
.00003	.79481
.16416	.33099
.53994	.77117
.00459	.34094
.15347	.58727
.32698	.32804
.51410	.36054

The figure below shows a histogram used to test for normality.



The figure below shows a normal P-P plot of regression standardised residual used to test for normality.



## APPENDIX 11: RELATION OF EPIPHYSEAL FUSION TO PUBERTAL PHASE IN THE MEDIAEVAL SAMPLES

- Pars lateralis to pars basilaris: Fused before puberty begins.
- Spheno-occipital synchondrosis: Partial fusion was found to occur in the Deceleration phase for Canterbury. However, one individual was found to be completely fused, but still in PHV. Maturation and Completion were missing for the York sample, but unfused individuals were found in Deceleration and completely fused individuals were found in PHV. Overall, fusion of the spheno-occipital appears to take place around PHV and Deceleration.
- Posterior synchondrosis of the atlas: Unfused Canterbury children were found in Pre-puberty and Acceleration. No partial fusion was recorded. Those who had completely fused spanned all pubertal phases. All unfused York individuals were recorded in Pre-puberty only.
- Dentoneural synchondrosis of the axis: Unfused and partially fused Canterbury individuals are only found in Pre-puberty. Completely fused Canterbury individuals are found in all pubertal phases. This is the same for York. The fusion of the dentoneural synchondrosis therefore takes place before the onset of puberty.
- Dentocentral and neurocentral junctions of the axis: Unfused Canterbury individuals were in Pre-puberty only. Partially fused juveniles spanned Pre-puberty to PHV and completely fused Canterbury individuals were in all pubertal phases. The mean pubertal phase at fusion (Stages 2 and 3) for the Canterbury group was the Acceleration phase (mean phase = 1.71, s.d. = 0.77). Unfused York juveniles were only in Pre-puberty, but partially fused individuals were in Pre-puberty and Acceleration. Completely fused York individuals were in all pubertal phases. The mean pubertal phase at fusion (Stages 2 and 3) for the York group was the Pre-puberty phase (mean phase = 1.46, s.d. = 0.52).
- Posterior synchondrosis of the axis: All unfused Canterbury children were in Pre-puberty. No data was available for partial fusion, but completely fused Canterbury skeletons were recorded in all pubertal phases. Data was limited for the York group.

**APPENDIX 12: SACRAL BODIES 1 & 2 CROSS-TABULATED WITH PUBERTAL  
PHASE AND FUSION STAGE FOR THE MEDIAEVAL SITES**

The table below shows skeletons recorded for the age at fusion of sacral bodies 1 and 2 cross-tabulated with the pubertal stage reached at the time of death. This table is for Mediaeval Canterbury, York, and East Lothian skeletons only. Frequencies are recorded as percentages.

<b>Group</b>	<b>Fusion stage</b>	<b>Age</b>	<b><i>n</i></b>	<b>Acceleration</b>	<b>PHV</b>	<b>Deceleration</b>	<b>Maturation</b>	<b>Completion</b>
<i>Canterbury</i>	1	16	3	33.3	66.7	-	-	-
	2	19	3	-	-	100.0	-	-
		21	6	-	16.7	16.7	33.3	33.3
		22	1	-	-	-	-	100.0
		25	2	-	-	-	-	100.0
		3	19	1	-	-	-	100.0
	3	21	2	-	-	-	-	100.0
		23	1	-	-	-	-	100.0
		24	1	-	-	-	-	100.0
		28	2	-	-	-	-	100.0
<i>York</i>	1	16	2	50.0	50.0	-	N/D	N/D
		18	1	-	-	100.0	N/D	N/D
	2	16	1	-	-	100.0	N/D	N/D
<i>East Lothian</i>	2	19	-	-	N/D	100.0	N/D	-
		22	-	-	N/D	-	N/D	100.0
	3	21	1	-	-	N/D	-	100.0

**APPENDIX 13: ADDITIONAL INFORMATION PERTAINING TO THE RELATION  
OF EPIPHYSEAL FUSION TO PUBERTAL PHASE IN THE APPENDICULAR  
SKELETON OF THE MEDIAEVAL SAMPLES**

- Medial epiphysis of the clavicle: Unfused Canterbury individuals were in all pubertal phases. However, those who were partially fused were recorded from Deceleration onwards and those who had completely fused were recorded from Maturation onwards. The mean pubertal phase Canterbury individuals were in at fusion (Stages 2 and 3) for the medial clavicle was Completion. Data was limited for the other sites, but East Lothian individuals that had completed puberty had also completed fusion.
- Lateral epiphysis of the clavicle: Unfused Canterbury individuals were in all pubertal phases except for Completion. Those in partial fusion were found in Maturation and Completion, whereas those who had completed puberty were in PHV onwards. The mean puberty phase at fusion (Stages 2 and 3) for Mediaeval Cantuarrians was Maturation (mean phase = 5.36, s.d. = 0.93). Data was limited for the other Mediaeval sites.
- Coracoid of scapula: Unfused Canterbury individuals were found in Pre-puberty to PHV. One partially fused individual was in PHV, and Canterbury individuals who had completely fused were in PHV onwards. The mean pubertal phase at fusion that Mediaeval Canterbury juveniles were in at fusion (Stages 2 and 3) was PHV (mean phase = 3.33, s.d. = 0.58). Unfused York individuals were recorded in Pre-puberty to PHV, and completely fused individuals were recorded from PHV onwards.
- Acromial epiphysis of scapula: Canterbury individuals who were unfused were in puberty phases up to Deceleration and those who had completely fused were recorded from PHV onwards.
- Medial border of scapula: Canterbury individuals who were unfused were in puberty phases up to PHV. The Deceleration phase was missing, but completely fused Canterbury individuals were recorded from Maturation onwards.

- Inferior angle of scapula: Unfused Canterbury individuals were in puberty phases Pre-puberty to Maturation, whereas completely fused Canterbury individuals were in Maturation and Completion.
- Medial epicondyle of humerus: Unfused Canterbury individuals were in puberty phases Pre-puberty to PHV. One partially fused individual was listed in PHV, whereas completely fused Canterbury individuals were recorded from PHV onwards. The mean pubertal phase that fusion (Stages 2 and 3) occurred for the Canterbury group is Deceleration (mean phase = 3.67, s.d. = 1.16). Maturation and Completion phases were missing for the York group, but unfused individuals were found up to PHV. One partially fused juvenile skeleton was found in Deceleration and all completely fused York individuals were in PHV onwards. The mean pubertal phase at fusion (Stages 2 and 3) for the York group was Deceleration (mean phase = 3.67, s.d. = 0.58). There were no significant differences in the mean pubertal phase at fusion between the two groups ( $U = 4.000, p = 0.814$ ).
- Distal composite epiphysis to the shaft of the humerus: Unfused Canterbury individuals were in Pre-puberty to PHV. One partially fused child was in Acceleration, and completely fused Canterbury individuals were in Acceleration onwards. The mean pubertal phase at fusion (Stages 2 and 3) for the Canterbury group was PHV (mean phase = 2.71, s.d. = 0.49). Maturation and Completion phases were missing for the York group, but unfused individuals were found up to Acceleration. Those who had completely fused were found in PHV onwards. The mean pubertal phase at fusion (Stages 2 and 3) for the York group was PHV (mean phase = 3.20, s.d. = 0.45). No significant differences were found in the mean pubertal phase at fusion between the two groups ( $U = 10.000, p = 0.109$ ).
- Proximal epiphysis of the humerus: Unfused Canterbury juvenile skeletons were found in Pre-puberty to Deceleration, partially fused skeletons were found in PHV to Maturation and completely fused skeletons were found from Deceleration onwards. The mean pubertal phase at fusion (Stages 2 and 3) for the Canterbury group was Maturation (s.d. = 0.88).

- Proximal epiphysis of the radius: Unfused Canterbury individuals were recorded in Pre-puberty to PHV, partially fused skeletons were recorded in PHV to Deceleration and those who had completely fused were in PHV onwards. The mean puberty phase at fusion (Stages 2 and 3) for the Canterbury group was PHV (mean phase = 3.17, s.d. = 0.41). Maturation and Completion phases were missing for the York group, but unfused individuals were found up to PHV. Partially fused individuals were in PHV and Deceleration and those who had completely fused were in PHV onwards. The mean pubertal phase at fusion (Stages 2 and 3) for the York group was Deceleration (mean phase = 3.50, s.d. = 0.57). No significant differences were found in the mean pubertal phase at fusion between the two groups ( $U = 8.000, p = 0.285$ ).
- Distal epiphysis of the ulna: Unfused Canterbury skeletons were found in Pre-puberty to Deceleration. Those who had partially fused were in Maturation only, and Canterbury skeletons who had completely fused were in Deceleration onwards. The mean pubertal phase at fusion (Stages 2 and 3) was Maturation (mean phase = 5.33, s.d. = 0.65) for the Canterbury group.
- Metacarpals 2-5, and the proximal and middle phalangeal epiphyses of the hand: Unfused Canterbury individuals were found in Pre-puberty to PHV. One skeleton that was partially fused was recorded in Pre-puberty and the other partially fused skeleton was recorded in Deceleration. Completely fused Canterbury individuals were recorded from Deceleration onwards. The mean pubertal phase at fusion (Stages 2 and 3) that Canterbury individuals were in was PHV (mean phase = 3.33, s.d. = 2.08).
- Ischiopubic ramus of the os coxae: Unfused Canterbury skeletons were recorded in Pre-puberty and Acceleration, whereas completely fused individuals were found in Acceleration onwards. The mean pubertal phase at fusion (Stages 2 and 3) was PHV (mean phase = 2.50, s.d. = 0.71) for the Canterbury group.
- Acetabulum of the os coxae: Unfused Canterbury skeletons were recorded in Pre-puberty and Acceleration. Those who had partially fused were in Acceleration and PHV and Cantuarians who had completed puberty at the time of their death were in PHV and beyond. The mean pubertal phase at fusion (Stages 2 and 3) for the Canterbury group

was PHV (s.d. = 0.58). Maturation and Completion were missing for the York group, but unfused skeletons were recorded in Pre-puberty and Acceleration, whereas completely fused skeletons were in PHV and beyond. The mean pubertal phase at fusion (Stages 2 and 3) for the York group was Deceleration (mean phase = 3.50, s.d. = 0.71). There were no significant differences in the mean pubertal phase at fusion between the two groups ( $U = 4.000, p = 0.294$ ).

- Femoral head: Unfused Canterbury individuals were found to be in Pre-puberty to PHV, partially fused individuals were recorded in PHV to Maturation and those who had completely fused were in PHV and beyond. The mean pubertal phase for fusion (Stages 2 and 3) for the Canterbury group was Maturation (mean phase = 4.56, s.d. = 1.13).
- Greater trochanter: Unfused Canterbury individuals were found in Pre-puberty to PHV. Those who were partially fused were in PHV and skeletons that had completely fused at the time of their death were in PHV and beyond. The mean pubertal phase at fusion (Stages 2 and 3) for the Canterbury group was Deceleration (mean phase = 3.67, s.d. = 1.16).
- Lesser trochanter: Unfused Canterbury skeletons were in Pre-puberty to PHV. One individual who was partially fused was in PHV and those who had completed fusion were in PHV onwards. The mean pubertal phase at fusion (Stages 2 and 3) for the Canterbury group was Deceleration (mean phase = 3.67, s.d. = 1.16). Maturation and Completion were missing from the York data, but unfused individuals were in Pre-puberty to PHV. One partially fused individual was in PHV, and one was in Deceleration. Only one York skeleton was recorded as completely fused and in PHV. The mean pubertal phase at fusion (Stages 2 and 3) for the York group was PHV (mean phase = 3.33, s.d. = 0.58). There was no significant difference in the mean pubertal phase at fusion between the two groups ( $U = 4.000, p = 0.796$ ).
- Distal epiphysis of the femur: Unfused Canterbury individuals were recorded from Pre-puberty to Deceleration. One partially fused individual was found in Deceleration, and one was found in Maturation, whereas completely fused skeletons were found in PHV

onwards. The mean pubertal phase for fusion (Stages 2 and 3) for the Canterbury group was Maturation (mean phase = 5.13, s.d. = 0.84).

- Proximal epiphysis of the tibia: Unfused Canterbury individuals were found in Pre-puberty to Deceleration. Those who were partially fused were found in PHV to Maturation. Completely fused Canterbury individuals were recorded from PHV onwards. The mean pubertal phase at fusion (Stages 2 and 3) was Maturation (mean phase = 4.86, s.d. = 1.07).
- Distal epiphysis of the tibia: Unfused Canterbury individuals were recorded from Pre-puberty to PHV. One partially fused individual was in PHV, and the other was in Deceleration. Those who had completed puberty were in PHV and above. The mean pubertal phase at fusion (Stages 2 and 3) for the Canterbury group was Maturation (mean phase = 4.71, s.d. = 1.11). Maturation and Completion were missing from the York group, as well as Stage three of fusion. However, York individuals in partial fusion were found in PHV and Deceleration.

---

**APPENDIX 14: ADDITIONAL INFORMATION PERTAINING TO THE RELATION  
OF EPIPHYSEAL FUSION TO PUBERTAL PHASE WITHIN THE  
ARCHAEOLOGICAL SAMPLES**

- Pars lateralis to pars basilaris: Fusion occurred before puberty commenced in all archaeological groups.
  
- Spheno-occipital synchondrosis: One unfused Roman individual was in the Deceleration phase. Roman skeletons that had completed fusion were in phases PHV and above. Two unfused Anglo-Saxons were also in Deceleration. One partially fused Anglo-Saxon was also recorded in Deceleration. This was the same for the Mediaeval and Post-Mediaeval samples. The mean pubertal phase for the fusion (Stages 2 and 3) of the spheno-occipital synchondrosis was the Maturation phase for the Anglo-Saxon group (mean phase = 4.50, s.d. = 0.71) and the Deceleration phase for the Mediaeval group (mean phase = 4.43, s.d. = 1.27). No significant differences were found in the mean pubertal phase for the fusion of the spheno-occipital synchondrosis when the Anglo-Saxon group was compared with the Mediaeval group ( $U = 6.500, p = 0.880$ ). Overall, it therefore appears that the fusion of the spheno-occipital synchondrosis occurs in the Deceleration phase of puberty, except for the Roman group, whereby one fused Roman was listed in PHV.
  
- Anterior arch of the atlas: Unfused Roman skeletons were in Pre-puberty and completely fused individuals were in all pubertal phases. This was the same for the Anglo-Saxon sample. The Anglo-Saxon sample also had one individual in partial fusion who was also recorded in Pre-puberty. Unfused Mediaeval skeletons were 92.3% in Pre-puberty and 7.7% in Acceleration. Those who were in partial fusion were in pre-puberty only and those who had completely fused were in all pubertal phases. Except for two Mediaeval children in Acceleration, the fusion of the anterior arch of the atlas can be said to fuse before puberty begins.
  
- Posterior synchondrosis of the atlas: Unfused Anglo-Saxons were in Pre-puberty only, whereas completely fused individuals were in all pubertal phases. Unfused Mediaeval

children were 88.2% in Pre-puberty and 11.8% in Acceleration, whereas those who had completely fused were in all pubertal phases. Overall, it can be said that for most children, fusion of the posterior synchondrosis occurs before puberty begins.

- Ossiculum terminale to the dens: Unfused Roman children were recorded in Pre-puberty only. Those who had completely fused were in all pubertal phases. Unfused and partially fused Anglo-Saxon children were also in Pre-puberty only and those who had completed fusion were the same as the Roman sample. The mean pubertal phase at fusion (Stages 2 and 3) for the Anglo-Saxon sample was Pre-puberty (mean phase = 1.40, s.d. = 0.55). Unfused and partially fused Mediaeval children were in Pre-puberty and Acceleration. Those who had completed fusion were in all pubertal phases. The mean pubertal phase at fusion (Stages 2 and 3) for the Mediaeval group was Acceleration (mean phase = 1.89, s.d. = 0.67). There were no significant differences in the mean pubertal phase at fusion of the ossiculum terminale to the dens between the Anglo-Saxon and Mediaeval groups ( $U = 70.500, p = 0.119$ ). Overall, it appears that children fuse their ossiculum terminale to the dens near the onset of puberty.
- Dentocentral and neurocentral junctions of the axis: Romans who had unfused (Stage 1) dentocentral and neurocentral junctions of the axis or where fusion was underway (Stage 2) for this site, were recorded in Pre-puberty only. Romans who had completed fusion (Stage 3) at the time of death were found in all pubertal phases. Anglo-Saxons who were undergoing fusion (Stage 2) of their dentocentral and neurocentral junctions were recorded in Pre-puberty to Acceleration. Anglo-Saxons who had completed fusion (Stage 3) of this site were recorded in all pubertal phases. The mean pubertal phase for the Anglo-Saxons when fusion was underway (Stage 2) was Pre-puberty (mean phase = 1.10, s.d. = 0.32). The mean pubertal phase for the Anglo-Saxons for the fusion (Stages 2 and 3) of the dentocentral and neurocentral junctions was also Pre-puberty (mean phase = 1.29, s.d. = 0.47). The Romans and Anglo-Saxons were found not to differ significantly ( $U = 4.500, p = 0.752$ ) in the mean pubertal phase when fusion was underway (Stage 2). These two groups were also found to not differ significantly ( $U = 11.000, p = 0.554$ ) in the pubertal phase at fusion (Stages 2 and 3) of the dentocentral and neurocentral junctions of the axis. Like the Romans, Mediaeval children who had unfused (Stage 1) dentocentral and neurocentral junctions were recorded in Pre-puberty

only. Where fusion was underway (Stage 2), Mediaeval skeletons were recorded in Pre-puberty to PHV. The mean pubertal phase for when fusion was underway was Pre-puberty (mean phase = 1.27, s.d. = 0.52). Mediaeval individuals who had completed fusion (Stage 3) at the time of death were recorded in all pubertal phases. The mean pubertal phase for the fusion (Stages 2 and 3) of the dentocentral and neurocentral junctions was the Acceleration phase (mean phase = 1.79, s.d. = 0.81). The Roman and Mediaeval groups were found to not differ significantly ( $U = 12.500, p = 0.581$ ) in the mean pubertal phase when fusion was underway (Stage 2). Nor were they found to differ significantly ( $U = 68.000, p = 0.658$ ) in the mean pubertal phase during fusion (Stages 2 and 3) of the dentocentral and neurocentral junctions. The Anglo-Saxon and Mediaeval groups were found to not differ significantly ( $U = 141.000, p = 0.329$ ) in the mean pubertal phase when fusion was underway (Stage 2). However, the mean pubertal phase at fusion (Stages 2 and 3) was **found to significantly differ** ( $U = 377.000, p = 0.026$ ) between the Anglo-Saxon and Mediaeval groups, in which fusion occurred during Pre-puberty for the Anglo-Saxons and Acceleration for the Mediaeval group.

- Dentoneural synchondrosis of the axis: Unfused Anglo-Saxons were found in Pre-puberty only and completely fused Anglo-Saxons were in all pubertal phases. This is the same for the Mediaeval group. The Mediaeval sample also had children recorded in partial fusion and these were also in Pre-puberty. The fusion of the dentoneural synchondrosis therefore fuses before the onset of puberty.
- Sacral bodies 1 and 2: Roman skeletons with unfused (Stage 1) sacral bodies 1 and 2 were found in Pre-puberty to PHV. One Roman was recorded in partial fusion (Stage 2) and was reported as having completed puberty. All Romans who had completed fusion (Stage 3) had completed puberty. Anglo-Saxons recorded as unfused (Stage 1) were in pubertal phases: Pre-puberty to Deceleration. When fusion was underway (Stage 2), Anglo-Saxons had been recorded in PHV and Maturation. The mean pubertal phase when fusion was underway was Completion (mean phase = 5.50, s.d. = 0.71). Puberty had not been reported for any Anglo-Saxons who had completed fusion (Stage 3) of their sacral bodies 1 and 2. Mediaeval skeletons with unfused (Stage 1) sacral bodies 1 and 2 were in Pre-puberty to Deceleration. Where fusion was underway (Stage 2), Medieval individuals were recorded in PHV to Completion. The mean pubertal

phase for when fusion was underway was Maturation (mean phase = 5.07, s.d. = 0.96). Medieval individuals who had completed fusion (Stage 3) had also completed puberty. No significant differences were found in the mean pubertal phase between the Roman and Mediaeval ( $U = 3.000, p = 0.299$ ) groups or the Anglo-Saxon and Mediaeval ( $U = 11.500, p = 0.579$ ) groups when fusion was underway (Stage 2), nor between the Roman and Mediaeval group ( $U = 14.000, p = 0.291$ ) for the fusion (Stages 2 and 3) of sacral bodies 1 and 2. The sacral bodies 1 and 2, therefore, appear to begin the process of fusion, in which fusion is underway (Stage 2) from PHV onwards, but it appears universal within this study, that all individuals who have completed fusion (Stage 3) of their sacral bodies 1 and 2 would have also completed puberty.

- Posterior synchondrosis of the axis: One partially fused Anglo-Saxon was recorded in Pre-puberty. Those who had completed fusion were in all pubertal phases. Unfused Mediaeval children were in Pre-puberty only. Those who had completed fusion were in all pubertal phases. Fusion of the posterior synchondrosis appears to occur before pubertal onset.
- Medial epiphysis of the clavicle: Unfused Romans were in every phase of puberty. Those partially fused were in Maturation and Completion, and completely fused Romans were in Completion only. Mean pubertal phase at fusion (Stages 2 and 3) was Completion (mean phase = 5.75, s.d. = 0.50). Unfused Anglo-Saxons were in all pubertal phases except for Completion and completely fused individuals were only in Completion. Unfused Mediaeval individuals were in all pubertal phases. Those who were partially fused were in Deceleration onwards and those who had completely fused were in Maturation and Completion. The mean pubertal phase at fusion (Stages 2 and 3) was Completion for the Mediaeval group (mean phase = 5.73, s.d. = 0.59). No significant differences in the mean pubertal phase at fusion (Stages 2 and 3) were found between the Roman and Mediaeval samples ( $U = 29.000, p = 0.888$ ). The medial epiphysis of the clavicle therefore appears to fuse after puberty has finished.
- Lateral epiphysis of the clavicle: Deceleration was missing from the Roman data, but unfused individuals spanned all pubertal phases, whereas completely fused individuals were only in Completion. Unfused Anglo-Saxons were in all pubertal phases except for

Completion. One partially fused Anglo-Saxon was in Acceleration and 33.3% of completely fused Anglo-Saxons were in PHV, and 66.7% in Completion. The mean pubertal phase at fusion (Stages 2 and 3) for the Anglo-Saxon sample was Deceleration (mean phase = 4.25, s.d. = 2.06). Unfused Mediaeval individuals spanned all pubertal phases. One partially fused Mediaeval skeleton was in Maturation and the other in Completion. Completely fused Mediaeval skeletons were recorded from PHV onwards. The mean pubertal phase at fusion (Stages 2 and 3) for the Mediaeval group was Maturation (mean phase = 5.40, s.d. = 0.91). No significant differences were found between the Anglo-Saxons and Mediaeval group for the mean pubertal phase at fusion of the lateral clavicle ( $U = 21.500, p = 0.341$ ).

- Coracoid of scapula: Unfused Romans were in phases Pre-puberty to PHV, whereas those who had completely fused were in PHV onwards. This is the same for the Anglo-Saxon and Mediaeval samples, except that the Mediaeval sample had data for partial fusion also. This data showed that partial fusion occurred in PHV.
- Acromial epiphysis of the scapula: Unfused Romans were recorded from Pre-puberty until Deceleration and completely fused Romans were recorded from Maturation onwards. Unfused Anglo-Saxons were the same as the Roman sample, but completely fused Anglo-Saxons were recorded from Deceleration onwards. Unfused Mediaeval juvenile skeletons were also recorded up until Deceleration but were recorded from PHV onwards. The Mediaeval group had the largest sample size, so it may be that fusion occurs around PHV.
- Medial border of scapula: Maturation was missing from the Anglo-Saxon sample, but unfused Anglo-Saxons were recorded from Pre-puberty until Deceleration, while completely fused Anglo-Saxons were recorded in Completion only. Unfused Mediaeval individuals were recorded from Pre-puberty to PHV, while completely fused Mediaeval individuals were recorded from Deceleration onwards.
- Inferior angle of the scapula: Maturation was unavailable for the Roman sample, but unfused Romans were recorded up until Deceleration and completely fused Romans were recorded in Completion. Maturation was also unavailable for the Anglo-Saxon

sample and unfused and completely fused skeletons followed the same pattern as the Romans. The Mediaeval group had unfused skeletons up until Maturation and fused individuals from Deceleration onwards. It is likely that the inferior angle fuses near the tail end of puberty.

- Medial epicondyle of the humerus: Unfused Romans were found from Pre-puberty to PHV, while completely fused Romans were in PHV onwards. Unfused Anglo-Saxons were the same as the Roman group. One partially fused skeleton was found in Acceleration and those who had completely fused before death were in Deceleration onwards. The mean pubertal phase at fusion (Stages 2 and 3) for the Anglo-Saxon sample was PHV (s.d. = 1.41). Unfused Mediaeval individuals were also recorded up until PHV. One partially fused skeleton was in PHV, and one was in Deceleration. Those who had completely fused were the same as the Roman sample. The mean pubertal phase at fusion (Stages 2 and 3) for the Mediaeval sample was Deceleration (mean phase = 3.86, s.d. = 0.90). No significant differences in the mean pubertal phase at fusion existed between the Anglo-Saxon and Mediaeval samples ( $U = 4.000$ ,  $p = 0.361$ ).
- Distal composite epiphysis of the humerus: Unfused Romans were found in Pre-puberty and Acceleration, while completely fused Romans were in PHV onwards. Unfused Anglo-Saxons were recorded up until PHV. Those who were partially fused were found in Acceleration and PHV, and completely fused Anglo-Saxons were recorded from PHV onwards. The mean pubertal phase at fusion (Stages 2 and 3) for the Anglo-Saxons was PHV (mean phase = 2.75, s.d. = 0.50). Unfused and partially fused Mediaeval skeletons were the same as the Anglo-Saxon sample, but completely fused Mediaeval individuals were recorded from Acceleration onwards. The mean pubertal phase at fusion (Stages 2 and 3) for the Mediaeval sample was PHV (mean phase = 2.94, s.d. = 0.43). No significant differences in the mean pubertal phase at fusion were apparent between the Anglo-Saxon and Mediaeval samples ( $U = 28.000$ ,  $p = 0.432$ ).
- Proximal epiphysis of the humerus: Unfused Romans were recorded up until Deceleration while those who had completely fused were recorded from Maturation onwards. Unfused Anglo-Saxons were listed from Pre-puberty to Deceleration. One

partially fused Anglo-Saxon was in PHV and the other in Deceleration. Those who had completely fused were the same as the Romans. The mean pubertal phase at fusion (Stages 2 and 3) was Maturation (mean phase = 4.75, s.d. = 1.50) for the Anglo-Saxon group. The Mediaeval sample was the same as the Anglo-Saxons for unfused skeletons, but partially fused Mediaeval skeletons were recorded from PHV to Maturation. Those who had completed fusion before death were recorded from Deceleration onwards. The mean pubertal phase for the fusion (Stages 2 and 3) of the proximal epiphysis of the humerus for the Mediaeval group is Maturation (mean phase = 5.07, s.d. = 0.88). There were no significant differences in the mean pubertal phase at fusion between the Anglo-Saxons and Mediaeval sample for the fusion of the proximal humerus ( $U = 27.500, p = 0.792$ ).

- Proximal epiphysis of the radius: Unfused Roman children were in Pre-puberty to PHV. One partially fused Roman was in PHV, and those who had completely fused were in PHV onwards. Unfused Anglo-Saxons were the same as the Roman children. However, partially fused Anglo-Saxons were recorded in Acceleration and Deceleration. Completely fused Anglo-Saxons were found from Deceleration onwards. The mean pubertal phase at fusion for the Anglo-Saxon group was Deceleration (mean phase = 3.50, s.d. = 1.000). No significant difference was found in the mean pubertal phase at fusion between the Roman and Anglo-Saxon groups ( $U = 2.000, p = 0.317$ ). Like the Romans and Anglo-Saxons, the Mediaeval group had unfused children in Pre-puberty to PHV. Partially fused Mediaeval skeletons were in PHV and Deceleration. Those who had completely fused were in PHV onwards. The mean pubertal phase at fusion for the Mediaeval sample was Deceleration (mean phase = 3.57, s.d. = 0.76). There were no significant differences between the mean pubertal phase at fusion of the Roman and Mediaeval samples ( $U = 8.000, p = 0.268$ ), nor the Mediaeval and Anglo-Saxon group ( $U = 26.000, p = 0.818$ ).
- Distal epiphysis of the ulna: Unfused Romans were found from Pre-puberty to Deceleration. One partially fused Roman was in Maturation and those who had completely fused were in Maturation onwards. The mean pubertal phase at fusion (Stages 2 and 3) for the Roman sample was Maturation (mean phase = 5.33, s.d. = 0.58). Unfused Anglo-Saxon children were the same as the Romans. One partially fused

Anglo-Saxon was recorded in Deceleration and those who had completely fused were in Maturation onwards. The mean pubertal phase at fusion (Stages 2 and 3) for the Anglo-Saxon sample was Maturation (mean phase = 5.33, s.d. = 1.16). There was no significant difference in the mean pubertal phase at fusion between the Roman and Anglo-Saxon samples ( $U = 4.000, p = 0.814$ ). Like the Romans and Anglo-Saxons, the Mediaeval sample was found in Pre-puberty to Deceleration for unfused children. Two partially fused Mediaeval skeletons were in Maturation and those who had completely fused were recorded from Deceleration onwards. The mean pubertal phase at fusion (Stages 2 and 3) for the Mediaeval sample was Maturation (mean phase = 5.38, s.d. = 0.65). No significant differences in the mean pubertal phase at fusion occurred between the Roman and Mediaeval samples ( $U = 18.000, p = 0.821$ ), nor the Anglo-Saxon and Mediaeval samples ( $U = 18.500, p = 0.882$ ).

- Metacarpals 2 – 5, proximal and middle phalangeal epiphyses of the hand: Unfused Romans were in pubertal phases Pre-puberty to Deceleration, while completely fused Romans were recorded from Maturation onwards. Unfused Anglo-Saxons were recorded from Pre-puberty to PHV. One partially fused Anglo-Saxon was in Deceleration and those that had completely fused were recorded from Deceleration onwards. The mean pubertal phase at fusion was Deceleration (s.d. = 0.000). Unfused Mediaeval individuals were recorded up to Deceleration. Partially and completely fused Mediaeval skeletons were the same as the Anglo-Saxons. The mean pubertal phase at fusion (Stages 2 and 3) was Deceleration (mean phase = 3.80, s.d. = 1.64) for the Mediaeval sample. There was no significant difference in the mean pubertal phase at fusion when the Anglo-Saxon and Mediaeval samples were compared ( $U = 6.000, p = 0.606$ ).
- Ischiopubic ramus of the os coxae: The Mediaeval group was missing data for the Maturation phase of puberty, but unfused children were recorded in Pre-puberty and Acceleration. Completely fused individuals were found in all pubertal phases. It is likely that fusion of the ischiopubic ramus occurs before pubertal onset or in the early stages of puberty.

- Acetabulum of the os coxae: The Roman group was missing data for the Deceleration phase of puberty, but unfused Romans were found up to PHV. Those who were completely fused were in PHV and beyond. Unfused Anglo-Saxons were also recorded up until PHV. One partially fused Anglo-Saxon was listed in Acceleration and those who had completely fused at the time of their death were recorded from Deceleration onwards. The mean pubertal phase at fusion (Stages 2 and 3) for the Anglo-Saxon sample was PHV (s.d. = 1.41). Unfused Mediaeval children also followed suit of the Romans and Anglo-Saxons. Partially fused Mediaeval skeletons were recorded in Acceleration and PHV, whereas those who were completely fused were recorded from PHV onwards. The mean pubertal phase at fusion (Stages 2 and 3) for the Mediaeval sample was PHV (mean phase = 3.11, s.d. = 0.60). There was no significant difference in the mean pubertal phase at fusion when the Anglo-Saxon and Mediaeval samples were compared ( $U = 8.500, p = 0.896$ ).
- Femoral head: Unfused Romans were recorded from Pre-puberty to PHV. Partially fused Romans were found in PHV and Deceleration, whereas those who had completely fused were in Maturation onwards. The mean pubertal phase at fusion (Stages 2 and 3) for the Roman sample was Deceleration (s.d. = 1.41). Unfused Anglo-Saxons were the same as the Roman sample. One partially fused Anglo-Saxon was listed in Deceleration and those who had completely fused were in Deceleration onwards. The mean pubertal phase at fusion (Stages 2 and 3) for the Anglo-Saxon sample was Deceleration (s.d. = 0.00). There was no significant difference in the mean pubertal phase at fusion when the Roman and Anglo-Saxon sample was compared ( $U = 4.500, p = 0.554$ ). Like unfused Romans and Anglo-Saxons, unfused Mediaeval skeletons were recorded up to PHV. Partially fused Mediaeval skeletons were recorded in PHV to Maturation and completely fused skeletons from PHV onwards. The mean pubertal phase at fusion (Stages 2 and 3) for the Mediaeval sample was Deceleration (mean phase = 4.42, s.d. = 1.00). There was no significant difference in the mean pubertal phase at fusion when the Roman and Mediaeval samples were compared ( $U = 17.500, p = 0.412$ ), nor the Anglo-Saxon and Mediaeval samples ( $U = 13.500, p = 0.478$ ).
- Greater trochanter of the femur: Unfused Romans were recorded from Pre-puberty to PHV. Partially fused Romans were found in PHV to Deceleration and those completely

fused were found in Maturation onwards. The mean pubertal phase at fusion (Stages 2 and 3) for the Roman group was Deceleration (s.d. = 1.41). Unfused Anglo-Saxons were in the same pubertal phases as the Romans. One partially fused Anglo-Saxon was in Deceleration and those who had completely fused were found from Deceleration onwards. There was no significant difference in the mean age at fusion when the Roman and Anglo-Saxon samples were compared ( $U = 1.500, p = 0.709$ ). Unfused and partially fused Mediaeval skeletons were the same as the Roman sample, but completely fused Mediaeval individuals were found from PHV onwards. The mean pubertal phase at fusion (Stages 2 and 3) for the Mediaeval sample was Deceleration (mean phase = 3.83, s.d. = 0.75). There was no significant difference in the mean pubertal phase when the Roman and Mediaeval samples were compared ( $U = 11.500, p = 0.909$ ), nor when the Anglo-Saxon and Mediaeval samples were compared ( $U = 2.500, p = 0.780$ ).

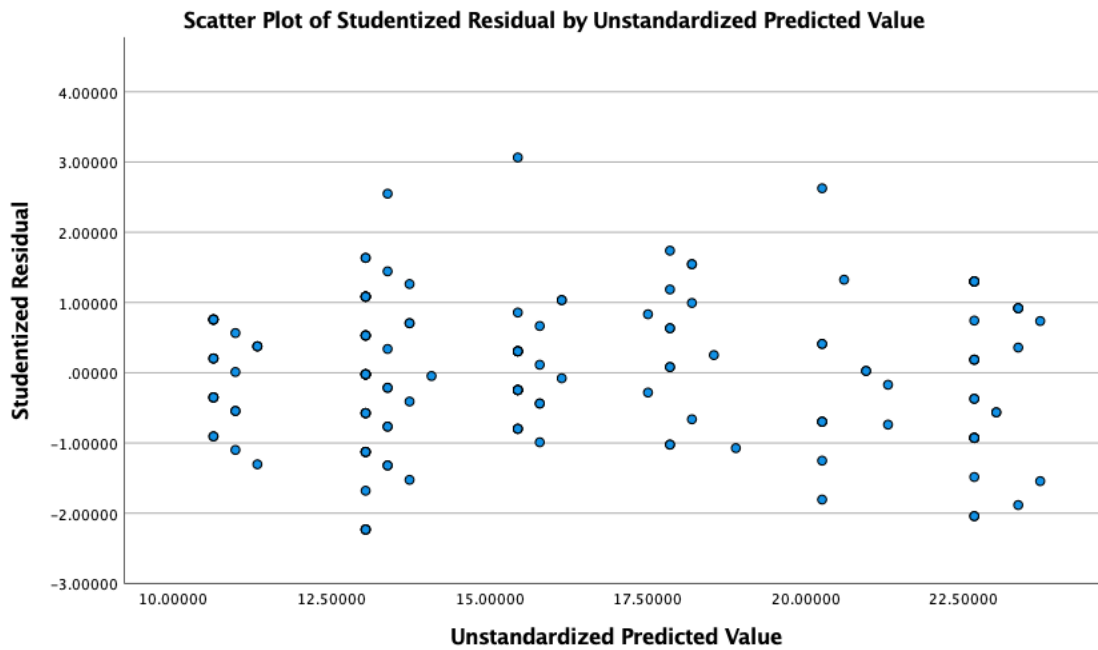
- Lesser trochanter of the femur: Unfused Romans were found from Pre-puberty to PHV. One partially fused Roman skeleton was recorded in PHV, whereas the other was recorded in Deceleration. Those who had completely fused at the time of their death were in Maturation and Completion. The mean pubertal phase at fusion (Stages 2 and 3) for the Roman group was Deceleration (mean phase = 4.33, s.d. = 1.53). Unfused Anglo-Saxons followed the same pattern as the Roman group. One partially fused Anglo-Saxon was listed in PHV and those who had completely fused were in Deceleration and beyond. The mean pubertal phase at fusion (Stages 2 and 3) was Deceleration (mean phase = 3.50, s.d. = 0.71) for the Anglo-Saxon sample. There was no significant difference in the mean pubertal phase at fusion (Stages 2 and 3) when the Roman and Anglo-Saxon samples were compared ( $U = 2.000, p = 0.543$ ). Unfused and partially fused Mediaeval skeletons followed the same pattern as the Roman sample. Those who had completely fused at the time of death were found in PHV onwards. The mean pubertal phase at fusion (Stages 2 and 3) was Deceleration (mean phase = 3.50, s.d. = 0.84). There was no significant difference in the mean pubertal phase at fusion between the Roman and Mediaeval samples ( $U = 5.500, p = 0.320$ ), nor the Anglo-Saxon and Mediaeval samples ( $U = 5.500, p = 0.847$ ).

- Distal epiphysis of the femur: The Deceleration phase was missing from the Roman data. Unfused Romans were recorded up to PHV, whereas completely fused individuals were recorded from Maturation onwards. Unfused Anglo-Saxons were found from Pre-puberty, whereas partially fused Anglo-Saxons were in Deceleration only. Those who had completely fused were found in Maturation and Completion. The mean pubertal phase at fusion (Stages 2 and 3) for the Anglo-Saxon sample was Maturation (s.d. = 1.16). Unfused Mediaeval skeletons were found from Pre-puberty to Deceleration. Partially fused Mediaeval skeletons were in Deceleration and Maturation, while those who had completely fused were in PHV onwards. The mean pubertal phase at fusion (Stages 2 and 3) was Maturation (s.d. = 0.87). There was no significant difference in the mean pubertal phase at fusion between the Mediaeval and Anglo-Saxon groups ( $U = 18.000, p = 1.000$ ).
- Proximal epiphysis of the tibia: Unfused Romans were recorded from Pre-puberty to PHV. One partially fused Roman was in PHV and the other in Deceleration. Those who had completely fused were found in Maturation and Completion. The mean pubertal phase at fusion (Stages 2 and 3) for the Roman group was Deceleration (mean phase = 4.33, s.d. = 1.53). Unfused Anglo-Saxons were the same as the Roman sample. Partially fused Romans were in Deceleration only and completely fused Romans were recorded from Deceleration onwards. The mean pubertal phase at fusion (Stages 2 and 3) for the Anglo-Saxon sample is Deceleration (s.d. = 0.000). There was no significant difference in the mean pubertal phase at fusion between the Roman and Anglo-Saxon samples ( $U = 4.500, p = 1.000$ ). Unfused Mediaeval skeletons were found from Pre-puberty until Deceleration. Partially fused Mediaeval individuals were in PHV to Maturation, whereas those who had completely fused were recorded from PHV onwards. The mean pubertal phase at fusion (Stages 2 and 3) for the Mediaeval samples was Maturation (mean phase = 4.75, s.d. = 1.04). There was no significant difference in the mean pubertal phase at fusion between the Roman and Mediaeval samples ( $U = 9.500, p = 0.599$ ), nor the Anglo-Saxon and Mediaeval samples ( $U = 6.000, p = 0.193$ ).
- Distal epiphysis of the tibia: The Deceleration phase was missing for the Roman sample. However, unfused Romans were found up until PHV and completely fused Romans were from Maturation onwards. Unfused Anglo-Saxons were also found up

until PHV, but completely fused Anglo-Saxons were found from Deceleration onwards. Unfused Mediaeval individuals were the same as the Romans and Anglo-Saxons. The Mediaeval sample had individuals in PHV and Deceleration for partial fusion and from PHV onwards for those who had completed fusion before death. The mean pubertal phase for the Mediaeval sample for the fusion of the distal epiphysis of the tibia was Deceleration (mean phase = 4.40, s.d. = 1.08).

## APPENDIX 15: MULTIVARIATE ANALYSIS OF PUBERTY WITHIN THE ARCHAEOLOGICAL SITES

The Scatterplot below shows the studentised deleted residuals and studentised residuals for puberty phase and age for all archaeological periods apart from the Iron Age to test the linear relationship and homoscedasticity.



The tables below gives the leverage points and Cook's Distance Values for the multiple regression.

<b>COO 1</b>	<b>LEV 1</b>
.00139	.00308
.00018	.00538
.02568	.00538
.00018	.00538
.00194	.01295
.00824	.00538
.00210	.01295
.00004	.00209
.00687	.00538
.00687	.00538
.00444	.00487
.00002	.00397
.00026	.01174
.00124	.00487
.00027	.00228

---

<b>COO 1</b>	<b>LEV 1</b>
.00075	.01174
.00000	.00487
.01011	.00487
.00000	.00487
.00353	.01174
.00107	.00487
.00000	.00487
.00107	.00487
.00027	.00228
.00093	.00994
.00444	.00487
.00353	.01174
.00444	.00487
.00479	.00487
.00268	.00994
.00000	.00487
.00444	.00487
.01796	.00994
.00000	.00487
.00017	.00228
.00479	.00487
.00107	.00487
.00780	.02019
.00027	.00228
.00479	.00487
.00353	.01174
.01999	.02019
.00027	.00228
.00353	.01174
.01880	.00487
.00124	.00487
.00002	.00397
.00353	.01174
.01011	.00487
.00140	.00397
.00017	.00228
.01536	.02019
.03782	.02019
.00032	.02019
.00502	.01174
.00124	.00487
.01536	.02019
.00502	.02019
.00017	.00228
.00213	.00228
.00184	.00228
.00075	.01174
.03782	.02019
.00780	.02019
.00444	.00487
.00363	.00397
.00032	.02019
.01880	.00487
.03804	.00994

---

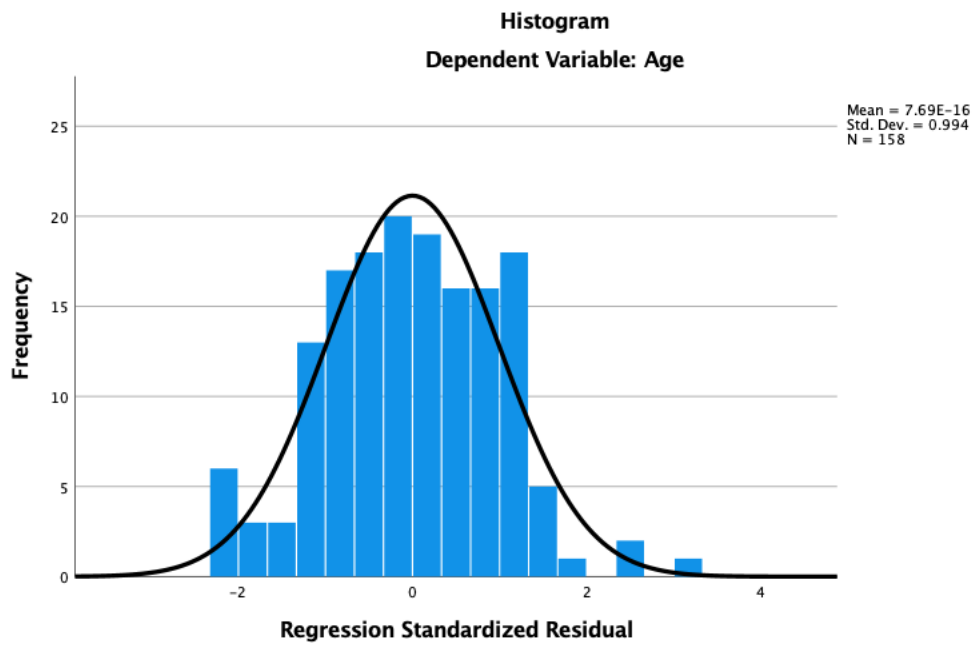
<b>COO 1</b>	<b>LEV 1</b>
.00017	.00228
.00124	.00487
.00502	.01174
.00075	.01174
.01049	.00397
.00107	.00487
.00124	.02019
.00017	.00228
.01536	.02019
.00268	.00994
.00780	.02019
.00488	.00397
.00093	.00994
.01536	.02019
.00780	.02019
.02720	.00228
.00026	.01174
.01536	.02019
.01880	.00487
.00444	.00487
.00268	.00994
.01536	.02019
.00863	.00994
.00479	.00487
.00032	.02019
.00075	.01174
.00027	.00228
.01064	.00487
.00000	.00487
.01880	.00487
.00353	.01174
.00000	.00487
.00000	.00487
.00363	.00397
.00026	.01174
.00107	.00487
.00027	.00228
.00017	.00228
.00184	.00228
.00184	.00228
.00498	.02275
.01138	.03249
.00001	.02363
.00167	.02275
.00498	.02275
.00919	.01876
.01595	.02275
.01138	.03249
.02196	.03101
.02319	.02275
.01138	.03249
.00184	.03101
.00919	.01876
.00045	.00538

---

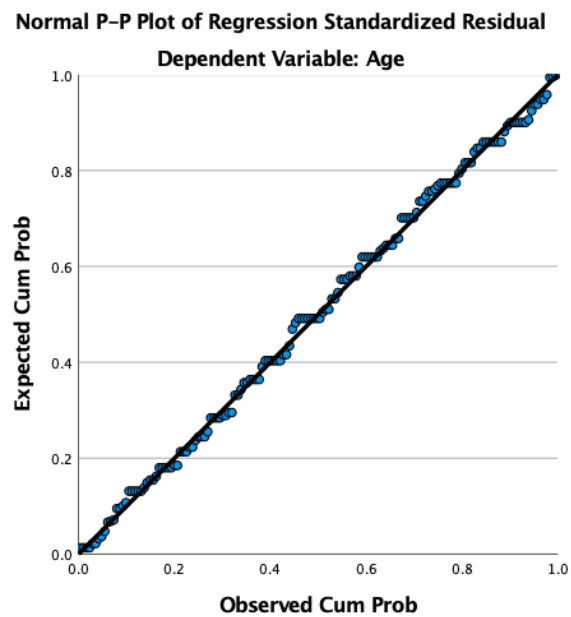
<b>COO 1</b>	<b>LEV 1</b>
.00232	.00538
.00873	.00836
.00790	.01295
.00126	.00209
.00277	.00209
.00001	.02363
.04772	.03249
.00055	.01906
.00184	.03101
.00184	.03101
.00005	.01876
.00174	.03249
.00076	.02171
.00757	.00308
.00757	.00308
.00124	.02019
.00444	.00487
.00140	.00397
.00479	.00487
.00668	.02171
.00780	.02019
.05993	.06393
.00005	.05697
.01368	.06393
.00064	.05577
.01201	.05577
.02369	.05189
.00262	.01791
.00194	.01295
.00262	.01791
.00313	.00308
.00000	.01295
.00054	.00209
.00232	.00538
.00054	.00209

---

The figure below shows a histogram to see if errors are normally distributed.



The figure below shows a normal p-p plot to check for any distributed errors.



## APPENDIX 16: ROMAN AND MEDIAEVAL AGES AT FUSION COMPARED TO PUBLISHED LITERATURE

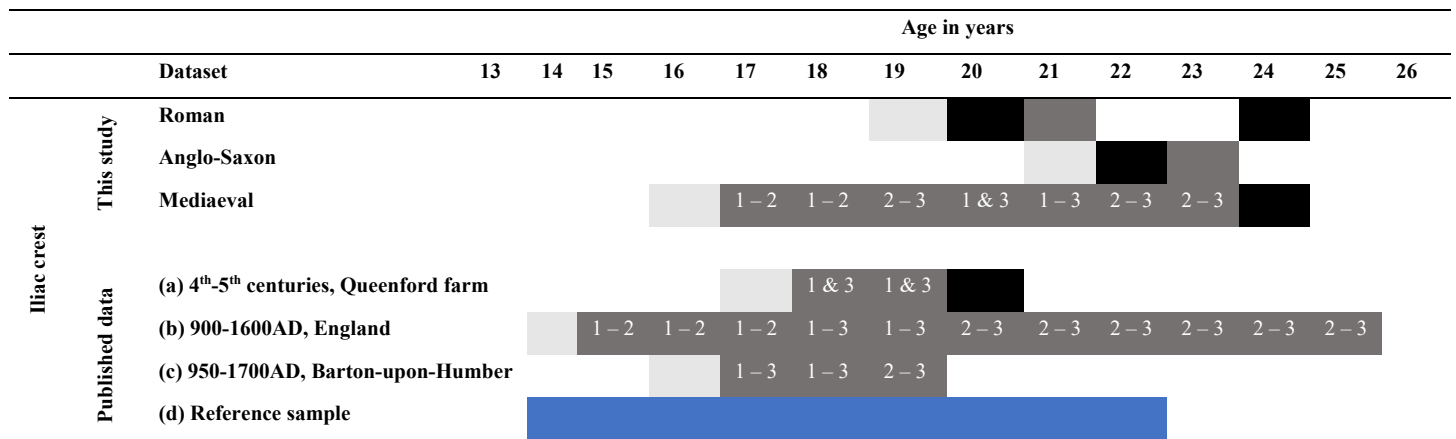
The figure below shows the fusion of the pars lateralis to the pars basilaris of the occipital bone of the skull split by primary data collected for this thesis and secondary data, which was taken from published literature. References are below. Light grey = unfused (Stage 1). Dark grey = partial fusion (Stage 2). Black = complete fusion (Stage 3). Stages of fusion may overlap due to variation in individuals. To keep the table simple, overlap of fusion stages is denoted by the white text. The Reference Sample is shown in blue as partial fusion (Stage 2) and complete fusion (Stage 3) are not distinguished in the text. References: (a) Mediaeval, Mistihalj, Former Yugoslavian-Albanian border, 1400-1475AD, dry bone (Redfield, 1970), (b) Post-Mediaeval/Modern reference sample (Schaefer et al., 2009).

			Age in years								
			3	4	5	6	7	8	9	10	
Pars lateralis to pars basilaris	This study	Anglo-Saxon				1 – 2	1 – 3	1 – 3			
		Mediaeval					1 & 3	1 & 3			
	Published data	(a) Mediaeval, Balkans									
		(b) Reference sample									

The figure below shows the fusion of the distal epiphysis of the radius split by primary data collected for this thesis and secondary data, which was taken from published literature. References are below. Light grey = unfused (Stage 1). Dark grey = partial fusion (Stage 2). Black = complete fusion (Stage 3). Stages of fusion may overlap due to variation in individuals. To keep the table simple, overlap of fusion stages is denoted by the white text. The Reference Sample is shown in blue as partial fusion (Stage 2), and complete fusion (Stage 3) are not distinguished in the text. References: (a) Roman, Queenford Farm, England, early 4<sup>th</sup> – 5<sup>th</sup> century AD, female data taken only, dry bone (Arthur et al., 2016), (b) Mediaeval, Barton-upon-Humber, England, 950-1700AD, dry bone (Shapland and Lewis, 2013), (c) Mediaeval, Various sites, England, 900-1600AD, dry bone (Shapland et al., 2015), (d) Post-Mediaeval/Modern reference sample (Schaefer et al., 2009).

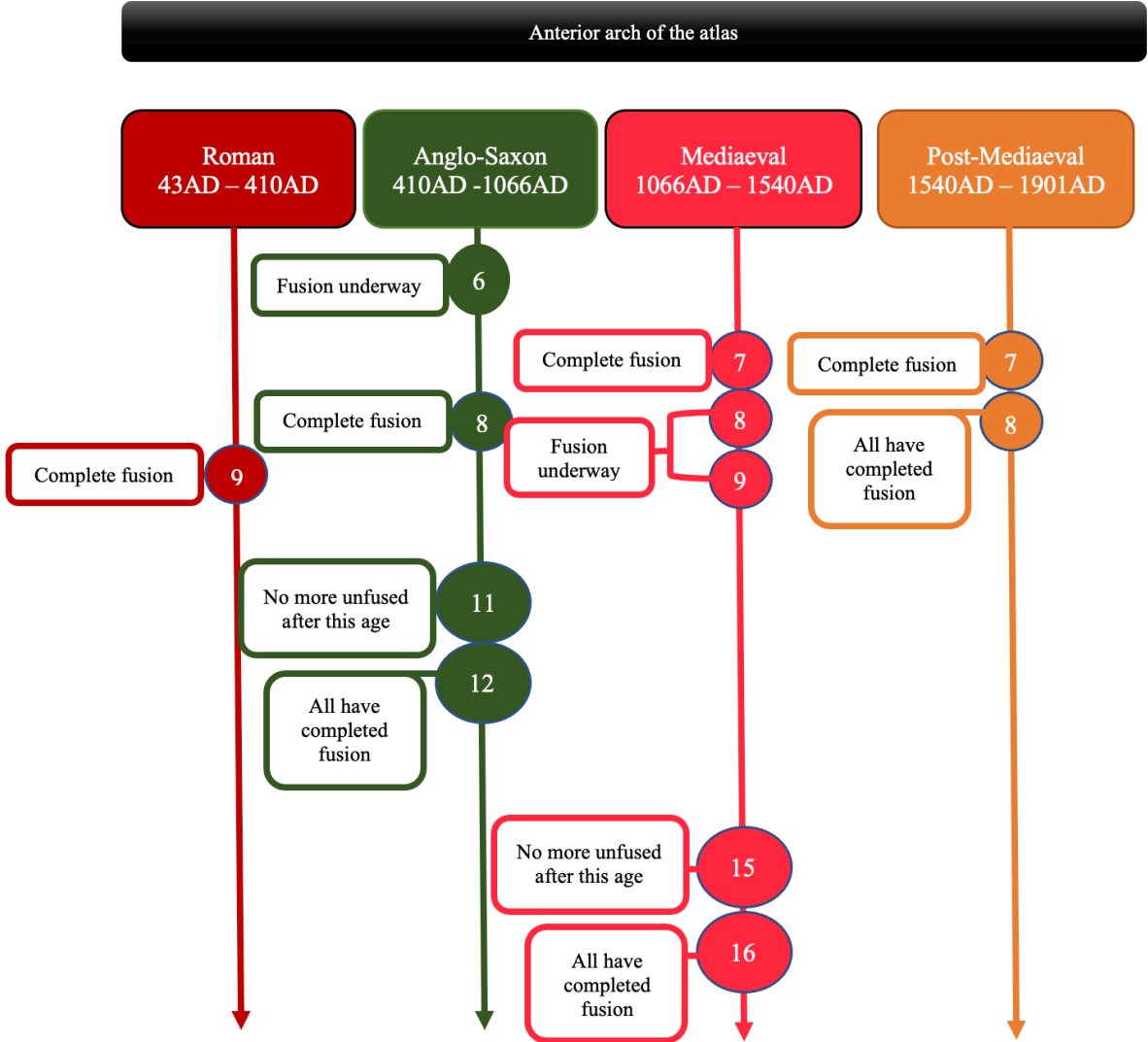


The figure below shows the fusion of the iliac crest of the os coxae split by primary data collected for this thesis and secondary data, which was taken from published literature. References are below. Light grey = unfused (Stage 1). Dark grey = partial fusion (Stage 2). Black = complete fusion (Stage 3). Stages of fusion may overlap due to variation in individuals. To keep the table simple, overlap of fusion stages is denoted by the white text. The Reference Sample is shown in blue as partial fusion (Stage 2) and complete fusion (Stage 3) are not distinguished in the text. References: (a) Roman, Queenford Farm, England, early 4<sup>th</sup>-5<sup>th</sup> century AD, dry bone (Arthur et al., 2016), (b) Mediaeval, Various sites, England, 900-1600AD, dry bone (Shapland et al., 2015), (c) Mediaeval, Barton-upon-Humber, England, 950-1700AD, dry bone (Shapland and Lewis, 2013), (d) Post-Mediaeval/ Modern reference sample (Schaefer et al., 2009).

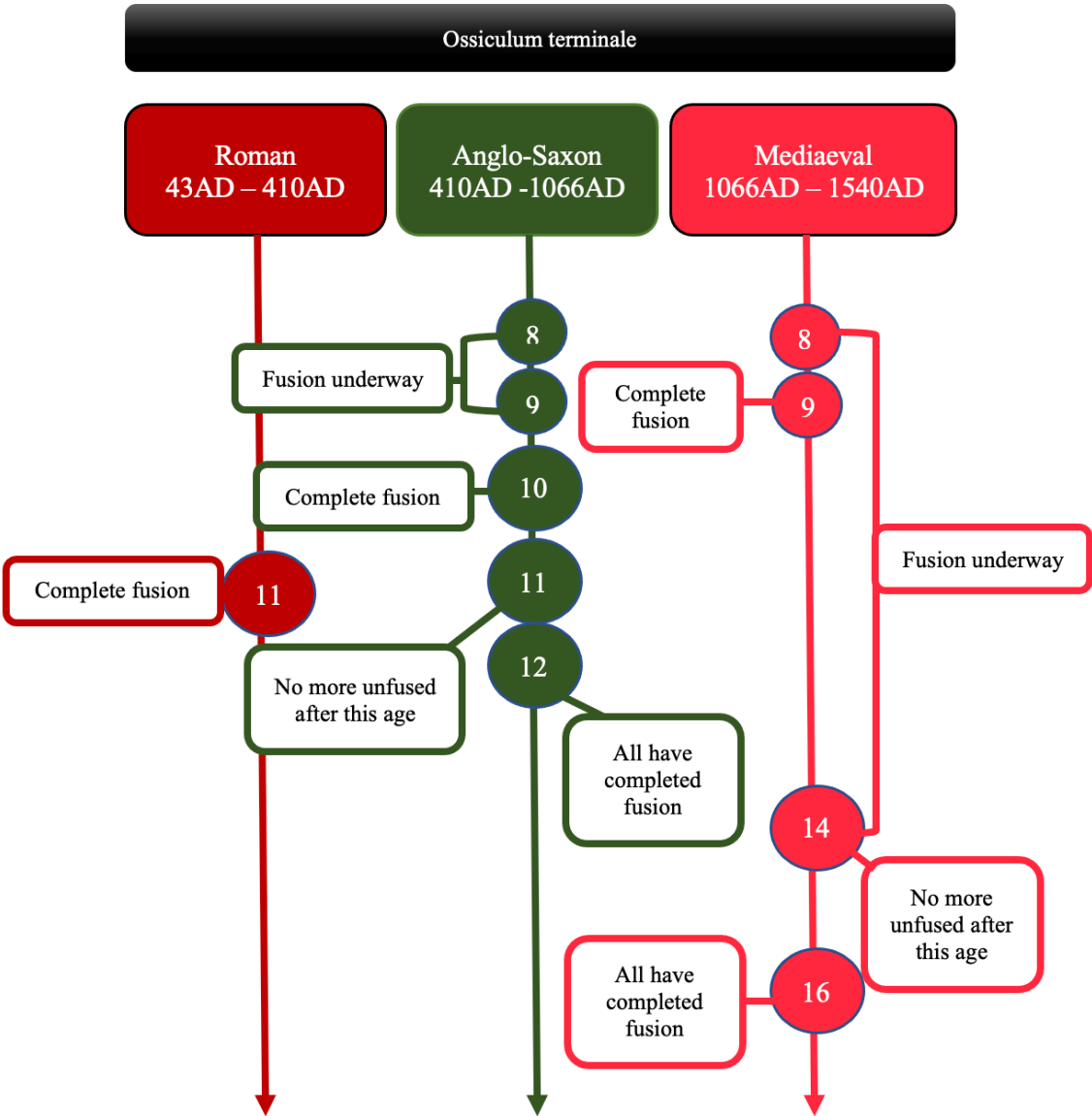


**APPENDIX 17: AGE-AT-FUSION ACROSS PERIODS IN FIGURE FORM**

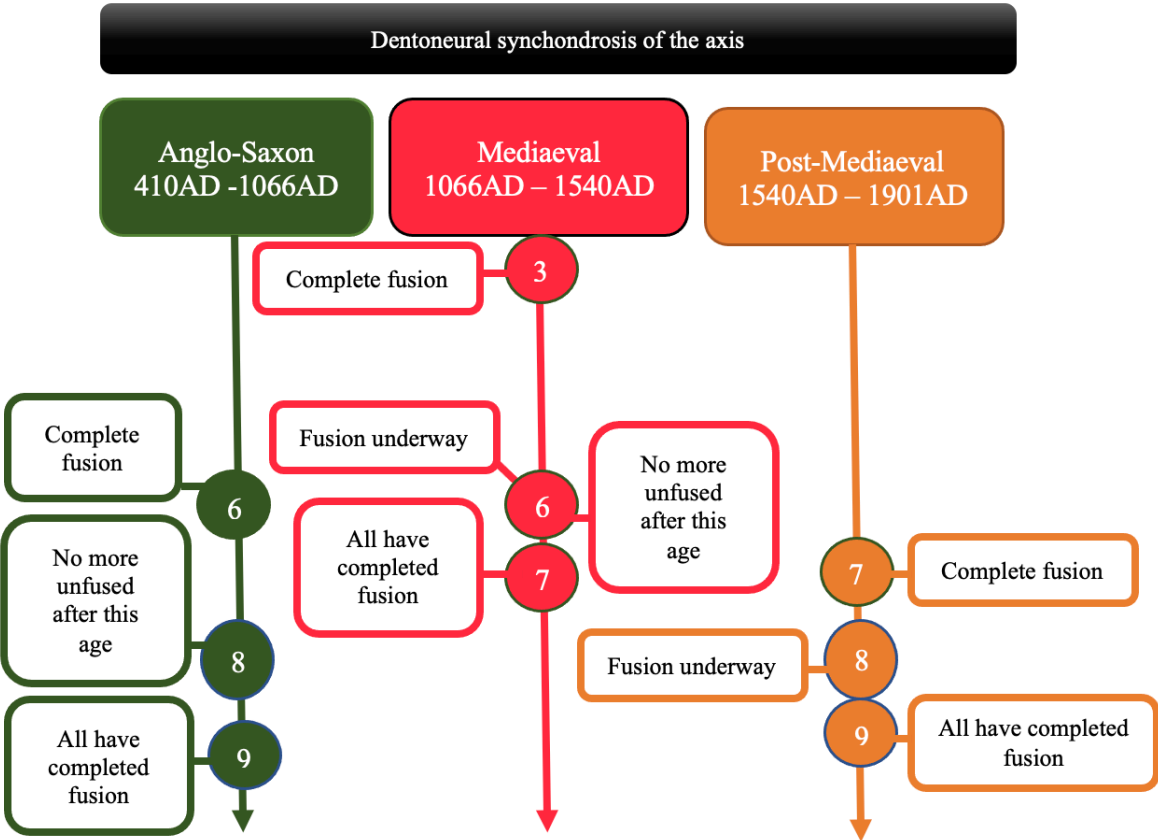
The figure below shows the fusion of the anterior arch of the atlas compared between the archaeological groups. Age in years is given in coloured circles.



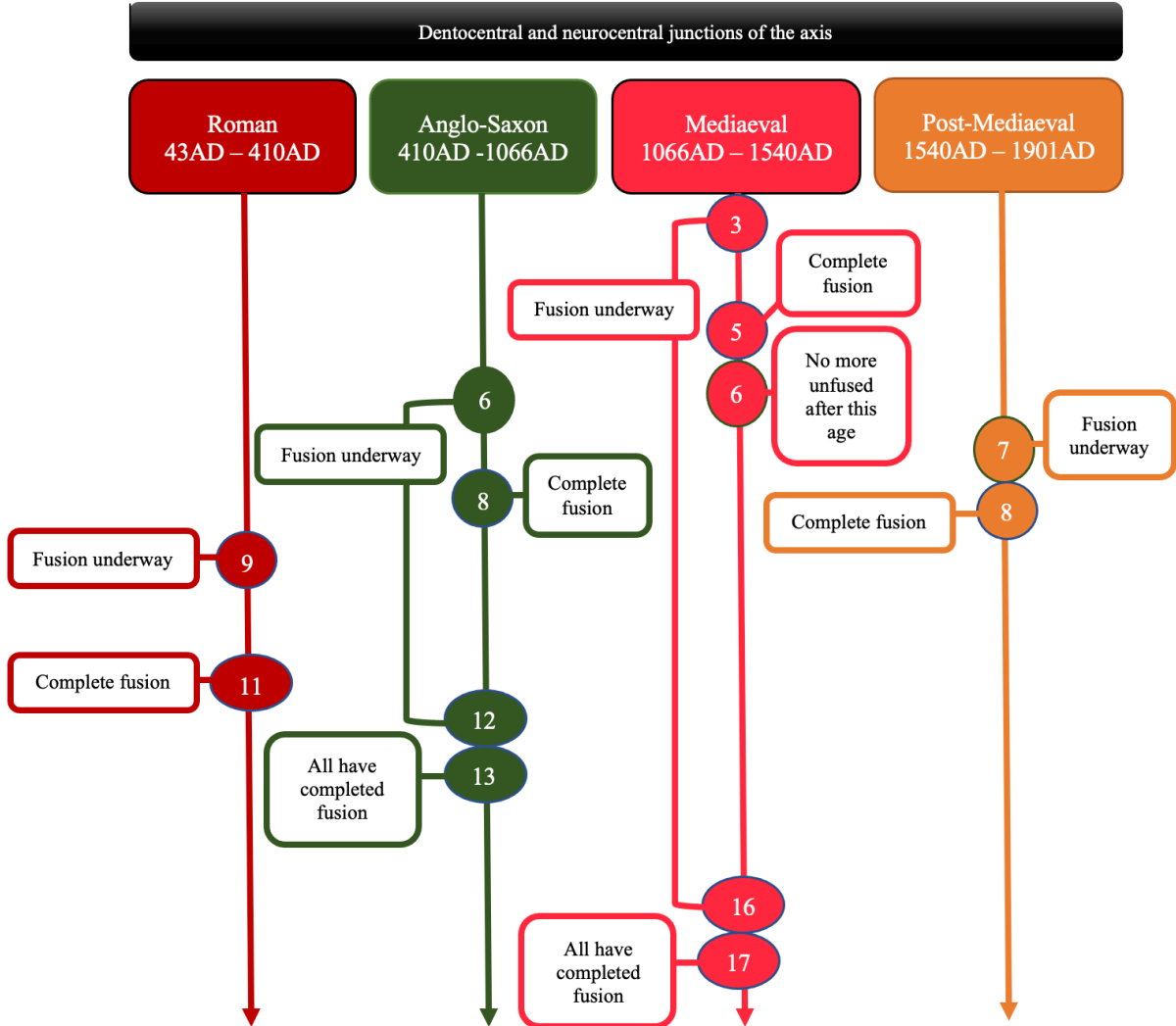
The figure below shows the fusion of the ossiculum terminale of the dens of the axis. Age in years is given in coloured circles.



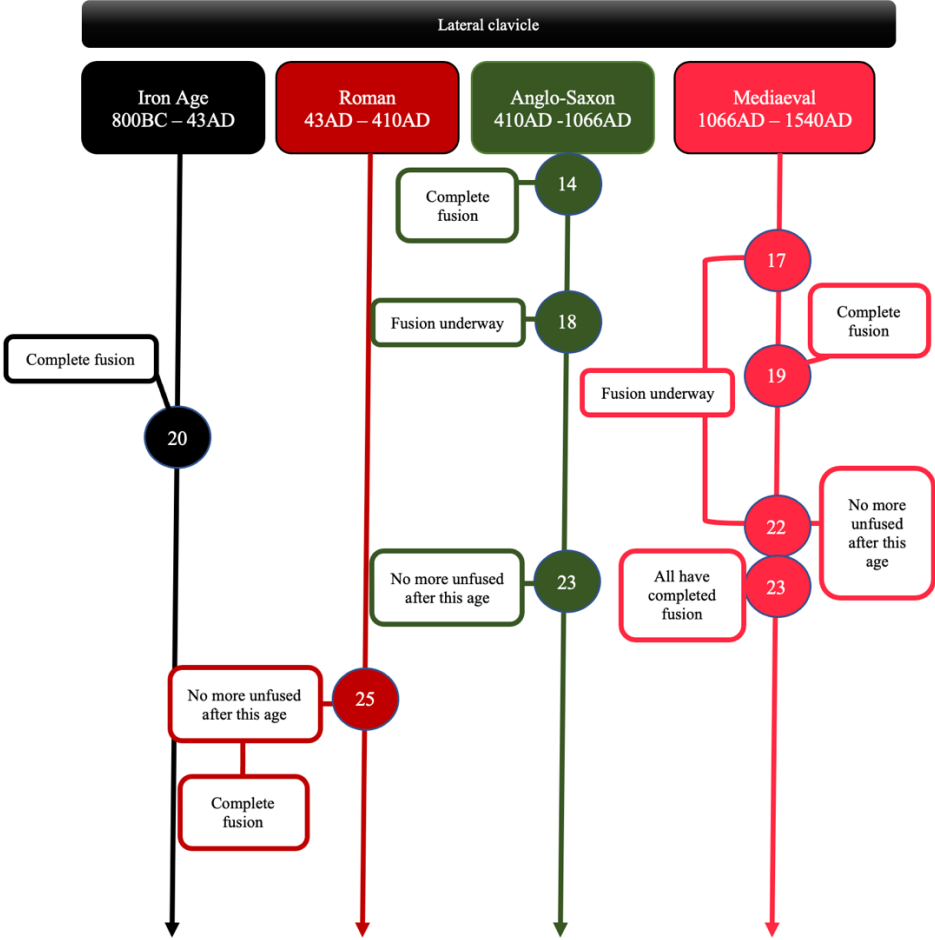
The figure below shows the fusion of the dentoneural synchondrosis of the axis. Age in years is given in coloured circles.



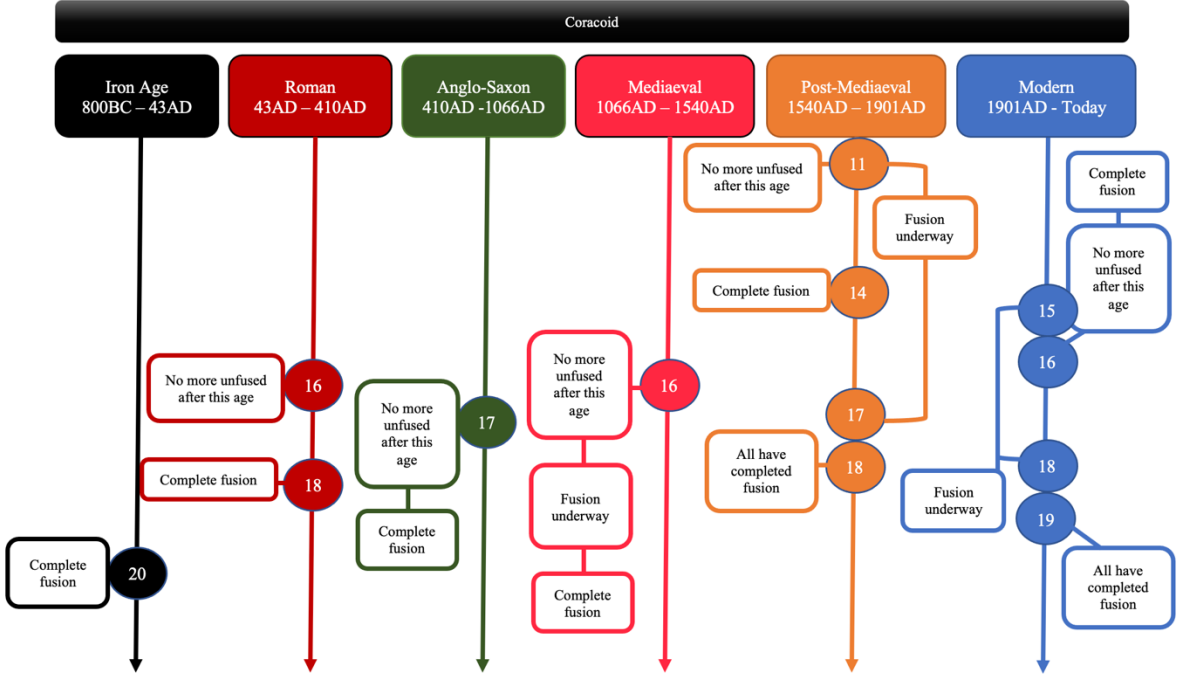
The figure below shows the fusion of the dentocentral and neurocentral junctions of the axis. Age in years is given in coloured circles.



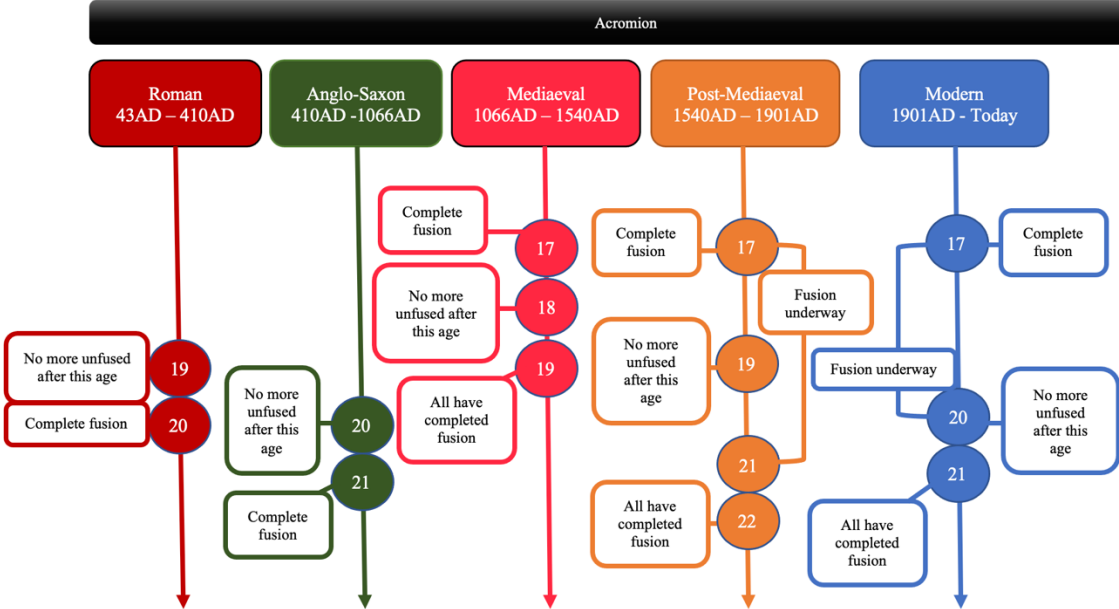
The figure below shows the fusion of the lateral clavicle compared between archaeological groups. Age in years is given in coloured circles.



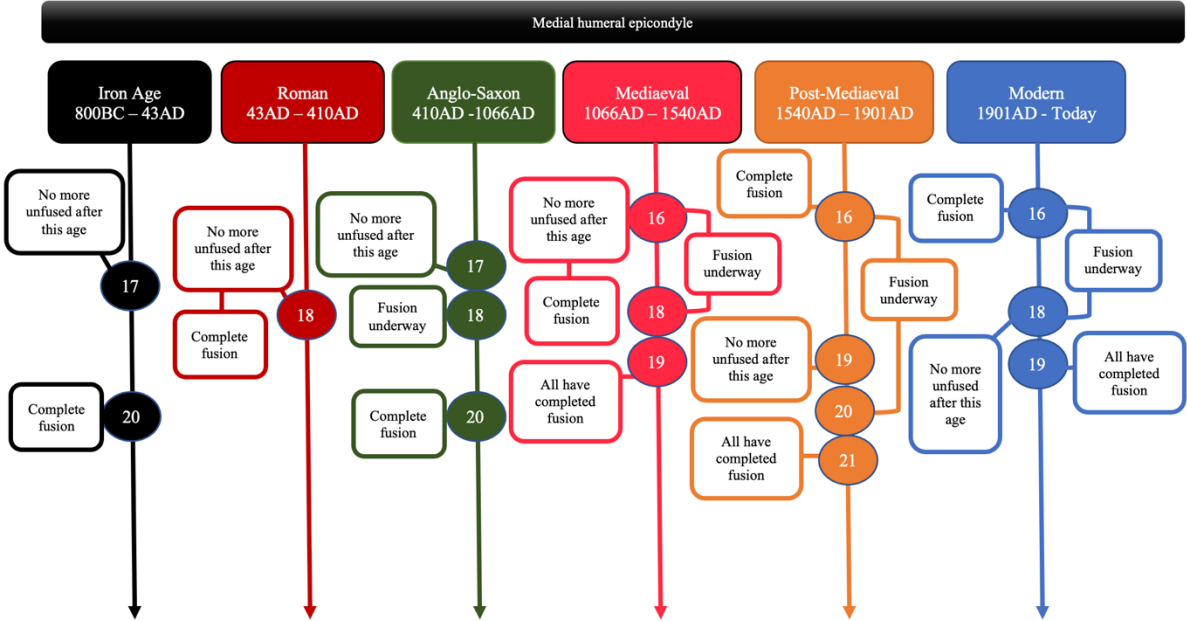
The figure below shows the fusion of the coracoid process of the scapula compared between archaeological groups. Age in years is given in coloured circles. Post-Mediaeval data is from 1826-1938AD Coimbra females, dry bone (Coqueugniot and Weaver, 2007), Modern data is from Bosnia, 1995AD (war victims from the fall of Srebrenica), males only, dry bone (Schaefer, 2008b).



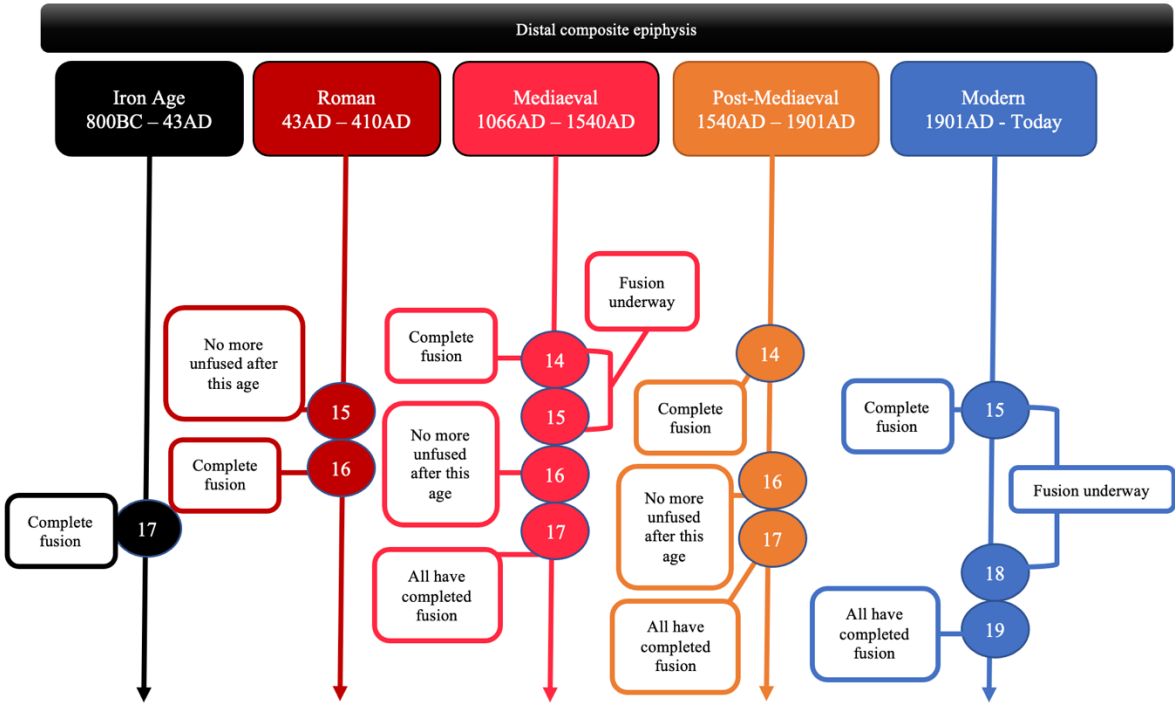
The figure below shows the fusion of the acromion of the scapula compared between archaeological groups. Age in years is given in coloured circles. Post-Mediaeval data is from 1826-1938AD Coimbra females, dry bone (Coqueugniot and Weaver, 2007), Modern data is from Bosnia, 1995AD (war victims from the fall of Srebrenica), males only, dry bone (Schaefer, 2008b).



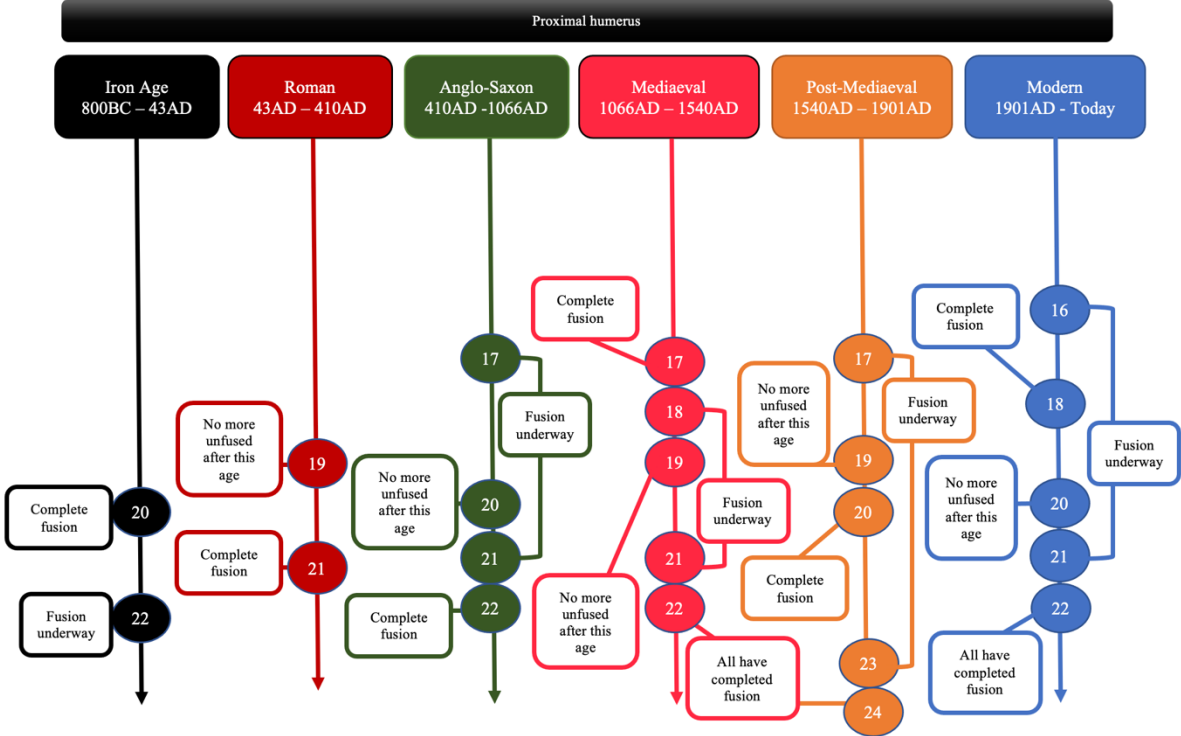
The figure below shows the fusion of the medial humeral epicondyle compared between archaeological groups. Age in years is given in coloured circles. Post-Mediaeval data is from 1826-1938AD Coimbra males, dry bone (Coqueugniot and Weaver, 2007), Modern data is from Bosnia, 1995AD (war victims from the fall of Srebrenica), males only, dry bone (Schaefer, 2008b).



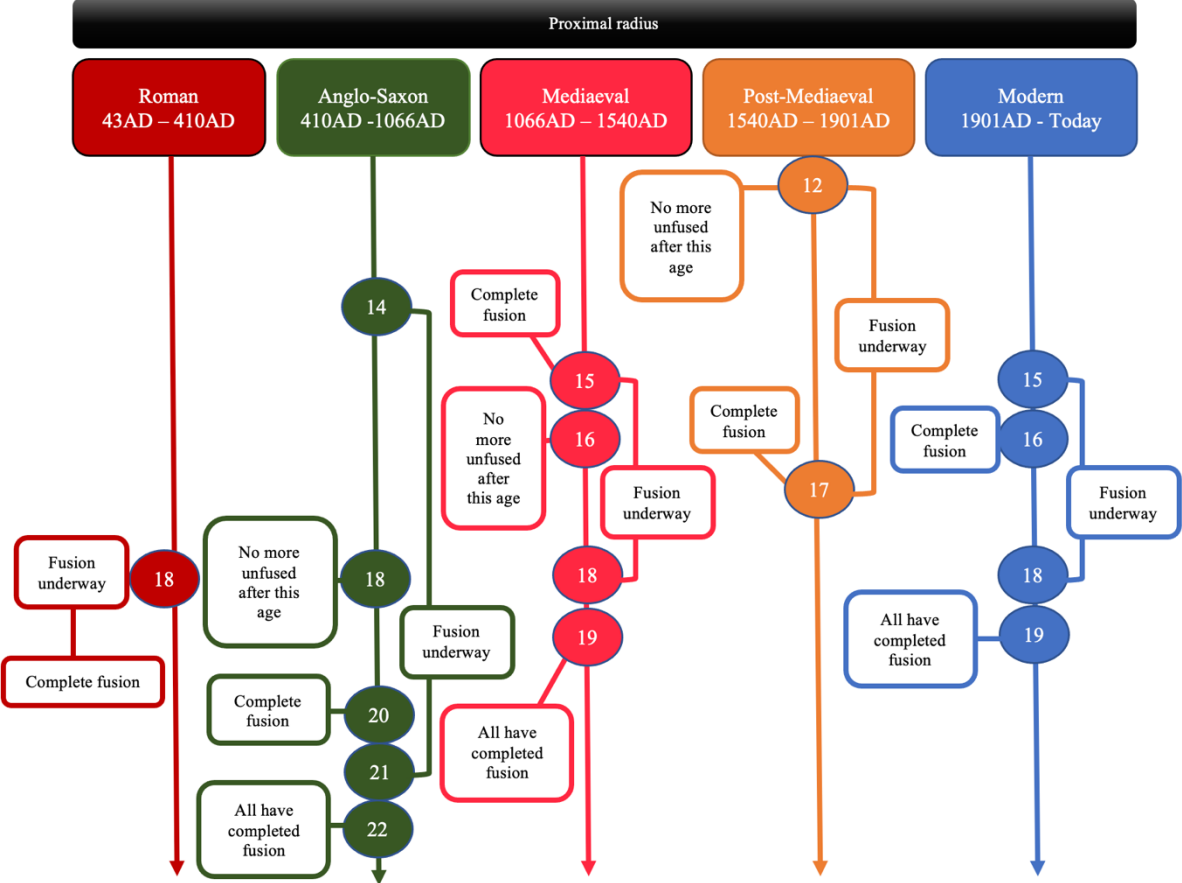
The figure below shows the fusion of the distal composite epiphysis of the humerus compared between archaeological groups. Age in years is given in coloured circles. Post-Mediaeval data is taken from 1887-1975AD Lisbon males, dry bone (Cardoso, 2008a), Modern data is from Bosnia, 1995AD (war victims from the fall of Srebrenica), males only, dry bone (Schaefer, 2008b).



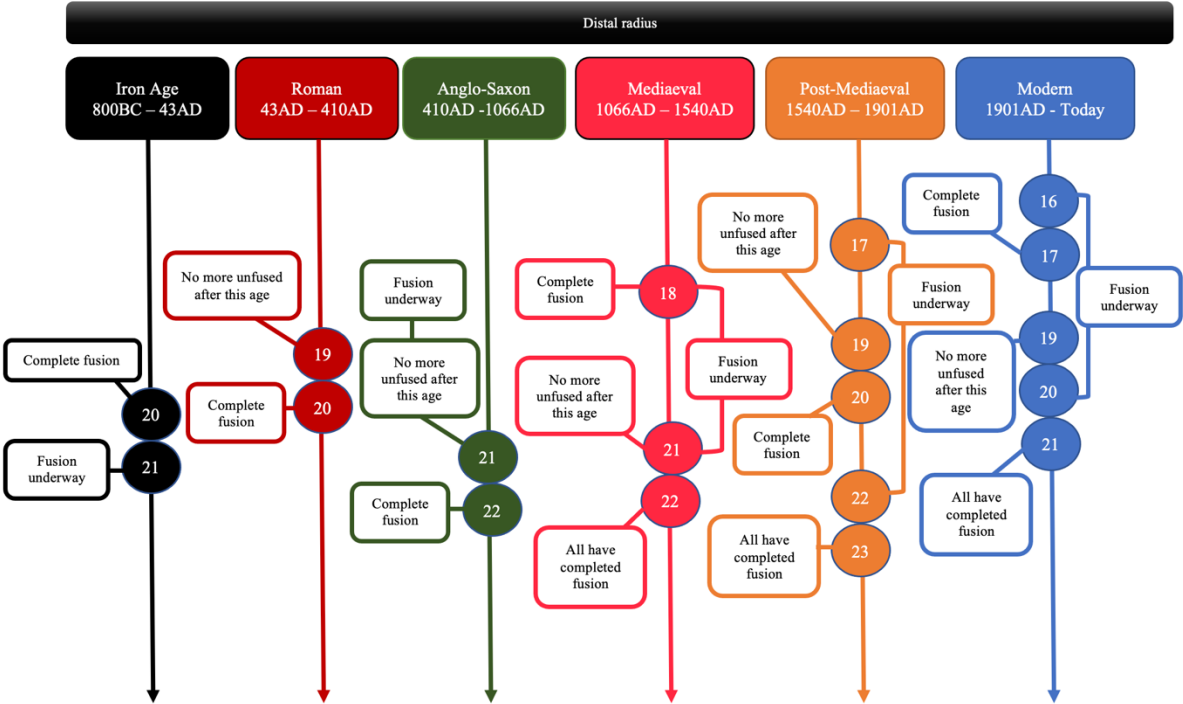
The figure below shows the fusion of the proximal humerus compared between archaeological groups. Age in years is given in coloured circles. Post-Mediaeval data is taken from 1826-1938AD Coimbra females (Coqueugniot and Weaver, 2007), Modern data is from Bosnia, 1995AD (war victims from the fall of Srebrenica), males only, dry bone (Schaefer, 2008b).



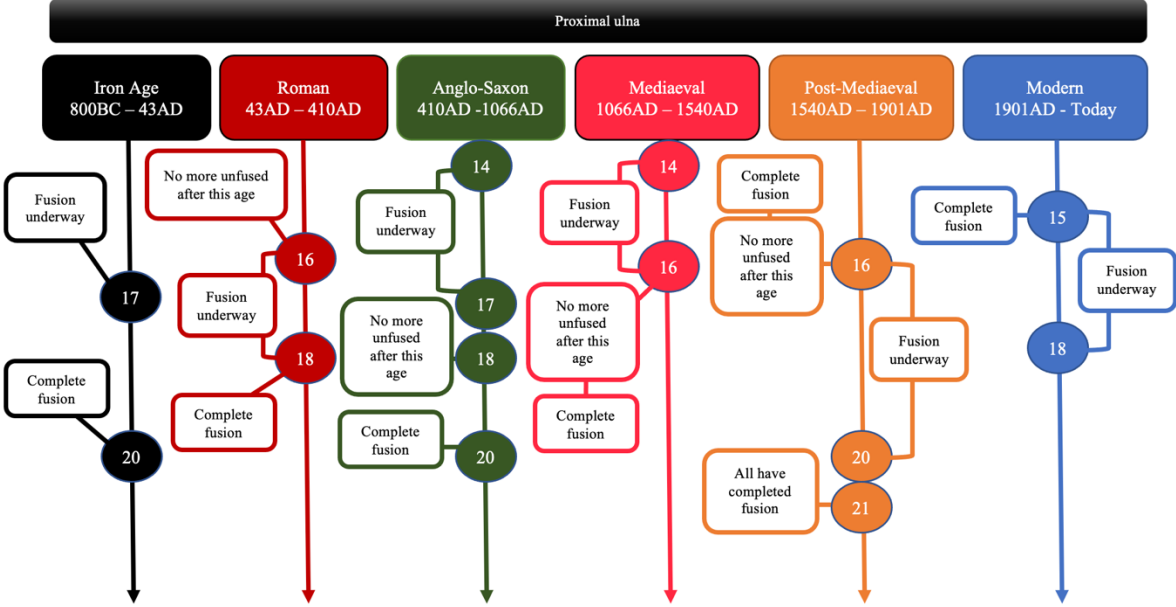
The figure below shows the fusion of the proximal radius compared between archaeological groups. Age in years is given in coloured circles. Post-Mediaeval data is taken from 1826-1938AD Coimbra females (Coqueugniot and Weaver, 2007), Modern data is from Bosnia, 1995AD (war victims from the fall of Srebrenica), males only, dry bone (Schaefer, 2008b).



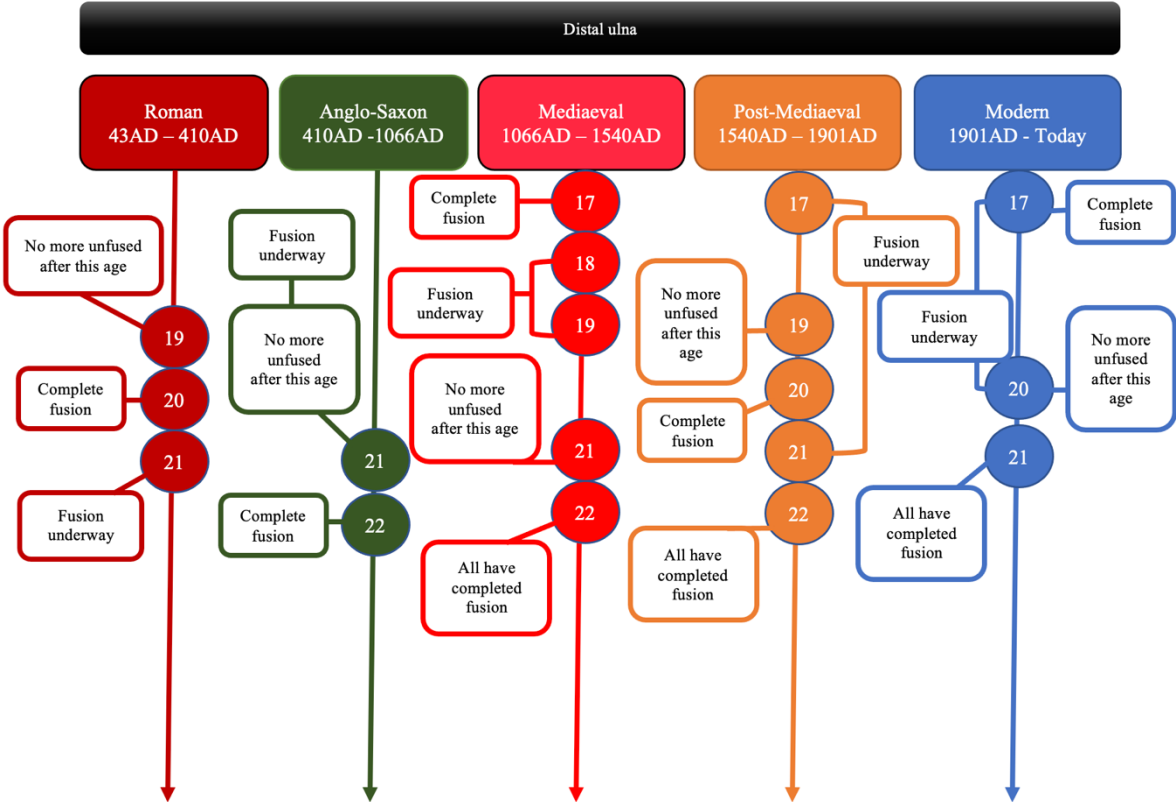
The figure below shows the fusion of the distal radius compared between archaeological groups. Age in years is given in coloured circles. Post-Mediaeval data is taken from 1826-1938AD Coimbra females (Coqueugniot and Weaver, 2007), Modern data is from Bosnia, 1995AD (war victims from the fall of Srebrenica), males only, dry bone (Schaefer, 2008b).



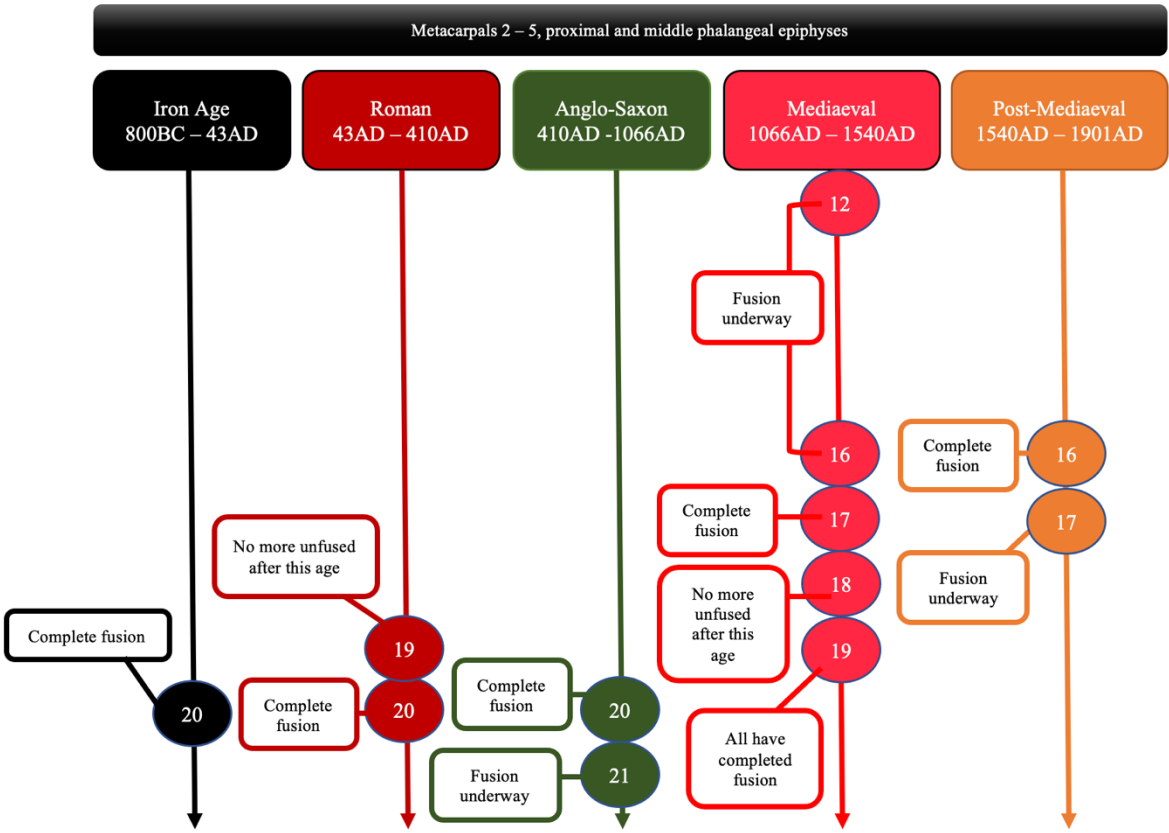
The figure below shows the fusion of the proximal ulna compared between archaeological groups. Age in years is given in coloured circles. Post-Mediaeval data is taken from 1826-1938AD Coimbra males (Coqueugniot and Weaver, 2007), Modern data is from Bosnia, 1995AD (war victims from the fall of Srebrenica), males only, dry bone (Schaefer, 2008b).



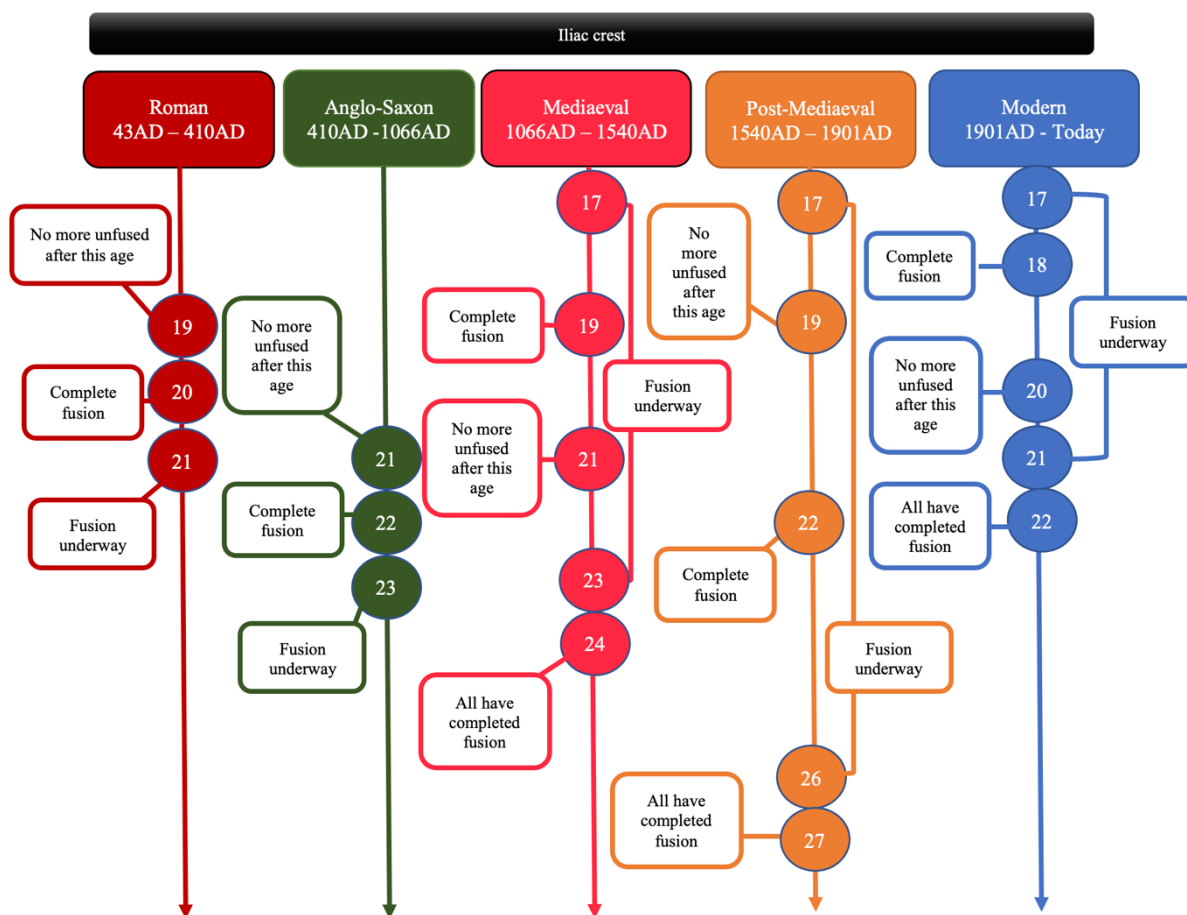
The figure below shows the fusion of the distal ulna compared between archaeological groups. Age in years given in coloured circles. Post-Mediaeval data is taken from 1826-1938AD Coimbra females (Coqueugniot and Weaver, 2007), Modern data is from Bosnia, 1995AD (war victims from the fall of Srebrenica), males only, dry bone (Schaefer, 2008b).



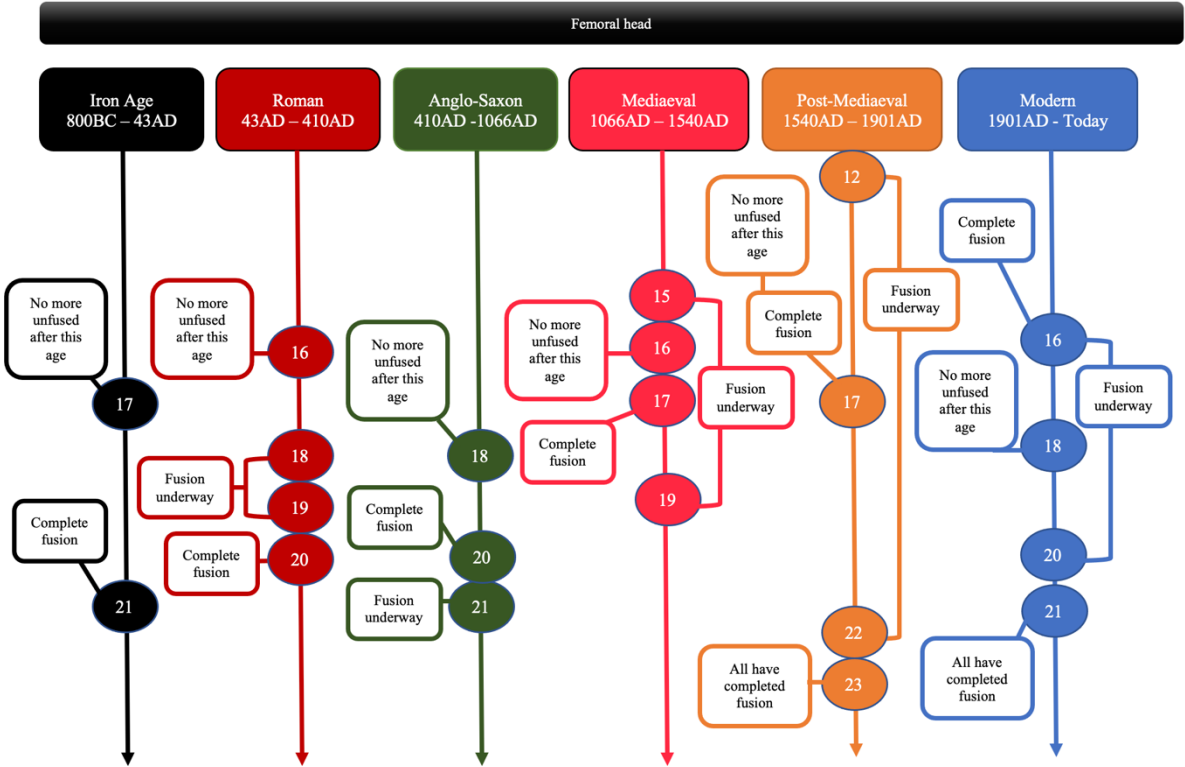
The figure below shows the fusion of the metacarpals 2 – 5, as well as the proximal and middle phalangeal epiphyses of the hand. Age in years is given in colour.



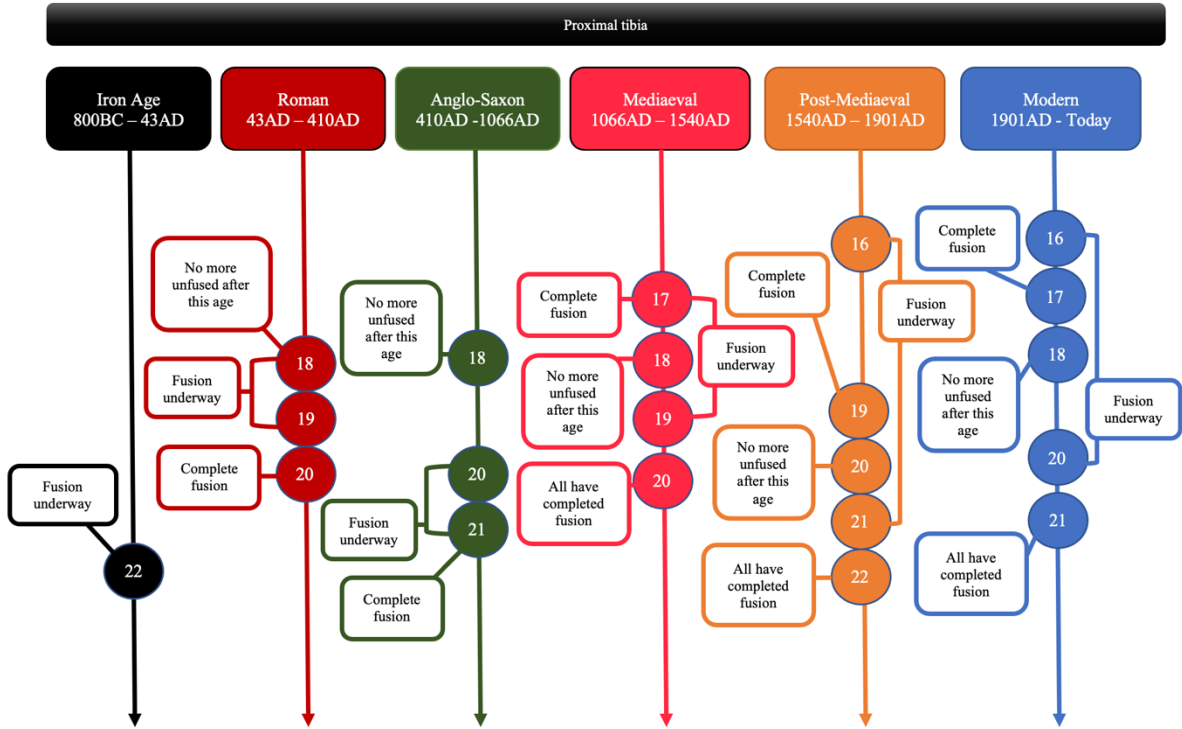
The figure below shows the fusion of the iliac crest compared between archaeological groups. Age in years given in coloured circles. Post-Mediaeval data is taken from 1826-1938AD Coimbra females (Coqueugniot and Weaver, 2007), Modern data is from Bosnia, 1995AD (war victims from the fall of Srebrenica), males only, dry bone (Schaefer, 2008b).



The figure below shows the fusion of the femoral head compared between archaeological groups. Age in years given in coloured circles. Post-Mediaeval data is taken from 1826-1938AD Coimbra females (Coqueugniot and Weaver, 2007), Modern data is from Bosnia, 1995AD (war victims from the fall of Srebrenica), males only, dry bone (Schaefer, 2008b).

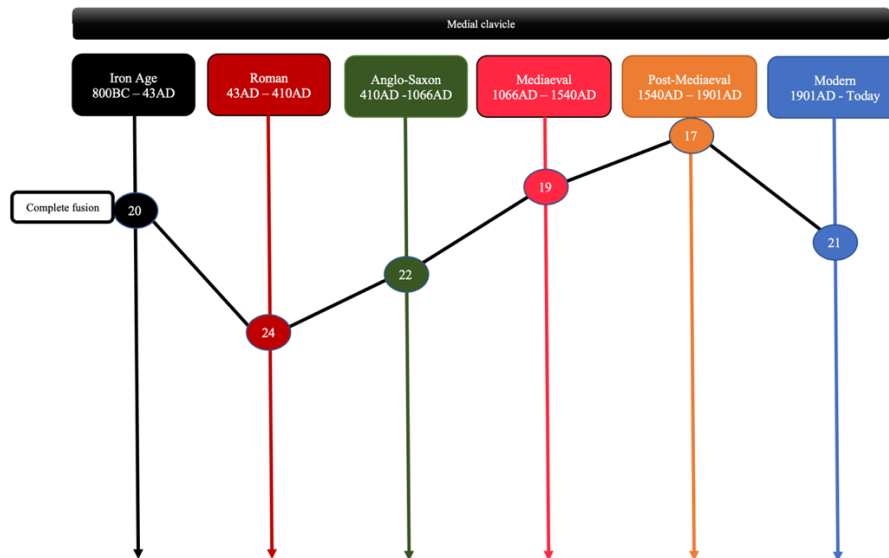


The figure below shows the fusion of the proximal tibia compared between archaeological groups. Age in years given in coloured circles. Post-Mediaeval data is taken from 1826-1938AD Coimbra males (Coqueugniot and Weaver, 2007), Modern data is from Bosnia, 1995AD (war victims from the fall of Srebrenica), males only, dry bone (Schaefer, 2008b).

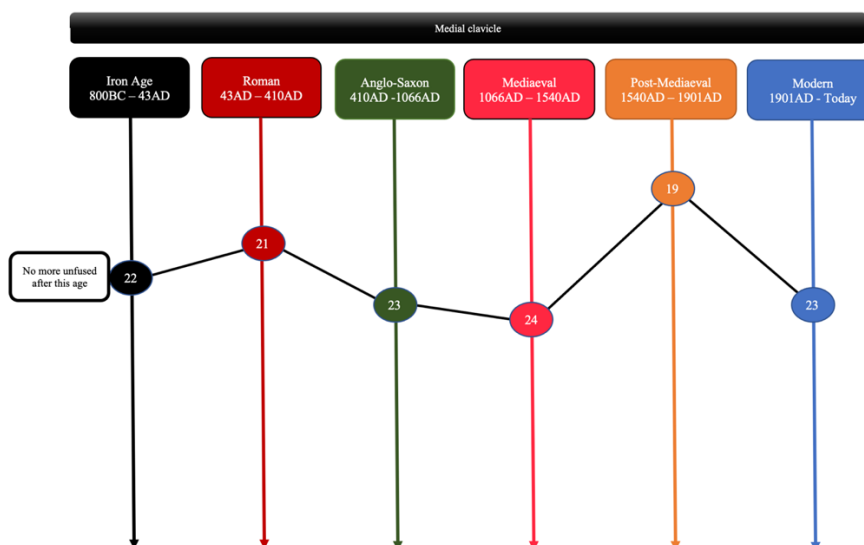


## APPENDIX 18: AGE-AT-FUSION ACROSS PERIODS FOR THE MEDIAL CLAVICLE

The figure below shows the complete fusion of the medial clavicle compared between archaeological groups. Age in years is given in coloured circles. Modern data is from Bosnia, 1995AD (war victims from the fall of Srebrenica), males only, dry bone (Schaefer, 2008b).



The figure below shows the latest age for when an individual remained unfused (Stage 1) for the medial clavicle compared between archaeological groups. Age in years is given in coloured circles. Modern data is from Bosnia, 1995AD (war victims from the fall of Srebrenica), males only, dry bone (Schaefer, 2008b).



Although the pattern for the age-at-fusion was not significant for the medial epiphysis of the clavicle, the differences in age was reviewed between the archaeological periods.

The Roman sample entered partial fusion (Stage 2) earlier than the Iron Age sample. The duration of fusion was shorter for the Romans, but Romans entered complete fusion (Stage 3) at a later age. It is possible that the deleterious effects of Romanisation and urbanisation (Redfern and Roberts, 2005; Redfern and Dewitte, 2011; Redfern et al., 2015; Arthur et al., 2016) discussed in **Section 8.3.1.** affected the skeletal maturation of the medial clavicle.

Iron Age to Roman:

Unfused = 22 to 21 ↓

Earliest age at complete fusion: 20 to 24 ↑

All have completed fusion: >30 to 26 ↓

The age an individual could remain unfused (Stage 1) increased from Roman to Anglo-Saxon, but individuals completed fusion (Stage 3) much earlier in the Anglo-Saxon sample for the medial clavicle. This may be due to the unrest of the Anglo-Saxon period, which may have affected growth and development. As, after Rome fell into chaos, troops left for the Empire and left England defenceless (Schama, 2009). Invaders attacked: Picts from central and northern Scotland, Gaelic Dal Riata from Ireland and peoples from across the sea (Schama, 2009). Romano-British towns were burned and sacked, and this raiding, along with a lack of governmental leadership caused the economy to collapse (Schama, 2009). The English abandoned the towns and great Roman buildings, such as the bath-houses, went into disrepair (Schama, 2009). Vikings later raided and Britons were taken as slaves (Schama, 2009). It is understandable why this period in time was known as the “dark ages.”

However, the medial epiphysis of the clavicle showed an opposite effect to much of the Anglo-Saxon significant data, in which the earliest age at complete fusion (Stage 3) decreased from the Roman to the Anglo-Saxon group. Although, an earlier age at maturation does not necessarily mean that the population was healthier (Prebeg and Bralić, 2000; Klepinger, 2001; Boynton-Jarrett and Harville, 2012; Dewitte and Lewis, 2020). However, earlier maturation is seen in tandem with positive trends in nutrition and healthcare (Malina et al., 1985; Tanner et al., 1997; Gafni and Baron, 2000; Calfee et al., 2010; Duren et al., 2015; Boeyer et al., 2018). Although, maturation that occurs too early is associated with health problems (Tanner, 1962; van Lenthe et al., 1996; Klein et al., 1998; Biro et al., 2001; Cameron and Demerath, 2002;

Wang, 2002; Demerath et al., 2004; Golub et al., 2008; Kaplowitz, 2008; Schooling et al., 2010; Hauspie and Roelants, 2012; Tremblay and Larivière, 2020). Since socioeconomic impact is said to have less of a ramification on later fusing epiphyses (Cardoso, 2008b), the fusion of the medial clavicle may have not felt the environmental consequences that younger individuals did during Anglo-Saxon times. However, during Roman times, increased frailty heterogeneity (unobserved factors that increase or decrease an individual's mortality risk) possibly occurred through new settlement types, new foods, and new culture (Redfern and Dewitte, 2011; Zarulli, 2016) and this may have had far-reaching effects on even some of the last epiphyses to fuse.

Roman to Anglo-Saxon:

Unfused = 21 to 23 ↑

Earliest age at complete fusion = 24 to 22 ↓

The age an individual could remain unfused (Stage 1) increased from the Anglo-Saxon to the Mediaeval period. The earliest age at complete fusion (Stage 3) decreased from the Anglo-Saxon to Mediaeval sample. The abundant harvests, low crime rates and technological innovations of the 12<sup>th</sup> century, in which many of the Mediaeval skeletons of this study are dated to, most likely allowed for a longer duration of fusion (i.e., individuals could remain unfused for longer) and earlier skeletal maturation (i.e., individuals can mature earlier).

Anglo-Saxon to Mediaeval:

Unfused = 23 to 24 ↑

Earliest age at complete fusion = 22 to 19 ↓

For the analysis of the medial clavicle, the Post-Mediaeval group was split into early and late phases. The Post-Mediaeval London data from the 17<sup>th</sup> and 19<sup>th</sup> century (Black and Scheuer, 1996) comprise the early Post-Mediaeval group. Partial fusion (Stage 2) occurred at an earlier age compared to the Mediaeval sample and age at complete fusion (Stage 3) was delayed.

Seventeenth-century Britain was a period of civil war, pestilence, crowded, urban living and poor nutrition (History Extra, 2016; Morrill, 2016; Zuvich, 2016; Appleby and Stahl-Timmins, 2018; Murel, 2021; English Heritage, 2022). During the 18<sup>th</sup> century, industrialisation called for more women to join the workforce and parents took up artificial weaning practices to balance home and work life (Nitsch et al., 2011). This resulted in many

children lacking in essential dietary components, which caused poor health and growth attainment (Nitsch et al., 2011). Britain's urbanisation made living conditions unhygienic, and the poor were not only cramped but had little access to fresh meat and vegetables (Mant and Roberts, 2015; Eggington, 2020). However, the rich were no better, with all socioeconomic classes reliant on a cariogenic diet (Mant and Roberts, 2015), in which tea, coffee and hot chocolate were imported in high demand, and sugar consumption and milled flour caused a decrease in mandibular measurements from Mediaeval to the Post-Mediaeval period, as well as an increase in caries (Corbett and Moore, 1976; Rando et al., 2014). The rich also partook in fashionable rearing practices, such as swaddling and the prevention of children going out in sunlight, so that both the infants of the rich and the poor would be subject to nutrient deficiency, leading to an early death or stunted growth and poor health in the coming years (Newman and Gowland, 2017; Newman et al., 2019). In fact, mortality rates increased for both infants and adults from industrialisation, and growth was stunted (Lewis, 1999, 2002, 2013).

Mediaeval to early Post-Mediaeval:

Unfused = 24 to 22 ↓

Earliest age at complete fusion: 19 to 25 ↑

The later Post-Mediaeval phase is based on the data recorded for this study, which was taken from a 19<sup>th</sup> century skeletal collection from Sheffield. Both the age an individual could remain unfused (Stage 1) and the earliest age an individual completed fusion (Stage 3) decreased from the early Post-Mediaeval phase. Nineteenth-century Britain saw an economic downturn (Nitsch et al., 2011). Many women were left out of work and without the extra income, the cost of living increased (Nitsch et al., 2011). This meant that many women were homebound and could not afford the cost of milk substitutes, meaning that there was a return to breastmilk (Nitsch et al., 2011). This was healthier for children. Then, by the 1820s, agricultural productivity was greatly improved and food prices fell, allowing the population to access a more nutritious diet (Oddy, 2003). However, sugar and processed foods were now entrenched in the diet. During the 18<sup>th</sup> and 19<sup>th</sup> centuries, soft white bread was bought from bakeries, fruit and vegetable intake decreased, and sweet tea, jam and bread became a lower-class staple (Corbett and Moore, 1976; Rando et al., 2014). This phase in British history may have been at odds. On the one hand, a return to breastmilk and better access to food may have helped to optimise growth and development. However, poor nutrition would be detrimental to health, and a tentative link exists between unhealthy foods and early maturation, in which energy-dense foods could cause

higher adiposity in individuals, which could then lead to earlier maturation (Biro et al., 2001; Pechey and Monsivais, 2016). At the same time, the 18<sup>th</sup> and 19<sup>th</sup> centuries saw a rise in air pollution, poor ventilation, overcrowding and poor sanitation in the industrialised British cities (Newman and Gowland, 2017). This may be why the pattern in the Later Post-Mediaeval phase is different to the other patterns seen between archaeological groups for the medial clavicle.

Early Post-Mediaeval to Later Post-Mediaeval:

Unfused = 22 to 19 ↓

Earliest age at complete fusion: 25 to 17 ↓

The Modern data in this analysis is provided by a 1995 AD Bosnian all-male skeletal collection (Schaefer, 2008b). In opposition to the Later Post-Mediaeval phase, the Modern group showed an increase in age in both those who remained unfused and the earliest age at complete fusion (Stage 3). These ages were similar to the fusion of the medial clavicle in other Modern datasets (Webb and Suchey, 1985; Langley-Shirley and Jantz, 2010). The age individuals could remain unfused (Stage 1) was comparable to the Iron Age (22 years), Anglo-Saxon (23 years) and Mediaeval sample (24 years). Fusion was also found to remain underway (Stage 2) long into the late twenties and early thirties, like the Iron Age group.

Post-Mediaeval to Modern:

Unfused = 19 to 23 ↑

Earliest age at complete fusion: 17 to 21 ↑